



BSAVA
BRITISH SMALL ANIMAL
VETERINARY ASSOCIATION

BSAVA Manual of Canine and Feline Thoracic Imaging



Edited by
**Tobias Schwarz
and Victoria
Johnson**



Contents

List of contributors		v
Foreword		vii
Preface		viii
1	Basics of thoracic radiography and radiology <i>Heike Rudolf, Olivier Taeymans and Victoria Johnson</i>	1
2	Basics of thoracic ultrasonography <i>Gabriela Seiler, Joanna Dukes-McEwan and Lorrie Gaschen</i>	20
3	Basics of thoracic computed tomography <i>Tobias Schwarz</i>	66
4	Basics of thoracic magnetic resonance imaging <i>Fraser McConnell</i>	71
5	Basics of thoracic nuclear medicine <i>Federica Morandi</i>	75
6	Basics of respiratory interventional radiology <i>Chick Weisse</i>	82
7	The heart and major vessels <i>Victoria Johnson, Kerstin Hansson, Wilfried Mai, Joanna Dukes-McEwan, Nola Lester, Tobias Schwarz, Peter Chapman and Federica Morandi</i>	86
8	The mediastinum <i>Elizabeth Baines</i>	177
9	The oesophagus <i>Wencke M. Wagner</i>	200
10	The trachea <i>Nicolette Hayward, Tobias Schwarz and Chick Weisse</i>	213
11	The bronchial tree <i>Panagiotis Mantis, Victoria Johnson and Federica Morandi</i>	228
12	The lung parenchyma <i>Wilfried Mai, Robert O'Brien, Peter Scrivani, Yael Porat-Mosenco, Emma Tobin, Gabriela Seiler, Fraser McConnell, Tobias Schwarz and Allison Zwingenberger</i>	242

13	The pleural space <i>Mairi Frame and Alison King</i>	321
14	The thoracic boundaries <i>Francisco Llabrés-Díaz, Audrey Petite, Jimmy Saunders and Tobias Schwarz</i>	340
Appendices		
1	M-mode echocardiography reference values for cats <i>Joanna Dukes-McEwan</i>	377
2	M-mode echocardiography reference values for dogs <i>Joanna Dukes-McEwan</i>	378
3	Conversion tables	385
4	Differential diagnoses for thoracic mineralization <i>Tobias Schwarz</i>	386
	Acknowledgements	388
	Index	389

Contributors

Elizabeth Baines MA VetMB DVR DipECVDI MRCVS

The Royal Veterinary College, University of London, Hawkshead Lane, North Mymms, Hatfield, Hertfordshire AL9 7TA, UK

Peter Chapman BVetMed DipECVIM-CA (Companion Animals) MRCVS

School of Veterinary Medicine, University of Pennsylvania, 3900 Delancey Street, Philadelphia, PA 19104, USA

Joanna Dukes-McEwan BVMS (Hons) MVM PhD DVC DipECVIM-CA(Companion Animals) MRCVS

Small Animal Teaching Hospital, University of Liverpool, Leahurst, Chester High Road, Wirral CH64 7TE, UK

Mairi Frame BVMS DVR DipECVDI MRCVS

Department of Veterinary Clinical Studies, Royal (Dick) School of Veterinary Studies, Easter Bush Veterinary Centre, Easter Bush, Roslin, Midlothian EH25 9RG, UK

Lorrie Gaschen PhD Dr.habil DVM DrMedVet DipECVDI

School of Veterinary Medicine, Louisiana State University, Baton Rouge, Louisiana, LO 70803, USA

Kerstin Hansson DVM CertVR DipECVDI PhD

Department of Clinical Sciences, Division of Diagnostic Imaging and Clinical Pathology, Swedish University of Agricultural Sciences, PO Box 7054, SE-750 07, Uppsala, Sweden

Nicolette Hayward BVM&S DVR DipECVDI MRCVS

Great Western Referrals, Unit 10, Berkshire House, County Park Business Park, Shrivenham Road, Swindon, SN1 2NR, UK

Victoria Johnson BVSc DVR DipECVDI MRCVS

Animal Health Trust, Lanwades Park, Kentford, Newmarket, Suffolk CB8 7UU, UK

Alison King BVMS MVM DVR PhD DipECVDI MRCVS

Division of Companion Animal Studies, School of Veterinary Medicine, University of Glasgow, Bearsden Road, Glasgow G78 4BQ, UK

Nola Lester BSc BVMS(Hons) DipACVR

School of Veterinary Clinical Science, Division of Veterinary and Biomedical Sciences, Murdoch University, South Street, Murdoch, 6150, Western Australia

Francisco Llabrés-Díaz DVM DVR DipECVDI MRCVS

Davies Veterinary Specialists, Manor Farm Business Park, Higham Gobion, Hertfordshire SG5 3HR, UK

Wilfried Mai DVM MS PhD DipACVR DipECVDI

School of Veterinary Medicine, University of Pennsylvania, 3900 Delancey Street, Philadelphia, PA 19104, USA

Panagiotis Mantis DVM FHEA DipECVDI MRCVS

The Royal Veterinary College, University of London, Hawkshead Lane, North Mymms, Hatfield, Hertfordshire AL9 7TA, UK

Fraser McConnell BVM&S DVR DipECVDI CertSAM MRCVS

Small Animal Teaching Hospital, University of Liverpool, Leahurst, Chester High Road, Wirral CH64 7TE, UK

Federica Morandi DrMedVet MS DipECVDI DipACVR
Department of Small Animal Clinical Sciences, C 247 Veterinary Teaching Hospital,
University of Tennessee, Knoxville, TN 37996, USA

Robert O'Brien DVM MS DipACVR
Department of Clinical Sciences, Kansas State University, Manhattan, KS 66506, USA

Audrey Petite DrMedVet DVDI DipECVDI MRCVS
Davies Veterinary Specialists, Manor Farm Business Park, Higham Gobion,
Hertfordshire SG5 3HR, UK

Yael Porat-Mosenco DVM DipECVDI
School of Veterinary Medicine, University of Pennsylvania, 3900 Delancey Street, Philadelphia,
PA 19104, USA

Heike Rudolf DrMedVet DVR DipECVDI
Veterinary Diagnostic Imaging, Rheinbach, Germany

Jimmy Saunders DVM PhD CertVR DipECVDI
Department of Medical Imaging of Domestic Animals, Faculty of Veterinary Medicine,
Ghent University, Salisburylaan 133, 9820 Merelbeke, Belgium

Tobias Schwarz MA DrMedVet DVR DipECVDI DipACVR MRCVS
Department of Surgical Sciences, School of Veterinary Medicine, University of Wisconsin-Madison,
2015 Linden Drive, Madison, WI 53706, USA

Peter Scrivani DVM DipACVR
Department of Clinical Sciences, PO Box 36, Cornell University College of Veterinary Medicine,
Ithaca, NY 14853, USA

Gabriela Seiler DrMedVet DipECVDI DipACVR
School of Veterinary Medicine, University of Pennsylvania, 3900 Delancey Street, Philadelphia,
PA 19104, USA

Olivier Taeymans DVM DipECVDI
Department of Medical Imaging of Domestic Animals, Faculty of Veterinary Medicine,
Ghent University, Salisburylaan 133, 9820 Merelbeke, Belgium

Emma Tobin MVB MVM CertVR DipECVDI
Faculty of Veterinary Medicine, University College Dublin, Belfield, Dublin 4, Republic of Ireland

Wenke M. Wagner BVSc(Hons) DrMedVet MMedVet(Diagnostic Imaging) DipECVDI
Department of Companion Animal Clinical Studies, Faculty of Veterinary Science, University of
Pretoria, Private Bag X04, Onderstepoort 0110, Republic of South Africa

Chick Weisse PhD DipACVS
School of Veterinary Medicine, University of Pennsylvania, 3900 Delancey Street, Philadelphia,
PA 19104, USA

Allison Zwingenberger DVM DipECVDI DipACVR MRCVS
Department of Surgical and Radiological Sciences, School of Veterinary Medicine,
University of California-Davis, 1 Shields Avenue, 2112 Tupper Hall, Davis, California, CA 95616, USA

Foreword

The 25 years that have passed since Peter Lord and I finished writing *Thoracic Radiography: a Text Atlas of Thoracic Diseases of the Dog and the Cat* have witnessed an enormous development in new physical examination technologies. These modern non-invasive methods offer an impressive array of possibilities to depict the thoracic structures. Therefore, updating our book on Thoracic Radiography became a necessity and became urgent after our book had sold out. On several occasions I encouraged my radiologist friends to take on the update of our book. Unfortunately, several attempts to find a publisher failed.

Therefore, I was very happy when in 2005 Victoria Johnson and Tobias Schwarz informed me that they had been approached by the BSAVA to co-edit a *Manual of Canine and Feline Thoracic Imaging*. They asked for my assistance because of their intention to include some pertinent material from our book. It appeared promising to me that two enterprising radiologists were willing to co-edit a new Manual on the principles of thoracic imaging. However, I cautioned the co-editors that designing and editing such a Manual might be a considerable challenge.

Now that the Manual is done I have the great honour and pleasure to write a Foreword. The intentions of the co-editors to create a modern, condensed and comprehensive thoracic imaging manual to be used by radiology residents, practitioners and students has been kept and even surpassed. Their ambitious project has been realized with the assistance of a number of very experienced and competent co-authors. The richly illustrated Manual impresses the reader by its systematic and logical arrangement of the contents, which facilitates the orientation and simplifies the search for a specific topic.

The first part of the Manual is devoted to the basics of the various thoracic imaging technologies. Radiography, which still remains the most popular diagnostic screening tool for the thorax, is discussed in great detail, including a short digress into contrast studies and digital radiography. In the following chapters core information is provided referring to the indications, to the respective importance of other methods of diagnosing thoracic diseases, to their examination techniques, risks and the inherent limitations of other imaging methods, such as thoracic ultrasonography, computed tomography, magnetic resonance imaging, nuclear medicine and interventional radiology.

The second part of the Manual is devoted to the radiographic anatomy of the thoracic body systems and the interpretation principles used to recognize and analyse diseased organs and thoracic regions. Numerous illustrations are provided to facilitate the recognition, the interpretation and comprehension of the radiographic abnormalities and signs of diseases discussed in the text. Since radiographic signs are ambiguous most of the time, lists of diseases that may be responsible for a particular sign are included. Contrast studies and/or the use of other imaging methods are recommended where indicated.

I congratulate the co-editors, the authors and the BSAVA team assisting them on the promising outcome of the Manual. This book should be ready at hand in every small animal radiology area.

Peter F. Suter
January 2008

Preface

Thoracic radiographs are relatively easy to obtain, but particularly difficult to interpret. Thus, they are a challenge to students, practitioners and radiologists alike. Despite rapid advances in the field of diagnostic imaging, thoracic radiographs still have incredible potential as a window to both thoracic and systemic disease and remain the first step towards diagnosis. Chest films are taken every day, in nearly every veterinary practice. Love them or loathe them – we all need to try and understand them! This Manual aims to show that a careful and logical approach should remove the mystery from all but the most challenging of cases.

Since the release of the invaluable *BSAVA Manual of Small Animal Diagnostic Imaging* edited by Professor Robin Lee in 1989 and 1995, there have been tremendous advances in diagnostic imaging. Ultrasonography is now widely available in veterinary practices, and many larger hospitals, referral and academic institutions are turning to CT, MRI, endoscopic ultrasonography and nuclear medicine to make a diagnosis of thoracic disease. Historically, radiology has been confined to disease diagnosis, but the advent of interventional radiology brings exciting inroads into therapeutic techniques. The Manual lays out when and how alternative imaging techniques are indicated to narrow down the differential list and to plan a therapeutic approach.

We were lucky enough to convince immensely talented radiologists, cardiologists, internists, surgeons and interventional radiologists from around the world to contribute to this Manual. Our aim was to ensure that the Manual was as up-to-date, accurate and comprehensive as possible. The Manual is organised into two sections: the first explaining the different imaging modalities and their correct usage; and the second illustrating the features of normalcy and disease of the main anatomical compartments of the thorax. We have tried to emphasise the more common conditions and their diagnosis, but also to provide the entire spectrum of thoracic diseases. High quality images of the interpretive principles and thoracic diseases are included in this Manual.

We would like to extend our sincerest thanks to the editorial team at Woodrow House, in particular Marion Jowett and Nicola Lloyd, for their hard work and seemingly never-ending patience; Samantha Elmhurst for the wonderful artwork; and all of the authors for their expertise and valuable time. We are also extremely grateful to Professor Peter Suter who has allowed us to reproduce many diagrams and tables from his book and who's work has had an incredible influence on us and veterinary radiology as a whole.

Tobias Schwarz
Victoria Johnson
January 2008

Basics of thoracic radiography and radiology

Heike Rudolf, Olivier Taeymans and Victoria Johnson

Introduction

Thoracic radiography is an essential tool in the investigation of both thoracic and systemic disease. Radiography remains a popular diagnostic screening tool for the thorax because:

- It is time- and cost-efficient
- It uses readily available equipment
- It is relatively easy to perform
- It usually does not require general anaesthesia
- It is non-invasive and causes relatively low stress to the patient
- It is unparalleled by any other diagnostic test for these characteristics.

Despite the fact that radiography is easy to perform, careful technique is required to ensure that high-quality films are obtained. Poor technique is a common reason for misdiagnosis. The first part of this chapter outlines the methods that should be used to obtain thoracic films and special techniques to enhance their diagnostic yield.

Although thoracic radiographs are easily obtained, the thorax remains a very difficult region to interpret. This is due to:

- The effects of superimposition
- The wide range of normal anatomical and physiological variations
- Wide overlap of radiographic features of physiological and pathological processes
- Similar imaging features for different diseases
- Lack of confirmation by other non-invasive tests.

This leaves the clinician in a dilemma where thoracic radiographs are concerned because radiography is the most practical test to perform, but results are difficult to interpret. The most challenging part of thoracic radiographic examination will always be the interpretation of the films. The second part of this chapter introduces some of the basic principles of thoracic radiology that apply to all anatomical regions. These are discussed in further detail in later chapters, but an early understanding of these principles will facilitate interpretation of the thoracic radiograph as a whole.

Basics of thoracic radiography

Indications

There are many indications for thoracic radiography (Figure 1.1) and these fall into two broad categories: the assessment of intrathoracic disease; and the screening and assessment of systemic disease. In general, thoracic radiography:

- Identifies the:
 - Presence of a disease
 - Location of a disease
 - Type of lesion
 - Extent of a lesion.
- Provides a list of potential or differential diagnoses
- Suggests additional procedures
- Documents the development/course of a lesion.

Indication	Cause
Coughing	Acute or chronic bronchitis Bronchopneumonia Allergic lung disease (feline asthma, allergic bronchitis, pulmonary infiltrate with eosinophilia) Bronchiectasis Left-sided heart failure (pulmonary congestion and oedema) <i>Filaroides osleri</i> infection <i>Aleurostrongylus abstrusus</i> infection (cats) Inhaled tracheal/bronchial foreign body Pressure on the airway (e.g. enlarged left atrium, pulmonary neoplasia) Pulmonary abscess/granuloma

1.1

Indications for thoracic radiography. This list is not exhaustive. (continues)

Dyspnoea	<p>Pleural and mediastinal disorders:</p> <ul style="list-style-type: none"> • Pleural effusions • Pneumothorax • Diaphragmatic rupture • Mediastinal masses (\pm pleural fluid) <p>Pulmonary disorders:</p> <ul style="list-style-type: none"> • Pulmonary oedema (acute or chronic left-sided heart failure) • Pulmonary haemorrhage (coagulopathies or trauma) • Bronchopneumonia • Feline asthma • Widespread pulmonary neoplasia (miliary metastases) • Paraquat poisoning • Pulmonary emphysema • Heartworm disease <p>Airway obstruction:</p> <ul style="list-style-type: none"> • Tracheal foreign body • <i>Filaroides osleri</i> infection • Intraluminal tracheal/bronchial tumour
Cardiovascular disease	<p>Murmurs in young dogs</p> <p>Murmurs in adults with associated circulatory impairment</p> <p>Congestive heart failure</p> <p>Unexplained alteration in cardiac rate or rhythm</p>
Thoracic trauma	<p>Pneumothorax or pneumomediastinum</p> <p>Pulmonary haemorrhage or contusion</p> <p>Haemothorax</p> <p>Diaphragmatic rupture</p> <p>Rib fractures</p>
Neoplasia	<p>Evaluation of primary thoracic and multicentric tumours</p> <p>Evaluation of pulmonary metastases</p>
Thoracic wall lesions	<p>Rib tumours</p> <p>Discharging sinuses</p> <p>Subcutaneous emphysema</p> <p>Thoracic deformity</p>
Regurgitation	<p>Megaesophagus</p> <p>Oesophageal foreign bodies</p> <p>Vascular ring anomalies</p> <p>Oesophageal stricture</p> <p>Oesophageal diverticuli</p> <p>Oesophageal and periesophageal neoplasia</p> <p>Oesophagitis</p> <p>Hiatal hernia</p>
Miscellaneous	<p>Pyrexia of unknown origin</p> <p>Assessment of lung changes in Cushing's syndrome</p>

1.1 (continued) Indications for thoracic radiography. This list is not exhaustive.

Restraint and patient preparation

Physical restraint and positioning aids

Animals presented for thoracic radiography are often afraid, in pain, dyspnoeic or all three. With considerate handling and verbal reassurance most patients can be restrained with a combination of positioning aids and sedation. The use of verbal commands such as 'sit', 'down' and 'stay' in the language the owner uses to address the dog are usually helpful. Calming words will help to reduce fear and stress. Gentle stroking of the ear during the positioning process will activate acupuncture points and further calm the animal. Gently swaying a cat from side to side in a ventrodorsal position has been advocated to disorientate the cat and keep it still for sufficient time to take an exposure. Muzzles are also useful for cats (Figure 1.2).



1.2 Fractious cats can be difficult to restrain while conscious. A cat muzzle is often extremely useful and many cats can be positioned using tape and sandbags once this is applied.

The following are commonly employed as positioning aids:

- Sandbags (Figure 1.3)
- Troughs or bean bags
- Foam wedges
- Ties and tape.



1.3 Many positioning aids are available. Sandbags should be heavy enough to provide adequate restraint. The internal sand or beans should be shifted to either end to avoid airway compromise.

In very young kittens and puppies, the use of an atraumatic clip on the back of the neck will sometimes keep the animal still whilst in lateral recumbency (mimicking the animal being carried by the queen/bitch).

It is important to realize that trying to obtain thoracic radiographs may occasionally be *fatal* in animals with severe thoracic disease:

- Consider whether it is essential to take radiographs at this time. Do the benefits outweigh the risks? Will it change your treatment plan? Would it be safer to stabilize the patient before obtaining radiographs?
- Consider which views are safest to obtain in your patient (see Standard radiographic views, below)
- Consider placing a dyspnoeic cat in a cardboard box to obtain a screening dorsoventral (DV) view (Figure 1.4). This entails minimal restraint or intervention and should keep the cat calmer.



1.4 A dyspnoeic animal should be handled with care. If a thoracic radiograph is considered essential in a stressed cat or small dog then a screening DV radiograph can be obtained through a cardboard box. The lid can be closed (provide airholes or oxygen supply) for further calming effect.

Manual restraint

In the UK the law provides strict guidelines on restraint for small animal radiography:

- No animal should be held for radiography unless there are good clinical indications why they cannot be restrained by other means. The use of anaesthesia or sedation and positioning aids should always be considered before recourse to manual restraint

- Manual restraint should only be used in exceptional circumstances and should not be permitted unless the X-ray machine is fitted with a light beam diaphragm.

In certain other countries regulations are more lenient; however, radiation protection should be considered paramount no matter what the legal requirements.

- A maximal distance from the primary beam should be maintained.
- Two people may be required so that each is as far away from the primary beam as possible (Figure 1.5).
- Appropriate personal dosimetry devices must be used.
- Appropriate personal protection, such as lead gowns, gloves and thyroid protectors, should be employed. These items should be stored properly and checked on a regular basis to ensure continued protection.
- Pregnant women and persons under the age of 18 should not be present.



1.5 In the UK manual restraint should only be used in **exceptional** circumstances. Two people may be required to hold the animal in order that each is a maximal distance from the primary beam. Protective clothing and personal dosimeters must be worn.

Chemical restraint

Sedation: This is highly recommended for thoracic radiography unless contraindicated by the clinical condition of the patient. Sedatives have a calming effect and induce drowsiness, making the animal more amenable to handling. The level of sedation should depend upon the demeanour and general health of the animal. Quiet surroundings are essential for sedation to take effect, not only immediately after administration but during the radiographic procedure as well. If the animal is in pain, sedation will not occur unless analgesics are also administered. The reader is referred to the *BSAVA Manual of Canine and Feline Anaesthesia and Analgesia* for appropriate sedative dosages and combinations.

Anaesthesia: This is not usually required for a standard radiographic procedure. Anaesthetic-induced changes, such as atelectasis, hinder interpretation and therefore it is advisable to avoid general anaesthesia when obtaining thoracic films. However, anaesthesia may be required in difficult patients to obtain appropriate and diagnostic-quality radiographs.

- The clinical condition of the patient should be taken into account before considering anaesthesia. Intubation and intravenous access are recommended.
- Repeated gentle inflation prior to obtaining radiographs and use of different body positions may assist in preventing or resolving atelectatic change to some degree.
- The use of anaesthesia for screening for pulmonary metastases is controversial. Some radiologists prefer inspiratory radiographs in non-anaesthetized patients and others advocate inflated radiographs under general anaesthesia. If inflated radiographs are obtained under anaesthesia, then the exposure factors must be reduced and great care must be taken to avoid or resolve atelectasis. Consideration must also be given to protective clothing and dosimetry for personnel.

The reader is referred to the *BSAVA Manual of Canine and Feline Anaesthesia and Analgesia* for appropriate anaesthetic protocols.

Technique

Radiographic technique is summarized in Figure 1.6.

Intensifying screens

Screens decrease the patient dose due to their ability to convert few absorbed X-ray photons into many light photons. This X-ray to light conversion efficiency is highest in the *rare earth screens*. The speed of a screen and its ability to record detail are in a reciprocal relationship; the faster the screen, the less detail it records. Screens allow the use of short exposure times and therefore reduce the likelihood of motion artefacts; the faster the screen, the shorter the exposure time. To balance speed and recorded detail, a *medium-speed* screen should be used in most situations for thoracic radiography.

Film

Most film has photosensitive emulsion on both sides ('double-sided emulsion'). The emulsion contains the light-sensitive crystals, and the size of the grains determines the speed of the film and its sensitivity to light. The film is wedged between two intensifying screens within the cassette, and it has to be sensitive to the type of light emitted by the screens.

Medium-speed film in association with medium-speed screens will usually result in a good thoracic radiographic image. The safelight in the darkroom has to be matched to the sensitivity spectrum of the film: amber light for blue and red light for blue/green sensitive films.

Exposure

An exposure chart should be employed to optimize the radiographic result. General principles for thoracic radiography are as follows:

- High kilovoltage (kV)
- Low milliampereseconds (mAs):
 - High mA
 - Short exposure times.

The kV dictates the energy of each photon (the *quality* of the X-ray beam) and the mAs dictates the number of photons emitted (the *quantity* of X-ray photons in the beam). A high kV is used in thoracic radiography as it gives a low-contrast image with a wide range of tones of grey, enabling better evaluation of lung detail. This effect occurs with a high kV due to:

- The high degree of penetration of the beam
- The predominance of the Compton effect
- The presence of scatter (undesirable).

Since both kV and mAs contribute to film blackening, the high kV is compensated for by a low mAs. An important additional reason to keep the mAs low is to limit exposure time, thereby avoiding motion unsharpness due to respiratory movements.

Centring, collimation and use of grids

Centring: Careful centring is important. This allows accurate collimation to the area under investigation, which in turn decreases scatter.

Problem	How to counteract it
Motion unsharpness	Exposure times between 1/20 and 1/120 second
Variation in diameter and density of the thorax	High kV setting to get a long scale of grey tones; position the head towards the cathode of the X-ray tube (Heel effect); use low mAs, 2.5–5 mAs
Scatter radiation	Fine-line grid (80–100 lines per inch, ratio 8:1) for all thoraces over 10 cm in diameter or high-speed Potter-Bucky grid
Positional artefacts, superimposition, distortion	Lateral: pull limbs forward, do not rotate caudal portion of thorax; centre beam over heart DV: sternbrae and spine must be exactly superimposed; centre beam near caudal border of scapula
Detail and contrast	Expose toward the end of inspiration; high kV, low mAs

1.6 Radiographic technique for examination of the thorax. (Adapted from Suter (1984) with permission.)

Collimation: A light beam is used to show the centre and exact configuration of the X-ray field. The X-ray beam is confined to the area of the body under investigation, which limits scatter formation in neighbouring tissue. The amount of scattered radiation produced by the area under investigation also depends on the thickness of the part being examined and the kV used.

Grids: A thorax thicker than 10 cm should be radiographed with a grid to reduce the effect of scattered radiation on the film. A grid gives improved film contrast. Grids absorb multidirectional X-rays (scatter) and part of the primary beam, so exposure factors must therefore be increased slightly when using a grid. A moving grid (Potter-Bucky) will eliminate grid lines from the final radiograph.

Whichever type of grid is used it is important to be aware that improper use will lead to artefacts (such as grid cut-off) and a compromised final image.

Inspiration or expiration?

The exposure should generally be made at the end of the inspiratory phase, when the lungs are fully expanded. Radiographs taken at end-expiration show a pulmonary opacity that approaches that of a pathological infiltrate. Inspiratory and expiratory views can be useful together to evaluate dynamic changes in the lung and trachea.

End-expiratory views are advisable in certain situations, for example:

- In the diagnosis of small amounts of pleural fluid or gas (see Chapter 13)
- In the identification of pulmonary fibrosis when the degree of lung expansion is compared on both inspiratory and expiratory views (see Chapter 12).

Standard radiographic views

Radiographic views should be referred to by the entrance and exit points of the X-ray beam through the patient. For example the term 'ventrodorsal' means that the beam entered the ventral aspect of the patient and exited the dorsal aspect of the patient. The exit point of the X-ray beam is also assumed to be synonymous with the side of recumbency of the patient. For example, the term ventrodorsal also implies that the animal was lying on its back when the radiograph was obtained.

Strictly speaking a lateral view obtained with the patient in left lateral recumbency (left side next to the table) should be referred to as a 'right lateral to left lateral' view. This terminology is unwieldy in practical situations, hence lateral views are commonly described only by the recumbent side:

- Patient in left lateral recumbency = left lateral
- Patient in right lateral recumbency = right lateral.

A complete radiographic evaluation of all thoracic organs, but in particular the lungs, requires three views: two opposite lateral views and one ventrodorsal (VD) or DV view. A set of two orthogonal views can be

regarded as a minimal standard for a routine thoracic examination. A single radiographic view will provide significantly less information than a two- or three-view study, but may be appropriate if the clinical condition of the patient dictates brevity of the examination. It should be kept in mind that radiography is a screening procedure. Choosing a single radiographic view to monitor a known condition may result in loss of information about unexpected pathology.

The minimum views that should be obtained in different clinical situations are:

- Right lateral and DV views for cardiac conditions
- Right lateral and VD views for lung pathology (especially assessment of the accessory lobe)
- Left lateral, right lateral and VD views for pulmonary metastases (see Chapter 12).

Lateral views: The right and left lateral views look different, provide different information and therefore both should be obtained (see Chapters 8 and 12). However, if the examination is limited to only one lateral view then the right lateral is usually preferable because:

- The diaphragm obscures less of the caudodorsal lung field
- The heart is in a more consistent position due to the cardiac notch of the lungs on the right side
- In inflated views of the chest, the right middle lobe will project itself between the heart and the sternum, resulting in better cardiac detail
- An enlargement of the sternal lymph node is more easily identified.

Technique for lateral recumbent views:

1. Position the animal in right or left lateral recumbency.
2. Place a sandbag over the neck with the sand distributed to either end of the bag so as not to obstruct the airway (Figure 1.7).
3. Gently pull the forelimbs forward and hold in place with sandbags or ties to avoid superimposition of the triceps muscles over the cranial lung lobes.

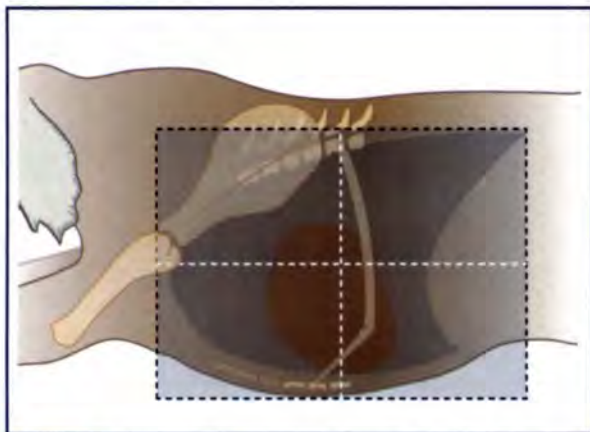


1.7 A dog positioned in left lateral recumbency for a thoracic radiograph. Note the full extension of the forelimbs and the use of a sandbag across the neck. The head and neck are gently extended. A foam pad has been placed under the head to make the dog comfortable. Some dogs will require a small foam wedge under the sternum to ensure that it is parallel to the spine.

4. Position a second sandbag over the hindquarters or wrap around the hindlimbs to ensure the animal remains in the required position.
5. Gently extend the head and neck to avoid positional variation of the trachea.
6. The sternum and vertebrae should be level with each other. This can be achieved by positioning a foam wedge under the sternum to elevate it to the required level (Figure 1.8). Barrel-chested dogs, such as English Bull Terriers, may require the foam wedge under the spine.
7. Centre the beam at the caudal aspect of the scapula and two-thirds of this distance down the chest (Figure 1.9).
8. Collimation should include the thoracic inlet and whole diaphragm (including part of the liver). Ventrally the sternum should be included. A common mistake is to extend dorsal collimation to the most dorsal skin surface of the animal. This is unnecessary, as inclusion of the spine will be sufficient to evaluate the entire dorsal lung fields.
9. Include a positional marker (right or left) in the collimated area.

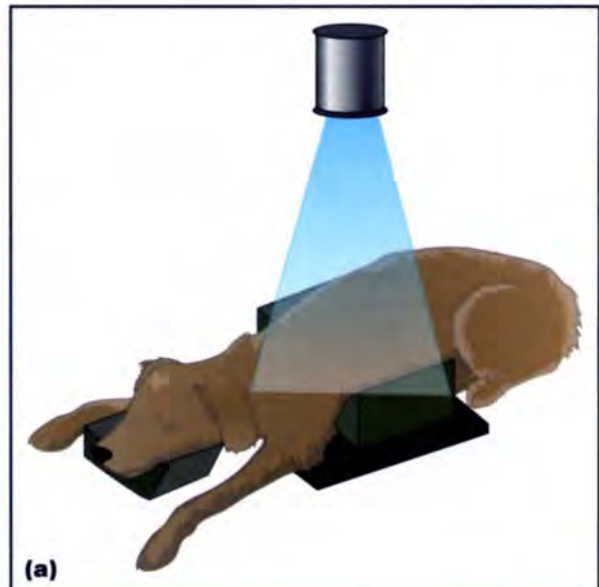


1.8 The use of foam wedges to achieve a parallel spine and sternum.



1.9 Location for centring point of the beam for a lateral thoracic radiograph.

Dorsoventral and ventrodorsal views: DV and VD radiographs are rarely both needed but each view has its advantages and disadvantages. On DV views the cardiac silhouette assumes a more standard appearance, is less magnified, and the caudal pulmonary arteries and veins are more easily identified surrounded by a gas-filled lung; this view is therefore often preferred in animals with heart disease. VD views are generally considered more useful for evaluation of the pulmonary parenchyma. There may be some situations where it is beneficial to obtain one or both views, and this is discussed in the relevant chapters. One of the most important technical aspects of any VD or DV view is to acquire it with the animal in a perfectly straight position (Figure 1.10). In sedated animals without manual restraint this is often most easily achieved with a DV view (natural sternal recumbency). However, in some deep-chested animals (such as the Afghan Hound) a straight VD view will be easier to obtain.



1.10 (a) Positioning for the DV view. (b) Positioning for the VD view.

It is important to note that the DV view is always preferable for animals in respiratory distress. This is a position the animal itself would assume as it allows:

- Full expansion of the rib cage during inspiration
- Positioning of the elbows away from the thorax
- Extension of the neck thereby allowing undisturbed airflow in the trachea.

Since different situations may require either a DV or a VD view, it is useful to be familiar with the acquisition as well as the interpretation of both image types.

Technique for DV view:

1. Position the animal in sternal recumbency with elbows to either side of the chest and the hindlimbs flexed, resulting in a crouching position (Figure 1.11).
2. Patient comfort is important and it may be helpful to support the hindfeet with sandbags to avoid slipping.
3. Narrow-chested breeds may be more comfortable with a slender foam block under the sternum.
4. Take great care to ensure that the animal is straight with sternum and vertebrae superimposed.
5. Gently extend the neck and if necessary rest it on a foam block.
6. Place a sandbag across the neck, taking care not to compromise the airway.
7. Centre the beam between the shoulder blades and at their caudal aspect.

8. Collimation should include the thoracic inlet, diaphragm and cranial abdomen, and the lateral aspects of the thorax.
9. Include a positional marker (right or left) in the collimated area.

Technique for VD view:

1. Place the animal in dorsal recumbency in a trough or bean bag.
2. Pull the forelimbs forward and fix them in position with sandbags (Figure 1.12).
3. Allow the hindlimbs to remain in a flexed ('frog leg') position, the stifles may be supported by foam blocks or by shifting the beans in the bean bag.
4. Alternatively, ties or tape may be used to secure the legs; care should be taken, however, that the animal is not uncomfortable and does not struggle or injure itself.
5. The vertebrae and sternum should be superimposed.
6. Centre the beam on the centre of the sternum.

Collimation and labelling are as described for the DV view.



1.11 Positioning for a DV radiograph. **(a)** The elbows are to either side of the chest and a sandbag has been used across the front feet and over the neck. **(b)** It can be helpful also to support the hindlegs with a sandbag. **(c)** The radiograph is centred at the caudal aspect of the shoulder blades in the midline. **(d)** A measurement is made from the centring point to determine the exposure to be set.



1.12 A dog positioned in a trough for a VD thoracic radiograph. Sandbags are used to pull the forelimbs cranially. A small foam wedge has been placed under the head to make the dog comfortable. Care has been taken to make sure that the sternum is vertically above the spine.

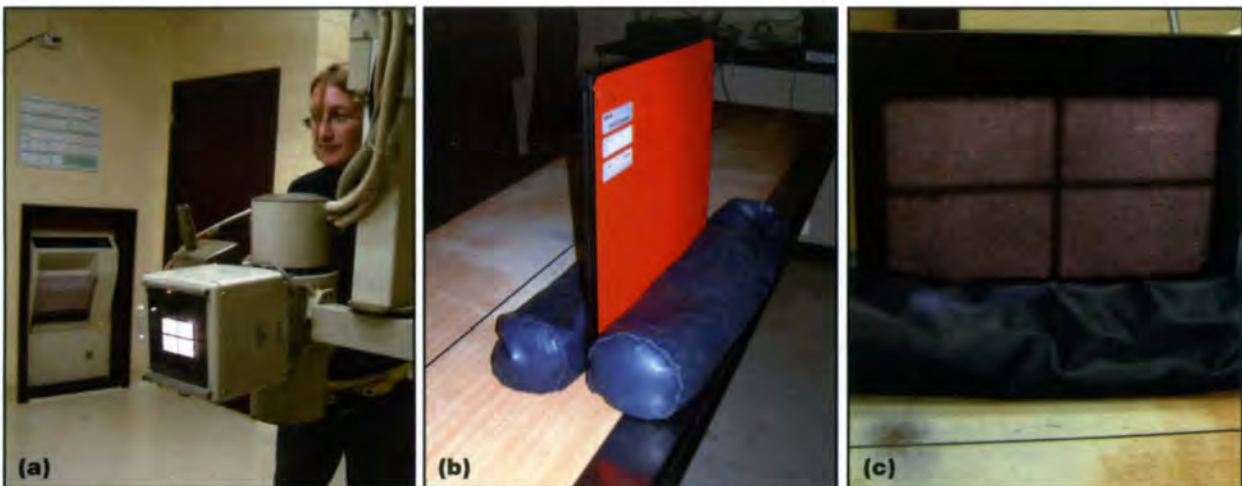
Supplementary views

Decubitus view or horizontal beam VD/DV view:

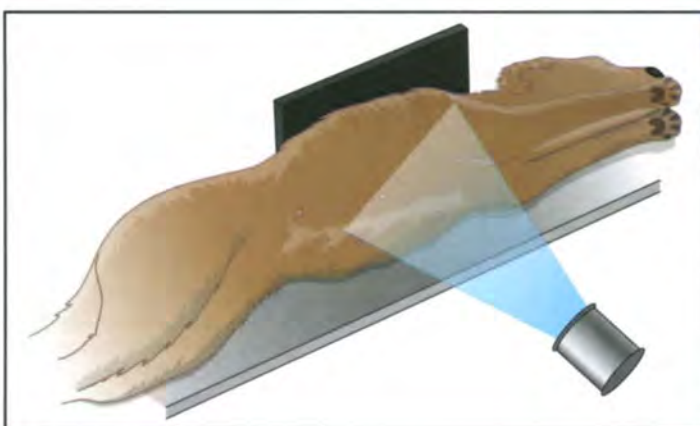
This is indicated in the detection of a small pneumothorax and small amounts of pleural effusion, and is also useful to skyline thoracic wall lesions. The decision as to whether to use left or right lateral recumbency will depend on the indication for obtaining this view. As with all horizontal beam views, radiation safety is paramount. Consideration must be given to personnel safety, where the beam is directed and suitable equipment (e.g. lead-backed cassettes).

The technique is as follows (Figures 1.13 and 1.14):

1. Position the patient in lateral recumbency and direct the beam horizontally by turning the X-ray tube head through 90 degrees.
2. Position the cassette against the spine or the sternum (it may have to be supported by



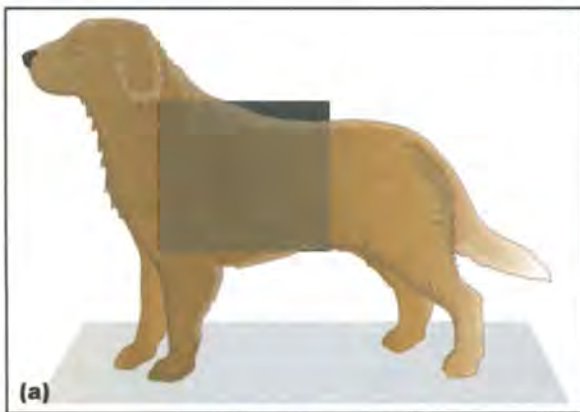
1.13 (a) In order to take a decubitus view a horizontal X-ray beam is required. Consideration should be given as to where the beam is aimed (e.g. thickness of wall behind). (b) A cassette can then be held in an upright position using sandbags. (c) An area of collimation is established. The dog is then positioned in lateral recumbency with the spine adjacent to the cassette. A foam wedge may be needed to elevate the patient. (d) Normal decubitus radiograph in a mature dog. The dog is in left lateral recumbency and the right lung is uppermost. The lung markings extend to the periphery of the lung and there is no evidence of pneumothorax.



1.14 Positioning for the decubitus view.

- sandbags or be positioned in a cassette holder to remain upright).
- It is important to maintain the usual film–focus distance (FFD).
 - If a grid is used, the tube head should be aligned carefully with respect to the grid in order to avoid artefact.

Horizontal beam standing view: This view is indicated in animals with severe respiratory compromise that cannot be positioned in lateral recumbency to obtain a lateral view (Figure 1.15). It is a useful position for the detection of pneumothorax, pleural effusion and gas–fluid interfaces of cysts or abscesses. This position, however, is less sensitive for the detection of small amounts of pleural effusion when compared with the decubitus lateral view described above. A similar view can also be achieved with the animal in sternal recumbency or in a sitting position. It may be easier to extend the front legs more adequately in sternal recumbency than in a standing position.



1.15 (a) Positioning and set-up for a horizontal beam standing lateral radiograph. (b) A horizontal beam standing view in a dog. In this example the cassette has been attached to a vertically suspended platform, but in practice it can be taped to a wall or suspended in a carrier bag from a drip stand.

The technique is as follows:

- Position the cassette in a cassette holder against the chest wall (alternatively, sandbags may be used if the animal is in sternal recumbency).

- Rotate the tube head 90 degrees and centre and collimate as for a lateral recumbent view.

The previous comments apply with respect to radiation safety, FFD and the use of grids.

Oblique VD/DV or lesion-oriented oblique view:

This is indicated for the assessment of lesions of the thoracic wall and for the demonstration of the oesophagus, avoiding its superimposition with the spine. The animal is positioned so that the lesion is projected tangentially (Figure 1.16); the degree of obliquity depends on the precise location of the lesion. The exposure factors must be reduced considerably compared with the exposure used for the straight VD/DV thorax view.



1.16 An oblique DV view.

Digital radiography

Two types of digital radiography exist: computed radiography (CR) and, more recently, direct radiography (DR). The method of detecting and processing the image in both CR and DR is completely different to that used in film–screen radiography. Digital radiography will become increasingly prevalent in clinical and radiographic practice over the next few years. It is important to be aware of the advantages and disadvantages that these modalities will bring.

Principles of computed radiography

CR uses a specialized cassette (imaging plate) and image reading device (Figure 1.17). The cassette does not contain a film wedged between two intensifying screens but rather a photostimulable phosphor plate. CR can be used with the existing X-ray tube, generator and table top.

The phosphor absorbs the X-ray energy and keeps it for a period of time. The exposed cassette is fed into the image reading device and a laser is used to release the stored energy in the form of luminescent light. A photomultiplier transforms the light into electrical signals where the different light intensities result in a digital picture. Once the plate



1.17 A CR image reading device. Many different brands and types are available.

is read, the information on it is erased by white light to prepare it for the next exposure. The digital image can now be manipulated or post-processed using a computer (Figure 1.18).



1.18 The final CR image on a viewing monitor. The resolution of the monitor is extremely important. Post-processing, such as enlargement, annotation and windowing, can be performed at this time.

The image reading process usually takes about 90 seconds, but each imaging plate must be processed one at a time. It is important to tell the image reading device which algorithm to use to process the image (i.e. a skeletal radiograph will be processed very differently to a thoracic radiograph).

Principles of direct radiography

DR can be compared with digital photography in that an immediate image is created on a screen without a processing step. The cassette, screen and film are replaced by a digital imaging sensor, which may be permanently fixed to the X-ray suite table, or attached by wires. It is possible that wireless systems may become available in the future.

An *immediate* image is generated on a screen once the imaging sensor is exposed. There is no need for processing or waiting. The digital image can then be manipulated or post-processed using a computer.

Advantages and disadvantages of digital radiography

It is important to realize that digital radiography gives one almost exactly the same information as a carefully obtained and processed film–screen radiograph. In fact, film–screen radiographs have better spatial resolution than digital radiographs. However, there are many important advantages of a digital system and these are discussed below.

Advantages:

- A wider range of exposures can be used without resulting in a non-diagnostic film, due to the increased latitude of digital systems. This results in a reduction of repeated radiographs due to poor exposure, therefore there is:
 - Increased radiation safety
 - Increased patient throughput.Repeats due to poor positioning or patient movement do not go away though!
- DR is quicker than film–screen radiography. CR processing may actually be slower (see comments below).
- Theoretical ability to use lower exposure factors than for conventional film–screen combinations. (However, note that digital radiography is generally more forgiving to overexposed than underexposed films and therefore the tendency may be to increase exposure factors over time.)
- Post-processing allows the viewing of individual lung areas at high magnification; it also allows the choice of different density curves to examine relatively underexposed areas, such as the vertebral column, in the same detail as the correctly exposed areas, such as the lung.
- Long-term cost reduction if a completely filmless system is attained.
- No lost films, no time wasted on filing or retrieving films.
- All the inherent advantages of digital images, e.g. ability to send images easily as email attachment.

Disadvantages:

- Expense, especially of the DR system. Savings with the new system will only be realized once a completely filmless state is achieved, and this requires increased initial outlay.
- Technology is rapidly evolving; therefore, a system may become quickly outdated.

- Need for special veterinary software: not all human systems are immediately adaptable to veterinary patients.
- The resolution depends on the quality of the monitor (2000 x 2000 pixels is the minimum). Monitors with better resolution are more expensive.
- CR and DR have certain artefacts that are not seen in film–screen radiography. This is not really a disadvantage as such: they just need to be understood and avoided.
- With CR, the throughput of films may actually decrease. In most systems, only one image can be processed every 90 seconds, compared with a film–screen processor where the process takes the same amount of time, but films can be introduced one after the other.
- Quality of erasing the image in the CR system depends on the type of equipment and, if poor, has dramatic repercussions on the quality of the following exposures and therefore the life of the system.
- The attaching wires in DR may get damaged or in the way during exposures.
- It may not be possible to take horizontal beam views with the fixed in-table DR systems.

Contrast radiography

Oesophagography

The oesophagus is normally not visible on survey radiographs, although it can be spontaneously outlined by an accumulation of air, fluid or solid food within its lumen. A detailed radiographic examination can only be performed after an opaque contrast medium has been administered (see also Chapter 9).

Indications:

- Intrinsic mass, foreign body.
- Megaoesophagus.
- Stricture, vascular ring anomaly.
- Oesophageal perforation.
- Oesophagitis.
- Diverticulum.
- Tracheo-oesophageal fistula.
- Dysphagia.
- Mediastinal mass.
- Hiatal hernia.

Choice of contrast medium:

Barium: Different types of barium can be used in the examination:

- Barium sulphate suspension. Should be used for initial examination. A 60% weight/volume suspension should be used. May not distend a dilated oesophagus or show a stricture. Does not adhere well to mucosa.
- Barium sulphate pastes or creams. Formulated for extreme radiopacity and to enable good adherence to oesophageal mucosa. Useful to evaluate foreign bodies and masses, but

generally of limited value in the dog and cat. Paste aspiration may lead to asphyxiation.

- Barium sulphate suspension plus food ('barium burger' usually one part barium to three parts canned food/kibble). Very useful to demonstrate even early oesophageal strictures, dilatations and regional motility disorders.

Barium contrast media are delicately equilibrated suspensions, which easily precipitate if mixed with water of less than optimal hardness. It is therefore best to use barium suspensions that are premixed in different concentrations by the manufacturer.

If barium is *aspirated* the consequences are usually limited as long as the volume is small. The aspirated barium usually coats only the trachea and is then removed by ciliary motion and coughing. Aspiration of barium into the alveoli may result in permanent visualization, but is unlikely to affect lung function. However, clinical signs seen are related to the volume and location of aspirated barium. Rare consequences include pneumonia and granulomatous reactions.

If an *oesophageal perforation* or *broncho-oesophageal fistula* is present or suspected then barium should not be used, as mediastinal complications such as adhesions and granuloma formation may result. In this situation *non-ionic iodinated contrast media alone* (no kibble/food, etc.) should be used. Ionic iodinated agents should also be avoided as aspiration of hypertonic contrast media can result in pulmonary oedema and possibly death.

Iodinated contrast media: Two main classes exist. Both types taste bitter and an oesophageal tube is usually required for administration. The types are:

- *Ionic* (hyperosmolar) iodinated contrast media, e.g. diatrizoate meglumine and diatrizoate sodium (Gastrografin®). Ionic forms are cheaper than non-ionic but may induce pulmonary oedema if aspirated. They may also cause severe dehydration in an already volume-depleted animal while passing through the gastrointestinal tract due to the hypertonicity of the agent
- *Non-ionic* (low osmolar) iodinated contrast media, e.g. iohexol (Omnipaque®). These have far fewer side effects but are more expensive than ionic agents. Iso-osmolar forms are also available but are even more expensive. Non-ionic contrast media must be used in cases where a gastrointestinal perforation or broncho-oesophageal fistula is suspected.

Air or other gas: This is also known as a negative contrast study or pneumo-oesophagram; it is not used routinely. It is occasionally useful, for example, to define an oesophageal mass (see Figure 9.21b, p. 209). Air embolism is a theoretically possible side effect, but is extremely unlikely.

Technique: Oesophagography is quick and easy to perform. No specific patient preparation is required, although a hungry patient may ease the job of

administering a contrast media/food mixture. The patient must be conscious. Sedation should be avoided as this may depress gastrointestinal motility; however, an extremely difficult patient may be given a low dose of a phenothiazine sedative.

Survey radiographs are a prerequisite; significant findings may be identified prior to contrast media administration (e.g. foreign body) and appropriate exposure factors can be selected.

The technique is as follows:

1. Administer approximately 10–20 ml of contrast medium orally to induce several complete swallows.
2. Start with barium sulphate suspension (liquid).
3. Obtain immediate lateral and VD (or DV) radiographs.
4. Then offer a barium/food mixture or place it in the mouth.
5. Repeat radiographs.

Lateral views are the most informative. The visibility of the thoracic inlet can be improved by moving one thoracic limb cranially and the other caudally. Additional information may be gained from an oblique VD view of the thoracic oesophagus: the beam should be angled 15–30 degrees from left ventral to right dorsal.

Fluoroscopy is required for the evaluation of functional disorders resulting in dysphagia (e.g. cricopharyngeal achalasia or pharyngeal incoordination). The evaluation of these disorders is beyond the scope of this manual. They should be investigated first with barium sulphate suspension followed by a mixture of barium and food/kibble. Extremely slow frame rates are required for meaningful assessment of swallowing disorders. Care should be taken when administering contrast media to animals with swallowing disorders to minimize the risk of aspiration.

A pneumo-oesophagram is carried out on an anaesthetized patient. The oesophagus is inflated with room air using a second endotracheal (ET) tube (with the cuff inflated).

Bronchography

The bronchial tree is outlined by coating its mucosal surface with a positive contrast medium (Figure 1.19). Nowadays this technique has been superseded by fiberoptic bronchoscopy and computed tomography (CT) and is considered obsolete.

Angiocardiography

With angiocardiography the chambers of the heart and the great vessels are seen due to the presence of intraluminal iodinated contrast medium. Angiocardiography can be performed in a non-selective (peripheral injection of contrast medium) or in a selective (injection into the cardiac chambers or great vessels) way. Further information on this technique is beyond the scope of this manual, but some examples of normal and abnormal angiographic studies are provided in Chapters 5 and 7.



1.19

A normal bronchogram of the left cranial lobar bronchus. Bronchography is now an obsolete technique.

Fluoroscopy

Fluoroscopy is a technique whereby X-rays are used to produce a real-time instantaneous image. The X-rays leaving the patient are received by an image intensifier and the final output is transmitted to a television screen. Images are recorded digitally or on videotape. Fluoroscopy adds a dynamic dimension to the thoracic examination and has many inherent advantages:

- Images can be viewed immediately – there is no delay for film processing
- Allows real-time investigation of movement, which is extremely useful for the assessment of functional abnormalities
- Synchronous timing of radiographic exposures in relation to a movement is unnecessary (e.g. gastro-oesophageal reflux)
- Invasive procedures can be performed quickly and under constant guidance
- Fluoroscopic images may be captured in a variety of ways. These may be analogue or digital and include cine, video, film or digital still-frame images
- If a digital system is used, subtraction images can be generated. This is extremely useful in interventional procedures.

Indications

- Dysphagia (e.g. pharyngeal or cricopharyngeal dysfunction).
- Oesophageal disorders (e.g. strictures, foreign body).
- Removal of oesophageal foreign bodies.
- Tracheal collapse.
- Tracheal stent placement.
- Sliding hernias (e.g. hiatal, lung).
- Evaluation of diaphragmatic paralysis.

- Angiocardiology and therapeutic procedures (e.g. balloon valvuloplasty).
- Biopsy guidance (e.g. lung biopsy).

Technique

Specific fluoroscopic examinations are discussed in the relevant chapters (see Chapters 6, 7, 9, 10 and 14).

Personnel are usually required to remain in the room for most fluoroscopic examinations because anaesthesia is contraindicated for most functional examinations, and interventional procedures require the presence of personnel by their very nature (Figure 1.20). Radiation safety is paramount. Due care and attention must therefore be given to correct protective clothing, position with regard to the X-ray tube, time limitation, lead curtaining and personal dosimetry. Fluoroscopy remains a hazardous examination method and therefore:

- Should be used sparingly
- Should never be employed for extended periods of time
- Indications must be selected carefully
- Numbers of personnel should be limited
- Manual restraint should be avoided:
 - Consider sedation or general anaesthesia if possible
 - Certain procedures may be performed with smaller animals restrained in a cardboard box. The box must be narrow to prevent turning and be close to the image intensifier.



1.20 An X-ray suite with an image intensifier for fluoroscopy. The image intensifier is pulled forward for use and the corresponding X-ray tube is underneath the table. The image is shown on the television screen. Many different types of fluoroscopy set-up exist.

Basics of thoracic radiology

Prerequisites for evaluation of thoracic radiographs

Interpreting thoracic radiographs is not an easy task, even for an experienced radiologist. The best approach

is to adopt a careful routine for viewing a series of thoracic films. The following is a suggested protocol:

- Your viewing area should be quiet and dark and an appropriate bright light should be available for viewing relatively overexposed regions of the films
- Do you have an adequate number of views?
- Is the animal well positioned and are the radiographs of diagnostic quality?
- What phase of respiration were the films acquired in?
- Does the phase of respiration alter between films? (This is useful to assess hyperinflation and air trapping, upper respiratory tract obstructions, tracheal collapse, fibrotic conditions, etc.)
- What is the body condition of the animal and how does this affect your interpretation of the film?
- What is the age of the animal and how does this affect your interpretation of the film?
- What is the breed of the animal and how does this affect your interpretation of the film?
- After reading the films, ask yourself whether further views would assist in your diagnosis (e.g. a decubitus view, an end-expiratory view, an additional lateral view).

Systematic evaluation of the thoracic radiograph

There are many appropriate techniques for reading radiographs. Some people prefer to assess anatomical structures or regions in a particular order (see below). Other people prefer to assess a film from top to bottom, or from the centre out, or from left to right. The important thing is to choose a technique that suits you and that covers every structure on the film, and then stick to it each time you look at a radiograph.

In a clinical setting you will usually be reading the radiograph with the patient history in mind. You may find it useful to look at films without prior knowledge of the clinical history of the patient whenever this is possible (e.g. reviewing films for a colleague). This helps to prevent bias and enables you to keep an open mind as to the abnormalities that may be present. It is then advisable to review the film in the light of the clinical information and finally to look again at the regions of the film that you considered to be normal. It is also valuable to discuss radiographs with colleagues and to look at them again later. All of these techniques may assist in reducing the inevitable number of errors in thoracic radiographic interpretation.

Anatomical

The following is a suggested route for reading a thoracic radiograph based on the patient's anatomy. Each of the Röntgen signs (see below) should be considered for each structure. Look at:

- The surrounding soft tissues
- The cranial abdomen and diaphragm
- The neck
- All bones
- The pleural space
- The mediastinum

- The trachea and carina
- The bronchi
- The cardiac silhouette
- The aorta, caudal vena cava and pulmonary vasculature
- The lung.

Many people find it useful to rotate the radiograph 90 degrees when assessing the ribs. By creating this unfamiliar way of looking at the radiograph the ribs appear to 'stand out' more to the observer (Figure 1.21).



1.21 The simple technique of rotating a radiograph 90 degrees to an unfamiliar position immediately enables the observer to assess the ribs and other skeletal structures more thoroughly.

Topographical

Alternatively, it is possible to assess thoracic radiographs by dividing up the image into different areas and assessing them step-by-step. This can be done as a cranial-to-caudal, central-to-peripheral approach or any other way ensuring that each part of the radiograph is assessed. One advantage of the topographical method is a less biased assessment because every area is evaluated out of its anatomical and physiological context. The disadvantage is the lack of this context, which makes it harder to develop a coherent description and meaningful diagnosis. Also, some important thoracic compartments are normally not visible (pleural space, mediastinum), and ensuring the absence of a structure is somewhat more awkward to encompass with a topographical search.

To some degree a topographical search is always part of an anatomical assessment plan (e.g. searching for nodules throughout the lungs).

Variations in radiographic anatomy

Enormous variation exists in the normal radiographic appearance of the thorax, especially in the dog. It is essential to consider these variable factors every time a radiograph is assessed. Some may be removed by repeating the exposure (e.g. a second attempt at obtaining an inspiratory rather than an expiratory film) but others are an inherent feature of the patient and cannot be altered (e.g. age, breed). Ignoring these normal variations will undoubtedly lead to hazardous interpretation and to possible misdiagnosis. These variations are also described in more detail in the respective anatomical chapters of this manual.

Breed, age, sex and body condition

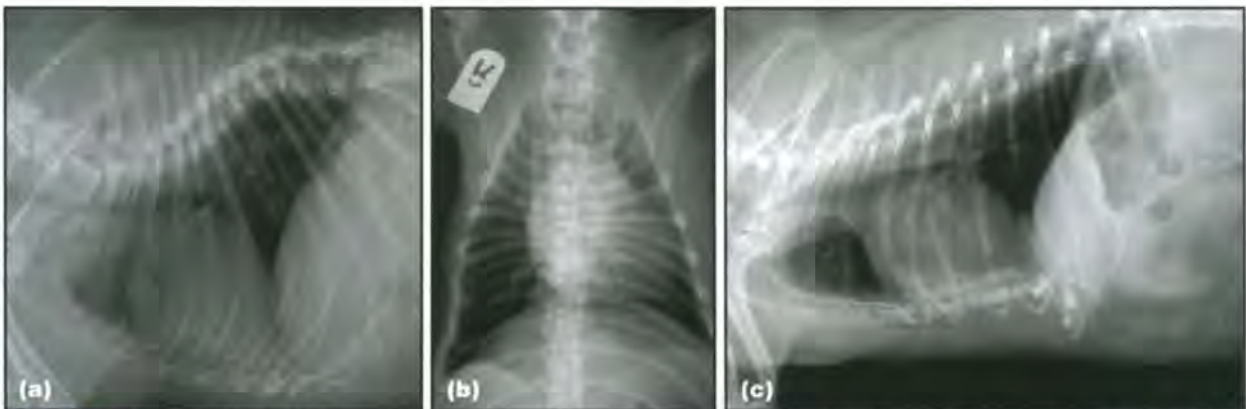
These factors have an important influence on the appearance of normal radiographic anatomy.

Breed: This has little influence on the normal appearance of a feline radiograph, but considerable impact on the evaluation of canine thoracic radiographs. Three main canine body types should be recognized:

- Deep, narrow-chested conformation (e.g. Afghan Hound, Irish Setter, Greyhound)
- Intermediate thoracic conformation (e.g. German Shepherd Dog, Boxer, Retriever, Standard Poodle)
- Wide, shallow conformation (e.g. Boston Terrier, Bulldog).

These conformational variations have importance in the evaluation of structures such as the mediastinum and cardiac silhouette. This is discussed later in the individual chapter sections.

Additional factors to consider are breed-related spinal abnormalities (e.g. wedge or butterfly vertebrae in screw-tailed breeds such as the French Bulldog) that can lead to kyphosis, scoliosis or lordosis (Figure 1.22). Sternal abnormalities (such as pectus excavatum) will also influence the radiographic appearance of the thorax. Alterations in the spinal or sternal



1.22 (a) Lateral and (b) VD radiographs of a French Bulldog. The dog has multiple spinal abnormalities, including wedge and butterfly vertebrae, lordosis and kyphosis. (c) A Lhaso Apso with a severe pectus excavatum. Such abnormalities make perfect positioning impossible and interpretation harder.

curvature may result in the projection of normal soft tissue structures over the lung fields. Chondrodystrophoid breeds (especially the Basset Hound) often have unusual costal cartilage and knobby costochondral junctions, which may appear nodule-like and create confusing shadows over the lung fields.

Age: Young animals have a detectable thymic shadow. This reaches a maximum size at about 4 months and then progressively involutes until it is no longer radiographically visible (usually not seen after the age of 6 months). Depending on the age of the animal, open physes may be seen in the skeleton.

Many old dogs (Figure 1.23) have varying degrees of spondylosis deformans, degenerative sternal changes, mineralized costochondral junctions, bronchial and tracheal rings, pulmonary osteomas and some degree of age-related fine interstitial lung patterns. Pleural thickening may also be seen in older animals.



1.23 Left lateral radiograph of an 11-year-old Labrador Retriever. Note the spondylosis deformans and degenerative changes in the sternum and fine interstitial lung pattern. These are age-related changes.

Older cats may have an elongated aorta and this is often accompanied by a cranially sloping cardiac silhouette. Fragmented costal cartilages are seen as a normal variation in some older cats.

Sex: Females often have prominent nipples (especially pregnant, in-season or older postparturient bitches) and these can be confused with pulmonary nodules when superimposed over the lung fields.

Body condition: Obesity influences the interpretation of many thoracic structures (Figure 1.24). Large amounts of fat will alter the appearance of the cardiac silhouette (mimicking cardiomegaly), widen the cranial mediastinum, create an overall increase in the opacity of the lung fields and separate the edge of the lung from the thoracic wall (mimicking a pleural effusion). Exposures should be increased for thoracic radiography in these animals, but despite this action considerable difficulty still exists in the interpretation of films from overweight patients.



1.24 DV radiograph of the thorax of an extremely fat dog. The large amount of pericardial fat is evident as a separate structure in this dog (between black and white arrows) but in many animals is not distinguishable and may mimic cardiomegaly. The cranial mediastinum is very wide due to the presence of fat and the lung fields are generally increased in opacity.

Emaciated animals will appear to have hyperlucent lung fields and exposures will need to be reduced in these animals to create a diagnostic radiograph. Structures such as the azygous vein may also be seen in a thin animal. This is especially the case in narrow-chested breeds such as the Greyhound. Severe emaciation can also result in microcardia (a small cardiac silhouette).

Respiratory phase

It is important to recognize the differences between radiographs obtained at full inspiration and those obtained during expiration. Figure 1.25 outlines the major differences and Figure 12.9 (p. 246) illustrates these principles.

Cardiac cycle

The influence of cardiac motion on a radiograph varies from animal to animal. Generally the edges of the cardiac silhouette should appear slightly hazy due to the presence of cardiac motion during the radiographic exposure, and a sharply marginated, enlarged cardiac silhouette should alert the clinician to the possibility of a pericardial effusion. The changes between systole and diastole are best seen in large dogs, on the DV view and with short exposure times. Near end-systole the ventricular area is small and the atria are well rounded and bulging out. At end-diastole the ventricles are larger and rounder and the atria less conspicuous. The main pulmonary artery varies a great deal during the cardiac cycle and will appear more prominent during systole.

Radiographic features	Inspiration	Expiration
Overall pulmonary radiolucency	Increased radiolucency Good contrast to vascular structures, bronchial walls and heart	Diminished radiolucency Poor contrast to vascular and bronchial walls; bronchial lumen may be seen
Lateral radiograph Retrosternal radiolucency (area of cranial lobes)	Slight separation of right ventricular margin from sternum Retrosternal radiolucency increased Ill defined ventral border of cranial vena cava (CrVC)	Extended contact between right ventricular margin and sternum Well defined ventral border of CrVC
Dorsocaudal lung region	Lumbodiaphragmatic recess ^a around T12 and open Distances from spine to carina and lumbodiaphragmatic recess ^a to caudal vena cava (CdVC) are increased	Lumbodiaphragmatic recess ^a around T11 and closed Distances from spine to carina and lumbodiaphragmatic recess ^a to CdVC are diminished
Postcardiac triangle between caudal heart border, ventral diaphragm and CdVC (accessory lobe area)	Minimal or no contact between heart and diaphragm Horizontal position of CdVC Radiolucent, large accessory lobe area Flattened diaphragm	Ventricular border and diaphragm intersect Caudally ascending position of CdVC Radiopaque, small accessory lobe area Rounded diaphragm
Relative and absolute cardiac size (cardiothoracic ratio)	Diminished (i.e. small cardiac size with respect to thoracic size)	Increased (i.e. larger cardiac size with respect to thoracic size)
Dorsoventral radiograph Changes of caudal thorax (the cranial thorax barely changes, or not at all, with respiration)	Caudal thorax widened and lengthened Diaphragmatic cupula approximately at T8–T10 Open costodiaphragmatic recesses ^b	Caudal thorax narrowed and shortened Diaphragmatic cupula approximately at T7–T8 Narrowed costodiaphragmatic recesses ^b
Cardiac size	Relatively and absolutely smaller than on expiration	Relatively and absolutely larger than on inspiration

1.25 Radiographic features of inspiration and expiration in dogs. ^a The lumbodiaphragmatic recess is the angular region between the diaphragm and the thoracolumbar spine on a lateral radiograph. ^b The costodiaphragmatic recess is the angular region between the diaphragm and the ribs on a DVVD radiograph. (Adapted from Suter (1984) with permission.)

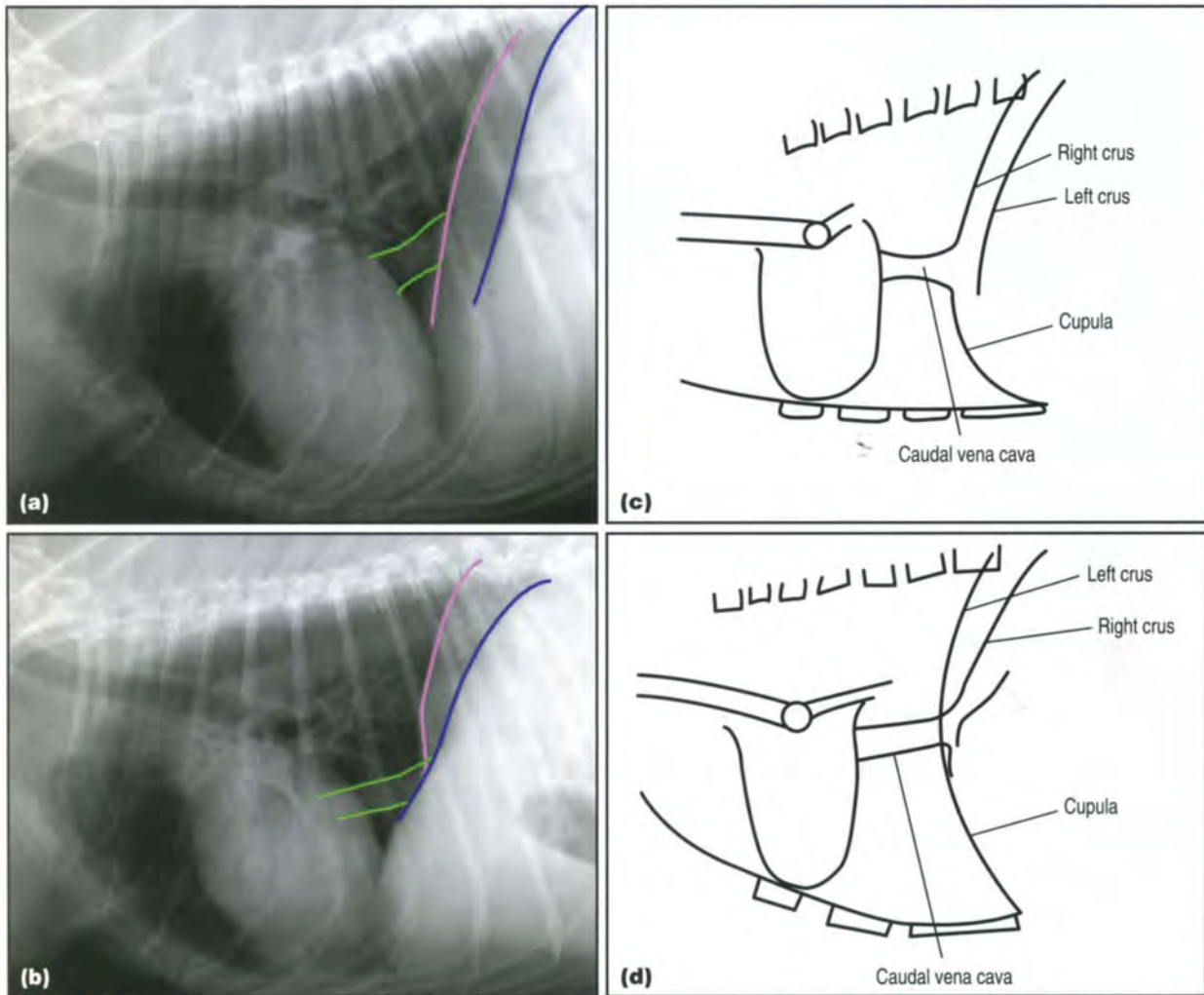
Body position

There are inherent differences between left and right lateral views and between DV and VD radiographs of the thorax. It is even possible to identify which view has been obtained based on the appearance

of certain anatomical structures on the film. These principles are shown in Figures 1.26, 1.27, 1.28 and 1.29. These differences are more pronounced in larger dogs than in small dogs and cats.

Structure	Right lateral	Left lateral
Diaphragm	The crura appear parallel	The crura appear "Y" shaped
Gastric gas shadow	Gas is present within the fundus, seen dorsally behind the left crus of the diaphragm	Gas is present ventrally within the pyloric antrum
Caudal vena cava	Seen to merge with the most cranial crus (the right crus)	Seen to pass the most cranial crus (left crus) and merge with the more caudal crus (the right crus)
Lung	Left lung is seen better	Right lung is seen better
Cardiac silhouette	More oval or egg-shaped	More rounded. The apex may be displaced slightly dorsally from the sternum
Cranial lobar pulmonary arteries and veins	Vessels overlap more frequently making it harder to distinguish left from right cranial lobar vessels	Easier to distinguish left from right cranial lobar vessels
Sternal lymph node	May be seen as a normal finding on this view with a mean length of 30 mm	Seen less frequently

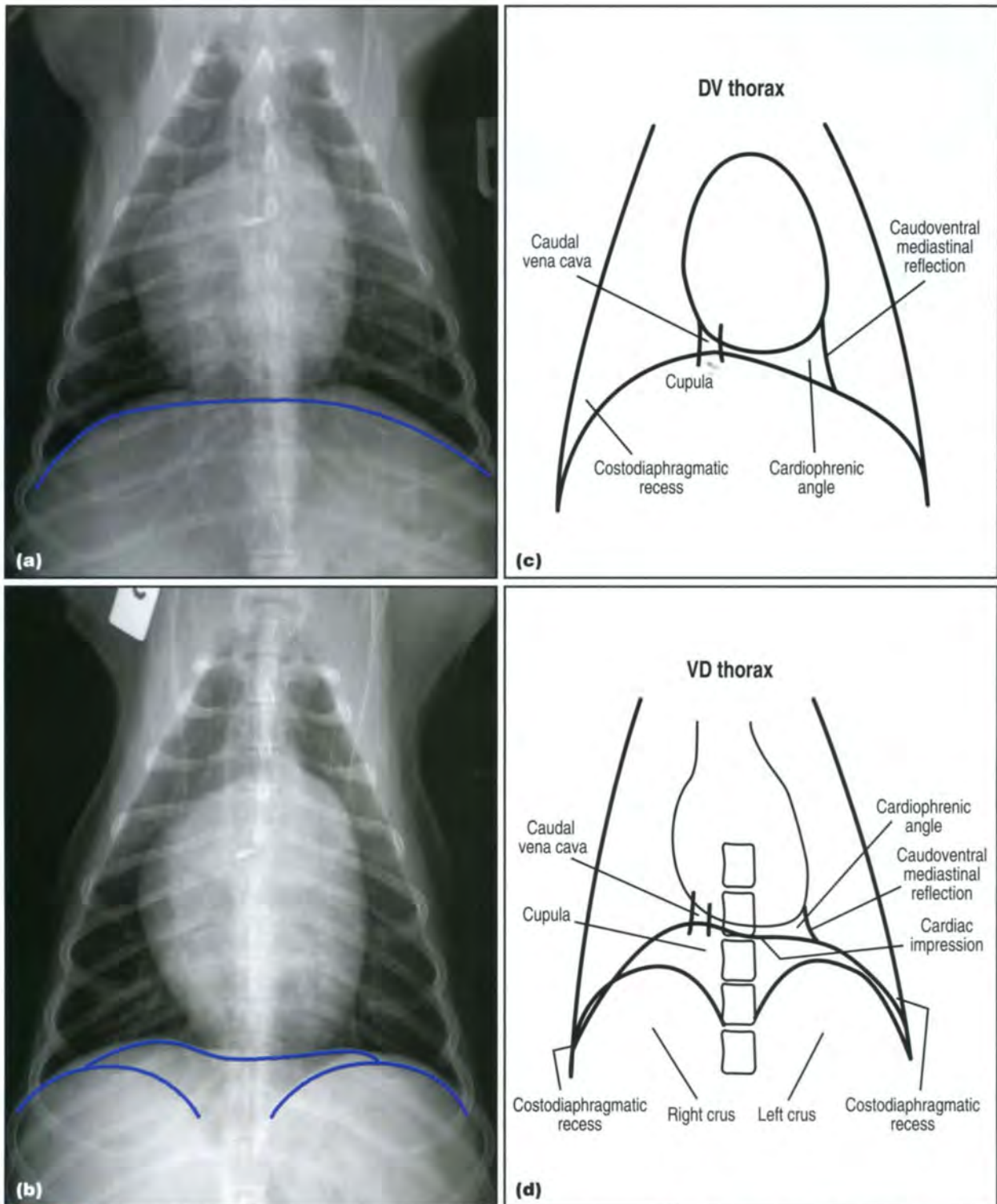
1.26 There are many differences between the left lateral recumbent and right lateral recumbent radiographs.



1.27 Normal **(a)** right lateral and **(b)** left lateral thoracic radiographs. Note the difference in appearance of the diaphragmatic crura (right crus = pink line, left crus = blue line). They appear parallel to one another in the right lateral view and form a 'Y' shape on the left lateral view. The caudal vena cava (green lines) merges with the right crus as it passes through the diaphragm. This is the more cranial crus on the right lateral view and the more caudal crus on the left lateral view (the abdominal contents push the lowermost crus forward). **(c)** Right lateral view. **(d)** Left lateral view. (c, d Adapted from Suter (1984) with permission.)

Structure	Ventrodorsal	Dorsoventral
Diaphragm	Crura are seen superimposed over the cupula giving a three-humped appearance	A single smooth curve of the cupula is seen
Gastric gas shadow	Gas present within the body (centrally) or the pyloric antrum (seen on the right side)	Gas present within the fundus (seen on the left side)
Aorta and major vessels	Changes in size tend to be more conspicuous. Also a greater length of the caudal vena cava is seen than on the DV view	Changes in size are not seen as easily
Lung	Accessory lobe seen better as heart moves more cranially. In general ventral lung fields are seen best	Accessory lobe less aerated due to cranial displacement of the midportion of the diaphragm. In general dorsal lung fields are seen best
Caudal lobar pulmonary arteries and veins	Not seen as easily as on the DV view	Seen more easily due to the well inflated surrounding lungs and the effect of magnification
Cardiac silhouette	Elongated, main pulmonary artery may appear bulging as a normal variation	More oval due to a more upright position

1.28 Thoracic structures appear different on VD and DV radiographs. It is important to be aware of these differences in order to interpret the radiograph correctly and avoid error.



1.29 Normal **(a)** DV and **(b)** VD thoracic radiographs. Note the differences in the diaphragmatic outline, which appears as three humps on the VD view but as one smooth curve on the DV view. **(c, d)** This principle is shown in the two schematics. (c, d Adapted from Suter (1984) with permission.)

Essential principles of interpretation

Border obliteration (silhouette) sign

The visibility of a radiographed object depends on the opacity difference between itself and its surroundings. If two (or more) structures of similar opacity are in direct contact with each other, they will be projected as one merged silhouette on a radiograph. The border

between them will not be visible radiographically. This disappearance of individual silhouettes is called the *border obliteration sign* (also known as border effacement). The alternative term *silhouette sign* is frequently used but confusing, since it does not clearly emphasize the loss of individual silhouettes.

Some examples of lost individual soft tissue silhouettes are:

- The heart completely surrounded by pleural fluid
- Lung vessels surrounded by consolidated lung.

Mass and mass effect

In diagnostic imaging, any space-occupying lesion is regarded as a *mass*, regardless of its origin and nature. Since the external boundaries of the thorax are limited (as in most other regions of the body), a mass can only grow by displacing and/or compressing other organs. As a result the displaced organs will be found in a different location. Should they be compressible, they will also assume an abnormal shape. This is called a *mass effect*. The mass effect is an essential diagnostic tool in situations where the mass itself is not clearly visible radiographically, but its position and origin can be assumed based on the magnitude and direction of the visible deviated and/or compressed organ.

An example is cardiomegaly with marked pleural effusion. The cardiac silhouette is no longer radiographically evident due to the border obliteration by the pleural fluid. Its size (mass effect) displaces the trachea dorsally on the lateral thoracic radiograph. This is a sign of cardiomegaly.

The term *mediastinal shift* (also known as cardiac shift) describes the mass effect on DV/VD radiographs. The cardiac silhouette may be displaced away from the midline by a mass, or may fall away from the midline towards a collapsed lung lobe (see also Chapter 8 for further information).

The term *extrapleural sign* is also an adaptation of the mass effect where a lung margin is locally deviated from a mass arising from the chest wall (ribs, soft tissues, sternal lymph node) (see also Chapter 13).

Röntgen signs

When each thoracic structure is evaluated radiographically, consideration should be given to the following characteristics for that organ:

- Size
- Shape
- Opacity
- Location
- Number
- Architecture
- Function.

This list is known as the Röntgen signs (named after Wilhelm Conrad Röntgen, who discovered

X-rays). The signs of architecture and function are only applicable in specific situations, i.e. a contrast study.

References and further reading

- Berry CR, Love NE and Thrall DE (2002) Neck and thorax – companion animals: Interpretation paradigms for the small animal thorax. In: *Textbook of Veterinary Diagnostic Radiology, 4th edn*, ed. DE Thrall, pp. 307–322. Saunders, Philadelphia
- Brawner WR and Bartels JE (1983) Contrast radiography of the digestive tract. Indications, techniques and complications. *Veterinary Clinics of North America: Small Animal Practice* **13**, 599–626
- Coleman MG, Warman CGA and Robson MC (2005) Dynamic cervical lung hernia in a dog with chronic airway disease. *Journal of Veterinary Internal Medicine* **19**, 103–105
- Curry TS III, Dowdey JE and Murray RC Jr (1990) Luminescent screens and photographic characteristics of X-ray film. In: *Christensen's Physics of Diagnostic Radiology, 4th edn*, ed. TS Curry III pp. 118–136 and 148–164. Lea & Febiger, Philadelphia
- Dennis R and Herrtage M (1995) The thorax. In: *BSAVA Manual of Small Animal Diagnostic Imaging, 2nd edn*, ed. R Lee, pp. 43–66. BSAVA Publications, Cheltenham
- Dennis R, Kirberger RM, Wingley RH and Barr FJ (2001) Lower respiratory tract; Cardiovascular system; Other thoracic structures – pleural cavity, mediastinum, thoracic oesophagus, thoracic wall. In: *Handbook of Small Animal Radiological Differential Diagnosis, 1st edn*, ed. R Dennis *et al.*, pp. 103–124, pp. 125–142 and 143–163. WB Saunders, London
- Garner M, Hennings SP, Jager HJ *et al.* (2000) Digital radiography versus conventional radiography in the chest imaging: diagnostic performance of a large area silicon flat panel detector in a clinical CT-controlled study. *American Journal of Radiology* **174**, 75–80
- Kirberger RM and Avner A (2006) The effect of positioning on the appearance of selected cranial thoracic structures in the dog. *Veterinary Radiology and Ultrasound* **47**, 61–68
- Kodak Ltd. (No year given) Intensifying screens and control of contrast. In: *Fundamentals of Radiographic Photography Book 2*, pp. 9–17 and 21–28. Kodak Limited, United Kingdom
- Martinelli M (2001) Digital imaging advances and the future. *Veterinary Clinics of North America: Equine Practice* **17**, 275–295
- Morgan JP (1993) Technique charts. In: *Techniques of Veterinary Radiography, 5th edn*, pp. 78–83. Iowa State University Press, Ames
- O'Brien RT (2001) *Thoracic Radiology for the Small Animal Practitioner*. Teton NewMedia, Jackson
- Owens J (1982) Principles of radiographic interpretation; The chest. In: *Radiographic Interpretation for the Small Animal Practitioner*, ed. DN Biery, pp. 1–8 and pp. 89–116. Ralston Purina Company, Missouri
- Seymour C and Duke-Novakovski T (2007) *BSAVA Manual of Canine and Feline Anaesthesia and Analgesia, 2nd edn*. BSAVA Publications, Gloucester
- Suter PF (1984) Normal radiographic anatomy and radiographic examination; Special procedures for the diagnosis of thoracic disease; Methods of radiographic interpretation, radiographic signs and dynamic factors in the radiographic diagnosis of thoracic diseases. In: *Thoracic Radiography: A Text Atlas of Thoracic Diseases of the Dog and Cat*, pp. 1–46, pp. 47–76 and pp. 77–126. Peter F. Suter, Wettswil, Switzerland
- Watrous BJ (2002) The Esophagus. In: *Textbook of Veterinary Diagnostic Radiology, 4th edn*, ed. DE Thrall, pp. 329–349. WB Saunders, Philadelphia
- www.animalinsides.com

Basics of thoracic ultrasonography

Gabriela Seiler, Joanna Dukes-McEwan and Lorrie Gaschen

General thoracic ultrasonography

Indications

Non-cardiac thoracic ultrasonography is increasingly used in veterinary medicine. Despite the fact that ultrasound waves are not able to penetrate air-containing lung, there are many applications of non-cardiac thoracic ultrasonography. A complete set of thoracic radiographs should be acquired initially and these are then used to determine the area of interest to be examined ultrasonographically.

Indications for thoracic ultrasonography include:

- Pleural effusion obscuring thoracic or mediastinal contents
- Mediastinal widening with suspicion of a mediastinal mass
- Lung consolidation
- Thoracic wall or pleural masses
- Suspicion of diaphragmatic hernia
- Suspicion of lung lobe torsion
- Diagnostic fine-needle aspiration or biopsy
- Therapeutic pleural fluid removal.

Restraint and patient preparation

Patients are routinely prepared by clipping the hair coat, cleaning the skin with alcohol and applying coupling gel. For fine-needle aspiration and biopsy procedures, aseptic preparation of the skin is required.

Most patients can be examined awake with minimal restraint, in lateral or dorsal recumbency. Dyspnoeic patients should be examined in the position they feel most comfortable with, in sternal recumbency or standing. In the absence of, or with minimal pleural effusion, scanning from the *dependent* side may be essential to identify heart, mediastinum or pulmonary masses or consolidations. General anaesthesia is required if biopsy specimens are taken of any thoracic structures in order to control respiratory movement. For fine-needle aspiration, sedation can be sufficient.

Coagulation profiles should also be obtained prior to ultrasound-guided biopsy procedures. These are generally not required for fine-needle aspiration techniques unless there is a clinical suspicion that a patient has a coagulopathy.

In most cases it is sufficient to clip the ventral half of the thorax along the sternum. The dorsal lung field is usually still aerated and causes too many artefacts to allow ultrasonographic evaluation. In selective cases

with dorsal lung or chest wall masses, the dorsal chest wall is also clipped, based on radiographic location of the lesion.

Technique

A non-cardiac thoracic ultrasound examination is usually targeted to an area of interest identified on survey radiographs. Depending on the location of the suspected lesion (mediastinum, thoracic wall, pulmonary parenchyma) different windows have to be used. These may be intercostal, parasternal, subcostal, transhepatic or via the thoracic inlet. Specific suggestions are provided below.

Equipment

- Small footprint transducer (sector, microconvex).
- Linear array transducers produce excellent images despite rib artefacts in cats and small dogs.
- Transducer frequency – as high as possible but with adequate depth penetration:
 - Small dogs, cats: 7.5–10 MHz
 - Large-breed dogs may require a 3.5–5 MHz transducer.

Examination method

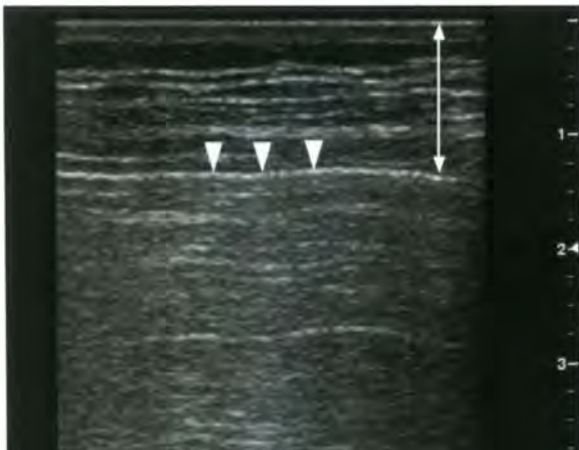
Using each intercostal space as a scan window, the thorax is examined in a dorsal and transverse plane, following the intercostal spaces as far dorsally as the aerated lungs allow. Both sides are routinely examined. The structures described below are identified.

Body wall, pleural and lung surface: Normal ribs are seen as round (in short axis) or linear (in long axis) structures with a distal acoustic shadowing (Figure 2.1). The surface of the ribs is smooth and hyperechoic, any interruption of the cortex is a sign of either rib fracture or lysis. The layers of the body wall result in a striated appearance of the tissue with medium echogenicity. The body wall is best examined using a linear transducer (Figures 2.1 and 2.2).

The pleural surface is seen as a bright hyperechoic line covering the lungs. The two layers are not seen separately in a small animal; only the visceral pleural surface of the lung is visible as a bright, smooth, continuous hyperechoic line (see Figure 2.2). It is very important to observe the movement of the pleural surface: normal pleura glides smoothly against the chest wall with respiration.



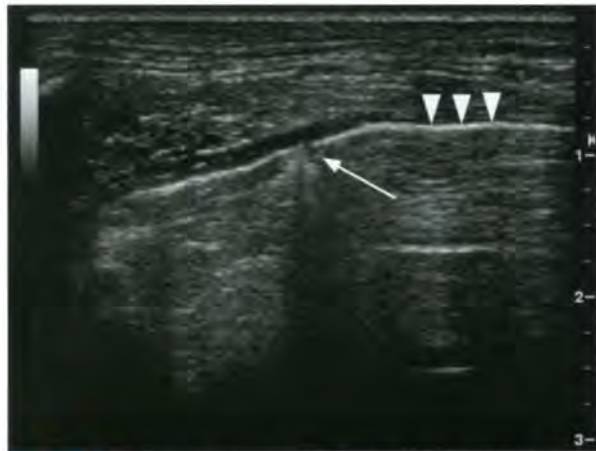
2.1 Dorsal image of the thorax of a normal adult Border Collie, using an 8 MHz microcurved transducer. The chest wall with subcutaneous fat and intercostal musculature is mainly hypoechoic with linear striations. The ribs (★) are seen in cross section and create a strong distal acoustic shadow. The lung surface presents as a bright hyperechoic line.



2.2 Transverse image of the dorsal eighth intercostal space of a normal adult Border Collie, using a 12 MHz linear transducer. Compared with Figure 2.1, the layers of the body wall (thin arrow) in the near field are shown with better resolution due to the high frequency and linear nature of the transducer. The lung surface is visible as a bright, continuous line (arrowheads). Distal to the lung surface, the attenuation of the sound waves results in shadowing with multiple horizontal echogenic lines, caused by reverberation artefacts.

On the lung surface almost all ultrasound waves are reflected by the soft tissue–gas interface, resulting in distal acoustic shadowing. The shadowing is inhomogenous ('dirty') due to multiple reverberation artefacts, seen as very echogenic linear echoes deep and parallel to the lung surface (see Figure 2.2). Reverberation artefacts are created by strong reflection of the ultrasound beam off the aerated lung tissue. Interruption of the normal 'dirty' shadowing and the presence of a column of densely spaced, small linear artefacts (comet tail artefacts) (Figure 2.3) are a result of focal non-aerated lung tissue or incidental peripheral mineralizations (benign pulmonary osteomas). Larger consolidations or nodules present as hypoechoic areas, interrupting the normal hyperechoic

lung surface (Figure 2.4). Observation of the respiratory movement and appearance of gas within a lesion allows differentiation between pulmonary and extrapulmonary origin of the lesion.



2.3 Transverse image of the dorsal lung field in a 10-year-old Boston Terrier with mild pleural effusion. The lung surface (arrowheads) is not completely smooth and there is a small area of consolidation present in the superficial lung tissue, producing closely spaced linear echoes distally. This is called a comet tail artefact (arrowed).



2.4 Right oblique intercostal view of the right caudal lung lobe in a 12-year-old Miniature Poodle bitch with metastatic mammary carcinoma. A round, hypoechoic nodule is present (arrowed), interrupting the normal lung surface (arrowhead). This would be amenable to fine-needle aspiration if required.

Mediastinum: Three different parts of the mediastinum are identified ultrasonographically: the cranial, middle (cardiac) and caudal mediastinum. The examination is limited to the ventral aspects as the dorsal mediastinum is usually surrounded by aerated lung.

The caudal mediastinum is very thin, accommodating the caudal vena cava, oesophagus and accessory lung lobe. These structures are best seen close to the diaphragm using a subcostal approach with the liver as the acoustic window. The most dorsal part of the caudal mediastinum containing the aorta and azygos vein is usually not accessible ultrasonographically. Using the heart or the cranioventral part

of the liver as an acoustic window, a portion of the caudoventral mediastinum can be seen in most animals (Figure 2.5). It contains variable amounts of fat. If pleural effusion is present, the caudoventral mediastinum can be seen as a thin undulating hyperechoic structure (Figure 2.6).



2.5 Parasternal sagittal view of the caudoventral thorax in an adult crossbreed dog, the transducer is placed just lateral to the last sternebra. Between the heart (a) and the liver (b), outlined by a curvilinear hyperechoic line representing the diaphragm–lung interface, a small triangular area of fat can be seen in the caudal mediastinum (c).



2.6 Oblique intercostal view of the right caudoventral thorax in a 5-year-old male Borzoi with pleural effusion secondary to idiopathic chylothorax. The heart (a) and a partially collapsed ventral tip of the right caudal lung lobe (b) are seen on the left. The caudal mediastinum is visible as an irregular, thin, hyperechoic structure (arrowed).

The cranial mediastinum can be examined through the thoracic inlet or using a parasternal intercostal window. The trachea and external jugular veins can be observed through the thoracic inlet. The trachea is easy to identify based on the structure of the cartilage rings, which give the trachea a rippled surface, and the air column within the trachea, which produces reverberation artefacts. The jugular veins are easily compressed and are bilateral tubular, anechoic structures close to the skin surface (Figure 2.7).



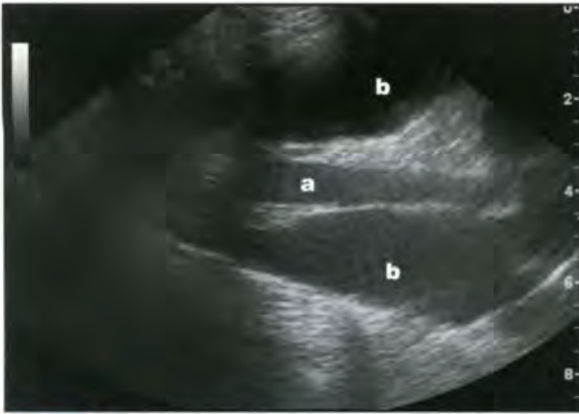
2.7 Sagittal oblique view with the curvilinear probe slightly to the right side in the thoracic inlet. The jugular vein (a) can be seen entering the thorax and the tip of the right cranial lung lobe (b) is visible (easier to identify when respiratory movement can be observed).

If an intercostal approach is chosen, it is important to pull the thoracic limb as far cranially as possible to access the cranial intercostal spaces. The transducer is placed just dorsal to the sternum and cranial to the heart.

In the presence of pleural effusion, the ventral portion of the cranial mediastinum is a thin stripe of echogenic tissue, depending on the amount of mediastinal fat, and can be examined quite easily for presence of lymphadenopathy or other masses (Figure 2.8). The cranial vena cava, if visible, is a good landmark to identify the surrounding mediastinum (Figure 2.9) and should be examined for evidence of thrombosis in animals with pleural effusion.



2.8 Dorsal image of the cranial thorax of an 8-year-old neutered male Domestic Shorthair cat with pleural effusion. The whole width of the cranial thorax can be examined: thoracic wall (a), pleural space with anechoic effusion (b), collapsed lung lobe (c), cranial mediastinum (d), which is very thin without evidence of lymphadenopathy or other masses, and the heart (e).



2.9 Dorsal image of the cranial thorax of a 12-year-old neutered male crossbreed dog with pleural effusion. The cranial vena cava (a) and surrounding mediastinum with some fat are seen between the fluid-filled left and right pleural spaces (b).

Normal sternal or mediastinal lymph nodes are not differentiated from the surrounding mediastinal fat. Mediastinal fat is fairly uniform and can be recognized by its coarse structure, poor margination and poor transmission of the ultrasound beam (Figure 2.10). Especially in brachycephalic breeds and obese animals, a large amount of fat can be observed in the mediastinum and should not be confused with a mediastinal mass. Most mediastinal masses or abnormal lymph nodes are hypoechoic or sometimes heterogenic, well defined and rounded (Figure 2.11).

In young animals, thymic tissue is present cranial to the heart, best seen from the left side. It has a granular, homogenous texture and contains a large amount of blood vessels.

Diaphragm: The normal diaphragm is normally not seen as a separate structure; the highly reflective hyperechoic lung interface blends in with the diaphragm. The diaphragm is only seen in its full thickness in cases of pleural and peritoneal effusion. A normal diaphragm has a smooth, curvilinear, continuous surface (Figure 2.12). Examination of the diaphragm is best performed with a subcostal approach, placing the transducer just behind the ribcage and examining the diaphragm in sagittal, dorsal and transverse planes. In the presence of pleural effusion, the cranial surface of the diaphragm can also be evaluated using an intercostal window. Care should be taken not to confuse consolidated lung tissue or pericardial fat with herniated abdominal organs; an ultrasound examination of the cranial abdominal organs usually helps to determine the origin of abnormal intrathoracic tissue.

Fine-needle aspiration and biopsy

Fine-needle aspiration

Twenty-two gauge needles of various lengths are usually used for diagnostic pleural fluid aspiration. In very cellular (seen as very echogenic) effusions larger gauge needles are sometimes necessary. Sedation is not usually required for this procedure. Appropriate collection devices (for cytology, culture, etc.) should be available.



2.10 Dorsal image of the cranial thorax of an obese dog, 2 cm dorsal to the sternum. The retrosternal fat is of medium echogenicity and without specific structures, apart from one hypoechoic tubular vessel. The thoracic wall is delineated with an arrow.



2.11 Transverse right intercostal view (dorsal is to the left). The tip of the right cranial lung lobe (a), creating reverberation artefacts, and enlarged, rounded and hypoechoic lymph node (b), surrounded by hyperechoic fat, and the sternum, creating a distal acoustic shadows (c) are seen. The thoracic wall is labelled (d).



2.12 Sagittal image of the diaphragm, using the liver as acoustic window in a normal large-breed dog. The curvilinear probe is placed directly caudal to the xiphoid and angled cranially. The diaphragm-lung interface is seen as a continuous, bright, curvilinear structure covering the surface of the liver (arrowed).

Therapeutic pleural fluid aspiration is performed under ultrasound guidance if the effusion is loculated and exact needle placement is the only method to drain the thorax adequately. A 16–22 gauge needle, depending on the size of the patient and the cellularity of the fluid, is connected to an extension set with a three-way stopcock. A large fluid pocket cranial or caudal to the heart is identified, and the position of the needle is constantly observed during the procedure to avoid laceration of lung tissue or obstruction of the needle by fibrin strands.

Fine-needle aspiration of mediastinal and thoracic wall masses, using a 22 gauge needle, is performed if an acoustic window for safe approach to the lesion can be found. Care should be taken to avoid large mediastinal vessels: colour Doppler ultrasonography can be used to identify a safe window.

Fine-needle aspiration of lung masses can only be performed if the lesion is superficial and not covered by more than 1–2 cm of aerated lung tissue. It is essential in these cases to localize the mass on survey radiographs before starting the procedure. A thin layer of air-filled lung tissue can be reduced by keeping the animal in lateral recumbency with the affected side down for 5–10 minutes. Atelectasis of the lung tissue is usually sufficient to visualize and sample the lesion either from the dependent or the non-dependent side, as the lung stays atelectatic for a few minutes.

Biopsy

Biopsies of mass lesions are always performed under general anaesthesia. It is important to control respiratory motion during the biopsy procedure whether the origin of the lesion is mediastinal or pulmonary or in the thoracic wall. A coagulation profile should be checked prior to the procedure. Fourteen to eighteen gauge automated or semiautomatic biopsy devices are most commonly used. The skin is aseptically prepared and a small incision is made with a scalpel blade. The depth of the lesion has to be measured and the length of the biopsy throw adjusted. Colour Doppler ultrasonography is useful to make sure no large vessels are in the biopsy path.

Complications

Pneumothorax can occur, more commonly after biopsy, but also after fine-needle aspiration of pulmonary lesions. It can be recognized immediately after or during the procedure if the lesion suddenly disappears and a broad hyperechoic layer appears directly underneath the chest wall with distal reverberation artefacts. This is similar to the appearance of a normal lung surface, but it *does not move* with respiration. The extent of the pneumothorax and lung collapse is best assessed radiographically. Even though pneumothorax is a rare complication, equipment to perform a therapeutic thoracocentesis should always be available during aspiration or biopsy techniques.

Haemorrhage is a very uncommon complication of thoracic interventional procedures and is usually minimal and self-limiting. Intervention is only required occasionally.

Echocardiography

Indications

Echocardiography (cardiac ultrasonography) has revolutionized the non-invasive assessment of cardiac disease. The ability of ultrasonography to discriminate between soft tissue (myocardium) and fluid (the blood pool) permits easy assessment of:

- The structure, size and relative proportions of the specific heart chambers and walls
- Heart valves
- Great vessels
- Cardiac performance (particularly systolic function)
- The presence of a pericardial effusion.

It should be appreciated that echocardiography is *complementary* to thoracic radiography. Both techniques are essential in the investigation of a cardiac patient, particularly in conditions associated with left-sided volume overload, as radiographs demonstrate the haemodynamic significance of this on the pulmonary vasculature and lung field.

- Quantitative echocardiography allows standard assessment of chamber size or wall measurements, which can be compared with reference values for the species, breed or size of animal, where these data are available. Measurements can be carried out on both two-dimensional (2D) and M-mode images.
- Doppler echocardiography demonstrates the direction, velocity and character of flow within the heart and great vessels. It is indicated for the identification of the cause of a heart murmur detected clinically, and for assessing its clinical significance.
- A complete systematic 2D, M-mode and Doppler echocardiographic examination will enable a diagnosis to be made and assessment of the severity of most acquired or congenital heart diseases in animals, without resorting to invasive procedures such as cardiac catheterization and angiography.

Restraint and patient preparation

Animals with life-threatening pulmonary oedema or arrhythmias should always be stabilized prior to an echocardiographic examination. Dyspnoeic cats should never be restrained in lateral recumbency. Treatment and stabilization over 24–48 hours may be required before a definitive diagnosis of cardiac disease can be made, once the patient is breathing normally. As ultrasonography is exquisitely sensitive at detecting fluid, rapid thoracic imaging of a dyspnoeic animal (in sternal recumbency) identifies whether a pleural effusion is responsible, which can then be drained.

The fur is clipped over the left and right thorax, over the area of the palpable cardiac impulse. If the subcostal view is to be utilized, a small square caudal to the xiphisternum should also be clipped. For more rapid acoustic contact, the clipped area can be soaked in surgical spirit before applying ultrasound coupling gel.

Animals are gently restrained in lateral recumbency (right then left). Cats, especially, should not feel over-restrained (they may need more than one handler restraining them). The lower fore- and hindlimbs should be held by the handler(s) to prevent the patient rising from the table, thus allowing the operator to keep equipment and transducers safe from damage. The animal should be comfortable, on bedding material, so they may actually fall asleep in quiet, calm conditions.

Chemical restraint is not normally required. As sedative drugs may influence heart rate, contractility, wall thickness and flow velocities, they are best avoided. However, it is appreciated that they may be indicated in uncooperative or very stressed patients. Similar drugs and dose rates in cardiac patients are used as for radiographic positioning:

- Suggested sedation for dogs with heart disease: intramuscular injection of acetylpromazine (0.02–0.03 mg/kg) with butorphanol (0.1–0.2 mg/kg) in same syringe
- Suggested sedation for cats with heart disease. Initially calm cat: intramuscular injection of acetylpromazine (0.05 mg/kg) with butorphanol (0.2 mg/kg) in same syringe. If the cat is extremely uncooperative, then an intramuscular injection of midazolam (0.2 mg/kg) and ketamine (5 mg/kg) in same syringe can be given. (Ketamine will increase heart rate, making assessment of diastolic function difficult.)

Electrocardiographic electrodes need to be applied. As a complete study takes a minimum of 30 minutes, it is preferable to use adhesive electrodes (on the main pads of the feet) rather than crocodile clips on the skin. Normally, a lead II is obtained to optimize complex size and recognition, with electrodes on the right forelimb and the left hindlimb, with the earth lead positioned wherever else is convenient (e.g. right hindlimb).

The right-sided views are used for 2D and M-mode images and measurements. Image quality is good as the heart is perpendicular to the ultrasound beam. For the right-handed operator, the animal remains in this position for the subcostal view.

The animal is turned over, still with sternum towards the operator, for the left-sided views. These give a 'vertical' heart, so image quality is less good, as structures other than the heart base are parallel to the ultrasound beam. However, alignment with intracardiac flow is optimized, facilitating Doppler studies. Access over several rib spaces (third to sixth) is required for all standard left-sided views; the animal may need to be repositioned during the course of the study, to permit access for all views.

Technique

The conventional standard display of images is that right-sided and basilar structures are displayed to the right of the screen (with a single exception: the left apical four-chamber view, which is displayed like a dorsoventral (DV) radiograph, with left to the right side of the screen). To achieve this, with the

operator's thumb on the transducer thumb-mark near the animal's sternum, the left–right image reverse facility of the ultrasound machine may be required.

2D (also known as B-mode) images represent a 'slice' through a complex, three-dimensional (3D) structure. Cardiac anatomy must be thoroughly appreciated to acquire and interpret these views; a model of the heart adjacent to the ultrasound machine can facilitate this. Most of the anatomy is appreciated from these 2D views. The standard 2D views are also essential:

- To position the M-mode cursor for M-mode studies
- For colour flow interrogation of the heart valves, septa and great vessels
- To position the spectral Doppler cursor (for pulsed wave (PW) or continuous wave (CW) Doppler) to record blood flow direction, velocity and character.

In general, the right parasternal (RPS) views are used to assess the anatomy and for M-mode studies. The left apical and left parasternal (LPS) views are used for Doppler studies. 2D images are described as being long-axis or short-axis, depending on whether the ventricular axis or aorta is being displayed in longitudinal or cross-sectional planes, respectively.

Equipment

A sector transducer (either mechanical or phased array) is required to image the heart through windows between the lung lobes and the rib spaces. A linear transducer or a curvilinear transducer with a large footprint is not appropriate, as it would not permit acquisition of images acquired by rotation or angulation.

A range of transducers, offering various frequencies, is normally required to scan veterinary patients:

- Cats and very small dogs require a 7.5 MHz transducer
- Medium-sized dogs require a 5.0 MHz transducer
- Giant breeds of dogs require a 2.5 MHz transducer
- The highest frequency transducer offering appropriate penetration should be selected, to optimize image resolution
- For Doppler studies, a lower frequency transducer may be required than that for optimal imaging; transducers may need to be changed during the course of the study.

A purpose-designed echo table should be used, with a hole or a wedge over which the animal lies in lateral recumbency. Images are acquired through the dependent chest wall. The hypostatic effects on the dependent lung minimize air interference on the cardiac images.

Cardiac software is required on the ultrasound machine. A simultaneous electrocardiogram (ECG) should be recorded with the images. Accurate measurement depends on defining phases of diastole or systole. Generally, end-diastolic measurements are taken at the start of the QRS complex. End-systolic measurements are taken at the end of the T wave (or at the smallest left ventricle (LV) cavity).

Standard 2D (B-mode) views of the heart

Acquisition of the standard RPS views is described and illustrated in Figure 2.13; the subcostal view is also shown. The corresponding observations, measurements and calculations are also indicated in Figure 2.13. Acquisition of the standard left apical and LPS views is described and illustrated in Figure 2.14.

M-mode echocardiography

M-mode measurements are just one-dimensional (1D). The images are motion–time graphs. Temporal resolution is very high (in contrast to 2D and spectral Doppler images). The M-mode cursor can be accurately positioned on the 2D image.

M-mode measurements need to be carefully and consistently acquired for them to be useful in patient follow-up or in comparison with reference values for the species, breed and weight, where these data are available. Acquisition of M-mode images and methods of measurement are detailed in Figure 2.15.

Doppler echocardiography

J. Christian Döppler originally defined the Doppler principle. This states that there is an apparent change in transmitted frequency, reflected back to the source off a target, which occurs as a result of the movement of the source or the target. This phenomenon is readily appreciated as a police car with siren noise approaches, then passes the observer; the sound is of higher frequency as it approaches, and lower frequency as it moves away from the observer. There are several practical applications, not least important of which is Doppler echocardiography.

In Doppler echocardiography, a pulse of sound is emitted from the transducer. This is reflected off moving targets within the heart, the red blood cells (RBCs). The apparent shift in frequency of the sound reflected back to the transducer is proportional to the velocity of the RBCs and their direction of movement. The software of a Doppler echocardiography machine converts this Doppler into an audible signal and a visual display, and velocity of the RBCs is calculated. The flow through each valve varies during the cardiac cycle; these events can be plotted against time (with the simultaneously recorded ECG). This gives the spectral Doppler trace, a velocity–time graph.

In PW Doppler, a sample volume may be positioned within the area of interest. A pulse of ultrasound waves is emitted by the crystal in the transducer. Only the RBCs in the area of interest are assessed; ultrasound waves are reflected back to the transducer before another pulse is transmitted. Because of the time required for sampling in this way, only low velocities can be measured. If blood is moving at a velocity exceeding the *Nyquist limit* of the machine settings, it is shown 'wrapped around' in the opposite direction; this is called *aliasing*. Aliasing, thus, results in directional ambiguity.

PW Doppler gives information about flow velocity and direction of flow (towards the observer is displayed above the baseline, away is displayed

below the baseline of the spectral trace). Character of flow is also illustrated with PW Doppler. Laminar flow, due to RBCs moving in 'sheets', uniformly accelerating and decelerating, is indicated by a clean 'envelope' (see Figure 2.16). Turbulent flow tends to occur at higher velocities, and whorls and eddies of flow, giving a filled in, less tidy signal on pulsed-wave spectra. PW Doppler may be limited at the depth of image being interrogated.

High pulse repetition frequency (HPRF) spectral Doppler describes additional sample volumes along the cursor line, as well as the region of interest at a particular valve. The transducer does not wait for a pulse of ultrasound waves to be reflected back prior to transmitting another pulse; this allows much higher velocities to be assessed and displayed in a spectrum by the machine without aliasing.

CW Doppler echocardiography also produces a spectral display. Ultrasound waves are continuously emitted from, and received back by, the transducer; the frequency shift is converted by the machine into a spectral signal that is not limited by aliasing, so very high velocities can be measured. Sampling is not specific to one region of interest; it is all along the cursor line. Most modern machines allow positioning of the CW cursor on a 2D image to ensure correct alignment with flow (steerable CW). Other CW transducers are stand-alone or ped-off probes – these are dependent on the operator directing it until the spectrum is optimized. CW Doppler is required for recording velocity of mitral regurgitant jets or very high velocities in aortic or pulmonic stenosis.

Colour flow: This is a specialized form of PW Doppler echocardiography. Within a sector, which can be directed over the area of interest within a 2D image, there is a large number of 'sample volumes' or pixels, which are individually colour-coded according to direction and character of flow.

On most ultrasound machines blood moving towards the transducer is colour-coded red. Blood moving away from the transducer is colour-coded blue (see Figure 2.16). Different colour shades may be present in some software packages to give an impression of flow velocity (the higher the velocity the brighter the hue). Again, the Nyquist limit can be exceeded and fast blood moving away from the transducer may have a normal blue outline, but an aliased core (of red) can be seen.

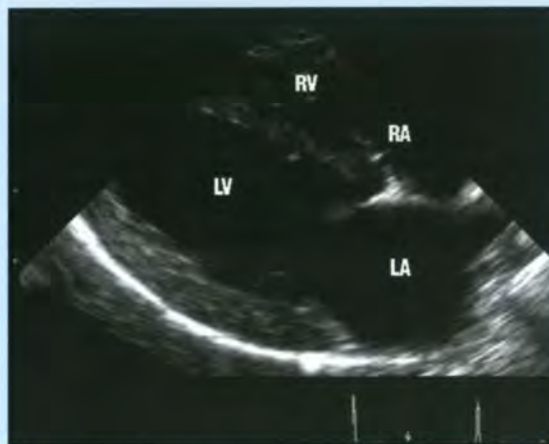
Most colour flow Doppler echocardiography machines have maps to indicate colour variance or turbulent flow; these are usually colour-coded green/yellow and have a 'speckled' or 'mosaic' appearance, e.g. such as may be seen in a mitral regurgitant jet.

Colour flow Doppler can rapidly screen for abnormal flow, such as a ventricular septal defect (VSD); the left-to-right shunting causes a turbulent jet to cross into the right ventricle (RV), usually just below the tricuspid valve. Imaging of this jet allows placement of a PW or steerable CW cursor over it to obtain a spectral signal, so that velocity may be accurately measured. Colour flow Doppler echocardiography may therefore be considered as a form of non-invasive angiography.

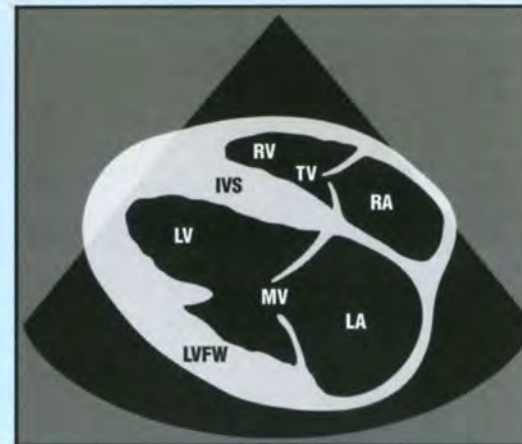
RPS long-axis four-chamber view

Acquisition of the view and assessments

- Operator thumb on thumb-mark of transducer
- Position transducer over where cardiac impulse is easily palpable
- Beam is directed approximately parallel to the ribs, directed towards the upper caudal scapula
- Slide up the intercostal space for a 'horizontal' heart (important before acquiring M-mode images) or slide down towards the sternum for a 'tipped' view (useful for colour flow screening)
- To image more of the right heart, the transducer may need to be moved one rib space cranially
- Check the IAS (anatomy and with colour flow Doppler)
- When determining LV shape and geometry, aim to optimize LV length and area, but note the true anatomical LV apex is not included
- Assess MV and check for MV prolapse
- Colour flow Doppler, check MV and TV



Normal Greyhound.



Observations, measurements and calculations

- Optimize LV length and area. 2D methods (e.g. *Simpson's rule*, see Figure 7.97, p. 137) can be used to trace the endocardial border of the LV (closing at the level of the mitral annulus) to determine *LV volumes in diastole and systole*
- An indication of whether the LV is rounded, such as in remodelling with disease, can be shown by calculating the *index of sphericity* (see Figure 7.96, p. 136). This is the ratio of LV diastolic length over 'width' (at chordal level, or use the M-mode dimension). (Normal ratio is >1.7. Increased sphericity if <1.7)
- In cats, regions of focal hypertrophy may be recognized (in HCM). These segments should be measured in diastole; a measurement of >6 mm defines LV hypertrophy in the adult cat
- Left atrial size can be measured in systole by measuring the maximal width of the LA parallel to the mitral annulus (see Figure 7.106a, p. 142)
- Assess the MV for the presence of mitral prolapse or flail (associated with myxomatous mitral valve disease and ruptured chordae tendinae, respectively)

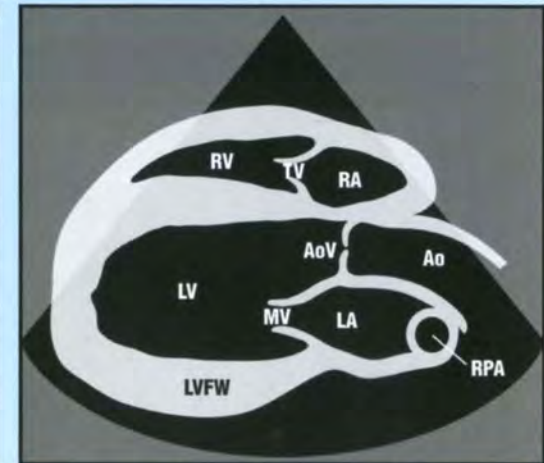


Collie cross with myxomatous degenerative mitral valve disease. In systole, parts of the valve 'balloon' on the left atrial side of the mitral annulus line. This is an abnormal finding.

2.13 RPS and subcostal views. amv = Anterior mitral valve leaflet; Ao = Aorta; AoV = Aortic valve; APM = Anterior papillary muscle; CW = Continuous wave; HCM = Hypertrophic cardiomyopathy; IAS = Interatrial septum; IVS = Interventricular septum; LA = Left atrium; LAu = Left auricular appendage; LPA = Left pulmonary artery; LV = Left ventricle; LVFW = Left ventricular free wall; LVOT = Left ventricular outflow tract; MPA = Main pulmonary artery; MV = Mitral valve; pmv = Posterior mitral valve leaflet; PPM = Posterior papillary muscle; PV = Pulmonic valve; PW = Pulsed wave; RA = Right atrium; RPA = Right pulmonary artery; RV = Right ventricle; RVOT = Right ventricular outflow tract; TV = Tricuspid valve; VSD = Ventricular septal defect. (Line diagrams adapted and reproduced from Boon (1998) with permission from the publisher) (continues)

RPS long-axis five-chamber view**Acquisition of the view and assessments**

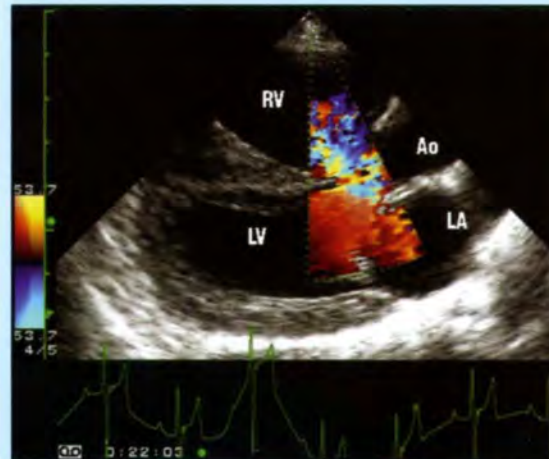
- From the four-chamber view, rotate the thumb about 10 degrees towards the animal's rump (anti-clockwise) and angle cranially
- The long-axis view of the Ao (i.e. 'chamber 5') should be clear
- Check LVOT and Ao for turbulence or aortic insufficiency with colour flow Doppler



Normal Greyhound, including the ascending Ao. The LAu (left image) or LA (right image) may be seen.

Observations, measurements and calculations

- The basal septum in cats with primary or secondary myocardial disease, or in aged cats, may be prominent or grossly hypertrophied (see Figure 7.104a, p. 141); measure diastolic wall thickness of this region, parallel to the endocardium
- Examine the subvalvular region, the aortic valves and the ascending aortic arch
- Exclude VSDs in membranous part of septum (but note that small VSDs may not be seen without colour flow Doppler)



Shetland Sheepdog, with colour flow Doppler over the base of the IVS. Turbulent flow from the LVOT into the RV in systole supports the presence of a VSD.

2.13

(continued) RPS and subcostal views. amv = Anterior mitral valve leaflet; Ao = Aorta; AoV = Aortic valve; APM = Anterior papillary muscle; CW = Continuous wave; HCM = Hypertrophic cardiomyopathy; IAS = Interatrial septum; IVS = Interventricular septum; LA = Left atrium; LAu = Left auricular appendage; LPA = Left pulmonary artery; LV = Left ventricle; LVFW = Left ventricular free wall; LVOT = Left ventricular outflow tract; MPA = Main pulmonary artery; MV = Mitral valve; pmv = Posterior mitral valve leaflet; PPM = Posterior papillary muscle; PV = Pulmonic valve; PW = Pulsed wave; RA = Right atrium; RPA = Right pulmonary artery; RV = Right ventricle; RVOT = Right ventricular outflow tract; TV = Tricuspid valve; VSD = Ventricular septal defect. (Line diagrams adapted and reproduced from Boon (1998) with permission from the publisher) (continues) ▶

RPS short-axis views

Acquisition of the view and assessments at the level of the chordae tendinae

- From the four-chamber view, with the heart as horizontal as possible, rotate the transducer 90 degrees anti-clockwise, towards the rump
- The LV is displayed in cross section, with the RV wrapped around the septum in a crescent shape
- Check the LV is rounded as normal. The septum may be flattened if RV pressure is increased (e.g. as in pulmonic stenosis)
- Slide or angle up the intercostal space to image at level of apex, level of papillary muscles and level of chordae tendinae. Aim for the LV to be symmetrical. The M-mode cursor can be positioned to bisect the LV cavity at the chordal level
- Note that during angling up from apex to base, as the heart is twisted, slightly more rotation is required towards the heart base

Observations, measurements and calculations

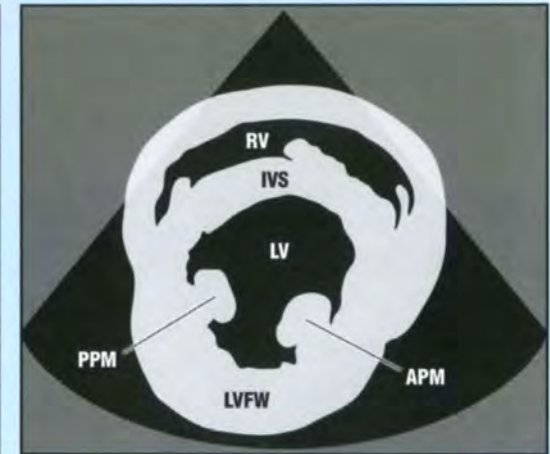
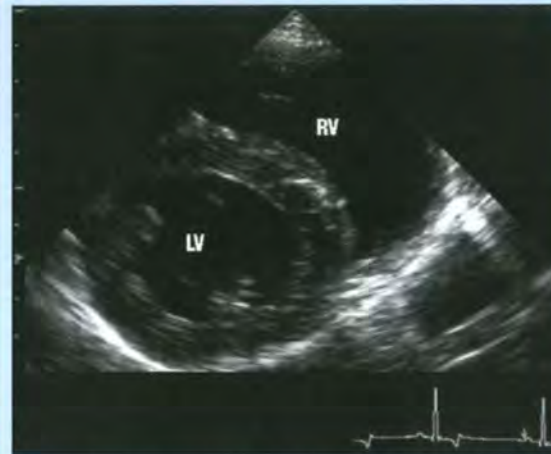
- At the level of chordae tendinae or papillary muscles, check normal relationship of LV and RV, and whether there is any septal flattening suggesting increased RV pressure
- In cats, can accurately measure the wall thickness in diastole to diagnose hypertrophy (>6 mm) (see Figure 7.104b, p. 141)
- Can make subjective assessment of papillary muscle hypertrophy (common in feline HCM)
- M-mode LV at chordae tendinae level

Acquisition of the view at the level of the MV

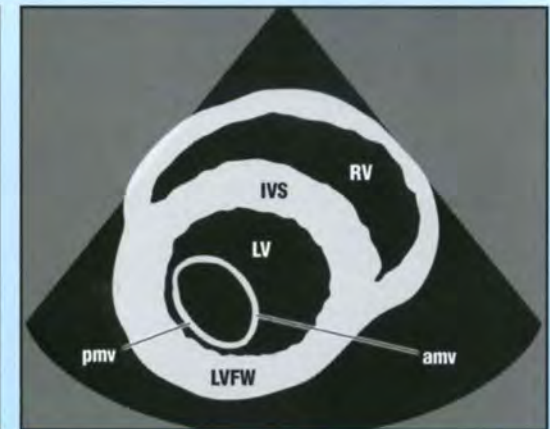
- Angle more dorsally to record the 'fish-mouth' view of the mitral valve, ensuring both anterior and posterior leaflets are imaged. Mitral M-mode studies can be positioned from this view

Observations, measurements and calculations

- Assess the MV leaflets
- Use to position the M-mode cursor for mitral M-mode



Left and right ventricles at the level of the chordae tendinae in a normal Greyhound.

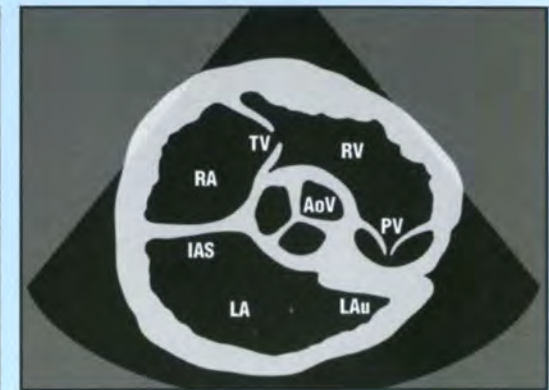


LV at MV level in a normal Greyhound.

2.13 (continued) RPS and subcostal views. amv = Anterior mitral valve leaflet; Ao = Aorta; AoV = Aortic valve; APM = Anterior papillary muscle; CW = Continuous wave; HCM = Hypertrophic cardiomyopathy; IAS = Interatrial septum; IVS = Interventricular septum; LA = Left atrium; LAu = Left auricular appendage; LPA = Left pulmonary artery; LV = Left ventricle; LVFW = Left ventricular free wall; LVOT = Left ventricular outflow tract; MPA = Main pulmonary artery; MV = Mitral valve; pmv = Posterior mitral valve leaflet; PPM = Posterior papillary muscle; PV = Pulmonic valve; PW = Pulsed wave; RA = Right atrium; RPA = Right pulmonary artery; RV = Right ventricle; RVOT = Right ventricular outflow tract; TV = Tricuspid valve; VSD = Ventricular septal defect. (Line diagrams adapted and reproduced from Boon (1998) with permission from the publisher) (continues)

RPS short-axis views**Acquisition of the view**

- With slightly more rotation and cranial angulation, the **short-axis view of the aorta**, central within the heart, is obtained, at AoV level (Mercedes Benz sign). As well as including AoV leaflets, optimize the LA with LAu



AoV level: when clearly seen, the aortic valves form a 'Mercedes Benz' sign.

Observations, measurements and calculations

At the level of aortic valves and LA:

- From a diastolic frame, measure the diameter of the Ao at valve level, and measure the left atrial size in the same dimension (avoiding ending measurement within pulmonary vein). The normal ratio of LA:Ao is <1.5
- Can also record M-mode of Ao (measured in diastole) to LA (measured in systole)



Left atrial enlargement, shown by ratio of the diastolic short-axis dimension of the LA, indexed to the aortic diameter in diastole. **(a)** AoV level, showing measurement in diastole of the aortic diameter (measurement 1) and the left atrial diameter, along the same plane (measurement 2). The ratio in this dog, with advanced myxomatous mitral valve disease, was $57.7/16.2 = 3.56$ (normal <1.5). **(b)** A cat with severe congestive heart failure due to end-stage HCM. AoV level, showing measurement in diastole of the aortic diameter (measurement 1) and the left atrial diameter, along the same plane (measurement 2). The ratio in this cat was $22.1/9.7 = 2.28$.

2.13

(continued) RPS and subcostal views. amv = Anterior mitral valve leaflet; Ao = Aorta; AoV = Aortic valve; APM = Anterior papillary muscle; CW = Continuous wave; HCM = Hypertrophic cardiomyopathy; IAS = Interatrial septum; IVS = Interventricular septum; LA = Left atrium; LAu = Left atricular appendage; LPA = Left pulmonary artery; LV = Left ventricle; LVFW = Left ventricular free wall; LVOT = Left ventricular outflow tract; MPA = Main pulmonary artery; MV = Mitral valve; pmv = Posterior mitral valve leaflet; PPM = Posterior papillary muscle; PV = Pulmonic valve; PW = Pulsed wave; RA = Right atrium; RPA = Right pulmonary artery; RV = Right ventricle; RVOT = Right ventricular outflow tract; TV = Tricuspid valve; VSD = Ventricular septal defect. (Line diagrams adapted and reproduced from Boon (1998) with permission from the publisher) (continues) ▶

RPS cranial long-axis view of aorta**Acquisition of the view**

- From short-axis Ao, rotate back clockwise until the Ao is seen in long-axis
- Alternatively, move a rib space forwards from the RPS five-chamber view

Observations, measurements and calculations

- From RPS cranial long-axis view of Ao, can assess aortic valves and subvalvular region, and whether there is any post-stenotic dilatation of the aortic arch
- Measure aortic diameter (systole: valve level or at sinotubular junction (junction of sinus of Valsalva with tubular Ao)) to enable calculation of cross-sectional area and forward stroke volume



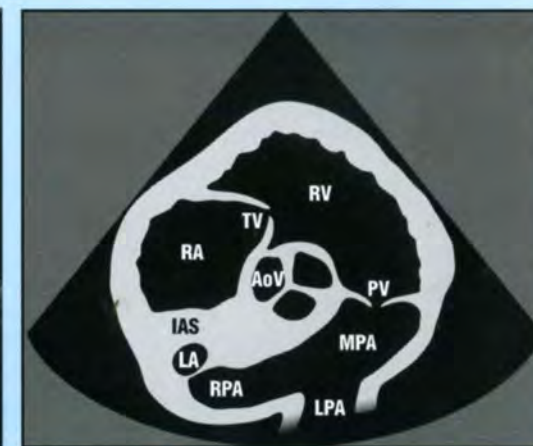
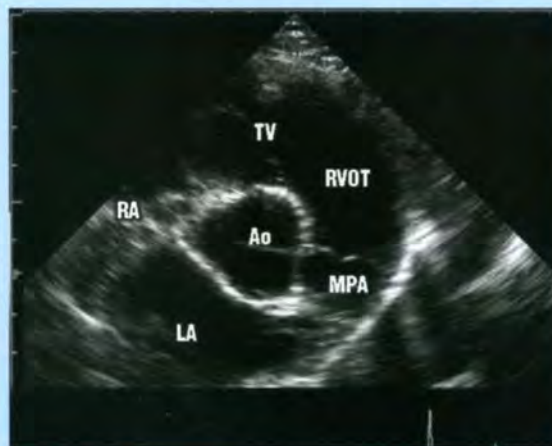
Aortic diameter can be measured at the sinotubular junction. From this, the aortic cross-sectional area can be calculated (πr^2).

RPS cranial short-axis view**Acquisition of the view and assessments**

- From a cranial view of the long-axis Ao, angle the transducer dorsally. The Ao will become short-axis, and a long-axis view of the RVOT and pulmonic valves is acquired (left image)
- Fan slightly more dorsally and cranially to optimize the pulmonary trunk and bifurcation of the MPA (right image)
- Colour flow Doppler for the pulmonic valves and pulmonary trunk

Observations, measurements and calculations

- Optimize for pulmonary trunk to assess pulmonic valves and pulmonary trunk
- Can measure MPA diameter, at valve level, in systole
- The diameter of the MPA should be equal to or smaller than the Ao. Increased diameter, with normal pulmonic valves, may suggest pulmonary hypertension
- This view is used for Doppler assessment of the pulmonic valves, pulmonary outflow and pulmonic insufficiency



AoV level, optimized for PV and proximal MPA in a normal Greyhound.

2.13

(continued) RPS and subcostal views. amv = Anterior mitral valve leaflet; Ao = Aorta; AoV = Aortic valve; APM = Anterior papillary muscle; CW = Continuous wave; HCM = Hypertrophic cardiomyopathy; IAS = Interatrial septum; IVS = Interventricular septum; LA = Left atrium; LAu = Left auricular appendage; LPA = Left pulmonary artery; LV = Left ventricle; LVFW = Left ventricular free wall; LVOT = Left ventricular outflow tract; MPA = Main pulmonary artery; MV = Mitral valve; pmv = Posterior mitral valve leaflet; PPM = Posterior papillary muscle; PV = Pulmonic valve; PW = Pulsed wave; RA = Right atrium; RPA = Right pulmonary artery; RV = Right ventricle; RVOT = Right ventricular outflow tract; TV = Tricuspid valve; VSD = Ventricular septal defect. (Line diagrams adapted and reproduced from Boon (1998) with permission from the publisher) (continues)

Subcostal view**Acquisition of the view**

- Position transducer caudal to the xiphisternum, angling cranially. The thumb is ventral, towards the operator. The depth of field needs to be increased for imaging the heart and ascending Ao beyond the liver and diaphragm. The transducer may need to be pushed into the cranial abdomen (which is not comfortable for most dogs). Slight rotation of the transducer results in opening up the Ao. The CW Doppler cursor can be used to position for aortic outflow peak velocity



The subcostal view for the Ao; transhepatic (liver-labelled) and transdiaphragmatic (diaphragm-labelled) view of the heart, which gives optimal alignment with the Ao, so peak aortic velocities can be measured.

Observations, measurements and calculations

- This view is used to be as parallel as possible to the aortic outflow. The Ao is central within the chest, and imaging from the midline optimizes alignment
- Spectral Doppler is used to record peak aortic velocity. In most dogs, peak aortic velocities are obtained from this view
- Note that a low-frequency transducer is required for the depth of penetration, and CW (rather than PW) Doppler may be required to obtain a signal at this depth

2.13

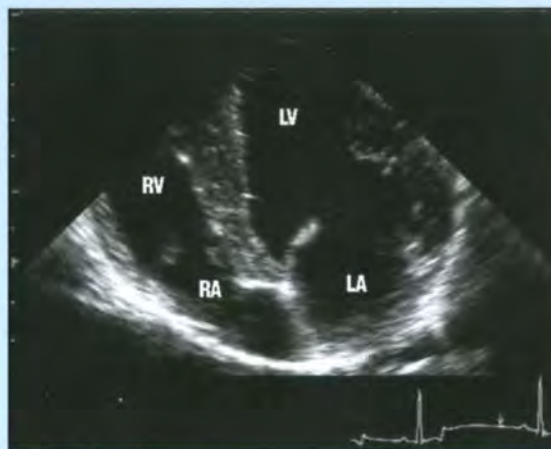
(continued) RPS and subcostal views. amv = Anterior mitral valve leaflet; Ao = Aorta; AoV = Aortic valve; APM = Anterior papillary muscle; CW = Continuous wave; HCM = Hypertrophic cardiomyopathy; IAS = Interatrial septum; IVS = Interventricular septum; LA = Left atrium; LAu = Left auricular appendage; LPA = Left pulmonary artery; LV = Left ventricle; LVFW = Left ventricular free wall; LVOT = Left ventricular outflow tract; MPA = Main pulmonary artery; MV = Mitral valve; pmv = Posterior mitral valve leaflet; PPM = Posterior papillary muscle; PV = Pulmonic valve; PW = Pulsed wave; RA = Right atrium; RPA = Right pulmonary artery; RV = Right ventricle; RVOT = Right ventricular outflow tract; TV = Tricuspid valve; VSD = Ventricular septal defect. (Line diagrams adapted and reproduced from Boon (1998) with permission from the publisher)

Left apical four-chamber view**Acquisition of the view**

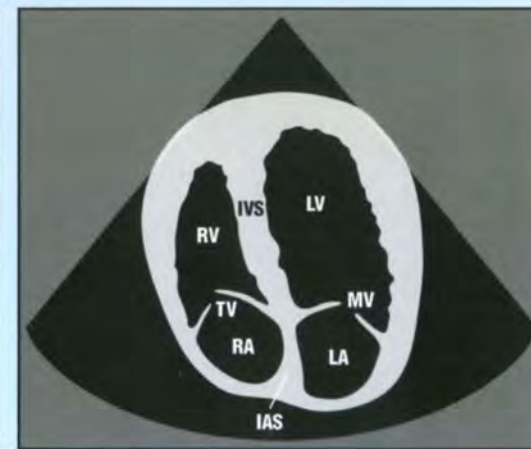
- Feel for the cardiac apex
- Position transducer with thumb about 30–45 degrees to the intercostal space, towards the head, angling dorsally
- To include the apex, move nearer the sternum, and possibly more caudally, to optimize LV length. Aim for a 'vertical' heart
- *Note: in all but very deep, narrow-chested breeds, the anatomical LV apex is not included, as it is more diaphragmatically directed*
- This view is used for mitral Doppler studies
- To include more right heart, move a rib space cranially (e.g. to record TV studies)

Observations, measurements and calculations

- Possibly use to assess LV length and volume (but apex not included)
- Colour flow Doppler interrogation of the MV and TV
- Spectral Doppler assessment of mitral and tricuspid inflow, and mitral and tricuspid regurgitation
- M-mode of mitral annulus motion
- Use for recording PW Doppler of pulmonary venous flow
- Use for calculation of mitral early flow propagation (V_p) with colour M-mode
- Use for pw-TDI studies of myocardial motion of longitudinal fibres at the mitral annulus



Normal Greyhound.

**Left apical five-chamber view****Acquisition of the view**

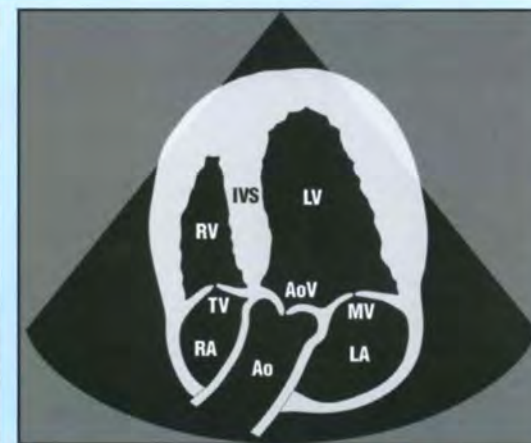
- From the left apical four-chamber view, rotate about 10 degrees anti-clockwise and angle cranially, to show the LVOT and Ao
- In some animals, alignment with aortic outflow is good from this view

Observations, measurements and calculations

- Assess colour variance of LVOT and Ao
- Colour flow and Doppler assessment of aortic insufficiency
- PW Doppler assessment of LVOT and aortic velocity



Normal Greyhound.

**2.14**

Left apical and LPS views. Ao = Aorta; AoV = Aortic valve; CW = Continuous wave; IAS = Interatrial septum; IVS = Interventricular septum; LA = Left atrium; LPA = Left pulmonary artery; LV = Left ventricle; LVFW = Left ventricular free wall; LVOT = Left ventricular outflow tract; MPA = Main pulmonary artery; MV = Mitral valve; PDA = Patent ductus arteriosus; PV = Pulmonic valve; PW = Pulsed wave; pw-TDI = Pulsed wave tissue Doppler imaging; RA = Right atrium; RPA = Right pulmonary artery; RV = Right ventricle; RVOT = Right ventricular outflow tract; TV = Tricuspid valve. (Line diagrams adapted and reproduced from Boon (1998) with permission from the publisher) (continues)

Left apical two-chamber view**Acquisition of the view**

- From the left apical four-chamber view, as far caudally as possible, rotate 90 degrees for the two-chamber view (LA and LV)

Observations, measurements and calculations

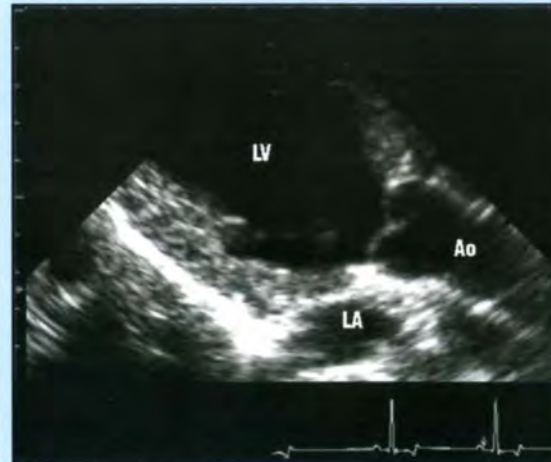
- Orthogonal long-axis view used for more accurate assessment of LV length and volume (e.g. full *Simpson's rule*)
- Sometimes used to assess mitral inflow or mitral regurgitation
- Can record mitral annulus motion at orthogonal points to those recorded in the four-chamber view

Left apical three-chamber view**Acquisition of the view**

- From the apical two-chamber view, angle cranially until the LVOT and Ao are apparent
- Normally, good alignment with aortic outflow is possible

Observations, measurements and calculations

- Assess colour variance of LVOT and Ao
- Colour flow and Doppler assessment of aortic insufficiency
- PW Doppler assessment of LVOT and aortic velocity to indicate whether there is step-up in velocity and/or to record peak aortic velocity



Normal Greyhound.

2.14

(continued) Left apical and LPS views. Ao = Aorta; AoV = Aortic valve; CW = Continuous wave; IAS = Interatrial septum; IVS = Interventricular septum; LA = Left atrium; LPA = Left pulmonary artery; LV = Left ventricle; LVFW = Left ventricular free wall; LVOT = Left ventricular outflow tract; MPA = Main pulmonary artery; MV = Mitral valve; PDA = Patent ductus arteriosus; PV = Pulmonic valve; PW = Pulsed wave; pw-TDI = Pulsed wave tissue Doppler imaging; RA = Right atrium; RPA = Right pulmonary artery; RV = Right ventricle; RVOT = Right ventricular outflow tract; TV = Tricuspid valve. (Line diagrams adapted and reproduced from Boon (1998) with permission from the publisher) (continues) ►

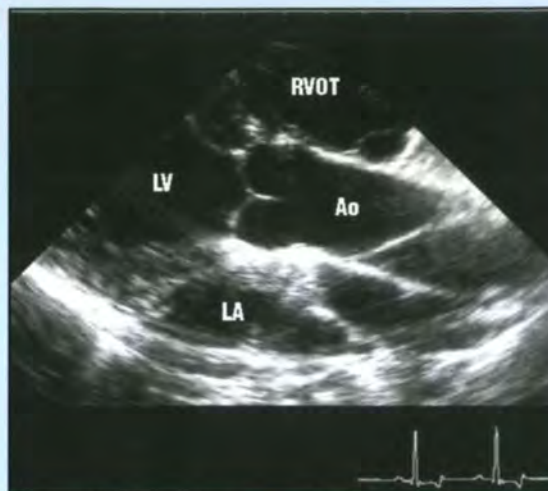
LPS cranial long-axis view

Acquisition of the view

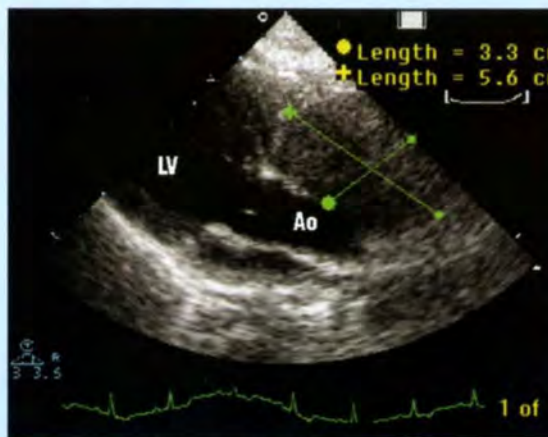
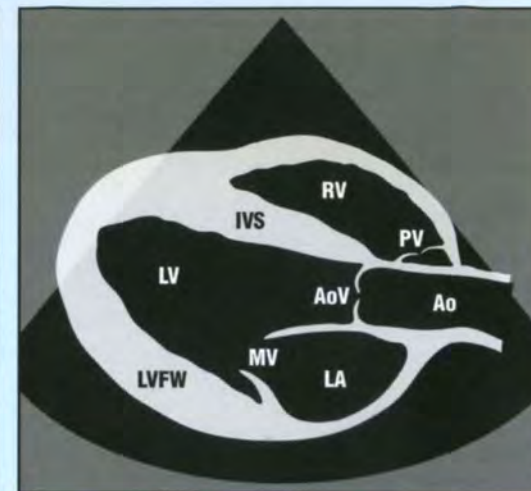
- Moving one to two rib spaces cranially, from the apical views, the ascending aortic arch can be assessed

Observations, measurements and calculations

- Used to assess for post-stenotic dilatation in aortic stenosis
- Search for periaortic masses
- Used to measure aortic diameter (to calculate forward stroke volume)



Normal Greyhound, optimized for the Ao.



Boxer with a periaortic mass, presumed to be a chemodectoma.

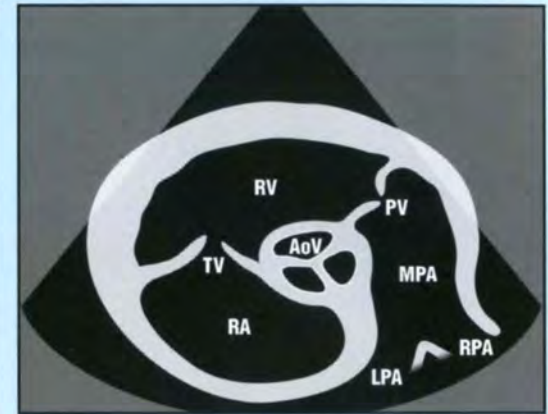
2.14 (continued) Left apical and LPS views. Ao = Aorta; AoV = Aortic valve; CW = Continuous wave; IAS = Interatrial septum; IVS = Interventricular septum; LA = Left atrium; LPA = Left pulmonary artery; LV = Left ventricle; LVFW = Left ventricular free wall; LVOT = Left ventricular outflow tract; MPA = Main pulmonary artery; MV = Mitral valve; PDA = Patent ductus arteriosus; PV = Pulmonic valve; PW = Pulsed wave; pw-TDI = Pulsed wave tissue Doppler imaging; RA = Right atrium; RPA = Right pulmonary artery; RV = Right ventricle; RVOT = Right ventricular outflow tract; TV = Tricuspid valve. (Line diagrams adapted and reproduced from Boon (1998) with permission from the publisher) (continues) ▶

LPS cranial short-axis view (aorta) optimizing pulmonary trunk**Acquisition of the view and assessments**

- From the long-axis Ao, angle dorsally (almost parallel with the chest wall) and slightly cranially; the Ao will become short-axis and the pulmonary trunk should be seen
- To optimize alignment with the pulmonary trunk, the transducer may need to be moved another rib space cranially
- This view can also be used to image the ductus of a PDA



Normal Greyhound, optimized for the MPA and its bifurcation.

**Observations, measurements and calculations**

- Used to align with pulmonic outflow, for colour flow and spectral Doppler assessment of PV
- Used to screen for PDA and align with PDA flow (colour flow and CW Doppler)



Optimized view for the MPA and ampulla entry of PDA into MPA, close to its bifurcation. Colour flow and spectral Doppler echocardiography confirmed the continuous, high-velocity flow characteristic of the ductus in this region.

2.14

(continued) Left apical and LPS views. Ao = Aorta; AoV = Aortic valve; CW = Continuous wave; IAS = Interatrial septum; IVS = Interventricular septum; LA = Left atrium; LPA = Left pulmonary artery; LV = Left ventricle; LVFW = Left ventricular free wall; LVOT = Left ventricular outflow tract; MPA = Main pulmonary artery; MV = Mitral valve; PDA = Patent ductus arteriosus; PV = Pulmonic valve; PW = Pulsed wave; pw-TDI = Pulsed wave tissue Doppler imaging; RA = Right atrium; RPA = Right pulmonary artery; RV = Right ventricle; RVOT = Right ventricular outflow tract; TV = Tricuspid valve. (Line diagrams adapted and reproduced from Boon (1998) with permission from the publisher)

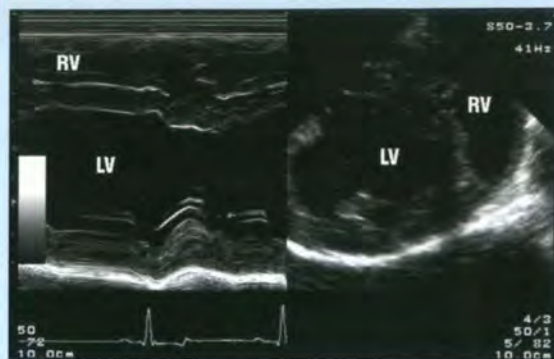
Left ventricular M-mode (chordae tendinae level)**Acquisition of the view**

- Make sure the RPS long-axis four-chamber view is as 'horizontal' as possible, with the M-mode cursor transecting chordae tendinae of both mitral valve leaflets. The cursor should be perpendicular with the endocardium of both the septum and the free wall
- Change to short-axis view and ensure the M-mode cursor bisects a symmetrical LV cavity
- Record M-mode tracing, ensuring endocardium on both sides of the septum, and the LVFW can be seen. Make sure papillary muscles are not transected. It is acceptable to see chordae within the LV cavity

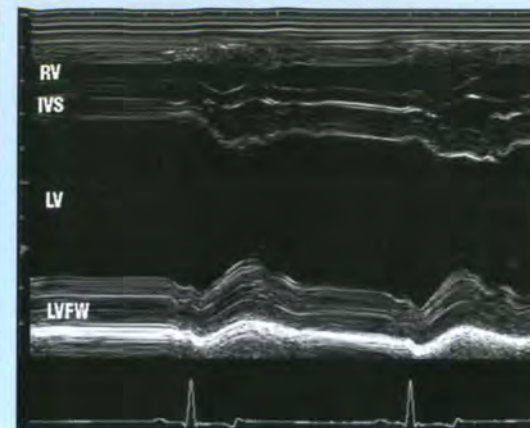
Measurements and calculations

- From still images, the standard LV measurements can be obtained
- An ECG is essential for accurate M-mode measurements. End-diastolic measurements are made at the start of the QRS complex; systolic measurements are made at the nadir of septal motion or the smallest LV dimension
- In obtaining measurements, use the 'leading edge to leading edge' technique, i.e. the endocardium nearest the transducer is included, but far endocardium is excluded. This ensures effects of gain and endocardial brightness do not influence measurements
- **Measurements:**
 - (a) IVS in diastole and systole (IVSd, IVSs)
 - (b) LVID in diastole and systole (LVIDd, LVIDs)
 - (c) LVFW in diastole and systole (LVFWd, LVFWs)
 - (d) RV may also be measured in diastole (RVd)
- **Calculations:** Fractional shortening (FS%):

$$FS\% = [(LVIDd - LVIDs)/LVIDd] \times 100$$



Positioning of the M-mode cursor, so it bisects the LV cavity (right). Everything along this cursor line is plotted against time to give the M-mode image.



Normal Greyhound, showing timing of systole associated with the ECG. Diastolic wall thickness and LV chamber dimension are measured at the start of the QRS complex. Systolic measurements are obtained at the nadir of septal motion (see Figure 2.17 for further information on assessment of M-mode measurements).

2.15

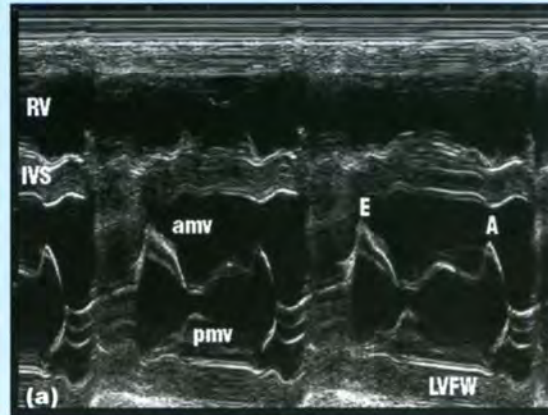
M-mode views, measurements and calculations. AF = Atrial fibrillation; amv = Anterior mitral valve leaflet; Ao = Aorta; DCM = Dilated cardiomyopathy; ET = Ejection time; HCM = Hypertrophic cardiomyopathy; IVS = Interventricular septum; LA = Left atrium; LAu = Left auricular appendage; LV = Left ventricle; LVFW = Left ventricular free wall; LVID = Left ventricular internal dimension; MA = Mitral annulus; MAM = Mitral annulus motion; PEP = Pre-ejection period; pmv = Posterior mitral valve leaflet; RV = Right ventricle; SAM = Systolic anterior motion. (continues)

Mitral valve M-mode**Acquisition of the view**

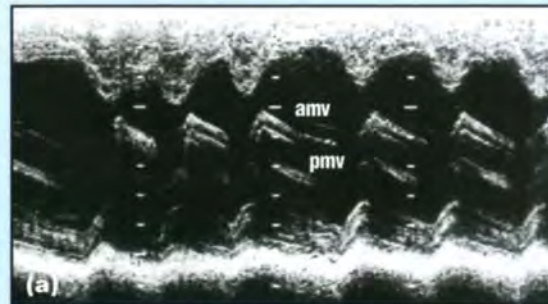
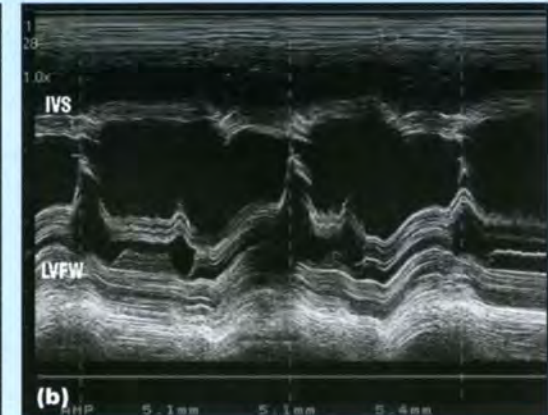
- From the fish-mouth view of the mitral valve, position the M-mode cursor, so it transects both leaflets in a symmetrical LV cavity
- Change to M-mode and record the excursions of the anterior and posterior leaflets with time
- An animal in sinus rhythm opens the valve twice: once in early diastole (E peak or E point of the anterior leaflet), with partial closure during diastasis; then during a late diastolic peak following the P wave on the ECG, corresponding to atrial emptying (A peak)
- The posterior leaflet should move to a lesser magnitude in the opposite direction, towards the LVFW
- Both leaflets are closed together in systole and course slightly anteriorly, towards the septum

Measurements and calculations

- Measurements include the mitral E point to septal separation. This distance may increase when the LV is rounded, or with reduced stroke volume (e.g. DCM; see Figure 7.99, p. 137). This distance should be <7 mm in any dog breed
- Due to the high temporal resolution of M-mode, the presence of SAM of the amv can be best appreciated and documented on this view (e.g. cats with hypertrophic obstructive cardiomyopathy) (see Figures 7.101, p. 139 and 7.108, p. 143)
- Diastolic flutter of the amv can be seen associated with significant aortic regurgitation
- Abnormal mitral valve movement, with the posterior leaflet failing to move in the opposite direction to the anterior leaflet, can be documented in mitral stenosis (e.g. mitral dysplasia in Bull Terriers)



(a) Normal Greyhound. Note that in sinus rhythm at normal heart rates, the anterior mitral valve moves towards the septum in early diastole (E peak), corresponding to passive LV filling, and is also associated with atrial contraction (A peak), following the P wave on the ECG. The pmv moves in the opposite direction, towards the LVFW. **(b)** German Shepherd Dog with severe aortic regurgitation associated with subaortic stenosis. Mitral valve leaflets were thickened due to concurrent mitral dysplasia. Note the diastolic flutter of the amv; a consequence of the aortic regurgitant jet affecting this leaflet in diastole.



(a) Bull Terrier with congenital mitral stenosis as part of mitral dysplasia. This dog had severe left atrial enlargement and AF, which meant that there was no A peak of anterior mitral motion. Note that the posterior leaflet is not moving in the opposite direction but tends to be dragged in the same direction as the anterior leaflet. **(b)** Cat with acquired mitral stenosis associated with HCM. In this case, the posterior leaflet appears immobile.

**2.15**

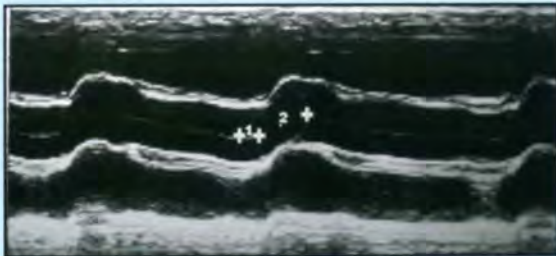
(continued) M-mode views, measurements and calculations. AF = Atrial fibrillation; amv = Anterior mitral valve leaflet; Ao = Aorta; DCM = Dilated cardiomyopathy; ET = Ejection time; HCM = Hypertrophic cardiomyopathy; IVS = Interventricular septum; LA = Left atrium; LAu = Left auricular appendage; LV = Left ventricle; LVFW = Left ventricular free wall; LVID = Left ventricular internal dimension; MA = Mitral annulus; MAM = Mitral annulus motion; PEP = Pre-ejection period; pmv = Posterior mitral valve leaflet; RV = Right ventricle; SAM = Systolic anterior motion. (continues)

M-mode at aortic valve level**Acquisition of the view**

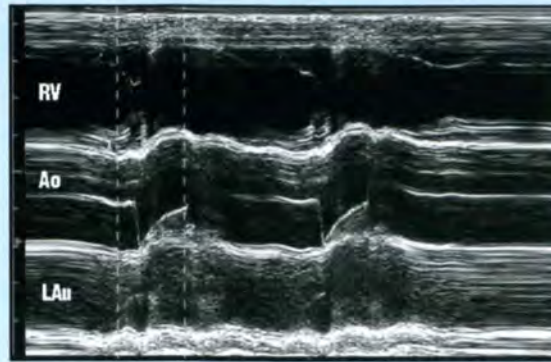
- From the cranial short-axis view of the aortic valve leaflets, position M-mode cursor through the centre of the Ao, and the LA/LAu
- Try to record the aortic valve leaflets throughout the cardiac cycle (normally only one is recorded in dogs)

Measurements and calculations

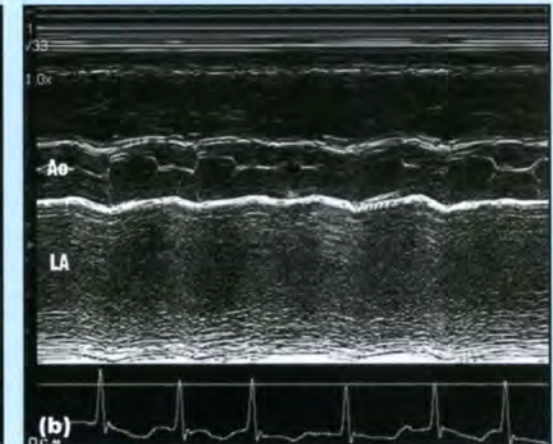
- Assess aortic root excursion in systole. In conditions of poor systolic function (e.g. DCM), the aortic root remains 'flat' during systole
- **Measurements:**
 - (a) Aortic diameter (diastole: start of QRS on ECG)
 - (b) LA (systole – maximal width)
- **Calculations:**
 - (a) M-mode LA:Ao ratio. *Note: it is difficult to consistently transect the same portion of the LA and LAu in different individuals, so 2D methods of assessing LA size are now preferred*
 - (b) Systolic time intervals:
 - Measure the PEP from the start of the QRS complex to opening of aortic valve
 - Measure the ET as the duration of aortic valve opening
 - The PEP:ET ratio is a sensitive indicator of systolic function. Normal ratio is 0.25–0.35



Great Dane. This view shows measurement of the systolic time intervals: PEP and ET. The PEP is measured from the start of the QRS complex to the opening of the aortic valves (measurement 1) (here 80 ms). The ET is the duration that the aortic valves open for (measurement 2) (here 195 ms). Both parameters are heart rate dependent. However, the PEP:ET ratio is relatively heart rate independent and is a sensitive indicator of systolic function. In this dog, the PEP:ET ratio was 0.41 (slightly higher than the reference values of 0.25–0.35).



Normal Greyhound. Note that the aortic root moves anteriorly during systole. The aortic valves transcribe a 'box' shape during systole. To calculate the left atrial to aortic root ratio, the aortic root diameter is measured in end-diastole (start of QRS complex) and the maximum left atrial dimension is measured during systole.



Cat with an unclassified cardiomyopathy with marked left atrial enlargement and systolic dysfunction. The cat was also in AF. **(a)** Cranial short-axis view of the aortic root and LA, indicating the 2D measurements. The M-mode cursor was positioned on this image: the aortic root and left atrial measurements are in a slightly different plane than the 2D measurements. **(b)** M-mode view of the aortic root (Ao) and the LA. This view also confirms the massive left atrial enlargement. Note also that the aortic root is 'flat' with minimal anterior excursion, providing additional evidence of the impaired systolic function. The AF is resulting in variable opening of the aortic valves, and there is also premature closure of the aortic valves during systole (the valves no longer transcribe a rectangular box). This finding is common in cases of impaired systolic function.

2.15

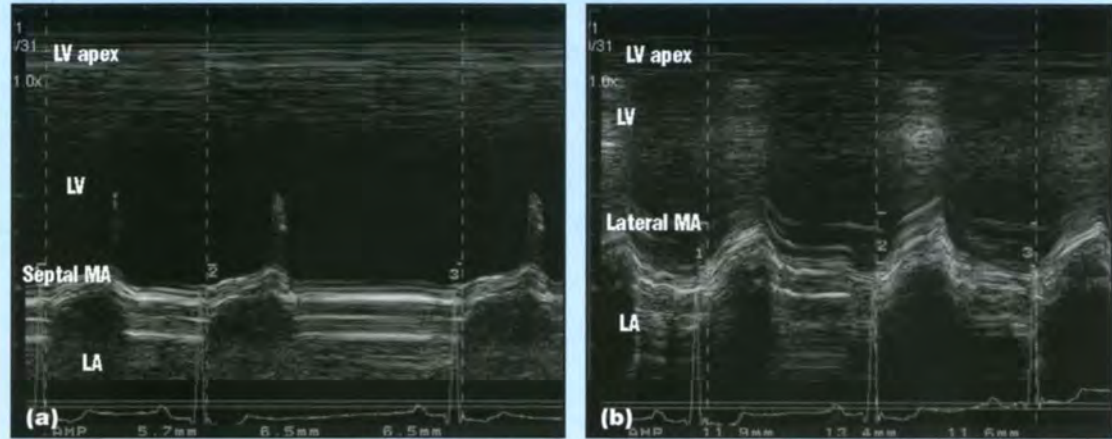
(continued) M-mode views, measurements and calculations. AF = Atrial fibrillation; amv = Anterior mitral valve leaflet; Ao = Aorta; DCM = Dilated cardiomyopathy; ET = Ejection time; HCM = Hypertrophic cardiomyopathy; IVS = Interventricular septum; LA = Left atrium; LAu = Left auricular appendage; LV = Left ventricle; LVFW = Left ventricular free wall; LVID = Left ventricular internal dimension; MA = Mitral annulus; MAM = Mitral annulus motion; PEP = Pre-ejection period; pmv = Posterior mitral valve leaflet; RV = Right ventricle; SAM = Systolic anterior motion. (continues)

Mitral annulus motion**Acquisition of the view**

- From the apical four-chamber view (or the orthogonal two-chamber view), position the M-mode cursor so it is perpendicular to the MA
- Record M-mode of MAM

Measurements and calculations

- Measure the magnitude of MAM, from end-diastole to systole
- This corresponds to longitudinal fibre shortening and apicobasilar contractility
- Regional wall motion may result in discordant readings from the two or four sampling points around the MA. Normally, the mean value is cited



Bull Terrier with mitral regurgitation due to mitral dysplasia. A left apical four-chamber view is acquired as vertically as possible, so the annulus is perpendicular to the ultrasound beam. An M-mode cursor is positioned at the annulus, at the point of attachment of the mitral valve, on both **(a)** the septal (anterior) leaflet side and **(b)** the lateral (posterior) side. The M-mode image transects the left ventricular cavity from apex to base, and the LA. Measurement of MAM is purely the magnitude of excursion between diastole and systole, as the MA moves towards the LV apex in systole, as a consequence of contraction of longitudinal fibres, resulting in the apicobasilar contractility of the heart. Normally, there is greater magnitude of movement from the lateral annulus.

2.15

(continued) M-mode views, measurements and calculations. AF = Atrial fibrillation; amv = Anterior mitral valve leaflet; Ao = Aorta; DCM = Dilated cardiomyopathy; ET = Ejection time; HCM = Hypertrophic cardiomyopathy; IVS = Interventricular septum; LA = Left atrium; LAu = Left auricular appendage; LV = Left ventricle; LVFW = Left ventricular free wall; LVID = Left ventricular internal dimension; MA = Mitral annulus; MAM = Mitral annulus motion; PEP = Pre-ejection period; pmv = Posterior mitral valve leaflet; RV = Right ventricle; SAM = Systolic anterior motion.

Importance of being aligned with flow: All Doppler echocardiography is dependent on positioning. It is very important for the cursor to be as parallel to blood flow as possible (and must be within 20 degrees). The reason for this can be understood from the *Doppler equation*.

The Doppler equation

$$f_2 = \frac{2f_0}{c} v \cos\theta$$

Where f_2 = reflected frequency
 f_0 = transmitted frequency
 v = maximal velocity
 c = velocity of ultrasound waves in blood
 θ = angle between ultrasound beam and direction of blood flow.

Rearranging the equation:

$$v = \frac{c}{2f_0 \cos\theta} f_2$$

As every attempt to be parallel to flow is made, θ is 0 degrees and the cosine of this = 1.

(θ must be <20 degrees for the angle factor to be ignored).

This allows the equation to be modified to:

$$v = \frac{c}{2f_0} f_2$$

As $\frac{c}{2}$ is constant:

$$v \propto \frac{f_2}{f_0}$$

i.e. the velocity of RBCs is proportional to the frequency shift between reflected and transmitted ultrasound waves.

It is very important to attempt to obtain maximal velocities, as these will represent best parallel alignment with flow. This may involve interrogating a valve from several different positions, e.g. aortic velocity in aortic stenosis from LPS and RPS views, and from subcostal views. The use of any angle correction facility on the machine is considered bad practice in cardiology. Despite apparent alignment in 2D, it may not be correct in 3D. Much of the learning curve in Doppler echocardiography is spent perfecting alignment with intracardiac flows.

Modified Bernoulli equation – non-invasive Doppler-derived pressure gradients: An estimate of pressure gradient (PG) across a valve, from the peak velocity of flow through that valve, can be determined using the modified Bernoulli equation. Thus, the severity of pulmonic stenosis or aortic stenosis can be assessed non-invasively, without selective cardiac catheterization.

Modified Bernoulli equation

$$PG = 4v^2$$

Where PG = pressure gradient (mmHg)
 v = maximal velocity (m/s)

Where the pressure of one chamber is known or assumed, the modified Bernoulli equation can be used to estimate pressure of the other side of a valve. For example, in aortic stenosis, if systolic blood pressure is recorded as 120 mmHg, and the PG derived from Doppler studies is 80 mmHg, then the LV systolic pressure must be 200 mmHg.

In the absence of pulmonic stenosis, and the presence of tricuspid regurgitation and pulmonic insufficiency jets, both systolic and diastolic pulmonary arterial pressure can be determined using the modified Bernoulli equation.

Practicalities of a complete Doppler study: Figure 2.16 gives the techniques for acquiring spectral Doppler studies from each heart valve, and the measurements which may be obtained.

Assessing cardiac function

In simplest terms, cardiac function can be divided into:

- Systolic function
- Diastolic function.

Doppler echocardiography can give a non-invasive method of assessing these, but it is important to be aware of the limitations of each technique.

Assessment of left ventricular systolic function

Figure 2.17 details the M-mode, 2D and Doppler methods of assessing systolic function, with advantages and limitations of each technique. To make an overall assessment of systolic function, an integrated approach is required, rather than relying on one single method.

Assessment of left ventricular diastolic function

The study of diastolic function ('diastology') requires recognition of the phases of diastole:

1. Isovolumic relaxation phase.
2. Early rapid filling of the LV (depending on LV active relaxation).
3. Diastasis.
4. Late LV filling, corresponding to left atrial contraction (following P wave of the ECG).

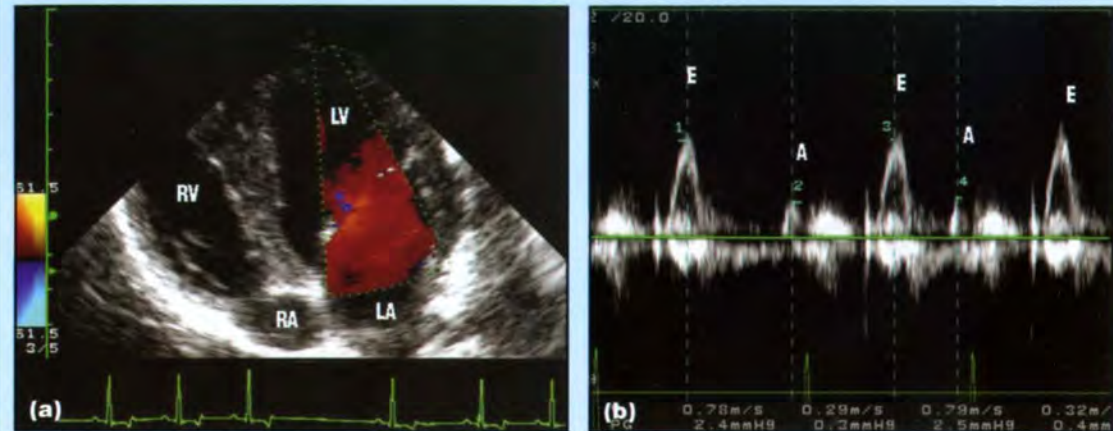
Most of the echocardiographically derived parameters of diastolic function will be preload and heart rate sensitive. Elevated filling pressures (left-sided congestive heart failure) or tachycardia may confound the interpretation of diastolic function.

Mitral inflow**Acquisition of image**

- From left apical view, make sure the heart is vertical and the cursor is aligned with the axis of the heart
- Put a colour flow region of interest over the mitral valve
- Position sample volume of the cursor between mitral valve leaflets cusps
- Record the mitral inflow pattern as a PW Doppler spectrum

Measurements and calculations

- From the mitral inflow PW Doppler spectrum, identify the E waves (early diastole) and A waves (associated with atrial contraction, following the P wave on the ECG)
- Measure peak E and A wave velocities
- Calculate mitral E and A ratio if needed
- There should be no respiratory variation in mitral inflow velocities (the presence of variation indicates increased ventricular interdependence, such as with pericardial disease).
- Other measurements include:
 - (a) Mitral E wave duration
 - (b) Mitral E wave deceleration time
 - (c) Mitral A wave duration



(a) From a left apical four-chamber view, a colour sample volume is placed over the mitral valve. Red indicates blood moving towards the transducer. **(b)** A PW Doppler sample volume is placed between the tips of the mitral valve to record mitral inflow. Note that for sinus rhythm there are two phases of diastolic filling, giving the two waves of mitral inflow. Early passive filling results in the E wave, and flow subsequent to atrial contraction gives the A wave (following the P wave of the ECG).

2.16

Spectral Doppler echocardiography. amv = Anterior mitral valve leaflet; Ao = Aorta; AoR = Aortic regurgitation; CW = Continuous wave; ET = Ejection time; HCM = Hypertrophic cardiomyopathy; HPRF = High pulse repetition frequency; LA = Left atrium; LAu = Left auricular appendage; LV = Left ventricle; LVOT = Left ventricular outflow tract; MPA = Main pulmonary artery; MR = Mitral regurgitation; PDA = Patent ductus arteriosus; PEP = Pre-ejection period; PG = Pressure gradient; PI = Pulmonic insufficiency; PW = Pulsed wave; RA = Right atrium; RV = Right ventricle; RVOT = Right ventricular outflow tract; SAM = Systolic anterior motion; TR = Tricuspid regurgitation; VSD = Ventricular septal defect; VTI = Velocity time integral. (continues) ▶

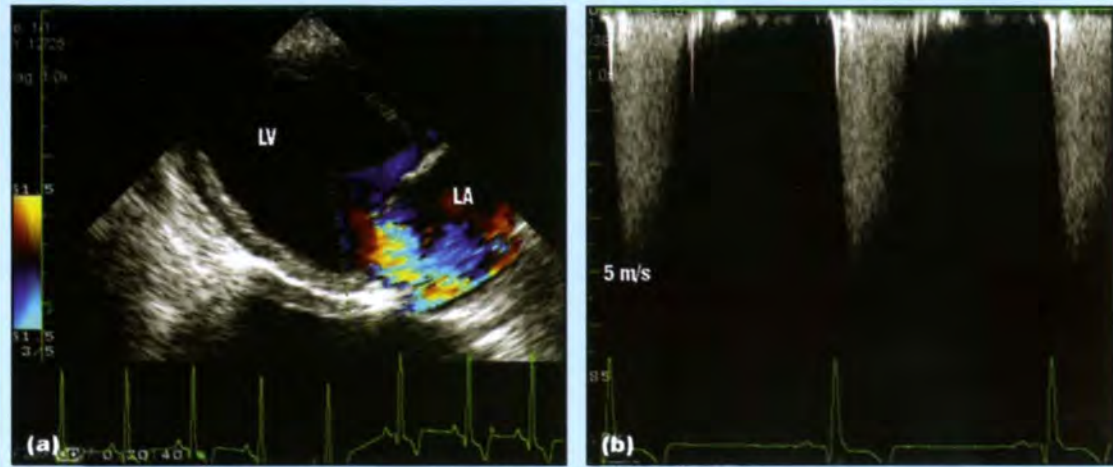
Mitral regurgitation

Acquisition of image

- Use colour flow Doppler to identify the direction and size of the MR jet
- Normally, alignment with the jet is best from the left apical four-chamber view
- Occasionally, with asymmetric jets, other views are acquired. In cats with MR due to SAM of the amv, the MR jet projects to the posteriolateral wall of the LA, and alignment may actually be optimal from the RPS four-chamber view
- Use CW Doppler to record the MR spectral signal. Make sure the velocity scale is set at over 4 m/s

Measurements and calculations

- From the colour flow signal, the severity of MR can be semiquantitatively assessed from jet area compared with LA area as: Trivial; + (<25% LA); 2+ (25–49% LA); 3+ (50–75% LA); or 4+ (>75% LA)
- Measure peak MR velocity (v)
- Use the modified Bernoulli equation to determine the PG ($= 4v^2$) between the LA and LV
- From the acceleration slope of the MR signal, $+dP/dt$ can be calculated (see Assessment of systolic function)
- From the deceleration slope of the MR signal, $-dP/dt$ can be calculated (see Assessment of diastolic function)



(a) RPS long-axis four-chamber view, indicating MR from a Whippet puppy with mitral dysplasia. The mosaic of colours (colour variance) are typical of turbulent flow on a velocity–variance colour flow map. The MR jet area can be compared with left atrial area for semiquantification of severity. However, this is difficult when the jet fits the dorsal wall of the LA and curls back (red) as in this example. **(b)** CW Doppler spectrum of a MR jet from a dog with myxomatous degenerative valvular disease. Note that the peak velocity is around 5 m/s, which reflects a normal, preserved PG between the LV and LA.

2.16

(continued) Spectral Doppler echocardiography. amv = Anterior mitral valve leaflet; Ao = Aorta; AoR = Aortic regurgitation; CW = Continuous wave; ET = Ejection time; HCM = Hypertrophic cardiomyopathy; HPRF = High pulse repetition frequency; LA = Left atrium; LAu = Left auricular appendage; LV = Left ventricle; LVOT = Left ventricular outflow tract; MPA = Main pulmonary artery; MR = Mitral regurgitation; PDA = Patent ductus arteriosus; PEP = Pre-ejection period; PG = Pressure gradient; PI = Pulmonic insufficiency; PW = Pulsed wave; RA = Right atrium; RV = Right ventricle; RVOT = Right ventricular outflow tract; SAM = Systolic anterior motion; TR = Tricuspid regurgitation; VSD = Ventricular septal defect; VTI = Velocity time integral. (continues)

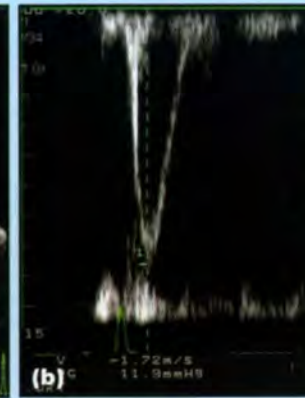
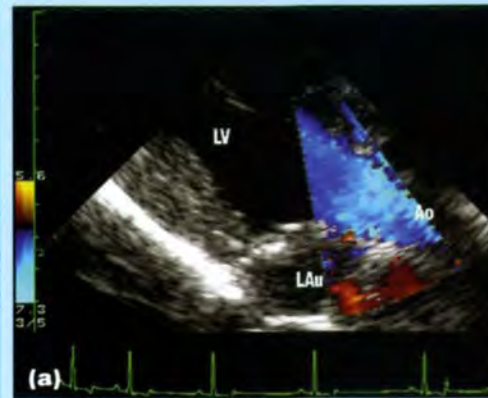
Aortic outflow

Acquisition of image and assessments

- Subcostal view, align CW cursor with the ascending Ao
- Record CW spectral Doppler. In most dogs, peak aortic velocities are obtained by this view
- In small dogs and with a low-frequency transducer, PW or HPRF PW signals may be possible
- Alignment for aortic outflow by the subcostal view is not usually good in cats
- Left apical view (three-chamber or five-chamber view). Work at getting the cursor as parallel as possible with aortic outflow (must be within 20 degrees)
- Use colour flow Doppler to assess the character of flow and any turbulence, and to identify the presence of any AoR
- Position the sample volume just beyond the aortic valves, within the Ao
- Record PW spectral Doppler signals of aortic outflow
- **Assessing step-up in velocity.** If aortic stenosis is suspected, the PW sample volume can be positioned in the LVOT before the possible obstruction, and the LVOT peak velocity recorded by PW spectral Doppler. The sample volume is then moved back into the Ao and the peak aortic velocity recorded beyond the valve. A significant step-up of velocity (>0.4 m/s) suggests increased aortic velocities are due to aortic stenosis and not a high output state (increased stroke volume)

Measurements and calculations

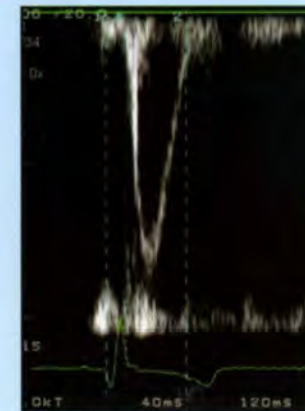
- Measure peak velocity of aortic flow (v)
- Calculate the PG across the aortic valve using the modified Bernoulli equation ($PG = 4v^2$)
- If aortic stenosis is present, it can be classified as mild ($PG < 40$ mmHg), moderate ($PG = 40-80$ mmHg) or severe ($PG > 80$ mmHg)
- Trace around the aortic outflow spectrum to measure the VTI. From this, the forward stroke volume can be calculated (see Figure 2.17)
- Systolic time intervals can be determined:
 - (a) PEP is start of QRS complex on ECG to onset of flow
 - (b) ET is the duration of the aortic outflow spectrum
- From the acceleration slope of the aortic spectrum, the following measurements can be made:
 - (a) Peak acceleration from the initial, steepest part of the slope (dv/dt max) (see Figure 2.17)
 - (b) Mean acceleration; the slope from baseline to peak velocity (dv/dt mean) (see Figure 2.17)
 - (c) Acceleration time



(a) Left apical three-chamber view optimizing alignment with aortic outflow. Blue indicates blood moving away from the transducer. **(b)** PW Doppler sample volume placed within the Ao, just beyond the aortic valves, to record aortic flow. Note that although the peak velocity is slightly above reference values at 1.72 m/s, there is no spectral dispersion and this spectral envelope indicates laminar flow.



CW Doppler spectrum obtained from a subcostal view of a Boxer with subaortic stenosis. Peak velocity was recorded at 4.12 m/s, corresponding to a PG between the LV and Ao of 68 mmHg, using the modified Bernoulli equation (moderately severe aortic stenosis).



PW Doppler spectrum of aortic outflow, showing measurements of the systolic time intervals, PEP and ET. The PEP is the start of the QRS complex to the onset of aortic flow. The ET is the duration of aortic flow. The PEP:ET ratio is relatively heart rate independent, and provides sensitive information about systolic function. The ratio here is 0.33, within the reference range of 0.25–0.35.

2.16 (continued) Spectral Doppler echocardiography. amv = Anterior mitral valve leaflet; Ao = Aorta; AoR = Aortic regurgitation; CW = Continuous wave; ET = Ejection time; HCM = Hypertrophic cardiomyopathy; HPRF = High pulse repetition frequency; LA = Left atrium; LAu = Left auricular appendage; LV = Left ventricle; LVOT = Left ventricular outflow tract; MPA = Main pulmonary artery; MR = Mitral regurgitation; PDA = Patent ductus arteriosus; PEP = Pre-ejection period; PG = Pressure gradient; PI = Pulmonic insufficiency; PW = Pulsed wave; RA = Right atrium; RV = Right ventricle; RVOT = Right ventricular outflow tract; SAM = Systolic anterior motion; TR = Tricuspid regurgitation; VSD = Ventricular septal defect; VTI = Velocity time integral. (continues) ▶

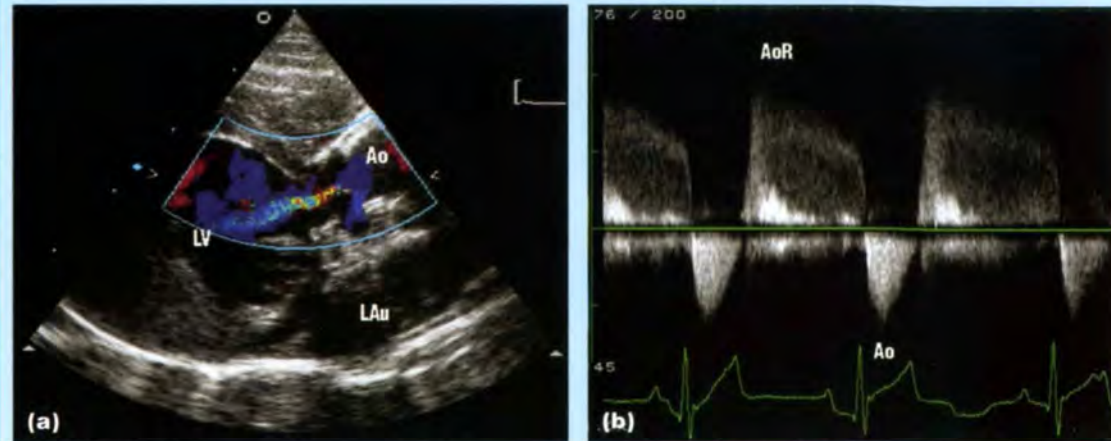
Aortic regurgitation

Acquisition of image

- Colour flow Doppler echocardiography is used to screen for the presence of AoR from the RPS five-chamber view, the right and left cranial long-axis views, examining the aortic valves, and the left apical three- and five-chamber views
- CW spectral Doppler recording of the diastolic AoR signal is obtained from the apical three- or five-chamber views, where alignment is optimized

Measurements and calculations

- The presence of AoR is suspicious in breeds of dogs susceptible to aortic stenosis. However, small amounts of AoR can be recognized in certain breeds such as Great Danes, without identified aortic valve pathology
- Measure peak AoR velocity
- Can determine the PG between the Ao and the LV in early diastole, provided alignment is good



(a) RPS long-axis five-chamber view in a Maine Coon cat with severe aortic stenosis. The aortic valves were also incompetent and the diastolic AoR jet is shown by colour flow mapping. **(b)** CW Doppler spectrum obtained from a left apical three-chamber view, optimizing alignment with the LVOT and Ao, in a German Shepherd Dog puppy with moderately severe subaortic stenosis. Aortic outflow is displayed below the baseline and AoR is displayed above the baseline.

2.16

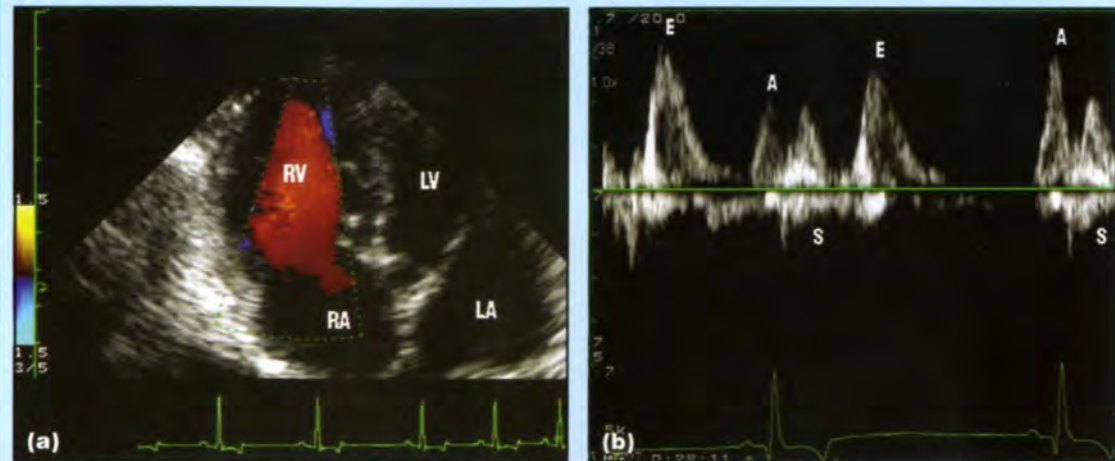
(continued) Spectral Doppler echocardiography. amv = Anterior mitral valve leaflet; Ao = Aorta; AoR = Aortic regurgitation; CW = Continuous wave; ET = Ejection time; HCM = Hypertrophic cardiomyopathy; HPRF = High pulse repetition frequency; LA = Left atrium; LAu = Left auricular appendage; LV = Left ventricle; LVOT = Left ventricular outflow tract; MPA = Main pulmonary artery; MR = Mitral regurgitation; PDA = Patent ductus arteriosus; PEP = Pre-ejection period; PG = Pressure gradient; PI = Pulmonic insufficiency; PW = Pulsed wave; RA = Right atrium; RV = Right ventricle; RVOT = Right ventricular outflow tract; SAM = Systolic anterior motion; TR = Tricuspid regurgitation; VSD = Ventricular septal defect; VTI = Velocity time integral. (continues)

Tricuspid inflow**Acquisition of image**

- The left apical four-chamber view is normally used to assess the tricuspid valve
- In some cases, the left cranial short-axis of the RVOT shows good tricuspid inflow
- Use colour flow Doppler to assess the valve
- Position the PW sample volume just within the leaflets of the tricuspid valve
- Record PW spectral Doppler of tricuspid inflow
- Note that there is normally considerable respiratory and heart rate variation in the tricuspid inflow pattern
- The ECG may be required to interpret the pattern: often a forward systolic wave, corresponding to right ventricular outflow, is recorded if the sample volume is within the RV side of the valve

Measurements and calculations

- Measure tricuspid valve E and A velocities
- The tricuspid E:A ratio can be calculated, but this will vary beat to beat due to the respiratory variation



(a) A left apical four-chamber view, optimized for alignment with tricuspid inflow (red). A PW Doppler sample volume is positioned at the tips of the tricuspid valve. **(b)** PW Doppler spectrum of tricuspid inflow. There is a peak corresponding to early passive RV filling, the E wave, and the A wave follows the P wave on the ECG, resulting in RV filling associated with atrial contraction. Note that in normal animals, the E and A wave velocities, and their ratio, show considerable respiratory variation. S shows some forward systolic flow towards the RVOT.

2.16 (continued) Spectral Doppler echocardiography. amv = Anterior mitral valve leaflet; Ao = Aorta; AoR = Aortic regurgitation; CW = Continuous wave; ET = Ejection time; HCM = Hypertrophic cardiomyopathy; HPRF = High pulse repetition frequency; LA = Left atrium; LAu = Left auricular appendage; LV = Left ventricle; LVOT = Left ventricular outflow tract; MPA = Main pulmonary artery; MR = Mitral regurgitation; PDA = Patent ductus arteriosus; PEP = Pre-ejection period; PG = Pressure gradient; PI = Pulmonic insufficiency; PW = Pulsed wave; RA = Right atrium; RV = Right ventricle; RVOT = Right ventricular outflow tract; SAM = Systolic anterior motion; TR = Tricuspid regurgitation; VSD = Ventricular septal defect; VTI = Velocity time integral. (continues) ▶

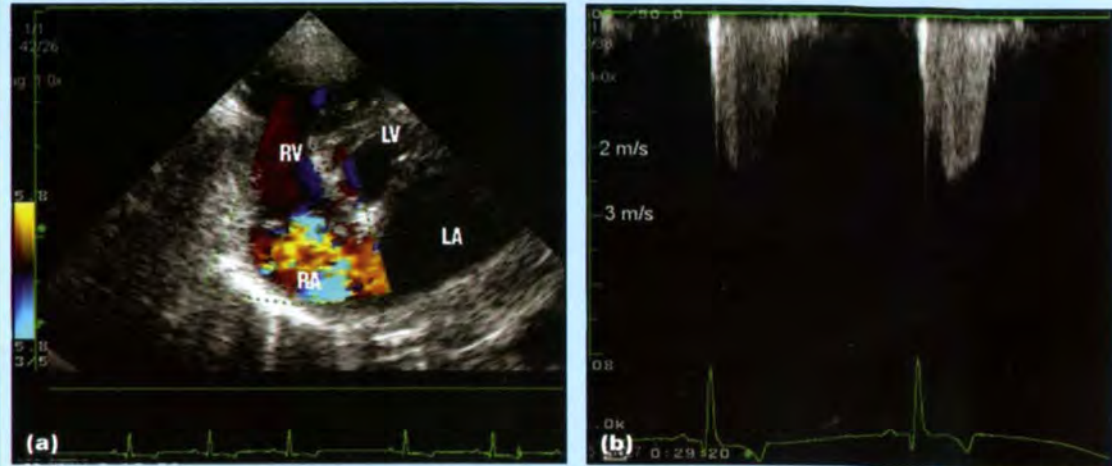
Tricuspid regurgitation

Acquisition of image

- Colour flow Doppler is used to assess the competence of the tricuspid valve from the RPS long-axis four-chamber view, the left apical four-chamber view and the left cranial short-axis view, optimizing the RA
- Use PW (or CW) spectral Doppler to align with the TR jet, and record the TR

Measurements and calculations

- Measure peak velocity of the TR jet (v)
- The PG between the RV and RA in systole can be calculated by the modified Bernoulli equation ($PG = 4v^2$) (normal <25 mmHg)
- In the absence of pulmonic stenosis, the derived RV pressure is approximately equal to pulmonary arterial systolic pressure (so the severity of pulmonary hypertension can be assessed non-invasively) (see Figure 7.124e, p. 151)



TR in a Cavalier King Charles Spaniel with myxomatous degenerative valvular disease. **(a)** Left apical four-chamber view optimized for alignment with the tricuspid valve. This systolic frame shows the severe TR by colour flow mapping. **(b)** CW spectral Doppler of the TR jet. Note that peak velocity of the TR jet is <2.5 m/s, which shows a normal PG between the RV and RA.

2.16

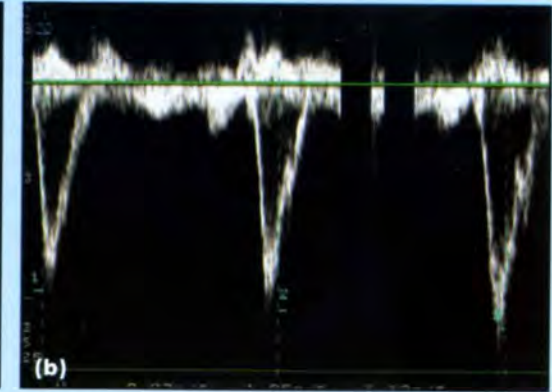
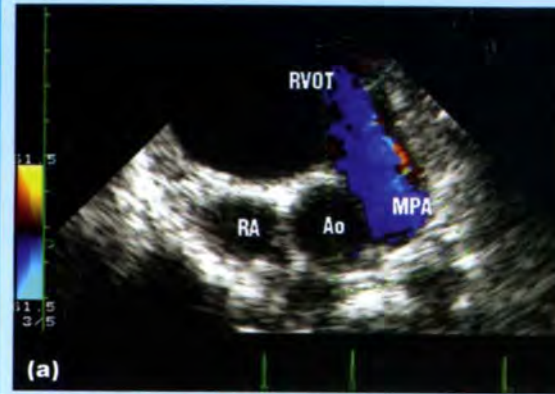
(continued) Spectral Doppler echocardiography. amv = Anterior mitral valve leaflet; Ao = Aorta; AoR = Aortic regurgitation; CW = Continuous wave; ET = Ejection time; HCM = Hypertrophic cardiomyopathy; HPRF = High pulse repetition frequency; LA = Left atrium; LAu = Left auricular appendage; LV = Left ventricle; LVOT = Left ventricular outflow tract; MPA = Main pulmonary artery; MR = Mitral regurgitation; PDA = Patent ductus arteriosus; PEP = Pre-ejection period; PG = Pressure gradient; PI = Pulmonic insufficiency; PW = Pulsed wave; RA = Right atrium; RV = Right ventricle; RVOT = Right ventricular outflow tract; SAM = Systolic anterior motion; TR = Tricuspid regurgitation; VSD = Ventricular septal defect; VTI = Velocity time integral. (continues)

Pulmonic outflow**Acquisition of image**

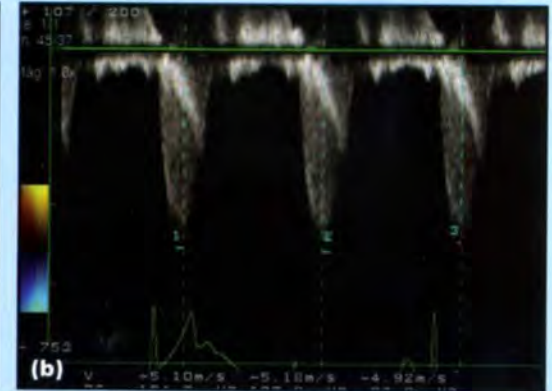
- Pulmonic valves are best imaged and assessed by colour flow Doppler from the right cranial short-axis view, optimizing the pulmonary trunk
- Note that the pulmonary trunk is difficult to become aligned with from this view, in most animals, as it wraps around the Ao
- Abnormalities of the RVOT are also best seen from this view (e.g. double-chambered RV)
- Some cats with HCM have dynamic RVOT obstruction, and the colour variance associated with this is best seen from the RPS cranial short-axis view. Spectral Doppler is guided from the colour flow signal to record the velocity of the RVOT
- Optimal alignment with pulmonary outflow is normally achieved from a left cranial short-axis view, optimizing the pulmonary trunk
- The sample volume is positioned just beyond the pulmonic valves within the pulmonary trunk, and PW spectral Doppler is recorded

Measurements and calculations

- Measure peak velocity of pulmonic flow
- The pulmonic outflow VTI is calculated by tracing around the pulmonic outflow spectrum
- The right ventricular stroke volume or cardiac output can be calculated, after determining the pulmonic cross-sectional area from the MPA diameter
- Shunt ratios, such as with a VSD, can be calculated
- Note that there should be no diastolic flow within the MPA. If diastolic flow is identified, it is important to search for a PDA



(a) LPS cranial view optimizing alignment with pulmonary outflow. (b) Positioning a PW Doppler sample volume just beyond the pulmonic valves allows recording of the pulmonic outflow.



RPS cranial short-axis views, optimizing the MPA in a Rottweiler with pulmonic stenosis. (a) Note the colour variance indicating high velocity and turbulent flow in the MPA. (b) CW spectral Doppler of the pulmonic outflow shows a mean peak velocity of 5.0 m/s, corresponding to a PG between the RV and MPA of 100 mmHg (modified Bernoulli equation), indicating severe pulmonic stenosis. Note that there is also a second, late accelerating peak of approximately half the peak velocity. This appearance on the spectrum is suggestive of concurrent dynamic infundibular obstruction.

2.16

(continued) Spectral Doppler echocardiography. amv = Anterior mitral valve leaflet; Ao = Aorta; AoR = Aortic regurgitation; CW = Continuous wave; ET = Ejection time; HCM = Hypertrophic cardiomyopathy; HPRF = High pulse repetition frequency; LA = Left atrium; LAu = Left auricular appendage; LV = Left ventricle; LVOT = Left ventricular outflow tract; MPA = Main pulmonary artery; MR = Mitral regurgitation; PDA = Patent ductus arteriosus; PEP = Pre-ejection period; PG = Pressure gradient; PI = Pulmonic insufficiency; PW = Pulsed wave; RA = Right atrium; RV = Right ventricle; RVOT = Right ventricular outflow tract; SAM = Systolic anterior motion; TR = Tricuspid regurgitation; VSD = Ventricular septal defect; VTI = Velocity time integral. (continues)

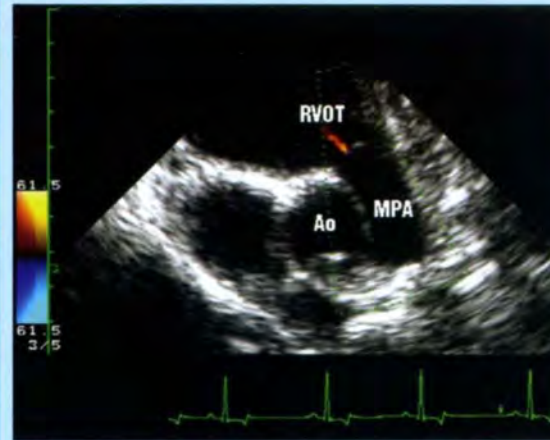
Pulmonic regurgitation/pulmonic insufficiency

Acquisition of image

- Pulmonic regurgitation is normally best identified from the RPS views using colour flow Doppler, as on the left side, the valve and RVOT are within the near field of the ultrasound image
- Note that it is normal physiologically to identify a trivial amount of pulmonic regurgitation. More significant amounts may be seen in association with pulmonic stenosis or pulmonary hypertension
- Position the PW sample volume within the PI jet in the RV, and record spectral Doppler

Measurements and calculations

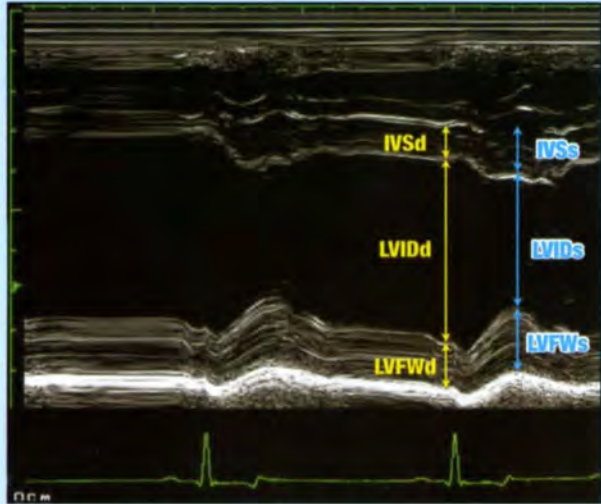
- Measure peak velocity of the PI jet (v)
- The modified Bernoulli equation is used to estimate the PG between the MPA and the RV in early diastole ($PG = 4v^2$)
- Thus, diastolic pulmonary arterial pressures can be estimated, which is useful to determine the severity of pulmonary hypertension, non-invasively
- The PI jet should gradually decelerate throughout diastole. Sudden deceleration, or termination prior to the end of diastole is consistent with pulmonary hypertension (see Figure 7.124f, p. 151)



LPS cranial view optimizing alignment with pulmonary outflow, showing a small jet of PI (red) in diastole. Such small jets are usually regarded as being physiological.

2.16

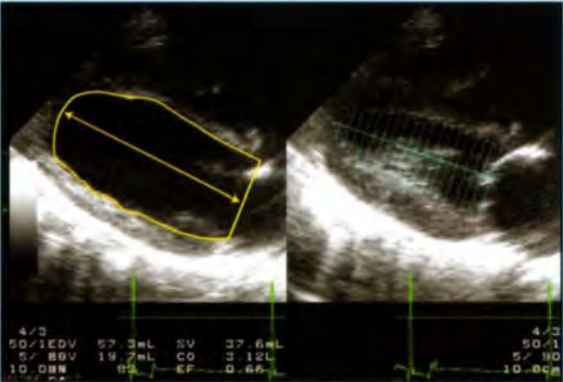
(continued) Spectral Doppler echocardiography. amv = Anterior mitral valve leaflet; Ao = Aorta; AoR = Aortic regurgitation; CW = Continuous wave; ET = Ejection time; HCM = Hypertrophic cardiomyopathy; HPRF = High pulse repetition frequency; LA = Left atrium; LAu = Left auricular appendage; LV = Left ventricle; LVOT = Left ventricular outflow tract; MPA = Main pulmonary artery; MR = Mitral regurgitation; PDA = Patent ductus arteriosus; PEP = Pre-ejection period; PG = Pressure gradient; PI = Pulmonic insufficiency; PW = Pulsed wave; RA = Right atrium; RV = Right ventricle; RVOT = Right ventricular outflow tract; SAM = Systolic anterior motion; TR = Tricuspid regurgitation; VSD = Ventricular septal defect; VTI = Velocity time integral.

Systolic function parameters	Calculations	Comments and limitations
M-mode assessment of systolic function		
Fractional shortening (FS) (%)	$FS = [(LVIDd - LVIDs)/LVIDd] \times 100\%$	 <p>Measurement of the LV M-mode. Diastolic measurements are taken at the end of diastole, at the start of the ECG QRS complex. Systolic measurements are taken at the nadir of septal motion (or the smallest LV cavity), which usually corresponds to the end of the T wave. Note the 'leading edge to leading edge' method of measurement: the proximal endocardium is included in each measurement, but not the distal endocardium. Thus, each measurement is not influenced by the effect of gain settings on endocardium thickness.</p> <ul style="list-style-type: none"> Note: this relies on normal wall motion It is a one-dimensional measurement It will give a falsely favourable impression of contractility in the presence of reduced afterload (e.g. severe MR)
Ejection fraction (EF) (%)	$EF = [(EDV - ESV)/EDV] \times 100\%$ Teicholz formula for calculating EDV (ESV) from LV M-mode dimensions: $EDV = [7/(2.4 + LVIDd)] \times LVIDd^3$ (for ESV, substitute LVIDd for LVIDs)	<ul style="list-style-type: none"> There are various formulae to derive LV volumes from M-mode dimensions, and therefore EF The Teicholz formula is usually more accurate than the others However, there is no advantage to these compared with M-mode when a single dimensional method is being used, and volumes derived are very inaccurate in a dilated, rounded LV chamber
Percentage thickening of the IVS or LVFW (%th IVS, %th LVFW)	$\%th\ IVS = (IVSs - IVSd)/IVSd \times 100\%$ $\%th\ LVFW = (LVFWs - LVFWd)/LVFWd \times 100\%$	

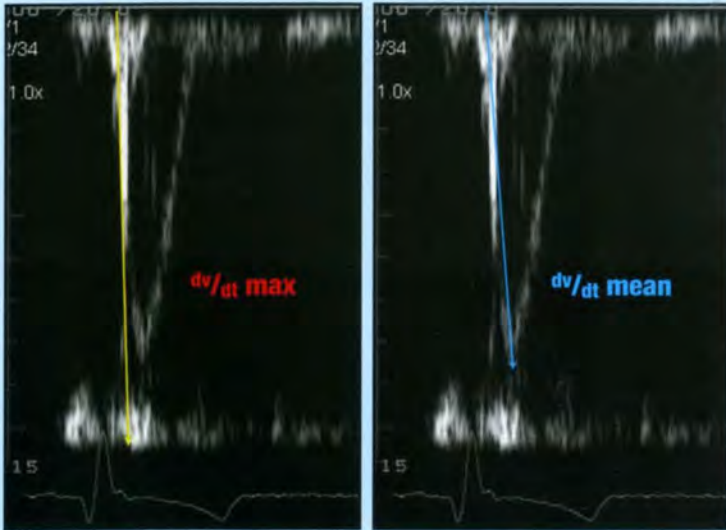
2.17 Assessment of systolic function. Ao = Aorta; Ao csa = Aortic cross-sectional area; CO = Cardiac output; CW = Continuous wave; DCM = Dilated cardiomyopathy; EDV = End-diastolic volume; EPSS = E point to septal separation; ESV = End-systolic volume; ET = Ejection time; HR = Heart rate; IVS = Interventricular septum; IVSd = Interventricular septal thickness in diastole; IVSs = Interventricular septal thickness in systole; LA = Left atrium; LV = Left ventricle; LVFW = Left ventricular free wall; LVFWd = Left ventricular free wall in diastole; LVFWs = Left ventricular free wall in systole; LVIDd = Left ventricular internal dimension in diastole; LVIDs = Left ventricular internal dimension in systole; MR = Mitral regurgitation; PEP = Pre-ejection period; PG = Pressure gradient; PW = Pulsed wave; SV = Stroke volume; VSD = Ventricular septal defect. (continues) ▶

Systolic function parameters	Calculations	Comments and limitations
M-mode assessment of systolic function continued		
Velocity of circumferential fibre shortening (Vcf)	$Vcf = FS/ET$ (FS as a fraction, not a percentage)	<ul style="list-style-type: none"> Units: circumferences/second This is another systolic time interval
Mitral M-mode EPSS <ul style="list-style-type: none"> Measure mitral E point, up to endocardium of the IVS 		<ul style="list-style-type: none"> Reduced CO, and therefore opening of the mitral valve leaflets, is one of the causes of increased EPSS in animals with impaired systolic function <div data-bbox="1048 427 1639 933" data-label="Image"> </div> <p>Measurement of the mitral EPSS (on anterior leaflet of mitral valve). This is simply the vertical distance between the two points. The EPSS should be <7 mm in any dog breed.</p>
Assessment of aortic root excursion		<ul style="list-style-type: none"> Subjective assessment of degree of anterior aortic root excursion during systole Animals with impaired contractility have flat aortic root motion (see Figure 2.15)
Systolic time intervals from aortic valve M-mode: <ul style="list-style-type: none"> Measure the PEP Measure the ET Can identify premature closure of aortic valves in some patients with severe systolic impairment 	Calculate the PEP:ET ratio	<ul style="list-style-type: none"> Normal PEP:ET ratio is 0.25–0.35 Systolic dysfunction evident when PEP:ET >0.4 (see Figure 2.15)

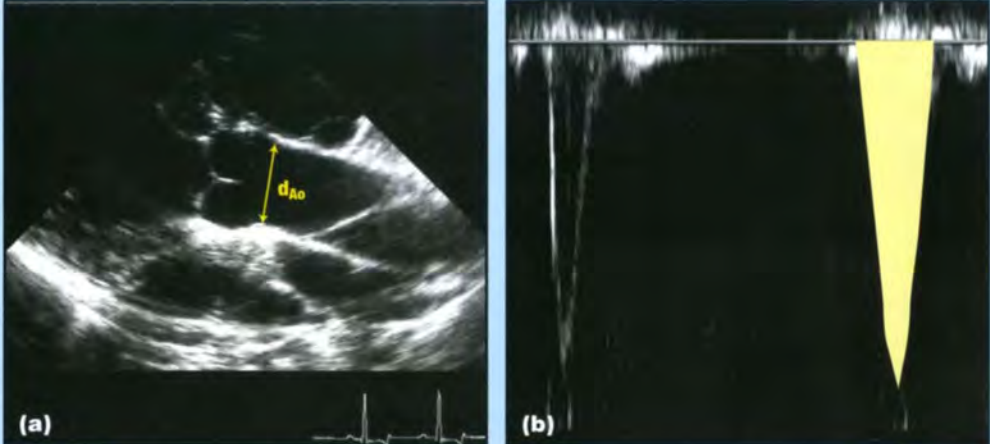
2.17 (continued) Assessment of systolic function. Ao = Aorta; Ao csa = Aortic cross-sectional area; CO = Cardiac output; CW = Continuous wave; DCM = Dilated cardiomyopathy; EDV = End-diastolic volume; EPSS = E point to septal separation; ESV = End-systolic volume; ET = Ejection time; HR = Heart rate; IVS = Interventricular septum; IVSd = Interventricular septal thickness in diastole; IVSs = Interventricular septal thickness in systole; LA = Left atrium; LV = Left ventricle; LVFW = Left ventricular free wall; LVFWd = Left ventricular free wall in diastole; LVFWs = Left ventricular free wall in systole; LVIDd = Left ventricular internal dimension in diastole; LVIDs = Left ventricular internal dimension in systole; MR = Mitral regurgitation; PEP = Pre-ejection period; PG = Pressure gradient; PW = Pulsed wave; SV = Stroke volume; VSD = Ventricular septal defect. (continues)

Systolic function parameters	Calculations	Comments and limitations
M-mode assessment of systolic function continued		
<p>Mitral annulus motion (MAM):</p> <ul style="list-style-type: none"> This is recorded from a vertical heart in a four- and a two-chamber view from the left apical windows (thus, four different points of the mitral annulus are assessed) The M-mode cursor is positioned at the mitral annulus, M-mode recorded and the maximum excursion from diastole to systole measured This corresponds to apicobasilar contractility of the longitudinal fibres 	Calculate the average motion, from the two or four points recorded	<ul style="list-style-type: none"> Need to be perpendicular to the mitral annulus Sometimes the lateral/posterior annulus is difficult to image due to lung interference Note if there is a wall motion abnormality at one of these points Normal mean MAM is >10 cm in medium and large breeds of dogs (see Figure 2.15)
2D assessment of LV systolic function		
Ejection fraction (EF) (%)	$EF = [(EDV - ESV)/EDV] \times 100\%$ <ul style="list-style-type: none"> Simpson's rule is the preferred formula to calculate the LV volumes in systole (ESV) and diastole (EDV), using the software on the ultrasound machine The LV length is divided into 20 discs. From the volume of each disc, the sum of discs corresponds to the LV volume The modified Simpson's rule only requires one plane of the LV (four-chamber view) The full Simpson's rule, as used for humans, requires the apical four- and two-chamber views (two orthogonal planes through the LV) 	 <p>2D-derived left ventricular volumes include Simpson's rule. These images are obtained from a Boxer with good systolic function and normal LV geometry. There is an end-diastolic frame on the left, and an end-systolic frame on the right. The yellow line shows the process of drawing around the endocardial border of the LV, closing at the mitral annulus. The length of the ventricle is then measured. For Simpson's rule, the software of the ultrasound machine divides the length into 20 discs. From the volume of each disc, the sum of discs gives the LV volume. The ultrasound machine software has done this on the right. Note that papillary muscles are just ignored if the image acquisition has failed to avoid them. In this example, the EDV is 57.3 ml, ESV is 19.7 ml and the EF is calculated at 0.66 (66%). Note the software has also calculated SV and CO.</p> <ul style="list-style-type: none"> There are several formulae for deriving LV volumes from the 2D images For all of these it is very important to optimize the LV length and area; a foreshortened LV will lead to marked underestimation of volumes In dogs, the RPS long-axis four-chamber view normally gives the maximum volumes, rather than the left apical view (as used in humans) Simpson's rule is the most accurate method of determining LV volumes, as it is independent of geometrical assumptions or wall motion abnormalities. Note: in conditions of reduced afterload, such as severe MR, the EF does not reflect contractility (see also Figure 7.97, p. 137)

2.17 (continued) Assessment of systolic function. Ao = Aorta; Ao csa = Aortic cross-sectional area; CO = Cardiac output; CW = Continuous wave; DCM = Dilated cardiomyopathy; EDV = End-diastolic volume; EPSS = E point to septal separation; ESV = End-systolic volume; ET = Ejection time; HR = Heart rate; IVS = Interventricular septum; IVSd = Interventricular septal thickness in diastole; IVSs = Interventricular septal thickness in systole; LA = Left atrium; LV = Left ventricle; LVFW = Left ventricular free wall; LVFWd = Left ventricular free wall in diastole; LVFWs = Left ventricular free wall in systole; LVIDd = Left ventricular internal dimension in diastole; LVIDs = Left ventricular internal dimension in systole; MR = Mitral regurgitation; PEP = Pre-ejection period; PG = Pressure gradient; PW = Pulsed wave; SV = Stroke volume; VSD = Ventricular septal defect. (continues)

Systolic function parameters	Calculations	Comments and limitations
2D assessment of LV systolic function continued		
End-systolic volume index (ESVI)	<ul style="list-style-type: none"> The ESV is determined, e.g. by Simpson's rule The animal's bodyweight is converted to body surface area in m² (see Appendix) Calculate the ESVI (ml/m²) 	<ul style="list-style-type: none"> Dogs with normal systolic function have an ESVI of <30 ml/m². Values significantly above this indicate impaired systolic function This is useful in the setting of reduced afterload such as severe MR, where FS and EF cannot be used to indicate contractility (see also Figure 7.97b, p. 137)
Doppler assessment of LV systolic function		
From aortic outflow: Peak aortic velocity: <ul style="list-style-type: none"> Measure peak velocity of aortic flow 		<ul style="list-style-type: none"> In the absence of aortic stenosis, peak velocity of aortic outflow correlates with systolic function (see Figure 2.16)
Aortic flow acceleration: <ul style="list-style-type: none"> Mean acceleration (dv/dt mean) is the slope from onset of aortic flow to peak velocity Maximum acceleration (dv/dt max) is the initial, steepest part of the slope 		<ul style="list-style-type: none"> Difficult to accurately measure, especially if very fast spectral Doppler sweep speeds are not available (>100 mm/s). This results in repeatability issues
		 <p>From a PW Doppler spectrum of aortic outflow, the steepest slope (left image) can be measured (dv/dt max). This slope is the peak acceleration of aortic outflow. It is easier to record the mean slope of aortic acceleration (dv/dt mean), with a line from onset of flow to peak velocity (right image). Both these measurements are correlated with LV systolic function provided there is no aortic stenosis.</p>

2.17 (continued) Assessment of systolic function. Ao = Aorta; Ao csa = Aortic cross-sectional area; CO = Cardiac output; CW = Continuous wave; DCM = Dilated cardiomyopathy; EDV = End-diastolic volume; EPSS = E point to septal separation; ESV = End-systolic volume; ET = Ejection time; HR = Heart rate; IVS = Interventricular septum; IVSd = Interventricular septal thickness in diastole; IVSs = Interventricular septal thickness in systole; LA = Left atrium; LV = Left ventricle; LVFW = Left ventricular free wall; LVFWd = Left ventricular free wall in diastole; LVFWs = Left ventricular free wall in systole; LVIDd = Left ventricular internal dimension in diastole; LVIDs = Left ventricular internal dimension in systole; MR = Mitral regurgitation; PEP = Pre-ejection period; PG = Pressure gradient; PW = Pulsed wave; SV = Stroke volume; VSD = Ventricular septal defect. (continues)

Systolic function parameters	Calculations	Comments and limitations
Doppler assessment of LV systolic function		
<p>From aortic outflow: <i>continued</i> Velocity time integral (VTI):</p> <ul style="list-style-type: none"> The aortic outflow spectrum is traced, and the area under its curve determined = VTI 	<p>Calculation of forward SV and CO:</p> <ul style="list-style-type: none"> $Ao\ csa = \pi (d/2)^2$ Forward SV = Ao csa x aortic VTI CO = SV x HR <p>Where, Ao csa is determined by measuring the aortic diameter (d) in systole (at valve level, or at sinotubular junction)</p> <p>HR is calculated from the ECG: HR = 60/R-R interval</p>	<ul style="list-style-type: none"> The VTI is also known as the stroke distance (units = cm)  <p>(a) RPS cranial long-axis view of the Ao, so that aortic diameter (d_{Ao}) can be measured. (b) PW spectral Doppler of aortic outflow. The area under the curve of a spectrum gives the VTI. Thus, forward SV can be calculated as shown.</p> <ul style="list-style-type: none"> In cases of severe MR, forward SV can be subtracted from total LV SV (e.g. from Simpson's rule: SV = EDV – ESV) to calculate MR volume and therefore, regurgitant fraction In cases of a shunt, such as a VSD, the pulmonic to systemic flow quotient can be calculated, where pulmonic outflow is calculated in a similar way, using pulmonic VTI and cross-sectional area of the pulmonic annulus
<p>Systolic time intervals:</p> <ul style="list-style-type: none"> The PEP is the start of the ECG QRS complex to the onset of aortic flow The ET is the duration of aortic flow 	<p>Calculate the PEP:ET ratio</p>	<ul style="list-style-type: none"> The PEP:ET ratio is an index of contractility, relatively independent of HR and load Normal ratio is 0.25–0.35 Values >0.4 suggest systolic dysfunction Check that values are similar to aortic M-mode-derived systolic time intervals before substituting. Some ultrasound machines may have a time delay in displaying spectral Doppler signals after the ECG, leading to a falsely high PEP and a large PEP:ET ratio (see Figure 2.16)

2.17 (continued) Assessment of systolic function. Ao = Aorta; Ao csa = Aortic cross-sectional area; CO = Cardiac output; CW = Continuous wave; DCM = Dilated cardiomyopathy; EDV = End-diastolic volume; EPSS = E point to septal separation; ESV = End-systolic volume; ET = Ejection time; HR = Heart rate; IVS = Interventricular septum; IVSd = Interventricular septal thickness in diastole; IVSs = Interventricular septal thickness in systole; LA = Left atrium; LV = Left ventricle; LVFW = Left ventricular free wall; LVFWd = Left ventricular free wall in diastole; LVFWs = Left ventricular free wall in systole; LVIDD = Left ventricular internal dimension in diastole; LVIDS = Left ventricular internal dimension in systole; MR = Mitral regurgitation; PEP = Pre-ejection period; PG = Pressure gradient; PW = Pulsed wave; SV = Stroke volume; VSD = Ventricular septal defect. (continues)

Systolic function parameters	Calculations	Comments and limitations
Doppler assessment of LV systolic function		
From mitral regurgitant jet: <ul style="list-style-type: none"> Measure peak velocity of MR jet 		<ul style="list-style-type: none"> MR jet velocity reflects the systolic PG between the LV and LA Where LA pressures are high (left heart failure) and/or in the presence of systolic impairment, this velocity will be reduced In dogs with DCM, MR velocity of <4/s is a negative prognostic indicator for survival
LV dP/dt from CW Doppler trace of MR jet: <ul style="list-style-type: none"> Good quality MR spectral Doppler signals are acquired They must have a clean acceleration slope 	<ul style="list-style-type: none"> From the acceleration slope of a MR spectral Doppler signal, two points are selected on this slope, e.g. at 1 m/s and at 3 m/s The modified Bernoulli equation is used to calculate the instantaneous PGs ($PG = 4v^2$) at these two points (i.e. 1 m/s = 4 mmHg, and 3 m/s = 36 mmHg) The pressure difference between them is calculated (in this example, $dP = 32$ mmHg) The time between the two points is measured (= dt) dP/dt can therefore be calculated 	 <ul style="list-style-type: none"> This is reported to correlate well with the gold standard of contractility, the catheterization-derived dP/dt It is difficult to measure short time durations accurately, unless the ultrasound machine is able to display spectral images at a very high sweep speed (>100 mm/s) <p>From the CW spectral Doppler of a clean MR jet, dP/dt can be calculated as shown. Note that the peak velocity is about 5.5 m/s from this dog with myxomatous degenerative mitral valve disease and adequate systolic function.</p>

2.17

(continued) Assessment of systolic function. Ao = Aorta; Ao csa = Aortic cross-sectional area; CO = Cardiac output; CW = Continuous wave; DCM = Dilated cardiomyopathy; EDV = End-diastolic volume; EPSS = E point to septal separation; ESV = End-systolic volume; ET = Ejection time; HR = Heart rate; IVS = Interventricular septum; IVSd = Interventricular septal thickness in diastole; IVSs = Interventricular septal thickness in systole; LA = Left atrium; LV = Left ventricle; LVFW = Left ventricular free wall; LVFWd = Left ventricular free wall in diastole; LVFWs = Left ventricular free wall in systole; LVIDd = Left ventricular internal dimension in diastole; LVIDs = Left ventricular internal dimension in systole; MR = Mitral regurgitation; PEP = Pre-ejection period; PG = Pressure gradient; PW = Pulsed wave; SV = Stroke volume; VSD = Ventricular septal defect.

Diastolic function parameter	Measurements and calculations	Comments and limitations
PW Doppler measurement of isovolumic relaxation time		
<ul style="list-style-type: none"> From an apical five-chamber view, use colour Doppler to show mitral inflow (red) and left ventricular outflow (blue) Position a large sample volume so both mitral inflow (above the baseline) and left ventricular outflow (below the baseline) are recorded at the maximum sweep speed possible; obtain PW signals It is useful if valve clicks are acquired on the PW signal to assist timing, but not essential. A CW spectral Doppler signal may assist acquisition of valve clicks 	<ul style="list-style-type: none"> Measure the time from end of left ventricular outflow to onset of mitral flow; this is the IVRT The measurement is affected by heart rate; the corresponding R-R interval should be recorded so measurements can be corrected for heart rate if appropriate 	<ul style="list-style-type: none"> It is difficult to measure small time durations accurately and repeatably IVRT should not be significantly influenced by respiration (if it increases in inspiration and decreases with expiration, constrictive pericardial disease may be suspected). For examples of measurement of IVRT in different disease states, see also Figure 7.112 (p. 144)
PW Doppler assessment of mitral inflow		
<ul style="list-style-type: none"> Mitral inflow E and A waves are recorded 	<ul style="list-style-type: none"> Measure peak velocity of mitral E and A waves The E wave deceleration time can also be measured (time from peak E until baseline) Mitral E wave and A wave durations can be measured The pressure half-time can be calculated using ultrasound machine software; this may be prolonged in the presence of mitral stenosis (uncommon) 	<ul style="list-style-type: none"> The ratio of E:A wave velocities should be >1 but <2 Ageing influences this ratio and decreases the E:A ratio A pattern of <i>abnormal relaxation</i> is identified by: <ol style="list-style-type: none"> E:A ratio <1 (i.e. increased dependence on atrial contraction for ventricular filling) Prolonged E wave deceleration time Prolonged IVRT <div style="display: flex; align-items: flex-start;">  <div style="margin-left: 10px;"> <p>Mitral inflow pattern from a Rottweiler with marked left ventricular concentric hypertrophy due to severe aortic stenosis. Note the A wave velocity exceeds the E wave (E:A reversal) and there is a long E wave deceleration time. These features are associated with abnormal relaxation of the LV.</p> </div> </div>

2.18 Assessment of diastolic function. AF = Atrial fibrillation; CW = Continuous wave; ET = Ejection time; HCM = Hypertrophic cardiomyopathy; HPRF = High pulse repetition frequency spectral Doppler ultrasonography; IMP = Index of myocardial performance; IVCT = Isovolumic contraction time; IVRT = Isovolumic relaxation time; LA = Left atrium; LPRF = Low pulse repetition frequency spectral Doppler ultrasonography; LV = Left ventricle; MR = Mitral regurgitation; MV = Mitral valve; MVC = Mitral valve closure; MVO = Mitral valve opening; PG = Pressure gradient; PVF = Pulmonary venous flow; PW = Pulsed wave; RV = Right ventricle; Vp = Propagation velocity of early filling; VTI = Velocity time integral. (continues)

Diastolic function parameter	Measurements and calculations	Comments and limitations
PW Doppler assessment of mitral inflow continued		
		<ul style="list-style-type: none"> As diseases such as feline HCM progress, and the LA pressure increases, then the early diastolic PG between the LA and LV is increased. Therefore, E wave velocities increase again, giving <i>pseudonormalization</i> of the mitral inflow pattern (E:A >1). <div data-bbox="1120 359 1646 949"> <p>The top panel shows a mitral inflow Doppler spectrum with a large E wave and a smaller A wave. The bottom panel shows a PVF Doppler spectrum with a large S wave and a smaller D wave, and a prominent Ar wave. Both panels include velocity scales and timing markers.</p> </div> <p>Cat in severe left-sided congestive heart failure due to end-stage HCM. Top: Mitral inflow with the normal E:A ratio, as E velocity > A velocity (pseudonormalization). However, there is a prolonged E wave deceleration time. Bottom: The PVF pattern confirms abnormal LV relaxation, with high Ar wave and S wave > D wave. Note the confirmation of elevated filling pressures as PVF Ar wave duration is > mitral A wave duration (see below).</p> <ul style="list-style-type: none"> <i>Restrictive filling</i> is due to increased LA pressures and a stiff, poorly compliant LV. It is identified by: <ol style="list-style-type: none"> E:A ratio > 2 Brief duration E wave, with short deceleration time Short IVRT In tachycardic animals, such as most cats in heart failure, or in animals with AF, mitral inflow is not useful for identifying diastolic dysfunction A vagal manoeuvre may separate E and A waves enough to separate them (e.g. gentle pressure on the nose in a cat). For more examples in feline myocardial disease, see Figures 7.110 and 7.111, p. 144

2.18 (continued) Assessment of diastolic function. AF = Atrial fibrillation; CW = Continuous wave; ET = Ejection time; HCM = Hypertrophic cardiomyopathy; HPRF = High pulse repetition frequency spectral Doppler ultrasonography; IMP = Index of myocardial performance; IVCT = Isovolumic contraction time; IVRT = Isovolumic relaxation time; LA = Left atrium; LPRF = Low pulse repetition frequency spectral Doppler ultrasonography; LV = Left ventricle; MR = Mitral regurgitation; MV = Mitral valve; MVC = Mitral valve closure; MVO = Mitral valve opening; PG = Pressure gradient; PVF = Pulmonary venous flow; PW = Pulsed wave; RV = Right ventricle; Vp = Propagation velocity of early filling; VTl = Velocity time integral. (continues)

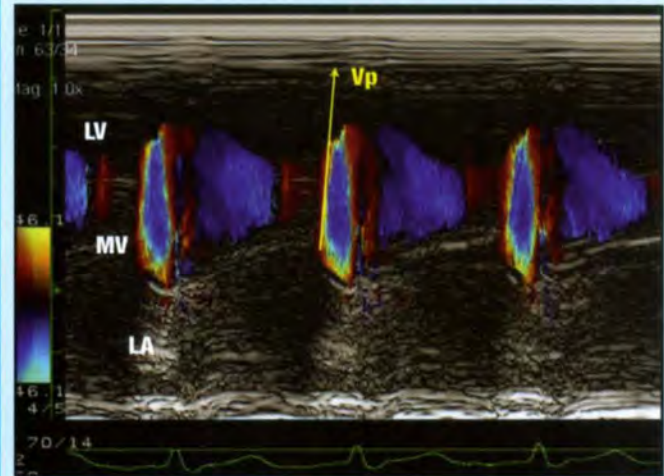
Diastolic function parameter	Measurements and calculations	Comments and limitations
PW Doppler assessment of pulmonary venous flow		
<ul style="list-style-type: none"> From an apical four-chamber view, a sample volume is positioned in one of the pulmonary veins (this is easier in animals with left-sided failure, as the veins are dilated) Ensuring LPRF is used (not HPRF), PVF is recorded. There are three major components to PVF: <ol style="list-style-type: none"> The atrial reversal wave (Ar). During atrial systole, retrograde flow in the pulmonary veins is detected following the P wave of the ECG Following atrial relaxation, some early forward flow is recorded (Se). During ventricular systole, the mitral annulus moves apically, and the main systolic (SI) PVF wave results. Although partial separation of Se and SI may be identified, in most animals, the peak S velocity is measured, and a single peak is usually recorded During diastole, the LA is merely a conduit between the pulmonary veins and the LV as it relaxes; this gives the diastolic (D) forward wave of the PVF pattern 	<ul style="list-style-type: none"> Measure peak velocity of S, D and Ar Measure the duration of Ar The durations of S and D can be measured D deceleration time can be measured The relevant R-R intervals should be measured as measurements will be influenced by heart rate The VTIs of S and D can be calculated by tracing the waveforms 	<ul style="list-style-type: none"> In normal animals, velocity $S < D$ In ageing animals, D may decrease, and reversal may be identified In <i>abnormal relaxation</i>, the S:D ratio is >1, and there is often a large Ar wave In a <i>restrictive filling pattern</i>, S velocity may be low, and D high but rapidly decelerating Ar may be normal or reduced (depending on atrial function) The mitral A wave duration may be compared with the PVF Ar wave In normal animals, A duration is greater than Ar duration In situations of elevated filling pressures, duration of Ar is greater than A (see above). For examples in feline myocardial disease, see Figure 7.113 (p. 145)
Diastolic function from mitral regurgitant jet		
<ul style="list-style-type: none"> LV $-dP/dt$ from CW Doppler trace of MR jet Good quality MR CW spectral Doppler signals are obtained 	<ul style="list-style-type: none"> From the deceleration slope of the signal, two points are identified, e.g. at 3 m/s and 1 m/s, corresponding to instantaneous LV:LA PGs at these two points of 36 mmHg and 4 mmHg. The pressure difference is therefore 32 mmHg ($= -dP$) The time between the two points is measured ($= dt$) $-dP/dt$ is then calculated 	<ul style="list-style-type: none"> No data of reference values available so far in the veterinary literature It is difficult to measure short time durations accurately, unless the ultrasound machine is able to display spectral images at a very high sweep speed (>100 mm/s)



A MR jet from a cat with HCM. If there is a clean deceleration slope, $-dP/dt$ can be calculated, as shown.

2.18 (continued) Assessment of diastolic function. AF = Atrial fibrillation; CW = Continuous wave; ET = Ejection time; HCM = Hypertrophic cardiomyopathy; HPRF = High pulse repetition frequency spectral Doppler ultrasonography; IMP = Index of myocardial performance; IVCT = Isovolumic contraction time; IVRT = Isovolumic relaxation time; LA = Left atrium; LPRF = Low pulse repetition frequency spectral Doppler ultrasonography; LV = Left ventricle; MR = Mitral regurgitation; MV = Mitral valve; MVC = Mitral valve closure; MVO = Mitral valve opening; PG = Pressure gradient; PVF = Pulmonary venous flow; PW = Pulsed wave; RV = Right ventricle; Vp = Propagation velocity of early filling; VTi = Velocity time integral. (continues) ▶

Diastolic function parameter	Measurements and calculations	Comments and limitations
Velocity of propagation of mitral inflow from mitral annulus towards the LV apex		
<ul style="list-style-type: none"> From the apical four-chamber view, colour flow Doppler is used to assess the column of blood corresponding to mitral inflow to the LV apex The colour Nyquist limit and/or baseline are altered so that there is a central aliased blue core in this colour signal The M-mode cursor is positioned within this column, aligning the M-mode cursor with the flow M-mode at maximum sweep speed is recorded. The distance this column of blood moves is plotted against time. This corresponds to the mitral inflow E wave as it courses towards the LV apex 	<ul style="list-style-type: none"> The slope of the wave front or the aliased core of this column is the velocity it moves from mitral annulus to the apex; this can be measured from M-mode software 	<ul style="list-style-type: none"> Normal (in cats) is about 64 cm/s The steeper the slope, the better the diastolic function. Lower velocities indicate impaired diastolic function (without separating abnormal relaxation from restrictive physiologies) The ratio of mitral E wave velocity to Vp correlates with LV end-diastolic pressures

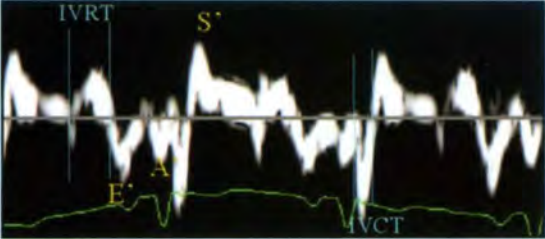
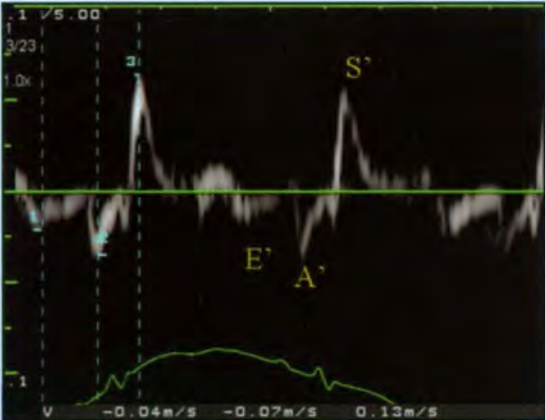


Colour M-mode taken from a left apical four-chamber view, with a colour sample volume from the MV towards the LV apex. The M-mode cursor is positioned within this column of blood of mitral inflow. M-mode shows the column of blood corresponding to early filling moving from the mitral annulus to the LV apex. The slope of this line (Vp) reflects the diastolic properties of the LV.

2.18 (continued) Assessment of diastolic function. AF = Atrial fibrillation; CW = Continuous wave; ET = Ejection time; HCM = Hypertrophic cardiomyopathy; HPRF = High pulse repetition frequency spectral Doppler ultrasonography; IMP = Index of myocardial performance; IVCT = Isovolumic contraction time; IVRT = Isovolumic relaxation time; LA = Left atrium; LPRF = Low pulse repetition frequency spectral Doppler ultrasonography; LV = Left ventricle; MR = Mitral regurgitation; MV = Mitral valve; MVC = Mitral valve closure; MVO = Mitral valve opening; PG = Pressure gradient; PVF = Pulmonary venous flow; PW = Pulsed wave; RV = Right ventricle; Vp = Propagation velocity of early filling; VTI = Velocity time integral. (continues)

Diastolic function parameter	Measurements and calculations	Comments and limitations
Index of myocardial performance (the Tei index)		
<ul style="list-style-type: none"> Mitral inflow is recorded, so that the time from mitral valve closure to opening is measured Aortic outflow is recorded to measure the ET 	<ul style="list-style-type: none"> $IMP = (IVCT + IVRT)/ET$ The time from mitral valve closure to mitral valve opening (MVC-MVO) = $IVCT + ET + IVRT$ To determine $IVCT + IVRT$, subtract ET from MVC-MVO IMP can then be calculated 	<ul style="list-style-type: none"> This is a combined index of systolic and diastolic function It could also be applied to the RV, from recordings of tricuspid inflow and pulmonic outflow <div data-bbox="1099 379 1624 1265"> <p>Top: Normal mitral inflow pattern. The time from MVC (end of A wave) to MVO (start of E wave) is measured. This represents $IVCT + ET + IVRT$.</p> <p>Bottom: ET is measured from aortic outflow. This can be subtracted from the MVC-MVO time. The IMP can then be calculated.</p> </div>

2.18 (continued) Assessment of diastolic function. AF = Atrial fibrillation; CW = Continuous wave; ET = Ejection time; HCM = Hypertrophic cardiomyopathy; HPRF = High pulse repetition frequency spectral Doppler ultrasonography; IMP = Index of myocardial performance; IVCT = Isovolumic contraction time; IVRT = Isovolumic relaxation time; LA = Left atrium; LPRF = Low pulse repetition frequency spectral Doppler ultrasonography; LV = Left ventricle; MR = Mitral regurgitation; MV = Mitral valve; MVC = Mitral valve closure; MVO = Mitral valve opening; PG = Pressure gradient; PVF = Pulmonary venous flow; PW = Pulsed wave; RV = Right ventricle; Vp = Propagation velocity of early filling; VTI = Velocity time integral.

Acquisition of image	Interpretation of image	Measurements and calculations
<ul style="list-style-type: none"> The left apical four-chamber view is acquired, ensuring the heart is as parallel with the ultrasound beam as possible. Longitudinal fibres at both the septal and lateral mitral annulus can be interrogated Position the sample volume at the annulus Change to pw-TDI Doppler, recording at maximum sweep speed 	<ul style="list-style-type: none"> There are three major phases to the longitudinal fibre motion: <ol style="list-style-type: none"> In systole, the longitudinal fibres contract from the mitral annulus towards the apex, giving an S' wave (the velocity of which is a parameter of systolic function) During early diastole, the active relaxation process of the longitudinal fibres gives the E' wave Following atrial contraction, the resulting changes in the longitudinal fibres give the A' wave There are also pw-TDI signals corresponding to IVC and IVR. These are biphasic, brief duration shifts in opposing directions from the preceding and following major waves; IVC is therefore positive/negative preceding the S' wave and IVR is negative/positive following S' and preceding E'. IVCT and IVRT can also be measured 	<ul style="list-style-type: none"> The S' wave velocity can be measured, which correlates with systolic function The E' and A' wave velocities can be measured  <p>Septal mitral annulus in a normal cat, positioned from the left apical four-chamber view. The velocities of the longitudinal fibres, resulting in apicobasilar movement of the heart are recorded. S' represents movement of the annulus towards the apex. E' indicates active relaxation (which will result in early LV filling). The A' reflects movements related to atrial contraction. The IVC and IVR phases are also evident.</p> <ul style="list-style-type: none"> The E':A' ratio may be <1 when there is abnormal relaxation, more likely to be identified in the septum than the LVFW. (This parameter is less influenced by loading conditions than the mitral E:A ratio)  <p>Lateral mitral annulus with pre-symptomatic HCM (detected during investigation of a heart murmur). There is evidence of abnormal relaxation, since the A' velocity (measurement 2) exceeds the E' velocity (measurement 1).</p> <ul style="list-style-type: none"> The ratio of mitral E wave velocity to E' velocity is relatively load-independent and corresponds to filling pressures. The normal ratio is about 8 in cats and humans, and a ratio above 15 predicts elevated filling pressures

2.19 Pulsed wave tissue Doppler imaging assessment of myocardial function. HCM = Hypertrophic cardiomyopathy; IVC = Isovolumic contraction; IVCT = Isovolumic contraction time; IVR = Isovolumic relaxation; IVRT = Isovolumic relaxation time; LV = Left ventricle; LVFW = Left ventricular free wall; pw-TDI = Pulsed wave tissue Doppler imaging.

PW Doppler assessment of diastolic function from isovolumic relaxation time (IVRT), mitral inflow and pulmonary venous flow (PVF) is shown in Figure 2.18. Additional parameters of diastolic function can be derived from mitral regurgitant jets ($-dP/dt$) and the velocity of propagation of left ventricular inflow towards the LV apex (V_p), and are also detailed in Figure 2.18.

Index of myocardial performance

The index of myocardial performance (IMP, also known as the Tei index), an index of combined systolic and diastolic function, has been proposed (see Figure 2.18).

Pulsed wave tissue Doppler imaging (pw-TDI)

Tissue Doppler echocardiography utilizes ultrasound machine settings which ignore the high-velocity, low-amplitude signals of the blood pool and record the high-amplitude, low-velocity signals of myocardial motion. The basic limitations of Doppler apply; only motion of fibres parallel with the ultrasound beam will have myocardial velocities recorded. Furthermore, velocities may be influenced by translational movement of the heart within the thorax. There are various applications of tissue Doppler, which are at the early investigational stage in veterinary echocardiography. However, pulsed wave tissue Doppler signals of the longitudinal fibres of the LV myocardium are relatively easy to acquire and interpret (Figure 2.19).

Summary of overall approach

A systematic and logical approach to obtaining standard echocardiographic images and measurements is essential in the evaluation of a cardiac patient. Following a systematic approach is more valuable than randomly surfing. Comparison with reference ranges is essential, although breed-specific reference ranges are currently sparse in the literature. Some canine breed-specific references are available for breeds susceptible to dilated cardiomyopathy (DCM). Assessment of overall left ventricular systolic performance requires integration of 2D, M-mode and Doppler methods. Assessment of diastolic function is still in its infancy in veterinary patients, although some reference data are available for cats. An integrated approach and comprehension of the influence of heart rate and loading condition are essential.

Endoscopic thoracic ultrasonography

Indications

Endoscopic ultrasonography (EUS) is a new modality in veterinary medicine with many potential indications and the ability to overcome some of the limitations of standard transthoracic ultrasonography. EUS is a versatile procedure that has evolved in human medicine from a purely diagnostic tool to an interventional and even therapeutic one.

Although standard transthoracic ultrasonography has become a valuable diagnostic procedure for the assessment of thoracic disease in small animals (see above), it is unrewarding for examining some intrathoracic anatomy. This includes the tracheobronchial

lymph nodes, the oesophagus and lesions in the caudal mediastinum. Furthermore, lesions not in contact with the thoracic wall are also difficult to visualize as they are hidden from view by the aerated lungs or bony thorax. Obesity poses an additional barrier. These obstacles to visualizing intrathoracic structures can be overcome by the use of EUS.

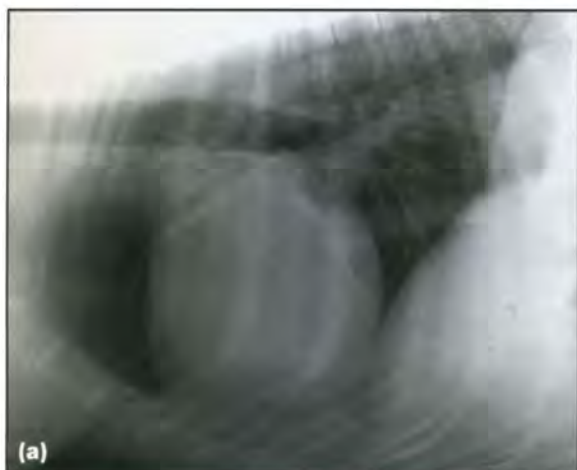
EUS is a form of endoluminal scanning which allows high-frequency ultrasound transducers to be brought directly to the region of interest via conventional endoscopes placed in the oesophagus. This imaging modality provides detailed images of pathological processes both within and outside of the oesophageal wall. It has found most success in humans for staging of lung, gastric and oesophageal cancer. Although originally designed to improve diagnostics in clinical human gastroenterology, applications for endoscopic ultrasound technology have evolved to become multifaceted and include thoracic imaging.

Potential veterinary indications for EUS of the thorax include:

- Dysphagia of unknown origin
- Tumour staging
- Evaluation of tracheobronchial lymph nodes
- Investigation and localization of radiographic soft tissue opacities that do not have contact with the thoracic wall
- Evaluation of intrathoracic paravertebral masses
- Cardiac imaging
- Assessment of infiltration of the oesophageal wall
- Differentiation of mediastinal *versus* pulmonary masses
- Detection of small amounts of pleural fluid
- EUS-guided fine-needle aspiration of intrathoracic and oesophageal lesions.

EUS examination of the thorax is advantageous for determining the origin of intrathoracic soft tissue lesions and masses. Soft tissue opacities in the caudal thorax may be of pulmonary, mediastinal, oesophageal or (para)vertebral origin. Observation of the movement of solid lesions during respiration under anaesthesia often provides a clue as to their origin. Pulmonary lesions move with the lung's direction during inspiration and expiration, whereas mediastinal lesions and vertebral lesions do not. It can also be determined whether solid lesions in the region of the caudal lung lobes have attachments to the lungs or the diaphragm by observing their excursions during respiration. In addition, radiographic lesions of soft tissue opacity can be differentiated as being solid or fluid-filled using EUS.

Pyrexia of unknown origin may be a potential indication for EUS of the thorax (Figure 2.20). Oesophageal and perioesophageal lesions can also be further examined with EUS (Figure 2.21). Determination of oesophageal wall involvement in solid and cavitary masses is very helpful for presurgical planning and prognosis. Endoscopic ultrasound-guided transoesophageal tissue sampling of pulmonary, perioesophageal, mediastinal and oesophageal wall lesions in both cats and dogs can also be performed.



2.20 (a) Lateral radiograph of a 76 kg, 5-year-old male neutered mixed-breed dog with recurrent pyrexia of unknown origin. The lungs were radiographically unremarkable and both transabdominal and transthoracic ultrasonography were unrewarding due to the large size of the dog. (b) Lateral radiograph of a normal cadaver, showing placement of the ultrasound endoscope for examination of the caudal lung lobes and mediastinum. (c) Endoscopic ultrasound image of the dog in (a), showing a heterogeneous space-occupying lesion within the right caudal lung lobe. The margins are irregular and there is an expansile nature to the lesion seen by the pattern of air surrounding it. Lobectomy was performed and a chronic suppurative process with foreign material at its centre was diagnosed histologically.



2.21 (a) Lateral radiograph of a 3 kg, 17-year-old female spayed cat with regurgitation and weight loss. A fairly well circumscribed soft tissue opaque lesion in the caudal thorax is shown with air-filled dilation of the oesophagus cranial to it. The lesion was shown to be midline on a ventrodorsal radiograph and suspected to be of mediastinal origin, most likely the oesophagus. (b) Endoscopic ultrasound image of a 5 cm homogenous space-occupying lesion (between white arrows), which involved the adjacent lung (+++) as well as the oesophageal wall. Cytology of an endoscopic ultrasound-guided fine-needle aspirate of the lesion resulted in the diagnosis of oesophageal adenocarcinoma.

In human medicine, transoesophageal EUS is considered to be superior to computed tomography (CT) in the detection of enlarged mediastinal lymph nodes. Malignant lymph nodes as small as 3 mm, which were not detected with CT, have been detected using EUS. The implementation of EUS and endoscopic ultrasound-guided fine-needle aspiration have allowed a less invasive and more cost-effective means of diagnosing metastasis in mediastinal disease compared with CT. The author [LG] has had similar experiences in dogs detecting tracheobronchial lymph nodes less than 1 cm; even those of considerable size (i.e. 6 cm) that were not visible radiographically were easily visualized with EUS. EUS may have potential in veterinary oncology for accurate staging of thoracic metastases.

Restraint and patient preparation

EUS, like conventional endoscopy or CT, requires general anaesthesia. Patients should be prepared as for any routine endoscopic procedure. Positioning

in left lateral recumbency is generally acceptable and once a position is adopted, it should be used repeatedly. This aids the beginning endosonographer in developing their endoscopic examination technique and recognition of important landmarks. Positioning in right lateral or sternal recumbency may be required, however, depending on location of the lesion.

Technique

Equipment

Ultrasound endoscopes are similar to conventional endoscopes but with an ultrasound transducer attached at the tip (Figure 2.22). They also include the standard endoscopic features: optic, light source, working channel and video capabilities.



2.22 Olympus video endoscope. The scope is 1.25 m long with a multifrequency (5–10 MHz) linear transducer, 11.8 mm outer scope diameter at the insertional end and a 2.8 mm biopsy channel. Note that the endoscope is side-viewing (optics mounted at the side rather than the tip).

Ultrasound endoscopes can either be purchased for attachment to a compatible ultrasound machine or as all-in-one dedicated units. Two types of multifrequency transducers are available, radial and linear. High-quality colour and power Doppler ultrasonography is available on most scopes. Both large- and small-breed dogs, as well as cats, can be examined with the endoscope (see Figure 2.22).

Examination method

In the EUS examination, intrathoracic structures are examined transoesophageally. Important landmarks include the thoracic inlet, cranial mediastinum and its great vessels, the base of the heart, bifurcation of the trachea, caudal vena cava, the thoracic vertebrae and intrathoracic aorta. Direct contact between the transducer and the oesophageal mucosa allows sufficient acoustic coupling in most cases. A condom-like stand-off balloon covering the transducer can be filled with water using the conventional buttons for suctioning and filling located on the scope handle.

Unlike conventional endoscopes, the echoendoscope has a much larger range of movement. The tip may be turned up to 90 degrees perpendicular to the long axis and in a 360 degree circle around it. This allows scanning in a large number of different planes.

Interpretation of the ultrasound views and anatomy is not as intuitive as in conventional transthoracic or transabdominal ultrasonography and a certain learning curve is required even for experienced ultrasonographers.

Fine-needle aspiration

Several aspiration needles of 22 gauge for solid organ sampling are available with a working handle. EUS can be used for fine-needle aspiration of various structures, including mediastinal and peri-oesophageal lymph nodes, aspiration of pleural fluid and pulmonary lesions. The aspiration technique is performed by endoscopic ultrasound-guided transoesophageal puncture and is generally performed with linear scanners. With radial scanners it is more difficult to visualize the tip of the needle because it appears only as a single point in the 360 degree image.

Many studies have been performed in humans and endoscopic ultrasound-guided fine-needle aspiration has been proven as feasible and safe. Bleeding, when it does occur, is usually self-limiting and appears as an echo-poor area adjacent to the sampled region. When this is detected, patients are typically treated with antibiotics and observed. Complications related to bacteraemia or infections have not been reported following transluminal fine-needle aspiration.

References and further reading

- Abbott JA and MacLean HN (2003) Comparison of Doppler-derived peak aortic velocities obtained from subcostal and apical transducer sites in healthy dogs. *Veterinary Radiology and Ultrasound* **44**, 695–698
- Affi A, Vazquez-Sequeiros E, Norton ID, Clain JE and Wiersma MJ (2001) Acute extraluminal hemorrhage associated with EUS-guided fine-needle aspiration: frequency and clinical significance. *Gastrointestinal Endoscopy* **53**, 221–225
- Bonagura JD (2000) Feline echocardiography. *Journal of Feline Medicine and Surgery* **2**, 147–151
- Bonagura JD, Miller MW and Darke PG (1998) Doppler echocardiography. I. Pulsed-wave and continuous-wave examinations. *Veterinary Clinics of North America: Small Animal Practice* **28**, 1325–1359
- Bonagura JD, O'Grady MR and Herring DS (1985) Echocardiography. Principles of interpretation. *Veterinary Clinics of North America: Small Animal Practice* **15**, 1177–1194
- Boon JA (1998) Appendix IV. Echocardiographic reference values. In: *Manual of Veterinary Echocardiography*, ed. JA Boon, pp. 453–473. Lippincott Williams & Wilkins, Philadelphia
- Bright JM, Herrtage ME and Schneider JF (1999) Pulsed Doppler assessment of left ventricular diastolic function in normal and cardiomyopathic cats. *Journal of the American Animal Hospital Association* **35**, 285–291
- Cornell CC, Kittleson MD, Della Torre P *et al.* (2004). Allometric scaling of M-mode cardiac measurements in normal adult dogs. *Journal of Veterinary Internal Medicine* **18**, 311–321
- Dancygier H, Lightdale CJ and Stevens PD (1999) Endoscopic ultrasonography of the upper gastrointestinal tract and colon. In: *Endosonography in Gastroenterology. Principles, Techniques, Findings*, ed. H Dancygier and CJ Lightdale, pp. 13–168. CJ Thieme, New York
- Dukes-McEwan J, French AT and Corcoran BM (2002) Doppler echocardiography in the dog: measurement variability and reproducibility. *Veterinary Radiology and Ultrasound* **43**, 144–152
- Gaschen L, Kircher P, Hoffmann G *et al.* (2003) Endosonographic diagnosis of intrathoracic lesions. *Veterinary Radiology and Ultrasound* **44**, 292–299
- Gaschen L, Kircher P and Lang J (2003) Endoscopic ultrasound instrumentation, applications in humans and potential veterinary applications. *Veterinary Radiology and Ultrasound* **44**, 665–680
- Gavaghan BJ, Kittleson MD, Fisher KJ, Kass PH and Gavaghan MA (1999) Quantification of left ventricular diastolic wall motion by Doppler tissue imaging in healthy cats and cats with cardiomyopathy. *American Journal of Veterinary Research* **60**, 1478–1486
- Gress FG, Hawes RH, Savides TJ, Ikenberry SO and Lehman GA (1997) Endoscopic ultrasound-guided fine-needle aspiration biopsy using linear array and radial scanning endosonography. *Gastrointestinal Endoscopy* **45**, 243–250
- Konde LJ and Spaulding K (1991) Sonographic evaluation of the cranial mediastinum in small animals. *Veterinary Radiology and Ultrasound* **32**, 178–184
- Lehmkuhl LB and Bonagura JD (1994) Comparison of transducer placement sites for Doppler echocardiography in dogs with subaortic

- stenosis. *American Journal of Veterinary Research* **55**, 192–198
- Mattoon JS and Nyland TG (2002) Thorax. In: *Veterinary Diagnostic Ultrasound, 2nd edn*, ed. TG Nyland and JS Mattoon, pp. 325–353. WB Saunders, Philadelphia
- Oyama MA (2004) Advances in echocardiography. *Veterinary Clinics of North America: Small Animal Practice* **34**, 1083–1104
- Reichle JK and Wisner ER (2000) Non-cardiac thoracic ultrasound in 75 feline and canine patients. *Veterinary Radiology and Ultrasound* **41**, 154–162
- Sahn DJ, DeMaria A, Kisslo J and Weyman A (1978) Recommendations regarding quantitation in M-mode echocardiography: results of a survey of echocardiographic measurements. *Circulation* **58**, 1072–1083
- Santilli RA and Bussadori C (1998) Doppler echocardiographic study of left ventricular diastole in non-anaesthetized healthy cats. *Veterinary Journal* **156**, 203–215
- Schiller NB, Shah PM, Crawford M *et al.* (1989). Recommendations for quantitation of the left ventricle by two-dimensional echocardiography. American Society of Echocardiography Committee on Standards, Subcommittee on Quantitation of Two-Dimensional Echocardiograms. *Journal of the American Society of Echocardiography* **2**, 358–367
- Schober KE, Luis Fuentes V and Bonagura JD (2003) Comparison between invasive hemodynamic measurements and non-invasive assessment of left ventricular diastolic function by use of Doppler echocardiography in healthy anesthetized cats. *American Journal of Veterinary Research* **64**, 93–103
- Thomas WP, Gaber CE, Jacobs GJ *et al.* (1993) Recommendations for standards in transthoracic two-dimensional echocardiography in the dog and cat. Echocardiography Committee of the Specialty of Cardiology, American College of Veterinary Internal Medicine. *Journal of Veterinary Internal Medicine* **7**, 247–252
- Tidwell AS (1998) Ultrasonography of the thorax (excluding the heart). *Veterinary Clinics of North America: Small Animal Practice* **28**, 993–1015
- Wood EF, O'Brien RT and Young KM (1998) Ultrasound-guided fine-needle aspiration of focal parenchymal lesions of the lung in dogs and cats. *Journal of Veterinary Internal Medicine* **12**, 338–342
- Yuill CD and O'Grady MR (1991) Doppler-derived velocity of blood flow across the cardiac valves in the normal dog. *Canadian Journal of Veterinary Research* **55**, 185–192
-

Basics of thoracic computed tomography

Tobias Schwarz

Indications

Computed tomography (CT) should be used in dogs and cats with suspected thoracic disease where other diagnostic imaging modalities, such as radiography and ultrasonography, fail to identify the cause and extent of the disease. CT is also indicated if the abnormalities cannot be clearly attributed to specific thoracic organs.

Thoracic wall

Determination of the extent of palpable thoracic wall masses is essential for surgical planning. This often cannot be determined accurately radiographically. Examples include vaccine-related feline fibrosarcomas or rib tumours with unknown expansion into the thoracic cavity (Figure 3.1).



3.1 Contrast-enhanced CT image of the cranial thorax of an 8-year-old Domestic Longhair cat with a mineralized sarcoma arising from the palmaroproximal aspect of the left scapula. This image is set with a narrow window (level 65 HU, width 187 HU) to emphasize the peripheral contrast enhancement of the mass at the expense of increased visibility of image noise and streak artefacts. The lungs cannot be appropriately assessed with this window.

Pleural space

CT can be useful to investigate further the following pleural abnormalities:

- Recurring/persistent pneumothorax. If no source of continuous gas leakage can be identified radiographically, CT can help to identify subpleural blebs and pulmonary bullae

- Pleural effusion and masses. CT can distinguish soft tissue masses from fluid and identify collapsed or consolidated lung lobes.

Mediastinum including heart and major vessels

CT is an excellent imaging modality for many mediastinal disorders, particularly if suspected lesions cannot be clearly differentiated radiographically or ultrasonographically. Cardiovascular CT is still in its infancy in veterinary medicine and only a few clinical applications have been developed so far. CT has been shown to be particularly useful to demonstrate:

- Sternal, cranial mediastinal and tracheobronchial lymphadenopathy, particularly in mild cases, for oncological staging and presurgical planning
- Cranial and caudal mediastinal masses (Figure 3.2) and cysts
- Oesophageal masses (spirocercosis, neoplasia)
- Aortic mineralization, aneurysm and parasitic infection (spirocercosis)
- Pericardial rupture and cardiac herniation
- Caval thrombosis and obstruction (Budd–Chiari-like syndrome)
- Heart base tumours
- Pneumomediastinum.

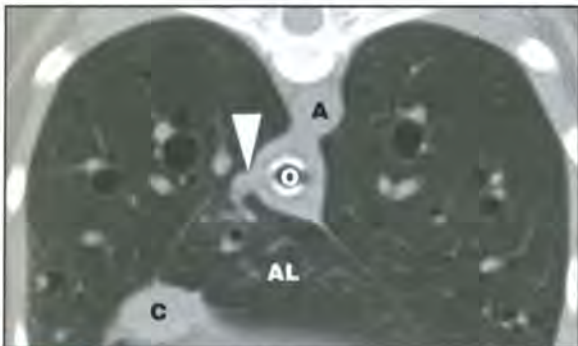


3.2 Contrast-enhanced CT image of the cranial mediastinum in a 6-year-old Labrador Retriever with an extraskelatal osteosarcoma. The image is set with a narrow window (level 70 HU, width 220 HU). The mass extended from the midcervical region to the cranial mediastinum where it deviated and compressed contrast-enhanced vessels, the trachea (T) and oesophagus (O). There is also compression of the cranial lung lobes.

Airways and lungs

CT is an excellent modality to investigate suspected airway and lung pathology where radiographic findings are non-specific in terms of underlying pathology, extent and severity. Particularly useful indications are:

- Tracheal collapse, obstruction and rupture
- Bronchial obstruction, rupture and thickening, peribronchial infiltrate
- Screening for metastatic lung lesions for oncological staging and presurgical planning (Figure 3.3)
- All interstitial lung diseases
- Exact location, nature and extent of pulmonary masses and bullae
- Pulmonary thromboembolism
- Lung lobe torsion
- Differentiation between collapsed and consolidated lung lobes.

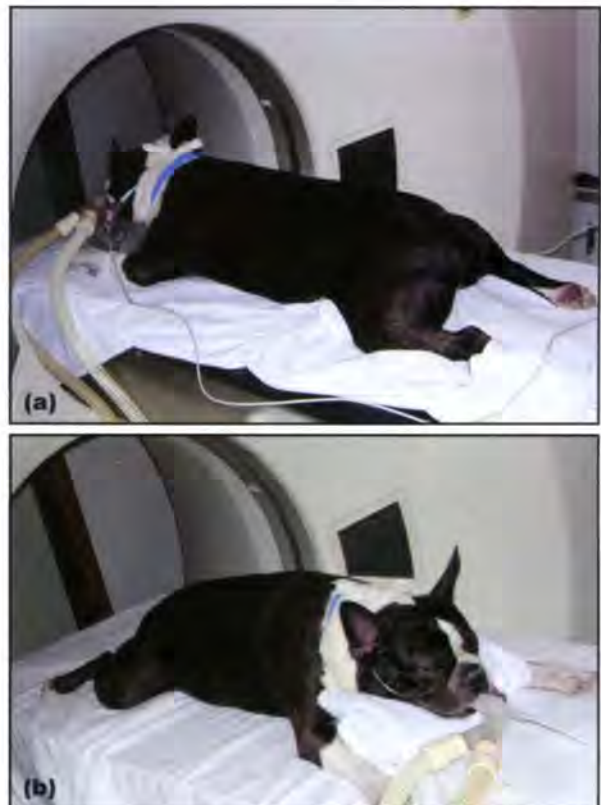


3.3 High-resolution CT image (1 mm slice width, 1 second rotation time, high spatial algorithm) of the caudal thorax of a 10-year-old Miniature Poodle with a salivary adenocarcinoma. The image is set with a centre in the negative HU range and a wide window (level -744 HU, width 2456 HU). There is a single small lung nodule (arrowhead) in the dorsal aspect of the accessory lung lobe (AL) assessed as a potential metastasis. This lesion was not seen on survey radiographs. A post-chemotherapy treatment follow-up CT examination four weeks later revealed no growth of the nodule. A = Aorta; C = Caudal vena cava; O = Oesophagus with oesophageal stethoscope.

Restraint and patient preparation

General anaesthesia is required for most thoracic CT examinations unless multislice CT scanners are available. Multislice scanners are capable of covering an entire thorax in a single breath-hold in humans and basically acquire multiple 'slices' for each gantry rotation. Inhalation anaesthesia is mandatory for most thoracic studies with the exception of tracheal CT where intubation could prohibit the diagnostic purpose of the scan. Depending on the site of the lesion, however, advancement of the endotracheal (ET) tube only to the cervical trachea may be sufficient.

Anaesthetic and monitoring equipment should preferentially be placed in a way that the tubes and lines connecting it to the patient do not cross the gantry of the CT scanner, since they do create major artefacts (Figure 3.4). In a 'head first' set-up this would mean placing the equipment behind the CT scanner,



3.4 (a) An anaesthetized Boston Terrier in ventral recumbency and 'head first' position on the CT table. Note the anaesthetic tubing and pulse oximetry cable crossing the gantry, which can create significant artefacts. (b) The dog now in a 'tail first' position. When the thorax is scanned, the anaesthetic equipment will not cross the gantry and artefacts are avoided. Note the extended forelegs to move them out the scanning area. ECG clips (not seen here) should be placed well cranial or caudal to the scanning area.

and in a 'tail first' set-up placing it in front of the scanning unit. Regardless of patient position, there should always be sufficient length of the connections to allow adequate bed movement during the scan.

CT is a modified X-ray technique that emits relatively high levels of ionizing radiation. Therefore, the patient restraint must be sufficient for all personnel to be able to leave the CT room for the duration of the scan (several minutes). It is imperative to anchor the patient securely to the CT table with large Velcro straps or other positioning devices designed for CT. Sandbags and other radiopaque positioning devices used in conventional radiography are usually not suitable for CT since they create major artefacts if located in the scan field, and have a tendency to fall off the CT table, which is much narrower than a conventional X-ray table.

Care must be taken to avoid overt restriction of thoracic expansion, particularly in patients that are already compromised in respiration. The use of a radiographic trough can be very helpful in this respect if the appropriate size is used (Figure 3.5). Self-adhesive tape is commonly used in CT to aid positioning of an animal under general anaesthesia. However, the tape can only be fixed to the moving bed which somewhat restricts its use for thoracic CT.



3.5 The canine muffin sign. Occasionally CT offers completely unexpected new vistas. This 4-year-old St Bernard dog was positioned for a thoracic CT scan in the largest trough available. The CT image of the caudal thorax reveals a muffin-shaped cross-sectional anatomy of the dog, indicating that the trough was not big enough and was potentially restricting respiration.

The patient should be positioned according to the nature of the study:

- In general, ventral recumbency works best for thoracic wall, pleural, mediastinal, cardiovascular and airway studies
- For lesions close to the thoracic spine, dorsal recumbency is preferred because the recumbent spine is not affected by respiratory movement
- For studies focusing on lung parenchyma, physiological hypostatic lung collapse during anaesthesia should be taken into account. For example, if ventral lung disease is suspected then dorsal recumbency would be preferable (if tolerated by the patient). This will avoid the development of atelectasis in the area of interest. If lung changes consistent with atelectasis are seen on initial CT images, the scan should be repeated with the patient positioned so that non-aerated lung lobes are non-dependent. In a case of hypostatic atelectasis the affected lung tissue will regain aeration, whereas it will remain atelectatic if pathologically altered (see Figure 12.86, p. 284)
- If CT-guided biopsy or aspiration is planned, then the patient should be positioned with the biopsy side up or on the side
- Whether the dog is positioned 'head first' or 'tail first' is of little consequence for a thoracic CT examination other than for the anaesthetic set-up (see above)
- The forelegs should be extended and placed parallel to the cervical spine. Leg extension can be secured with the help of tape. Metallic monitoring devices, such as electrocardiogram (ECG) clips, should be positioned outside of the scan area.

Respiratory control is critical for a diagnostic CT examination. Due to the relatively long exposure time for each CT image, respiratory motion would otherwise render most studies non-diagnostic. There are several strategies to achieve this:

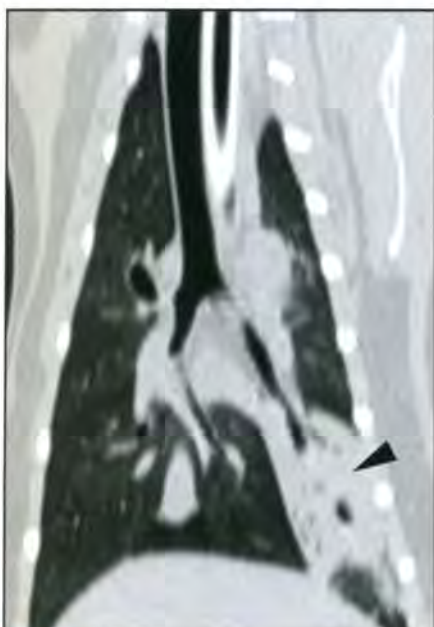
- *Natural respiratory pause imaging.* Each exposure is taken manually at the onset of the respiratory pause at end-expiration. Tape markers on the patient can be helpful to identify the pause in the respiratory cycle. This is technically the simplest method and sometimes the only practical means to achieve a diagnostic scan. However, it is difficult to achieve consistently high image quality. It cannot be used for a helical CT scan
- *Induced respiratory pause imaging.* The patient should be rigorously hyperventilated for several minutes until immediately prior to the start of the scan. Most patients will then not breathe for 30–60 seconds, which is sufficient for most CT scans to be completed. This is the most commonly used technique for helical thoracic CT scans in animals. The scan can also be interrupted should breathing commence and the manoeuvre is then repeated. Prolonged apnoea can be difficult to achieve with certain anaesthetic systems. Hyperventilation should not be performed unless it is safe to do so
- *End-inspiratory breath-hold imaging* is the standard for most human lung CT studies but is difficult to achieve with animals, who are rarely trained to hold their breath on command! Maintaining a breath-hold at inspiration can be achieved with a specific anaesthetic set-up that allows complete X-ray shielding for the monitoring anaesthetist
- *Pharmacological control of respiration* has been mainly used in research studies so far. In expert hands it can be a valuable tool.

Technique

Techniques for thoracic CT depend on the organ of interest. A study on a single animal may include several image sequences in order to evaluate the pulmonary parenchyma, mediastinal structures, ribs and thoracic wall.

- For *mediastinal and other soft tissue structures* a thick slice width (such as 5 mm) and a narrow window (window width 180–300 HU, window level 50–100 HU) should be used. The same is true for any contrast medium enhanced study to maximize contrast resolution (see Figures 3.1 and 3.2).
- For *high-resolution pulmonary parenchymal imaging* a narrow slice width (1 mm), high kVp and mA, high-resolution reconstruction algorithms and small field of view should be chosen. A wide window (window width 1500–3000 HU, window level –800 to –400 HU) should be used for viewing (see Figure 3.3).

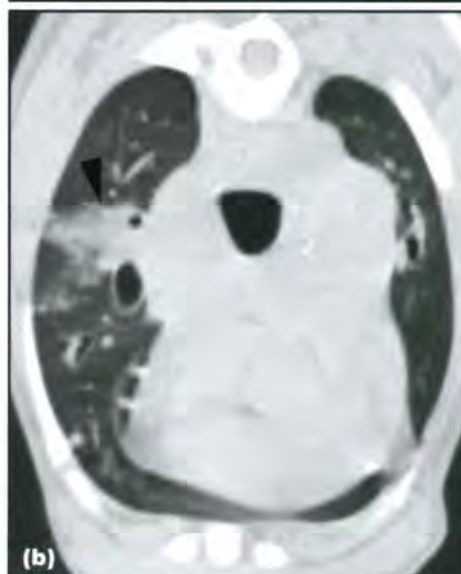
- For CT screening of pulmonary metastatic disease, a high-resolution technique can be used to achieve maximal detail of potential lung nodules (1 mm slice width, pitch of 2, helical respiratory pause imaging). This technique can produce tube cooling issues and prolonged scanning time. Sufficient detail can also be achieved with thicker slices (5 mm, pitch of 1.4) but the exact threshold of detectable nodule size with the different techniques has not been established.
- The tube rotation time should be kept at minimum (usually 1 second) for any thoracic study to reduce the effect of motion.
- Helical scanning is superior to axial scanning to achieve a maximum number of images free of motion artefact.
- If axial CT is used with thin slice image techniques, it may be sufficient to leave a larger slice gap to limit examination time.
- If induced respiratory pause imaging is used to control respiration (see above), then it is always advantageous to scan the thorax in a caudocranial direction. This way the area of the highest respiratory motion amplitude is scanned first, when the patient is still apnoeic.
- Sagittal and dorsal reconstructions are very useful to assess lesions identified on transverse images if a high image quality can be achieved. The image quality of orthogonal reconstructions depends on the slice width and interval (pitch in helical CT) and is far superior with multislice CT units (Figure 3.6).



3.6 Dorsal plane CT image of an 11-year-old Domestic Shorthair cat with a cavitated tumour in its left caudal lung lobe (arrowhead). The image was reconstructed from a helical CT series with 1 mm slice thickness and a pitch of 1, resulting in an image resolution close to the axial plane images. The main advantages of this plane are the better alignment of the lesion with the bronchial and vascular tree and the increased viewing area.

CT-assisted fine-needle aspiration

CT-assisted fine-needle aspiration (Figure 3.7) is a valuable diagnostic tool where samples via direct or ultrasound-guided techniques cannot be obtained, such as from lesions that are surrounded by aerated lung. Compared with ultrasound-guided fine-needle aspiration, the sampling is not performed under real-time imaging control and the set-up is more time-consuming. The manual technique involves several steps:



3.7 (a) Mid-thoracic CT image of a 3-year-old crossbred dog with perihilar lymphadenopathy, demonstrating the set-up for a CT-assisted transpulmonary fine-needle lymph node aspiration. The needle is supported by a box, aligned with the image plane and advanced subcutaneously (left side of image). A black streak artefact emanates from the needle tip. From this image, the depth and angle of needle advancement can be planned and the aspirate then pursued accordingly. (b) Recheck CT scan. There is a small area of pulmonary haemorrhage along the previous needle track (arrowhead) and a small pneumothorax (small amount of free gas dorsal aspect right hemithorax). The dog recovered uneventfully from anaesthesia and a granulomatous lymphadenopathy was diagnosed.

1. Identify lesion with CT scan and surgically prepare adjacent chest wall.
2. Place and secure syringe with needle along the axial plane of the patient with tip inserted subcutaneously. The laser light in the gantry should be used to exactly line up the needle with the axial plane.
3. CT scan the area of interest of anaesthetized patient with preliminary placed needle.
4. Assess from CT image the anticipated angle and depth of needle placement in order to hit the target and avoid vital structures.
5. It is beneficial to hyperventilate patient prior to the procedure to create a prolonged respiratory pause to minimize the chance of lung laceration.
6. Advance needle, harvest sample and retrieve needle as planned without direct CT monitoring.
7. Repeat entire procedure for next sample.
8. Recheck CT scan for complications (bleeding, pneumothorax).

Advanced CT units have automated biopsy guide arms, which allow precise sampling under real-time

imaging control. The author does not recommend obtaining full-core thoracic biopsy samples with the above described technique.

References and further reading

- Johnson VS, Corcoran BM, Wotton PR, Schwarz T and Sullivan M (2005) Thoracic high-resolution computed tomographic findings in dogs with canine idiopathic pulmonary fibrosis. *Journal of Small Animal Practice* **46**, 381–388
- Johnson VS, Ramsey IK, Thompson H *et al.* (2004) Thoracic high-resolution computed tomography in the diagnosis of metastatic carcinoma. *Journal of Small Animal Practice* **44**, 134–143
- Nemanic S, London CA and Wisner ER (2006) Comparison of thoracic radiographs and single breath-hold helical CT for detection of pulmonary nodules in dogs with metastatic neoplasia. *Journal of Veterinary Internal Medicine* **20**, 508–515
- Schwarz LA and Tidwell AS (1999) Alternative imaging of the lung. *Clinical Techniques in Small Animal Practice* **14**, 187–206
- Schwarz T (2002) General principles in CT image planning. *The European Association of Veterinary Diagnostic Imaging Yearbook 2002*, 9–23
- Schwarz T (2003) General principles for interpreting CT studies. *The European Association of Veterinary Diagnostic Imaging Yearbook 2003*, 9–17
- Vignoli M, Ohlerth S, Rossi F *et al.* (2004) Computed tomography-guided fine-needle aspiration and tissue-core biopsy of bone lesions in small animals. *Veterinary Radiology and Ultrasound* **45**, 125–130
-

Basics of thoracic magnetic resonance imaging

Fraser McConnell

Indications

The principal indication for magnetic resonance imaging (MRI) of thoracic disease in small animals is the evaluation of thoracic masses. MRI is of particular value for presurgical planning due to the excellent soft tissue contrast it provides and its ability to obtain images in any plane.

Thoracic wall

MRI is indicated for investigation of thoracic wall masses. It is valuable if contemplating extensive surgery, e.g. chest wall resection (Figure 4.1).



4.1 Transverse T2-weighted image of a dog with a soft tissue sarcoma arising from the chest wall. A cod liver oil capsule (arrowed) has been placed over the area of swelling to aid localization. The tumour is the medium strong signal tissue adjacent to the oil capsule.

Pleural space

MRI may be used for investigating causes of pleural effusion if a diagnosis is not reached with conventional imaging.

Mediastinum including heart and major vessels

Indications include:

- Investigation of mediastinal masses for lesion extent and involvement of major thoracic structures (Figure 4.2)



4.2 Dorsal plane T2-weighted image of an 11-year-old cat with dyspnoea. There is a cranial mediastinal mass (arrowheads), pleural fluid and lung lobe torsion (left cranial lobe). Compare the swollen, hyperintense left cranial lung lobe (arrowed) with the normal right cranial lobe (*). MRI allowed more accurate assessment of the thoracic pathology than conventional radiology or ultrasonography.

- Complex cardiac malformations (when diagnosis is not possible with echocardiography or if contemplating surgery)
- Vascular malformations.

The use of MRI to evaluate small animal cardiac function has been reported in experimental studies but has so far only limited clinical veterinary application. MRI allows more accurate quantification of cardiac volumes and function compared with echocardiography but is considerably more expensive. To evaluate the blood vessels MR angiography (MRA) may be used.

Airways and lungs

MRI of the lung is rarely performed compared with computed tomography (CT), due to an inherently low signal from lung and artefacts. Ventilation scans may be performed by using inhaled hyperpolarized inert gases, such as helium, but are not used clinically in veterinary medicine as they require specialized equipment. Lung perfusion scans may be performed using MRA but currently offer little advantage over other imaging modalities (CT, nuclear medicine or angiography) for this purpose in small animals.

Limitations and comparison with computed tomography

As MRI for small animals requires general anaesthesia, its use in severe cardiac or respiratory disease is limited.

Whilst it is non-invasive, there are some hazards associated with MRI. Metallic implants within the patient may move or heat up and will cause artefacts if they are near or within the field of view. This is particularly important in MRI units with high field strength.

- Hip replacement prostheses and bone implants rarely cause problems for thoracic MRI.
- Animals with potentially mobile metal within the body (e.g. gunshot, foreign bodies) should be screened radiographically prior to MRI.
- Animals with a pacemaker should not undergo MRI unless the implant is known to be MRI-compatible as the magnetic field may interfere with pacemaker function.
- Microchips may cause artefacts, leading to distortion of the images in the adjacent area. This may be a problem if evaluating lesions near the thoracic spine (e.g. injection site sarcomas).

Motion artefacts (cardiac, respiratory) can be a limiting factor in thoracic MRI. Possible remedies include:

- Fast imaging sequences (e.g. single shot techniques)
- Physiological gating.

Low and mid-field systems (<0.5 Tesla) can be used for the evaluation of thoracic masses but are limited in their capabilities for cardiovascular imaging. A comparison of CT and MRI is given in Figure 4.3.

Factor	Helical CT	MRI
Soft tissue detail	Moderate	Excellent
Choice of image planes	Limited	Unlimited
Image acquisition time	Seconds	Minutes
Cost	High	Very high
Preferred organs	Lung, airways, bone	Soft tissue masses, heart

4.3 Comparison of thoracic CT and MRI.

Restraint and patient preparation

General anaesthesia is required for all MRI studies to prevent motion artefacts. There are certain requirements for general anaesthesia and patient restraint:

- Special MRI-compatible (non-ferrous) monitoring and anaesthetic equipment
- Peripheral venous catheter placed for administration of contrast media
- Meticulous check for and removal of extraneous metallic objects (collars, leads, harness, etc.) prior to entering the scanning room

- Ensuring adequate length of anaesthetic tubing and monitoring equipment for anticipated patient position.

Generally, the preferred positioning for thoracic MRI is 'tail first' (depending upon the arrangement of the connection between the radio frequency (RF) coil and the scanner) and sternal recumbency in order to:

- Minimize the distance between the animal and the anaesthetic machine and prevent kinking of the breathing circuit
- Minimize dependency-related lung atelectasis
- Allow best comparison between left and right hemithorax (equal atelectasis).

For chest wall lesions, movement artefacts due to respiration may be reduced by positioning the animal in lateral recumbency with the lesion dependent. This reduces motion of the dependent surface but results in distortion of the superficial tissues. Deep-chested dogs (e.g. Great Danes, Irish Wolfhounds) usually need to be positioned in lateral recumbency to fit into the scanner. Care should be taken to ensure the animal is straight and not rotated.

Cats and small dogs (<10 kg) may be positioned in sternal recumbency within an extremity coil. For medium-sized dogs (10–20 kg) a human head coil may be used. For large dogs (>20 kg) a torso coil is used. Dedicated surface (cardiac) coils are not required for routine imaging but may be used for cardiac imaging.

To aid localization a mineral oil capsule may be taped to the surface of the lesion (see Figure 4.1).

If physiological gating is being performed then the bellows, pulse oximeter or electrocardiogram (ECG) should be placed before sending the animal into the bore of the magnet.

The animal should be positioned so that the area of interest is centred within the coil and laser lights on the scanner are used to identify this landmark. For general thoracic imaging, centring just caudal to the scapula is suitable. For chest wall masses the landmark should be set on the centre of the lesion.

Technique

A three-plane localizing scan is obtained first. If the animal is seen to be poorly positioned it should be repositioned and the localizing scan repeated. Additional slices are then prescribed from the localizer images. Images should be obtained in dorsal, sagittal and transverse planes. When prescribing slices, care should be taken to ensure that transverse slices are perpendicular and sagittal images are parallel to the long axis of the patient.

The choice of sequence depends upon the purpose of the study:

- Standard T1- and T2-weighted fast-spin echo sequences for evaluation of thoracic masses. T2-weighted images are useful for most conditions as these have maximum soft tissue contrast

- T1-weighted images are useful for anatomical imaging and allow the use of intravenous contrast media (gadolinium chelates) to define margins of masses and vascularized tissue
- A variety of pulse sequences (e.g. gradient-echo, phase-contrast sequences, true FISP) can be used to assess cardiac function or structure
- Fat suppression techniques (e.g. STIR sequence or spectral fat saturation) may be of benefit for the evaluation of fatty lesions and pathology involving muscle or bone.

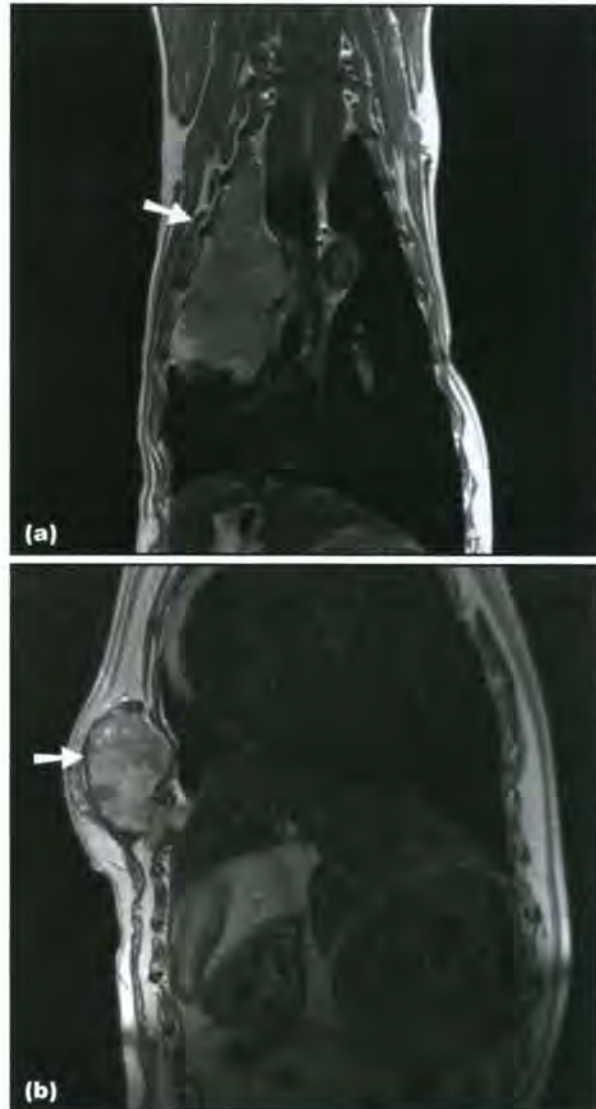
Slice thickness and field of view will vary depending on the area of interest and patient size. Field of view should be just larger than the diameter of the body where the images are being obtained to prevent phase wrap (where tissue outwith the field of view is superimposed on tissue within the field of view). If a small field of view is wanted, oversampling (no phase wrap) can be used.

- Generally 4–5 mm slice thickness is adequate for most cats and dogs.
- For chest wall and mediastinal disease, ideally all images in three planes should be obtained with slices oriented to the long axis of the animal.
- For cardiac imaging slices are oriented to the heart to give either long- or short-axis images.
- Correct identification of rib numbers may be difficult from sagittal and transverse images. A dorsal plane image, extending from the spine ventrally to include the dorsal aspect of the ribs, allows correct identification of the rib numbers (if this is important).

Motion artefacts due to respiration and pulsation from the heart and great vessels are common. Both occur predominately in the phase encoding direction and result in ghosting and severe degradation of image quality:

- For lateral chest wall lesions, dorsal plane images should have phase encoding set craniocaudal, and transverse images should have phase encoding dorsoventral
- For dorsal or ventral chest wall lesions phase encoding should be right–left for transverse plane images. Artefacts are less common on sagittal plane images
- If peripheral thoracic lesions are being imaged, application of pre-saturation bands (satbands) over the heart reduces artefact by reducing the signal from the heart
- Motion artefacts may be more pronounced on long echo time images (T2-weighted). This may be reduced (at the expense of increasing acquisition time) by using multiple excitations (NEX)
- Short echo time sequences and fast imaging (gradient-echo, echo-planar or single-shot) sequences reduce motion artefacts.

Respiratory motion may be minimized by using respiratory gating, where the scan acquisition is related to the respiratory cycle (Figure 4.4). This requires the



4.4 (a) Dorsal plane T2-weighted image of a dog with a primary lung tumour of the right middle lobe (arrowed). This image was acquired using respiratory gating. (b) Dorsal T2-weighted image of a dog with a chest wall tumour (arrowed). This image was acquired without respiratory gating. Note the reduction in motion artefacts and better image quality in (a) compared with (b). Scan times with gating were six times longer than without gating.

use of a band with bellows attached, which is placed around the chest and detects respiratory motion. Images are obtained at set points of the respiratory cycle. This may be ineffective in smaller animals as the movement of the chest wall is too small to be detected by the bellows. A disadvantage of respiratory gating is increased scan times.

Cardiac gating is required for cardiac MRI. This allows data to be obtained at one point of the cardiac cycle (Figure 4.5). It may be performed using MRI-compatible electrodes connected to the gating control on the scanner or using the pulse oximeter built into the scanner. In small animals the low height of the R wave on the ECG may make it difficult for the computer to obtain accurate timing. The pulse oximeter placed on the tongue usually works and avoids the need to have ECG cables in the region of the coil. Ventilator



4.5 Dorsal plane MR image of a Golden Retriever with pulmonary arterial thrombosis. Compare the large hypointense thrombus within the right pulmonary artery (arrowed) with the normal left pulmonary artery (arrowhead). This image was acquired using cardiac gating to minimize motion artefact.

settings for frequent low-amplitude chest excursions are preferred to avoid major artefacts associated with deeper respirations.

MRA can be performed with or without contrast media. Contrast-enhanced MRA is occasionally useful and gives better quality angiograms compared with non-contrast techniques (especially if there is turbulent or slow blood flow) as there is a greater signal to noise ratio and greater contrast compared with background tissues. If performing contrast-enhanced MRA a double or triple dose of gadolinium is used and ideally should be injected using a power injector to obtain a tight bolus.

References and further reading

- McRobbie DW, Moore EA, Graves MJ and Prince MR (2003) Cardiac MRI. In: *MRI From Picture to Proton*, pp. 278–299. Cambridge University Press, Cambridge
- McRobbie DW, Moore EA, Graves MJ and Prince MR (2003) MR angiography. In: *MRI From Picture to Proton*, pp. 255–277. Cambridge University Press, Cambridge
- Poustchi-Amin M, Gutierrez FR, Brown JJ *et al.* (2003), Performing cardiac MR imaging: an overview. *Magnetic Resonance Imaging Clinics of North America* **11**, 1–18
- Tidwell AS and Jones JC (1999) Advanced imaging concepts: a pictorial glossary of CT and MRI technology. *Clinical Techniques in Small Animal Practice* **14**, 65–111
- Westbrook C (1999) *Handbook of MRI Technique, 2nd edn*. Blackwell Science, Oxford

Basics of thoracic nuclear medicine

Federica Morandi

Introduction

Nuclear medicine, or nuclear scintigraphy, is a branch of medical imaging that uses radiopharmaceuticals (pharmaceuticals labelled to radioactive atoms) to evaluate physiological processes and diagnose a variety of diseases. Nuclear medicine differs from other imaging modalities in that it shows primarily the function of the system being investigated, as opposed to its anatomy. During scintigraphic studies, images are created using a radiation detector (the gamma camera) after the application of a radiopharmaceutical of choice (e.g. rectal, intravenous). Because scintigraphy employs radioactive compounds, radiation safety is of the utmost importance, both when handling the radiopharmaceutical dose and the animal being injected, as well as with waste products, such as urine and faeces. In small animal thoracic diagnostic nuclear medicine, the typical radiopharmaceutical dose is small (ranging between a minimum of 30 and a maximum of 740 MBq), resulting in minimal exposure from the animals and their excreta. Nevertheless, adherence to national radiation safety regulations is mandatory.

Indications

Indications for first pass radionuclide angiocardio-graphy using sodium ^{99m}Tc -pertechnetate ($\text{Na}^{99m}\text{TcO}_4$), ^{99m}Tc -DTPA or ^{99m}Tc -mebrofenin include:

- Diagnosis of congenital cardiac shunt and determination of the direction of shunting (left-to-right *versus* right-to-left); especially useful in cases where radiographic and echocardiographic findings are questionable or equivocal
- Quantification of left-to-right cardiac shunts
- Follow-up evaluation after surgical correction of a shunt (patent ductus arteriosus, PDA).

Indications for pulmonary scintigraphy using ^{99m}Tc -MAA include:

- Evaluation of pulmonary perfusion in cases of suspected pulmonary thromboemboli (PTE)
- Evaluation and quantification of right-to-left shunts (reverse PDA, tetralogy of Fallot)
- Follow-up evaluation after surgical correction of a shunt (reverse PDA).

Indications for ciliary scintigraphy using ^{99m}Tc -MAA include:

- Evaluation of mucociliary function (ciliary dyskinesia).

Indications for static images using sodium ^{99m}Tc -pertechnetate scintigraphy include:

- Evaluation of cranial mediastinal masses (determining whether or not a mass is thyroidal in origin).

Restraint and patient preparation

First pass radionuclide angiocardio-graphy

This study is easy and quick to perform and does not require sedation or general anaesthesia; however, sedation may be used in particularly fractious animals. Prior to the study, radiographs of the thorax should be obtained to make sure that the animal is not in left heart failure, since left heart failure will render the study invalid. An animal with evidence of pulmonary oedema and/or pulmonary venous congestion should be treated until resolution of the decompensation, before attempting the study.

The radionuclide must be injected intravenously in a bolus fashion; therefore, prior to the study, a large-gauge, short-length intravenous catheter must be placed in the cephalic vein.

The animal is positioned in left lateral recumbency over the gamma camera and restrained by one (or two) assistants. It is vital that the animal remains still during the few seconds of the dynamic acquisition of the first pass, or the study will be non-diagnostic.

Pulmonary scintigraphy

No sedation or anaesthesia is necessary; however, sedation may be used in particularly fractious animals.

It is important to assess whether the animal may have pulmonary hypertension. Pulmonary hypertension is a relative contraindication for the use of ^{99m}Tc -MAA, since the particles will occlude a portion of the pulmonary capillary bed and, therefore, could potentially exacerbate this condition. If pulmonary hypertension is suspected, the particle dose must be reduced as much as possible. In cases of severe pulmonary hypertension, the study risks must be weighed against the benefit of achieving a diagnosis.

When evaluating for PTE, radiographs of the thorax should be obtained immediately prior to the study and used in conjunction with the scintigraphic images for interpretation. This is especially important

because ventilation scintigraphy using inert radioactive gases or ^{99m}Tc-DTPA radioaerosol is virtually never performed in practice due to its technical difficulty and radiation safety concerns.

Since the MAA particles can adhere to plastic tubing, it is best to inject directly into the vein, and no intravenous catheter is needed.

The animal can be restrained in opposite lateral, dorsal and ventral recumbency over the gamma camera by an assistant.

^{99m}Tc-MAA scintigraphy for evaluation of mucociliary function

General anaesthesia is necessary and a short endotracheal (ET) tube must be used to ensure that the tube terminates no further than the thoracic inlet. Radiographs can be obtained immediately prior to the study to confirm the position of the ET tube.

^{99m}Tc-pertechnetate scintigraphy for evaluation of cranial mediastinal masses

Anaesthesia is not necessary, but sedation is generally required. If the study includes images of the thyroid using a pinhole collimator, then anaesthesia is needed. An intravenous catheter should be placed in the cephalic or saphenous vein to facilitate the administration of the radionuclide. The animal can be restrained in opposite lateral, dorsal and ventral recumbency over the gamma camera by an assistant.

It is important to remember that if the animal has recently undergone a contrast study with intravenous injection of iodinated contrast media, the scintigraphy will be negative because iodine reduces thyroid uptake of ^{99m}Tc-pertechnetate: a delay of 3–4 weeks is recommended from the time of intravenous iodinated contrast media injection to the time of scintigraphy to avoid a false-negative result.

Technique

First pass radionuclide angiocardiology

The set-up for first pass radionuclide angiocardiology is easy and the acquisition time itself is short. Most commercially available nuclear medicine software have a programme that permits the calculation of

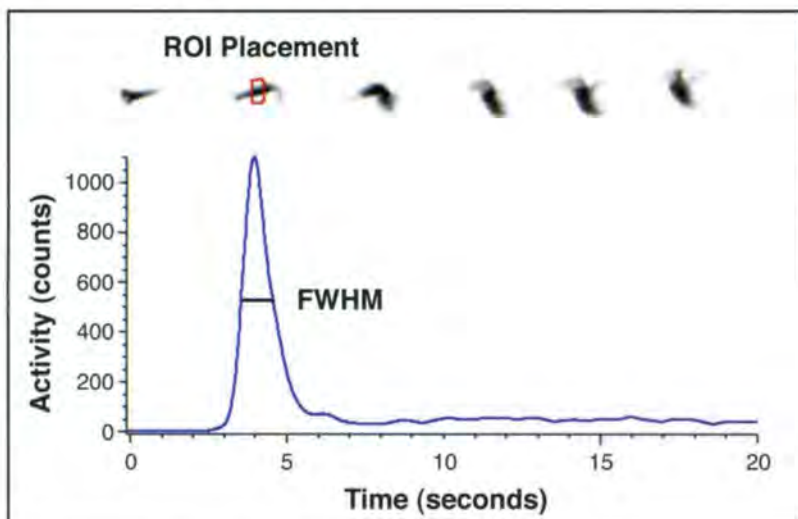
QP:QS, which allows for quantification of the magnitude of the shunt. Although the precise steps for image analysis will vary slightly depending on the software used, the principle behind the analysis is the same.

The only requirement for the radiopharmaceutical used in this study is that it must flow passively through the central circulation of the heart and lung. ^{99m}Tc-pertechnetate is the most commonly used radionuclide; ^{99m}Tc-DTPA or ^{99m}Tc-mebrofenin are also frequently used, especially if rapid clearance from the soft tissues is needed, for instance if the study needs to be repeated on the same day. A dose of 185–740 MBq is adequate for a dog; 74–185 MBq is sufficient for a cat.

It is necessary to set up a dynamic acquisition, with at least four (ideally eight) frames per second in order to have temporal resolution of the various phases of the cardiac cycle. A total acquisition time of 60 seconds is more than adequate. A low-energy, all-purpose collimator is used; matrix size is set at 64×64×16 or 128×128×16.

After positioning the patient on the gamma camera in left lateral recumbency and centring over the heart, the dynamic acquisition is started simultaneously with the bolus injection. To perform the injection, it is best to use a short extension tube connected to the intravenous catheter, and a three-way stopcock connecting the extension tube to the syringe containing the radiopharmaceutical dose and to a syringe of saline solution. The radiopharmaceutical can be loaded in the extension tube (it is important that the volume of radiopharmaceutical is no larger than the volume of the extension tube) and injected as a bolus using the saline flush.

Before analysing the study, it is necessary to perform a control step to ensure that the injection was performed in a bolus fashion and that the study is of acceptable quality. To do this, a region of interest (ROI) is drawn over the cranial vena cava (CrVC) from which the computer creates a time activity curve (TAC) that plots the counts in the CrVC ROI over time. An acceptable bolus shows a curve with a tall peak and a narrow base, with the width of the peak at half the maximum counts (full width half maximum, FWHM) measuring <2 seconds (Figure 5.1).



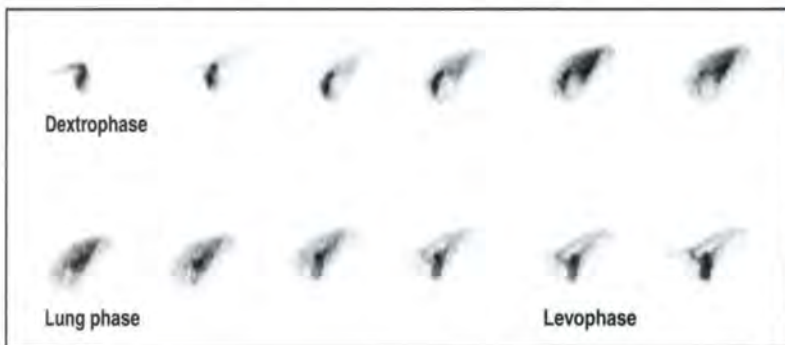
5.1 TAC from the CrVC in a normal dog illustrating a good bolus injection. The curve was obtained by drawing a ROI over the CrVC and plotting the counts in the ROI (y axis) over time in seconds (x axis). Notice the tall and narrow-based peak of the curve. The width of the peak at 50% of the peak maximum height (full width half maximum, FWHM) is 1 second, indicating an excellent bolus.

The evaluation of the study starts with a visual inspection: a normal first pass study is characterized by sequential passage of the radionuclide through the CrVC, right atrium, right ventricle (dextrophase), pulmonary arteries, lung, pulmonary veins (lung phase), left atrium, left ventricle and aorta (levophase). During the levophase, it should be possible to see the aorta clearly, because the lungs should be almost completely clear of the radiopharmaceutical (Figure 5.2).

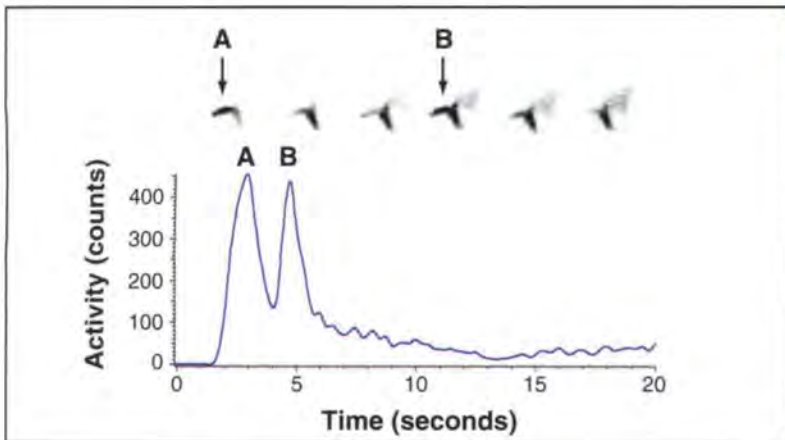
In a left-to-right shunt, the lungs do not clear because of recirculation of the radiopharmaceutical through the shunt into the pulmonary circulation. It should be noted that incomplete clearance of the lungs is also observed when the animal is in left heart failure, therefore evaluation of thoracic radiographs prior to the study is mandatory to rule out this differential. In addition, if the injection of radiopharmaceutical is

performed too slowly, the effect will be to simulate slow lung clearance; moreover, if too much pressure is used during the injection, the bolus can split between the cephalic or omobrachial vein and the axillobrachial vein, creating a double peak in the TAC, which may mimic a recirculation peak (Figure 5.3). In a right-to-left shunt, the aorta becomes visible at the same time as the pulmonary arteries.

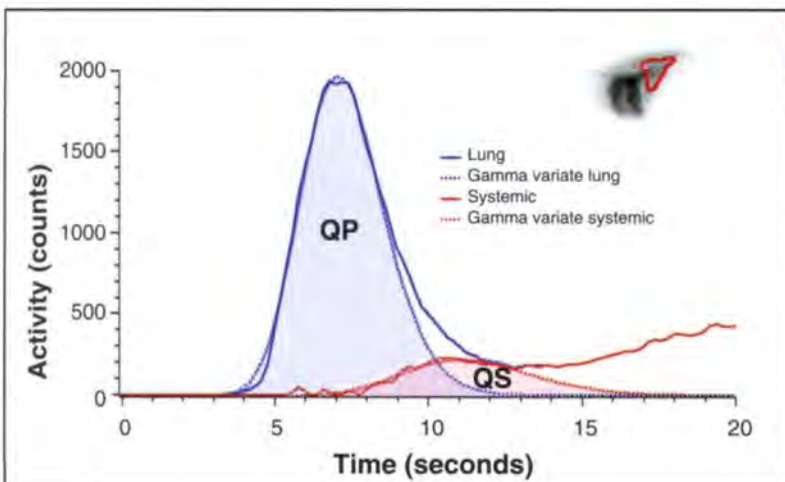
Quantitative analysis is performed by calculating the QP:QS. This is done by drawing a ROI over the caudodorsal lung field, avoiding the aorta, main pulmonary vessels and liver, and asking the computer to create a TAC that displays the lung counts over time. In a normal animal, there will be a peak as the bolus travels through the lungs, followed by a rapid fall (Figure 5.4). In an animal with a left-to-right shunt, a second peak is visible immediately after the first one,



5.2 Left lateral images illustrating a normal first pass radionuclide angiogram in a dog. The images are taken at a rate of 4 frames per second, representing the 3 seconds immediately after the intravenous injection of ^{99m}Tc -DTPA. The radionuclide outlines the CrVC, (top left), right heart, lungs, left heart and aorta. Notice that the margins of the aorta are distinct and the lung field clears completely (last two images, bottom right) during the levophase.



5.3 TAC from the CrVC in a normal dog illustrating a split bolus. This is an example of a biphasic bolus: the first peak in the TAC (A) is followed by a second peak (B), which may be erroneously interpreted as a recirculation peak compatible with a left-to-right shunt. This mistake is easily avoided by evaluating the TAC in conjunction with the dynamic acquisition.



5.4 Pulmonary TAC (blue) in a normal dog showing an initial increase and successive sharp fall of the pulmonary counts as the radioactive bolus passes through the pulmonary circulation (QP). The curve in red represents systemic activity in the lungs (QS), which is due to blood flow in the bronchial branches of the broncho-oesophageal artery. The dotted lines represent fitted curves, which were generated by the computer during the analysis and calculation of QP:QS ratio. The image in the top right corner illustrates positioning of the pulmonary ROI in the caudodorsal aspect of the lungs.

representing the recirculation of radionuclide into the lungs through the shunt (Figure 5.5). The computer software can then calculate a ratio of the area under the first pulmonary curve (QP) and the second recirculation (systemic) curve (QS). In a normal animal, the QP:QS ratio is <1.2 . It has been shown that the QP:QS ratio correlates well with percent of shunt. A QP:QS ratio of about 3, for instance, corresponds to a shunt fraction of about 50%.

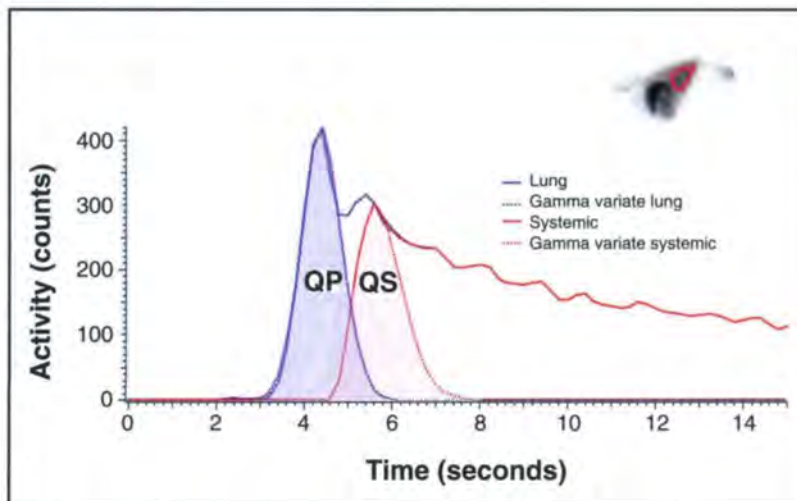
If the nuclear medicine computer does not have software for QP:QS analysis, an alternative procedure is to calculate the C2:C1 ratio. To calculate the C2:C1 ratio, a ROI is placed in the caudodorsal lung field in the same way as for QP:QS analysis, and a lung TAC is created. From the TAC, it is necessary to identify three points: C1, the maximum pulmonary counts, obtained at the peak of the pulmonary curve; Tmax, the time from the initial appearance of the bolus until the peak of the pulmonary curve (C1); and C2, the pulmonary counts at $2 \times T_{max}$ (Figure 5.6). A normal

C1:C2 ratio is <0.5 (the counts at C2 have to be less than half the counts at C1). While this method is easy to use, it is less accurate than the QP:QS ratio in distinguishing normal animals from animals that have a left-to-right shunt; that is, C2:C1 ratios in normal animals overlap with those of animals with left-to-right shunts to a much greater degree than the respective QP:QS values.

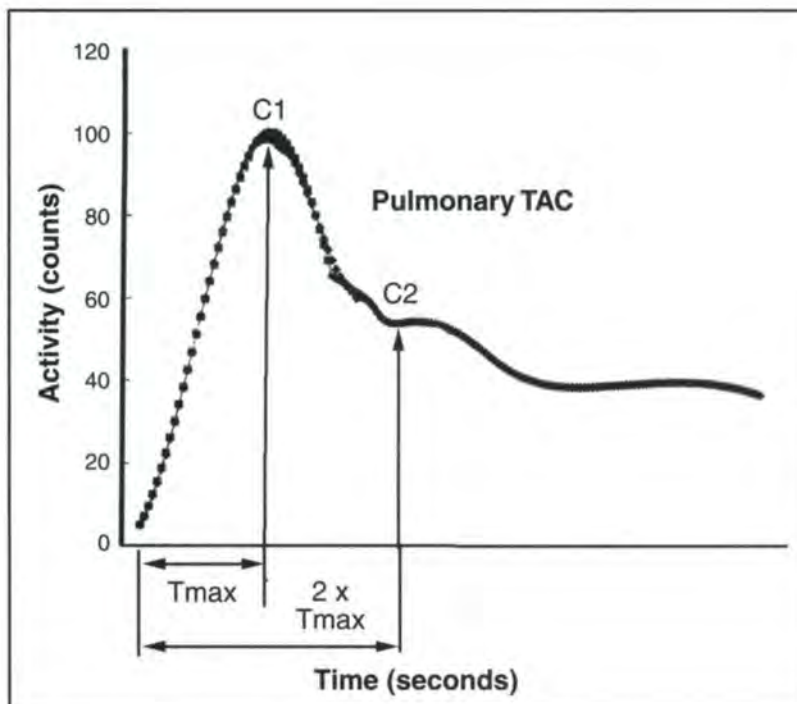
Pulmonary scintigraphy

Pulmonary scintigraphy for the evaluation of PTE and right-to-left shunts is easily performed and requires only the acquisition of static images; no particular software is necessary for image analysis.

Pulmonary perfusion imaging using the radiopharmaceutical ^{99m}Tc -MAA is based on physical blockade of the MAA particles in the first capillary bed encountered after intravenous injection. Because the MAA particles have a mean diameter of 10–40 μm , in a normal animal they lodge in the pulmonary capillaries



5.5 Pulmonary TAC in a dog with a left-to-right shunt. The curve was generated in the same way as the one in Figure 5.4. Notice the large systemic peak (QS), indicating recirculation of the radiopharmaceutical through the left-to-right shunt.



5.6 TAC in a dog with a left-to-right shunt, showing the reference points necessary for calculation of the C2:C1 ratio. C1 is the point of maximum pulmonary counts; Tmax is the time after the beginning of the pulmonary upslope at which C1 occurs; C2 is the point on the curve at $2 \times T_{max}$. The C2:C1 ratio in normal dogs should be <0.5 .

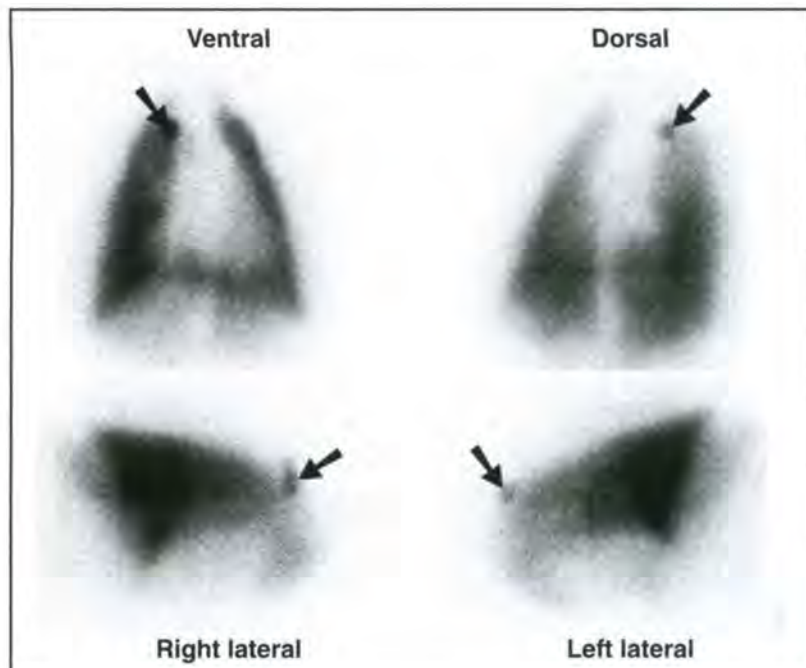
and their distribution is proportional to blood flow. The particles have a biological half-life of 4–6 hours, after which they are removed by pulmonary macrophages. The capillary embolization is therefore reversible.

A dose of 17.5 MBq is adequate for a cat or small dog, with up to 74 MBq for a large dog. For this particular radiopharmaceutical, it is important to estimate how many particles will be injected into the patient. Most commercially available kits contain 4–12 million particles: the typical dose in a 70 kg human patient is 1/10 of the kit, which is estimated to result in embolization of <0.1% of the pulmonary capillaries. In small animals, no more than 1/10 to 1/20 of the kit should be used. It is especially important to use the smallest possible particle dose when evaluating for a possible right-to-left shunt, and when pulmonary hypertension is suspected. In cases of documented severe pulmonary hypertension, the study is contraindicated. It is also better not to perform the study if adequate particle dilution cannot be reached, for instance in a very small dog or cat.

As the particles remain in position for several hours, the intravenous injection can be performed away from the gamma camera. It is better to image 1–5 minutes after the injection because as time elapses, some particles begin to be removed by macrophages, and the label begins to dissociate.

The radiopharmaceutical should be injected directly into the cephalic or saphenous vein; ^{99m}Tc-MAA has a tendency to form clots when mixed with blood in the syringe prior to injection, which can happen if the operator has difficulty in finding a vein and blood is withdrawn and allowed to remain in the syringe for a short period of time. The ^{99m}Tc-MAA clot does not represent a danger for the animal, but it will localize to the lungs creating an artefactual 'hot spot' that can be confusing during image interpretation (Figure 5.7). It is best to perform the injection with the animal in sternal recumbency to avoid collapse of the recumbent lung and ensure even distribution

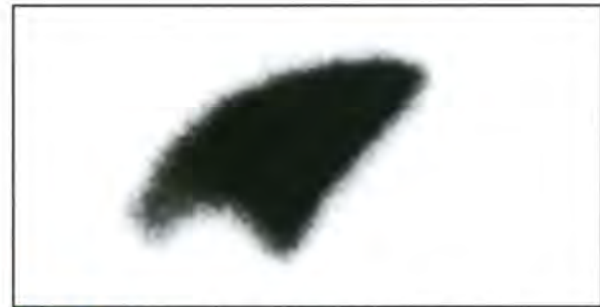
5.7 Pulmonary perfusion study in a dog presented for evaluation of possible PTE. Note the small but intense focus of activity in the apex of the right cranial lung lobe (arrowed). This was a ^{99m}Tc-MAA clot.



to the lung fields; it is important to remember that the distribution is proportional to blood flow.

When investigating possible right-to-left shunts, static right and left lateral, ventral and dorsal images of the whole body should be acquired. When the study is performed to evaluate for PTE, images are limited to the thorax and include additional oblique views. Matrix size is set at 256x256x16. Images should be acquired for 250,000–500,000 counts. A low-energy, all-purpose collimator is adequate.

In a normal animal, radioactivity is distributed exclusively to the lungs fields which have homogenous intensity (Figure 5.8). In animals with right-to-left shunts, radioactivity is seen in the systemic circulation and is especially noticeable in the capillaries of the renal cortices and cerebral hemispheres. In patients with PTE, wedge-shaped pleural-based perfusion defects are present, with the corresponding radiographs being normal or occasionally showing focal oligoemia and smaller than normal pulmonary vessels. Shunt fraction can be easily calculated by dividing the total extrapulmonary counts by the total body counts.



5.8 Left lateral view of the lungs of a normal dog after intravenous injection of approximately 37 MBq of ^{99m}Tc-MAA. Notice the uniform radiopharmaceutical distribution within the lungs, with no evidence of distribution outside the pulmonary capillaries. The smooth photopenic area seen cranioventrally represents the cardiac notch.

^{99m}Tc-MAA scintigraphy for evaluation of mucociliary function

Scintigraphy with ^{99m}Tc-MAA can also be used for the evaluation of mucociliary function in cases of suspected ciliary dyskinesia. The study is easy to perform, does not require specific software for image analysis, but does require general anaesthesia.

The animal is positioned in ventral recumbency on a table and the gamma camera positioned immediately dorsal to it and centred over the thorax. A low-energy, all-purpose collimator is adequate. A short ET tube must be used so that the tube does not interfere with ^{99m}Tc-MAA movement; a 90 degree connector with port is ideal to connect the ET tube to the anaesthetic machine.

Two external radioactive markers (⁵⁷Co or ^{99m}Tc) are placed along the side of the animal, one at the level of the caudal margin of the scapula or fifth intercostal space (which corresponds to the location of the carina), and the other 20 cm cranially. These markers will assist in the accurate deposition of the ^{99m}Tc-MAA droplet.

A sleeved catheter must be used to deposit a droplet of ^{99m}Tc-MAA at the tracheal bifurcation: a 10 Fr male urinary catheter with the tip removed works well as the outer sleeve, and a 5 Fr catheter can be used as the inner catheter. A small droplet of ^{99m}Tc-MAA (<30 MBq in 30 µl volume) is aspirated into the inner catheter; the inner catheter is then withdrawn into the outer catheter to avoid contamination of the trachea during positioning. The catheter is then advanced into the ET tube through the port at the right angle connection, or the anaesthetic machine is momentarily disconnected to allow placement of the catheter. The catheter is advanced until the radioactive ^{99m}Tc-MAA droplet is just cranial to the level of the caudal external radioactive marker (level of the carina); the persistence scope is used to assess the location of the catheter with respect to the external radioactive markers. The internal catheter is then advanced about 1 cm beyond the outer sleeve and a small volume of air is injected,

resulting in deposition of the radioactive droplet in the trachea. At this point the inner catheter is retracted into the outer catheter, the catheters are removed together from the trachea and, if necessary, the anaesthetic machine is reconnected.

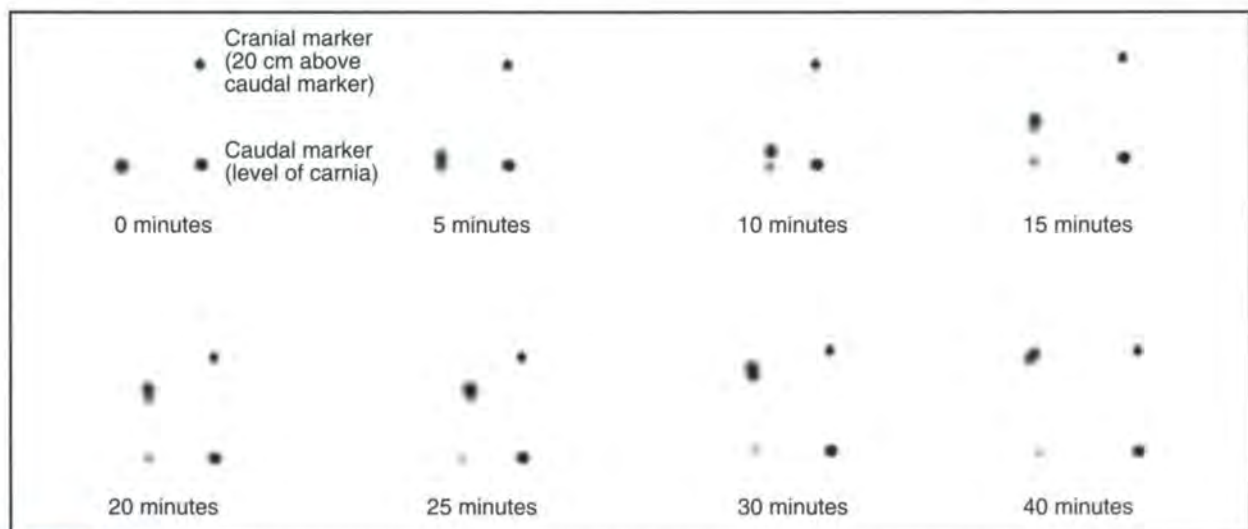
A series of 60 seconds dorsal static images is then acquired, starting just after radiopharmaceutical deposition, and then every 5 minutes for a total of 40 minutes afterwards. Matrix size is set at 256x256x16.

In a normal animal, the radiopharmaceutical droplet is cleared by the mucociliary apparatus and moves cranially as a discrete 'hot spot' (Figure 5.9). Movement usually starts 1–2 minutes after deposition. Sometimes a residual lower-intensity focus remains at the original site of deposition. In an animal with non-functional cilia, there will be no movement throughout the entire study. This is an 'all or nothing' type of evaluation: either the droplet moves, or it does not. The velocity at which the droplet moves varies greatly from animal to animal, even in healthy dogs and cats in the same age groups.

^{99m}Tc-pertechnetate scintigraphy for evaluation of cranial mediastinal masses

^{99m}Tc-pertechnetate scintigraphy can be used in the evaluation of cranial mediastinal masses, to determine whether a mass detected radiographically and/or ultrasonographically is thyroidal in origin. The technique is the same as for thyroid scintigraphy.

The administered dose is 74–185 MBq of ^{99m}Tc-pertechnetate in the dog and 37–148 MBq in the cat. A low-energy, all-purpose collimator is used; matrix size is set at 256x256x16. Image acquisition is best performed 20–30 minutes after injection. The animal is placed over the gamma camera and opposite lateral, ventral and possibly dorsal static images of the thorax are acquired for a minimum of 250,000 counts. A mass of thyroidal origin will show radionuclide uptake much like the thyroid gland does.



5.9 Mucociliary scan in a normal dog. The two static foci of radioactivity to the right of each image represent external markers positioned at the caudal border of the scapula and 20 cm cranial to it. The images are dorsal views obtained at 0, 5, 10, 15, 20, 25, 30 and 40 minutes after deposition of a small droplet of ^{99m}Tc-MAA just cranial to the carina. The radioactive droplet is at the level of the caudal external marker at 0 minutes (top left image); subsequently, the droplet moves cranially and is almost at the level of the cranial marker at 40 minutes (bottom right image).

References and further reading

- Alderson PO and Martin EC (1987) Pulmonary embolism: diagnosis with multiple imaging modalities. *Radiology* **164**, 297–312
- Bahr A, Miller M and Gordon S (2002) First pass nuclear angiocardigraphy in the evaluation of patent ductus arteriosus in dogs. *Journal of Veterinary Internal Medicine* **16**, 74–79
- Brawner WR and Daniel GB (1993) Nuclear imaging. *Veterinary Clinics of North America: Small Animal Practice* **23**, 379–398
- Daniel GB and Berry CR (2006) Pulmonary and mucociliary scintigraphy. In: *Textbook of Veterinary Nuclear Medicine, 2nd edn*, ed. GB Daniel and CR Berry, pp. 303–327. ACVR Publications, Tennessee
- Daniel GB and Brawner WB (2006) Thyroid scintigraphy. In: *Textbook of Veterinary Nuclear Medicine, 2nd edn*, ed. GB Daniel and CR Berry, pp. 181–198. ACVR Publications, Tennessee
- Daniel GB and Bright JM (1999) Nuclear imaging, computed tomography and magnetic resonance imaging of the heart. In: *Textbook of Canine and Feline Cardiology*, ed. PR Fox, D Sisson and NS Moise, pp. 193–203. WB Saunders, Philadelphia
- Daniel GB and Morandi F (2006) First pass radionuclide angiocardigraphy. In: *Textbook of Veterinary Nuclear Medicine, 2nd edn*, ed. GB Daniel and CR Berry, pp. 257–273. ACVR Publications, Tennessee
- Morandi F, Daniel GB, Gompf RE and Bahr A (2004) Diagnosis of congenital right-to-left shunts with ^{99m}Tc -MAA. *Veterinary Radiology and Ultrasound* **45**, 97–102
- Thrall DE, Badertscher RR, Lewis RE and McCall JW (1979) Scintigraphic evaluation of pulmonary perfusion in dogs experimentally infected with *Dirofilaria immitis*. *American Journal of Veterinary Research* **40**, 1426–1432
- Wolff RK (1987) Comparison of two methods of measuring tracheal mucous velocity in anesthetized Beagle dogs. *American Review of Respiratory Disease* **20**, 137–142
-

Basics of respiratory interventional radiology

Chick Weisse

General indications and limitations

Interventional radiology (IR) involves the use of contemporary imaging modalities, such as radiography, fluoroscopy and computed tomography (CT) to gain access to specific structures in order to deliver different materials for therapeutic purposes. These techniques are routinely used in human medicine; despite potential applications, however, these procedures have not yet been widely adopted in veterinary medicine. This chapter focuses on the use of IR techniques for tracheal diseases. The relatively high morbidity and mortality rates associated with surgery of the cervical and intrathoracic trachea make IR techniques particularly well suited for this location.

Advantages

The use of IR techniques in veterinary patients offers a number of advantages compared with more traditional therapies:

- Minimally invasive procedures reduce perioperative morbidity and mortality, and shorten anaesthesia and hospitalization times. Some less equipment-intensive procedures can result in reduced costs as well
- Alternative treatment options for certain patients in which traditional therapies have failed or are unavailable, declined or contraindicated.

Disadvantages

- Some degree of technical expertise required.
- Specialized equipment required.

The majority of IR procedures performed within the trachea are not equipment-intensive, and most are carried out on non-emergency cases so the necessary equipment can be purchased when needed. In addition, for those who do not have fluoroscopy readily available, some of these techniques have been performed with endoscopic guidance or rapidly obtained digital radiography alone.

Equipment

As tracheal IR procedures are performed through the endotracheal (ET) tube, traditional sterile operating rooms are not required. The majority of these types of procedures can be performed in clean radiography/

angiography suites whilst wearing sterile latex gloves. In general, the largest diameter ET tube possible should be selected (at least 4 mm inner diameter) to facilitate unrestricted passage of devices through the tube whilst permitting simultaneous oxygen delivery and ventilation during the procedure. An ET tube with a radiopaque line or markers should always be used when possible, to help avoid inadvertent deployment of stents within the tube. The use of sterile ET tubes is debatable and not routinely required by the author as the trachea is not generally considered a sterile environment.

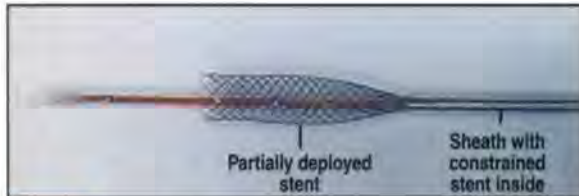
Radiation exposure during conventional or C-arm fluoroscopy can be substantial. The operator should review radiation safety guidelines, minimize exposure time and maximize shielding and distance from the beam as well as X-ray beam collimation. Those present during the procedure should always wear full lead gowns and lead thyroid shields, and only stay in the non-shielded parts of the room if their presence is essential during the radiological exposure. A traditional fluoroscopy unit is sufficient for the majority of tracheal IR procedures currently performed. A C-arm fluoroscopy unit has the advantage of mobility of the image intensifier, permitting multiple tangential views without moving the patient.

A general review of IR equipment is beyond the scope of this chapter, but a brief discussion of certain devices is necessary to understand how these procedures are performed:

- *Guidewires.* These are flexible, often angle-tipped and hydrophilic (slippery) coated wires used to gain access to different structures under direct fluoroscopic visualization
- *Catheters.* These are long (typically 65–100 cm) and designed to be advanced over a guidewire. For IR procedures, 'marker catheters' with radiopaque centimetre markings are typically used in order to calculate radiographic magnification and determine the length and diameter of both the normal and narrowed tracheal segments
- *Stents.* These devices are designed to hold the tracheal lumen open in the presence of tracheal collapse, stenosis or malignant obstruction. Self-expanding metallic stents (SEMSs) are most commonly used in veterinary patients. These devices are typically made of nitinol

(nickel–titanium alloy) or stainless steel and are compressed on to very narrow delivery systems, which can be introduced through the ET tube and placed across a narrowed area. Upon release, the stent resumes its original dimensions within the tracheal lumen (Figure 6.1)

- *Snares/stone baskets.* These devices are similar to their endoscopic counterparts (and are often used interchangeably) and are used to retrieve tracheal foreign bodies under fluoroscopic guidance.



6.1 Nitinol mesh self-expanding metallic stent, for intraluminal tracheal stenting, and delivery system during partial deployment

Tracheal collapse

Mild to moderate cases of tracheal collapse can usually be controlled with medications including anti-inflammatories, cough suppressants, sedatives/tranquillizers and bronchodilators. In addition, weight loss, restricted exercise and removal of second-hand smoke or inhaled allergens can further palliate symptoms. Those patients that have failed to respond to aggressive medical and environmental management, and have had other causes of respiratory disease either treated or ruled out, become candidates for surgical or interventional treatment. The decision to perform surgery or stenting is a complicated and unresolved one. Regardless, all animals should receive aggressive medical and environmental management before considering either of these treatment options. Patients must be treated on an individual basis; however, some basic guidelines can be used:

- Surgical rings should be considered when cervical tracheal collapse is present
- Intraluminal stent placement should be considered in a geriatric patient or in a patient with excessive co-morbidities (extensive cardiac or pulmonary disease, endocrinopathies, etc.) in which prolonged anaesthesia or healing could preclude more invasive surgery
- Avoid intraluminal stent placement in younger animals as long-term follow-up (>5 years) in tracheal stented animals has not yet been completed
- If only intrathoracic tracheal collapse is present then surgery is unlikely to resolve the problem and will probably be associated with excessive morbidity; therefore, an intraluminal stent should be considered
- Patients with both cervical and intrathoracic tracheal collapse can be managed with either a

single long stent spanning both segments, or with surgical rings in the cervical trachea and a stent for the intrathoracic trachea

- Use of intraluminal tracheal stents in patients with bronchial collapse is currently debatable. Placement of stents within collapsing mainstem bronchi will not address collapse of more distal bronchi so are not typically performed; however, tracheal stents in these patients may offer significant palliation.

Various surgical techniques have been described; however, the currently recommended surgical therapy for patients with extrathoracic tracheal collapse is extraluminal polypropylene ring prostheses; this is associated with a relatively high morbidity and mortality.

Advantages of stenting

- Minimal invasiveness.
- Shorter anaesthesia times.
- Access to the entire intrathoracic trachea.

Reported side effects

- Stent shortening.
- Excessive granulation/inflammatory tissue.
- Progressive tracheal collapse.
- Stent fracture.

Technique

A complete description of the technique used for tracheal stent placement is beyond the scope of this chapter.

Extent of collapse

Real-time fluoroscopy should be performed in the awake patient to determine the extent of collapse. When possible, coughing is induced to observe the results of the extreme dynamic airway pressures normally experienced by the patient. Bronchial collapse can often be identified with fluoroscopy as well and should be noted when present.

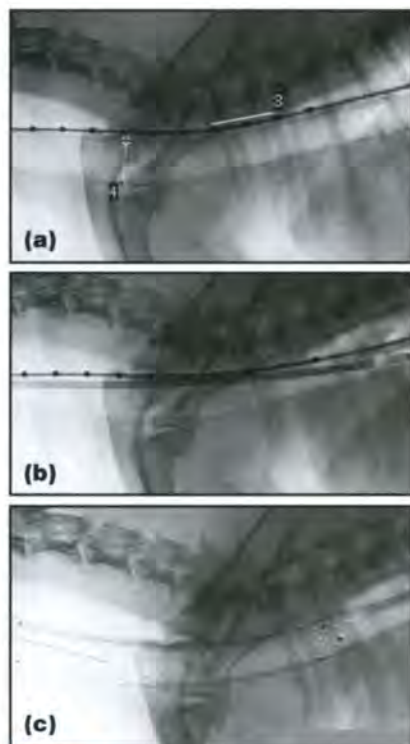
Patient preparation

A rapid induction and recovery are preferred when possible. Premedications are not routinely used; however, an antitussive/sedative combination can be effective if intravenous catheterization causes excessive anxiety and/or distress. Preoxygenation of the patient is routinely performed and, unless contraindicated, a combination of intravenous propofol and diazepam is used with minimal inhalant anaesthesia concentrations. Perioperative antibiotic use for these procedures is debatable and chosen on an individual basis. Unless contraindicated, these patients typically receive one perioperative dose of dexamethasone (0.1–0.25 mg/kg i.v.).

Tracheal and stent sizing

The patient is placed under general anaesthesia and positioned in lateral recumbency. A hydrophilic guidewire and marker catheter combination are placed within the mouth and the guidewire is

advanced down the oesophagus under fluoroscopic guidance. The marker catheter is advanced over the wire and positioned within the oesophagus over the pre-determined level of tracheal narrowing. Positive pressure ventilation of 20 cmH₂O is maintained to achieve maximal tracheal dilation while a radiograph is obtained. The radiopaque catheter markings are used to extrapolate the maximal tracheal diameter and the length of stent necessary, accounting for radiographic magnification (Figure 6.2a).



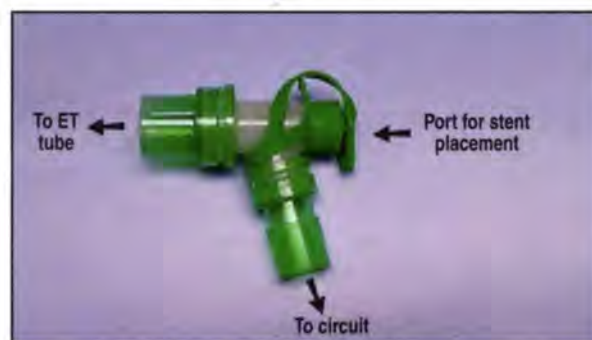
6.2 Serial lateral thoracic fluoroscopic images during tracheal sizing and stent placement. **(a)** Using positive pressure ventilation and an oesophageal marker catheter, measurements are taken to establish the maximal tracheal diameter. **(b)** The stent delivery system is advanced into the trachea. Note that the cervical and intrathoracic trachea are in line to facilitate unimpeded passage of the stent. **(c)** Restoration of a patent trachea immediately following placement of an intraluminal tracheal stent.

The tracheal stent chosen should have a diameter approximately 15–20% greater than the maximal tracheal diameter and a length approximately 2 cm longer than the area of narrowing (to span approximately 1 cm cranial and 1 cm caudal to the area of collapse).

Stent placement

Deployment properties vary depending upon the design of the stent. Some stents shorten significantly upon deployment and some stents are reconstrainable to some degree (can be recaptured within the delivery system before full deployment). The operator MUST read the manufacturer's instructions in order to understand the specific properties of the stent being used for a particular case. Once the stent has been chosen, it is removed from its packaging using sterile

technique and prepared and flushed with saline according to manufacturer recommendations. A right-angle bronchoscope adapter is attached to the ET tube to facilitate unrestricted passage of the stent delivery system through the tube while maintaining the anaesthetic circuit (Figure 6.3). The constrained, radiopaque stent is easily visualized under fluoroscopy. Once the distal end of the stent has been positioned appropriately, stent deployment can proceed (see Figure 6.2b). Following stent deployment, the delivery system is carefully removed under fluoroscopic guidance to avoid excessive contact with the unconstrained stent. Subsequent radiographs are necessary to document the final position of the stent within the trachea (see Figure 6.2c).



6.3 Bronchoscope adapter used to maintain a complete anaesthetic circuit whilst passing the stent delivery system through the bronchoscope opening and down the ET tube.

Recovery

The patient typically recovers in an intensive care unit setting and is provided with supplemental oxygenation as needed. Butorphanol (0.1–0.2 mg/kg i.v.) and/or acepromazine (0.005–0.01 mg/kg i.v.) are often useful to facilitate a smooth recovery.

Postoperative care and follow-up

Patients are routinely discharged 1 or 2 days after stenting with a 3–6-week tapering dose of prednisone (initial dose of 1–2 mg/kg/day orally), continued anti-tussive therapy (hydrocodone 0.25 mg/kg orally q6–12h or higher doses if tolerated) and a course of broad-spectrum, oral antibiotics. Owners should anticipate an initial dry cough that improves over the following 3–4 weeks. Aggressive medical management of coughing is imperative for a good long-term outcome and the majority of patients will require life-long medication following tracheal stenting. The initial recheck examination is approximately 2 weeks after stenting or sooner if problems arise. Repeat examinations are performed regularly (every 3–6 months if possible, sooner if the patient's clinical signs worsen).

Malignant or benign airway obstruction

Veterinary patients can present with advanced stages of malignancy in which traditional therapies such as surgery, chemotherapy or radiation therapy are associated with excessive morbidity, cost or poor

outcome. Presenting clinical signs may be associated with the tumour location and subsequent local effects rather than the systemic effects of the tumour burden, e.g. a tracheal tumour resulting in subsequent airway obstruction (Figure 6.4). Benign conditions can also result in subsequent tracheal stricture formation, leading to progressive airway obstruction. The techniques described above have been used for the treatment of tracheal malignancies or stenoses secondary to trauma when surgical procedures were declined, not indicated, or expected to result in excessive morbidity or mortality. The author has placed stents for intrinsic malignant tracheal obstructions; however, tracheal stents could also provide palliation for extrinsic compression of the airways.

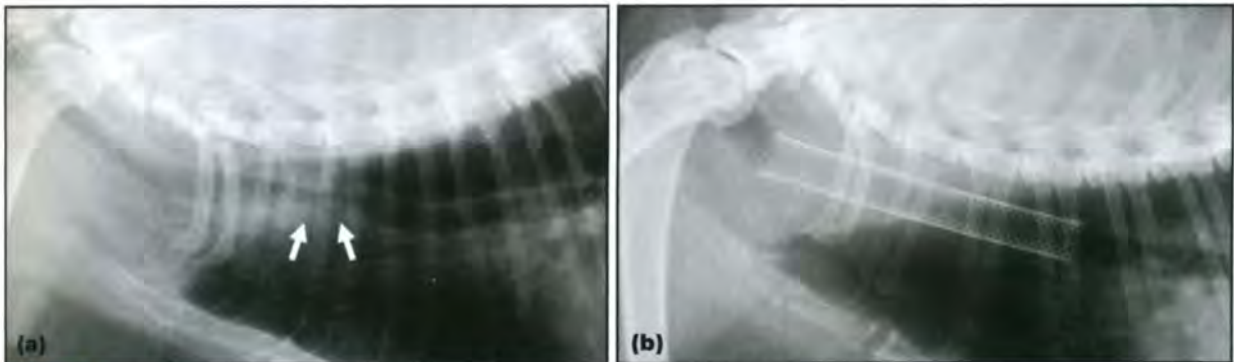
Tracheal foreign bodies

IR techniques are useful for retrieval of obstructive tracheal or bronchial foreign bodies, particularly in

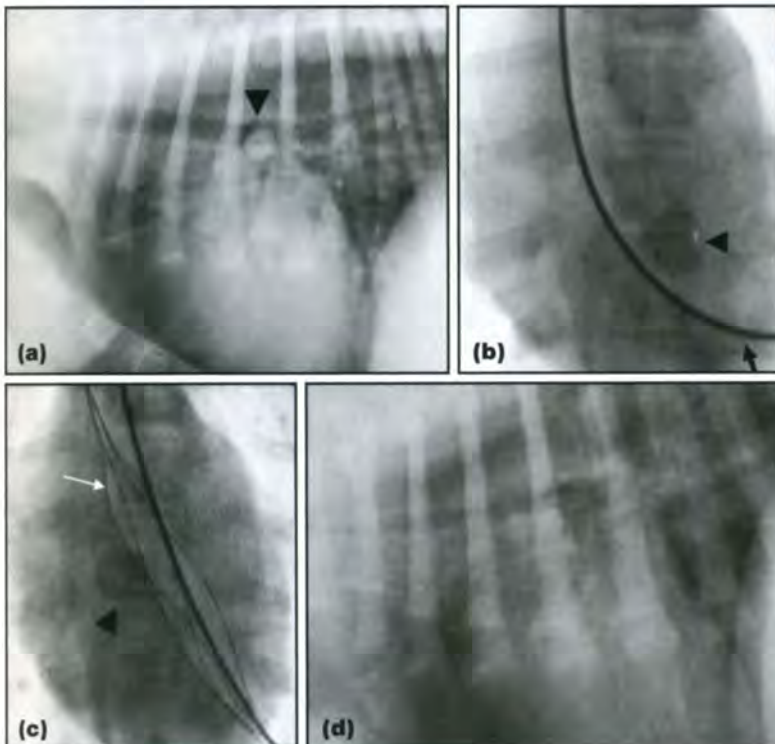
very small patients where surgery or endoscopy would be either dangerous or impossible. Occasionally, tracheal diameter restrictions require extubation before tracheoscopy/bronchoscopy can be performed. The endoscopes used are often occlusive in these small patients, impairing adequate ventilation. The techniques described above allow passage of very narrow snares or stone baskets through a bronchoscope adapter and ET tube while a complete anaesthetic circuit is maintained (Figure 6.5).

References and further reading

- Buback JL, Boothe HW and Hobson HP (1996) Surgical treatment of tracheal collapse in dogs: 90 cases (1983–1993). *Journal of the American Veterinary Medical Association* **208**, 380–384
- Moritz A, Schneider M and Bauer N (2004) Management of advanced tracheal collapse in dogs using intraluminal self-expanding biliary wall stents. *Journal of Veterinary Internal Medicine* **18**, 31–42
- Radlinsky MG, Fossum TW, Waler MA *et al.* (1997). Evaluation of the palmaz stent in the trachea and mainstem bronchi of normal dogs. *Veterinary Surgery* **26**, 99–107



6.4 Lateral thoracic radiographs of a cat with tracheal carcinoma. **(a)** Note the intrathoracic tracheal narrowing (arrowed) due to the tumour. **(b)** The tracheal lumen has been restored immediately following placement of an intraluminal stent.



6.5 Radiographic and fluoroscopic images of an 8-week-old Boxer puppy with a 'plastic bead' tracheobronchial foreign body. **(a)** Lateral radiograph demonstrating the large radiopaque foreign body at the level of the carina (arrowhead). **(b)** Ventrodorsal fluoroscopic image (inverse greyscale) showing the foreign body (arrowhead) in left mainstem bronchus and the guidewire (arrowed). **(c)** Ventrodorsal fluoroscopic image (inverse greyscale) showing the stone basket (arrowed) in left mainstem bronchus before grabbing the foreign body now located in right mainstem bronchus (arrowhead). **(d)** Lateral thoracic radiograph immediately following retrieval of the foreign body.

The heart and major vessels

Victoria Johnson, Kerstin Hansson, Wilfried Mai,
Joanna Dukes-McEwan, Nola Lester, Tobias Schwarz,
Peter Chapman and Federica Morandi

Radiographic anatomy

A thorough understanding of anatomy is an essential part of diagnostic imaging of the heart and cardiovascular system. This section covers the normal physiological and radiographic anatomy of the heart and the major vessels. An introduction to performing radiographic cardiac mensuration is also provided. The following section on interpretive principles covers the radiographic assessment of cardiac chamber enlargement, major vessel enlargement and differential diagnoses.

A full discussion of the ultrasonographic anatomy of the heart is beyond the scope of this manual. Chapter 2 provides information on performing an echocardiographic examination.

Basic cardiac anatomy

The heart is the largest mediastinal organ and its anatomy is complex. The heart develops from paired endocardial tubes that arise from splanchnic mesoderm. These gradually fuse and undergo elongation, various dilatations and constrictions, and finally partition into chambers to form the heart. A full description of the embryological origin of the heart is beyond the scope of this chapter, but a good understanding of cardiac formation will improve understanding of congenital heart disease.

Partitioning of the heart results in four chambers (right and left atria and right and left ventricles) and two great arteries (the aorta and main pulmonary artery):

- Blood enters the right atrium (RA) from the cranial and caudal venae cavae and the coronary sinus
- Blood leaves the right ventricle (RV) via the main pulmonary artery
- Blood enters the left atrium (LA) from the pulmonary veins
- Blood leaves the left ventricle (LV) via the aorta.

Valves divide the chambers. Each valve has a fibrous annulus and a number of cusps or leaflets. The atria are separated from the ventricles by atrioventricular valves: the mitral valve on the left and the tricuspid valve on the right. Both atrioventricular valves have two cusps and the term 'tricuspid' is a misnomer derived from human terminology. The ventricles are separated from the major arteries by semilunar valves (both have three cusps); the aortic on the left and the pulmonic on the right.

The four chambers of the heart are encased within the pericardium or pericardial sac. There are two layers forming the pericardium:

- The *fibrous* pericardium – a strong external layer
- The *serous* pericardium – a thin lining that covers the heart. This is divided into parietal and visceral layers and there is a small amount of lubricating fluid between these layers.

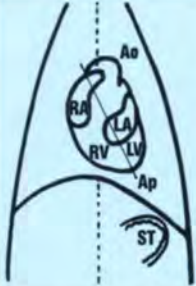
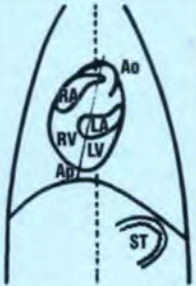
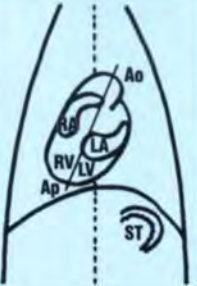
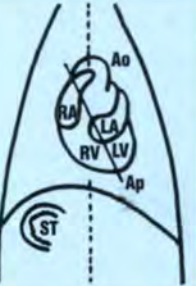
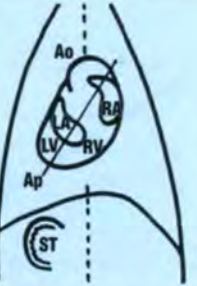
The heart itself is supplied with blood by the coronary arteries. The left and right main coronary arteries arise from the root of the aorta. Venous drainage is via the coronary veins and the coronary sinus.

Normal cardiac radiographic anatomy

The heart dominates a thoracic radiograph as it is the largest single soft tissue opacity in the thorax. It sits within the mediastinum from approximately the third to the sixth intercostal space. The larger, more dorsal part of the heart is known as the *base* and the smaller, more ventral part is known as the *apex*.

In the lateral view the apex is formed by the interventricular septum (IVS). The heart lies at an angle within the thorax (easily seen on the lateral view) with the apex positioned more caudally than the base. The apex usually points towards the *left* on a dorsoventral/ventrodorsal (DV/VD) view. Variation in the location of the apex on a DV/VD view may be extrinsic (e.g. due to alteration in lung volume) or intrinsic (a congenital malpositioning of the heart). The latter may be an incidental finding or associated with other pathological abnormalities (e.g. situs inversus in Kartagener's syndrome) (Figures 7.1 and 7.2).

The actual outline of the heart is not seen on a radiograph. Instead, the term *cardiac silhouette* is used to include the heart, pericardium, pericardial contents (such as fat and a small amount of fluid) and the origin of the aorta and main pulmonary artery. This is in contrast to an echocardiographic examination where the heart, origin of the major vessels, pericardium and pericardial contents are seen as separate structures. The outline of the cardiac silhouette is smooth, and details such as the coronary grooves and the separation of atria from the ventricles are *not seen*. The coronary arteries and veins are also not seen radiographically. However, it is possible to infer the location of the major chambers on a radiograph and to identify pathological changes in their size to some extent (see below).

	Levoposition	Dextroposition	Dextroversion	Levocardia	Dextrocardia
Cause	Normal	Displacement or congenital malposition	Congenital malposition	Congenital malposition	Congenital malposition
Location of viscera	Situs solitus	Situs solitus	Situs solitus	Partial situs inversus	Total situs inversus
Image					
Description	Normal situation in dogs and cats The heart is located slightly to the left and the apex points towards the left	Normal variant The apex is positioned more towards the right than normal. May be extrinsic (e.g. due to mediastinal shift) or intrinsic (actual embryological abnormality)	Congenital abnormality where the heart is positioned in the right side of the thorax Dextroversion also means that the heart is 'twisted' with the LV lying in the correct left-sided position but lying anterior to the RV	Heart is positioned on the left side of the thorax Mirror image arrangement of the abdominal viscera	Heart is positioned on the right side of the thorax Mirror image arrangement of the thoracic and abdominal viscera The most important of the positional abnormalities. Other congenital cardiac abnormalities may be present. May be seen as part of Kartagener's syndrome along with bronchiectasis and recurrent sinusitis

Definitions:

Dextrocardia – location of the heart in the right side of the thorax, the apex pointing towards the right. The cardiac chambers are reversed
 Dextroposition – displacement towards the right
 Dextroversion – version (turning) to the right. In terms of the heart, dextroversion means the location of the heart in the right thorax, the LV lying in the correct position on the left but lying cranial to the RV
 Levocardia – location of the heart in the left side of the thorax, the apex pointing towards the left
 Levoposition – displacement towards the left
 Situs inversus – the thoracic and abdominal viscera are reversed (i.e. a mirror image of the normal arrangement)
 Situs solitus – the thoracic and abdominal viscera are in a normal location
 There is some controversy over the exact definitions but those listed above are most commonly accepted

7.1 Cardiac position as seen on a DV radiograph. Variation in position may be a normal variant or a congenital abnormality. Some of the reported congenital abnormalities are included; many other variants are possible. Ao = Aorta; Ap = Apex; LA = Left atrium; LV = Left ventricle; RA = Right atrium; Right ventricle; ST = Stomach. (Line diagrams adapted from Suter (1984) with permission)

The central and ventral margins of the cardiac silhouette are easily outlined on a radiograph as these areas are surrounded by contrasting air in the lungs. It is not possible to outline the margins of the heart in the area of the heart base as the surrounding soft tissues, i.e. the major blood vessels (aorta, main pulmonary artery and pulmonary veins) and lymph nodes, have the same radiographic opacity. It is often difficult radiographically to appreciate changes and

pathology in this region, and ultrasonography and computed tomography (CT) are useful as alternative imaging modalities.

Many factors alter the appearance of a normal cardiac silhouette on a radiograph and this is a major source of misdiagnosis and confusion in thoracic radiography. These include tremendous variation with *breed*, as well as variation with respiratory phase, age and body condition and radiographic view (see below).



7.2 Dextroposition identified as an incidental finding in a dog. The cardiac silhouette and apex are located more in the right hemithorax than in the left and there is no evidence to suggest that this is associated with a mediastinal shift. Note the normal aorta (arrowed) on the left and the gastric fundus (St) also seen on the left; there is no suggestion of a situs inversus in this dog.

Identifying the cardiac chambers

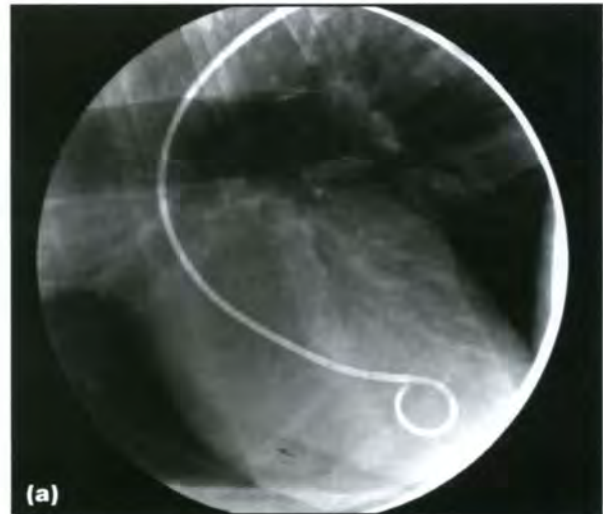
The internal chambers of the heart and the lumens of the great vessels can only be visualized on a radiograph with the administration of positive contrast media. This is known as angiocardiography (see Chapter 1). However, it is possible to use the location of the borders of the various chambers to assess cardiac or great vessel enlargement on a standard radiographic series.

Normal angiocardiograms are very useful in understanding the location of the chambers within the shadow of the cardiac silhouette (Figures 7.3 and 7.4). These have been used to formulate useful diagrams showing the radiographic location of the cardiac chambers (Figures 7.5 and 7.6).

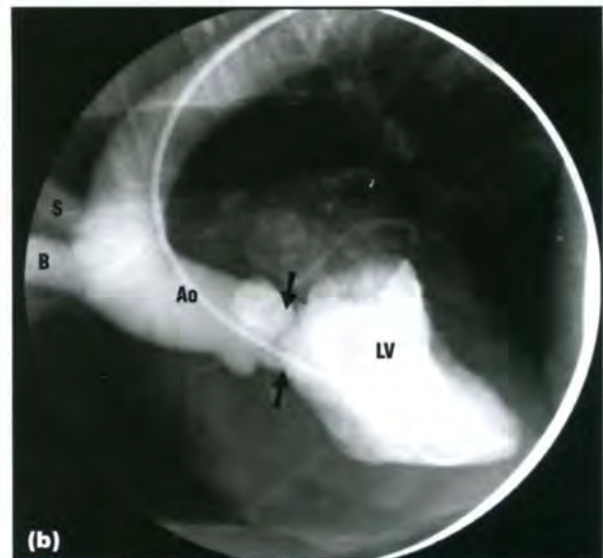
The presence of pericardial effusion usually precludes the evaluation of changes in specific cardiac chambers.

Some basic rules help in the assessment of cardiac chambers:

- In the dog the LV and LA are located on the left and caudal aspect of the heart; the RV and RA are located on the right and cranial aspect of the heart
- The position of the cardiac apex can be used to separate the right and left sides of the heart
- On a lateral view the RV is cranial to the apex and on a VD/DV view it is to the right. The reverse is true for the LV



(a)



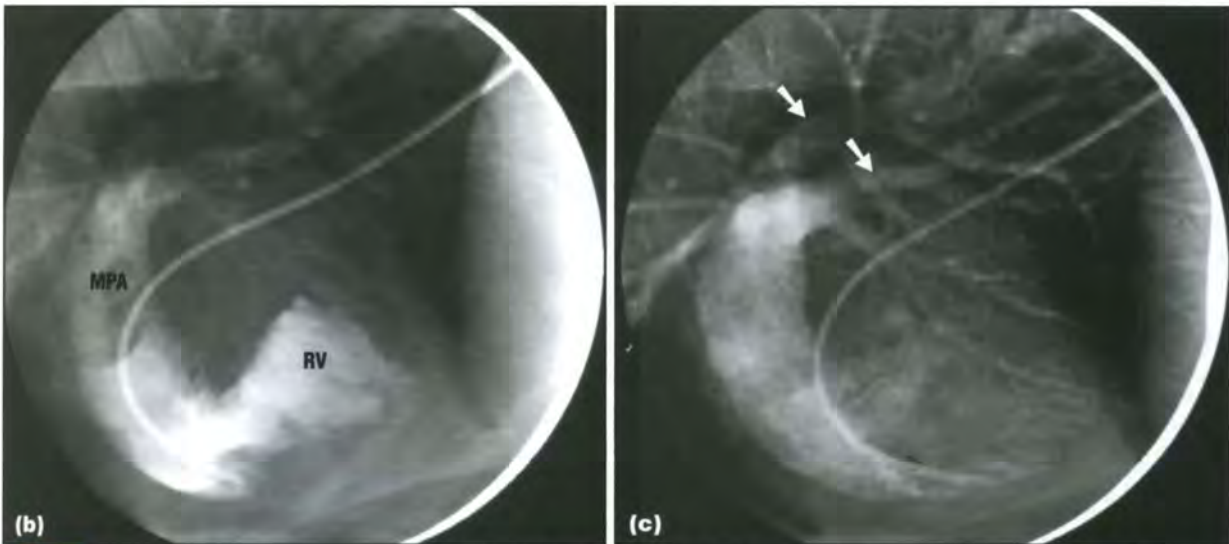
(b)

7.3 Normal left-sided angiocardiogram of a 5-year-old Golden Retriever. **(a)** The catheter has been placed into the LV via the femoral artery and aorta ready for the contrast medium injection. **(b)** Positive contrast medium outlines the LV, aortic valve (arrowed), ascending aorta (Ao), brachiocephalic trunk (B) and left subclavian artery (S). (Courtesy of J. Buchanan)

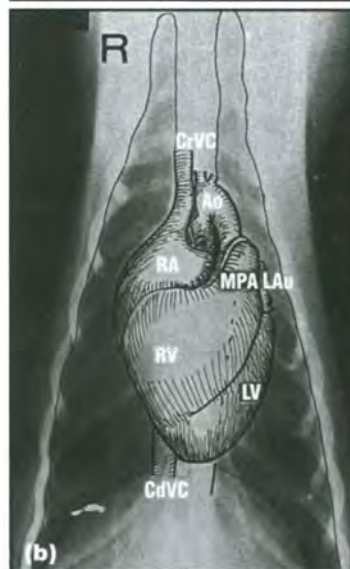
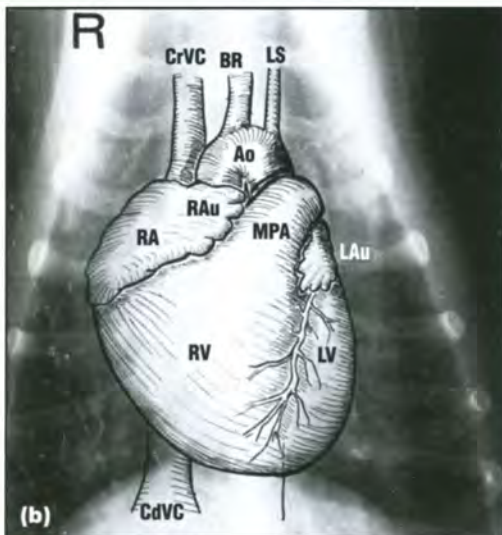
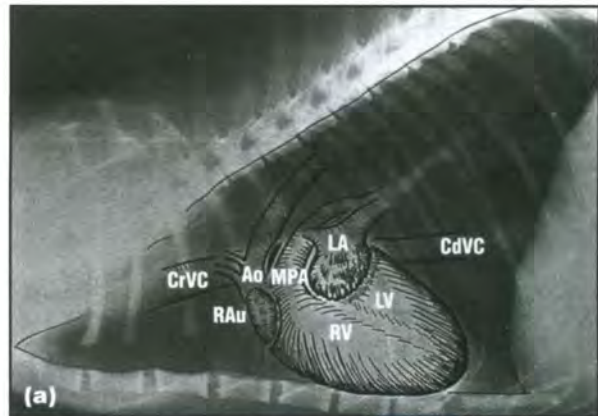
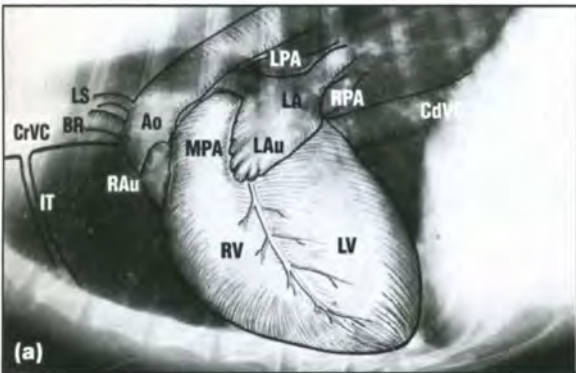


(a)

7.4 Normal right-sided angiocardiogram of the dog in Figure 7.3. **(a)** The catheter has been placed into the RV via the CdVC ready for the contrast medium injection. (Courtesy of J. Buchanan) (continues) ▶



7.4 (continued) Normal right-sided angiogram of the dog in Figure 7.3. **(b)** Positive contrast medium is present within the RV and has started to enter the RVOT and main pulmonary artery (MPA). **(c)** The contrast medium has now reached the left and right pulmonary artery branches (arrowed) and the smaller pulmonary arterial branches in the lungs. (Courtesy of J. Buchanan)



7.6 Location of the cardiac chambers on thoracic radiographs of a cat. **(a)** Lateral view. **(b)** Ventral view. Ao = Aortic arch; CdVC = Caudal vena cava; CrVC = Cranial vena cava; LA = Left atrium; LAu = Left auricular appendage; LV = Left ventricle; MPA = Main pulmonary artery; RA = Right atrium; RAu = Right auricular appendage; RV = Right ventricle. (Reproduced from Suter (1984) with permission)

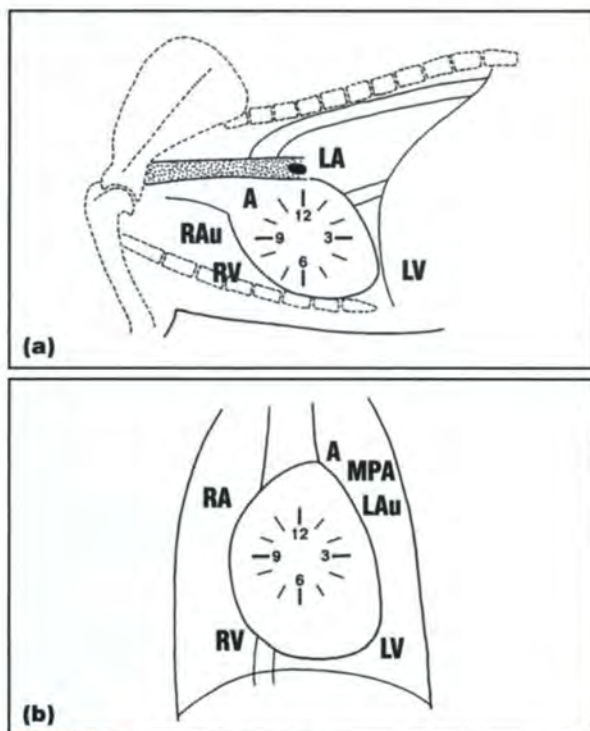
7.5 Location of the cardiac chambers on thoracic radiographs of a dog. **(a)** Lateral view. **(b)** Ventral view. Ao = Aortic arch; BR = Brachiocephalic trunk; CdVC = Caudal vena cava; CrVC = Cranial vena cava; IT = Internal thoracic arteries and veins; LA = Left atrium; LAu = Left auricular appendage; LPA = Left pulmonary artery; LS = Left subclavian artery; LV = Left ventricle; MPA = Main pulmonary artery; RA = Right atrium; RAu = Right auricular appendage; RPA = Right pulmonary artery; RV = Right ventricle. (Reproduced from Suter (1984) with permission)

- The exact apical point can be difficult to determine due to the variation in cardiac position. This can sometimes make evaluation of left-versus right-sided enlargement difficult
- The two atria are located dorsal to the level of the caudal vena cava (CdVC) on a lateral view

- The dorsal and caudodorsal borders of the LA do not have a distinct outline as the pulmonary veins enter in this area and the right pulmonary artery also overlaps this region.

Clock face analogy

A clock face analogy has been used to identify specific chamber locations on a radiograph. The clock numbers are used to indicate the approximate position of the chambers and great vessels (Figure 7.7).



7.7 Clock face analogy identifying the location of the cardiac chambers. **(a)** Lateral view. **(b)** DV view. A = Aorta; LA = Left atrium; LAu = Left auricular appendage; LV = Left ventricle; MPA = Main pulmonary artery; RA = Right atrium; RAu = Right auricular appendage; RV = Right ventricle. (Reproduced from Dennis *et al.* (2001) with permission from the publisher)

Lateral view

- 12.00–02.00 o'clock: left atrium
- 02.00–05.00 o'clock: left ventricle
- 05.00–09.00 o'clock: right ventricle
- 09.00–10.00 o'clock: main pulmonary artery and right auricular appendage
- 10.00–11.00 o'clock: aortic arch

Dorsoventral view

- 11.00–01.00 o'clock: aortic arch
- 01.00–02.00 o'clock: main pulmonary artery
- 02.30–03.00 o'clock: left auricular appendage
- 02.00–05.00 o'clock: left ventricle
- 05.00–09.00 o'clock: right ventricle
- 09.00–11.00 o'clock: right atrium

Species differences

- On a VD/DV view the cardiac apex points more to the left in the dog. In the cat the apex is more variable, but usually closer to the midline.
- In the dog the left auricular appendage (LAu) is located at 02.30–03.00 o'clock on the DV/VD view. In the cat the LA and LAu are located at 01.00–02.00 o'clock on this view and the main pulmonary artery may be cranial to this or not seen at all.
- In the cat the more cranial location of the LA may make it difficult to see on the lateral view.
- In the dog, when the LA is enlarged on the DV/VD view it is superimposed over the cardiac silhouette in the 05.00–07.00 o'clock position (between the caudal mainstem bronchi), whereas in the cat, it is located more cranially at the 01.00–02.00 o'clock position. This explains the so-called 'valentine heart shape' seen only in the cat and created by left ± right atrial enlargement.

Factors affecting cardiac size and appearance

Many factors can alter the appearance of the normal heart on a radiograph. It is extremely important to be aware of the influence of these factors to avoid the misdiagnosis of normal anatomical variation as disease. These include breed, pericardial fat, age, body position, respiratory phase and cardiac cycle.

Species difference

- The normal canine heart shows substantial breed-associated variations in size and shape. The normal feline heart is generally unaffected by breed (Figure 7.8).
- Variation in cardiac shape and size with body position is an important consideration in the dog. Generally size and shape alteration with body position are negligible in the cat.



7.8 The normal cardiac silhouette in a cat is fairly constant between different breeds. **(a)** It is a neat ovoid shape on lateral views. (continues)



7.8 (continued) The normal cardiac silhouette in a cat is fairly constant between different breeds. **(b)** The cardiac silhouette is also ovoid on the DV view. Alteration in cardiac shape is useful in radiographic diagnosis of cardiac disease in the cat.

Breed

The canine heart varies tremendously between different dog breeds; breed-associated conformational variation is the single most important cause of variation in the normal canine cardiac silhouette. A

basic outline of these differences is shown in Figures 7.9 and 7.10; however, there are many more variations that cannot be listed here. A good understanding of these differences is paramount to allow better cardiac assessment in thoracic radiography. It may be useful to build up a collection of normal thoracic radiographs of different breeds for easy reference.

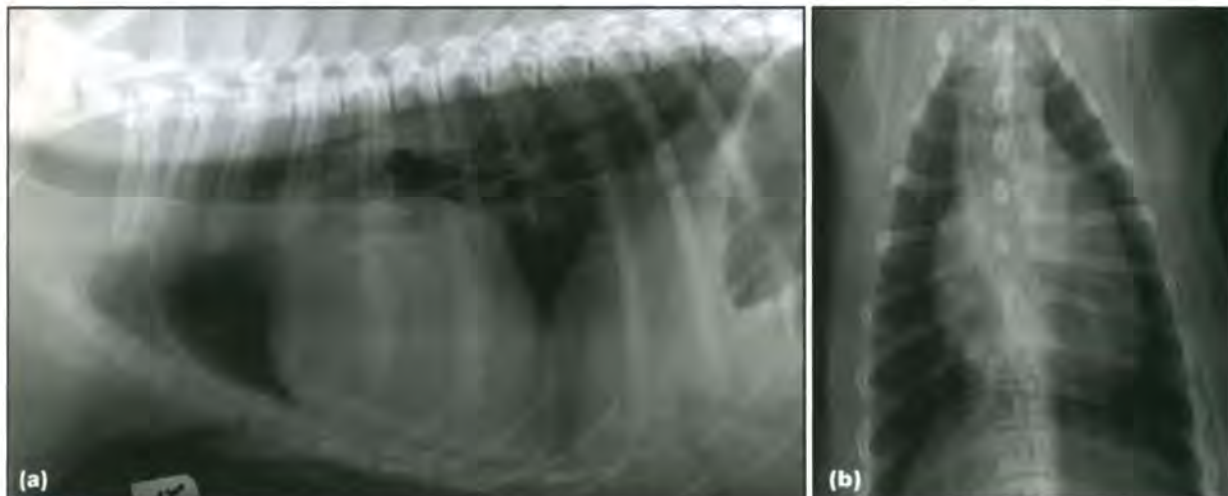
Pericardial fat

An incorrect diagnosis of cardiomegaly is often made in animals with a large amount of *pericardial fat* (see also Figure 1.24, p. 15). Pericardial fat contributes to the overall size of the cardiac silhouette but it is often possible to identify the presence of fat on careful inspection. Pericardial fat has a lower opacity compared with the heart and often the cardiac margin is not as sharp. The latter is due to the gradual change in opacity from soft tissue (heart) to fat to air-filled lung, rather than the sharp soft tissue–air interface seen in thinner animals. Altering radiographic technique may also assist in identification of pericardial fat.

In the cat, pericardial fat is seen better in DV/VD rather than lateral radiographs. Pericardial fat should be suspected if a large amount of falciform fat is present, and may have a characteristic triangular corner on the right cranial margin of the cardiac silhouette on the DV/VD view (Figure 7.11).

Thorax type	Lateral view	Dorsoventral view
Wide shallow (e.g. Dachshund, Shi-Tzu, Boston Terrier, Bulldog)	Shorter rounder cardiac silhouette at a large inclination to the spine Cardiac silhouette has a long contact area with the sternum (mimicking right-sided cardiomegaly)	Rounded right and left ventricular borders Apex is usually well to the left of the spine
Deep narrow (e.g. Greyhound, Afghan Hound, Whippet)	Long oval heart with a vertical position in the thorax (almost perpendicular to the spine)	Almost circular cardiac silhouette due to upright position of heart in thorax Apex is close to median plane
Intermediate (e.g. German Shepherd Dog, Labrador Retriever)	Heart appears ovoid or lop-sided egg-shaped	Heart appears similar to lateral view Apex is usually slightly to the left of the spine

7.9 Variation in the appearance of the cardiac silhouette with thoracic shape.



7.10 The cardiac silhouette varies markedly between different dog breeds. **(a)** Lateral and **(b)** DV radiographs of a normal Golden Retriever. This breed often appears to have right-sided cardiomegaly on the lateral view due to the large amount of sternal contact (similar to wide shallow-chested dog breeds) and the rectangular shape of the cardiac silhouette. On the DV view the cardiac size appears normal and the apex is moderately displaced into the left hemithorax. (continues)



7.10 (continued) The cardiac silhouette varies markedly between different dog breeds. **(c)** Lateral radiograph of a normal Dobermann. The cardiac silhouette is extremely upright due to the deep narrow-chested nature of this breed. **(d)** DV radiograph of a normal Greyhound. The cardiac silhouette is very rounded in shape (compared with b) and the apex lies in the midline.



7.11 DV radiograph of an obese Domestic Shorthair cat. Note the triangular soft tissue opacity border effacing the right side of the cardiac silhouette (arrowed). This is due to a large amount of pericardial fat (even though it appears as a soft tissue opacity and should not be confused with pathology). A CT examination confirmed that no lung changes were present in this cat.

Age

Young dogs appear to have large hearts. This is, in part, due to the relatively small size of the thoracic cavity. Thus, it is particularly important to take into account shape changes as well as overall cardiac size in younger animals.

About 40% of cats over 10 years old have a cranially sloping cardiac silhouette with increased sternal contact (Figure 7.12). The reason for this is



7.12 Left lateral view of a clinically normal 12-year-old cat. In about 40% of older cats the heart has a more horizontal, cranially sloping position.

poorly understood and no association with increased cardiac size has been found. It is considered likely to be associated with age-related changes in thoracic conformation.

Body position

Variation in body position will cause variations in the appearance of the cardiac silhouette due to the effects of gravity. Consistency in the radiographic technique is important in assessment of sequential radiographs and helps to avoid misinterpretation. Generally right lateral and DV radiographs are acquired for radiographic assessment of cardiac disease (see Chapter 1).

Regardless of view, the cardiac silhouette is always slightly larger than the heart itself due to the effects of magnification. Specific changes in the appearance of the canine cardiac silhouette on different radiographic views are given in Figure 7.13 (see also Figures 1.27, p. 17 and 1.29, p. 18).

Right lateral
Cardiac silhouette shape and position of apex are more consistent May have a longer sternal contact area than on left lateral view
Left lateral
Cardiac silhouette is more rounded Apex may be displaced slightly dorsally from the sternum
Dorsoventral
Cardiac silhouette shape and position of apex are more consistent Cardiac silhouette is more oval The apex is more to the left on DV views
Ventrodorsal
Cardiac silhouette is more elongated Apex may be more in the midline May see bulge in position of main pulmonary artery

7.13 Variation in the appearance of the cardiac silhouette with body position.

Respiratory phase

Expiratory radiographs create a false impression of cardiomegaly as the overall thoracic size is decreased, whilst the cardiac size stays the same (for examples of inspiratory and expiratory radiographs see Figure 12.9, p. 246). Sternal contact increases at expiration, which exacerbates the impression of cardiomegaly; there is also a small but real increase in cardiac size during expiration.

At expiration the cardiac silhouette can be more difficult to outline cranially due to adjacent mediastinal fat and caudally due to overlapping of the diaphragm. In addition, loss of air content in the lung tissue contacting the cardiac silhouette creates a surrounding hazy indistinct zone.

The effects of all of these changes are exaggerated in older, obese and shallow-breathing dogs.

Cardiac cycle

Variations due to cardiac cycle seldom cause major changes or radiographic misinterpretation. They are most easily seen in large-breed dogs and dogs with a slow heart rate.

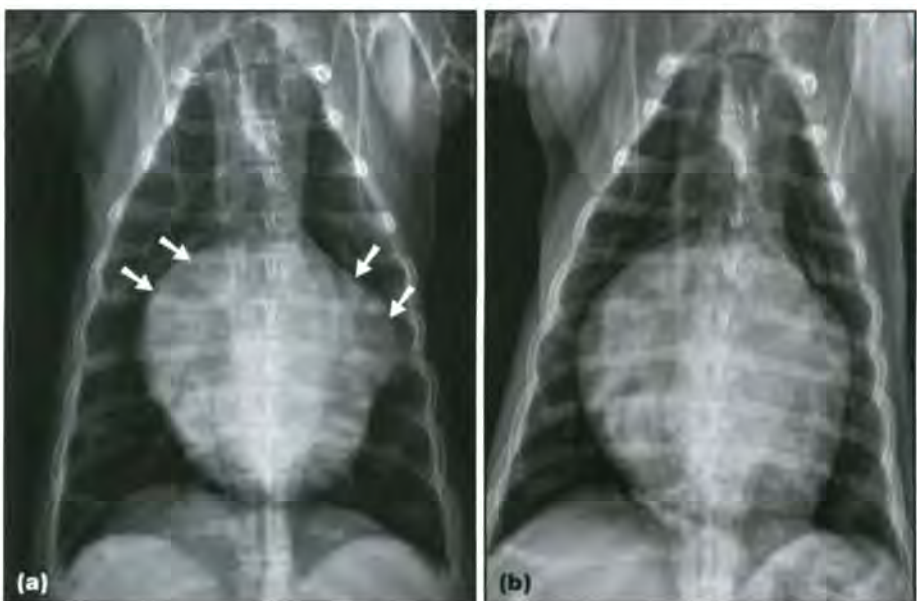
Most radiographs are exposed during ventricular diastole simply because it is longer than systole. Near the end of ventricular systole the atrial borders can be rounded and bulging and the ventricles may appear as slightly smaller with a narrow 'V' instead of 'U' shape (Figure 7.14). On VD/DV views the main pulmonary artery can be more prominent in systole. One report suggested that there was less alteration in shape due to cardiac cycle on the VD view than the DV view in cats.

Measuring the cardiac silhouette

It is important to be able to assess cardiac size radiographically and many techniques have evolved in order to do this. Note that radiographs are often inaccurate in the assessment of heart size and identification of specific chamber enlargement. Ultrasonography remains the gold standard for chamber size assessment (see Chapter 2).

Guidelines for cardiac size

Numerous papers have been published on the subject of quantifying the normal heart size and various methods are in use. These techniques have many limitations and should only be used in combination with a good understanding of the normal sources of variation in the cardiac silhouette. A good general principle is that the heart should be considered radiographically normal unless there is an obvious change in size or shape. Note also that a radiographically normal heart by no means excludes cardiac disease.



7.14 VD views of the thorax of a Cavalier King Charles Spaniel with cardiomegaly obtained at different phases of the cardiac cycle. Note the difference in the appearance of the heart. **(a)** Systole: the ventricles are smaller and the atria are dilated (arrows show the RA and LAu) **(b)** Diastole: the entire heart is more rounded and the atrial and auricular appendage bulges are not as prominent. The changes in this dog are also exacerbated by slight differences in respiratory phase.

Canine cardiac size: rules of thumb

- On a lateral view the cardiac length (apex to base) should be approximately 70% of the dorsal to ventral distance of the thoracic cavity.
- The width (craniocaudal dimension) should be between 2.5 (deep-chested breeds) and 3.5 (round-chested breeds) intercostal spaces.
- Cardiac width on a DV view is usually 60–65% of the thoracic width and no more than two-thirds of the thoracic width at the widest point of the cardiac silhouette on a VD view.

Feline cardiac size: rules of thumb

- In cats the width of the cardiac silhouette should be no more than 2–2.5 intercostal spaces in width on the lateral view.
- On the lateral view the maximal width should be approximately the same as the distance between the cranial border of the fifth rib and the caudal border of the seventh rib.

Vertebral heart score/vertebral heart size

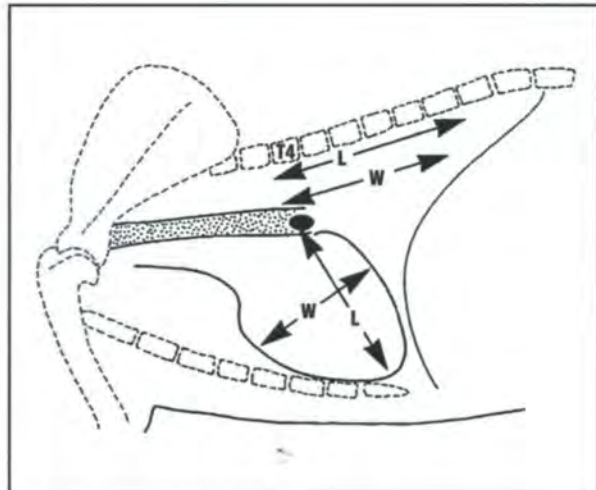
A novel system of cardiac measurement was proposed in 1995, which aimed to circumvent the limitations in other methods attributable to inherent breed variation in cardiac size. It is called the vertebral (or Buchanan) heart score (VHS). In this technique the long and short axes of the cardiac silhouette are measured on a lateral view and totalled. They are then scaled against the thoracic vertebral column (Figures 7.15 and 7.16).

The VHS is useful for those new to evaluating cardiac size on radiographs and also for the sequential assessment of cardiac size on repeat radiographs of the same patient. It has not been proven to be superior to subjective assessment. The suggested mean value for dogs in the original multibreed study was $9.7 \pm 0.5v$ (8.5–10.5v) (v: vertebrae). However, considerable breed variation exists even in the VHS, and later studies have established breed-specific normals (see Figure 7.16b).

Trachea and carina position

The location of the trachea and carina can be useful in assessing cardiac size and chamber enlargement (Figure 7.17). On a lateral radiograph the trachea diverges from the thoracic spine. The angle of divergence is fairly standard amongst cat breeds but shows variation between dog breeds. The greatest angle is seen in deep-chested dogs, whereas in shallow-chested breeds the trachea may be almost parallel to the spine. This should not be erroneously interpreted as representing cardiac enlargement.

Just cranial to the tracheal bifurcation there is a normal *ventral bend* in the trachea (Figure 7.18). This is often lost in animals with left-sided cardiac enlargement; however, it may not be present in normal, shallow, round-chested dog breeds.



7.15 Technique to perform a VHS on a lateral radiograph. L = Length of the cardiac silhouette; T4 = Fourth thoracic vertebra; W = Width of the cardiac silhouette. (Reproduced from Dennis *et al.* (2001) with permission from the publisher)

(a) How to perform a vertebral heart score

1. Take a well positioned lateral recumbent thoracic radiograph.
2. Measure the distance between the ventral aspect of the carina and cardiac apex.
3. Mark this on a piece of paper, with your starting point as a corner and mark along the edge to record the length.
4. Take a second measurement, perpendicular to the first at the widest point of the cardiac silhouette.
5. Mark this on the same piece of paper with the same starting point and on the same edge of the paper.
6. Hold the paper adjacent to the thoracic spine on the same radiograph with the starting point level with the cranial endplate of T4.
7. Count vertebral bodies along the spine (to the nearest 0.1 of a vertebra) until you reach your first mark. Note this figure.
8. Repeat step 7 counting to your second mark this time, being careful to start from T4 again. Note the second figure.
9. Add the two figures to get the VHS.

(b) Normal vertebral heart score

Dog breed-specific values

- Boxer: $11.6 \pm 0.8 v$
- Cavalier King Charles Spaniel: $10.6 \pm 0.5 v$
- Dobermann: $10.0 \pm 0.6 v$
- German Shepherd Dog: $9.7 \pm 0.7 v$
- Labrador Retriever: $10.8 \pm 0.6 v$
- Whippet: $11.0 \pm 0.5 v$
- Yorkshire Terrier: $9.7 \pm 0.5 v$

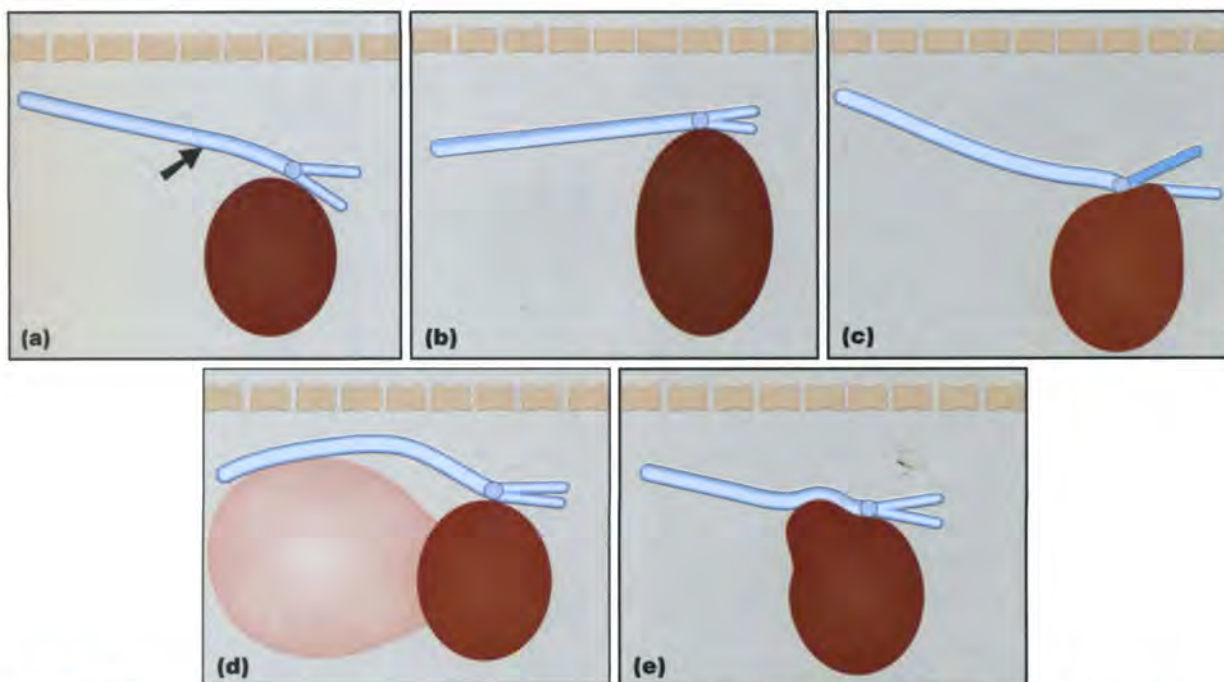
Puppies

Have VHS values within the same 8.5–10.5 v range

Cats

$7.5 \pm 0.3 v$ on a lateral view
(The cardiac width on a DV/VD view is $3.4 \pm 0.25 v$ if measured perpendicular to the long axis)

7.16 (a) How to perform a VHS. (b) Normal VHS. v = Vertebrae.



7.17 Basic principles of tracheal and bronchial displacement on the lateral radiograph. The positions of the trachea, carina and caudal mainstem bronchi can be very useful to assess cardiac chamber enlargement. In this series of figures the changes in tracheal and bronchial position on a lateral radiograph are illustrated for various conditions. Note that there is also variation in tracheal position between different breeds of dogs. **(a)** Normal. The trachea and caudal mainstem bronchi have a gentle ventral divergence from the thoracic spine. Note the normal ventral bend (arrowed) in the trachea just cranial to the carina. **(b)** Left ventricular enlargement in isolation. The LV elevates the entire trachea when it is enlarged and there is loss of the normal ventral bend cranial to the carina. **(c)** Left atrial enlargement in isolation. The LA creates a triangular or wedge-shaped soft tissue opacity at the caudal border of the cardiac silhouette and pushes the left caudal mainstem bronchus (shown in dark blue) dorsally. **(d)** The effect of a cranial mediastinal mass is shown for comparison. A cranial mediastinal mass (shown in pink) can elevate the trachea cranial to the carina anywhere along its length. Depending on the size and location of the mass, this may be focal elevation or more commonly elevation of the entire pre-cardiac trachea. The cardiac size will be normal. **(e)** Right atrial enlargement or right atrial mass in isolation. It is very rare to see severe focal right atrial enlargement. An enlarged RA can focally elevate the trachea cranial to the carina. (Note that a heart base mass can also elevate the trachea in this position but usually has a different appearance on the DV/VD view; see Cardiac neoplasia.)

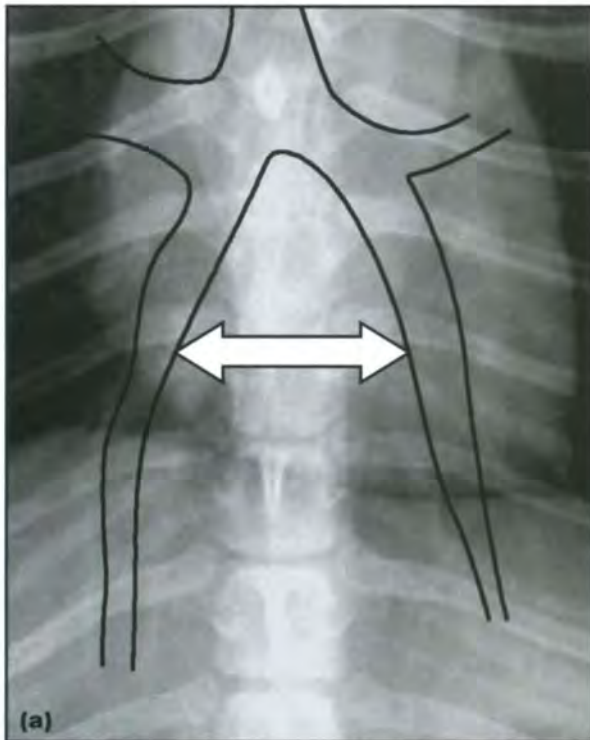


7.18 Close-up of a lateral thoracic radiograph of a dog demonstrating the normal appearance of the caudal trachea. Note the normal ventral bend (black arrow) cranial to the carina, and the two caudal mainstem bronchi almost level with one another (white arrows point to their dorsal margins).

The carina should be located at the fourth or fifth intercostal space. The round radiolucent ring-like structures extending out from the trachea are cross-sectional views of either the left or the right cranial mainstem bronchus (see Chapters 10 and 11). On a VD/DV view the angle between the left and right mainstem bronchi is around 60 degrees at the bifurcation. The mainstem bronchi should create an upsidedown V shape on this view (Figure 7.19).

Pericardial fat stripe

It can be difficult to assess cardiac size when a pleural effusion is present. Fat present between the fibrous pericardium and the pericardial mediastinal pleura may remain visible on the lateral view in animals with pleural effusion. This is known as the *pericardial fat stripe* and may aid radiographic assessment of the heart in animals with pleural fluid (Figure 7.20).



7.19 (a) Close-up of a DV radiograph of a normal dog at the level of the heart. The bronchial tree is shown with black lines. The angle between the left and right caudal mainstem bronchi (shown by the arrow) should be about 60 degrees and form an upside-down V shape. This does vary somewhat with breed, but an increased angle or splayed appearance ('cowboy legs' sign) suggests left atrial or tracheobronchial lymph node enlargement. (b) Postmortem bronchography image showing the normal angle between the caudal mainstem bronchi. (Courtesy of B. Hopper)



7.20 (a) Lateral thoracic radiograph of a cat with a small volume of pleural fluid associated with feline leukaemia virus infection. A narrow lucent line is visible in a position compatible with the cranial aspect of the heart (arrowed). Together with the position of the trachea and the caudal aspect of the cardiac silhouette, this line has the effect of completing a normal appearing cardiac silhouette. (b) Lateral thoracic radiograph of a different cat with a larger volume of pleural fluid. In this instance, the position and size of the pericardial fat stripe, relative to the position of the trachea, suggests enlargement of the cardiac silhouette. Ultrasonography subsequently confirmed marked HCM (and ruled out a mediastinal mass). (Reproduced from Lamb (2000) with permission from *Veterinary Radiology and Ultrasound*)

Normal major vessel physiological and radiographic anatomy

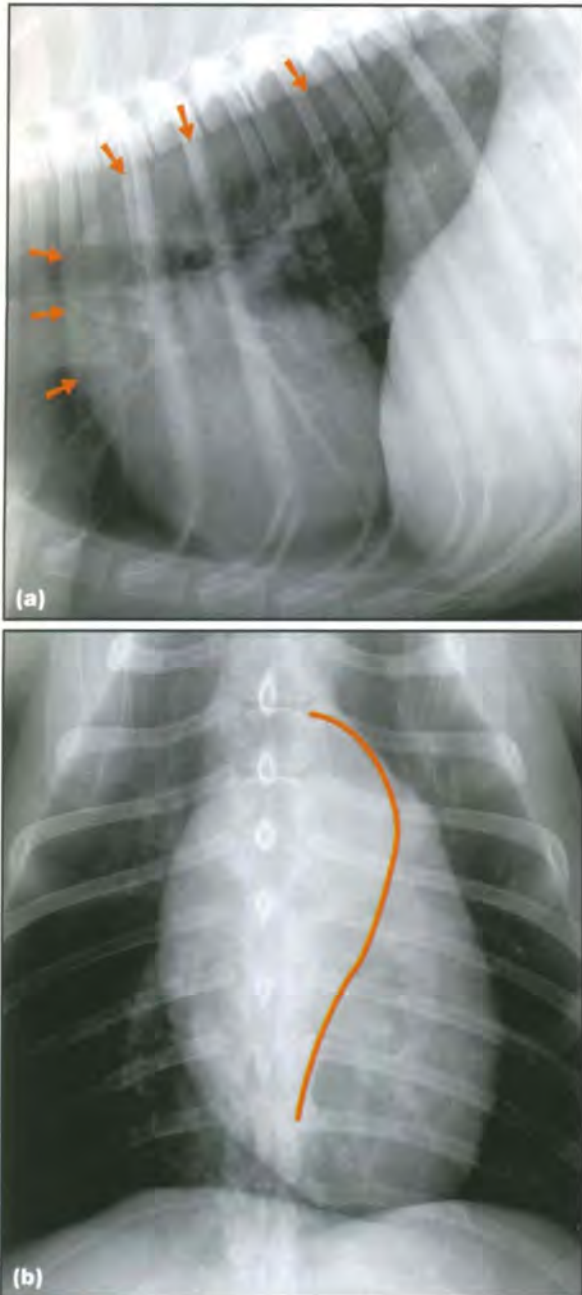
Aorta

The aorta is divided into three sections:

- The ascending aorta: short and arises from the cranial aspect of the heart. Has the same orientation as the LV
- The aortic arch (or transverse arch): short and curves caudally. Gives rise to the brachiocephalic trunk and left subclavian artery
- The descending aorta: long and can be divided into thoracic and abdominal portions.

The aortic isthmus is the junction of the ascending aorta and the aortic arch. The ascending aorta contributes to the cranial heart base area and cannot be seen clearly due to superimposition (see Figure

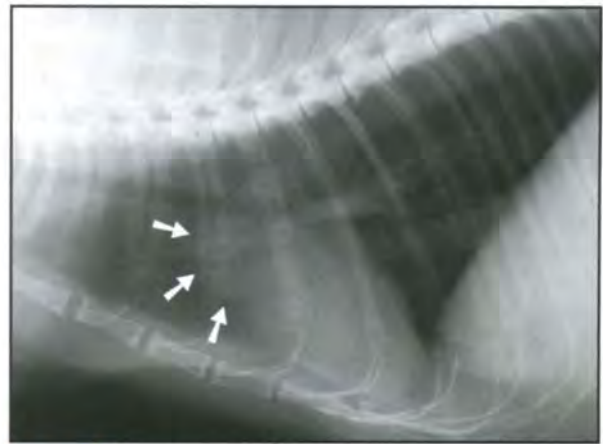
7.3). The aortic arch and descending aorta are identified on both lateral and DV/VD views. (Figure 7.21). In the normal animal the left border of the descending aorta is identified on the VD/DV view.



7.21 (a) Lateral and (b) DV radiographs of a dog showing the normal location and appearance of the aorta (orange arrows in (a); orange line in (b)).

The aortic diameter is similar to the height of adjacent vertebral bodies; aortic size does not alter in association with hypovolaemia or volume overload (unlike the CdVC).

A focal bulge in the aorta (sometimes also referred to as an elongated, redundant or tortuous aorta) at the aortic isthmus may be seen in a proportion of older cats (Figure 7.22). One study found that this was present in 28% of older (>10 years) cats. The change does not appear to be associated with systemic hypertension or hyperthyroidism.

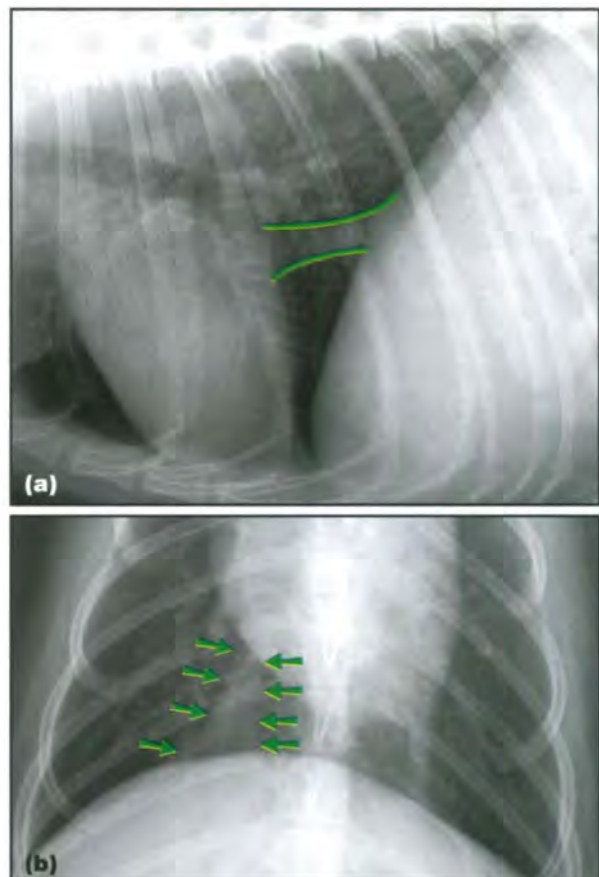


7.22 Lateral thoracic radiograph of an aged cat. Note the focal bulge in the aorta (arrowed).

Caudal vena cava

The CdVC receives blood from the abdomen, pelvis and hindlimbs. The final abdominal tributaries are the hepatic veins. The CdVC enters the thorax by crossing the diaphragm on the right side within the plica vena cava. It then traverses between the accessory and right caudal lung lobes to enter the RA dorsal to the inlet of the coronary sinus. It lies in close association with the right phrenic nerve.

The majority of the intrathoracic CdVC is easily seen on radiographs (Figure 7.23). On the lateral view the CdVC crosses the caudal half of the right ventricu-



7.23 Close-ups of (a) lateral and (b) DV radiographs of a dog showing the normal size and location of the CdVC (green lines in (a); arrows in (b)).

lar border and can often be seen overlapping the cardiac silhouette for a short distance. On VD/DV views it is seen to the right of the median plane between the caudal right border of the heart and the diaphragm.

The diameter of the CdVC is highly variable due to variations in intrathoracic pressure during respiration and stage in the cardiac cycle. It may also vary in pathological conditions such as right-sided heart disease, hypovolaemia or CdVC obstructive conditions (caval syndrome, masses, etc.; see Acquired vascular diseases). Enlargement of the CdVC is more likely to suggest right-sided heart disease in the dog when:

- CdVC:Ao >1.5 (strongly suggestive of right-sided heart abnormality)
- CdVC:VL >1.3
- CdVC:R4 >3.5.

Where Ao = aorta; CdVC = the greatest diameter of the CdVC not overlapping the heart or diaphragm; R4 = diameter of the right fourth thoracic rib just ventral to the spine; and VL = the length of the thoracic vertebra over the tracheal bifurcation. A word of caution: there was shown to be considerable overlap in the CdVC:Ao ratio between normal patients and those with right-sided heart disease.

Cranial vena cava

The cranial vena cava (CrVC) receives blood from the head, neck, thoracic wall and forelimbs. The axillary veins (from the forelimbs), together with the internal and external jugular veins, converge to form the right and left brachiocephalic veins. These then unite to create the CrVC. It travels in the cranial mediastinum and receives the costocervical and internal thoracic veins, as well as the azygos vein just cranial to the RA; it finally empties into the RA.

The CrVC is not seen as an individual structure on a radiograph unless a pneumomediastinum is present. It forms the ventral border of the cranial mediastinum on the lateral view.

Azygos vein

The azygos vein forms from the first lumbar veins and passes through the aortic hiatus into the thorax. It then receives intercostal, subcostal, oesophageal and broncho-oesophageal veins and terminates in the CrVC. It is not seen on a radiograph unless a severe pneumomediastinum is present or it is markedly enlarged. It then appears as a wavy vessel immediately ventral to the thoracic spine, receiving tributaries from every intervertebral space (Figure 7.24). It may rarely be seen in very deep-chested, narrow breeds, such as the Greyhound, in the absence of a pneumomediastinum.

Thoracic duct

The thoracic duct originates between the diaphragmatic crura. It has a variable course within the thorax but usually courses cranially along the right dorsal border of the aorta. Its termination is variable but it usually enters the CrVC or left jugular vein.

The thoracic duct is not seen on radiographs. It can be identified using radiographic or CT lymphangiography or on heavily T2-weighted magnetic resonance (MR) images.



7.24 Close-up of a lateral thoracic radiograph of a dog with a severe pneumomediastinum after trauma. The azygos vein (Az) is visible as a narrow soft tissue opacity tube ventral to the spine and dorsal to the aorta (Ao), receiving tributary vessels from each intervertebral space (small white arrows).

Main pulmonary artery

The main pulmonary artery arises from the pulmonary valve and arches dorsally and caudally. It splits into right and left pulmonary arteries immediately caudal to the level of the aortic root. These then form further branches within the left and right lung. The ligamentum arteriosum (the ductus arteriosus in fetal life) joins the proximal part of the left pulmonary artery.

The main pulmonary artery is usually not seen on a lateral radiograph as it is superimposed on the cardiac silhouette. On occasion it may be identified as a round soft tissue opacity located immediately ventral to the carina, and should not be confused with a nodule in this location (see Figure 7.38b). The left and right branches may be radiographically identified on the lateral view. The left branch runs slightly more cranial and also dorsal to the right branch. On VD/DV views the main pulmonary artery contributes to the cranial left cardiac silhouette (Figure 7.25). It appears more prominent during systole and also on a VD view compared with a DV view. This should not be interpreted as pathology. The left and right main branches are initially superimposed on the heart, but further along their course the caudal lobar right and left pulmonary arteries are seen as tubular soft tissue structures coursing caudolaterally in association with the lateral aspects of the caudal mainstem bronchi.

Cranial lobar pulmonary arteries and veins

Useful tip

In order to remember the location of the pulmonary veins compared with the arteries use the rhyme:

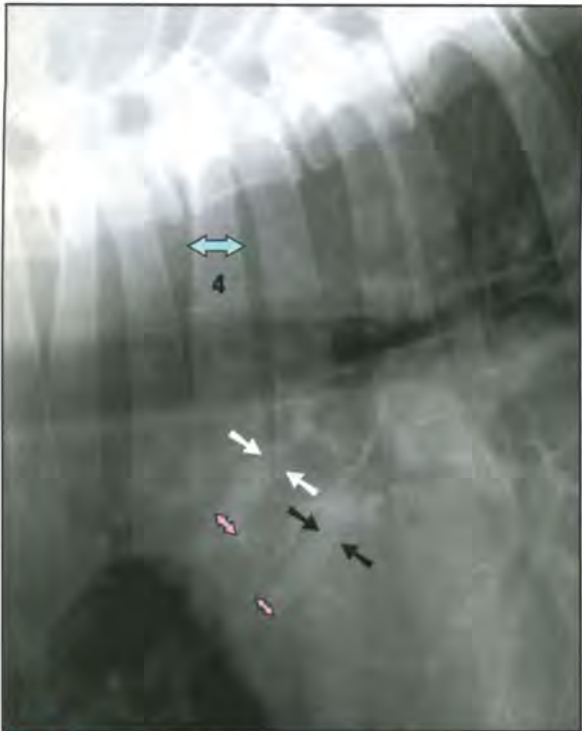
"Veins are ventral and central"

(i.e. veins are ventral to arteries on the lateral view and central to the arteries on the VD view).



7.25 VD thoracic radiograph of a normal dog. The main pulmonary artery appears as a small focal bulge at the 01.00–02.00 o'clock location (arrowed). This can be a normal finding on a VD view, or when an exposure is made during systole, and should not be interpreted as disease.

The arteries and veins to the cranial lung lobes can be seen on lateral views with the arteries dorsal to the veins (Figure 7.26). They are best separated on the left lateral view. Arteries follow the bronchial tree



7.26 Close-up of a lateral radiograph of a dog showing the cranial lobar pulmonary vessels, the artery is shown with small white arrows and the vein with small black arrows. These vessels should be no greater than the narrowest part of the third or fourth rib (turquoise arrow) where they cross the rib (pink arrow).

closely, but the veins may not be as closely associated with the bronchi. Arteries are often slightly curved and often better defined compared with the veins. Normally, the artery and vein of each pair is approximately the same size.

Various rules exist for the measurement of cranial lobar vessel size on the lateral view (see below) but a good general rule of thumb is that *no cranial lobar vessel should be greater than the narrowest part of the third or fourth rib where it crosses the rib.*

Rules for cranial lobar pulmonary vascular size in the dog and cat (lateral radiographs)

Dog

In the dog the cranial lobar pulmonary vessels should be approximately the same in size. The ratio of the diameter of the artery or vein to the proximal third of the fourth rib, at the level of the fourth intercostal space is $0.73 (\pm 0.24)$ with a 95% confidence interval of 0.26–1.2.

These vessels should be considered enlarged when greater than 1.2 times the proximal third of the fourth rib at the fourth intercostal space.

OR

The cranial lobar pulmonary arteries should not be larger than the diameter of the proximal third of the third rib on the lateral radiograph.

Cat

In the cat the right cranial lobar artery should be 0.5–1.0 times the proximal third of the fourth rib (mean artery:rib ratio of 0.70) when measured at the level of the fourth rib. The cranial lobe veins should be 0.2 cm (± 0.03 cm) in diameter at the same point.

Caudal lobar pulmonary arteries and veins

On VD/DV views the caudal pulmonary arteries are located lateral to the veins and can be traced cranially towards the main pulmonary artery segment (Figure 7.27). Caudal lobar pulmonary arteries and veins are more easily identified on DV views due to the presence of surrounding aerated lung and the effects of magnification. The veins are medially located and run towards the LA, which is located centrally in the cardiac silhouette between the mainstem bronchi.

Rules for caudal lobar pulmonary vascular size in the dog and cat (DV radiographs)

The pulmonary artery and vein of each caudal lobe should be similar in size.

The diameter of the artery or vein should be no greater than the width of the ninth rib where they cross it (anecdotal).

In the cat, a cut-off for pulmonary arterial enlargement of 1.6 times the ninth rib has been suggested in assessment of heartworm disease.



7.27 Close-up of a VD radiograph of a dog showing the right caudal lobar pulmonary vessels as they cross the eighth and ninth ribs. The artery is shown with small white arrows and the vein with small black arrows. The vessels are measured where they cross the ninth rib (rib measurements shown by turquoise arrows and the vessel measurements are shown by pink arrows).

Interpretive principles

Thoracic radiographs are extremely useful in the evaluation of the patient with cardiovascular disease. However, it should be noted that radiography and echocardiography are complementary techniques and it is important to understand the limitations and benefits of these two imaging modalities in the assessment of cardiac disease.

In simple terms, echocardiography is far more accurate in identifying chamber enlargement and other structural abnormalities than radiographs. Echocardiography also provides vital functional information that cannot be obtained radiographically. However, radiographs remain indispensable in the evaluation of pulmonary vascular and parenchymal changes secondary to heart disease. For example, a radiograph will quickly reveal evidence of pulmonary venous congestion and/or cardiogenic pulmonary oedema in left-sided failure, or pleural effusion in right-sided failure. Thoracic radiographs are also extremely valuable in monitoring the progress of therapy in heart failure.

Chapter 2 and the Appendices provide further information on echocardiographic technique and normal echocardiographic measurements.

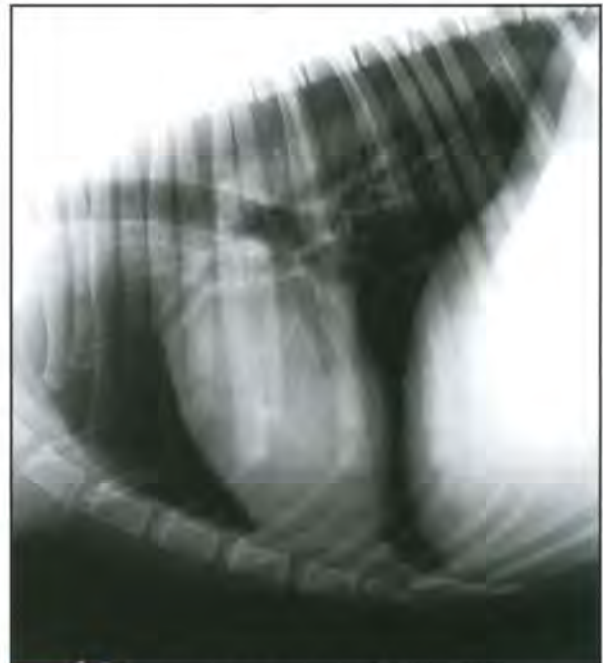
This section covers the radiographic features of specific cardiac chamber and major vessel enlargement. The evaluation of congestive heart failure is also covered here. It is important to have a good knowledge of cardiac anatomy, physiology and pathophysiology when approaching a thoracic

radiograph for the evaluation of cardiac disease. It should be remembered that when radiographic changes are present they do not show the disease itself, but rather the haemodynamic consequences of the condition.

Microcardia

Radiographic features

- Cardiac silhouette is narrow and pointed on the lateral view and narrow on the DV/VD view (Figure 7.28).
- Apex may lose contact with the sternum.
- There may be small pulmonary arteries and veins.
- Lung fields may be hyperlucent (without hyperinflation) depending on the cause of the microcardia.
- CdVC may be narrow.



7.28 Microcardia in a dog with Addison's disease (hypoadrenocorticism). Note the narrow pointed appearance of the cardiac silhouette.

Differential diagnoses

- Hypovolaemia: shock, dehydration. Lung fields are also underperfused and CdVC may be small (Figure 7.29).
- Addison's disease (hypoadrenocorticism). Heart is actually physically smaller due to chronic electrolyte abnormalities with or without hypovolaemia and shock in an acute Addisonian crisis.
- Emaciation.
- Atrophic myopathies.
- Artefactual, such as pneumothorax, deep-chested dogs, deep inspiration or pulmonary underinflation.



7.29 Lateral radiograph of an extremely dehydrated dog. The CdVC is narrow (arrowed), the lung fields are hyperlucent, and the cardiac silhouette is small and pointed.

Normal radiographic cardiac size

Some cardiac diseases may not produce any apparent radiographic changes. Examples are:

- Endocarditis
- Concentric ventricular hypertrophy:
 - Aortic stenosis
 - Pulmonic stenosis
 - Hypertrophic cardiomyopathy (HCM).
- Other myocardial disease:
 - Acute myocardial failure
 - Early or mild myocarditis
 - Myocardial neoplasia.
- Acute ruptured chordae tendinae
- Small atrial septal defect (ASD), ventricular septal defect (VSD) or patent ductus arteriosus (PDA)
- Some types of pericardial disease:
 - Constrictive pericarditis
 - Acute traumatic haemopericardium.
- Arrhythmias
- Overzealous use of diuretic therapy in heart disease.

Cardiac chamber enlargement

The limitations of radiographs for the evaluation of specific cardiac chamber size have already been discussed. Often more than one chamber will be enlarged and this will complicate interpretation of changes in the cardiac silhouette. It should be emphasized that artefactual chamber and major vessel enlargement will be seen on poorly positioned radiographs and that the utmost care should be taken in obtaining perfectly straight views.

In the following section the DV view is described rather than the VD view, as the former is more commonly obtained in cardiac patients.

Concentric and eccentric hypertrophy: what is the difference?

Ventricular hypertrophy may occur in response to:

- Increased systolic pressure (a pressure overload) leading to *concentric* hypertrophy: the ventricular wall gets thicker and the lumen size remains normal (or reduced)
- Increased diastolic pressure and volume (a volume overload) leading to *eccentric* hypertrophy (also known as *dilatation*): the ventricular wall remains a normal size and the lumen size increases.

The different types of hypertrophy have implications for radiographic interpretation. Concentric hypertrophy can be extremely difficult to recognize on a radiograph, whereas eccentric hypertrophy is more easily seen. Note that in contrast to the ventricles, only *atria* usually show *dilatation* in cardiac disease.

Right atrium

Right atrial enlargement is very uncommon in isolation and is also difficult to see radiographically unless it is severe (Figure 7.30).

Lateral view:

- Focal bulge on cranial aspect of cardiac silhouette just ventral to the terminal trachea (cranial to the carina).
- May even push the trachea dorsally at this point if large enough or a right atrial mass is present.
- May merge with an enlarged RV.

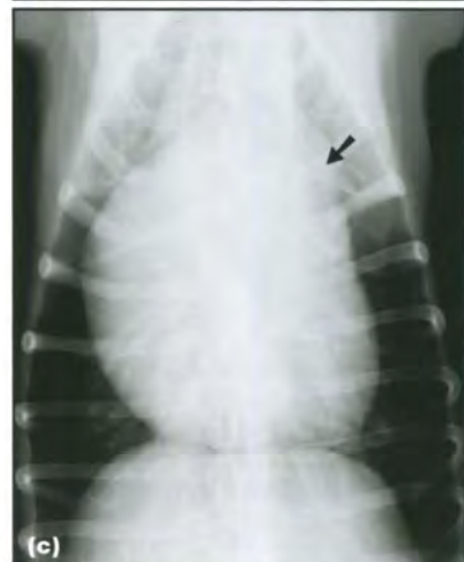
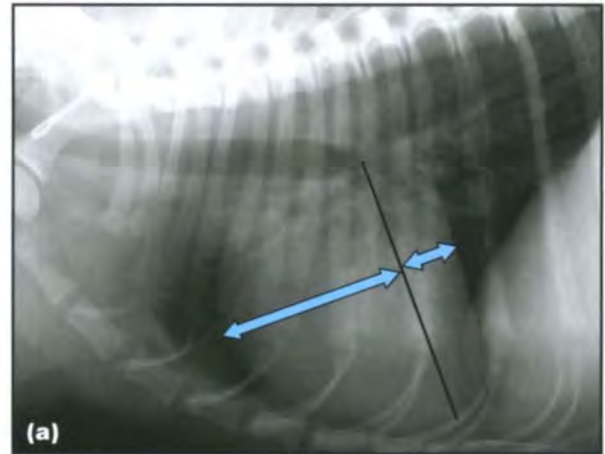
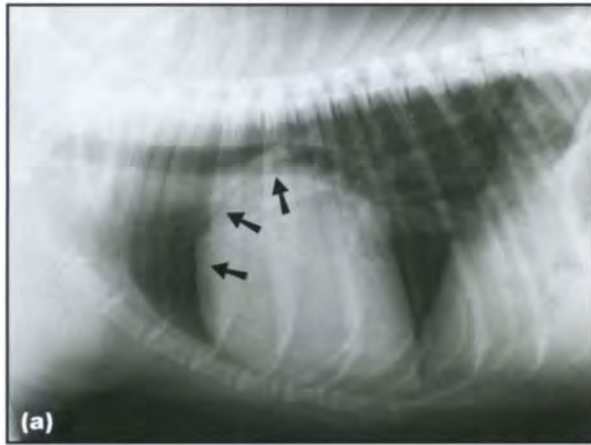
Dorsoventral view:

- Bulge in cardiac silhouette at 09.00 – 11.00 o'clock.
- May merge with an enlarged RV.

Right ventricle

Right ventricular enlargement is commonly overdiagnosed on thoracic radiographs. This is partly because the shallow-chested conformation of many dog breeds can mimic certain features of right-sided cardiomegaly (such as increased sternal contact). Great care must be taken to differentiate breed variation from true right-sided cardiac enlargement. When truly present, right ventricular enlargement is often accompanied by left-sided changes and right atrial enlargement, and may be hard to identify as a single entity (Figure 7.31).

Lateral view: To evaluate the size of the RV, a line can be drawn from the carina to the cardiac apex; approximately two-thirds of the cardiac silhouette should lie cranial to this line and one-third caudal to it. An increased cranial component (e.g. four-fifths



7.30 (a) Lateral and (b) DV radiographs of a 1-year-old Kelpie cross dog and (c) DV view of an 8-month-old Golden Retriever, both with tricuspid dysplasia. The RA is enlarged on all views (arrowed). Some right ventricular enlargement is also contributing to the appearance of the cardiac silhouette.

7.31 (a) Lateral and (b) DV radiographs of a dog with a moderately enlarged RV. In (a) when a line is dropped from the carina to the apex, approximately three quarters of the cardiac silhouette lies in front of the line and one quarter lies caudal to it. In (b) the cardiac silhouette has a reverse D-shaped appearance. Note that an enlarged RA is also contributing to the shape changes. (c) DV thoracic radiograph from a different dog with severe right-sided enlargement due to heartworm disease. There is a reverse D-shaped silhouette seen in this patient. The main pulmonary artery (arrowed) is also enlarged.

cranial and one-fifth caudal to the line) suggests right-sided enlargement. Rotation of the cardiac apex caudodorsally away from the sternum (i.e. pointing more towards the liver than the sternum) is a sensitive sign of right ventricular enlargement but is not always present. Right ventricular (or atrial) enlargement may displace the trachea dorsally over the heart base and cranial to the carina, but the trachea will still maintain its normal terminal ventral bend (unlike in left ventricular enlargement).

Other findings with RV enlargement include widening of the cardiac silhouette (non-specific) and increased cardiosternal contact (non-specific and not very useful: do not rely on this in isolation).

Dorsoventral view: This is often more reliable than the lateral view for evaluation of right-sided enlargement. Findings include:

- Increased size of the cardiac silhouette on the right side of the thorax
- Reduced distance between the right cardiac border and the right thoracic wall
- A typical 'reversed D' shape
- On occasion, the apex may be pushed towards the left, creating the false impression of left-sided cardiomegaly.

Left atrium

Radiographs are very useful in identifying left atrial enlargement, and generally sensitive for moderate to severe dilatation (Figure 7.32).

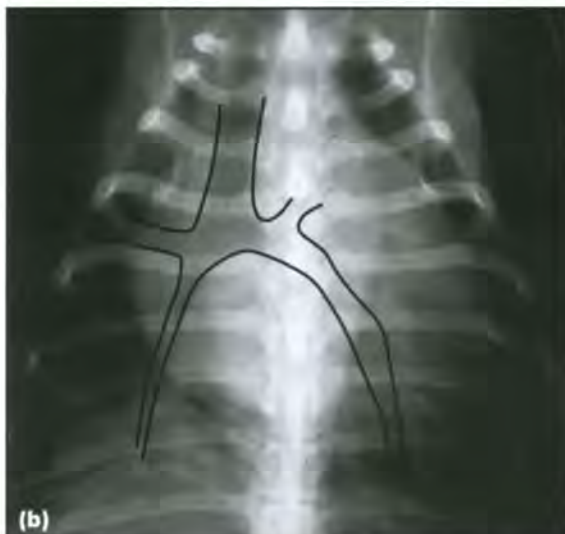
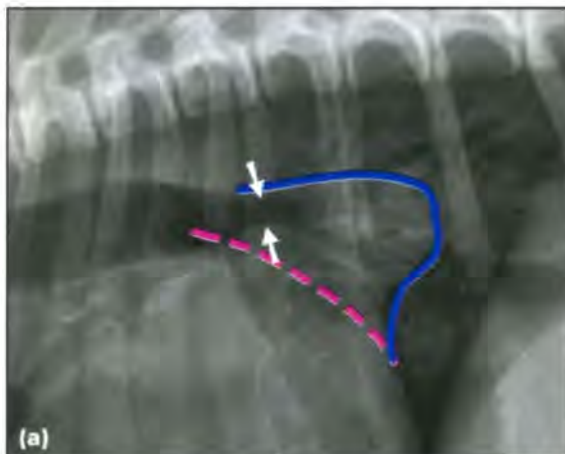
Lateral view:

Dogs:

- Elevation (with or without compression) of the left caudal mainstem bronchus (seen as a separation of the two caudal mainstem bronchi) (see also Figure 8.10a, p. 181).
- Loss of the normal gentle cranial curvature of the caudal margin of the cardiac silhouette. Instead, the caudodorsal margin of the cardiac silhouette becomes straight and then eventually triangular, forming a left atrial 'tent' or 'wedge'.
- Increased height of the caudodorsal border of the heart.
- Enlarged pulmonary veins may be seen entering the LA as indistinct nodular opacities in this region.

Cats:

- The LA is situated more cranially than in dogs and it is harder to identify on the lateral view.



7.32 (a) Close-up of a lateral thoracic radiograph showing moderate left atrial enlargement in a Dachshund. The left atrial outline is forming a bulging convex shape (blue line). The shape of the normal LA is shown for comparison (pink dashed line). Due to the enlargement of the LA the left mainstem bronchus is depressed (arrowed). (b) DV radiograph of a dog with marked left atrial enlargement. The increased size of the LA has separated the caudal mainstem bronchi (black lines show the outline of the bronchial tree). (c) Left atrial enlargement in the cat produces a bulge at the cranial left aspect of the cardiac silhouette on the DV/VD view. When this is accompanied by an apical shift to the right a valentine heart shape results. This is evident in this DV view of a cat with HCM.

Dorsoventral view:

Dogs:

- The enlarged LA is projected over the cardiac silhouette at the 05.00–07.00 o'clock position (between the caudal mainstem bronchi) on the DV/VD view. This results in divergence (or splaying) of the caudal mainstem bronchi (also known as the 'cowboy legs' sign). (This must be differentiated from enlargement of the middle tracheobronchial lymph node which will produce divergence of the caudal mainstem bronchi on a DV/VD view, but will push them *ventrally* on a lateral view; see Figure 8.10a, p. 181).
- A large LA may also create a 'double density' or more correctly, 'double opacity' sign on this view. This is the presence of two differing soft tissue opacities between the caudal mainstem bronchi, one more opaque than the other. This results from superimposition of the enlarged atrium summing with the ventricle and producing more attenuation of the X-ray beam.
- An enlarged LAu may be seen at 02.30–03.00 o'clock position.

Cats:

- The more cranial location means that an enlarged LA and LAu are seen at the left cranial border of the cardiac silhouette (even as cranial as the 01.00–02.00 o'clock position).
- A severely enlarged LA will bulge towards the left and can cause a shift of the cardiac apex to the right. Right atrial enlargement may also be present. This can create the appearance of a valentine-shaped heart.

Left ventricle

Left ventricular enlargement due to eccentric hypertrophy is usually easily recognized on a radiograph, whereas enlargement due to concentric hypertrophy is difficult to identify. This is important as animals with severe left-sided concentric hypertrophy (e.g. aortic stenosis) may have radiographically normal cardiac silhouettes.

Left ventricular enlargement is often accompanied by left atrial enlargement and also right-sided changes.

Lateral view:

- Tracheal elevation (of the *entire* trachea and with loss of the normal terminal ventral bend) (Figure 7.33).
- Caudal border becomes straighter (or less commonly rounder) than usual.

Dorsoventral view:

- Increased length of cardiac silhouette.
- Other signs are not as reliable.
- Cardiac apex may be more displaced into left hemithorax.
- Apex becomes rounder.



7.33 Lateral radiograph of a dog with severe left ventricular and left atrial enlargement due to DCM. Note the tracheal position and the left atrial tent (or wedge). (Courtesy of B. Hopper)

Generalized cardiomegaly

The entire cardiac silhouette may appear enlarged in many diseases and this is called generalized cardiomegaly. It is difficult (and usually inaccurate) to detect mild generalized cardiomegaly unless previous radiographs are available from the same patient. A moderate to severe generalized cardiomegaly is seen as an increase in width and height on the lateral view, and width and length on the DV view (Figure 7.34). The heart may also appear more generally rounded than usual. Care should be taken to try and distinguish generalized cardiomegaly from pericardial effusion (see below).



7.34 (a) Lateral radiograph of a middle-aged crossbreed dog with generalized cardiomegaly, secondary to endocardiosis. (continues) ▶



7.34 (continued) **(b)** DV radiograph of a middle-aged crossbreed dog with generalized cardiomegaly, secondary to endocardiosis.

Pericardial enlargement

Any increase in pericardial content or thickness can create the appearance of generalized, rounded (or globoid) enlargement of the cardiac silhouette. The commonest cause is the presence of pericardial effusion (for further information see Pericardial diseases).

Pericardial effusion can be distinguished from generalized cardiomegaly using:

- Ultrasonography (quick, accurate and extremely easy to perform for this distinction). Anechoic effusion peripheral to heart
- Radiographs (not nearly as reliable and not recommended):
 - Sharp border of cardiac silhouette in pericardial effusion compared with blurry border in generalized cardiomegaly (the normal movement blur of the beating heart is not recognized when it is encased in a fluid-filled pericardium) (Figure 7.35)
 - No individual chamber enlargement recognized in pericardial effusion (but often the case for generalized cardiomegaly as well by definition)
 - Lung fields are generally underperfused due to the effects of tamponade (may see pulmonary venous distension in generalized cardiomegaly)
 - Evidence of right-sided heart failure in pericardial effusion (but may also be present with generalized heart disease).

Changes in the major vessels

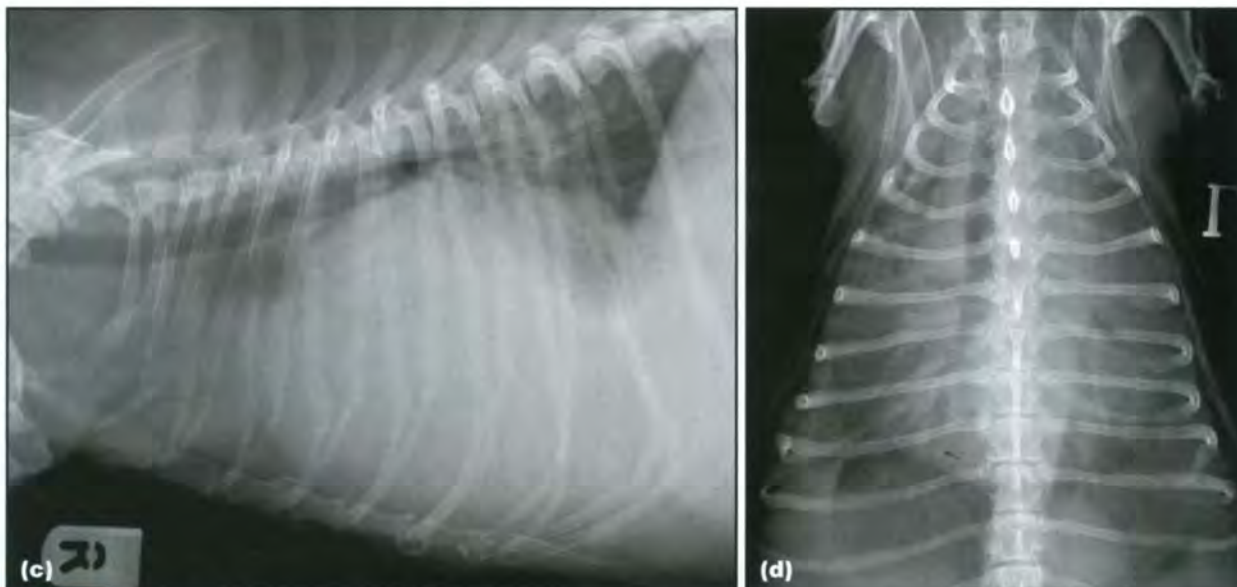
Aorta

Entire aortic arch enlarged:

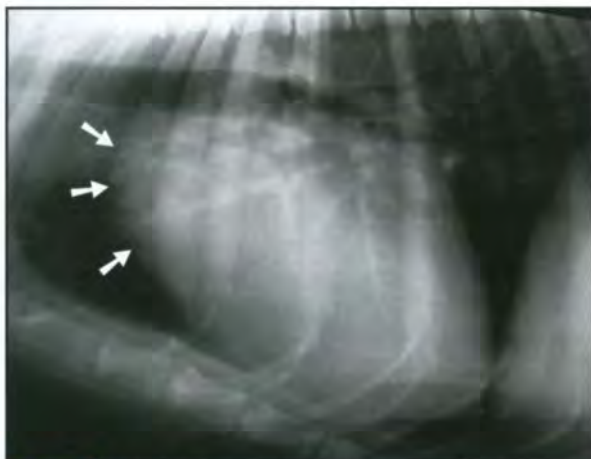
- Seen as a focal bulge on the cranial aspect of the heart on the lateral view.
- *Seen as widening of the caudal part of the cranial mediastinum on the DV view.*
- Possible causes:
 - Subaortic stenosis (or less commonly valvular), resulting in turbulence and post-stenotic dilatation (Figure 7.36; see also Figure 7.64)
 - Age-related change in the cat (see Figure 7.22).



7.35 **(a)** Lateral and **(b)** DV radiographs of a dog with a pericardial effusion. The cardiac silhouette is globoid on both views and careful observation reveals sharp margins. This makes pericardial effusion more likely than generalized cardiomegaly. (continues)



7.35 (continued) **(c)** Lateral and **(d)** DV radiographs of a dog with pericardial effusion and right-sided heart failure. The cardiac silhouette is massively enlarged and globoid on both views. A pleural effusion is present due to the right-sided heart failure.



7.36 Lateral radiograph of a dog with subaortic stenosis. The entire aortic arch is enlarged (arrowed). This was confirmed on the DV view.

Descending part of the aortic arch enlarged:

- Usually only seen on the DV view as a focal bulge when the left lateral border of the aorta is traced from caudal to cranial.
- May be seen as a bulge at the classic 11.00–01.00 o'clock location on the DV view and an apparent elongation of the cardiac silhouette.
- Possible causes: PDA (see Figure 7.46a).

Other aortic enlargements or abnormalities:

- Aortic aneurysm:
 - Secondary to *Spirocerca lupi* infection (see Figure 9.20, p. 209)
 - Dissecting aortic aneurysms have been reported in dogs and cats
 - Ductus aneurysm or ductus diverticulum.
- Coarctation of the aorta with post-stenotic dilatation (see Figure 7.90).

- Redundant aorta:
 - Aged cats
 - Brachycephalic dogs
 - Congenital hypothyroidism.
- Abnormal location:
 - Situs inversus
 - Vascular ring anomalies (persistent right aortic arch most commonly).
- Calcification or mineralization of the aorta:
 - Incidental non-significant aortic mineralization in dogs (more common in older dogs and Rottweilers) (see Figure 7.37 and Appendix)
 - Primary or secondary hyperparathyroidism
 - Hypervitaminosis D
 - Lymphoma
 - Hyperadrenocorticism
 - *S. lupi* infection
 - Arteriosclerosis.
- Aortic body tumour (see Cardiac neoplasia, below).



7.37 Incidental aortic calcification identified on the lateral thoracic radiograph of a 10-year-old Weimaraner. The calcification is seen as a wavy opaque line over the cranial border of the cardiac silhouette (arrowed).

Caudal vena cava

The normal size of the CdVC is described above. Caution should be used when diagnosing changes in CdVC size on a radiograph. Caval size varies markedly with respiratory and cardiac cycle and thoracic and abdominal pressures. Changes in caval size should not be diagnosed from a single film. A genuine alteration in size will be seen on *repeated* radiographs.

Wide caudal vena cava:

- Right-sided heart failure.
- Cardiac tamponade.
- Constrictive pericarditis.
- Obstruction of the CdVC from the level of the hepatic veins to the level of the RA (Budd–Chiari-like syndrome):
 - Thrombosis
 - Caval syndrome associated with heartworm disease
 - Compression or invasion of the cava by tumours or other masses (see Figure 7.162)
 - Trauma-induced stricture
 - Fibrosis
 - Diaphragmatic hernia
 - Congenital cardiac (e.g. cor triatriatum dexter) or caval (e.g. membranous obstruction) anomalies.

Narrow caudal vena cava:

- Shock.
- Hypovolaemia (see Figure 7.29).
- Addison’s disease (hypoadrenocorticism).
- Artefactual (pulmonary hyperinflation).

Mineralized caudal vena cava: This is rare. Causes include:

- Mineralized masses (see Figure 7.162)
- Other dystrophic mineralization

- Metastatic mineralization (hyperadrenocorticism, secondary hyperparathyroidism, etc.).

Segmental aplasia of the caudal vena cava: This is a rare congenital anomaly where part of the CdVC is missing and blood returns to the heart via the azygous vein. A markedly enlarged azygous vein will be identified.

Persistent left cranial vena cava: This is relatively common and only really of significance when performing cardiac catheterization or thoracic surgery. The left CrVC persists from fetal life and drains into the coronary sinus.

Main pulmonary artery

Dilatation of the main pulmonary artery is difficult to detect on lateral views due to superimposition over the cardiac silhouette. The DV view will show an enlarged main pulmonary artery as a bulge at the 01.00–02.00 o’clock position.

Enlarged main pulmonary artery segment:

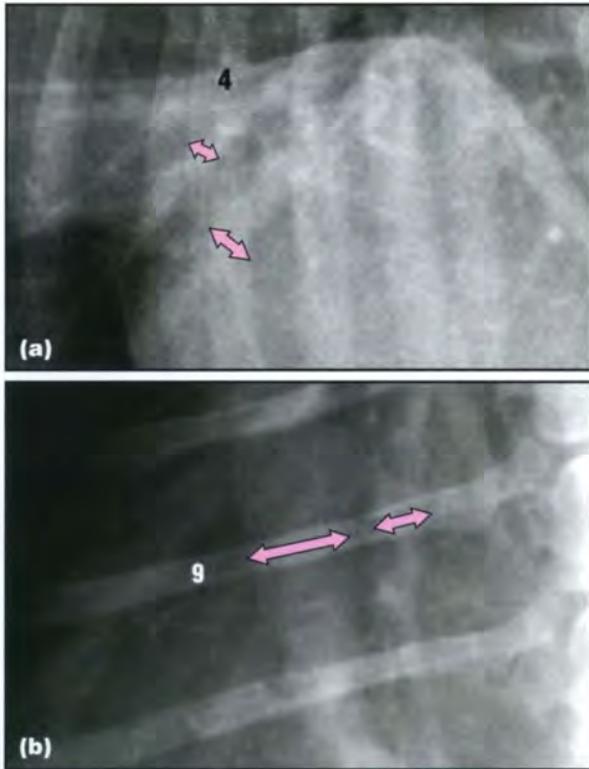
- Pulmonic stenosis: post-stenotic dilatation (Figure 7.38).
- Increased circulating volume due to PDA, ASD or VSD.
- Pulmonary hypertension.
- Severe heartworm disease or angiostrongylosis.
- Artefactual:
 - VD position
 - Systole
 - Positional rotation.

Pulmonary arteries and veins

Methods of assessing pulmonary artery and vein size are described above. Examples of pulmonary arterial and venous enlargement are shown in Figure 7.39. Figure 7.40 gives differential diagnoses for variations in pulmonary vascular size.



7.38 (a) Enlarged main pulmonary artery seen as a bulge at the 01.00–02.00 o’clock position in a dog with pulmonic stenosis (arrowed). **(b)** The main pulmonary artery may mimic a nodule on the lateral radiograph when an end-on view is obtained. This may occur, on occasion, in normal dogs or, as in this case, when the main pulmonary artery is enlarged. This is a dog with heartworm disease. The end-on main pulmonary artery is shown with arrows. The radiograph is slightly rotated.



7.39 Pulmonary arterial and venous enlargement. The main pulmonary artery and vein measurements are shown by pink arrows and the rib number is also shown. **(a)** Moderately enlarged cranial lobar pulmonary veins on a close-up of a lateral radiograph of a dog with heart failure. **(b)** Massively enlarged right caudal lobar main pulmonary artery on a DV view of a dog with heartworm disease.

Small pulmonary arteries and veins

- Dehydration
- Shock
- Hypoadrenocorticism
- Positive pressure ventilation (and other causes of pulmonary hyperinflation)
- Pericardial effusion with tamponade
- Constrictive pericarditis
- Severe pulmonic stenosis
- Right-to-left shunts (tetralogy of Fallot, reverse PDA)
- Focal due to pulmonary thromboembolism

Large pulmonary arteries

- Pulmonary hypertension
- Pulmonary thromboembolism
- Heartworm disease
- Left-to-right shunts (PDA, VSD, ASD)
- Angiostrongylosis (but often not a feature)
- Peripheral arteriovenous fistula

Large pulmonary veins

- Left heart failure
- (In right-to-left shunts the veins may appear larger as the arteries are small)

Large pulmonary arteries and veins

- Left heart failure
- Left-to-right shunts (PDA, VSD, ASD)
- Excessive intravenous fluid administration

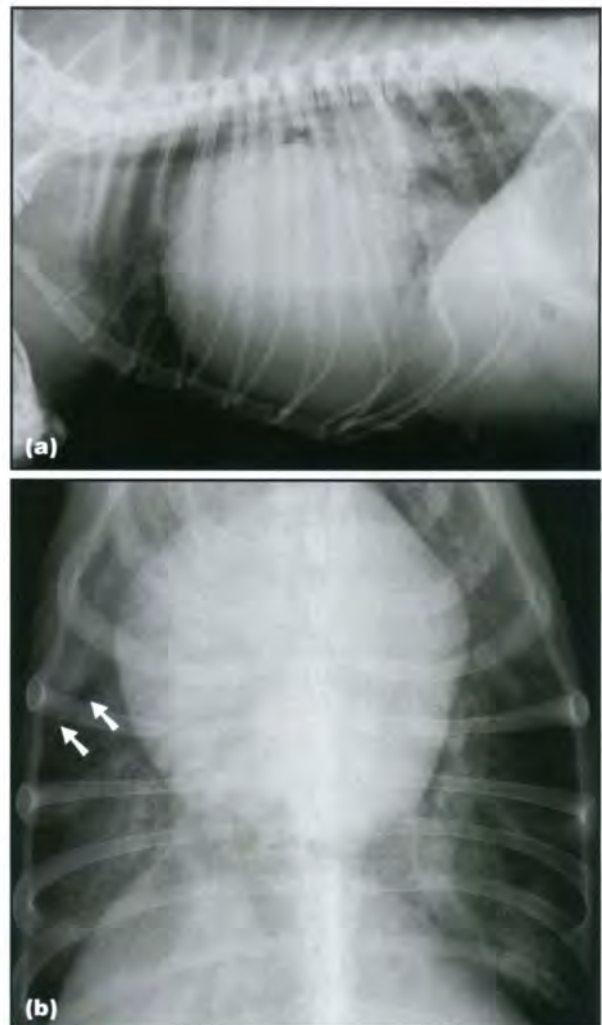
7.40 Differential diagnoses for variations in pulmonary vascular size in the dog and cat.

Heart failure

Heart failure can be defined in many ways. One definition is that heart failure is the end result of severe heart disease and is a clinical syndrome, resulting in systolic and/or diastolic dysfunction severe enough to overwhelm the cardiovascular system's compensatory mechanisms. Congestion, oedema, poor peripheral perfusion and/or systemic hypertension result. Radiographic examination provides an invaluable insight into the presence and severity of heart failure.

Radiographic features of left-sided heart failure in the dog

Cardiogenic pulmonary oedema is seen (see also Chapter 12) (Figure 7.41):



7.41 Left-sided heart failure in the dog. **(a)** Lateral radiograph of the same dog as in Figure 7.33 whose marked left atrial and ventricular enlargement is now accompanied by left-sided heart failure. An increase in opacity is evident in the perihilar and caudodorsal regions, due to the presence of cardiogenic alveolar oedema. The CdVC is also wide, due to accompanying right-sided heart disease. **(b)** DV view. An alveolar infiltrate is present in both left and right caudal lobes. The right caudal lobe is often an early location for oedema in left heart failure. A pleural line is seen between the right middle and caudal lobes (arrowed) and represents a small amount of pleural effusion also present in this patient.

- Varies from faint interstitial infiltrate to severe alveolar pattern (see Chapter 12)
- Usually first seen in the perihilar region on the lateral view, though the right caudal lobe is also often a predilection site (seen on the DV view)
- Usually extends from a central to more peripheral location.

Note that severe left-sided heart disease *must also be present* to make the diagnosis of left-sided heart failure. Non-cardiogenic pulmonary oedema may mimic the radiographic appearance (see Chapter 12). One complicating situation is that of an acute onset of heart failure, such as secondary to ruptured chordae tendinae. In this situation substantial left-sided cardiomegaly may not be present. Echocardiographic examination will provide an accurate diagnosis.

Radiographic features of left-sided heart failure in the cat

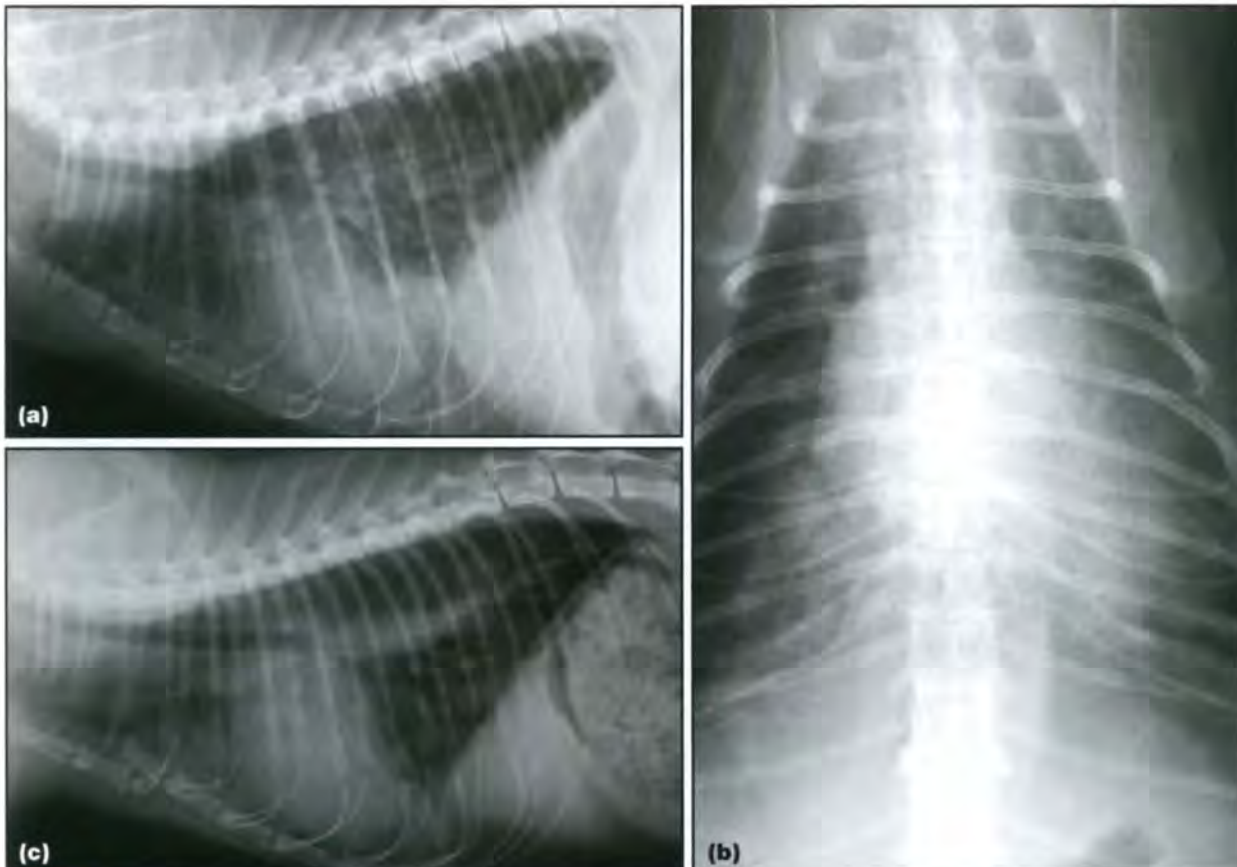
- Cardiogenic pulmonary oedema (see also Chapter 12) (Figure 7.42). May appear similar to that in the dog or may appear as patchy unevenly distributed opacities throughout the lung fields.

The variable appearance of cardiogenic oedema in the cat makes the diagnosis harder.

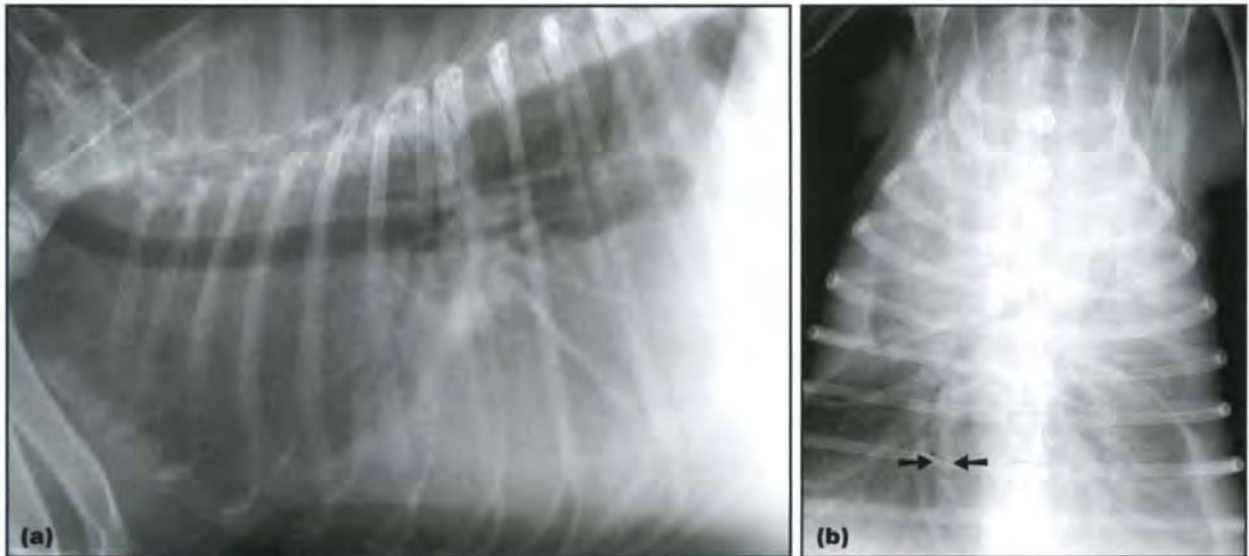
- Pleural effusion. In the cat, pleural effusion may be seen in left-sided heart failure. This is poorly understood, but is thought to be due to an anatomical variation in visceral pleural drainage.

Radiographic features of right-sided heart failure in the dog and cat

- Pleural effusion (Figure 7.43):
 - Note that right heart failure is a *rare* cause of pleural effusion in the cat
 - Pleural effusion in both dogs and cats is usually a combination of both left- and right-sided failure
 - It is important to identify severe right-sided cardiac disease in order to attribute a pleural effusion to right-sided heart failure.
- Wide CdVC; see previous comments on CdVC size.
- Hepatomegaly.
- Ascites (peritoneal effusion).
- Pericardial effusion may also result from right-sided heart failure.



7.42 Left-sided heart failure in the cat. **(a)** Diffuse, patchy ill defined opacities (almost appear nodular) are scattered throughout the lung fields on this lateral radiograph. In some regions there is a granular interstitial infiltrate. There is a small volume of pleural effusion, recognized by the rounding and retraction of the dorsocaudal tips of the lung lobes. **(b)** DV radiograph. There is an ill defined increase in opacity in the central parts of both caudal lung lobes due to cardiogenic pulmonary oedema. The small pleural effusion is also evident. **(c)** Lateral radiograph of another cat with left-sided heart failure. The pulmonary vessels are enlarged. In this cat a more diffuse interstitial pattern is present, more marked just cranioventral to the cardiac silhouette. The cardiac silhouette is tall. A pleural fissure line suggests the presence of a small pleural effusion. An incidental old sternal injury is present between the third and fourth sternbrae.



7.43 (a) Lateral and (b) DV radiographs of a dog with right-sided heart failure. A large volume of pleural effusion is present, obscuring the cardiac silhouette. The dog also has ascites and an enlarged liver (not seen on these radiographs). An enlarged right pulmonary caudal lobar vein (arrowed) suggests that pulmonary venous congestion may also be present due to left-sided heart disease. It is not possible to identify the cause of the effusion from these radiographs and further work-up would be required to confirm right-sided heart failure.

Congenital cardiovascular diseases

Congenital cardiovascular diseases are anomalies of the heart and great vessels that have been present since birth. This definition applies even if the condition

is not identified until later in life. A wide variety of congenital diseases exists and it is beyond the scope of this manual to explore all of these conditions. Figure 7.44 lists the congenital abnormalities that have been reported in the dog and cat.

Effect of defect	Primary causes of the defect in the dog	Primary causes of the defect in the cat
Volume overload (systemic to pulmonary (left-to-right) shunting)	<p>Common:</p> <ul style="list-style-type: none"> • PDA • VSD • Mitral dysplasia • Tricuspid dysplasia <p>Uncommon:</p> <ul style="list-style-type: none"> • ASD • Endocardial cushion defect • (Pseudo) truncus arteriosus • Valvular regurgitation • Pulmonic insufficiency • Aortic insufficiency 	<p>Common:</p> <ul style="list-style-type: none"> • VSD • PDA • ASD • Endocardial cushion defect • Mitral dysplasia • Tricuspid dysplasia <p>Uncommon:</p> <ul style="list-style-type: none"> • Truncus arteriosus • Valvular regurgitation
Pressure overload	<p>Common:</p> <ul style="list-style-type: none"> • Pulmonic stenosis • Subaortic stenosis <p>Uncommon:</p> <ul style="list-style-type: none"> • Valvular aortic stenosis • Coarctation and interruption of the aorta • Cor triatriatum dexter 	<p>Common:</p> <ul style="list-style-type: none"> • Dynamic subaortic stenosis <p>Uncommon:</p> <ul style="list-style-type: none"> • Pulmonic stenosis • Pulmonary artery branch stenosis • Fixed subaortic stenosis • Valvular aortic stenosis • Cor triatriatum dexter • Cor triatriatum sinister
Cyanosis	<p>Common:</p> <ul style="list-style-type: none"> • Tetralogy of Fallot <p>Uncommon:</p> <ul style="list-style-type: none"> • Pulmonary to systemic shunting (VSD) • Pulmonary to systemic shunting (PDA) • Tricuspid atresia/right ventricular hypoplasia • Double outlet RV • Transposition of the great vessels • Truncus arteriosus • Aortopulmonary window 	<p>Common:</p> <ul style="list-style-type: none"> • Tetralogy of Fallot • Endocardial cushion defect <p>Uncommon:</p> <ul style="list-style-type: none"> • Pulmonary to systemic shunting (VSD) • Pulmonary to systemic shunting (PDA) • Double outlet RV • Truncus arteriosus

7.44 Pathophysiological classification of congenital defects. (continues)

Effect of defect	Primary causes of the defect in the dog	Primary causes of the defect in the cat
Miscellaneous cardiac and vascular defects	<p>Common:</p> <ul style="list-style-type: none"> • Peritoneopericardial diaphragmatic hernia • Persistent right aortic arch • Persistent left CrVC <p>Uncommon:</p> <ul style="list-style-type: none"> • Endocardial fibroelastosis • Pericardial defects • Anomalous pulmonary venous return • Double aortic arch • Retroesophageal left subclavian artery • Situs inversus 	<p>Common:</p> <ul style="list-style-type: none"> • Peritoneopericardial diaphragmatic hernia • Endocardial fibroelastosis <p>Uncommon:</p> <ul style="list-style-type: none"> • Persistent right aortic arch • Anomalous RA

7.44 (continued) Pathophysiological classification of congenital defects.

In this section, the radiographic, angiocardio-graphic, echocardiographic and scintigraphic features are described for the main congenital cardiac conditions in the dog and cat. It should be noted that in most cases of congenital cardiac disease, only echocardiography (with Doppler evaluation) and radiographs are required as part of the work-up.

It should be noted that cats tend to get more complex combinations of congenital abnormalities than dogs and careful, skilled echocardiographic assessment is vital in this species.

Patent ductus arteriosus

PDA is the most common congenital cardiac disease in dogs. Small-breed dogs (including, but not limited to, Chihuahua, Maltese, Poodle, Pomeranian, Bichon Frisé, Shetland Sheepdog) and German Shepherd Dogs are predisposed. Bitches are more affected than dogs. Cats are also affected but the condition is less common than in dogs.

The ductus arteriosus is an important part of normal fetal circulation. It extends from the main pulmonary artery to the descending aorta and in the fetus functions to divert blood away from the lungs back into the systemic circulation. After birth, pulmonary vascular resistance falls and flow in the ductus reverses. The ductus then closes by constriction of smooth muscle within its wall, brought about by increased arterial oxygen tension that inhibits local prostaglandin release. The ductus is usually closed by 7–10 days after birth. It remains in the adult as the ligamentum arteriosum.

PDA results from failure of normal closure of the ductus arteriosus, resulting in a shunting vessel between the descending aorta and the main pulmonary artery.

There are three main types of PDA:

- The mildest form of the condition results in closure of the ductus at the pulmonary arterial end only. This produces a clinically insignificant blind-ended pouch called a 'ductus diverticulum'. *No shunting* of blood occurs and this anomaly may only be identified as an incidental finding on postmortem
- The commonest clinically presenting patent ductus is a complete tapering funnel-shaped tube with blood shunting from *left-to-right*. Volume overloading of the *left side* of the heart causes left atrial dilatation and left ventricular dilatation and hypertrophy

- The third and least common form for the ductus to take is a non-tapering cylindrical tunnel. This is associated with persistent postnatal pulmonary hypertension and *bidirectional* or *right-to-left shunting* (Eisenmenger's syndrome). These are sometimes known as 'reversed PDAs' and are discussed further, below. The condition results in decreased pulmonary blood flow, a normal to small LV and right ventricular concentric hypertrophy.

Left-to-right shunting

Clinically, a left-to-right shunting PDA is characterized by a continuous machinery-type heart murmur (continuous systolo-diastolic murmur) heard best over the main pulmonary artery. A bounding or 'waterhammer' arterial pulse may also be present.

Most animals are usually asymptomatic when the murmur is discovered. Surgical ligation is recommended in almost all cases.

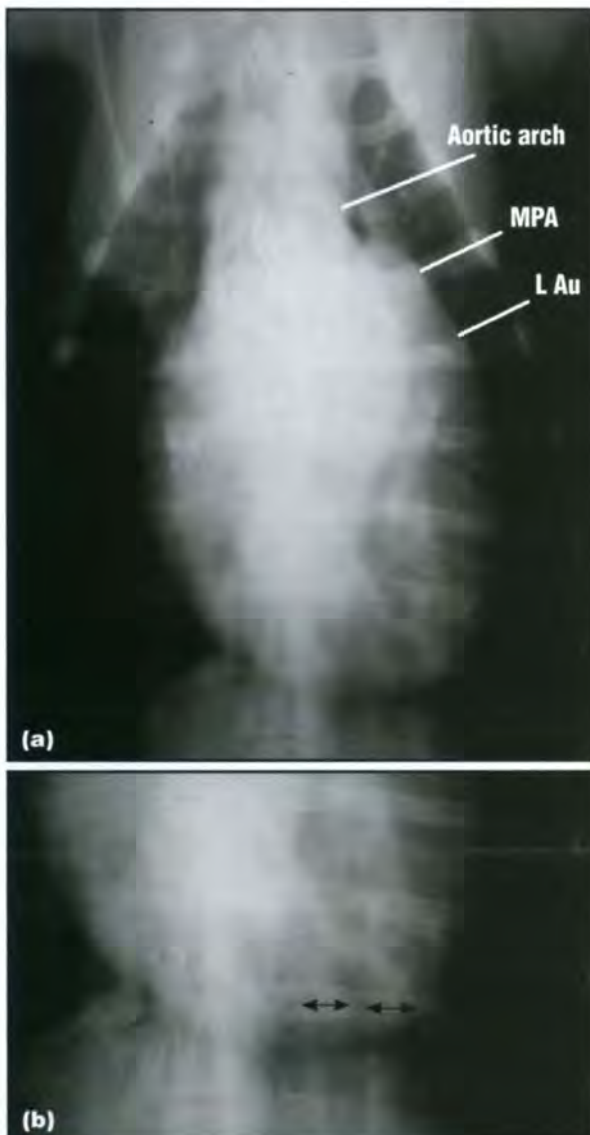
Radiography: Radiographic findings include:

- Lateral view (Figure 7.45):
 - Classically left-sided changes are present, but generalized cardiomegaly may be seen



7.45 Lateral view of the thorax of a 3-month-old male puppy with PDA. There is mainly left-sided cardiomegaly with left atrial tent formation. Both the arteries and veins to the cranial lung lobes were enlarged (difficult to see on this image), which is a sign of a left-to-right shunt.

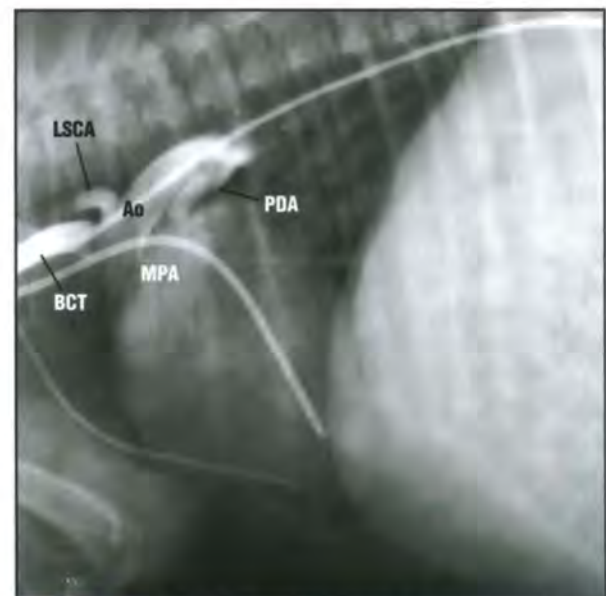
- Prominent aortic arch
- Prominent LA
- Left ventricular enlargement, leading to straightening of the caudal margin of the heart
- Increased vascular lung pattern, with increased size of both the pulmonary arteries and veins; very distally located vessels are visible due to enlargement (the vascular pattern is due to increased blood flow to the lung, caused by the left-to-right shunt)
- Eventually signs of left-sided cardiac failure, with pulmonary oedema.
- DV view (Figure 7.46):
 - Elongated cardiac silhouette
 - In cats the left apex may be displaced into the right hemithorax
- Prominence of the aortic arch, pulmonary trunk and LAu at 11.00–01.00, 01.00–02.00 and 02.00–03.00 o'clock, respectively: this triad has been reported to be pathognomonic for PDA but is not present in all patients (only around 20% of cases)
- Occasionally an aortic bulge ('ductus bump') may be seen near the level of the ductus. This is caused by the abrupt narrowing of the descending aorta beyond the level of the ductus origin
- Enlarged LA with splayed caudal mainstem bronchi with or without double opacity sign
- Increased vascular lung pattern (Figure 7.46b)
- Eventually signs of left-sided cardiac failure.



7.46 (a) DV view of the thorax of a dog with PDA. The cardiac silhouette is very long in a craniocaudal direction and there is bulging of the aortic arch, main pulmonary artery (MPA) and left auricular appendage (LAu). (b) Close-up of (a) showing the left caudal thorax. The artery and vein to the left caudal lung lobe (arrowed) have a diameter wider than the width of the ninth rib where they cross it. This is consistent with left-to-right shunting as seen with PDA.

Angiocardiography: This is usually unnecessary, but should be performed if echocardiography is inconclusive or additional congenital complications are suspected. It is performed by selective catheterization of the aorta, via either a carotid or a femoral approach: contrast medium is injected when the tip of the catheter is just distal to the aortic valve.

- With left-to-right shunting, contrast medium is seen both in the aorta and the main pulmonary artery and its branches immediately after injection.
- The ductus arteriosus can sometimes be identified: the aortic orifice is located on the left ventral aspect of the aorta distal to the left subclavian artery, then extending cranioventrally and to the left to its pulmonic orifice (Figure 7.47).



7.47 Angiocardiogram demonstrating a left-to-right shunt through a PDA in a dog. The contrast medium was injected in the aorta and the opacified ductus is seen (PDA). The contrast medium is opacifying the main pulmonary artery (MPA) at the same time as the aorta (Ao). BCT = Brachiocephalic trunk; LSCA = Left subclavian artery. (Courtesy of J. Buchanan)

- Often the ductus itself is not identified on angiocardiograms, due to partial superimposition of the aorta and main pulmonary artery. Dilatation of the aorta at the usual location of the shunt is a hint that the left-to-right shunting is due to a PDA.

Echocardiography: Ultrasonography is useful both for confirmation of diagnosis and to evaluate the consequences of the PDA on cardiac function. The ductus itself can be seen from either the right parasternal (RPS) short-axis or left parasternal (LPS) cranial window (Figure 7.48). In some cases the ductus is not seen on transthoracic echocardiograms but will be visualized with transoesophageal echocardiography.

Very early in the disease, no changes in chamber size or cardiac function are identified. Later on, the following can be observed:

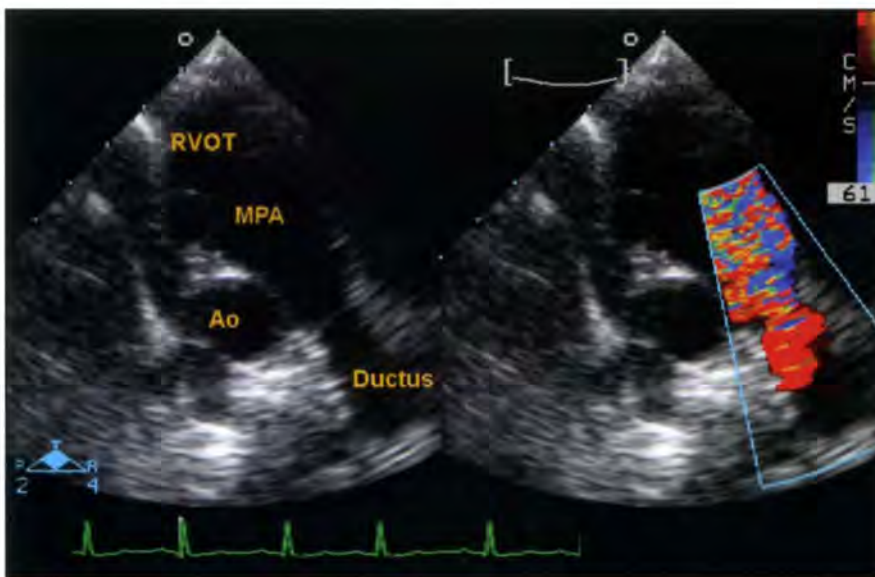
- Left atrial dilatation
- Aortic dilatation
- Main pulmonary artery dilatation
- Left ventricular hypertrophy and dilatation

- Decreased myocardial contractility (decreased fractional shortening, increased E point to septal separation (EPSS), increased left ventricular end-systolic dimensions).

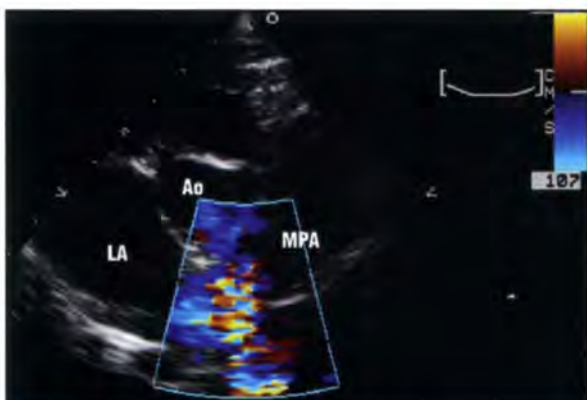
Doppler studies: If the ductus is visualized, then high-velocity turbulent flow from the aorta, through the ductus and into the main pulmonary artery can be observed (Figure 7.49). Otherwise diagnosis is based on other characteristic Doppler findings:

- Main pulmonary artery: continuous high-velocity ductal flow towards the pulmonic valve (up to 4.5–5 m/s) (Figure 7.50)
- Left ventricular outflow tract (LVOT): mild increase in outflow velocity (but usually <2.5 m/s)
- Mild aortic and pulmonic insufficiency.

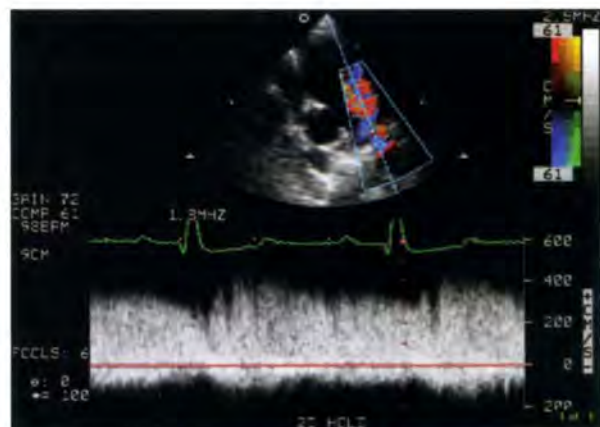
Care should be taken to distinguish PDA from similar congenital abnormalities, such as an aortopulmonary window (which usually results in Eisenmenger's physiology) or an anomalous systemic-to-main pulmonary artery shunt. These conditions are very rare and are beyond the scope of this manual.



7.48 LPS echocardiogram in a dog with a PDA, optimized for visualization of the ductus. The 2D image on the left demonstrates the appearance of the ductus itself at its connection with the main pulmonary artery (MPA). The aorta (Ao) and right ventricular outflow tract (RVOT) are also shown. The colour Doppler image on the right was acquired simultaneously and turbulent flow is evident within the ductus. (© J. Dukes-McEwan)



7.49 RPS short-axis echocardiogram of the heart base in a dog with a PDA. Colour Doppler shows turbulent flow in the main pulmonary artery (MPA), corresponding to the shunting of blood from the aorta (Ao). LA = Left atrium. (Courtesy of M. Sleeper)



7.50 CW Doppler trace acquired via a LPS window in a dog with a PDA. The cursor is aligned with the ductus and continuous flow is evident throughout systole and diastole. (© J. Dukes-McEwan)

Scintigraphy: Observations with first pass radionuclide angiocardiology include:

- Prolongation of the radioactivity within the lungs with incomplete clearance of the lungs during the levophase
- Lack of lung clearance in the levophase, causing partial or complete obliteration of the borders of the aorta (Figure 7.51)
- QP:QS ratio >1.2.

Right-to-left shunting

Occasionally, *right-to-left* shunting occurs through a PDA due to high pulmonary vascular resistance. This is thought to occur because the non-tapering tubular shape of the ductus in these animals permits aortic pressures to be transmitted to the pulmonary arterial system. The resulting extremely increased pulmonary perfusion eventually leads to intimal arteriolar damage and muscular proliferation, causing marked pulmonary hypertension and reversed flow through the ductus arteriosus (Eisenmenger's syndrome). This change has usually been shown to occur in the first few weeks of life. The pulmonary vascular changes are poorly understood, but are known to be irreversible, thereby precluding surgical treatment for this condition.

The anomaly is quite different in presentation to a left-to-right shunting PDA. Clinical signs include fatigue, shortness of breath and weakness. No murmur or only a soft systolic murmur is heard on auscultation and a split second heart sound may be detected. Differential cyanosis may be seen with normal pink cranial mucous membranes but cyanotic caudal mucous membranes, due to the fact that the PDA originates distal to the brachiocephalic trunk and left subclavian artery. The animal may be polycythaemic.

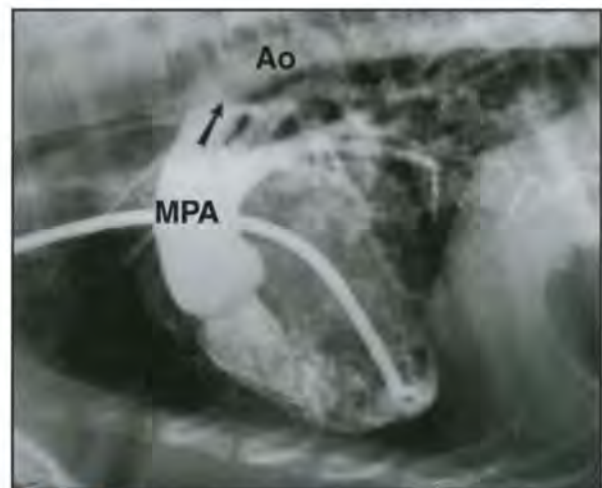
Radiography: Radiographic findings include:

- Right heart enlargement on both lateral and DV views

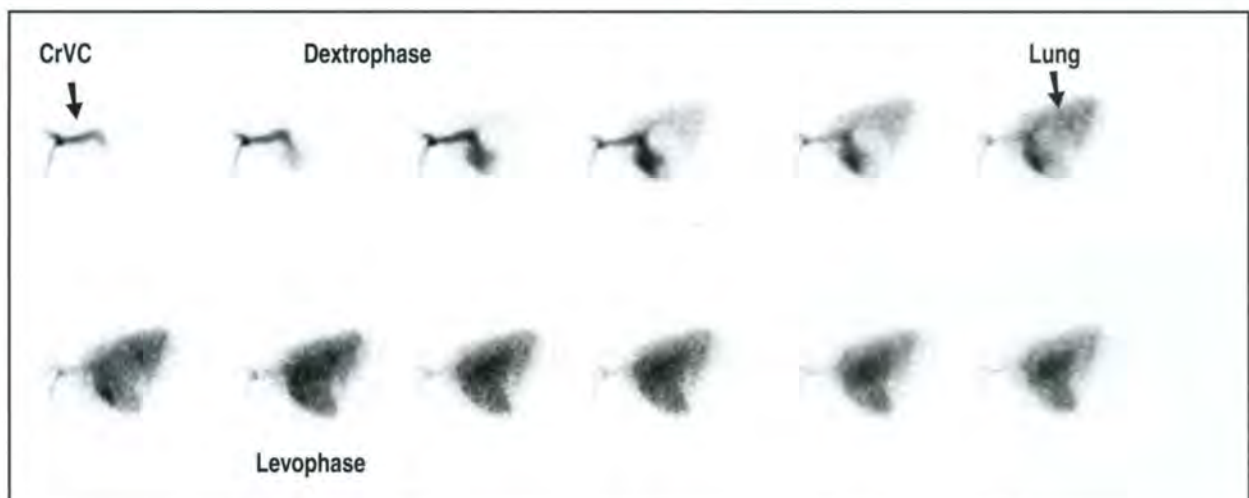
- Dilatation of the main pulmonary artery (seen best on the DV view)
- A 'ductus bump' may be seen
- Underperfusion of the lung fields may be evident (hypovascular pattern, hyperlucent lung fields).

Angiocardiography:

- Right-to-left shunting can be demonstrated by an injection of contrast medium in the RV or main pulmonary artery.
- The contrast medium then shunts from the main pulmonary artery to the descending aorta through the wide ductus (Figure 7.52).
- Pulmonary arteries may be normal or appear tortuous.
- Left-sided injections may show an extensive broncho-oesophageal collateral circulation.



7.52 Angiocardiogram demonstrating a right-to-left shunt through a PDA in a case where significant pulmonary hypertension was present. The contrast medium was injected in the RV, and the aorta (Ao) is opacified at the same time as the main pulmonary artery (MPA). The region of the PDA is indicated by the arrow. (Courtesy of J. Buchanan)



7.51 Left lateral images obtained at four frames per second during a first pass radionuclide angiogram in an 8-month-old Poodle with a left-to-right PDA. Notice the lack of clearance of the lungs in the levophase consistent with pulmonary recirculation; the aorta is never visible. The LA and LV are enlarged, consistent with volume overload. CrVC = Cranial vena cava.

Echocardiography: Echocardiographic findings include:

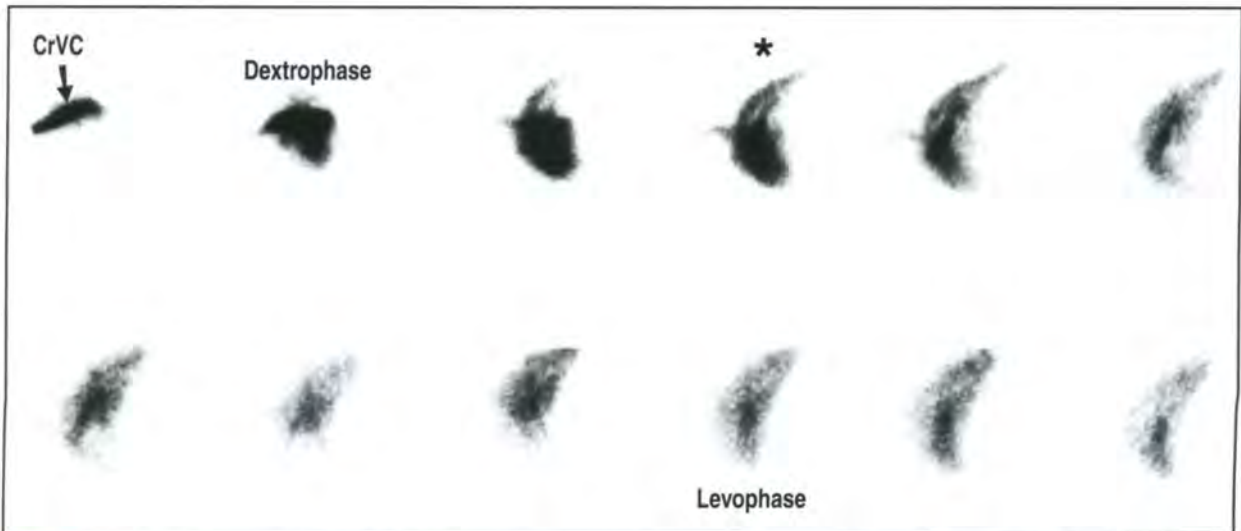
- Enlarged main pulmonary artery
- Concentric hypertrophy of the RV
- May identify a wide tube-like ductus.

Doppler studies: Evidence of pulmonary hypertension is seen (tricuspid or pulmonic insufficiency jets, with increased pressure gradients (PGs) suggesting pulmonary hypertension).

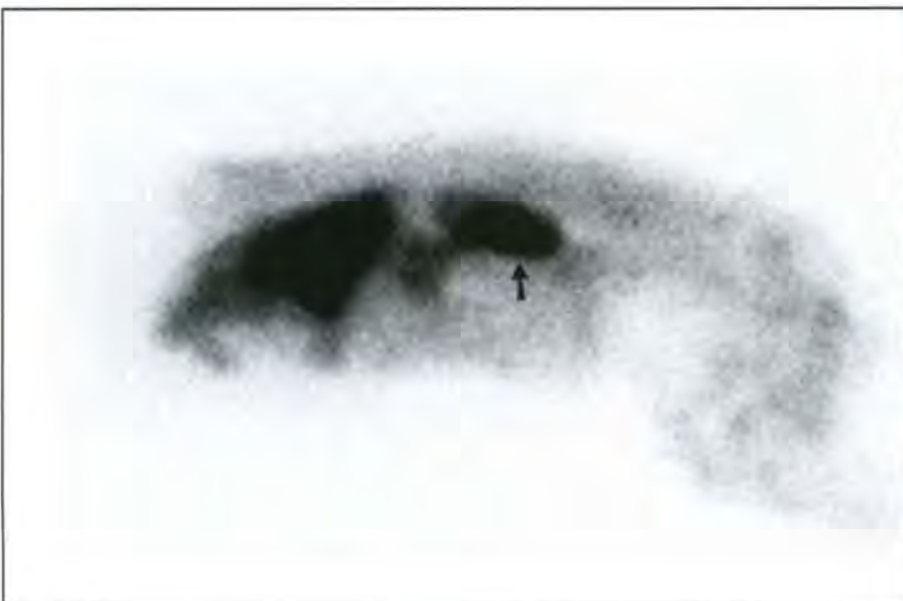
Contrast echocardiography: This is extremely useful in confirming the right-to-left shunt and easy to perform. Agitated sterile saline is injected into a cephalic or saphenous vein. The descending aorta is observed for bubbles confirming shunting; this is best seen in the caudal abdomen, ventral to the spine.

Scintigraphy:

- First pass radionuclide angiography:
 - In cases of reverse PDA, there is simultaneous appearance of the aorta and pulmonary arteries after the dextrophase as the radionuclide passes into the lungs (Figure 7.53)
 - It is not possible to distinguish a reverse PDA from tetralogy of Fallot on the basis of a first pass study alone.
- Scintigraphy with ^{99m}Tc-MAA. In cases of reverse PDA, activity is seen outside the lungs with clear visualization of the renal cortices; however, there is no activity in the neck, head and cerebral cortex due to the location of the shunt caudal to the brachiocephalic trunk and left subclavian artery, thereby allowing differentiation from tetralogy of Fallot (Figure 7.54).



7.53 Left lateral images obtained at four frames per second during first pass radionuclide angiogram in a 6-month-old Collie with a right-to-left shunt. Notice the simultaneous visualization of the main pulmonary artery and aorta (*). A final diagnosis was not reached in this case as the owner elected euthanasia without necropsy. CrVC = Cranial vena cava.



7.54 Whole body composite lateral static image of a 1-year-old Toy Poodle with polycythaemia, obtained 5 minutes after intravenous injection of ^{99m}Tc-MAA. The patient's head is to the left of the image. Note the extrapulmonary distribution of the radiopharmaceutical, with marked uptake at the level of the kidneys (arrowed). Notice also the sharp cut-off at the level of the front limbs, with no radiopharmaceutical distribution to the neck, head and brain. This is consistent with a reverse PDA, in which the radioactive particles are shunted from the pulmonary to the systemic circulation caudal to the brachiocephalic trunk and left subclavian arteries.

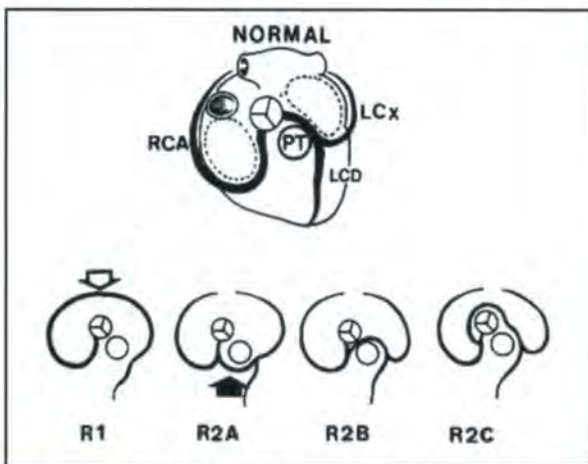
Pulmonic stenosis

Pulmonic stenosis encompasses any obstruction of blood flow from the RV to the main pulmonary artery. The prevalence is higher in English Bulldogs, but also Beagles, Boxers, Chihuahuas, Schnauzers and all terriers. Pulmonic stenosis is a rare condition in cats. The condition usually occurs in isolation but on occasion other cardiac anomalies, such as tricuspid dysplasia, ASD, patent foramen ovale or VSD, may be present.

The stenosis may occur at different levels:

- **Valvular stenosis** (most common form): a variety of anomalies may occur including hypoplasia of the valve, thickened valve leaflets, asymmetric valve leaflets and incomplete commissural separation. A fibrous ring may also be present below the valve
- **Subvalvular stenosis** (less common): a specific form of this occurs in English Bulldogs and Boxers due to an anomalous origin of the left main coronary artery (Figure 7.55). Many variations are possible, but most commonly the left and right coronary arteries branch from a single large coronary artery that arises from the right aortic sinus of Valsalva and wraps around the right ventricular outflow tract (RVOT). These cases cannot be treated with balloon valvuloplasty
- **Supravalvular stenosis** (rare): may be seen more often in Giant Schnauzers.

The stenosis leads to a pressure overload and concentric hypertrophy of the RV. This in turn leads to decreased right ventricular diastolic compliance, ventricular filling impairment and increased right atrial



7.55 Normal coronary artery distribution in dogs and humans, and common patterns of single right coronary artery in the latter. In the type R1 pattern, the right coronary artery (RCA) continues as a single vessel and crosses the caudal crux of the atrioventricular sulcus (open arrow), then continues as the left circumflex (LCx) and left caudal descending (LCD) arteries. In type 2 patterns, the single vessel branches shortly after leaving the aorta. Sub-classifications are made depending on whether the crossing vessel (solid arrow) passes cranial to the pulmonary trunk (PT) (R2A), between the aorta and pulmonary trunk (R2B) or caudal to the aorta (R2C). (Reproduced from Buchanan (1990) with permission from the *Journal of the American Veterinary Medical Association*)

pressure. Tricuspid regurgitation may result and further raises right atrial pressure with eventual right-sided heart failure.

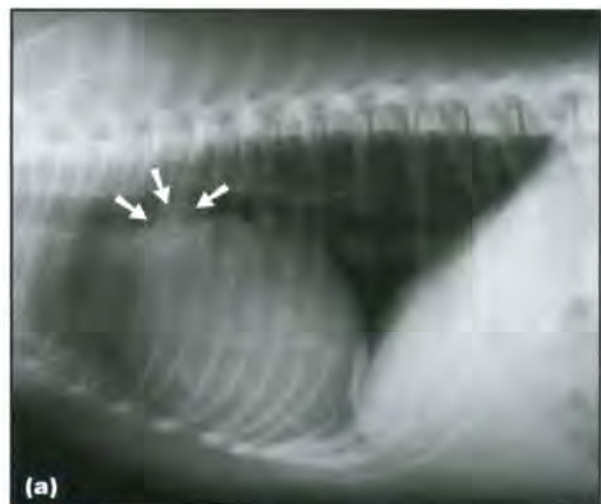
The condition is usually asymptomatic at the time of diagnosis. However, it eventually leads to exercise intolerance, syncope and possible right-sided heart failure if functional tricuspid insufficiency is present. On clinical examination pulmonic stenosis is characterized by a left-sided systolic heart murmur, most audible at the heart base (ejection type of murmur).

Therapy for the condition includes both medical and surgical options and the appropriate choice depends on the severity of the stenosis and the clinical status of the patient. The condition should be monitored over time as some dogs can gradually develop more severe obstructions.

Radiography

Radiographic findings include:

- **Right-sided cardiomegaly:**
 - Increased sternal contact on the lateral view (moderate) (Figure 7.56a)
 - Rounding of the heart with reverse D shape on the DV view (moderate) (Figure 7.56b).
- Prominence of the main pulmonary artery (post-stenotic dilatation), best seen on the DV view (between 01.00 and 02.00 o'clock) (Figure 7.56b)
- In a minority of dogs, the dilated post-stenotic main pulmonary artery segment is seen superimposed over the caudal trachea on the lateral view. This has been termed the 'hat sign' (Figure 7.56a)
- In very severe cases, pulmonary hyperlucency and small pulmonary vessels (due to decreased pulmonary arterial outflow) may be seen



7.56 West Highland White Terrier with pulmonic stenosis. **(a)** Lateral view of the thorax. There is rounding of the cranioventral border of the heart and increased sternal contact, consistent with right-sided cardiomegaly. The dilated post-stenotic main pulmonary artery segment is seen protruding dorsally from the heart base (arrowed) and is superimposed over the ventral aspect of the caudal trachea. This feature has been termed the 'hat sign'. (Courtesy of J. Buchanan) (continues)



7.56 (continued) West Highland White Terrier with pulmonic stenosis. **(b)** VD view of the thorax. The cardiac silhouette has a reversed D shape, consistent with right-sided cardiomegaly. There is also a soft tissue opacity bulging out of the cardiac silhouette at the left fourth intercostal space, between 01.00 and 02.00 o'clock, consistent with dilatation of the main pulmonary artery. A catheter is present in preparation for an angiogram. (Courtesy of J. Buchanan)

- There may be signs of right-sided cardiac failure: right ventricular and atrial enlargement, enlarged CdVC, hepatomegaly, ascites and pleural effusion.

Angiocardiography: This is not usually used for diagnosis but is often used prior to surgical intervention. Diagnosis can be established after selective catheterization of the RVOT using a jugular approach. Right atrial injections of contrast medium are not suitable for the diagnosis of pulmonic stenosis, since the pulmonic valve area is usually superimposed upon the opacified RA.

- Stenosis is visible at the level of the valve, the infundibulum or at the subvalvular level (muscular hypertrophy, creating a filling defect in the outflow tract) (Figure 7.57a).
- Post-stenotic dilatation of the main pulmonary artery can be identified (Figures 7.57ab).
- In cases of functional tricuspid insufficiency, regurgitation of contrast medium is seen from the RV to the RA.

- In English Bulldogs and Boxers, it is vital to search for an abnormal origin of the left coronary artery as an underlying cause of the stenosis (see Figure 7.55). Ideally, coronary arteriography should be performed. Alternatively, the aortic root and coronary arteries should be examined in the late levophase after a right ventricular injection of contrast medium, or just after a left ventricular injection of contrast medium. In affected animals a single coronary artery is seen wrapping around the RVOT and a right coronary artery branches from this single artery a few millimetres distal to its aortic origin (Figure 7.58).



7.57 Angiocardiogram after injection of contrast medium in the RV. Same dog as Figure 7.56. **(a)** On the lateral view the main pulmonary artery is opacified and there is a clear narrowing at the level of the infundibulum as well as post-stenotic dilatation of the main pulmonary artery. **(b)** On the VD view the main pulmonary artery is opacified and there is a clear dilatation. (Courtesy of J. Buchanan)



7.58 Angiocardiogram in a Bulldog with a pulmonic stenosis. The contrast medium injection was made in the LVOT in order to opacify the aorta and the coronary arteries. A single coronary artery (arrowed) is seen, which then branches into a right and left coronary artery. (Courtesy of J. Buchanan)

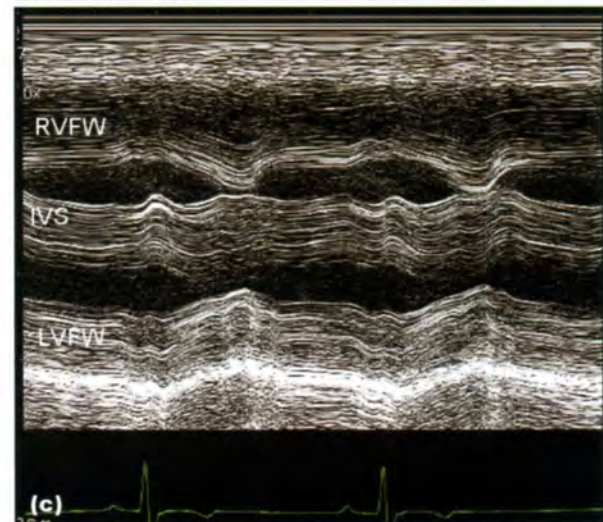
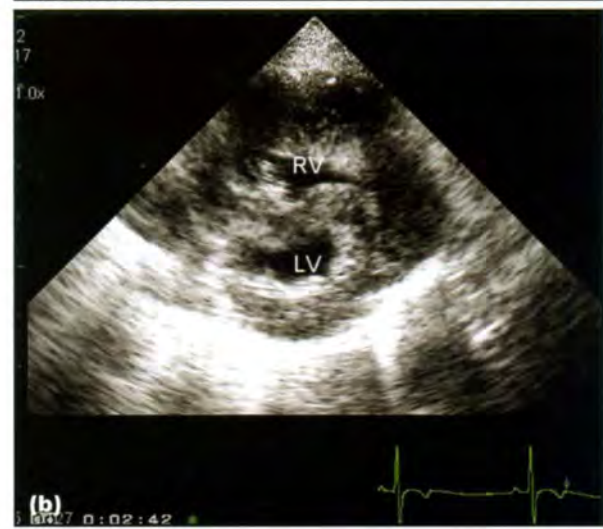
Echocardiography

Echocardiography is useful to confirm the diagnosis and to grade the severity of the stenosis. Findings include:

- Concentric hypertrophy of the RV (Figure 7.59), secondary to pressure overload on the RV. Seen as a thickening of the right ventricular free wall that can approach or exceed the thickness of the left ventricular free wall
- Prominent right ventricular papillary muscles are sometimes visible
- Flattening of the IVS due to the elevated right ventricular pressure. On M-mode images, paradoxical motion of the septum may be seen (Figure 7.60)

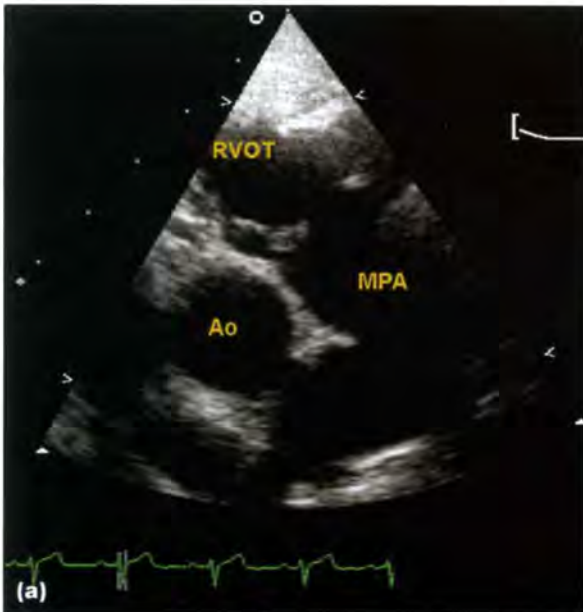


7.59 RPS short-axis echocardiogram at the level of the ventricles in a dog with pulmonic stenosis. There is a clear concentric hypertrophy of the right ventricle (RV) and flattening of the IVS, secondary to the pressure overload on the RV. LV = Left ventricle.



7.60 (a) RPS long-axis four-chamber view from a Lhasa Apso with pulmonic stenosis. Note the right ventricular hypertrophy and the right atrial enlargement. (b) RPS short-axis view at the level of the papillary muscles. The right ventricular free wall is markedly thickened and the IVS is flattened. (c) An M-mode echocardiogram acquired from the level shown in (b). Paradoxical motion of the IVS is present. IVS = Interventricular septum; LA = Left atrium; LV = Left ventricle; LVFW = Left ventricular free wall; RA = Right atrium; RV = Right ventricle; RVFW = Right ventricular free wall. (© J. Duker-McEwan)

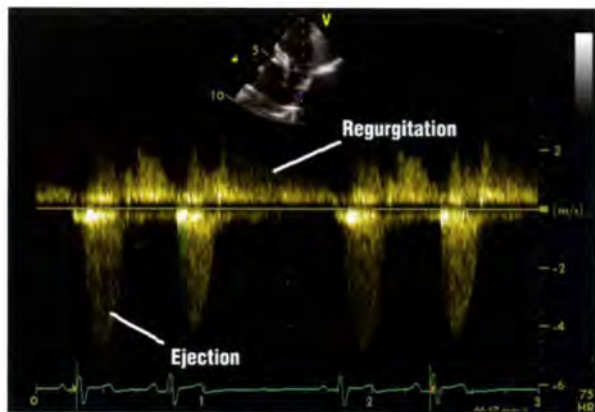
- **Abnormal pulmonic valve (Figure 7.61):**
 - Thickened, with a limited systolic excursion
 - Hyperechoic
 - If the valve leaflets are fused, occasionally ballooning can be seen during systole.
- Abnormal subvalvular region: discrete subvalvular fibrous ring may also be seen as well as generalized infundibular hypertrophy
- Post-stenotic dilatation of the main pulmonary artery distal to the valve
- Possible right atrial dilatation (and occasionally right ventricular dilatation).



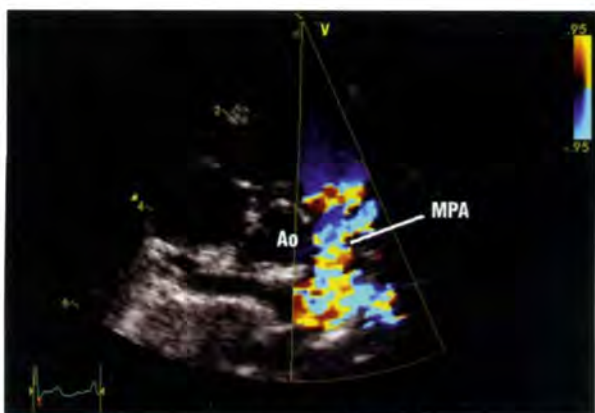
7.61 (a) LPS view optimized for the right ventricular outflow tract (RVOT) in a crossbred Labrador Retriever with pulmonic stenosis. Markedly thickened pulmonic valve leaflets are seen and there is a prominent post-stenotic dilatation of the main pulmonary artery (MPA). The aorta (Ao) is also seen in short axis. (b) LPS short-axis view. The pulmonic valve is seen in short axis during diastole. The valve leaflets (arrowed) are thickened and echogenic. The aorta is also seen on this image. (© J. Dukes-McEwan)

Doppler studies:

- **Accelerated ejection velocity** through the pulmonic valve (Figure 7.62). Care should be taken to achieve parallel alignment and to use continuous wave (CW) Doppler to achieve accurate velocity measurements.
- **Turbulent** ejection flow in the main pulmonary artery (Figure 7.63). Possible mild to moderate **pulmonary insufficiency** (diastolic back-flow from the main pulmonary artery to the RV) (Figure 7.62).
- The severity of the obstruction can be estimated by accurate measurement of the **peak flow velocity** through the main pulmonary artery. This is then used to calculate the instantaneous PG across the obstruction using the modified Bernoulli equation. The PG may be used to grade the severity of the stenosis, though it should be noted that the reliability of this measurement may vary with myocardial contractility and sedation/ anaesthesia:
 - Mild: <50 mmHg
 - Moderate: 50–80 mmHg



7.62 Spectral Doppler study of the main pulmonary artery in a dog with pulmonic stenosis. There is an increased velocity of the ejection flow, which is higher than 4 m/s. There is also a diastolic regurgitation from the main pulmonary artery to the RV due to some pulmonic insufficiency. (Courtesy of M. Oyama)



7.63 Colour Doppler study of the main pulmonary artery in a dog with pulmonic stenosis. There is a turbulent flow in the main pulmonary artery during systole as indicated by a mosaic-like colour display of the flow. Ao = Aorta; MPA = Main pulmonary artery. (Courtesy of M. Oyama)

- Severe: >80 mmHg. Such animals are likely to develop right-sided cardiac failure early and are candidates for balloon valvuloplasty.
- *Tricuspid insufficiency*. Measurement of this may also be useful to assess the degree of stenosis when accurate measurement of main pulmonary artery velocity cannot be obtained.

Aortic stenosis

The vast majority of aortic stenosis occurs in the *subvalvular* region (subvalvular aortic stenosis). This is the most common congenital cardiac malformation in large-breed dogs. *Valvular* stenosis (thickened valves and hypoplastic annulus) is rare, but Bull Terriers are predisposed. A bicuspid valve may also rarely cause a mild valvular stenosis. *Supravalvular* stenosis is also very rare. The remainder of this section relates to subvalvular aortic stenosis.

Large-breed dogs are more commonly affected by subvalvular aortic stenosis. Breed predisposition includes Golden Retrievers, Newfoundlands, German Shepherd Dogs, Boxers, Rottweilers and English Bull Terriers. It occurs occasionally in cats. The condition may be accompanied by other congenital cardiac disorders, such as mitral valve dysplasia and PDA.

The lesion is usually a fixed ridge or ring of fibrous tissue in the LVOT just below the aortic valve. The outflow obstruction leads to increased left ventricular systolic pressure, and concentric left ventricular hypertrophy results. A post-stenotic dilatation of the aorta and sometimes brachiocephalic trunk occurs. Mild aortic regurgitation is often present. Animals with subvalvular aortic stenosis are predisposed to aortic endocarditis, abnormal coronary arterial flow and myocardial infarctions.

The functional and clinical consequences vary with the severity of the obstruction. This ranges from minor obstructions with minimal hypertrophy and no clinical signs, to significant obstructions with concentric hypertrophy of the LV, left-sided heart failure, syncope or sudden death.

Radiography

Radiography is often unremarkable in mild cases. Changes may be seen in more severe cases:

- Lateral view (Figure 7.64a):
 - Elongated cardiac silhouette, with dorsally displaced trachea and carina and straightened caudal margin of the heart due to left ventricular enlargement
 - Prominent ascending aorta and aortic arch (post-stenotic dilatation)
 - Sometimes mild left atrial enlargement (if severe, suggests concurrent mitral regurgitation)
 - In cases with left-sided heart failure: left atrial dilatation, pulmonary venous congestion and pulmonary oedema.
- DV view (Figure 7.64b):
 - Rounding of the left contour of the heart

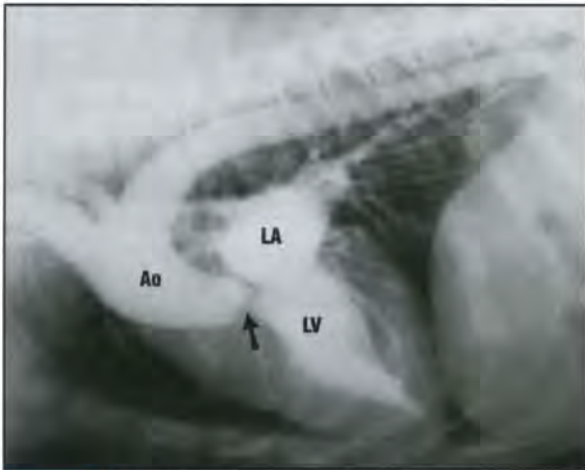


7.64 (a) Lateral view of the thorax in a dog with aortic stenosis. There is a marked rounding and bulging of the cardiac silhouette cranially in the region of the aortic arch. (b) VD view of the thorax. There is a marked bulge of the aortic arch visible between 11.00 and 01.00 o'clock (arrowed).

- Aortic bulge at the 11.00–01.00 o'clock position
- There may be left atrial enlargement (see above)
- In cases with left-sided heart failure: left atrial dilatation, pulmonary venous congestion and pulmonary oedema.

Angiocardiography:

- Subaortic stenosis is demonstrated by a left ventricular injection of contrast medium.
- Narrowing of the outflow tract is usually obvious on lateral views (Figure 7.65).
- Varying degrees of post-stenotic dilatation of the ascending aorta can be identified: in a normal dog, the maximum diameter of the ascending aorta distal to the sinus of Valsalva is always less than the diameter of the sinus of Valsalva.



7.65 Angiocardiogram in a dog with subaortic stenosis. The contrast medium was injected in the RA and this is the levophase of the study, 7 seconds after injection of the contrast medium. There is clear narrowing of the subaortic region (arrowed) and mild post-stenotic dilatation of the aorta. Some degree of concentric hypertrophy of the LV can also be appreciated on this view. Ao = Aorta; LA = Left atrium; LV = Left ventricle. (Courtesy of J. Buchanan)

Echocardiography

It can be extremely difficult to detect mild aortic stenosis with standard echocardiography. Subtle or no changes may be seen.

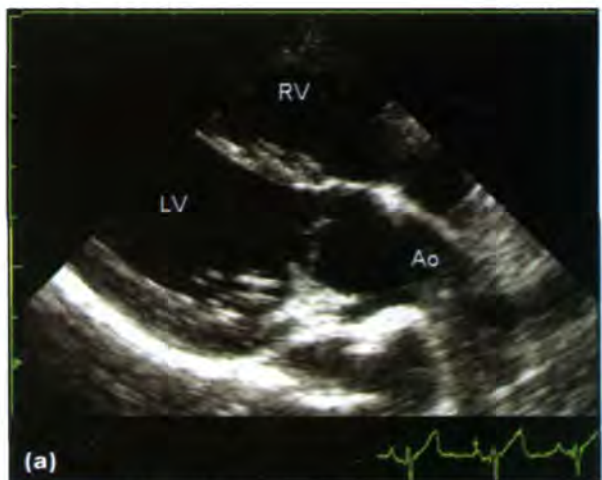
- Moderate to severe cases:
 - Left ventricular concentric hypertrophy is seen, with thickening of the left ventricular free wall and IVS (Figure 7.66a)
 - Hyperechoic ridge or circumferential ring of hyperechoic tissue in the region of the LVOT (Figure 7.66b and 7.67)
 - Post-stenotic dilatation of the ascending aorta.
- Severe cases as above plus:
 - Hyperechoic papillary muscles and endocardial surface due to areas of myocardial ischaemia and subsequent fibrosis
 - If there is mitral regurgitation, left atrial enlargement may be observed
 - Systolic anterior motion of the mitral valve may be seen in animals with concurrent mitral dysplasia.

Doppler studies: These are important in diagnosis and are characterized by high-velocity turbulent aortic flow (see Figure 7.67). The maximum normal aortic velocity in most dogs is 1.7 m/s. However, higher velocities can be seen in normal dogs and also breeds with slightly reduced LVOT size (e.g. Boxers, Golden Retrievers, Bull Terriers). Note also that conditions of excitement and stress will increase the velocity, and myocardial failure will reduce it.

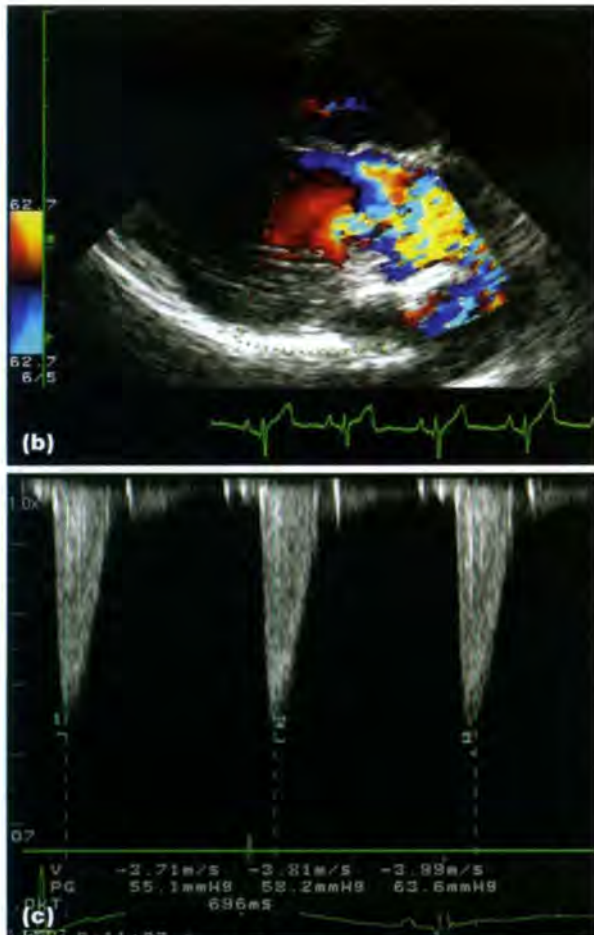
Subcostal (retroxiphoid) views are ideal for good alignment and accurate estimation of aortic velocities, although they are difficult to achieve in larger breed dogs due to the distance between the transducer and the LVOT; CW Doppler should be used.



7.66 (a) RPS short-axis echocardiogram at the level of the papillary muscles in a dog with subaortic stenosis. There is concentric hypertrophy of the left ventricle. The papillary muscles are more prominent than normal. The left ventricular cavity is reduced in this image acquired in diastole. (b) RPS five-chamber view of a Maine Coon cat with valvular and supravalvular aortic stenosis. Two focal regions of narrowing are identified in the LVOT and there is dilatation of the post-stenotic aorta (Ao). LV = Left ventricle. (© J. Dukes-McEwan)



7.67 (a) RPS five-chamber view from a German Shepherd Dog with subvalvular aortic stenosis. Note the prominent ridge in close proximity to and just below the aortic valve. Ao = Aorta; LV = Left ventricle; RV = Right ventricle. (© J. Dukes-McEwan) (continues)



7.67 (continued) **(b)** RPS five-chamber view, showing a colour Doppler map of the aortic outflow during systole. Note the turbulent flow within the aorta due to the stenosis. **(c)** CW Doppler trace from the aorta obtained from a subcostal position. A maximal aortic velocity of 3.99 m/s was recorded. The maximal aortic velocity in most dogs is 1.7 m/s. Ao = Aorta; LV = Left ventricle; RV = Right ventricle. (© J. Duker-McEwan)

- The diagnosis is reinforced when increased velocities show rapid focal acceleration in the LVOT and/or are accompanied by turbulent flow and anatomical lesions.
- Calculation of the PG across the stenosis (using the maximal aortic velocity) may be used for grading severity and estimating prognosis:
 - Dogs with maximal PG of <50 mmHg and minimal ventricular hypertrophy are more likely to lead normal lives
 - Dogs with maximal PG of >125 mmHg are very likely to develop serious complications or die suddenly.
- Mitral inflow studies may show an increased A wave during diastole (decreased E:A ratio) due to loss of compliance in the hypertrophied LV.
- Functional mitral regurgitation might be present in severe cases and those with concurrent mitral dysplasia. When present, it usually has a higher velocity than normal due to increased left ventricular pressure (and hence increased PG between the LV and the LA).

Ventricular septal defect

VSD is a common congenital disorder in both dogs and cats. Breed predispositions include English Springer Spaniels, West Highland White Terriers and Lakeland Terriers, amongst others. VSD is known to have a genetic basis in the Keeshond with malformations of the conotruncal septum.

Anomalous development of any part of the ventricular septal components may lead to a VSD (see above). However, most commonly the defect occurs at the point of fusion of the membranous and muscular parts of the septum, resulting in a perimembranous lesion. Thus, the defect is most often located 'high' or dorsally on the septum. Occasionally, the defect occurs lower down in the muscular part of the septum.

On the *left* side the defect is usually located in the subaortic septum, just below the aortic valve and typically between the right coronary and non-coronary cusps. On the *right* side the location is more variable. Typically, the VSD opens under the septal cusp of the tricuspid valve (also known as infracristal or under the crista supraventricularis). Less commonly, the opening on the right is in a more cranial location and opens directly into the RVOT above the tricuspid valve (also known as supracristal or above the crista supraventricularis). The full classification of VSDs is complex and is beyond the scope of this manual.

The septal defect allows *left-to-right* shunting of blood unless other significant abnormalities are present, which result in shunt reversal (such as pulmonic stenosis, tricuspid dysplasia or severe pulmonary arterial hypertension). Pathophysiological and clinical effects of the VSD depend upon the size and location of the defect, and the presence or absence of associated malformations. VSDs may be classed as resistive or non-resistive:

- *Resistive* VSDs are small and provide resistance to flow between the right and left sides
- *Non-resistive* VSDs are large (approximately the same size as the aortic orifice), and there is no resistance to flow between the two sides.

The most common type of VSD in the dog is a *small resistive* VSD. However, these are often large enough to have clinical significance. With resistive lesions the flow across the defect depends both on its size and the pressure difference between the left and right sides. Blood is shunted from the high pressure left side to the right side across the defect (in the absence of other abnormalities).

In most cases it has been shown that the shunted volume moves directly into the RVOT, hence right-sided enlargement is not usually a feature of the condition. The shunted blood then enters the pulmonary circulation and finally returns to the left side of the heart. This results in *overcirculation of the pulmonary system and left-sided heart enlargement* (eccentric hypertrophy) if the shunt is significant. If left ventricular end-diastolic pressure increases sufficiently as a result, then left-sided heart failure will ensue.

Less commonly, the defect is lower in the septum and a significant volume of shunted blood enters the RV, rather than exiting immediately via the outflow tract. In this case, right-sided heart enlargement may occur.

Non-resistive VSDs result in the two ventricles functioning as a single chamber. The volume of blood that is shunted, and the direction that it is shunted in, depends purely on the difference between the systemic and pulmonary resistance. In most cases the systemic resistance is much higher and a huge left-to-right shunt occurs. However, this large shunt to the pulmonary circulation will result in increased pulmonary pressure. The RV hypertrophies concentrically in response to this. Both ventricles also hypertrophy eccentrically.

If pulmonary hypertension worsens (pulmonary vascular pathology, reactive pulmonary hypertension) then there will be increased resistance to the right ventricular outflow. The shunt fraction from left-to-right will decrease and eventually shunt reversal may occur should right ventricular systolic pressures exceed left ventricular systolic pressures. The latter is known as *Eisenmenger's complex*; and right-to-left shunting and cyanosis are observed.

The clinical presentation, prognosis and recommended treatment vary enormously with the type of VSD. In general, small, uncomplicated VSDs have a good prognosis and clinical signs may not be seen. Animals with larger shunts and cardiomegaly have a poorer prognosis. Those with Eisenmenger's complex have a very guarded long-term prognosis.

Radiography

Radiographic findings include:

- Small defects: thoracic radiographs can be totally normal
- Larger defects: left atrial and left ventricular enlargement with or without increased vascular pattern in the lungs (Figure 7.68)
- In cases with left-sided congestive heart failure: pulmonary oedema
- In cases with biventricular heart failure: pulmonary oedema, pleural and peritoneal effusion
- Varying degrees of right ventricular and main pulmonary artery enlargement are also possible, depending on the level and size of the defect (as explained above)
- Main pulmonary arterial enlargement and an underperfused lung periphery suggests pulmonary hypertension or pulmonic stenosis and shunt reversal.

Angiocardiography: VSDs with left-to-right shunts are best demonstrated by injection of contrast medium in the LV (Figure 7.69):

- The left ventricular opening is usually high in the ventricular septum, in the outflow tract just below the aortic valve
- The right ventricular opening is usually just under the cranial part of the septal leaflet of the tricuspid valve
- Shunting usually occurs only in systole, as in diastole the PG between both ventricles almost equals zero.



7.68 Thorax of a cat with a VSD. **(a)** Lateral view. There is generalized cardiomegaly and a marked increase in the vascular pattern of the lungs, which is consistent with left-to-right shunting. The cat had a pectus excavatum, making accurate positioning difficult. **(b)** VD view. There is moderate generalized cardiomegaly and enlargement of the caudal pulmonary lobar arteries and veins.



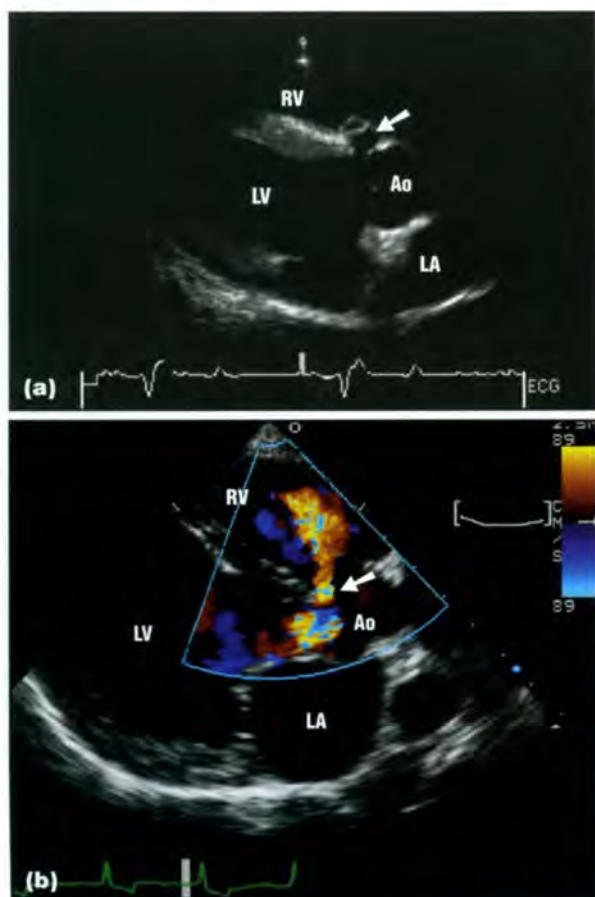
7.69 Angiocardiogram in a dog with a VSD. The contrast medium was injected in the LV and shunting can be seen from the LV to the RV through a membranous VSD (arrowed). There is also eccentric hypertrophy of the LV. The LA also appears dilated. (Courtesy of J. Buchanan)

VSDs with right-to-left shunts secondary to pulmonary hypertension (Eisenmenger's complex) are best demonstrated by injection of contrast medium in the RV; there is evidence of passage of contrast medium into the LV immediately after the injection into the RV, and simultaneous opacification of the aorta and main pulmonary artery. This condition can be difficult to differentiate from a tetralogy of Fallot.

Echocardiography

Echocardiographic findings include:

- Visualization of the septal defect may be possible, usually on a RPS long-axis five-chamber view, just below the root of the aorta (Figure 7.70a)
- Signs of eccentric hypertrophy of the left heart may be visible: left ventricular and left atrial dilatation (Figure 7.70ab)
- Right ventricular hypertrophy and/or dilatation can also be seen, depending on the nature of the VSD (Figure 7.70b).

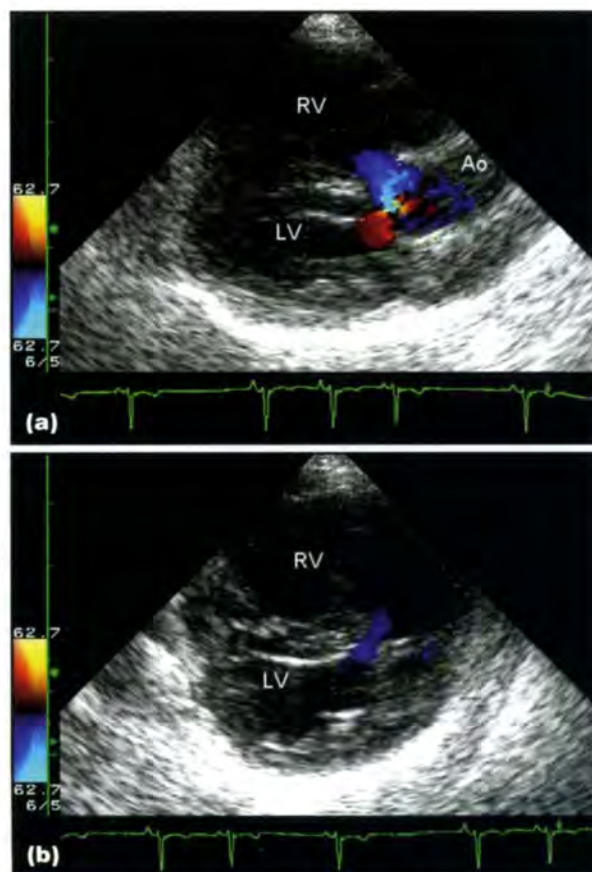


7.70 (a) RPS long-axis echocardiogram in a dog with a VSD. The defect is clearly visible (arrowed). There is mild left ventricular and atrial dilatation. (Courtesy of M. Oyama) (b) Colour Doppler study in a dog with a VSD. On this RPS long-axis echocardiogram, shunting is clearly seen as a turbulent flow through the defect from the LV to the RV (arrowed). There is left ventricular and atrial dilatation as well as right ventricular dilatation. Ao = Aorta; LA = Left atrium; LV = Left ventricle; RV = Right ventricle. (Courtesy of M. Sleeper)

Doppler studies: Colour Doppler investigation is extremely useful to identify VSDs (see Figures 7.70b and 7.71). Shunting through the defect can be demonstrated using Doppler studies, revealing high-velocity and turbulent systolic flow through the defect; the direction of shunting can also be assessed.

The usual velocity of the flow through an uncomplicated small resistive defect (the most common type in dogs) with normal left and right ventricular pressures is ≥ 4.5 m/s. A lower velocity should raise suspicion for increased right ventricular systolic pressure (pulmonary hypertension, pulmonic stenosis, etc.). Occasionally, there is secondary functional aortic regurgitation (due to the proximity of the defect to the insertion of the septal aortic leaflet) and this can be documented on Doppler examination.

Contrast echocardiography: Right-to-left shunts can be assessed using an ultrasound bubble study: an intravenous injection of vigorously shaken saline is performed. If a right-to-left shunt is present, echogenic gas bubbles appear simultaneously in the right and left cardiac cavities after injection.



7.71 (a) RPS long-axis five-chamber view from a Cavalier King Charles Spaniel with a VSD and Eisenmenger's complex. The blood flows from right-to-left across the defect in this case (seen as blue on the colour Doppler map). (b) RPS short-axis view at the level of the ventricles. The small right-to-left shunting VSD is identified by colour Doppler as flow from the RV to the LV. This can be a subtle finding and is easily missed unless a careful and thorough examination is undertaken. Ao = Aorta; LV = Left ventricle; RV = Right ventricle. (© J. Dukes-McEwan)

Scintigraphy

The scintigraphic findings using first pass radionuclide angiocardiology include:

- Prolongation of the radioactivity within the lungs with incomplete clearance of the lungs during the levophase
- Lack of lung clearance in the levophase, causing partial or complete obliteration of the borders of the aorta
- In a medium to large VSD, reappearance of the RV during the levophase due to shunting of the radiopharmaceutical through the defect, allowing differentiation from a PDA (Figure 7.72)
- QP:QS ratio >1.2.

Atrial septal defect

ASDs are uncommon congenital abnormalities in the dog. Breeds at risk include the Samoyed, Boxer, Newfoundland and Old English Sheepdog. They are also infrequently seen in cats (mostly endocardial cushion defects).

ASDs can occur at three main locations:

- High in the atrial septum, near the entrance of the pulmonary veins. These are *sinus venosus* ASDs and are very rare
- In the middle of the septum. These are *ostium secundum* ASDs and are the most common type. They vary in size. Some authors consider a patent foramen ovale to be a small ostium secundum defect. Conversely, other authors do not consider a patent foramen ovale to be a true ASD, as the atrial septum forms normally but the foramen walls are pushed apart, usually by conditions that increase right atrial pressure
- At the base of the septum. These are either *ostium primum* defects or *endocardial cushion* defects. Various types of endocardial cushion defects exist and they are often accompanied by abnormal atrioventricular

valve development. These defects are usually big and are more commonly reported in cats. A complete endocardial cushion defect comprises a large ASD in the lower atrial septum, a high VSD and fusion of the septal leaflets of the two atrioventricular valves. This results in a communication between all four cardiac chambers and is also known as an *atrioventricular valve canal defect*.

Most ASDs are associated with left-to-right shunting, unless there is a reason for reversal of the flow, with increased right atrial pressure (pulmonic or tricuspid valve malformation or pulmonary hypertension). Just as with VSDs, the defect may be classed as resistive or non-resistive.

The shunting occurs during diastole. Large defects result in significant left-to-right shunting and eccentric hypertrophy of the RV, pulmonary overcirculation and sometimes right atrial dilatation. Right-sided heart failure may result.

If left atrial enlargement is identified then the examiner should look for an additional defect, such as an endocardial cushion defect with mitral regurgitation. These animals may develop left-sided or bilateral heart failure.

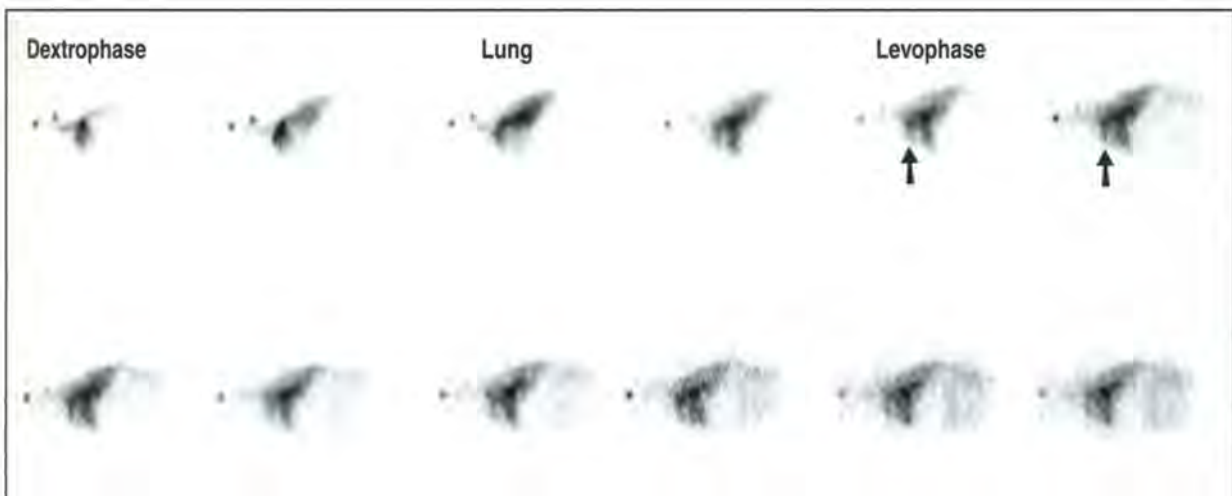
Shunt reversal may occur in certain conditions, such as pulmonic stenosis or pulmonary hypertension (Eisenmenger's syndrome/physiology).

Most ASDs are not clinically significant and treatment is usually not necessary.

Radiography

Radiographic findings include:

- Often normal radiographs
- Right-sided cardiomegaly: dilatation of the RV with or without dilatation of the RA (Figure 7.73)
- There may be enlarged pulmonary arteries
- Left atrial changes are seen with some endocardial cushion defects.



7.72 Left lateral images obtained at four frames per second during first pass radionuclide angiogram in a 1-year-old cat with a VSD. Notice the lack of clearance of the lungs in the levophase and the lack of distinction of the margins of the aorta, consistent with pulmonary recirculation in a left-to-right shunt. In this case, reappearance of the RV in the levophase (arrowed) indicates a VSD.



7.73 DV view of the thorax in a dog with an ASD. There is mild rounding of the cardiac silhouette in the region of the RA, between 09.00 and 11.00 o'clock.

Angiocardiography: Uncomplicated ASDs are demonstrated using left atrial injections of contrast medium. The study reveals abnormal shunting of the contrast material from the LA to the RA, through the septal defect. In cyanotic animals, where right-to-left shunting is suspected, the septal defect can be demonstrated using a right atrial injection of contrast medium.

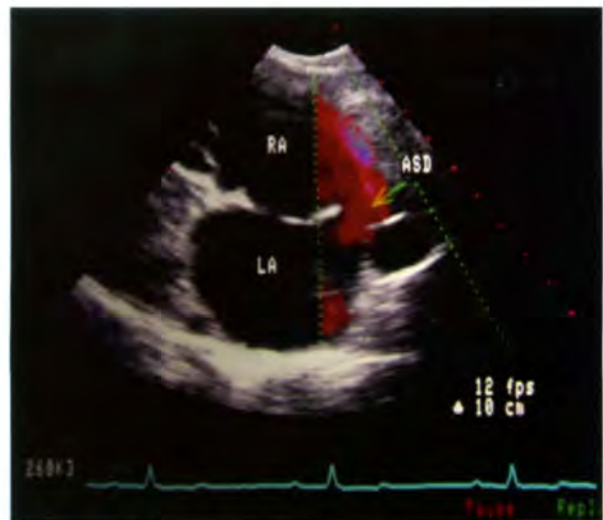
Echocardiography

Septal defects can be identified at various locations. They are best seen using a RPS long-axis four-chamber view (Figure 7.74). However, it is important to be aware that the thin nature of the septum and ultrasound beam orientation may result in the false appearance of a defect. Doppler studies must be used for confirmation (Figure 7.75). There may also be:



7.74 RPS long-axis echocardiogram in a dog with an ASD. The defect is clearly seen as an interruption of the echogenic line of the interatrial septum (arrowed). LA = Left atrium; LV = Left ventricle; RA = Right atrium.

- Right atrial dilatation
- Right ventricular eccentric hypertrophy
- Atrioventricular valve abnormalities, possibly with high VSD ± left atrial dilatation in endocardial cushion defects (Figure 7.76).



7.75 RPS long-axis four-chamber view of a Boxer with an ostium secundum type ASD. Flow across the defect is identified. ASD = Atrial septal defect; LA = Left atrium; RA = Right atrium. (© J. Duker-McEwan)



7.76 RPS four-chamber echocardiogram of a cat with an endocardial cushion defect. A large VSD and ASD are present. LA = Left atrium; LV = Left ventricle; RA = Right atrium; RV = Right ventricle. (© J. Duker-McEwan)

Doppler studies: Doppler should always be used to confirm the abnormal flow through the septal defect, usually from left-to-right (best demonstrated on the RPS long-axis four-chamber view).

Occasionally, there is increased velocity of the blood flow through the pulmonic valve, due to an increased volume of flow through a normal valve, associated with left-to-right shunting. On clinical examination this can be identified as a murmur of 'relative pulmonic stenosis'. There may also be evidence of additional defects (e.g. mitral regurgitation in some endocardial cushion defects).

Scintigraphy

Scintigraphic findings with first pass radionuclide angiocardiography include:

- Prolongation of the radioactivity within the lungs with incomplete clearance of the lungs during the levophase
- Lack of lung clearance in the levophase, causing partial or complete obliteration of the borders of the aorta
- In the case of a large defect, potential reappearance of the RA and/or RV; this has not yet been documented
- QP:QS ratio >1.2.

Mitral valve dysplasia

This condition is frequently encountered in dogs, especially Great Danes, English Bull Terriers, German Shepherd Dogs, Mastiffs, Golden Retrievers and Newfoundlands. Cats are also affected and mitral dysplasia may be the most common congenital cardiac defect in this species.

The disease encompasses any combination of malformed valve leaflet or cusps, abnormal chordae tendinae (short, absent or too long) and abnormal papillary muscles (fused, abnormally positioned). Concurrent cardiac abnormalities may be noted in dogs, such as subvalvular aortic stenosis. Most commonly the abnormality is associated with systolic mitral regurgitation. Valvular insufficiency leads to volume overloading, and atrial and ventricular dilatation. Left-sided congestive heart failure may eventually result. Mitral stenosis can also occur and in dogs is seen in the Bull Terrier.

Animals may be asymptomatic or can present with exercise intolerance or even left-sided heart failure. A holosystolic murmur will be heard over the left apex (or left sternal border in cats). The prognosis is variable and influenced by the presence of heart failure.

Radiography

Radiographic changes are very similar to those of acquired mitral insufficiency secondary to mitral endocardiosis:

- Left atrial and left ventricular enlargement (Figure 7.77)



7.77 Lateral view of the thorax in a dog with mitral valve dysplasia. There is a marked dilatation of the LA, creating a prominent bulge between 12.00 and 03.00 o'clock.

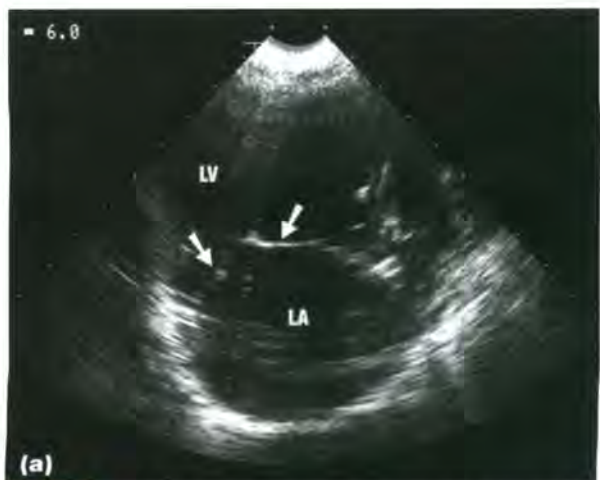
- Enlargement of the pulmonary veins
- At the stage of cardiac failure: cardiogenic pulmonary oedema (\pm pleural effusion in cats)
- Mitral stenosis should be considered when the atrium is markedly enlarged but not accompanied by changes in the ventricle.

Angiocardiography: This is generally not useful for diagnosis of mitral valve dysplasia. Mitral regurgitation is demonstrated by left ventricular injection of contrast medium. Prominent left atrial dilatation accompanied by left ventricular dilatation will usually be identified. Mitral stenosis is best demonstrated using a left atrial injection of contrast medium (performed by transeptal catheterization) but is certainly difficult to recognize.

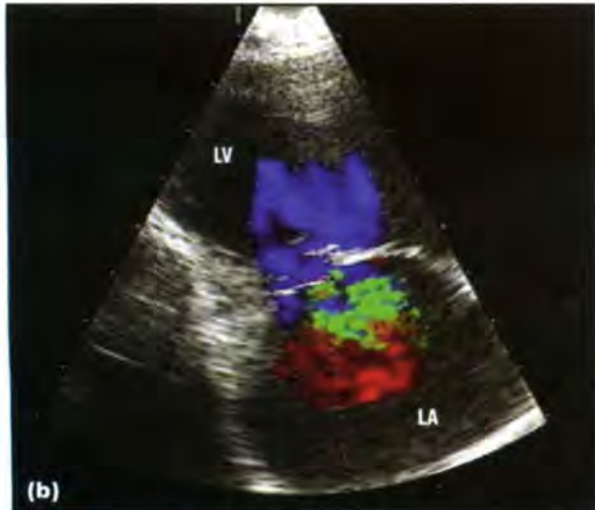
Echocardiography

Echocardiographic findings include:

- Left atrial and ventricular enlargement (Figure 7.78)
- Abnormal mitral apparatus:
 - Malformed valve leaflet or cusps (thickened, hyperechoic)
 - Hyperechoic chordae tendinae, which can be short, absent or too long
 - Abnormal papillary muscles (fused or abnormally positioned)
 - Abnormal motion of the mitral leaflets: may appear rigid, lack of diastolic opening (potentially leading to mitral stenosis) (Figure 7.78a).
- If there is mitral regurgitation (most cases), in the early stage of the disease M-mode examination (at the transventricular level) shows a hyperkinetic ventricle with an increased fractional shortening as the regurgitation volume into the low-pressure LA assists rapid emptying of the LV.
- Left ventricular function may deteriorate over time.



7.78 (a) Left apical echocardiogram of a dog with mitral valve dysplasia, presenting with both mitral stenosis and regurgitation as a functional consequence of the valvular malformation. There is marked dilatation of the LA. Note the lack of opening of the mitral valve leaflets, leading to a mitral stenosis (arrowed) in this diastolic image. LA = Left atrium; LV = Left ventricle. (continues) ▶



7.78 (continued) **(b)** Left apical echocardiogram colour Doppler study in systole. There is a mitral regurgitation with a high-velocity, turbulent flow. LA = Left atrium; LV = Left ventricle.

Doppler studies:

- High-velocity systolic regurgitant flow from the LV to the LA, best demonstrated using a left apical window (see Figure 7.78b).
- When mitral stenosis is present, an abnormally prolonged high-velocity jet will be noted from the atrium into the ventricle during diastole. There will be acceleration of the A wave (atrial systole) of ventricular filling and a decrease in the E:A ratio.

Tricuspid valve dysplasia

This condition is mostly observed in dogs, with larger breeds such as Labrador Retrievers most commonly affected (especially males). The condition is also seen in cats.

Tricuspid valve dysplasia is characterized by malformed tricuspid leaflets, chordae tendinae and/or papillary muscles. Occasionally, valvular stenoses may occur. Additional congenital cardiac anomalies may be present, such as pulmonic stenosis or ASD.

Ebstein's anomaly is a rare form of tricuspid valve dysplasia. In this condition the base of the cusps of the abnormal tricuspid valve are displaced distally into the ventricle and part of the RV is therefore 'atrialized'.

Clinical signs are usually not apparent early on in the condition. A holosystolic murmur will be identified over the tricuspid valve region. Eventually right-sided cardiac failure may result (e.g. hepatomegaly, ascites and distension of the jugular veins).

Radiography

Radiographic findings include:

- Right ventricular and right atrial dilatation (Figure 7.79)
- Often a marked apex shift to the left is noted
- The cardiac enlargement can be impressive and almost appear globoid
- Valvular stenosis should be considered when the atrium is markedly enlarged but not accompanied by changes in the ventricle



7.79 Lateral view of the thorax in a puppy with tricuspid valve dysplasia. Right-sided cardiomegaly is evident.

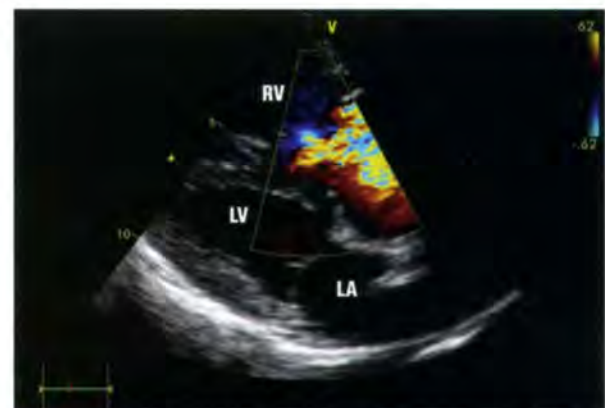
- There may be enlargement of the CdVC
- Hepatomegaly and ascites, resulting in increased opacity and decreased serosal detail in the cranial abdomen, may be noted.

Angiocardiography: Contrast studies are not very useful in the diagnosis and/or management of tricuspid valve malformations. They can demonstrate right atrial and right ventricular enlargement. Tricuspid regurgitation can be demonstrated by a right ventricular injection of contrast medium.

Echocardiography

Echocardiographic findings include:

- Right ventricular dilatation (unless the valve is stenotic) (Figure 7.80)
- Right atrial dilatation
- Abnormal papillary muscles (may find large fused papillary muscle instead of the small discrete muscles)
- Abnormal conformation of the tricuspid valve:
 - Hypoechoic leaflets and chordae tendinae
 - Decreased motion of the tricuspid leaflets
 - Decreased separation from the right ventricular free wall and/or IVS

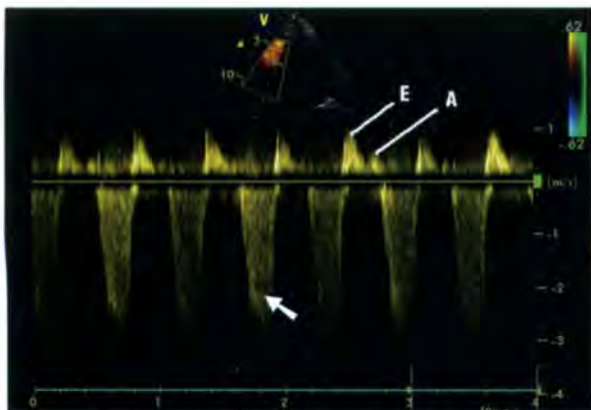


7.80 RPS long-axis echocardiogram in a dog with tricuspid valve dysplasia. Marked dilatation of the right cardiac chambers is evident. The RV is almost larger than the LV and the IVS is flat and pushed to the left side of the heart. Colour Doppler shows a turbulent high-velocity tricuspid regurgitation. LA = Left atrium; LV = Left ventricle; RV = Right ventricle. (Courtesy of M. Oyama)

- Apical implantation of the tricuspid valves with a seemingly reduced right ventricular cavity and a seemingly enlarged RA (right ventricular ‘atrialization’ – Ebstein’s anomaly).
- Right ventricular dilatation is evident on two-dimensional (2D) or transventricular M-mode images – it is usually accompanied by a flattening or paradoxical motion of the IVS due to the increased pressure in the RV (Figure 7.80).

Doppler studies:

- A high-velocity regurgitant flow from the RV to the RA can best be demonstrated using a left apical window (see Figures 7.80 and 7.81).
- The severity of the disease correlates to the extent of regurgitation into the RA.
- The PG is usually in the order of 30 mmHg.
- When pulmonary hypertension is present the regurgitation flow is usually of very high velocity (>3 m/s).
- When stenosis is present, an abnormally prolonged high-velocity jet will be noted from the atrium into the ventricle during diastole.



7.81 Spectral Doppler study of the tricuspid valve in a dog with tricuspid dysplasia. There is a systolic high-velocity tricuspid regurgitation reaching 3 m/s (arrowed). A = Normal diastolic inflow A wave; E = Normal diastolic inflow E wave. (Courtesy of M. Oyama)

Tetralogy of Fallot

Tetralogy of Fallot is a complex congenital disorder, resulting from a failure of the conotruncal septum to align properly at the embryonic stage. The Keeshond and English Bulldog are predisposed and the condition is also seen in cats. Tetralogy of Fallot is the most common cause of cyanotic cardiac disease in young animals.

The disease is characterized by four features:

- Pulmonic stenosis leading to right ventricular outflow obstruction (main pulmonary artery atresia may also be present)
- Secondary right ventricular hypertrophy
- A subaortic VSD
- Dextroposition of the aorta (rightward positioning or overriding aorta).

The right ventricular outflow obstruction and increased right ventricular pressure lead to shunting of blood from the right side to the left via the septal defect. Deoxygenated blood mixes with left-sided oxygenated blood and hypoxaemia results. The LA and LV are small and the pulmonary arteries and veins are underperfused. The bronchial arteries increase the systemic collateral circulation that they provide to the lungs.

Animals present with exercise intolerance, failure to grow, shortness of breath, syncope, cyanosis and secondary polycythaemia. Note that since shunting occurs at the level of the ventricles the cyanosis is generalized and not differential as in reverse PDA. Medical and surgical treatment options exist and the prognosis is variable.

Radiography

Radiographic findings include:

- The overall size of the heart is usually small to normal
- Right ventricular enlargement may be apparent (Figure 7.82)
- The overriding of the aorta may produce a loss of the cranial indentation on the cardiac silhouette on the lateral view (Figure 7.82)
- The main pulmonary artery is not enlarged (unlike the situation in pulmonic stenosis without a septal defect)
- Hypovascularization of the lungs may be identified: hyperlucent lung fields, decreased size of the pulmonary lobar vessels (Figure 7.82).

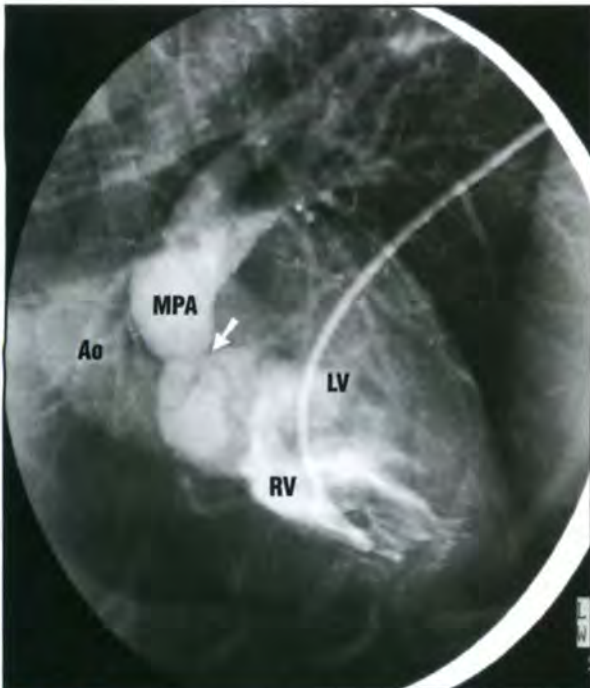


7.82 Lateral view of the thorax in a dog with tetralogy of Fallot. There is mild right-sided cardiomegaly. Note also the loss of the cranial indentation (or waist) of the cardiac silhouette, which is probably secondary to the overriding of the aorta. The changes are subtle. Diffuse hyperlucency of the lung fields is identified due to hypovascularization.

Angiocardiography: Angiocardiography can be useful to confirm the diagnosis but is usually unnecessary if a careful echocardiographic examination is performed.

It can be difficult to differentiate a tetralogy of Fallot from a VSD with reversed shunt direction (right-to-left) secondary to pulmonary hypertension (Eisenmenger’s complex):

- In both cases, after a right ventricular injection of contrast medium, there will be simultaneous opacification of the main pulmonary artery and ascending aorta
- In tetralogy of Fallot, narrowing of the main pulmonary artery with post-stenotic dilatation or hypoplasia of the main pulmonary artery should be looked for (Figure 7.83). This will assist in differentiation from a reversed VSD (in which the RVOT, main pulmonary artery and its branches appear normal in size and will fill up with contrast medium)
- Note that pulmonic stenosis in combination with an isolated right-to-left shunting VSD can be extremely difficult to differentiate from a tetralogy of Fallot in all imaging studies.



7.83 Angiocardiogram in a dog with tetralogy of Fallot. The contrast medium was injected in the RV. There is narrowing of the main pulmonary artery at the infundibular level (arrowed) and there is simultaneous opacification of the main pulmonary artery and the aorta, which means that there is a right-to-left shunt. Ao = Aorta; LV = Left ventricle; MPA = Main pulmonary artery; RV = Right ventricle. (Courtesy of J. Buchanan)

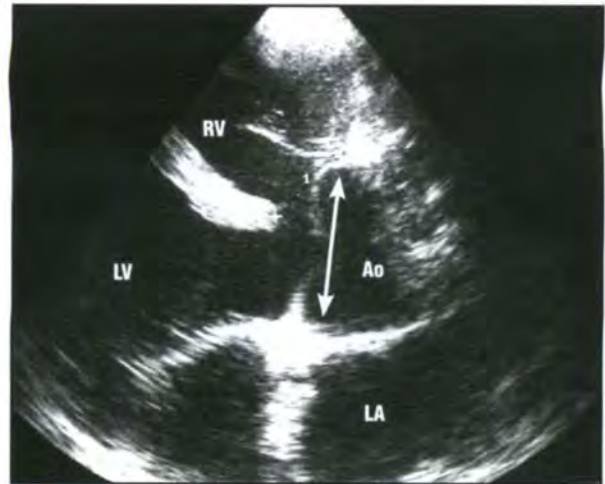
Echocardiography

Echocardiographic findings include:

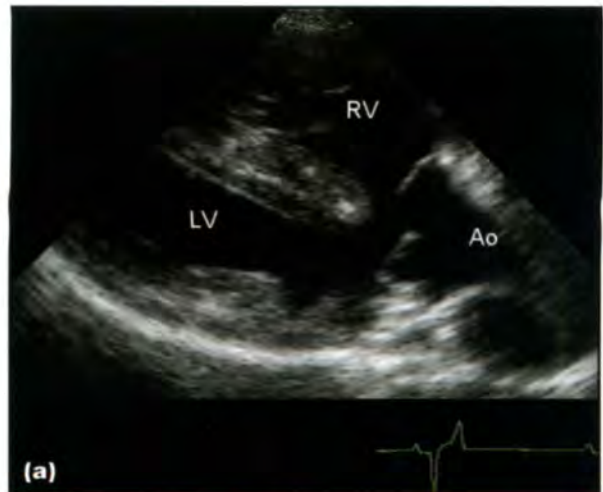
- Right ventricular hypertrophy
- High and often large VSD
- Aorta 'overriding' the IVS (Figures 7.84 and 7.85)
- Pulmonic stenosis (Figure 7.85b)
- Reduced dimensions of the LA and LV.

Doppler studies: Doppler findings include (Figure 7.86):

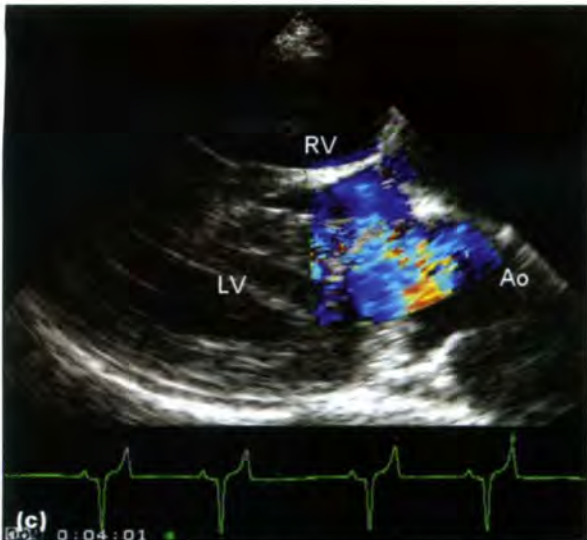
- A low-velocity systolic flow from the RV to the LV through the septal defect
- A high-velocity turbulent flow across the pulmonic stenosis.



7.84 RPS long-axis echocardiogram in a dog with tetralogy of Fallot. There is overriding of the aorta (double-headed arrow) over the IVS. A VSD is created by this abnormal position of the aorta. Ao = Aorta; LA = Left atrium; LV = Left ventricle; RV = Right ventricle.



7.85 (a) RPS long-axis five-chamber echocardiogram of a Border Collie with tetralogy of Fallot. The aorta is overriding or dextraposed and a high VSD is present. (b) RPS short-axis view obtained at the level of the heart base and optimized for the RVOT. The pulmonic valve is stenotic and the valves are thickened and echogenic. The main pulmonary artery is hypoplastic. Ao = Aorta; LV = Left ventricle; MPA = Main pulmonary artery; RV = Right ventricle; RVOT = Right ventricular outflow tract. (© J. Dukes-McEwan) (continues)



7.85 (c) RPS long-axis five-chamber view with colour Doppler. Blood is shunting from right-to-left across the VSD. Ao = Aorta; LV = Left ventricle; RV = Right ventricle. (© J. Dukcs-McEwan)

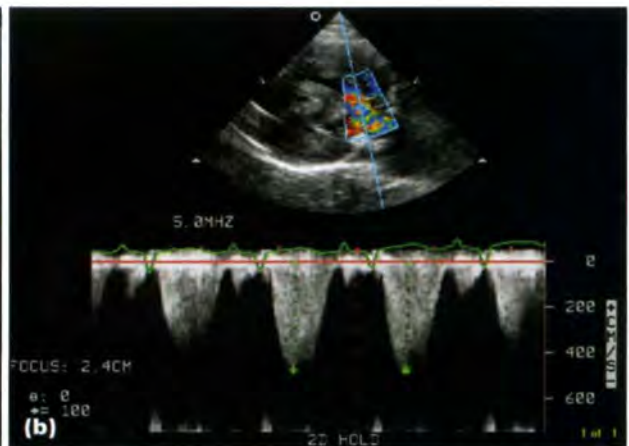
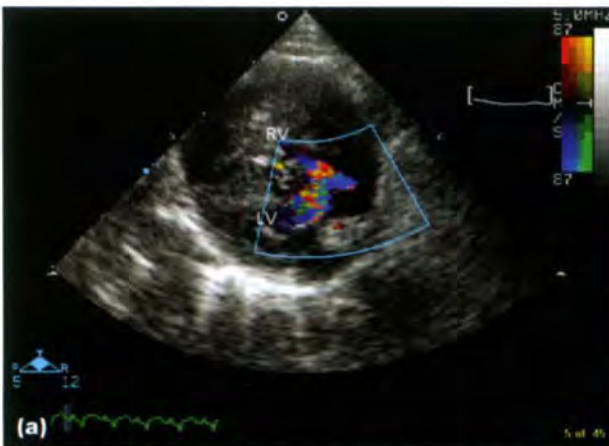
Scintigraphy

Scintigraphic findings in first pass radionuclide angiocardiology include simultaneous appearance of the aorta and pulmonary arteries after the dextrorphase. It is not possible to distinguish tetralogy of Fallot from a reverse PDA on the basis of a first pass study alone.

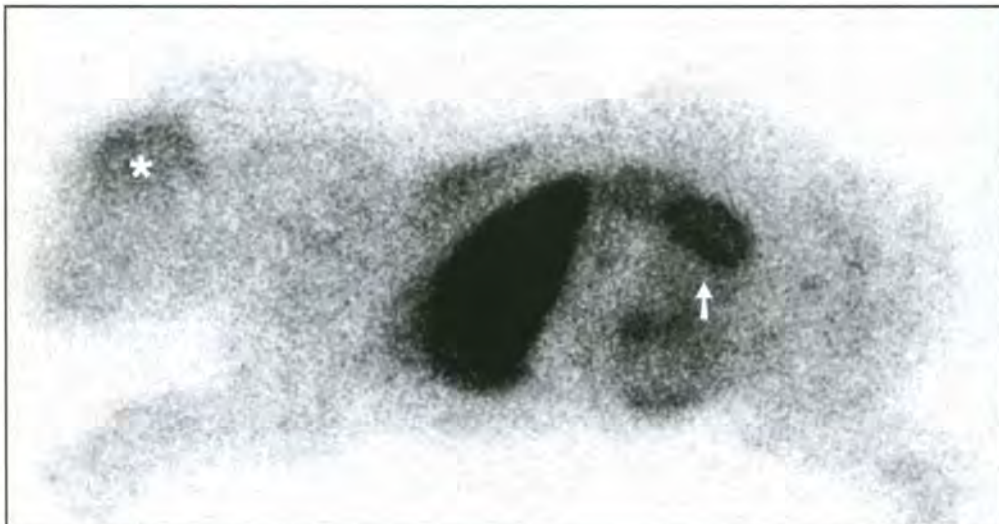
Scintigraphy with ^{99m}Tc-MAA shows activity outside the lungs with prominent uptake in the renal and cerebral cortices, the latter finding allowing differentiation from a reverse PDA (Figure 7.87).

Vascular ring anomaly

A vascular ring anomaly results from an abnormal embryonic development of the primordial aortic arches (aortic arches III, IV or VI) around the embryonic pharynx. This leads to postnatal constriction of the thoracic oesophagus and development of a secondary megaesophagus (see also Chapter 8). Dogs and cats are affected; in dogs, German Shepherd Dogs and Irish Setters are predisposed to this condition.



7.86 (a) RPS short-axis view of a Domestic Shorthair cat with a tetralogy of Fallot. A high VSD is present and the colour flow map documents the right-to-left flow. **(b)** CW Doppler shows the right-to-left flow across the septal defect. LV = Left ventricle; RV = Right ventricle. (© J. Dukcs-McEwan)



7.87 Whole body composite left lateral static image of a 4-month-old English Bulldog obtained 5 minutes after intravenous injection of ^{99m}Tc-MAA. Notice the extrapulmonary distribution of the radiopharmaceutical, with marked uptake at the level of the renal cortices (arrowed), as well as the cerebral cortex (*); compare with Figure 7.54. The diagnosis was tetralogy of Fallot.

A spectrum of abnormalities may be encountered, the most common ones being:

- Persistence of the right fourth aortic arch (PRAA) with a left-sided ligamentum arteriosum (most common anomaly) and/or a retro-oesophageal left subclavian artery
- Double aortic arches
- Normal fourth aortic arch with retro-oesophageal (aberrant) right subclavian artery (usually not a major problem from a clinical stand-point).

Rarely, a PDA is associated with a vascular ring anomaly.

Radiography

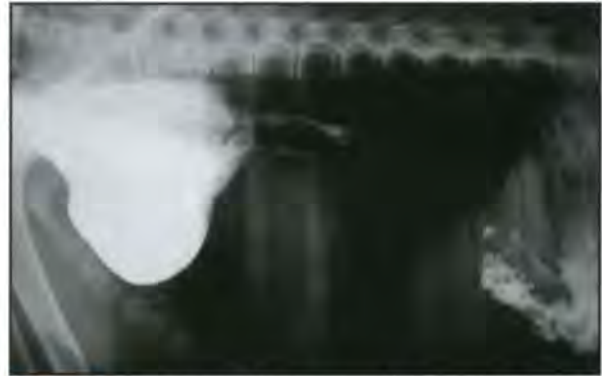
Radiographic findings include:

- If the vascular ring anomaly has entrapped the oesophagus, then oesophageal dilatation may be seen cranial to the heart base. Oesophagography may be required to identify this
- A soft tissue or heterogenous granular opacity, cranial to the heart base with general ventral displacement of the trachea may be seen on survey radiographs (Figure 7.88)
- There may be a ventral alveolar pattern if aspiration pneumonia has occurred
- Moderate or marked focal leftward curvature of the trachea near the cranial border of the heart in DV or VD radiographs (see Figure 9.18, p. 208) is a reliable sign of PRAA in young dogs with consistent clinical signs (as opposed to the normal right-sided tracheal curvature in normal animals)
- In cases of PRAA the leftward margin of the descending aorta is not visible
- If a well defined, normal left descending aortic margin is clearly identified on the VD or DV view, a less common vascular ring anomaly may be suspected: angiography is warranted in such cases, to confirm the diagnosis and plan the best surgical approach.



7.88 Lateral view of the thorax of a dog with a PRAA. Note the gas accumulation in the cranial portion of the thoracic oesophagus (black arrow) on this survey radiograph. There is mineralized material in the cranioventral thorax (white arrow), which represents material accumulating in the distended oesophagus cranial to the vascular anomaly. (Courtesy of J. Buchanan)

Oesophagography: Oesophageal contrast studies show accumulation of the contrast medium in a distended oesophagus cranial to the heart base and abrupt tapering at the level of the sixth pair of ribs (Figure 7.89). Occasionally, the oesophageal dilatation is generalized and these cases carry the worst prognosis (see Chapters 1 and 9 for more information).



7.89 Lateral view of the thorax of a dog with a PRAA, after oral administration of barium sulphate. There is accumulation of the contrast medium in a distended oesophagus cranial to the heart base and abrupt tapering at the level of the heart base. (Courtesy of J. Buchanan)

Angiocardiography: This is not necessary in all cases, as an adequate presurgical diagnosis of vascular ring constriction of the oesophagus can be made with barium studies of the oesophagus. It may be valuable to identify animals that have a normal left fourth aortic arch but abnormal formation of the right fourth and/or right sixth aortic arch: in these cases a right thoracotomy is the best surgical approach as opposed to the more common left approach.

A left ventricular injection of contrast medium is usually performed:

- Persistent right fourth aortic arch is more consistently demonstrated on DV views, where the opacified aortic arch can be seen coursing to the right of the trachea
- A retro-oesophageal left subclavian artery can be demonstrated in lateral views as it courses cranially from its origin dorsally and to the left of the aorta at about the level where the thoracic aorta begins to parallel the vertebral column. The persistent left subclavian artery compresses the oesophagus dorsally when it begins running ventrally to the thoracic inlet.

Cor triatriatum sinister and dexter

Cor triatriatum is a rare congenital defect that manifests as a partitioned RA (cor triatriatum dexter, CTD) or even less commonly, a partitioned LA (cor triatriatum sinister, CTS):

- CTD is caused by failure of the right sinus venosus valve to regress during embryogenesis
- CTS is caused by an abnormal connection of the LA with the pulmonary veins.

The condition is rare but well documented in dogs. It is extremely rare in cats.

In both CTD and CTS, there is a membrane dividing the atrium into two compartments, resulting in abnormal venous return to the affected atrium (CdVC in the case of CTD and pulmonary veins in the case of CTS). The degree of venous pressure elevation depends on the degree to which the dividing membrane is perforated. If the degree of obstruction is significant then subsequent cardiac failure will occur. This will be left-sided failure in CTS and right-sided failure in CTD. In the latter there may only be congestion of the caudal half of the body (i.e. ascites and hepatomegaly, but no jugular distension) and in this way the condition may mimic a Budd–Chiari-like syndrome (see later).

Note that supravulvar mitral stenosis (SMS) closely resembles CTS. The only difference is the level of the obstructing membrane. In SMS the obstruction is distal to the foramen ovale and LAu enlargement will occur; in CTS the obstruction is proximal to the foramen ovale and the LAu is therefore downstream and does not enlarge.

Radiography

Radiographic findings include:

- CTD:
 - Marked dilatation of the RA, creating a soft tissue opacity bulge between 09.00 and 11.00 o'clock on the VD and lateral views
 - Dilatation of the CdVC
 - There may be hepatomegaly and peritoneal effusion (right-sided cardiac failure).
- CTS:
 - Left atrial dilatation
 - Pulmonary venous enlargement
 - There may be cardiogenic pulmonary oedema (left-sided cardiac failure).

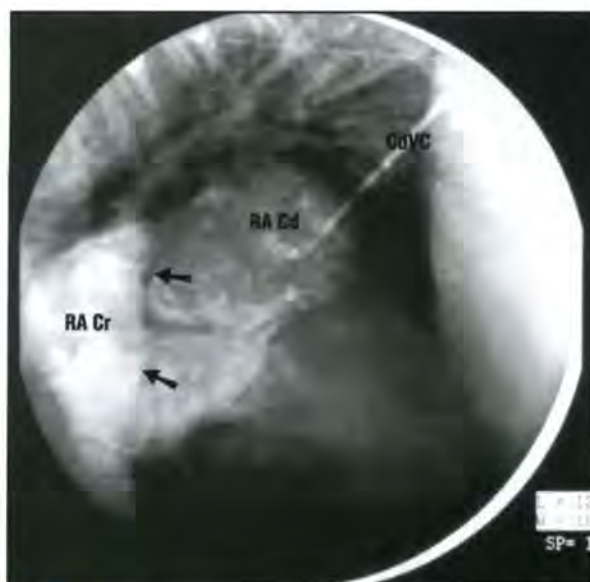
Angiocardiography:

- CTD: injection of contrast medium in the CdVC might reveal an obstruction to venous return at the level of the RA, with saccular dilatation of the caudal RA (Figure 7.90).
- CTS: selective angiography is difficult as the dividing membrane in the LA makes it difficult to opacify the entire LA. Non-selective angiocardiography at the late phase (levophase) can provide more information, revealing that the large soft tissue opacity corresponds to a saccular dilatation of the LA, which occasionally will appear bilobed (Figure 7.91).

Echocardiography

Echocardiographic findings include:

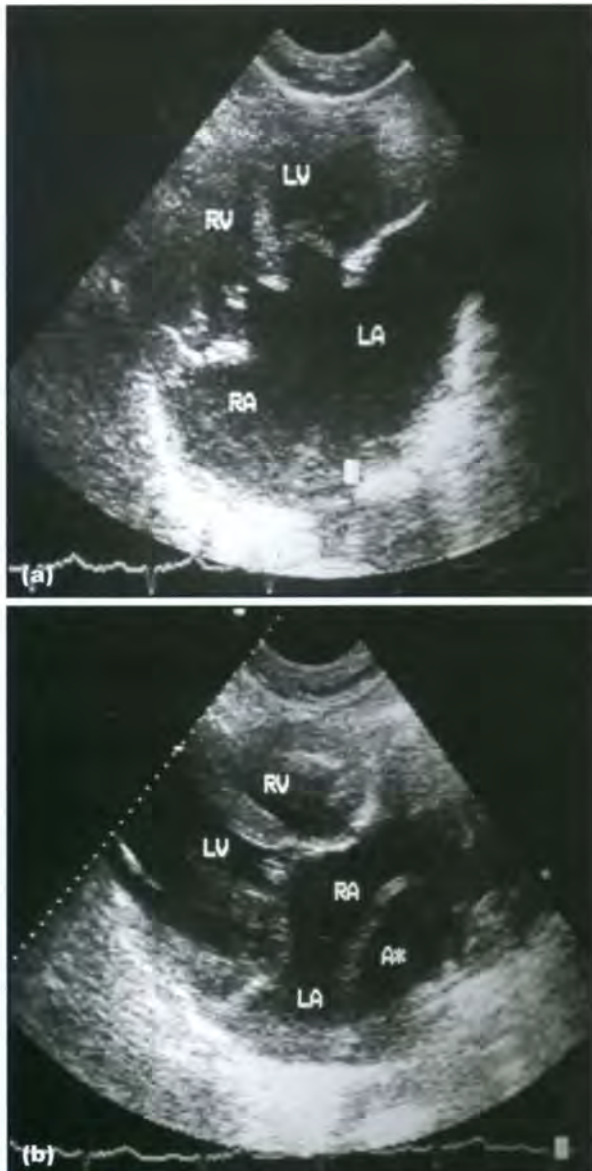
- CTD:
 - Echocardiography can provide the diagnosis of CTD
 - Right atrial dilatation without other obvious changes is seen
 - A thin membrane can be seen in the caudal RA, dividing the atrium into a larger cranial compartment and a smaller caudal compartment
- CTS:
 - The caudal compartment includes the entrance of the CdVC, which is distended
 - Turbulent venous inflow can be seen through the membrane using Doppler studies.
- CTS:
 - Echocardiography can provide the diagnosis of CTS (Figure 7.92)
 - A visible partition of the LA is seen



7.90 Angiocardiogram in a dog with CTD. The contrast medium was injected in the CdVC. The RA is markedly dilated and there is a linear filling defect, corresponding to the dividing membrane (arrowed). CdVC = Caudal vena cava; RA Cd = Caudal section of the right atrium; RA Cr = Cranial section of the right atrium. (Courtesy of J. Buchanan)



7.91 Angiocardiogram in a cat with CTS. The contrast medium was injected in the RV after catheterization of the jugular vein. A levophase image is presented, where the contrast medium has reached the left atrium (LA). The LA is enlarged and a linear filling defect is visible in its lumen, corresponding to the dividing membrane (arrowed). (Courtesy of J. Buchanan)



7.92 (a) Left apical four-chamber echocardiogram of a cat with an endocardial cushion defect and an unusual cor triatriatum. On this view the large confluent ASDs and VSDs are evident. (b) RPS long-axis view. The ASD can be seen and within the common atrium an additional thin dividing membrane is evident, creating an extra chamber (A*). This was considered to be a CTS; however, the decision as to whether the lesion is left- or right-sided is a difficult one when a common atrium is present. LA = Left atrium; LV = Left ventricle; RA = Right atrium; RV = Right ventricle. (© J. Dukes-McEwan)

- The perforations in the dividing membrane are occasionally identified
- Doppler studies reveal a turbulent venous flow through the dividing membrane.

Aortic coarctation

Aortic coarctation is a very rare condition in dogs and even more rare in cats. The disease consists of a narrowing of the aortic lumen that usually occurs at the aortic isthmus, the segment of the aorta between the origin of the left subclavian artery and the insertion of the ductus arteriosus.

It is believed to be due to spreading of the specialized contractile ductal tissue into the aorta to form a sling around it, which after birth becomes part of an obstructive curtain of tissue. The narrowing is responsible for obstruction to the flow into the descending aorta and aneurysmal dilatation of the aorta distal to the obstruction. The narrowing process takes weeks to develop, which leaves time for the LV to adjust to the increased pressure load and for collateral circulation to develop; this is why there are often no clinical signs associated with the disease.

Radiography

Radiographic findings are non-specific:

- An exaggerated and enlarged aortic arch is visible, creating a soft tissue opacity bulging out from the mediastinum into the left cranial thorax
- The trachea can be displaced ventrally (lateral view) and to the right (VD or DV view) by the soft tissue opacity
- Notching of the ribs (small indentation surrounded by fine rim of sclerotic bone) is highly suggestive of aortic coarctation in humans and has also been reported in dogs. It occurs due to enlargement of the intercostal arteries. These carry collateral circulation in a retrograde direction from both the costocervical trunk and internal thoracic arteries to supply the distal aorta.

Angiocardiography: Cardiac catheterization and aortography are indicated to localize accurately the site of obstruction, determine the length of the coarctation and identify associated malformations (Figure 7.93).



7.93 Lateral view of the thorax in a dog with aortic coarctation. Contrast medium was injected in the aortic arch after catheterization of the femoral artery. There is narrowing of the aorta distal to the origin of the left subclavian artery, followed by marked dilatation of the aorta after the stenosis. The catheter is seen curving around in the dilated portion of the aorta. (Courtesy of M. Herrtage)

Echocardiography

Echocardiography does not allow the diagnosis of aortic coarctation, though endo-oesophageal echocardiography might be helpful. Echocardiography can rule out the presence of associated cardiac anomalies, such as a VSD.

Myocardial diseases

Cardiomyopathies are defined as diseases of the myocardium associated with cardiac dysfunction. They may be primary or secondary to another insult. In making a diagnosis of idiopathic cardiomyopathy, active exclusion of inflammatory, infiltrative, metabolic, endocrine, nutritional, pulmonary, systemic hypertensive, toxic and other conditions is required. Specific secondary cardiomyopathies may be subdivided according to their aetiology (e.g. hyperthyroid cardiomyopathy).

Idiopathic cardiomyopathies are further subdivided according to their morphological (echocardiographic) appearance and dysfunction, according to the World Health Organization, and include:

- Dilated cardiomyopathy (DCM)
- Arrhythmogenic right ventricular cardiomyopathy (ARVC)
- Hypertrophic cardiomyopathy (HCM)
- Restrictive cardiomyopathy (RCM).

Canine myocardial disease

Dilated cardiomyopathy

- DCM is characterized by left-sided or four-chamber dilatation and impaired left ventricular systolic function.
- DCM is a major cause of morbidity and mortality in various large and giant breeds of dog, including Deerhounds, Dobermanns, Great Danes, Irish Wolfhounds, Newfoundlands, St Bernards and spaniel breeds (Cocker and American Cocker, English Springer).
- Presentation is usually associated with the onset of congestive heart failure, with coughing or dyspnoea. Exercise intolerance may be marked. It may be associated with episodic tachyarrhythmias, such as ventricular tachycardia, resulting in syncopal episodes.
- There is a long, presymptomatic phase of this disease and the onset of congestive heart failure is merely the 'tip of the iceberg'.
- Clinical findings may be subtle. Arrhythmias, such as atrial fibrillation, may be present. A soft murmur may be detected, due to mitral regurgitation, secondary to dilatation of the mitral annulus. Diastolic gallops may be detected in the decompensated animal.
- Imaging is essential to making the diagnosis of DCM. It demonstrates the chamber dilatation and impaired systolic function. However, it also has an important role in excluding other cardiac conditions, which may secondarily result in congestive heart failure or poor output signs. In the presymptomatic dog, from a breed or family with DCM prevalence, echocardiographic screening may be requested prior to breeding.

Radiography: Thoracic radiographs should be obtained in all dogs where left-sided congestive heart failure is suspected clinically, or is imminent.

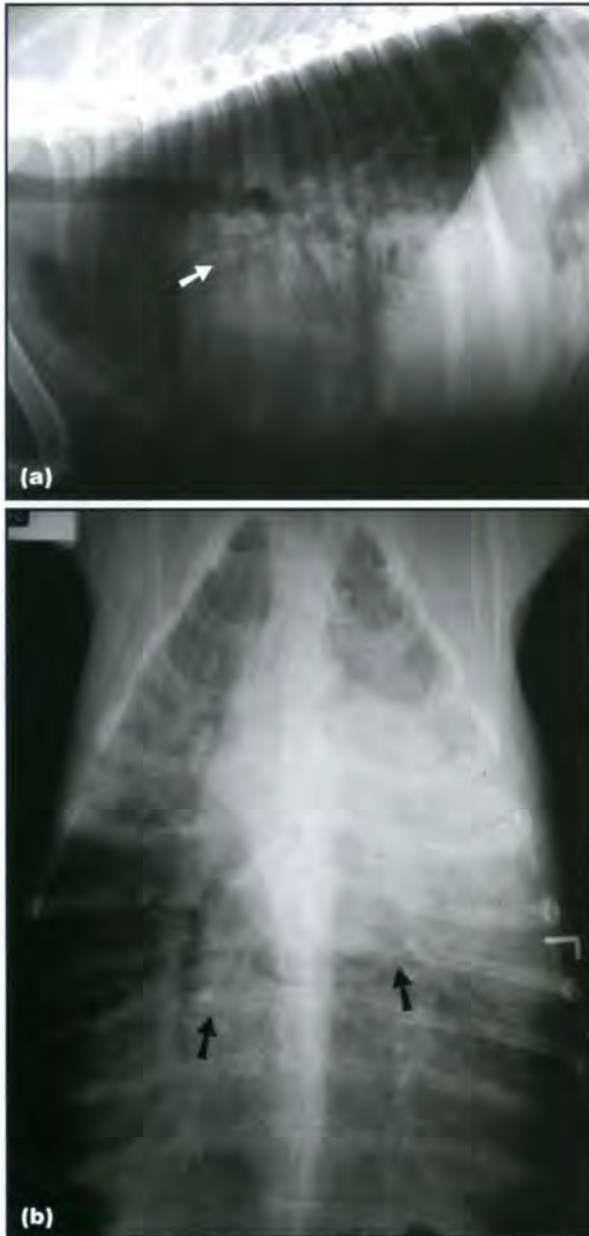
Radiographs are exquisitely sensitive at documenting the volume load associated with left-sided congestive heart failure (pulmonary oedema). A pulmonary infiltrate associated with left atrial enlargement and pulmonary venous congestion is consistent with cardiogenic pulmonary oedema (Figures 7.94 and 7.95).

In clinical symptomatic DCM, the cardiac silhouette is almost always abnormal. Possible findings include:

- Left atrial and left ventricular enlargement
- Right atrial and right ventricular enlargement
- The cardiac silhouette may have a sharp 'static' outline with severe systolic function (loss of normal systolic–diastolic movement blur with each cardiac cycle). The concomitant presence of left atrial enlargement helps distinguish this from a pericardial effusion



7.94 (a) Right lateral and (b) DV thoracic radiographs from a Cocker Spaniel, which presented with coughing and dyspnoea. There is generalized cardiomegaly with left atrial enlargement. Pulmonary venous distension is apparent. There is a mixed interstitial–alveolar infiltrate, consistent with pulmonary oedema. Echocardiography confirmed that this dog had DCM, resulting in the left-sided congestive heart failure.



7.95 (a) Right lateral and (b) DV thoracic radiographs from a Doberman, which presented with a history of several weeks coughing, recent syncopal episodes and then dyspnoea. DCM in the Doberman is not associated with radiographic evidence of massive cardiomegaly, but there is left atrial and left ventricular enlargement. Note the pulmonary venous distension (arrowed) and the predominantly perihilar mixed interstitial and alveolar infiltrate.

- In left-sided congestive failure:
 - Triad of signs: LA enlargement, pulmonary venous distension and pulmonary infiltrate
 - The pulmonary infiltrate due to pulmonary oedema is normally predominantly perihilar. It may be interstitial, alveolar or mixed.
- In right-sided congestive failure:
 - Evidence of abdominal effusion (ascites) in the cranial abdomen
 - Distended CdVC
 - Pleural effusion

- Note: in a dog with cardiomegaly presenting with predominantly right-sided congestive heart failure, pericardial effusion *must* be excluded. DCM normally presents with left-sided congestive failure.

In presymptomatic ('occult') DCM, the lung field and pulmonary vasculature are usually unremarkable. The cardiac silhouette may or may not show signs of generalized cardiomegaly or specific chamber enlargement. Radiographs are not useful in screening for presymptomatic DCM. They are useful in determining whether or not the dog is likely to show clinical signs in the near future.

Echocardiography (including Doppler studies): 2D and M-mode echocardiography are normally sufficient to make the diagnosis of DCM. However, since the stringent diagnosis of DCM requires the active exclusion of other congenital or acquired cardiac disease, colour flow and Doppler echocardiography are indicated. Furthermore, Doppler studies are required for identifying and classifying abnormalities in diastolic function, and for supporting the presence of systolic function. Guidelines for the robust diagnosis of DCM have recently been proposed.

2D echocardiographic abnormalities in DCM typically include:

- Subjective findings include LV dilatation with relatively thin walls and poor contractility
- A rounded LV chamber (increased sphericity)
 - LV diastolic length:LV diastolic width at chordae tendinae level (= M-mode left ventricular internal dimension in diastole, LVIDd) <1.65 (Figure 7.96)
- End-systolic volume index >30 ml/m² (confirms systolic dysfunction and chamber dilatation) (Figure 7.97b)
- Ejection fraction <40% (Figure 7.97)
- The LA is dilated in symptomatic dogs
- The right-sided chambers may or may not be dilated.



7.96 Calculation of the index of sphericity. (a) On a RPS long-axis view, every attempt is made to optimize the LV length. From a frozen image (diastolic frame: start of QRS complex), a measurement is taken from the mitral annulus to the apex of the LV. The diastolic LV length in this example is 77.8 mm. (continues) ▶



7.96 (continued) Calculation of the index of sphericity. **(b)** The diastolic 'width' of the LV, at chordal level, is the M-mode diastolic chamber dimension (here 64.3 mm). In this example, the index of sphericity is the LV length (diastole)/LV width (diastole) = 77.8/64.3 = 1.21 (normal >1.7). The ventricle is confirmed as being abnormally rounded.



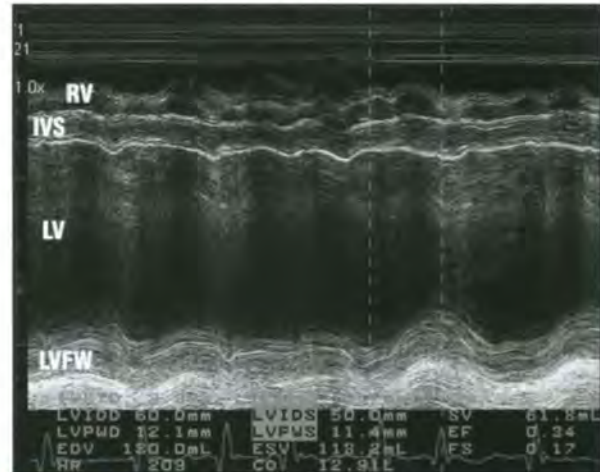
7.97 Simpson's rule to calculate LV volume from a RPS long-axis four-chamber view. Every attempt should be made to optimize the LV chamber length and area. The LV chamber endocardium is traced around, closing at the mitral annulus, in both diastole and systole. A length from the mitral annulus to the LV apex is drawn. The ultrasound machine software divides this length into 20 divisions, considered as discs. The volume of each disc is calculated, and the sum of volumes of the discs gives the overall LV volume, relatively independent of geometrical assumptions. Both **(a)** end-diastolic volume (EDV) and **(b)** end-systolic volume (ESV) are calculated. The ejection fraction is calculated as (EDV-ESV)/EDV (usually expressed as a percentage) (normal >50%). The dog's body surface area (BSA) can be calculated. The end-systolic volume index (ESVI) is the ESV/BSA (normal <30 ml/m²). The ejection fraction is low and the ESVI is increased in DCM, as in this Boxer.



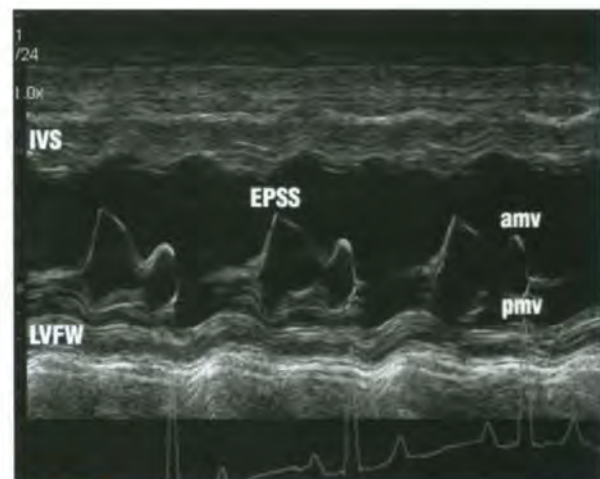
M-mode echocardiographic abnormalities in DCM include:

- Increased LVIDd and left ventricular internal dimension in systole (LVIDs) for size or breed-based reference ranges (Figure 7.98)

- Relative wall thickness (left ventricular free wall in diastole, LVFWd:LVIDd) is decreased
- Fractional shortening <20%
- Increased mitral valve M-mode EPSS (Figure 7.99)
- Reduced aortic root systolic excursion on aortic M-modes, and possibly premature closure of aortic valve
- The LA may be enlarged in symptomatic dogs (increased M-mode LA:Ao ratio)
- Systolic time intervals: M-mode aortic pre-ejection period (PEP):ejection time (ET) >0.4.



7.98 LV M-mode obtained from a Doberman with DCM, indicating marked hypokinesia of the LV, proportionately thin walls and a dilated LV chamber. The LV diastolic and systolic measurements can be compared with reference values for breed, where known. This dog has atrial fibrillation. IVS = Interventricular septum; LV = Left ventricle; LVFW = Left ventricular free wall; RV = Right ventricle.



7.99 M-mode obtained at mitral valve level from a Leonberger with preclinical DCM. The anterior leaflet of the mitral valve (amv) moves towards the septum (IVS), and the posterior leaflet (pmv) moves towards the free wall of the LV (LVFW). In normal sinus rhythm, the amv opens twice in diastole: once early (E peak) corresponding to rapid LV filling, and once corresponding to atrial contraction (A peak). The E point to septal separation (EPSS) should not exceed 7 mm in any breed. It increases in DCM due to LV dilatation and rounding, and also because of reduced stroke volume.

Findings with Doppler studies in DCM include:

- Colour flow Doppler may identify mitral and/or tricuspid regurgitation, without grossly abnormal valve apparatus, due to stretch of the atrioventricular annuli
- Mitral regurgitant velocity may be lower than normal, due to impaired LV systolic function and elevated LA pressures, giving a reduced systolic PG between the LV and LA. Mitral regurgitant velocity <4 m/s is associated with poor prognosis
- Aortic velocity and velocity time integrals may be lower than normal, due to systolic dysfunction
- Aortic PEP:ET ratio may be increased (>0.4)
- The assessment of diastolic function is important to provide prognostic information. Dogs with a restrictive physiology have reduced survival.

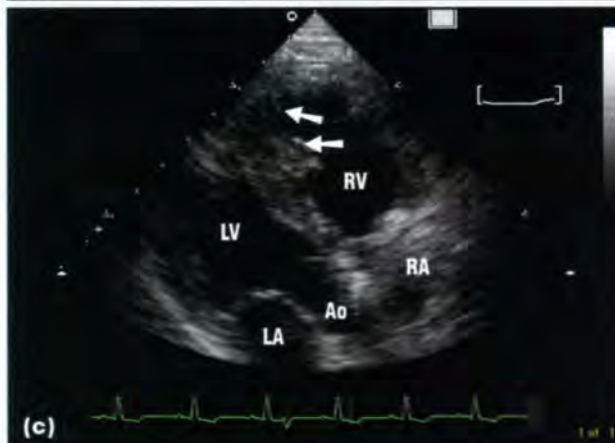
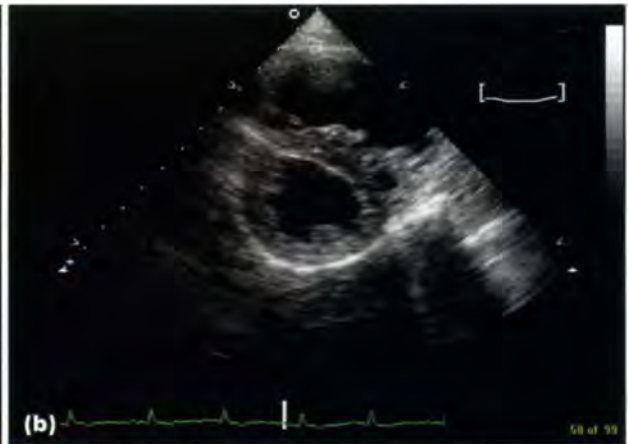
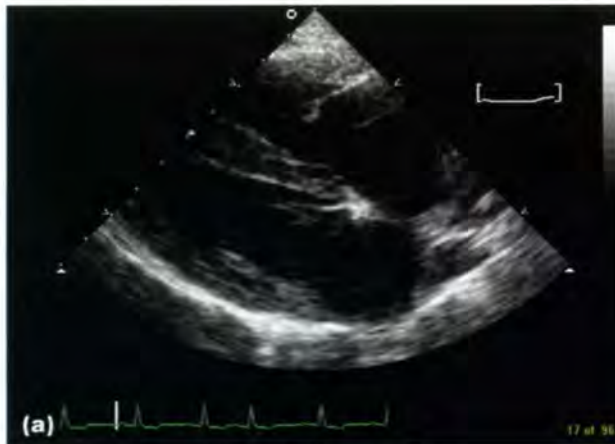
If dogs are screened for presymptomatic DCM, various echocardiographic abnormalities may be identified, such as impaired systolic function prior to unequivocal evidence of LV dilatation. Other cases may have LV enlargement with apparently preserved systolic function. The systolic time interval, PEP:ET ratio, appears to offer the best discrimination between normal and affected dogs. Serial evaluation is required to confirm that these echocardiographic findings precede the development of DCM, and a scoring system has been proposed to monitor these cases.

Boxer cardiomyopathy or arrhythmogenic right ventricular cardiomyopathy

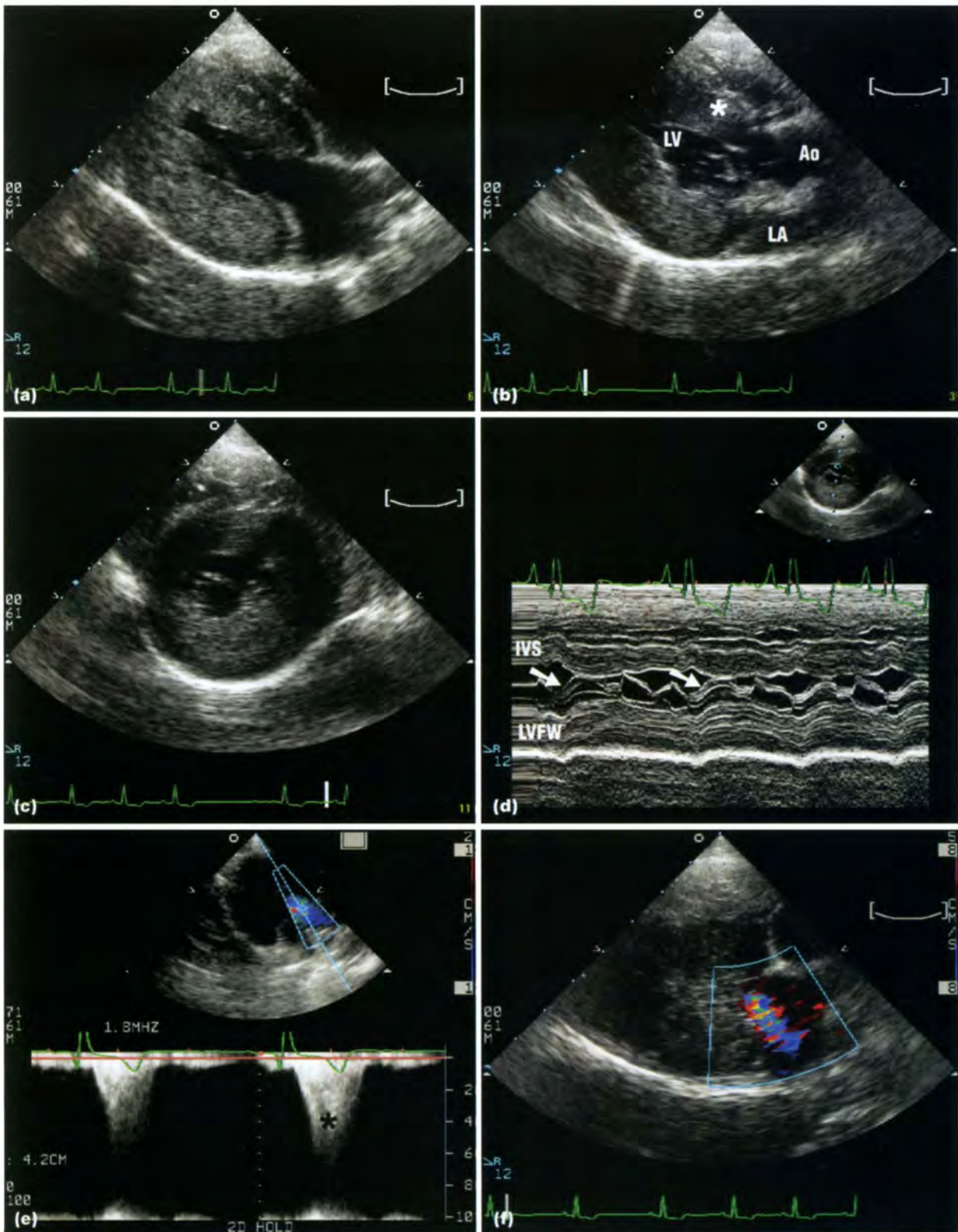
Boxer dogs with cardiomyopathy may present with the classical findings of DCM, as described above. Until recently, this was the most common presentation in UK and European Boxers (see Figures 7.96 and 7.97). In contrast, North American Boxers are reported to present with malignant ventricular arrhythmias, of right ventricular origin, with minimal changes initially on echocardiography, although systolic dysfunction and LV dilatation can occur later in the course of the disease. This form is now being increasingly recognized in the UK and Europe. In some affected Boxers, the RV may appear dilated (Figure 7.100) with dysplastic RV apical papillary muscles (Figure 7.100c). However, in many Boxers there may be no echocardiographic evidence of structural abnormalities, despite severe ventricular arrhythmias.

Hypertrophic cardiomyopathy

HCM is rare in dogs, although it has been documented. Echocardiographic features are similar to those described in cats (see below). One unusual condition, which may represent a form of HCM, is *dynamic LVOT obstruction*, due to *systolic anterior motion* of the anterior mitral valve leaflet (Figure 7.101). This has been described in young, growing dogs. They may outgrow this lesion. It must be distinguished from subaortic stenosis with associated dynamic obstruction.



7.100 ARVC in a Boxer, which presented collapsed with ventricular tachycardia. The arrhythmia was treated. **(a)** RPS long-axis view and **(b)** short-axis view show dilatation of the RA and RV. **(c)** Apical sternal RPS view shows dysplastic papillary muscles in the RV apex (arrowed). Ao = Aorta; LA = Left atrium; LV = Left ventricle; RA = Right atrium; RV = Right ventricle.



7.101 Images from a 2-year-old Border Terrier with frequent syncopal episodes of excitement and a heart murmur. A diagnosis was made of HCM. There is marked concentric hypertrophy of the LV, evident from **(a)** the RPS long-axis four-chamber view, **(b)** the five-chamber view and **(c)** the short-axis view. There is no evidence of gross abnormality of the aortic valves, LVOT or the ascending aorta on the five-chamber view (b). However, in (b) the mitral valve anterior leaflet in this early systolic frame is shown moving towards the basal septum (\star) (where endocardial thickening may be consistent with a 'kissing' lesion). **(d)** The presence of systolic anterior motion (SAM) of the anterior mitral valve leaflet (arrowed) is confirmed by the superior temporal resolution of M-mode at mitral valve level. SAM results in dynamic LVOT obstruction. **(e)** This can be documented from a left apical view. There is increased aortic outflow velocity with a biphasic acceleration slope (\star). In this example, CW Doppler shows aortic peak velocities to be >6 m/s. **(f)** SAM also results in mitral valve incompetence and colour flow Doppler typically shows an eccentric MR jet, coursing towards the posterior-lateral wall of the LA. Ao = Aorta; IVS = Interventricular septum; LA = Left atrium; LV = Left ventricle; LVFW = Left ventricular free wall.

Feline myocardial disease

Cats as a species display the plethora of primary myocardial diseases, classified by the World Health Organization. Imaging, particularly Doppler echocardiography, plays a vital role in determining the definitive diagnosis. Ancillary diagnostic techniques are required to exclude conditions which may secondarily affect the myocardium (blood pressure measurement, clinical pathology, etc.).

Hypertrophic cardiomyopathy

HCM is the most common form of myocardial disease affecting cats. It is genetically transmitted as an acquired, autosomal dominant trait (proven in Maine Coons). It is characterized by concentric left ventricular hypertrophy, which may be regional or asymmetrical. The wall thickness:LV chamber diameter ratio (= relative wall thickness) is greatly increased. Evidence of diastolic dysfunction is documented by Doppler studies. This is manifested by progressive left atrial enlargement.

Symptomatic cats present with signs of left-sided congestive heart failure (dyspnoea due to pulmonary oedema). This is often of sudden onset, and may be preceded by a stressful incident or fluid loading. There is a long presymptomatic phase. Affected cats may fortuitously have a heart murmur detected, which leads to an early diagnosis. Other cats may be detected by echocardiographic screening schemes in breeds, such as Maine Coons and Persians.

Radiography: This is indicated to identify the haemodynamic consequences of heart disease, with evidence of increased left-sided filling pressures:

- Left atrial enlargement
- Pulmonary venous distension

- Pulmonary infiltrate, which may affect any region of the lung field, and be patchy, interstitial, alveolar or mixed. This is consistent with pulmonary oedema (Figure 7.102).

Radiography does not differentiate between the various myocardial diseases. In asymptomatic HCM, there may be no gross radiographic evidence of cardiomegaly or specific chamber enlargement. In symptomatic HCM, left atrial enlargement is evident. Radiographically, apparent biatrial enlargement may be documented, but in most cases, echocardiography shows that the marked left atrial enlargement pushes the interatrial septum and the right atrial wall more to the right and cranially, giving this impression on the cardiac silhouette. The apparent biatrial enlargement gives the classical 'valentine' shaped heart on the DV view (Figure 7.102b). A pleural effusion may be present, associated with biventricular failure.

Doppler echocardiography: This is the imaging modality of choice to distinguish between the various forms of myocardial disease. The following 2D and M-mode findings (Figure 7.103) are typical in HCM:

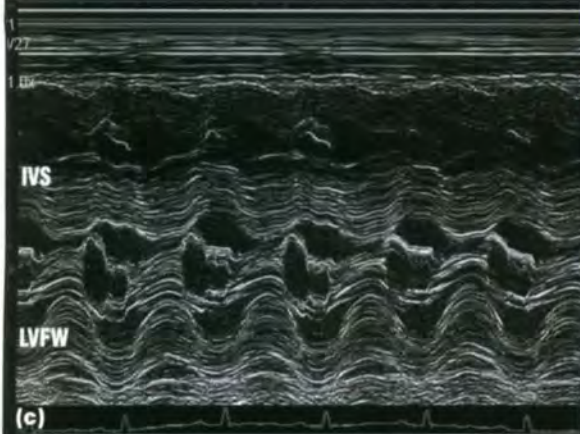
- Generalized or focal, symmetrical or asymmetric hypertrophy, with diastolic wall thickness ≥ 6 mm (Figure 7.104)
- The LV chamber diameter may be normal or small
- Subjective impression that the papillary muscles are hypertrophied
- LA size may be normal (Figure 7.105) or dilated (Figure 7.106)
- Systolic function is normally preserved; fractional shortening can often be $>45\%$, indicating a hyperkinetic LV, due to the low wall stress (Figure 7.107).



7.102 (a) Right lateral and (b) DV thoracic radiographs from a cat, which presented with apparently sudden onset left-sided congestive heart failure. There is marked left atrial enlargement and dilatation of the LAu, which on the DV view results in the appearance of a 'valentine heart'. Both pulmonary arteries and veins are dilated (pulmonary hypertension may be secondary to left-sided failure in the cat). The pulmonary infiltrate associated with cardiogenic pulmonary oedema in the cat can be patchy and variable in distribution, as indicated here. This cat also has radiographic evidence of pericardial fat.

Parameter	Normal	HCM	RCM	DCM
Interventricular septum in diastole (IVSd)	3.5–5.0 mm	>6 mm	Normal or mild increase	Normal or reduced
LV free wall in diastole (LVFWd)	3.5–4.5 mm	>6 mm	Normal or mild increase	Normal or reduced
Left ventricular internal dimension in diastole (LVIDd)	14–15 mm	Normal or reduced	Normal or mild increase	>16 mm
Left ventricular internal dimension in systole (LVIDs)	7.0–8.5 mm	Normal or reduced	Normal or mild increase	>9 mm
Fractional shortening (FS)	30–50%	Normal or increased	Normal	<25%
Mitral M-mode	E point (on anterior leaflet of mitral valve) to septal separation (EPSS) <2 mm	Normal EPSS ± systolic anterior motion	Normal or mildly increased EPSS	Increased EPSS
Mitral E:A ratio	>1<2	Impaired relaxation: <1 May be pseudonormal or restrictive, depending on stage of disease	Restrictive filling pattern: E>>A	Normal or restrictive, depending on stage of the disease
E deceleration time	60 ms	>65 ms	<55 ms	Normal or decreased
Isovolumic relaxation time (IVRT)	55–60 ms	>60 ms	<55 ms	Normal or decreased
Pulmonary venous flow (PVF) S:D velocity ratio	<1 (unless aged cat)	S:D>1	S:D<<1	Low S (<0.2 m/s), S:D<<1
PVF Ar velocity	<0.2 m/s	Normal or increased	Normal, increased or decreased	Normal or decreased
PVF Ar duration:mitral A duration	<1	Normal or >1, depending on stage of disease	>1 in cats with congestive heart failure (CHF)	>1 in cats with CHF

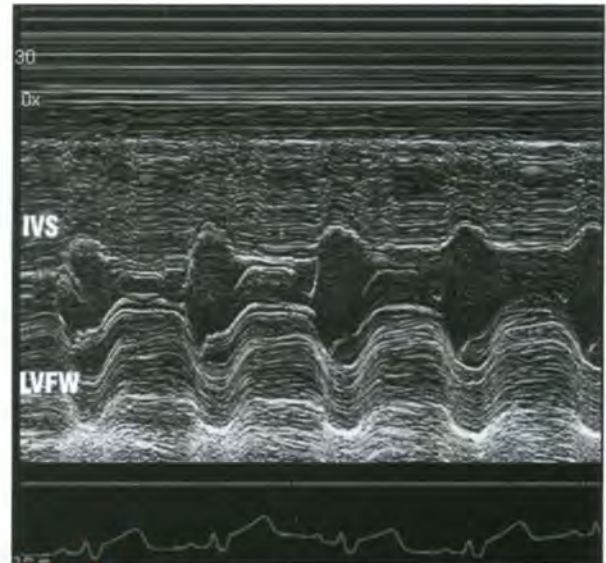
7.103 Typical echocardiographic findings in feline myocardial disease based on 2D and M-mode criteria and assessment of diastolic function.



7.104 Images from a 2-year-old British Shorthair cat with HCM. There is marked concentric hypertrophy of the LV. **(a)** The basal septal bulge may result in turbulence or increased velocity of LV outflow. If the basal septal bulge exceeds 6 mm in diastole, this confirms the presence of significant hypertrophy. **(b)** A short-axis view can be used to measure wall thickness at the chordal level, ensuring that papillary muscles are not inadvertently included. Diastolic wall thicknesses over 6 mm confirm hypertrophy, as here. **(c)** The M-mode in feline HCM typically has a cluttered appearance, particularly at mitral valve level. Ao = Aorta; IVS = Interventricular septum; LA = Left atrium; LVFW = Left ventricular free wall.



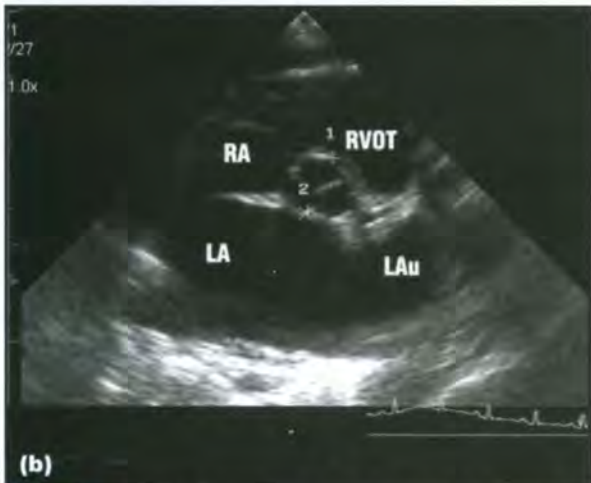
7.105 Left atrial dilatation is a consequence of significant diastolic dysfunction and elevated filling pressures in the cat. In cats with asymptomatic HCM, the left atrial size may still be normal. From a RPS long-axis four-chamber view, the maximum width of the LA, parallel to the mitral annulus, can be measured (normal <16 mm).



7.107 M-mode of a cat with HCM, showing the concentric hypertrophy and the apparent hyperkinesis of the LV. IVS = Interventricular septum; LVFW = Left ventricular free wall.



(a)



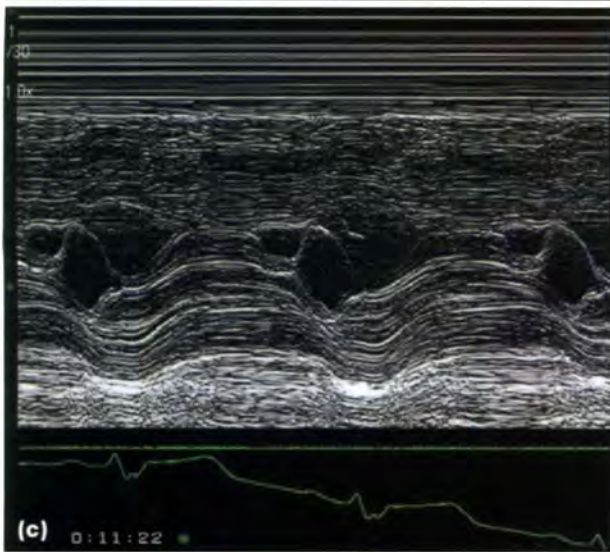
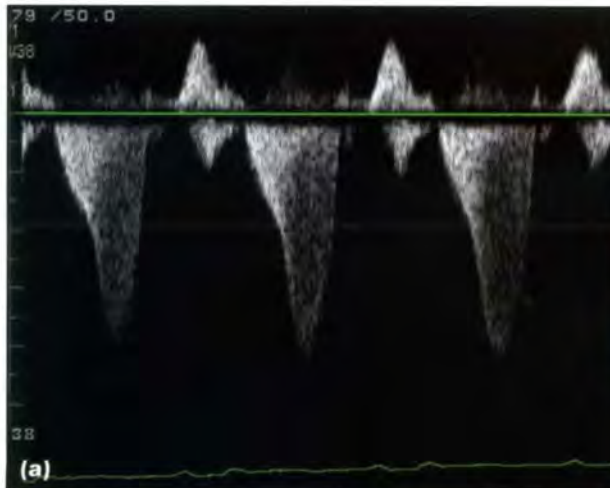
(b)

7.106 This is the same cat as in Figure 7.104. The LA is grossly dilated, both measured from (a) a RPS long-axis four-chamber view and (b) assessing the 2D short-axis LA:aortic root ratio in diastole. The ratio is 2.55 (normal <1.5). LA = Left atrium; LAu = Left auricular appendage; RA = Right atrium; RVOT = Right ventricular outflow tract.

Hypertrophic (obstructive) cardiomyopathy: This term is reserved for forms of HCM where dynamic obstruction of the LVOT is documented by echocardiography. A simplified series of events leading to this finding include:

- Turbulence of flow in the LVOT as blood travels around a basal septal bulge associated with the hypertrophy. This may be recognized as colour variance in the LVOT
- This may result in a Venturi effect on the anterior mitral valve leaflet, which is 'sucked' into the LVOT during systole. This further narrows the LVOT
- The LVOT and aortic velocities may then be increased, with abnormal biphasic acceleration on spectral Doppler, giving a scimitar shape (Figure 7.108a)
- The mitral valve is therefore incompetent, and typically, an eccentric jet of mitral regurgitation, coursing towards the posteriolateral LA wall, is recorded by colour flow Doppler (Figure 7.108b)
- Other factors are almost certainly involved in systolic anterior motion of the mitral valve, such as altered papillary muscle alignment
- Systolic anterior motion can be confirmed by mitral M-mode (Figure 7.108c). Normally, the temporal resolution of 2D is not sufficient to confirm this in real time.

Hypertrophic (obstructive) cardiomyopathy (HOCM) is frequently diagnosed in asymptomatic cats, due to the identification of a heart murmur. The murmur is due to mitral regurgitation or LVOT obstruction, and it may be variable depending upon how relaxed or stressed the cat is. It may not be possible to document HOCM in a sedated or very relaxed cat during echocardiography.



7.108 Evidence of dynamic LVOT obstruction due to systolic anterior motion (SAM) of the anterior mitral valve leaflet, leads to the diagnosis of HOCM. **(a)** There is increased and turbulent LVOT velocity, with a biphasic acceleration slope (so-called 'scimitar' shape); in this example the aortic outflow velocity is around 4 m/s. **(b)** RPS long-axis five-chamber view. The presence of SAM leads to mitral incompetence, with an eccentric mitral regurgitant jet coursing towards the posterior-lateral wall of the LA, as well as colour variance in the LVOT. **(c)** SAM is best confirmed by mitral M-mode.

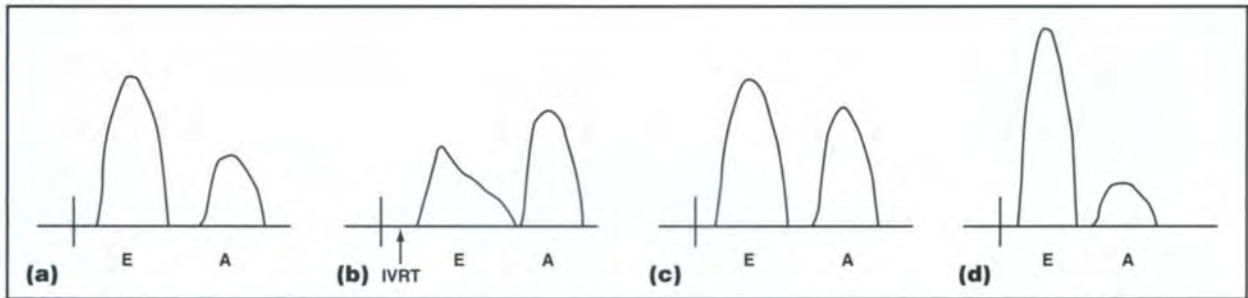
Pulsed wave Doppler assessment of diastolic function: Diastolic function can be classified by studies of:

- Mitral inflow
- Isovolumic relaxation time (IVRT)
- Pulmonary venous flow (PVF)
- Mitral inflow propagation (Vp)
- Tissue Doppler imaging.

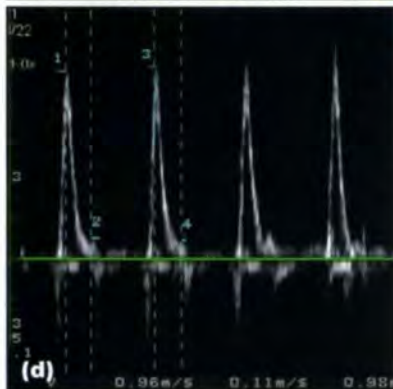
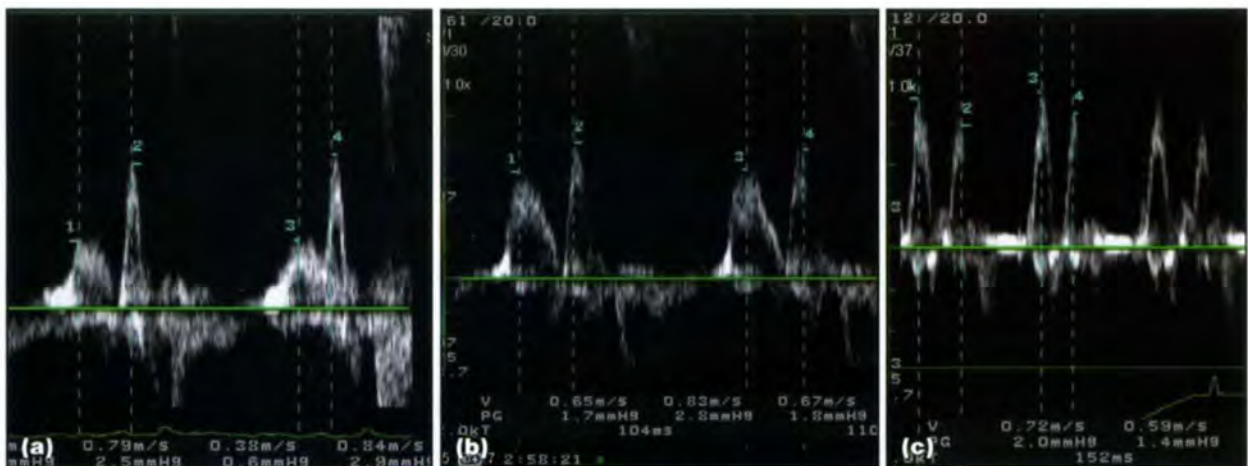
The typical findings in feline HCM patients at various stages of the disease are documented in Figure 7.109. The mitral inflow patterns are illustrated in Figures 7.110 and 7.111. Corresponding abnormalities in diastolic dysfunction are illustrated for IVRT (Figure 7.112) and PVF (Figure 7.113).

Condition	Mitral inflow	IVRT	PVF
Asymptomatic HCM. Abnormal LV relaxation	<ul style="list-style-type: none"> • E:A <1 • Prolonged E deceleration time (>65 ms) 	Long IVRT (>60 ms)	<ul style="list-style-type: none"> • S>D • Increased Ar
Progressive increase in LA-LV PG (increased filling pressures), so E wave velocity increases and exceeds A (pseudonormalization)	<ul style="list-style-type: none"> • E:A >1 • E deceleration time normal or prolonged 	IVRT long or normal	<ul style="list-style-type: none"> • S>D • Usually increased Ar velocity
With disease progression, LA pressure increases further, and the LV may become less compliant. Results in restrictive physiology	<ul style="list-style-type: none"> • E:A >2 • E deceleration time short (<55 ms) 	IVRT short (<55 ms)	<ul style="list-style-type: none"> • Low S • Increased D • Ar can be normal if atrial function preserved or low velocity • Prolonged Ar duration (greater than mitral A duration)

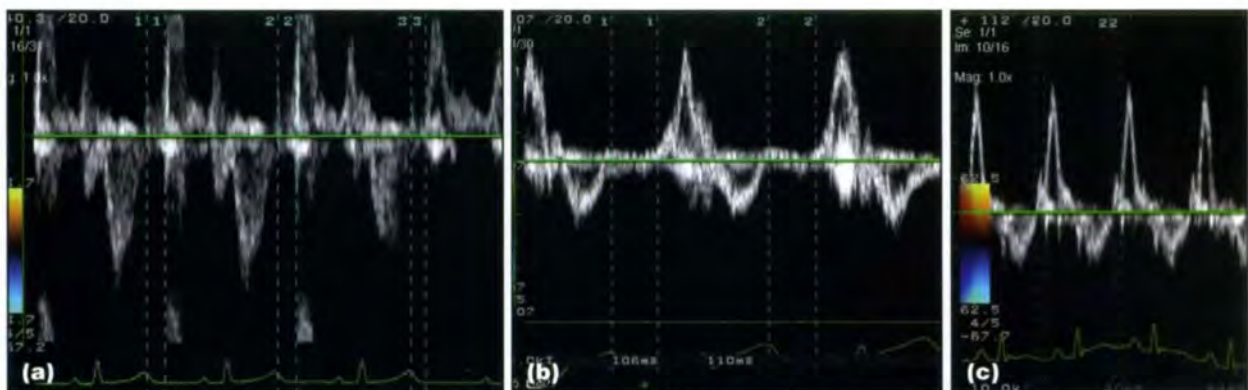
7.109 Criteria for the classification of diastolic abnormalities recognized in feline myocardial disease, such as HCM. Note the theoretical progression of disease from the first row downwards, as LA pressure and filling pressures increase and the LV becomes less compliant.



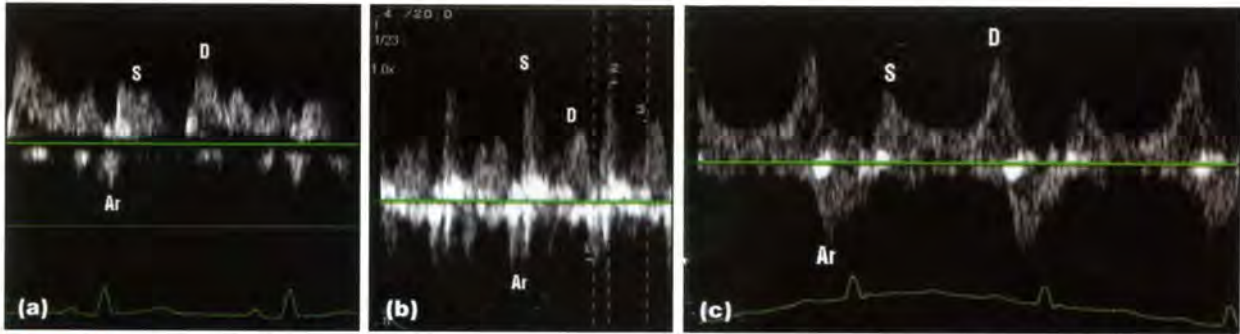
7.110 Mitral inflow patterns. **(a)** Normal mitral inflow with E wave velocity <2 but $>1 \times$ A wave velocity. **(b)** Abnormal relaxation. As active relaxation (lusitropy) of the LV is compromised, E wave velocity is reduced and E wave deceleration time is prolonged. IVRT is prolonged. Atrial contraction is important to achieve ventricular filling. **(c)** With evolution of the disease, left atrial pressures increase and E wave velocity increases, giving a relatively normal E:A ratio again (pseudonormalization). **(d)** Further worsening of the disease, with high left atrial pressure and a stiff, poorly compliant LV, can result in a high E wave velocity, short E wave deceleration time and E:A velocity ratio of >2 (restrictive filling pattern).



7.111 Mitral inflow patterns from cats with myocardial disease. **(a)** A cat with HOCM, which presented for investigation of an asymptomatic heart murmur. Note the abnormal relaxation pattern (E<A; prolonged E deceleration time). **(b)** Re-evaluation 6 months later. The cat was still asymptomatic but there is evidence of increased LA pressure; the E wave velocity is increased, although, there is still E:A reversal and evidence of abnormal relaxation. **(c)** A cat with pseudonormalization. Note that although the LA pressures have increased, the abnormal relaxation is now masked, and other methods are required to document the diastolic dysfunction. **(d)** A cat with severe biventricular failure and a RCM. A restrictive filling pattern with probable LA dysfunction is shown, with E>>A, low velocity A wave and short E wave deceleration time.



7.112 Measurement of IVRT in cats with myocardial disease. **(a)** Normal cat, with time measurement from aortic valve closure to onset of mitral flow. **(b)** A cat with abnormal relaxation time, showing increased IVRT (>65 ms). **(c)** A cat with a restrictive filling time, showing very short IVRT (<55 ms).



7.113 Assessment of PVF pattern in cats with myocardial disease. **(a)** Normal, middle-aged cat with $D > S$. **(b)** A cat with abnormal relaxation, with increased S wave (measurement 2) and lower D wave (measurement 3) velocity, but increased velocity of the Ar wave (measurement 1). **(c)** A cat with a restrictive filling pattern, with normal atrial function (increased Ar wave). D wave velocity exceeds S, and D deceleration is rapid.

Restrictive cardiomyopathy

RCM is much more poorly understood than other forms of cardiomyopathy in the cat. It is characterized by relatively normal wall thickness, LV chamber size and systolic function, but marked left atrial enlargement is apparent. The pathophysiology is associated with reduced LV compliance and diastolic dysfunction. With elevated filling pressures, there is a restrictive filling pattern on mitral inflow (however, note that this diastolic abnormality is not specific for RCM).

There are two main forms:

- An endomyocardial form: believed to be post-inflammatory (feline endomyocarditis). There is irregular endocardial thickening
- A myocardial form: the initiating factor is unknown and the endocardium appears normal.

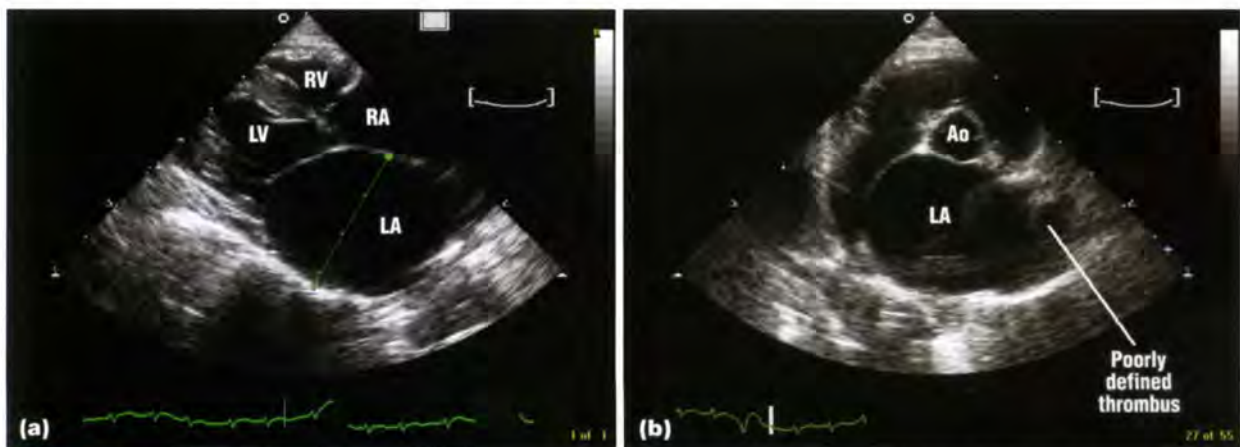
A consequence of the marked left atrial enlargement may be thromboembolism. RCM is usually not detected until the cat presents with left-sided congestive heart failure or thromboembolic complications.

Radiography: This does not differentiate between the various myocardial diseases. In RCM, there is usually dramatic left atrial enlargement (which may appear radiographically to reflect biatrial enlargement). Signs

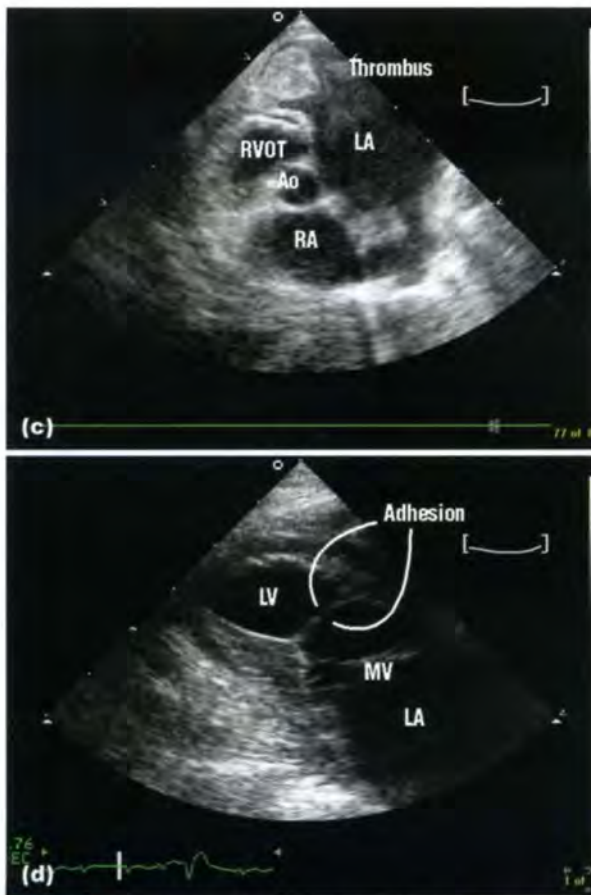
of left-sided congestive heart failure include pulmonary venous distension and a pulmonary infiltrate.

Doppler echocardiography: Echocardiographic findings include:

- There is a marked left atrial enlargement (Figure 7.114a)
- An organized thrombus may be apparent in the LA or LAu
- Spontaneous echocontrast of blood within the LA may be seen, giving the impression of swirling 'smoke'. This represents a prothrombotic state (Figure 7.114c)
- The LV has relatively preserved systolic function, and relatively normal LV dimensions and wall thickness
- This is a disease of diastolic dysfunction. Detailed Doppler assessment of myocardial function is consistent with a restrictive physiology (see Figures 7.103 and 7.109)
- In the endomyocardial form of RCM, adhesions may be seen crossing the LV chamber and the endocardium may appear irregularly thickened (Figure 7.114d)
- In the myocardial form of RCM, the myocardium and endocardium echotexture appear unremarkable.



7.114 Marked left atrial enlargement is apparent in this example of a RCM, both from **(a)** the RPS long-axis four-chamber view (33 mm diameter) and **(b)** the RPS short-axis view at the level of the aortic valves. In the short-axis view, there is a poorly defined thrombus in the LAu with a real-time image showing spontaneous echocontrast in the LA. This cat had atrial fibrillation with occasional ventricular premature complexes. Ao = Aorta; LA = Left atrium; LV = Left ventricle; MV = Mitral valve; RA = Right atrium; RV = Right ventricle; RVOT = Right ventricular outflow tract. (continues)



7.114 (continued) **(c)** A modified LPS cranial view, optimized for the LAu. The thrombus in the LAu can be seen with spontaneous echocontrast appearing as 'smoke', swirling in the junction of the LAu and LA. **(d)** RPS four-chamber view of the LV showing an irregular endocardium, particularly on the septum, and a probable adhesion crossing the LV chamber. Ao = Aorta; LA = Left atrium; LV = Left ventricle; MV = Mitral valve; RA = Right atrium; RV = Right ventricle; RVOT = Right ventricular outflow tract.

Dilated cardiomyopathy

DCM is now rarely diagnosed in the cat; it used to be one of the most common forms of feline myocardial disease prior to taurine deficiency being implicated in this disease in the late 1980s. The nutritional history of any cat diagnosed with this condition should be ascertained. DCM may be familial in certain breeds of cat, such as the Abyssinian.

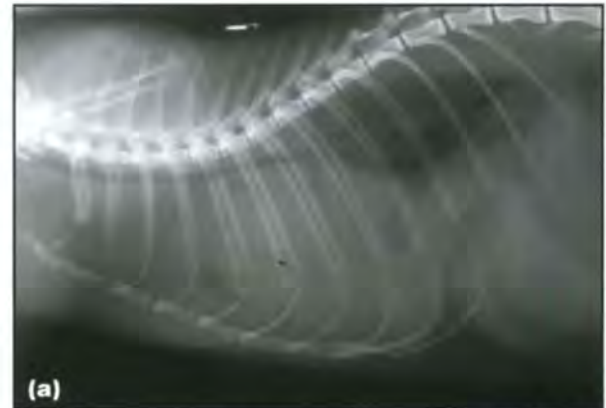
Presymptomatic disease is not normally recognized. Cats usually present with severe, biventricular failure with cardiogenic shock. They, therefore, must be stabilized prior to carrying out diagnostic tests. It must be appreciated that myocardial dysfunction and LV dilatation may be an end-stage consequence of a variety of primary and secondary cardiomyopathies in the cat (e.g. HCM, thyrotoxic cardiomyopathy).

Radiography: Radiographic findings include:

- Affected cats often have a pleural effusion, so assessment of the lung fields and cardiac silhouette is compromised (Figure 7.115)

- There is generalized cardiomegaly and the LV apex may appear to be rounded.

Radiographic findings do not distinguish between the various forms of myocardial disease.

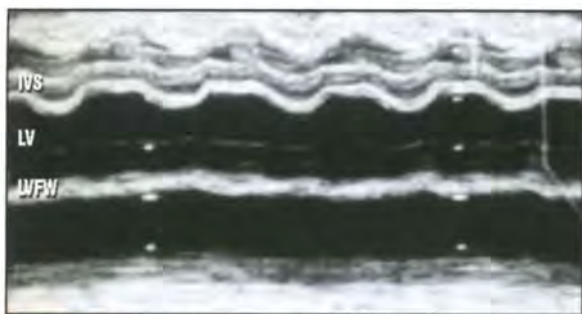


7.115 **(a)** Right lateral and **(b)** DV thoracic radiographs from a cat with DCM. There is a significant pleural effusion, masking detail of the cardiac silhouette and the lung fields. From the degree of tracheal elevation, the cardiac silhouette appears to show marked generalized enlargement.

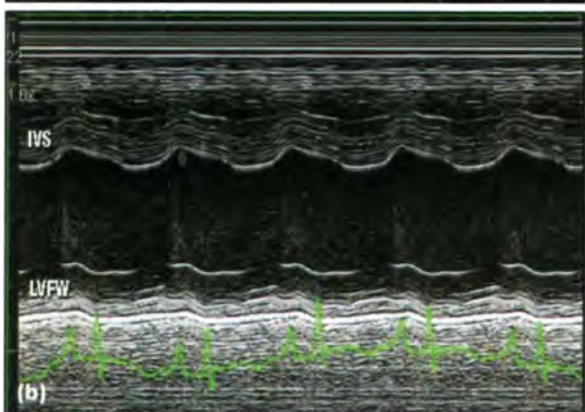
Doppler echocardiography: Similar changes are described as listed for canine DCM:

- The LV is dilated in both diastole and systole (see Figures 7.103 and 7.116) and systolic function is impaired. Wall thickness is normal or reduced
- There may be mitral and/or tricuspid regurgitation, secondary to stretch of the atrioventricular annulus.

An example of a cat with myocardial dysfunction, secondary to untreated hyperthyroidism and possibly associated with myocardial infarction, is shown in Figure 7.117.



7.116 M-mode of a cat with DCM from 1988, showing a pleural effusion and marked hypokinesis, especially of the left ventricular free wall (LVFW). IVS = Interventricular septum; LV = Left ventricle.



7.117 Images from an elderly cat with untreated, probably long-standing, hyperthyroidism. **(a)** The RPS long-axis four-chamber view shows four-chamber dilatation. **(b)** In real time, the LV was noticeably hypokinetic, which is indicated on the M-mode. Notice that the left ventricular free wall (LVFW) is not functioning on the M-mode, and the wall is thin. A segmental region of posterior wall thinning, corresponding to the M-mode sampling, is shown in (a) (*). This may correspond to a myocardial infarct (although postmortem confirmation was not achieved in this cat). IVS = Interventricular septum.

Arrhythmogenic right ventricular cardiomyopathy
Feline ARVC has been recently described. The disease is histopathologically characterized by fibrofatty replacement and infiltration in the myocardium, most pronounced in the RV. Affected cats may or may not

show malignant ventricular arrhythmias. They may show ascites as a manifestation of right-sided congestive heart failure.

Radiography: Radiographic findings include:

- Changes may show evidence of right-sided congestive heart failure or biventricular failure
- Ascites in association with a dilated CdVC indicate that the abdominal effusion is associated with right-sided congestive failure (Figure 7.118). A pleural effusion may also be present
- There may or may not be radiographic evidence of left-sided congestive heart failure.

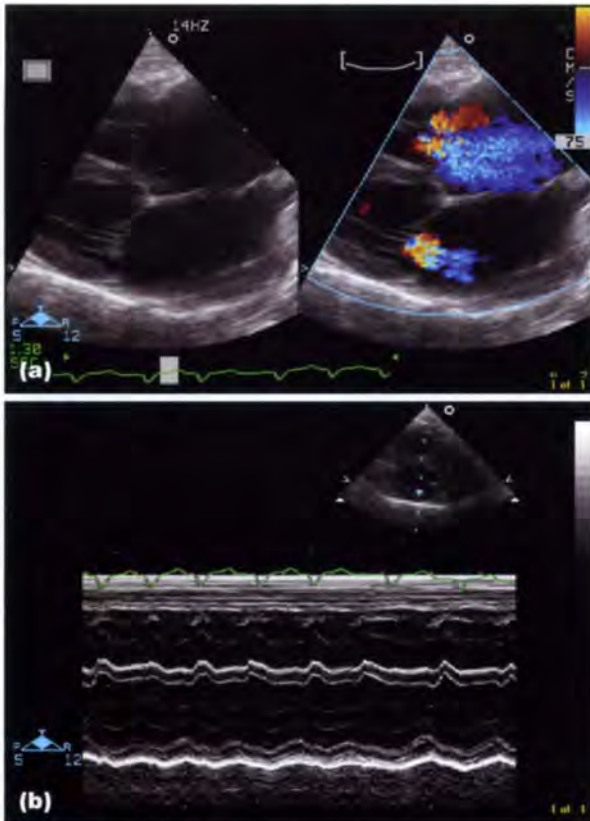


7.118 **(a)** Right lateral radiograph from a cat later confirmed to have ARVC. Ascites with the dilated CdVC indicates radiographic support for right-sided congestive heart failure. From this view (no DV available) there appears to be predominantly right-sided enlargement, resulting in cardiomegaly. **(b)** RPS long-axis four-chamber view, indicating marked right atrial and right ventricular enlargement.

Doppler echocardiography: Echocardiographic findings include:

- There is marked right-sided RA and RV dilatation (see Figure 7.118b)
- Tricuspid regurgitation may be evident due to stretch of the tricuspid annulus (Figure 7.119a). ARVC must be distinguished from tricuspid dysplasia (which will usually show an immature age of onset compared with the middle- or older-age onset in ARVC)

- A hallmark of this condition is evidence of dysplastic papillary muscles within the RV apex (the transducer needs to be moved far enough caudally and sternally to appreciate this feature from the RPS long-axis view)
- Variable changes affect the LV. In advanced disease, the LV also becomes dilated and hypokinetic (Figure 7.119b).



7.119 (a) RPS long-axis four-chamber view of a cat with ARVC. Colour flow mapping indicates the presence of tricuspid and mitral regurgitation due to stretch of the atrioventricular annuli, secondary to myocardial disease, although the RV is predominantly affected. (b) M-mode, showing dilatation of both ventricles and impaired LV systolic function. This cat was in atrial fibrillation.

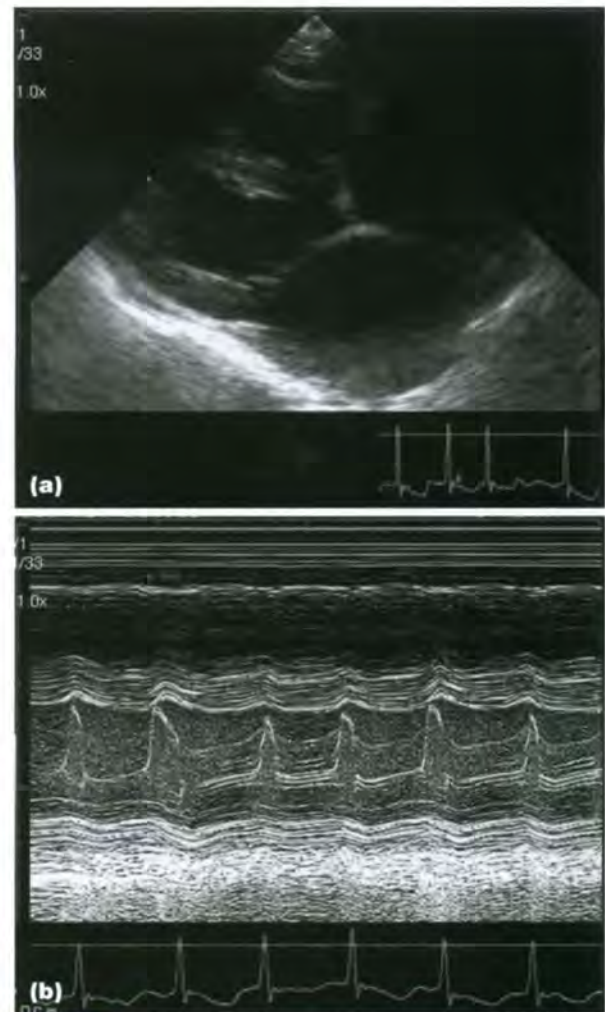
Unclassified cardiomyopathy

The findings with feline myocardial disease can be diverse. In some cats, the echocardiographic findings do not neatly fall into one of the above categories. For example, the wall thickness may be normal, but systolic function is impaired and there is evidence of abnormal relaxation (Figure 7.120). It is perfectly acceptable to categorize these cats as unclassified. It should be borne in mind that this may represent a heterogenous group.

Radiographic findings reflect the presence of congestive heart failure, and echocardiographic findings will have features from more than one of the above groups.

Secondary myocardial disease

The myocardium is influenced by other systemic factors. These include:



7.120 (a) The RPS long-axis four-chamber view and (b) M-mode, including the mitral valve, show mild chamber dilatation and impaired LV systolic function. There is also a restrictive filling pattern. This cat was categorized as having an UCM. This cat was also in atrial fibrillation.

- Systemic hypertension
- Hyperthyroidism
- Hypothyroidism
- Chronic renal failure
- Acromegaly
- Respiratory disease.

These may result in significant cardiac disease or congestive heart failure. Diagnostic tests other than imaging are required to make the diagnosis of a secondary myocardial disease.

Systemic causes of myocardial depression

In the presence of impaired systolic function, it should not be merely presumed that this represents, for example, a preclinical phase of DCM. Conditions which should be excluded are:

- Tachyarrhythmia. An animal which is tachycardic (e.g. supraventricular tachycardia) may develop a phenotype similar to DCM (called a tachycardiomyopathy). Control of rate (and/or rhythm) should result in improved systolic function

- Assessment of systolic function or chamber dimensions should not be carried out in the presence of a dysrhythmia, if possible. Altered electrical activation of the ventricles or abnormal rate can give misleading results
- Hypothyroidism. There have been several case reports of dogs with hypothyroidism and DCM, with improvement in systolic function associated with thyroid supplementation. It is not clear that the association is cause and effect; many breeds show prevalence of both conditions
- Systemically ill animals may show myocardial depression possibly associated with elevated cytokine levels.

Systemic hypertension

Systemic hypertension results in increased afterload (arterial resistance) on the LV; LV pressure then increases to maintain cardiac output. To normalize wall stress, concentric LV hypertrophy occurs. Therefore, the walls are thick and the LV chamber may be proportionately small.

Systemic hypertension is normally believed to be secondary to a primary problem in animals. Essential hypertension is considered to be rare. Conditions which may result in hypertension include:

- Chronic renal failure
- Hyperthyroidism
- Hyperadrenocorticism
- Acromegaly
- Pheochromocytoma
- Hyperaldosteronism (Conn's syndrome).

Note that some of these conditions are associated with factors that have a direct trophic effect on the myocardium (see previously), so not all changes are related to the hypertension.

Radiography: Thoracic radiographs may be unremarkable where there is just concentric LV hypertrophy in the absence of left atrial enlargement. If the underlying disease and hypertension leads to left-sided congestive heart failure, there will be left atrial enlargement, pulmonary venous distension and a pulmonary infiltrate consistent with pulmonary oedema.

Doppler echocardiography: 2D and M-mode echocardiographic findings will be similar to those described for HCM.

- Abnormalities of relaxation may be apparent with gross hypertrophy.
- In older dogs, systemic hypertension may result in accelerated progression of degenerative valvular disease.
- Mitral regurgitation is often of high velocity (increased PG between the LV and LA).

Pulmonary hypertension (cor pulmonale)

Pulmonary hypertension is a consequence of primary respiratory disease or abnormalities of the pulmonary vasculature. Mild degrees of pulmonary hypertension are recognized in brachycephalic breeds of dogs and in obesity (Pickwickian syndrome).

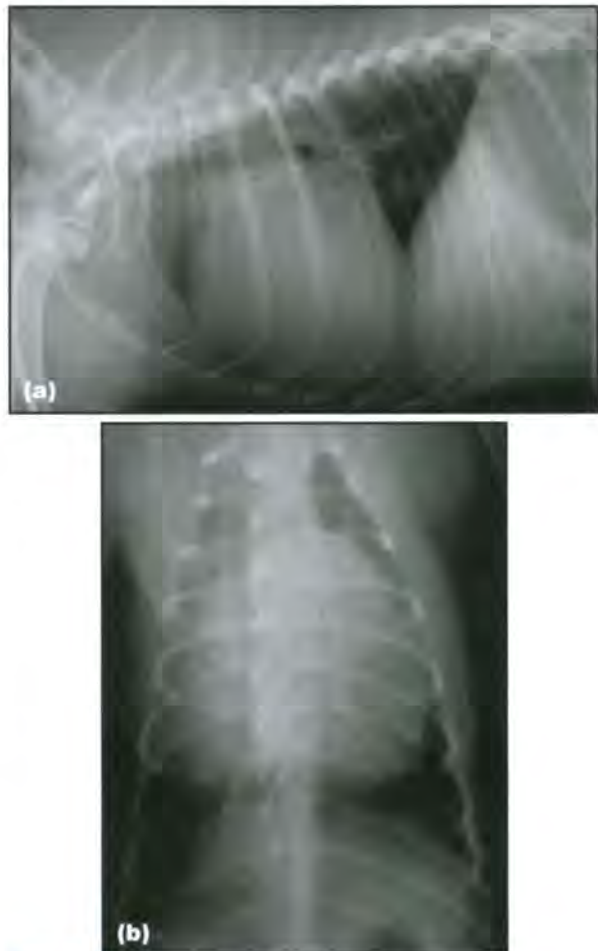
Severe pulmonary parenchymal disease, such as idiopathic pulmonary fibrosis in West Highland White Terriers, can result in more significant pulmonary hypertension, although the cardiac manifestations are not usually clinically relevant to the presentation. Pulmonary vascular disease may be secondary to parasitism, such as *Dirofilaria immitis* or *Angiostrongylus vasorum* infection.

Pulmonary vascular disease may be a consequence of an initially left-to-right shunting congenital heart disease, leading to Eisenmenger's physiology (e.g. reverse-shunting PDA or VSD). It is the pulmonary hypertension which results in reversal of the shunting from the pulmonary into the systemic circulation, for those phases of the cardiac cycle where pulmonary pressures exceed systemic pressures, resulting in cyanosis.

Sometimes, the cause of the pulmonary vascular disease is unknown (essential or primary pulmonary hypertension).

Radiography: Radiographic findings include:

- Evidence of pulmonary hypertension, including right heart enlargement (Figure 7.121)



7.121 (a) Right lateral and (b) DV thoracic radiographs from a Cavalier King Charles Spaniel with presumed idiopathic (essential) pulmonary hypertension, as other common causes of pulmonary hypertension had been actively excluded. There is marked right-sided enlargement, resulting in generalized cardiomegaly. (The DV view is slightly rotated.)

- If pulmonary hypertension is associated with respiratory disease, abnormalities of the lung field should be apparent (Figure 7.122)
- Evidence of pulmonary vascular disease may include dilated, tortuous or 'pruned' appearance to the pulmonary arteries (particularly in heartworm disease) (Figure 7.123).

Doppler echocardiography: Echocardiographic findings include:

- Pulmonary hypertension is associated with right ventricular enlargement. The RV is both dilated and concentrically hypertrophied (Figure 7.124a)
- As RV pressure is increased, the IVS appears flattened, which may be most apparent on the RPS short-axis view (Figure 7.124ab)
- Commonly, there is also right atrial enlargement (Figure 7.124a)
- The main pulmonary artery is frequently dilated (wider than the aortic diameter) (Figure 7.124c)

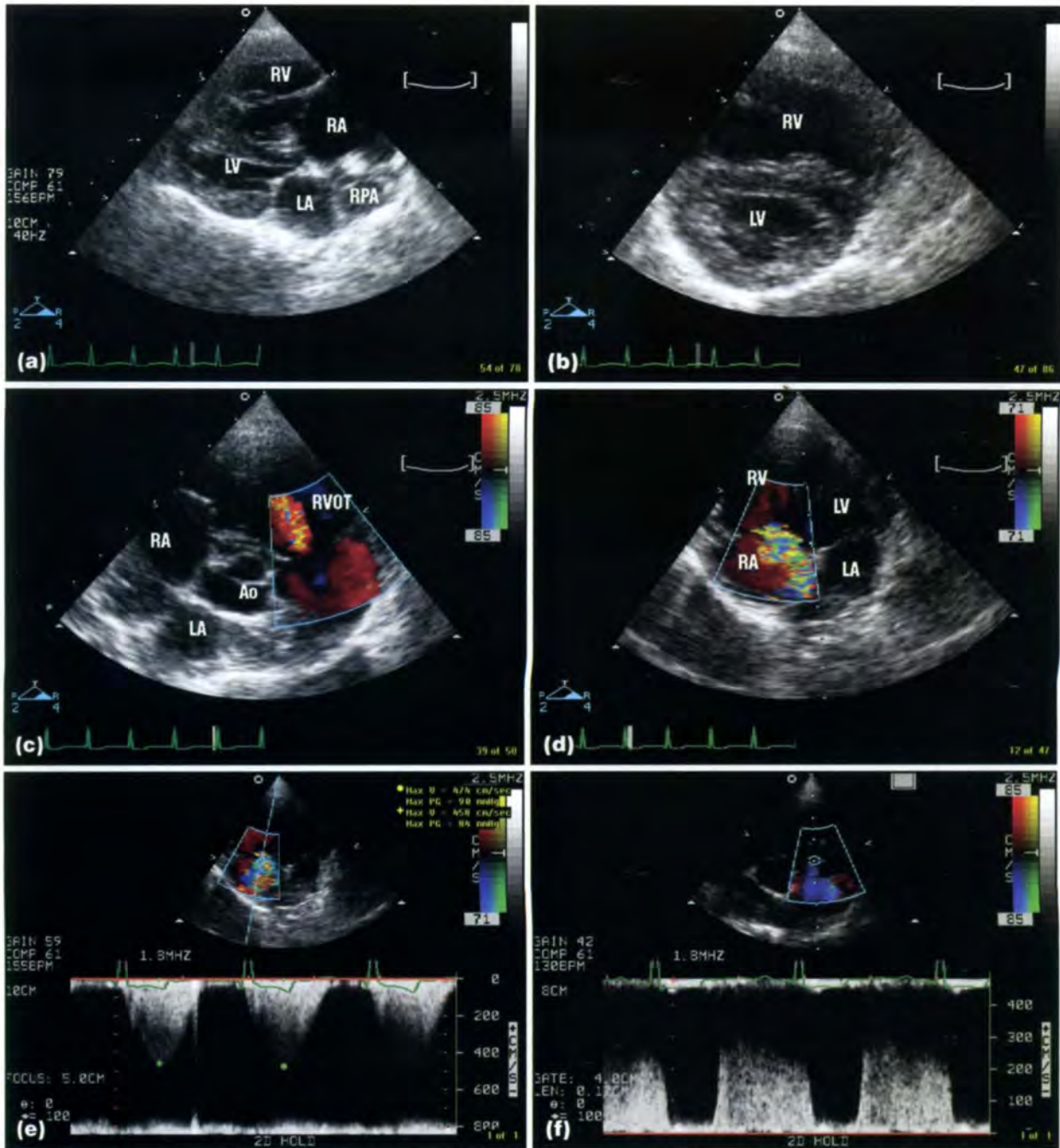
- A detailed Doppler echocardiographic examination, including intravenously administered echocontrast to demonstrate any right-to-left shunts, is indicated to actively exclude structural heart disease, which may result in pulmonary hypertension
- Tricuspid regurgitation (Figure 7.124d) and pulmonic insufficiency (Figure 7.124c) are commonly both present, whatever the cause of pulmonary hypertension
- In the absence of pulmonic stenosis, the tricuspid regurgitant velocity can indicate, by the modified Bernoulli equation, the systolic PG between the RV and RA, and therefore the systolic main pulmonary artery pressure. Thus, a non-invasive determination of systolic pulmonary arterial pressure is possible (Figure 7.124e)
- In the presence of pulmonic regurgitation, the velocity of this jet indicates the diastolic PG between the main pulmonary artery and RV. Thus, non-invasive estimation of diastolic pulmonary arterial pressure is possible (Figure 7.124f).



7.122 (a) Right lateral and (b) DV thoracic radiographs from a West Highland White Terrier with idiopathic pulmonary fibrosis and echocardiographically confirmed pulmonary hypertension. The radiographs show mild right heart enlargement. The cardiac silhouette and pulmonary vasculature are masked by a gross, generalized, interstitial opacity throughout the lung fields.



7.123 (a) Right lateral and (b) DV thoracic radiographs from a dog with *Dirofilaria immitis* infection (heartworm). The pulmonary arteries are markedly dilated and tortuous (arrowed). (Courtesy of M. Sullivan)



7.124 Images from a 5-year-old Cavalier King Charles Spaniel with a PDA associated with pulmonary hypertension, presented with ascites and other evidence of right-sided congestive heart failure. **(a)** RPS long-axis four-chamber view shows marked right atrial and right ventricular dilatation, with concentric hypertrophy of the RV wall. The IVS is flattened, which is also appreciated on **(b)** the RPS short-axis view. The right branch of the pulmonary artery (RPA) is also markedly dilated as it courses around the base of the heart. **(c)** The RPS cranial view shows the dilated pulmonary trunk with marked pulmonary insufficiency. **(d)** The left apical four-chamber view shows tricuspid regurgitation by colour flow Doppler. **(e)** Mean CW Doppler recorded velocity of the tricuspid regurgitant jet is 4.6 m/s. By the modified Bernoulli equation, there is a systolic PG ($4v^2$) between the RV and RA of 84 mmHg. Therefore, pulmonary arterial systolic pressure is at least 90 mmHg (since normal right atrial pressure is about 6 mmHg). **(f)** The mean velocity of pulmonary regurgitation is 3.4 m/s (recorded from a RPS cranial view). Therefore, the diastolic PG between the main pulmonary artery and RV is 46 mmHg. Thus, the systolic/diastolic pulmonary pressures are estimated to be at least 90/46 mmHg (but this is an underestimate as the dog is in right-sided failure; RA and RV filling pressures will be increased). This has an impact on the PDA flow. There is some left-to-right diastolic flow but in systole, no flow was evident ('balanced' PDA as a consequence of the pulmonary hypertension). Ao = Aorta; LA = Left atrium; LV = Left ventricle; RA = Right atrium; RV = Right ventricle; RVOT = Right ventricular outflow tract.

Myocardial infiltrative disease

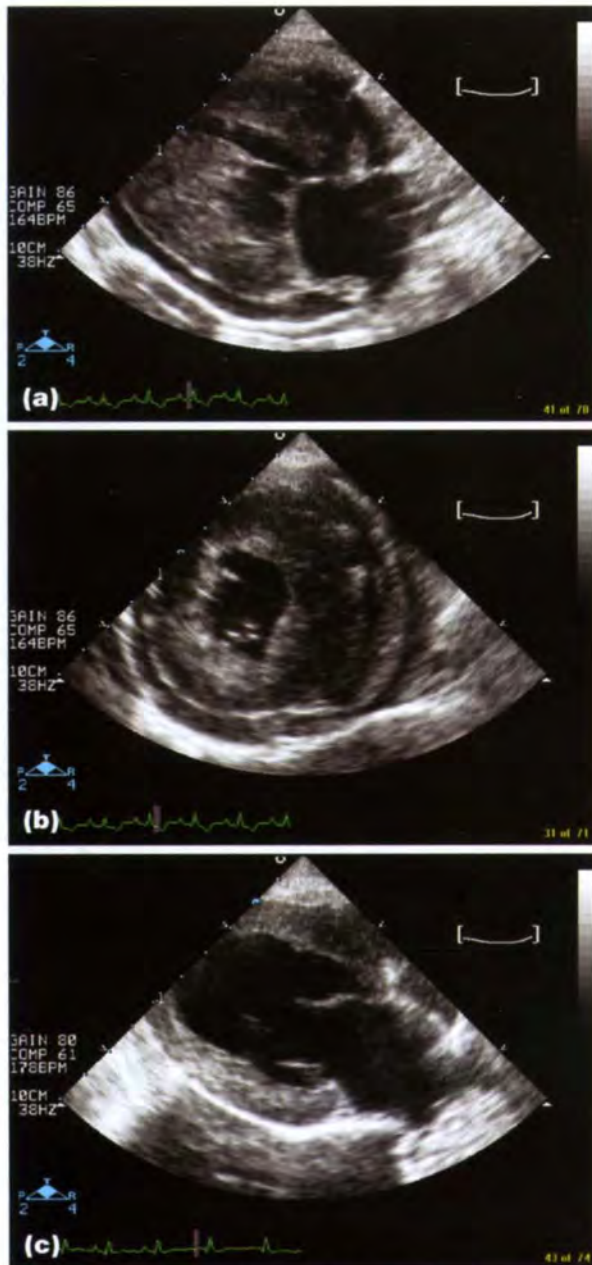
Unusually, the myocardium can be affected by infiltration. These infiltrations are normally neoplastic, such as lymphoma.

Other, non-cardiac signs usually result in the presentation of the patient. Cardiac dysrhythmias, such as ventricular tachycardia, may be clinically important.

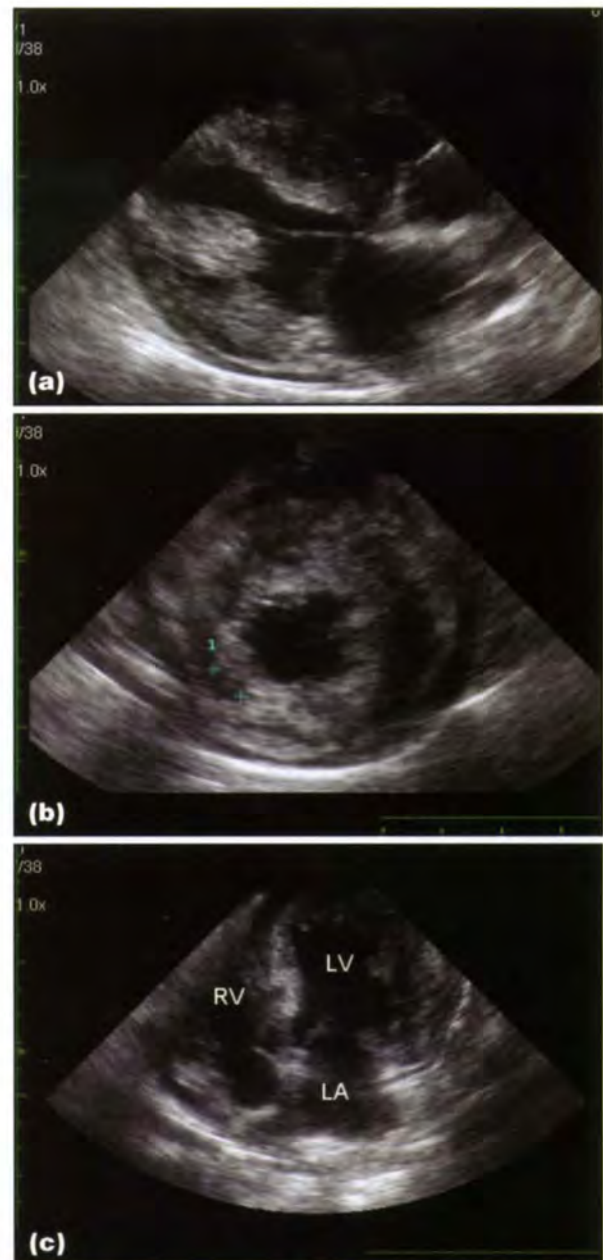
Radiography: Thoracic radiographs may or may not indicate any abnormalities in the cardiac silhouette. Radiographs may reflect the presence of the primary lesion.

Doppler echocardiography: Echocardiographic findings include:

- Infiltration into the myocardium is usually generalized and results in the impression of thickened myocardial walls (Figures 7.125 and 7.126)



7.125 (a) RPS long-axis four-chamber view and (b) short-axis view from a crossbred dog. The myocardium appears thickened but with a heterogeneous patchy increased echogenicity. There is a small amount of pericardial effusion. This was sampled and cytology confirmed the diagnosis of cardiac lymphoma. (c) After 9 days of staged chemotherapy, reduction in the thickness of the walls could be seen.



7.126 Images from an 11-year-old male Golden Retriever, which presented collapsed, anaemic and with paroxysmal ventricular tachycardia. (a) The RPS long-axis four-chamber view, (b) short-axis view and (c) left apical four-chamber view all show evidence of thickened myocardial walls, with disrupted architecture, and numerous hypoechoic lesions of various sizes. (d) Postmortem examination showed the entire myocardium was affected by a disseminated haemangiosarcoma. LA = Left atrium; LV = Left ventricle; RV = Right ventricle. (Courtesy of R. Irvine)

- The normal myocardial echotexture is disrupted and it may appear to be hyperechoic, or show focal hypoechoic regions, or a general 'moth-eaten' appearance
- Both systolic and diastolic dysfunction may be evident as a consequence of the infiltrate.

Acquired valvular disease

A list of the differential diagnoses of acquired valvular regurgitation is presented in Figure 7.127.

<p>Mitral valve</p> <p>Small regurgitant jet may be incidental finding Myxomatous valvular degeneration Endocarditis Secondary to left ventricular enlargement Widespread arteriosclerosis with myocardial infarcts (Undiscovered congenital heart disease)</p>
<p>Tricuspid valve</p> <p>Small regurgitant jet may be incidental finding Myxomatous valvular degeneration Main pulmonary artery hypertension Secondary to right ventricular enlargement Rarely endocarditis (Undiscovered congenital heart disease)</p>
<p>Pulmonic valve</p> <p>Low degree insufficiency as a common incidental finding Secondary to pulmonary artery hypertension Secondary to pulmonary artery dilatation (e.g. heartworm disease) (Undiscovered congenital heart disease)</p>
<p>Aortic valve</p> <p>Low degree insufficiency as an occasional incidental finding Endocarditis Annuloaortic ectasia (idiopathic dilatation of proximal aorta and aortic annulus) (very rare) (Undiscovered congenital heart disease)</p>

7.127 Differential diagnoses for acquired valvular regurgitation.

Myxomatous atrioventricular valvular degeneration

Myxomatous atrioventricular valvular degeneration (also known as endocardiosis, chronic degenerative valvular disease) is the most common acquired cardiac disease in small-breed dogs. Commonly affected breeds include the Papillon, Cavalier King Charles Spaniel, Poodle and Chihuahua. Myxomatous atrioventricular valvular degeneration is uncommon in dogs under the age of 5 years old. The condition is also seen in large-breed dogs and is rarely seen in cats. The aetiology is unknown but the condition is likely to be hereditary in small dog breeds.

The condition may affect either the mitral or the tricuspid valve. Each of these valves consists of two large leaflets (one mural and one septal) and sometimes smaller commissural cusps between the leaflets. Tough fibrous cords called chordae tendinae attach the components of the valve to the papillary

muscles. The leaflets have chordae tendinae from both papillary muscles attached to them, the commissural cusps have chordae tendinae from only one papillary muscle.

The pathological changes in myxomatous atrioventricular valvular degeneration can involve the leaflets and the chordae tendinae. The valve leaflets become thickened (most marked at the free edge) and redundant. The thickening may extend to nodular change. The chordae tendinae may also become thickened where they attach to the valve. Eventually they may rupture and result in flail of the valve leaflet.

The clinical presentation of the disease varies from a soft heart murmur to end-stage heart disease and failure. Large dogs may be less tolerant and have a more drastic progression of the condition.

Radiography

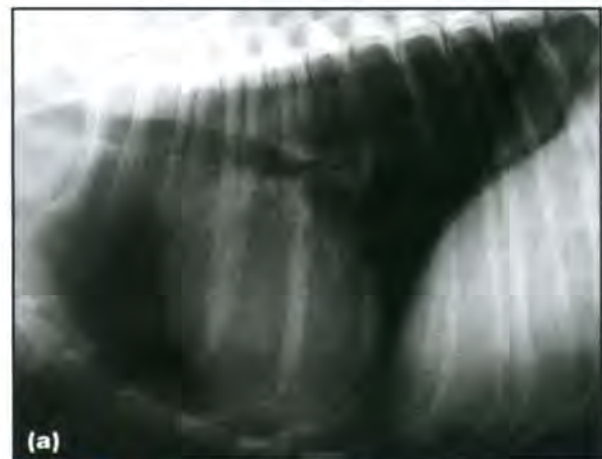
There is marked variation in radiographic features, depending on the progression of the disease (Figure 7.128). The major features include:

- Left atrial enlargement (one of earliest and most consistent signs)
- Left ventricular enlargement
- Right atrial and ventricular enlargement, depending on the degree of tricuspid involvement.

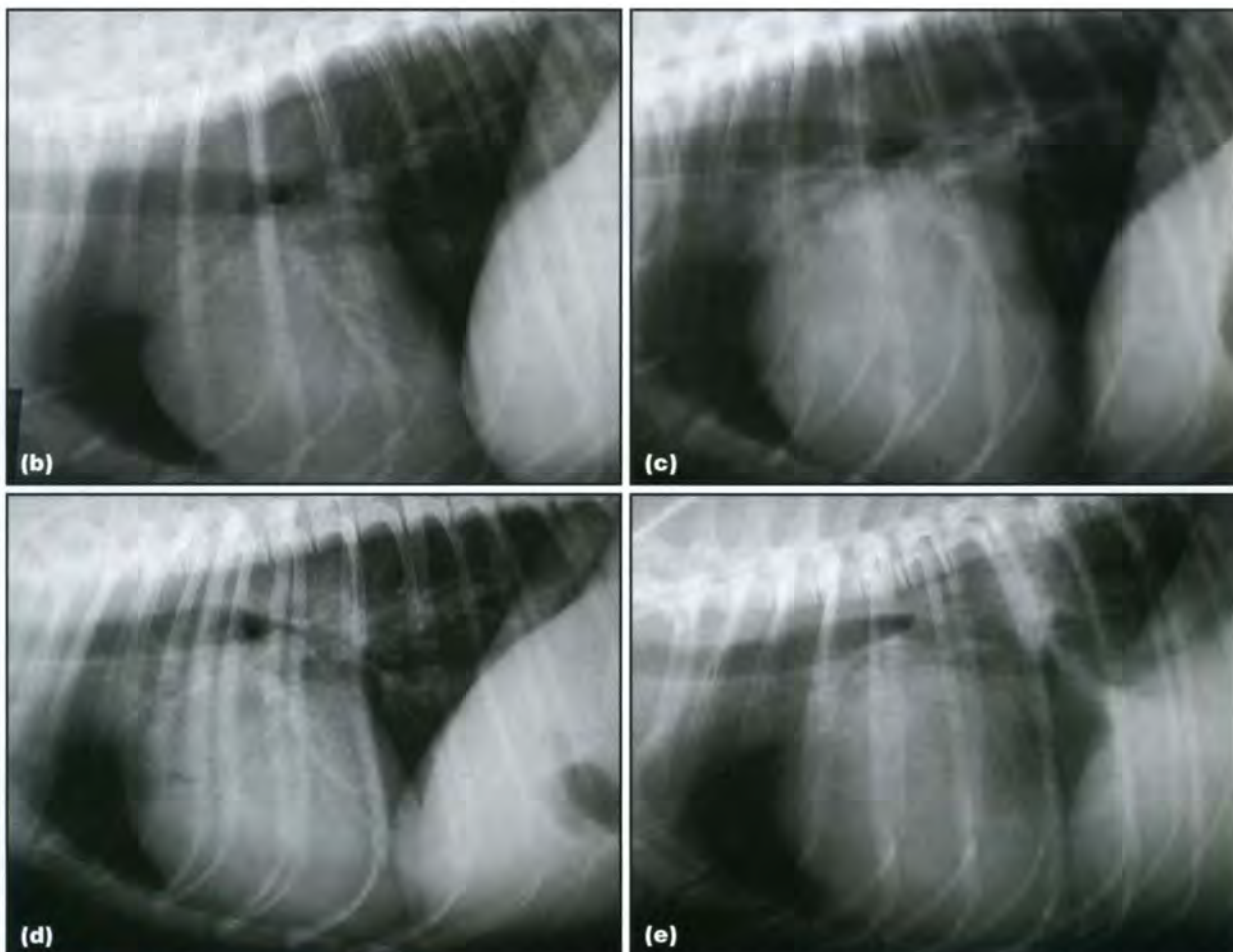
There may also be:

- Pulmonary venous congestion (enlarged pulmonary veins)
- Evidence of left-sided heart failure: interstitial or alveolar pattern representing oedema. Supporting evidence of pulmonary venous congestion and left-sided enlargement is useful
- Evidence of right-sided heart failure.

Contrast studies: Angiocardiography has been replaced by echocardiography.



7.128 A series of five lateral radiographs obtained over a period of 4 years in a middle-aged Cavalier King Charles Spaniel with confirmed endocardiosis. **(a)** Normal. The initial view was obtained when a soft systolic murmur consistent with mitral regurgitation was detected on clinical examination. No significant abnormalities are present on this film. The disease progressed over the following 4 years and left-sided and eventually generalized cardiomegaly developed. (continues)



7.128 (continued) A series of five lateral radiographs obtained over a period of 4 years in a middle-aged Cavalier King Charles Spaniel with confirmed endocardiosis. **(b)** Slight cardiomegaly. **(c)** Moderate cardiomegaly. **(d)** Moderate cardiomegaly and congestive heart failure. Note that left-sided heart failure and a perihilar alveolar infiltrate are evident on this film. **(e)** Severe cardiomegaly and congestive heart failure. The heart failure was treated but recurred.

Echocardiography

Echocardiography is useful to confirm the diagnosis and assess systolic function. It cannot be used to identify heart failure, hence radiography and ultrasonography are complementary techniques in the evaluation of this condition. It is important to examine the entire valve as the lesions may be unevenly spread.

- Early signs include a systolic bulging of the valve leaflet(s) with or without regurgitation.
- This progresses to thickening of the leaflet, most pronounced at the tip (Figure 7.129). The leaflet may appear thickened, nodular or club-like. Changes are often more pronounced on the septal leaflet. Note that the valvular changes in large-breed dogs may not appear obvious, yet severe disease may still be present.
- Thickening of the chordae tendinae.
- Flail leaflet (Figure 7.130):
 - Mild to moderate: the tip of the leaflet moves into the LA during systole
 - Severe: the entire leaflet moves into the LA during systole.
- Enlarged LA (Figure 7.131). It is very important to assess left atrial size as this parameter reflects severity (except in cases of acute chordae tendinae rupture).
- LV and M-mode parameters:
 - Mild mitral myxomatous valvular degeneration does not lead to abnormal left ventricular size
 - However, with time the left ventricular end-diastolic short-axis dimension increases but the end-systolic dimension remains the same. This is the result of *eccentric hypertrophy* seen in moderate to severe disease
 - It is important to note that with moderate to severe mitral regurgitation the values of ejection phase indices (e.g. fractional shortening, ejection fraction, velocity of circumferential fibre shortening) are often *increased*. This is due to the rapid regurgitation of left ventricular blood into the low pressure LA during systole
 - Hyperdynamic wall motion will be seen (Figure 7.132)

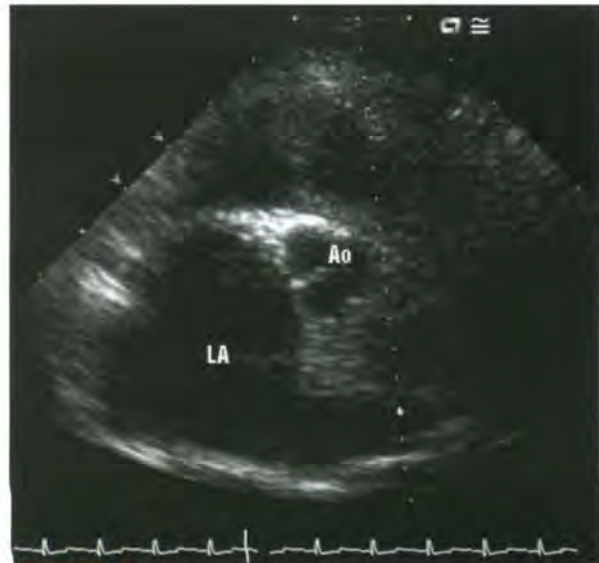
- Small-breed dogs often have a fractional shortening percentage of greater than 50% with severe mitral regurgitation. Hence, if a normal fractional shortening (or other ejection phase index) is identified in a small-breed dog with severe mitral valvular disease, then *reduced myocardial contractility is present*
- End-systolic volume indices more accurately assess myocardial contractility
- Breed differences: note that myocardial failure is more severe and develops earlier in large-breed dogs with myxomatous mitral valvular degeneration. Also note that large dogs usually have a fractional shortening percentage within the 25–40% range with severe mitral regurgitation.
- Right ventricular and right atrial enlargement, depending on the degree of tricuspid disease.



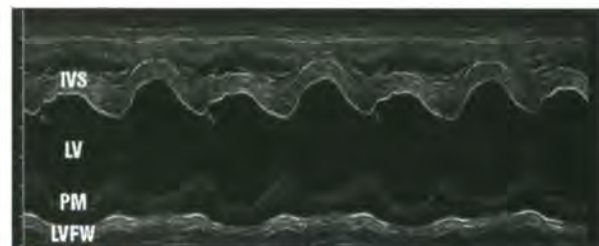
7.129 RPS long-axis echocardiogram, optimized for visualization of the mitral valve in a dog with myxomatous mitral valve degeneration. A thickened region is present at the tips of both valve leaflets creating a 'club-like' appearance (arrows show the thickened region on the septal leaflet). LA = Left atrium; LV = Left ventricle.



7.130 A flail leaflet is seen in this dog with myxomatous mitral valve degeneration. Note that the septal leaflet is displaced above the level of the valve annulus. This image was acquired during systole. LA = Left atrium; LV = Left ventricle.



7.131 RPS short-axis view at the heart base in a dog with myxomatous mitral valve degeneration. Normally the ratio of left atrium (LA) to aortic (Ao) diameter at this level should be no greater than 1.5:1; in this case the atrium is enlarged. The size of the LA is an important indicator of disease severity.



7.132 An M-mode echocardiogram obtained from a RPS short-axis view at the level of the papillary muscles. Note the hyperkinetic motion of the IVS, secondary to the rapid regurgitation of left ventricular blood into the low pressure LA during systole. IVS = Interventricular septum; LV = Left ventricle; LVFW = Left ventricular free wall; PM = Edge of papillary muscle that was included in the image.

Doppler studies:

- Valvular insufficiency (mitral, tricuspid) (Figure 7.133). Note that a small jet near the mitral valve should not be over interpreted as this can be seen in normal dogs.
- Typically the mitral regurgitant jet is 5–6 m/s in dogs without myocardial failure. The speed of the jet depends on the pressure differences between the LA and LV:
 - Systemic hypertension *increases* jet velocity
 - Systemic hypotension, a large orifice, dramatic increases in left atrial pressure and systolic failure all *decrease* jet velocity.
- An increased tricuspid regurgitant jet velocity (≥ 2.8 m/s) indicates pulmonary hypertension. Pulmonary oedema, secondary to severe mitral disease or other causes of pulmonary hypertension should be considered. Pulmonic stenosis will also increase the velocity of a tricuspid regurgitant jet, but other changes will be present (see Congenital heart disease, above).



7.133 Colour and spectral Doppler echocardiograms of two dogs with myxomatous mitral valve disease. **(a)** A large jet of mitral regurgitation, extending to the wall of the LA. **(b)** CW spectral Doppler tracing from a dog with mitral regurgitation. The cursor was placed in the mitral regurgitant jet. LA = Left atrium; LV = Left ventricle; MR = Mitral regurgitation.

- The size of the mitral regurgitant jet can be compared with the size of the LA and is useful in assessing the severity of the disease.
- Additional Doppler techniques have been described, but left atrial size remains a more reliable parameter for the evaluation of the disease severity.
- Mitral diastolic filling velocity is usually increased when significant mitral regurgitation is present.
- Doppler parameters of systolic function can be assessed (see Chapter 2).

Infective endocarditis

Infective endocarditis involves bacterial infection and inflammation of the cardiac valves in almost all cases, though strictly speaking the term refers to any infection of the endocardial surface of the heart. Transient or persistent bacteraemia is the most common aetiology. The condition is seen mainly in

medium to large pure-breed dogs and rarely in cats. German Shepherd Dogs may be over-represented. The mitral valve and aortic valve are the most commonly affected in both species.

Bacteria colonize the valve and create vegetative lesions or destroy the valve, both of which lead to valvular regurgitation. Less commonly the valve may narrow and become stenotic. Organisms reported in canine endocarditis include *Staphylococcus aureus*, haemolytic and non-haemolytic streptococci and *Escherichia coli*. Rarer isolates include *Corynebacterium*, *Pseudomonas*, *Erysipelothrix* and infection with the proteobacteria *Bartonella vinsonii*.

Clinical presentation of the condition varies. Clinical signs include lethargy, pyrexia, weakness, anorexia, gastrointestinal disease and lameness. A heart murmur is usually, but not always, present. A recent onset of a murmur, pyrexia and the presence of lameness should increase the index of suspicion for infective endocarditis. Blood cultures are used to confirm the diagnosis of bacteraemia, but are not always sensitive.

Radiography

Radiography may show left-sided cardiac enlargement in chronic cases. Contrast studies have been superseded by echocardiography.

Echocardiography

This is extremely useful in diagnosis:

- Visualization of vegetations. Vary from small nodules to large florid cauliflower-like masses (Figure 7.134). The valve lesions can look identical to those in myxomatous valvular degeneration
- Infective endocarditis lesions are usually solitary and more echogenic. History and signalment are helpful in distinguishing the two:
 - Myxomatous mitral valve degeneration: small breed, older, chronic history of murmur, pyrexia, systemically well



7.134 **(a)** Long-axis RPS view of a mixed breed dog with bacterial endocarditis of the mitral valve, secondary to a snake bite. Large florid masses are present on the valve leaflets. LA = Left atrium; LV = Left ventricle. (continues)



7.134 (continued) **(b)** Short-axis RPS view of a mixed breed dog with bacterial endocarditis of the mitral valve, secondary to a snake bite. Large floriid masses are present on the valve leaflets. LV = Left ventricle.

- Infective endocarditis: large breed, recent onset of murmur, pyrexia, systemic illness.
- Valvular destruction in the absence of vegetations may also be present. Seen as a defect in the valve and consequent regurgitation
- Abnormal valvular motion.

Doppler studies: Depending upon which valve is involved, aortic or mitral valve regurgitation may be seen.

Aortic and pulmonic insufficiency

There are many congenital diseases that result in clinically significant pulmonic or aortic insufficiency (see Congenital heart disease). However, both pulmonic and aortic insufficiency may also be seen as non-clinically significant findings in acquired conditions. This is especially the case for pulmonic insufficiency, which is an incidental finding in many dogs. Myxomatous degeneration of the valve leaflets has also been described in both locations, but is very unlikely to result in clinical signs.

Other acquired diseases that may result in aortic and pulmonic insufficiency are:

- Aortic – infectious endocarditis (see above)
- Pulmonic – pulmonary hypertension, main pulmonary artery dilatation (e.g. heartworm).

Radiography

There are no significant radiographic changes. Contrast studies are not necessary.

Echocardiography

Pulmonic insufficiency:

- A small flame-like jet of pulmonic insufficiency is commonly seen in clinically normal dogs (Figure 7.135). The maximal velocity is usually 1 m/s.



7.135 RPS short-axis echocardiogram at the heart base. A flame-like small jet of pulmonic insufficiency was identified in this 2-year-old Flat Coated Retriever. This was considered to be a clinically insignificant finding. The pulmonic valve and outflow velocity were normal. MPA = Main pulmonary artery; RVOT = Right ventricular outflow tract.

- Pulmonary hypertension should be considered when the jet velocity is ≥ 2.2 m/s.
- Pulmonic stenosis will also give a high-velocity jet (see Congenital heart disease).

Aortic insufficiency:

- A small flame-like jet of aortic insufficiency is occasionally seen in clinically normal dogs (Figure 7.136).
- A large jet should alert suspicion of subaortic or aortic stenosis (see Congenital heart disease) and requires further investigation.



7.136 A tiny jet of aortic insufficiency identified on a RPS long-axis view (optimized for the aorta) in a 7-year-old Border Collie cross breed dog. This insufficiency was considered to be a clinically insignificant finding. Ao = Aorta; LV = Left ventricle.

Traumatic valvular disease

Traumatic rupture of the chordae tendinae or papillary muscles may occur and has been reported in dogs and cats secondary to falling from a height or other blunt thoracic trauma. The result is acute onset mitral or tricuspid regurgitation.

Radiography

Varying degrees of chamber enlargement may be seen, depending on the time elapsed since the injury occurred, the extent of injury and whether the mitral or tricuspid valve was involved. Animals with left-sided injury develop rapid onset pulmonary oedema (see Figure 12.21, p. 252).

Echocardiography

Features seen include:

- Structural abnormalities depending on the extent of the injury:
 - Flail leaflet
 - Partial separation of the leaflet(s) of the valve from the valve annulus (Figure 7.137)
 - Abnormal papillary muscles.
- Extensive regurgitant jet from either the mitral or tricuspid valve
- Enlarged left atrial or right atrial dimensions (depending on which valve is involved).

Pericardial diseases

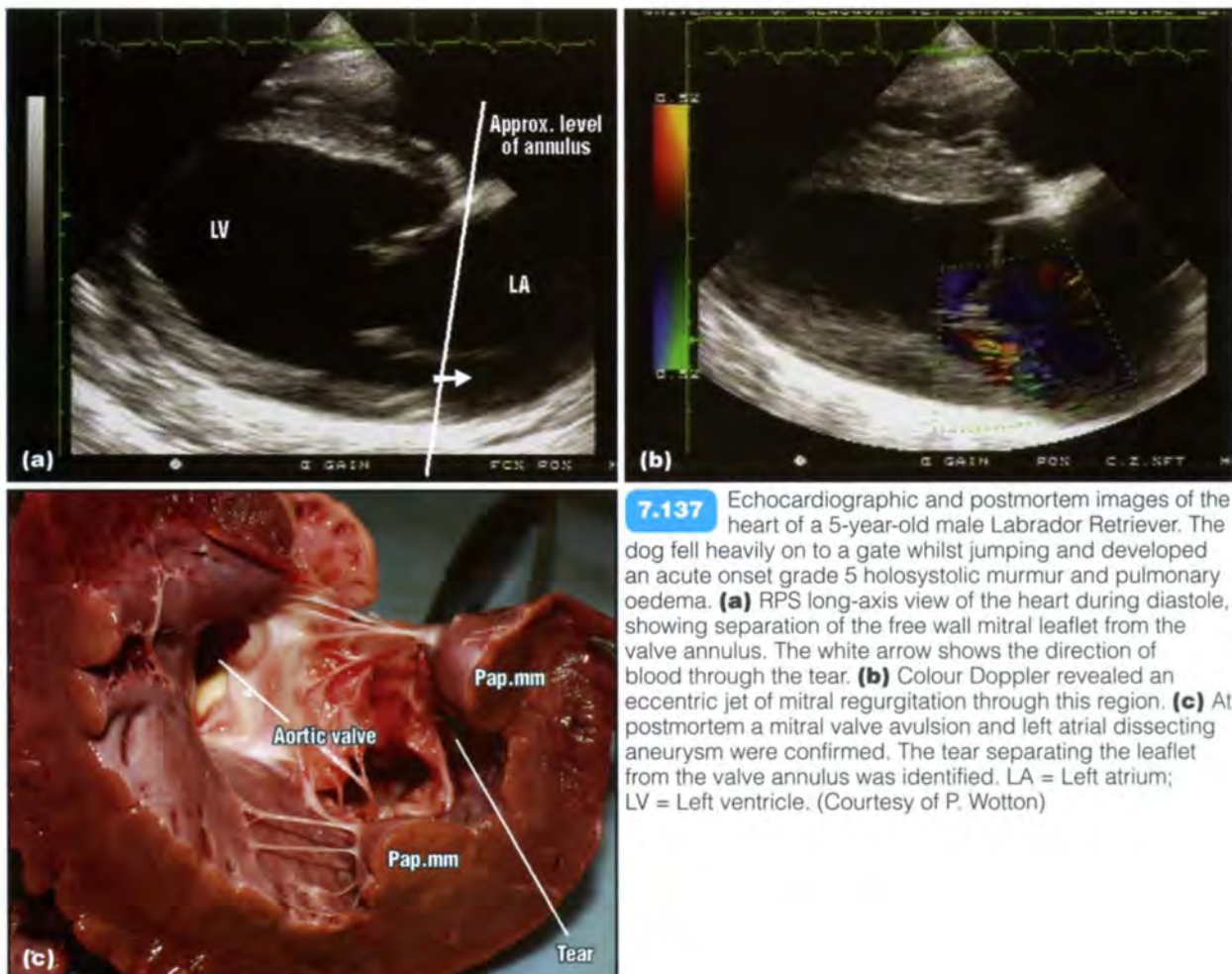
Pericardial effusion and cardiac tamponade

Pericardial effusion is the most common pericardial disease seen in small animals. Fluid can accumulate in the pericardial sac due to a variety of disorders that can be systemic, cardiac or pericardial in origin. All generally produce the same end result of cardiac tamponade and congestive heart failure.

Cardiac tamponade can be defined as compression of the heart due to collection of blood or fluid in the pericardial sac.

The effusion can be classed as a pure transudate, modified transudate, exudate or haemorrhagic (just as in other areas of the body). Chronic effusions can reach large volumes before clinical signs occur as the pericardium is able to slowly enlarge. More acute pericardial effusions (such as those which occur with left atrial rupture) can produce severe tamponade at small volumes (florid tamponade) and even result in death.

Pericardial effusion may be seen in any dog or cat but older large-breed dogs are predisposed. Clinical signs include lethargy, respiratory distress, anorexia, collapse and abdominal distension. Evidence of right-sided heart failure is usually



identified on clinical examination. Heart sounds are muffled on auscultation, pulses are weak and pulsus paradoxus may be present.

Causes of pericardial effusion

The most common causes of pericardial effusion include (see also Cardiac neoplasia):

- Cardiac haemangiosarcoma
- Idiopathic pericardial effusion
- Heart base neoplasia
- Mesothelioma
- Congestive heart failure
- Other (see below).

Cardiac haemangiosarcoma:

- Most common cause of pericardial effusion in dogs in retrospective studies.
- Older dogs, average weight 32 kg.
- Golden Retrievers and German Shepherd Dogs are over-represented.
- By the time of diagnosis, cardiac haemangiosarcoma has usually metastasized and should be considered a systemic disease.
- Effusion is haemorrhagic but does not clot.

Idiopathic pericardial effusion: By definition this is an effusion where no underlying cause is identified. It must be a cautious diagnosis as small mass lesions and mesothelioma may be missed on echocardiographic examination and fluid analysis. The features include:

- Older dogs
- Golden Retrievers are over-represented
- The aetiology is poorly understood
- Fluid appears haemorrhagic usually but does not clot.

Heart base neoplasia:

- Usually aortic body tumours.
- Older dogs.
- Brachycephalic breeds are predisposed. It may be associated with chronic hypoxia inducing hyperplasia and neoplasia of the chemoreceptors in these breeds.
- Rarely reported in cats.
- May metastasize to lung, LA, pericardium and kidney.
- The effusion varies but is often haemorrhagic.

Mesothelioma:

- May be a more common cause of pericardial effusion than originally thought.
- There is no breed predisposition; occasionally seen in the cat.
- This is a difficult diagnosis to make even with histopathology.

- Mesothelioma is a diffuse neoplasm of the pericardium and cannot be diagnosed on echocardiography.
- Fluid analysis cannot distinguish between idiopathic pericardial effusion and mesothelioma.
- One paper reports that accumulation of significant amounts of fluid within 120 days of pericardectomy increases suspicion of mesothelioma.

Other:

- Congestive heart failure. Often present in right-sided heart failure but rarely of clinical significance.
- Feline infectious peritonitis (FIP).
- Coagulopathy:
 - Rarely results in significant tamponade
 - Reported in both dogs and cats.
- Left atrial rupture (uncommon cause):
 - Small-breed dogs with chronic myxomatous mitral valve degeneration
 - Acute tamponade and life-threatening condition
 - Effusion will be haemorrhagic and will clot
 - Clots and fluid seen on echocardiography.
- Trauma. Rare, fluid will be haemorrhagic and will clot.
- Uraemia. Has been reported in both dogs and cats.
- Septic pericarditis (rare):
 - Migrating foreign bodies, such as grass awns
 - Bite wounds
 - Fungal disease – coccidioidomycosis, one case of aspergillosis.
- Constrictive pericarditis (see below).
- Cardiac lymphoma. Rare, reported in dogs and cats, pericardial fluid will give diagnosis.
- Cardiac rhabdomyosarcoma. Rare, reported in dogs and cats.

Pericardial effusion in the cat: This is most commonly part of a more generalized disease:

- Congestive heart failure
- FIP
- Lymphoma.

Symptomatic pericardial effusion in the cat is uncommon. A recent study found that congestive heart failure was the most common cause of pericardial effusion in the cat.

Radiography

Findings vary with the amount of fluid and the rate at which it developed. Rapid accumulation of fluid may cause tamponade without radiographic signs of cardiomegaly. The classic appearance is a generally enlarged and globoid cardiac silhouette with (Figure 7.138):

- Sharply defined margins
- No specific chamber enlargement.



7.138 DV radiograph of a dog with a large volume pericardial effusion. Note the extremely sharp margins of the cardiac silhouette. This is often a clue to the presence of a pericardial effusion in a dog with globoid cardiomegaly.

A careful examination for heart base masses and right atrial mass effect should be performed; however, often no radiographic evidence is seen. A search for pulmonary metastases and thoracic lymphadenopathy should be performed. There may be hypoperfused lung fields due to tamponade and radiographic features of right-sided heart failure.

Contrast studies have been replaced by echocardiography.

Echocardiography

This is the diagnostic technique of choice; it is easy, accurate and non-invasive.

Important tip

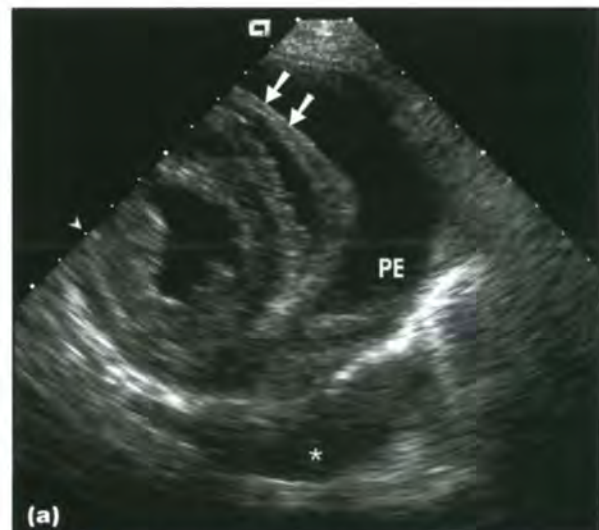
The ultrasound examination should be performed *before* draining the pericardial effusion to improve the chance of visualizing a mass lesion.

- Pericardial effusion is seen as an *anechoic* (to slightly echoic, depending on type) *circular* region surrounding the heart. The pericardium is seen as a thin hyperechoic line surrounding the fluid (Figure 7.139).
- Pleural fluid can occasionally mimic pericardial effusion:
 - Pleural effusion is more diffuse and the edges of lung lobes and the mediastinal structures will be outlined by fluid (see Chapter 13)
 - Pericardial effusion is more abundant at the apex and is scant or absent behind the LA. Pleural effusion will surround the LA.



7.139 RPS long-axis echocardiogram of a 7-year-old Golden Retriever with pericardial effusion. The effusion was identified as an anechoic region (PE) surrounding the heart and encased by a thin hyperechoic rim of pericardium (arrowed). A small volume pleural effusion was also present in this dog in association with right-sided heart failure. This is seen as an anechoic region surrounding a collapsed lung lobe tip (L) in the foreground.

- The heart may swing in the pericardial effusion.
- Cardiac tamponade (Figure 7.140):
 - This affects the lower pressure right side more than the left
 - There is late diastolic to systolic inversion of the RA and diastolic collapse of the RV.



7.140 A pericardial effusion can produce cardiac tamponade. **(a)** RPS short-axis echocardiogram at the level of the papillary muscles in a dog with a pericardial effusion (PE). The image was obtained during diastole and the RV shows collapse (arrowed) due to the pericardial pressure exceeding the intraventricular pressure. This confirms cardiac tamponade. A small pleural effusion was also present in this dog (*). (continues)



7.140 (continued) A pericardial effusion can produce cardiac tamponade. **(b)** RPS short-axis echocardiogram at the level of the papillary muscles in another dog with pericardial effusion. This dog does not show any evidence of tamponade as the RV did not collapse during diastole. Note that the atria should also be examined for evidence of collapse indicating tamponade.

- Identification of mass lesions:
 - An extremely careful search should be performed from both LPS and RPS approaches. The tip of the right auricular appendage (RAu) should be visualized (Figure 7.141) and the search should extend dorsally until the aorta and main pulmonary artery are no longer seen (Figure 7.142)



7.141 It is extremely important to visualize the tip of the right auricular appendage (RAu) when evaluating patients for neoplastic causes of pericardial effusion. No mass was identified in this dog (compare with Figure 7.149). The auricular wall is thickened and slightly irregular. This is a RPS view of the heart base optimized for the RAu. LPS cranial views are also useful to examine the RAu.



7.142 It is very important to perform a thorough examination in order to identify heart base masses. They often surround the ascending aorta; this is a difficult area to assess due to the surrounding air-filled lung. **(a)** RPS short-axis view of the heart base showing the aorta (Ao) and main pulmonary artery (MPA). The operator should continue to obtain views more dorsally from this location (until imaging is no longer possible) in a search for a heart base mass. This dog had a pericardial effusion (PE) but no mass was identified. **(b)** LPS four-chamber view. It is important to obtain LPS views and optimize imaging for the heart base (in the far field). No mass was identified in this dog.

- A negative examination does not rule out neoplasia
- Haemangiosarcomas are often found in the RAu or RA (see Figure 7.149)
- Mass lesions surrounding the aorta and main pulmonary artery are commonly chemodectomas
- Mesothelioma will not be seen
- Care should be taken not to diagnose intrapericardial thrombi as mass lesions, but it can be impossible to differentiate between them.

Constrictive and effusive–constrictive pericarditis

Constrictive pericarditis is characterized by a thickened, fibrotic and non-distensible pericardial sac. Two forms have been described: *constrictive* (fusion of the visceral and parietal serous pericardial layers) and *effusive–constrictive* (constriction by the visceral pericardium plus a small volume pericardial effusion). The latter is more common in dogs.

The condition can develop secondary to chronic idiopathic effusion, mycotic pericarditis, chronic septic pericarditis, foreign body reactions, traumatic pericardial haemorrhage and intrapericardial neoplasia. The stiff pericardium will limit ventricular diastolic filling abruptly in mid diastole. Animals present in right-sided heart failure with ascites and jugular venous distension.

Radiography

Radiography may or may not be helpful:

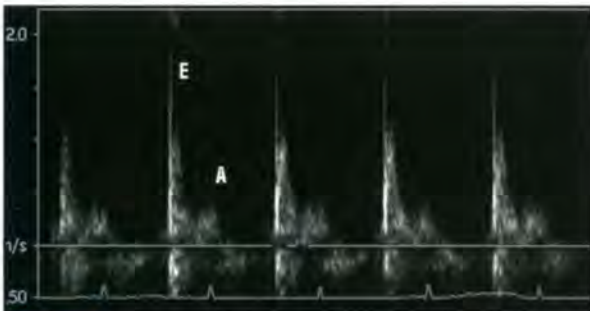
- Cardiac silhouette can be normal or enlarged, depending on the presence and amount of pericardial fluid
- Enlarged CdVC
- Pleural fluid is often seen
- Hepatomegaly and ascites.

Echocardiography

Echocardiographic findings include:

- Cardiac tamponade with only a *small* (millilitres) pericardial effusion
- Diagnosis can be extremely difficult in the absence of a pericardial effusion (constrictive form)
- Occasionally, the pericardium may appear thickened if effusion is present
- Signs of right-sided heart failure (pleural effusion, enlarged CdVC).

Doppler studies: Mitral and tricuspid inflow (E and A waves) may show a restrictive pattern (see Myocardial diseases and Figure 7.143).



7.143 Constrictive pericarditis will lead to a restrictive pattern of ventricular filling. This image shows mitral E and A waves from a cat with constrictive pericarditis, secondary to a foreign body and pyothorax. The E wave is markedly enlarged compared with the A wave.

Peritoneopericardial diaphragmatic hernia

Peritoneopericardial diaphragmatic hernia (PPDH) is the most common congenital pericardial anomaly in

both dogs and cats. This condition is extensively covered in Chapter 14 in the section on diaphragmatic hernias and so will not be discussed here.

Pericardial cysts

Pericardial cysts are rare in dogs and cats. There have been reports of unilocular or multilocular pericardial cyst-like masses in young dogs. These have most often been found to represent organized haematomas. Cysts may also be composed of encapsulated adipose tissue from the omentum or falciform ligament when examined histologically. In many cases the cyst is connected to a fatty pedicle, which enters the diaphragm through a small PPDH. Incarceration of hepatic cysts within the pericardium have been reported in a cat with PPDH.

True endothelium-/epithelium- or mesothelium-lined cysts occur in humans but are extremely rare in the dog and have not been reported in the cat.

Clinical signs of pericardial cysts include abdominal distension, dyspnoea and anorexia. Most cases have concomitant pericardial effusion (see above).

Radiography

Radiographic findings depend on the size and position of the cyst:

- Small cysts are not seen radiographically
- Large cysts can cause bulging of the cardiac silhouette in the location of the cyst
- If the pericardial sac also contains fluid the cardiac silhouette will have a globoid shape
- Other features of PPDH may also be present if this is co-existing.

Contrast studies: Pneumopericardiography has been described. Cysts were seen as mass-like lesions within the pericardial sac. This technique has been superseded by ultrasound examination.

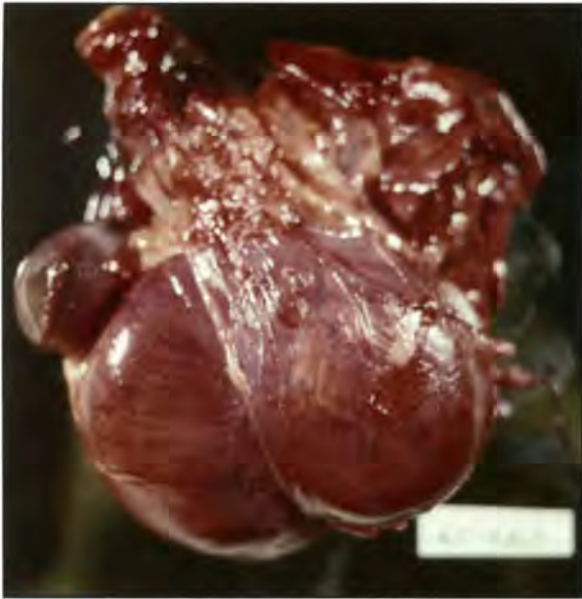
Echocardiography

This is extremely useful in evaluating pericardial content:

- Single or multiple anechoic thin-walled cyst-like structures within the pericardium
- There may be pericardial effusion
- There may be co-existing PPDH.

Pericardial defects

Pericardial defects are rare in dogs. Defects may be as extensive as a congenital absence of the pericardial sac (extremely rare) or may be smaller partial defects in varying locations. The aetiology is unknown; congenital, inflammatory, traumatic and necrotic causes have all been considered. Defects ventral to the level of the phrenic nerve are thought unlikely to be congenital. Parts of the heart may herniate through the defect, including part or all of an atrium or myocardial tissue (Figure 7.144). If myocardial tissue becomes incarcerated then ischaemia, necrosis and shock can develop without specific clinical signs. Pericardial defects are most often incidental postmortem diagnoses.



7.144 Necropsied canine heart with herniation and incarceration of the RV through a large pericardial defect. (Courtesy of J. Buchanan)

Radiography

The defect itself is *not* seen. Radiographic signs depend on the size of the rupture and the presence of herniated parts of the heart.

- A protruding soft tissue opacity mass(es) is seen bulging out from the contour of the RA, the RV or possibly left atrial area (Figure 7.145a).
- A pericardial defect should be considered as a differential for a *mediastinal mass* with a border that effaces with the cardiac silhouette.
- Fluctuations in size may be seen on repeated thoracic radiographs and provide a clue that this is not a typical solid mediastinal mass.

Contrast studies: A non-selective venogram is a fairly simple technique to assist in the diagnosis. This should be performed via the right jugular vein and an immediate lateral radiograph obtained (Figure 7.145b).

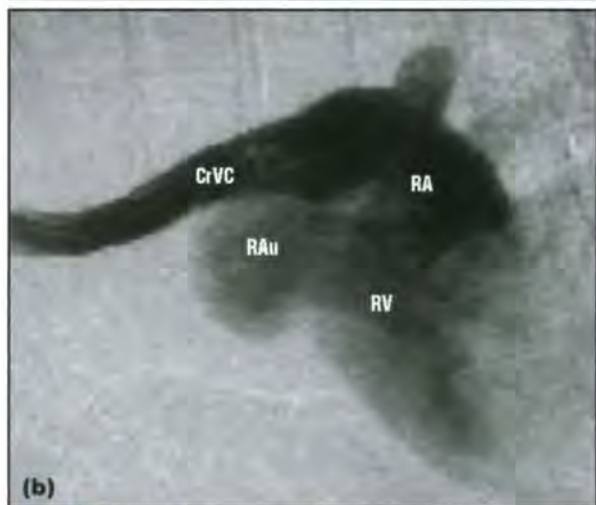
Echocardiography

This may not be very helpful in diagnosis.

- In the case of RAu herniation, there is marked right atrial dilatation but with an inability to define the margins due to lung interference.
- Changes related to the anomaly may not be seen.
- In the case of cardiac apex incarceration in a cardiac defect, left ventricular dilatation and poor myocardial contractility will be seen.

Computed tomography

CT angiography has been used successfully to confirm herniation of cardiac structures (RAu) through the pericardial defect.



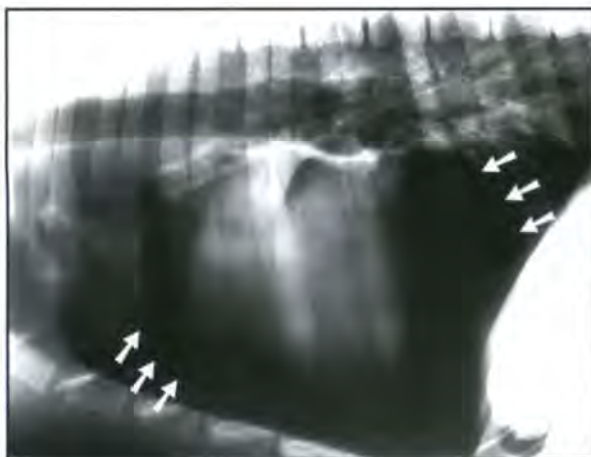
7.145 (a) Lateral thoracic radiograph of a 13-year-old Lhasa Apso with an ovoid mass (★) arising from the cranial cardiac silhouette. This was a herniation of the RAu through a pericardial defect. (b) Jugular venography (digital subtraction fluoroscopy) demonstrates vascular contrast medium in the cranial vena cava (CrVC), entering the right atrium (RA) and the right ventricle (RV) and the herniated right auricular appendage (RAu).

Pneumopericardium

This is a very rare condition that has been diagnosed secondary to trauma and in association with pneumothorax. It can also be seen in combination with bronchial or pulmonary parenchymal tears and pneumomediastinum. Theoretically, an infection with a gas-producing organism may produce a pneumopericardium.

Radiography

Air must be seen surrounding the entire heart and outline the atria and the intrapericardial parts of the aorta and main pulmonary artery in order to diagnose a pneumopericardium (Figure 7.146). Pneumothorax with air surrounding the pericardium may look like pneumopericardium and is much more common. A horizontal beam (decubitus) view centred on the heart may help to differentiate between air in the pericardial sac and pneumothorax.



7.146 Lateral radiograph of a dog with an iatrogenic pneumopericardium (arrowed) after surgery to repair a PPDH. Note that the air is constrained by the pericardial sac and that it outlines the major vessels, i.e. the actual heart is seen.

Computed tomography

CT may be used to confirm the diagnosis, but is probably unnecessary. It may be useful when trying to identify the primary cause.

Cardiac neoplasia

Cardiac neoplasia is rare in the dog and is seen even less in the cat. The types of neoplasia seen vary between the two species (Figure 7.147). The most common type of cardiac neoplasia in dogs is haemangiosarcoma and in cats is lymphoma. Clinical signs vary with the type of tumour, location and presence of a pericardial effusion. Cardiac neoplasia generally has a poor prognosis.

Dogs	
Primary:	<ul style="list-style-type: none"> • Haemangiosarcoma (primary or metastatic) • Chemodectoma • Mesothelioma • Others (undifferentiated sarcoma, myxoma, ectopic thyroid carcinoma, fibroma, fibrosarcoma, rhabdomyosarcoma, chondrosarcoma, osteosarcoma, granular cell tumour)
Metastatic neoplasia	
Cats	
Primary:	<ul style="list-style-type: none"> • Lymphoma most commonly (generally considered systemic) • Mesothelioma (very rare in this species) • Chemodectoma (very rare in this species)
Metastatic neoplasia:	<ul style="list-style-type: none"> • Haemangiosarcoma (generally not involving the RAu) • Metastatic carcinomas (pulmonary, mammary gland, salivary gland) • Oral melanoma and squamous cell carcinoma • Mast cell tumour

7.147 Differences between canine and feline cardiac neoplasia.

Radiographs are insensitive for the detection of cardiac neoplasia. Intrapericardial masses need to reach a substantial size before they produce any radiographic size and shape changes in the cardiac silhouette. Ultrasonography is much more valuable in evaluating the presence of cardiac masses but, as described in the section on pericardial diseases, small masses may be missed, particularly in the absence of pericardial effusion. An extremely careful examination is required from both LPS and RPS windows and in long and short axis. Every attempt should be made to visualize the entire RA and the tip of the auricular appendage. CT is also extremely useful, particularly in the evaluation of heart base masses.

Right atrial or auricular neoplasia

The most common right atrial neoplasm is haemangiosarcoma. This may be primary or metastatic and older German Shepherd Dogs and Golden Retrievers are predisposed. Canine haemangiosarcoma has usually metastasized by the time of diagnosis, and the lungs, spleen and liver in particular should be examined for evidence of metastatic disease. Animals usually present with a haemorrhagic non-clotting pericardial effusion (see Pericardial diseases).

Other right atrial or auricular masses have been reported and include benign lesions such as thrombi.

Radiography

- There are usually radiographic features of pericardial effusion.
- It is unusual to see focal right atrial enlargement.
- The lungs should be evaluated for evidence of metastasis (most commonly these are poorly defined small coalescing nodules (see Figure 12.56, p. 268), less commonly they are well circumscribed nodules or an alveolar infiltrate secondary to haemorrhage).
- Hepatosplenomegaly may be seen: in this case right-sided heart disease or metastatic neoplasia should be considered.

Echocardiography

Echocardiographic findings include:

- Pericardial effusion may be seen
- Mass lesion (Figures 7.148 and 7.149):
 - Can arise from the RAu, the right atrial lateral wall or the junction between the RA and RV
 - Projects into the pericardium or less commonly into the atrium or auricular appendage
 - Haemangiosarcoma lesions usually appear hypoechoic and mottled due to cavitations.

Computed tomography

This is useful to evaluate for the presence of a mass when ultrasonography is not conclusive or a pericardial effusion has been drained. It can also be useful for evaluating metastatic lung disease.



7.148 RPS short-axis echocardiogram at the level of the heart base in a dog with a RAu haemangiosarcoma. The view has been optimized to best show the mass. The lesion is moderately cavitary (arrowed) and is outlined by pericardial effusion. RA = Right atrium. (Courtesy of B. Hopper)



7.149 RPS short-axis echocardiogram in a 9-year-old German Shepherd Dog at the level of the heart base. The view is optimized to show a RAu mass (arrowed). The mass is within the tip of the RAu and is outlined by pericardial effusion. CdVC = Caudal vena cava; RA = Right atrium.

Heart base neoplasia

Heart base masses are usually chemodectomas, but ectopic thyroid and parathyroid tumours may be found less commonly in this location. Chemodectomas (also known as non-chromaffin paragangliomas, members of the APUDoma (amine precursor uptake and decarboxylation) group of neoplasms) are tumours of the aortic bodies. These are congregations of neuroendocrine cells responsible for detecting blood pressure changes. Brachycephalic breeds are predisposed to chemodectomas and this is thought to have an association with chronic hypoxia.

Occasionally, chemodectomas are seen in other locations, such as the cranial mediastinum. In the heart, they wrap around the aortic root and main

pulmonary artery. They are locally invasive and expansile. Metastasis is seen in dogs and cats but is not common (occurs in approximately 10–20% dogs) and is slow to occur. Metastatic sites include the lung, LA, pericardium, liver and kidney.

Radiography

Radiographic findings include:

- There is often minimal or no change in the appearance of the cardiac silhouette
- Mass border effacing or silhouetting with cranial aspect of the cardiac silhouette
- Focal elevation of the terminal (caudal) part of the trachea on the lateral view (Figure 7.150)
- Focal deviation of the terminal trachea on the DV/VD view in association with a soft tissue mass
- There may be radiographic features of pericardial effusion.



7.150 (a) Right lateral and (b) DV views of an 11-year-old mixed breed dog with a heart base tumour. Note the focal cranial and right-sided deviation of the trachea at the heart base and cranial to the carina (arrowed). (continues)



7.150 (continued) **(c)** RPS short-axis echocardiogram. There is a hypoechoic mass (M) lesion surrounding the ascending aorta (A). This was a heart base mass, most likely to be a chemodectoma, but no confirmation was obtained.

Echocardiography

Echocardiographic findings include:

- Pericardial effusion may be seen
- Mass lesion (Figure 7.150c):
 - Extends around ascending aorta, though may be invasive and involve other areas of the heart
 - Usually homogenous and moderately echoic.

Computed tomography

A contrast-enhancing mass is seen around the ascending aorta (Figure 7.151). The mass is usually well defined and easily visualized using this imaging modality.

Other cardiac neoplasia

Mesothelioma

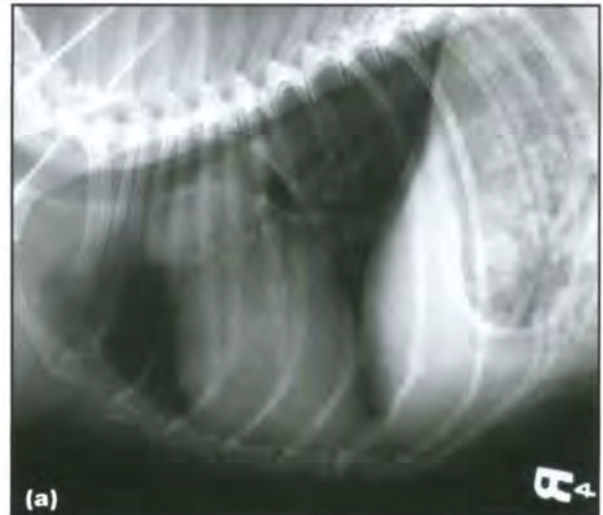
Imaging techniques will identify a pericardial effusion (significant amounts of fluid within 120 days of pericardectomy increases suspicion of mesothelioma). Mesothelioma is likely to be underdiagnosed as it is a difficult diagnosis to establish antemortem. It is a diffuse neoplasm so there is no specific mass lesion identified on imaging (see also Pericardial effusions, above).

Myxoma

This is a rare benign neoplasm which has been reported in the dog and cat. It is usually gelatinous in nature but ossifying myxomas may also occur. Myxomas are often right-sided but they have also been reported on the left (Figure 7.152). A right atrial malignant *myxosarcoma* has also been reported.

Lymphoma

This is the most common cardiac neoplasm in cats, and it is also seen in dogs. Unlike other cardiac neoplasms, examination of the pericardial effusion (if present) usually provides the diagnosis. It can be confused with myocardial disease (see Myocardial diseases and Figure 7.125).



7.151 **(a)** Right lateral radiograph and **(b)** transverse CT (post-contrast) image at the level of the mid-heart from a 10-year-old male neutered Cavalier King Charles Spaniel with a heart base mass. The CT image shows a heterogeneously enhancing mass (M) wrapping around the aorta (A) and main pulmonary artery (MPA). **(c)** The dorsal reconstruction was of further use in defining the margins of the mass (M).



7.152 LPS four-chamber view of a dog with a left atrial myxoma. A homogenous echogenic mass is seen within the LA and part of the LAu (arrowed). LV = Left ventricle; RA = Right atrium; RV = Right ventricle.

Lymphoma appears as myocardial thickening, with or without hypoechoic mottled areas. This appearance is also seen in other myocardial infiltrative diseases (e.g. haemangiosarcoma).

Acquired vascular diseases

Dirofilariasis

Heartworm disease, caused by the nematode *Dirofilaria immitis*, affects both dogs and cats in endemic regions. The parasite has a worldwide distribution, primarily in tropical and subtropical regions but with an increasing prevalence in temperate regions, particularly where there is a high urban (and pet) density and appropriate mosquito vectors. The life cycle of the parasite is similar in dogs and cats, but the parasite takes longer to reach patency in cats. Cats are also inherently more resistant to infection.

Adult heartworms live in the pulmonary arteries and in severe infections may also be present in the RV. Microfilariae produced by the adult female heartworm are released into the circulation. These are then ingested by feeding female mosquitos in which they undergo several moults to form an infective stage transmitted by the mosquito into another canine or feline host. About 3 months later the parasite reaches an immature adult stage and enters the vascular system. It then migrates to the heart and lungs where it matures into the adult worm. The pulmonary arterial response to heartworms in the cat is more severe than that in the dog, and in general the clinical manifestations of the disease tend to be more severe in this species.

The manifestations of heartworm disease depend on the number of worms, the chronicity of infection and on interactions between the parasite and host. Most dogs with heartworm infection are asymptomatic. Presenting signs in symptomatic dogs may include lethargy, coughing, poor condition, ascites and syncope. More serious consequences of heartworm disease, such as parasitic eosinophilic pneumonitis, may occur. Rare complications include eosinophilic granulomatosis, thromboembolic disease, pulmonary hypertension, glomerulonephritis, caval syndrome and disseminated intravascular coagulation (DIC).

Clinical signs in cats are often chronic and non-specific. These include anorexia, weight loss, vomiting, dyspnoea and coughing.

More acute signs are usually due to aberrant worm migration (more common in cats than dogs) or worm embolization, and include shock, salivation, haemoptysis, neurological signs, vomiting, syncope and even death.

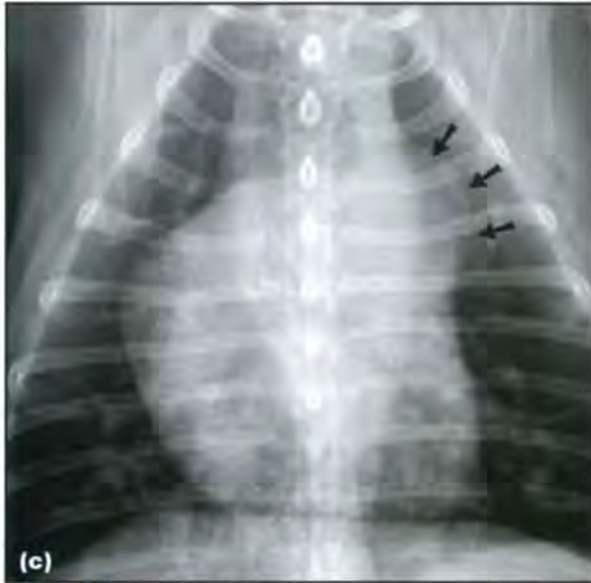
Radiography

Radiographic findings include:

- Dogs (Figure 7.153). Changes primarily reflect the pulmonary hypertension that results from physical obstruction to outflow by adult worms living in the RV and pulmonary outflow tract, as well as changes to the walls of the pulmonary arteries:
 - Enlargement of the right side of the heart ('reverse D' appearance on VD/DV view)
 - Enlargement of the main pulmonary artery segment



7.153 (a) Lateral and (b) VD thoracic radiographs of a 12-year-old male Golden Retriever with heartworm disease. The pulmonary arteries are extremely enlarged and tortuous (arrowed). The cardiac silhouette is rounded and right-sided cardiomegaly is present. Incidental tiny metallic opacities represent lead shot from a previous injury. (continues)



7.153 (continued) **(c)** DV thoracic radiograph of a 4-year-old Staffordshire Bull Terrier with heartworm disease. This radiograph was acquired 3 months after treatment for caval syndrome and heartworm disease but severe right-sided cardiac enlargement and main pulmonary artery enlargement (arrowed) are still evident.

- Enlargement and tortuosity of the (particularly caudal) lobar pulmonary arteries
- Right heart failure may be evident in advanced disease
- There may be diffuse bronchointerstitial pulmonary pattern due to eosinophilic infiltrates associated with an allergic response
- Patchy dense interstitial to alveolar infiltrates may be seen, associated with pulmonary thromboembolism.
- Cats (Figure 7.154):
 - Most commonly *enlargement* of the caudal lobar pulmonary arteries (>1.6 times the ninth rib on the VD view)
 - Tortuosity of these vessels and enlargement of the right side of the heart is much less common than in dogs
 - Bronchointerstitial or even alveolar pulmonary infiltrates and pulmonary hyperinflation, mimicking feline bronchial disease have also been reported
 - Changes may also be seen in cats that ultimately resist heartworm infection and are eventually negative for the disease.

Contrast studies: Angiography is rarely necessary, but may demonstrate the cardiac chamber and pulmonary vascular changes typical of heartworm disease, and differentiate it from other cardiovascular diseases (Figure 7.155).

- Adult worms may be seen as linear filling defects within the contrast medium-filled peripheral pulmonary arteries.
- Changes that may be better demonstrated with contrast studies include main pulmonary artery segment dilatation (not usually demonstrated on survey films of cats due to the medial location



7.154 VD view of a 7-year-old Domestic Medium-hair cat with heartworm disease, showing moderate to severe enlargement and lack of tapering of the caudal lobar pulmonary arteries (arrowed).



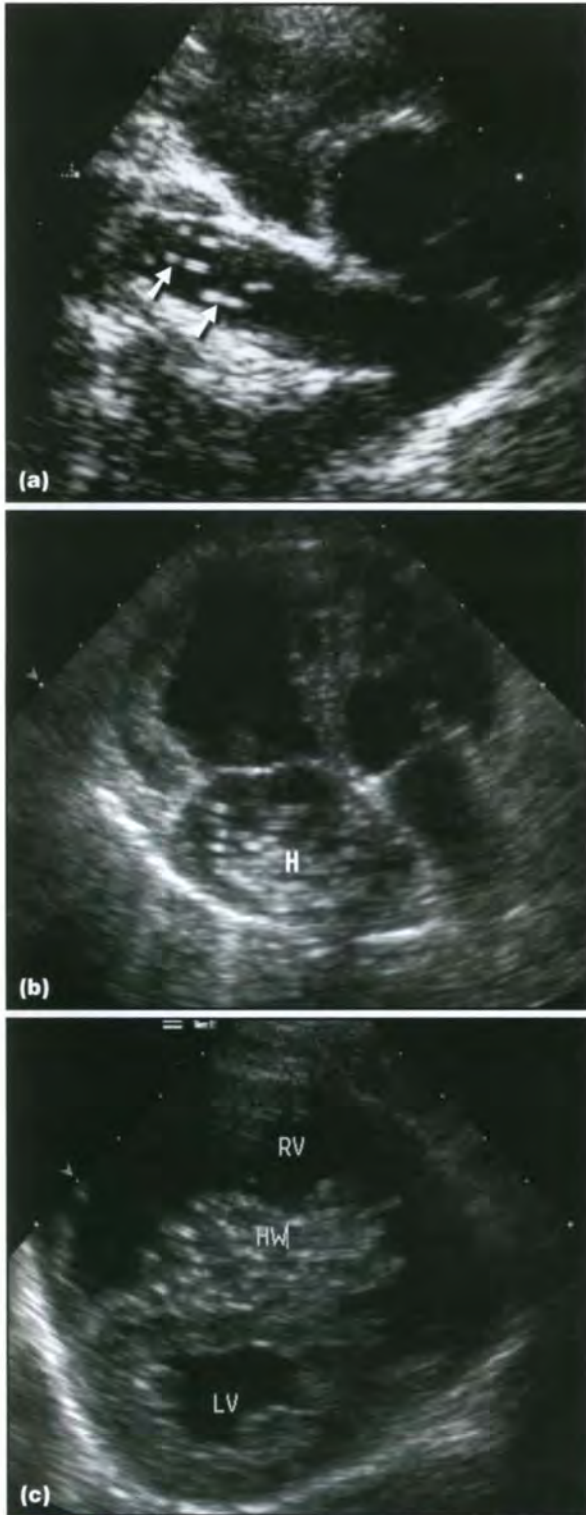
7.155 Selective angiogram in a dog with chronic heartworm disease. Several catheters are present but the angiogram has been performed via a catheter in the main pulmonary artery. The contrast medium fills a markedly dilated main pulmonary artery and its branches. The caudal lobar pulmonary arteries are also tortuous and truncated.

of the vessel) as well as pulmonary arterial enlargement (hilar region), tortuosity and loss of the normal tapering toward the periphery.

Echocardiography

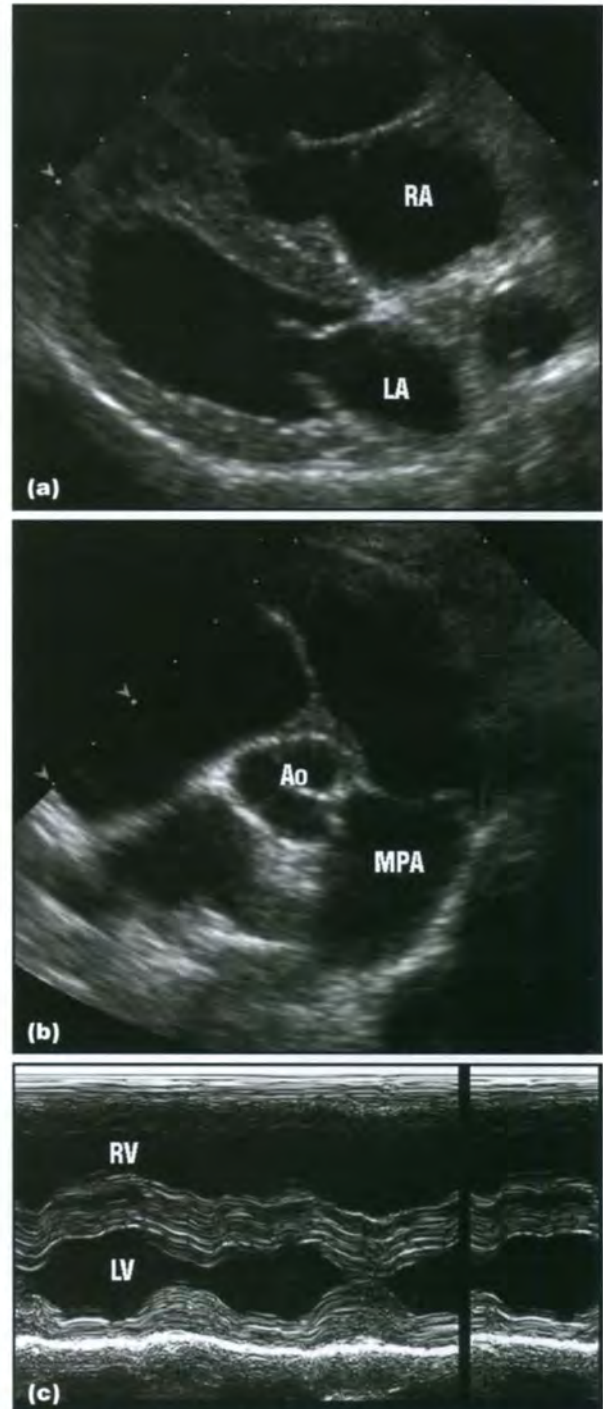
Ultrasonography can be a useful adjunctive test in dogs, and can provide definitive evidence of infection in cats when other tests are equivocal.

- Adult worms in dogs are usually present in the pulmonary arteries and, thus, may not be seen on ultrasound examination.
- However, they may be found in the main pulmonary artery, the proximal right and left caudal lobar arteries (Figure 7.156a), and occasionally the RA, RV or across the tricuspid valve (Figure 7.156bc). The latter has particularly been described in dogs with caval syndrome.
- On 2D echocardiography adult worms appear as strongly echogenic short parallel lines.



7.156 (a) RPS short-axis ultrasound image of the heart base and pulmonary arteries of a 7-year-old male neutered mixed breed dog. Several adult worms are identified in the right pulmonary artery (arrowed). (b) LPS long-axis four-chamber echocardiogram of a 4-year-old Staffordshire Bull Terrier with caval syndrome due to heartworm disease. A large mass of adult heartworms (H) is present in an enlarged RA. They are identified as parallel echogenic lines. (c) RPS short-axis echocardiogram obtained at the level of the papillary muscles in the same dog as (b). During diastole the worms were seen to move through the tricuspid valve and into the enlarged RV. HW = Heartworm mass; LV = Left ventricle; RV = Right ventricle.

Supportive echocardiographic findings of the diagnosis in the absence of visible adult worms include (Figure 7.157):



7.157 (a) RPS long-axis echocardiogram of the same dog as in Figure 7.156b after heartworm removal. Note the enlarged right atrium (RA) and compare its size to that of the left atrium (LA). (b) RPS short-axis echocardiogram obtained at the heart base and optimized for the main pulmonary artery (MPA). The main pulmonary artery is enlarged both before and after the pulmonic valve. Usually, the main pulmonary artery is close to the diameter of the aorta (Ao) at this level. (c) M-mode echocardiogram obtained at the level of the papillary muscles from a RPS location. The right ventricle (RV) is markedly dilated. The left ventricle (LV) is also marked for comparison.

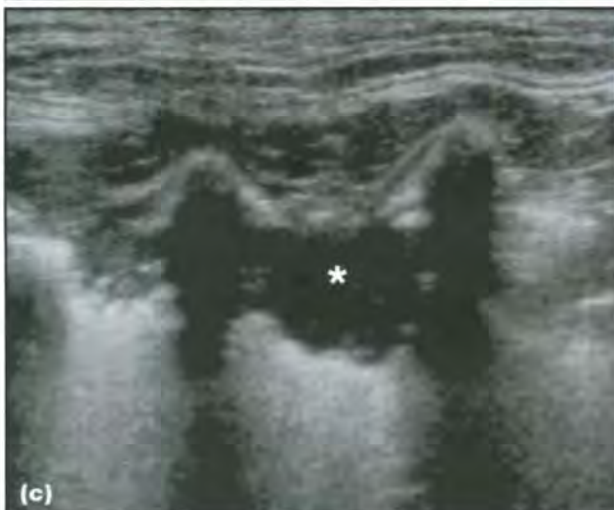
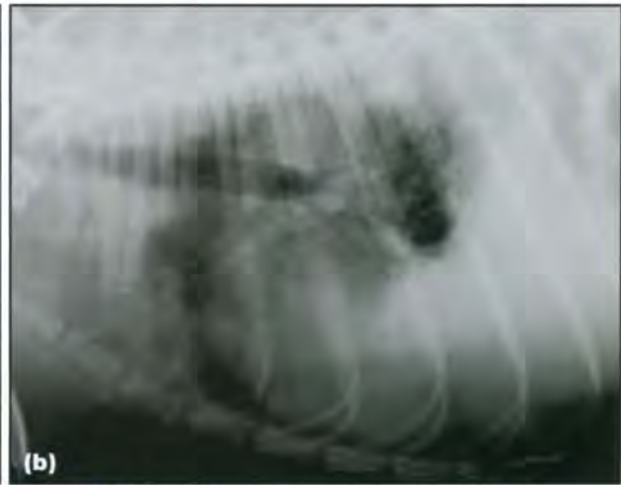
- Right ventricular eccentric hypertrophy
- Right atrial and main pulmonary artery dilatation
- Septal flattening and paradoxical motion
- Tricuspid regurgitation can be identified in dogs with advanced pulmonary hypertension or if adult worms are present across the valves.

Angiostrongylosis

Angiostrongylus vasorum is a metastrongylid nematode that infects domestic dogs. *A. vasorum* has a worldwide distribution and within Europe is endemic in southern England, France, Ireland and Denmark. Foxes are presumed to act as a wildlife reservoir for the parasite. The adult worm is oviparous and lives in the right side of the heart or the pulmonary arteries, from where the eggs are carried to the pulmonary capillaries. The eggs hatch and first-stage (L1) larvae migrate through the alveolar epithelium, are coughed up, swallowed and passed in the faeces. The life cycle is indirect and larvae undergo subsequent moults within a molluscan intermediate host, to become third-stage (L3) larvae. When a dog ingests an intermediate host, infective L3 larvae are liberated into the dog's small intestine. The L3 larvae undergo two further moults in the mesenteric lymph nodes and the L5 larvae migrate via the liver to the right side of the heart, completing the life cycle.

The most common clinical signs associated with angiostrongylosis are coughing and dyspnoea caused by the inflammatory response to the eggs and migrating larvae at the level of the alveolar membrane. The second common manifestation of angiostrongylosis is a coagulopathy. Subcutaneous, mucosal and internal haemorrhages may all be seen. Neurological signs associated with cerebral haemorrhage may also occur. Bleeding may occur with or without concurrent respiratory disease and the pathogenesis of the coagulopathy is undetermined. A minority of dogs suffer collapse episodes or sudden death, possibly due to aberrant larval migration into the myocardium. The majority of affected dogs are young and Cavalier King Charles Spaniels appear particularly predisposed to clinical disease.

Angiostrongylosis should be suspected in any young dog presenting with compatible clinical signs and a typical radiographic pattern (see below). The diagnosis is confirmed by demonstrating the presence of L1 larvae in the faeces or airway cytology samples. Other diagnostic findings are variable. Eosinophilic inflammation in airway cytology samples is less common than might be expected. The results of coagulation function testing are inconsistent and in some cases may be normal.



7.158 (a) Right lateral thoracic radiograph of a 6-year-old spayed Golden Retriever bitch with angiostrongylosis, showing a patchy, peripheral alveolar pattern. A pleural fissure line can also be seen. (b) Right lateral thoracic radiograph of a 5-year-old Cocker Spaniel with angiostrongylosis. The peripheral alveolar pattern is more severe in this case. (c) Thoracic ultrasound image from the same dog as in (b) obtained with a linear transducer via an intercostal approach. A peripheral hypoechoic consolidated region of lung (*) is identified. Ultrasound-guided aspiration of this region confirmed the diagnosis of angiostrongylosis.

Radiography

Significant thoracic radiographic abnormalities are present in almost all clinically affected dogs (Figure 7.158):

- Most common findings are alveolar infiltrate and bronchial thickening (seen in approximately 80% and 70% of dogs, respectively). Typically, the alveolar infiltrate has a multifocal or peripheral distribution. Less commonly a mild, generalized interstitial pattern may be seen
- Note that the same thoracic radiographic changes are also seen in most dogs with *A. vasorum*-associated coagulopathy, even in the absence of clinical signs of respiratory disease
- Less common findings include a small volume pleural effusion and right ventricular enlargement
- Although *A. vasorum* is a pulmonary vascular parasite, significant radiographic changes affecting the pulmonary arteries are not usually seen
- Radiographic improvement may lag behind clinical resolution
- Residual alveolar infiltrate may still be present 1 month after successful treatment and an interstitial pattern may persist for up to 3 months.

Ultrasonography

The ultrasonographic findings with *A. vasorum* have not been specifically described:

- Evidence of right-sided cardiac enlargement and pulmonary hypertension may be seen
- *A. vasorum* larvae may be identified in ultrasound-guided fine needle aspirates of the lung (Figure 7.158c)
- In one case report, reversible pulmonary hypertension was reported in a dog with a right-to-left shunting ASD and angiostrongylosis. Pulmonary hypertension and shunt direction reversed after treatment.

Idiopathic pulmonary hypertension

Idiopathic pulmonary hypertension is a syndrome characterized by increased pulmonary arterial pressure due to hypertrophy of the tunica muscularis and tunica intima with no primary or discernible cause. The condition may be suspected in patients presenting with respiratory and right-sided heart disease in which no underlying cardiac or pulmonary disease can be demonstrated. In advanced disease, cor pulmonale and signs of right-sided heart failure (hepatomegaly, ascites, jugular pulse) may result due to prolonged pressure overload.

Radiography

Radiographic findings include:

- Features common to pulmonary hypertensive patterns and include enlargement of the right heart and main pulmonary artery segment, and enlarged lobar pulmonary arteries in the hilar region that taper rapidly toward the periphery

- The peripheral lung parenchyma may appear hyperlucent due to poor perfusion
- Features such as variable diameter and saccular dilatations of the peripheral vasculature and pulmonary parenchymal infiltrates associated with hypertension due to other causes (chronic heartworm disease, pulmonary thromboembolism) are absent with idiopathic disease.

Echocardiography

Ultrasonographic findings include:

- Doppler ultrasound studies can be used to document increased velocity of right-sided regurgitant fractions. In the absence of pulmonic stenosis, pulmonic insufficiency velocity ≥ 2.2 m/s and/or tricuspid regurgitant velocity ≥ 2.8 m/s is reported to be indicative of pulmonary hypertension
- Additional echocardiographic findings include eccentric right ventricular hypertrophy, paradoxical septal motion and main pulmonary artery enlargement.

Pulmonary thromboembolism

Pulmonary thromboembolism (PTE) results in interruption of the blood supply to a portion of the lung due to obstruction of a pulmonary artery(ies) by embolic material (blood clots, parasites, tumour fragments, bacterial aggregates, bone marrow fat, etc.) delivered by the blood stream. Primary thrombosis (formation *in situ*) may result from local stasis, turbulent blood flow or vascular injury. Hypercoagulable states, such as those that exist with glomerulonephritis, Cushing's disease, pancreatitis or DIC, also predispose to thrombus formation in both the pulmonary and systemic circulation.

The consequences of PTE depend on the magnitude of the obstruction and the pre-existing condition; they may range from insignificant to severe ventilation-perfusion mismatching, development of pulmonary hypertension and right heart failure.

Radiography

Most commonly there are no survey radiographic abnormalities.

- Enlargement of the hilar portion of the pulmonary arteries may be identified; there may be abrupt reduction in size or termination.
- Poor perfusion to part or all of a lung lobe may result in a hyperlucent appearance in the absence of hyperinflation.
- There may be atelectasis of a lung lobe, resulting in a mediastinal shift and displacement of the diaphragm.
- Focal pleural effusion may be seen around the affected lobe.
- Occasionally, there are peripheral triangular areas of consolidated lung extending to the pleural margin, particularly in the caudal lung lobes.

Contrast studies: Pulmonary angiography may delineate abrupt termination or filling defects in large pulmonary arterial segments, or areas of decreased

or absent perfusion. Interpretation may be difficult in lungs with abnormal findings on plain films; abnormal perfusion to areas of lung that appear radiographically normal is much less equivocal.

Computed tomography

Helical CT angiography is a standard examination for suspected thromboembolism in humans. In dogs it is a useful and efficient technique to detect arterial thrombi in first- and second-order pulmonary arteries. Thrombi in subsegmental vessels may be too small to image reliably. An automatic power injector is required for a post-contrast scan. Multislice CT gives superior results.

Technique:

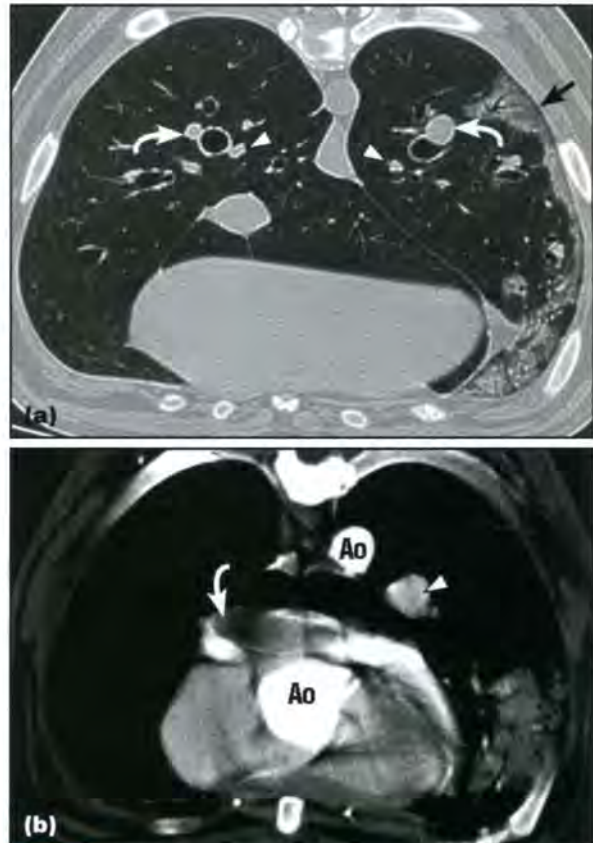
- Respiratory control is essential (see Chapter 3) as patients with PTE are often hyperpnoeic. If panting cannot be stopped for about 30 seconds, do not proceed with scanning. Image blur will render the examination non-diagnostic otherwise.
- Pre-contrast CT scan: thin-slice high-resolution axial lung CT scan with 5 mm slice gap.
- Post-contrast imaging:
 - A large volume of low concentration non-ionic contrast medium should be used to extend the arterial phase (e.g. 4 ml/kg of 200 mg iodine/ml contrast medium)
 - Fast rate (e.g. 4 ml/second) injection via cephalic venous catheter
 - Scanning should be started approximately 5 seconds after the start of the injection
 - Time scan length according to duration of injection to ensure arterial filling
 - Helical scan settings with 2 or 3 mm slice width and interval, mediastinal window, soft tissue algorithm.
- Depending on the speed of the CT scanner, it is sometimes necessary to perform two arterial phase scans; one from the hilus scanning cranially and one from the hilus scanning caudally. The bolus can be divided or an additional contrast medium dose can be given, if safe to do so.

Computed tomography findings:

- Pre-contrast lung CT (Figure 7.159a):
 - Abnormally large (thrombosed) and/or small (hypovolaemic) pulmonary arteries, small pulmonary veins
 - Wedge-shaped peripheral consolidated lung tissue due to infarction.
- Post-contrast CT angiography (Figure 7.159b)
 - Arterial filling defects
 - Note that subsegmental embolism cannot be ruled out in case of normal CT scan.

Magnetic resonance imaging

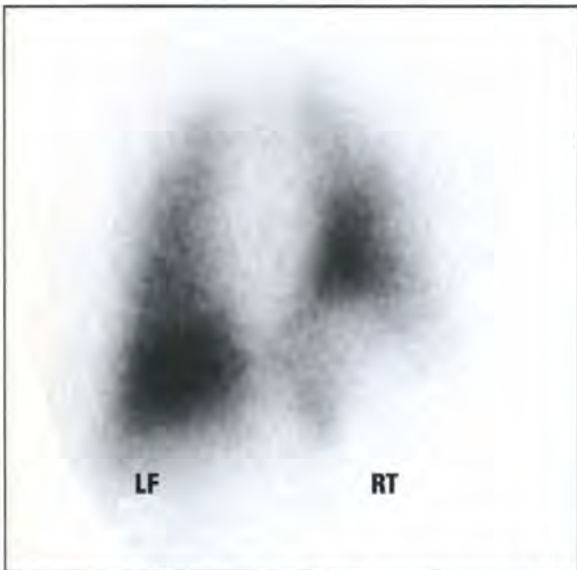
Contrast-enhanced magnetic resonance angiography (MRA) is a minimally invasive development in human medicine for evaluation of the pulmonary vascular system.



7.159 (a) Pre-contrast high-resolution CT image of the lung of a 9-year-old Rottweiler with PTE at the level of the accessory lung lobe. Note the wedge-shaped peripheral pulmonary consolidation (straight black arrow) and distended lobar artery (anti-clockwise white bent arrow) of the left caudal lung lobe, the diminished size of the right caudal lung lobe lobar artery (clockwise bent arrow), and both left and right caudal lung lobe lobar veins (arrowheads). Left of dog is right side of image. (b) Post-contrast CT angiography image at the level of the main pulmonary artery. Notice the large contrast medium filling defect in the main pulmonary artery (bent arrow) and left pulmonary artery (arrowhead). This large thrombus extended caudally, distending the diameter of the main pulmonary artery and resulting in peripheral oligoemia. Ao = Aorta (seen as two circles as both the aortic arch and descending aorta are seen in cross section at this level)

Scintigraphy

- The classic appearance of PTE is photopenic, wedge-shaped, pleural based defects with a lobar or subsegmental distribution (Figure 7.160).
- Sometimes there is lack of distribution in an entire lobe, indicative of the occlusion of a major lobar artery (Figure 7.161).
- Multiple small emboli, resulting in a mottled perfusion pattern, are common in dogs with heartworm disease.
- Normal or hyperlucent corresponding radiographs confirm a diagnosis of high probability of PTE.
- A corresponding normal ventilation scan confirms the diagnosis of PTE but this is very rarely obtained in small animals.



7.160 Dorsal static image of the lungs in a middle-aged, mixed breed dog with Cushing's disease presented for evaluation of possible PTE. The image was obtained 10 minutes after intravenous injection of ^{99m}Tc -MAA. Thoracic radiographs obtained immediately prior to scintigraphy were unremarkable. Note the large wedge-shaped photopenic area, which occupies the majority of the right caudal lung lobe, consistent with a large lobar pulmonary embolus.



7.161 Ventral (left of image) and dorsal (right of image) static images of the lungs obtained 5 minutes after intravenous injection of ^{99m}Tc -MAA in a 4-year-old Beagle with heartworm disease. Thoracic radiographs obtained immediately prior to scintigraphy showed no focal pulmonary parenchymal abnormalities. Notice the complete lack of blood flow to the right cranial, caudal and accessory lobes, with minimal perfusion to the right middle lobe (arrowed). There is also a pleural based, wedge-shaped defect along the diaphragmatic border of the left caudal lobe, best seen in the ventral view.

Budd–Chiari-like syndrome

In animals, this term describes post-sinusoidal hypertension and the development of a high-protein peritoneal effusion due to the obstruction of hepatic venous return to the heart. The obstruction may involve the:

- Junction of the hepatic veins with the CdVC
- CdVC itself between the entry of the hepatic veins and the heart
- RA.

Causes include thrombosis, caval syndrome associated with heartworm disease, compression or invasion of the cava by tumours or other masses,

trauma-induced stricture, fibrosis, diaphragmatic hernia and congenital cardiac (e.g. CTD) or caval (e.g. membranous obstruction) anomalies.

Radiography

Other than ascites, radiographic features are not specific. Absence (congenital) of the CdVC, masses, hernias or other abnormalities in the region of the caudal mediastinum, diaphragm or liver may be seen.

Contrast studies: A caudal vena cavagram (lateral saphenous injection) may demonstrate invasion, compression or obstruction of the CdVC.

Ultrasonography

Abdominal ultrasonography may identify abnormalities of the liver or the abdominal portion of the CdVC. Doppler interrogation may identify abnormal or retrograde flow. Colour Doppler evaluation of the hepatic veins and CdVC provides the most information regarding the presence and direction of blood flow within the hepatic veins and CdVC.

Computed tomography

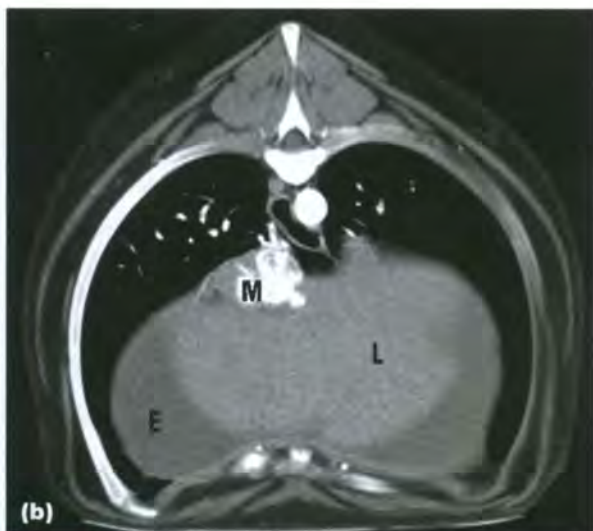
CT may demonstrate structural abnormalities or masses (Figure 7.162). CT angiography may be necessary to demonstrate vascular abnormalities.

Cranial vena cava syndrome

CrVC syndrome results from obstruction of the CrVC with resulting impairment of the venous return from the cranial parts of the body to the heart. Reported causes include great vessel invasion/compression (tumour, e.g. thymoma), granuloma (e.g. blastomycosis) and thromboembolism. Predisposing factors include conditions that contribute to a hypercoagulable state (immune-mediated disease, sepsis, glomerulonephritis, cardiac disease, neoplasia, corticosteroid administration, central venous catheters with these pre-existing conditions).



7.162 (a) Post-contrast transverse CT scan (soft tissue algorithm and window) of a 6-year-old male neutered Labrador Retriever with a Budd–Chiari-like syndrome due to a CdVC mass. The image was obtained caudal to the heart. The mass (M) is seen as a large soft tissue attenuating structure with a small amount of contrast medium within the CdVC ventral to it. There is also atelectasis of the ventral tip of the right caudal lung lobe. (continues)



7.162 (continued) **(b)** A more caudal image from the same CT series. The caudal part of the mass (M) has large regions of mineralization (these were also hyperdense pre-contrast administration). The peritoneal effusion (E) is evident on this image, surrounding the liver lobes (L).

The clinical signs include symmetrical, simultaneous swelling of the head, neck and forelimbs.

Radiography

Radiographs may be normal or may demonstrate the cause of the obstruction (e.g. cranial mediastinal mass).

Contrast studies: Angiography may demonstrate intraluminal filling defects, extraluminal compressive masses or other causes of CrVC obstruction. Non-selective angiography via the jugular vein is preferred but may be difficult in the face of swelling of the soft tissues of the neck; cephalic vein administration of contrast medium should also provide excellent opacification (Figure 7.163).



7.163 Lateral view of an 11-year-old spayed Labrador Retriever bitch with recurrence of severe oedema of the head, neck and forelimbs 1 week after removal of a thymoma. Non-selective angiography via the cephalic vein demonstrated a large intraluminal filling defect (arrowed) consistent with a thrombus in the CrVC at the level of the costocervical vein. A repeat angiogram 2 weeks later showed the thrombus to be approximately half the size. (Courtesy of D. Davies)

Ultrasonography

In the presence of radiographic abnormalities of the cranial mediastinum, ultrasonography may provide additional information with regard to masses or other abnormalities. If thoracic radiographs are normal, ultrasonography is unlikely to provide additional information and angiography is recommended.

Computed tomography

CT angiography may provide an alternative means of evaluating the CrVC for filling defects or compressive lesions.

Coronary artery diseases

The right and left coronary arteries arise from the aortic bulb immediately distal to the aortic valve and supply the muscle of the heart (Figure 7.164). Coronary artery disease is extremely important in humans but rare in dogs and cats. A brief discussion of coronary disease in the dog and cat is given here.



7.164 A selective coronary angiogram with the contrast medium injection made just beyond the level of the aortic valve in a normal dog. This dog has the normal arrangement of left and right coronary arteries. (Courtesy of J. Buchanan)

Congenital anomalies

There is variation in the anatomical pattern of the right and left coronary arteries. Five types of coronary arterial patterns have been identified in the dog (see Figure 7.55). Anomalous origin of the left coronary artery can lead to subvalvular pulmonic stenosis in English Bulldogs and Boxers. For surgical or interventional radiological correction of subvalvular pulmonic stenosis, exact knowledge of the anatomical pattern is required.

Angiography: Selective coronary angiography is required to identify the coronary artery pattern (Figure 7.165).



7.165 A selective coronary angiogram in a 5-month-old Bulldog bitch puppy. A single right coronary artery is present and resulted in pulmonic stenosis. (Courtesy of J. Buchanan)

Coronary arterial and ischaemic heart disease

Ischaemic heart disease is rare in dogs and cats. Myocardial infarction can occur secondary to atherosclerosis or other forms of *arteriosclerosis* in both the dog and cat. *Arteriosclerosis* is arterial wall hardening, loss of elasticity and thickening, leading to luminal narrowing. Specific forms of arteriosclerosis include:

- Lipid deposition and thickening of the intimal cell layers within arteries (*atherosclerosis*)
- Calcification of the tunica media of muscular arteries
- Thickening of the walls of small arteries or arterioles due to cell proliferation or hyaline deposition (*arteriolosclerosis*).

Atherosclerosis has been strongly associated with diabetes mellitus and hypothyroidism (but not with hyperadrenocorticism). Mineralization of the walls of the coronary arteries may occur in chronic cases of arteriosclerosis. The gradual occlusion of the coronary arteries leads to myocardial ischaemia, myocardial infarction and fibrosis. The outcome may be sudden death, acute or chronic heart failure.

Ischaemic heart disease has been postulated as a cause of sudden death during anaesthesia or sedation. Myocardial infarction (generally left ventricular free wall) has also been reported secondary to HCM in the cat. Ischaemic heart disease can also rarely occur as a result of incarceration of the LV in a pericardial defect (congenital) or tear (traumatic) with strangulation of one or both coronary arteries (see Figure 7.144).

Imaging findings: Survey radiographs may reveal coronary artery mineralization in dogs (Figure 7.166). It can be difficult radiographically to distinguish coronary mineralization from aortic mineralization without the use of angiography. Coronary angiography is the diagnostic technique of choice, but is seldom used in animals.



7.166 Postmortem radiograph from a dog with mineralized coronary arteries due to atherosclerosis. The dog also had hypothyroidism, which has been strongly linked with this condition.

With echocardiography, ischaemic myocardium can show thinning, regional hypokinesis or akinesis and reduced or absent contractility.

References and further reading

- Allema AR (2003) Abdominal, thoracic, and pericardial effusions. *Veterinary Clinics of North America: Small Animal Practice* **33**, 89–118
- Basso C, Fox PR, Meurs KM *et al.* (2004) Arrhythmogenic right ventricular cardiomyopathy causing sudden cardiac death in boxer dogs: a new animal model of human disease. *Circulation* **109**, 1180–1185
- Baty CJ (2004) Feline hypertrophic cardiomyopathy: an update. *Veterinary Clinics of North America: Small Animal Practice* **34**, 1227–1234
- Beardow AW and Buchanan JW (1993) Chronic mitral valve disease in cavalier King Charles spaniels: 95 cases (1987–1991). *Journal of American Veterinary Medical Association* **7**, 1023–1029
- Berg RJ, Wingfield WE and Hoopes PJ (1984) Idiopathic hemorrhagic pericardial effusion in eight dogs. *Journal of American Veterinary Medical Association* **185**, 988–992
- Boag AK, Lamb CR, Chapman PS and Boswood A (2004) Radiographic findings in 16 dogs infected with *Angiostrongylus vasorum*. *Veterinary Record* **154**, 426–430
- Bright JM, Herrtage ME and Schneider JF (1999) Pulsed Doppler assessment of left ventricular diastolic function in normal and cardiomyopathic cats. *Journal of the American Animal Hospital Association* **35**, 285–291
- Bright JM and Mears E (1997) Chronic heart disease and its management. *Veterinary Clinics of North America: Small Animal Practice* **6**, 1305–1329 Erratum in *Veterinary Clinics of North America: Small Animal Practice* (1998) **1** x–xi
- Bright JM, Toal RL and Blackford LA (1990) Right ventricular outflow

- obstruction caused by primary cardiac neoplasia. Clinical features in two dogs. *Journal of Veterinary Internal Medicine* **4**, 12–16
- Buchanan JW (1990) Pulmonic stenosis caused by single coronary artery in dogs: four cases (1965–1984). *Journal of the American Veterinary Medical Association* **196**, 115–120
- Buchanan JW (1999) Prevalence of cardiovascular disorders. In: *Textbook of Canine and Feline Cardiology: Principles and Clinical Practice, 2nd edn*, ed. PR Fox, D Sisson and NS Moise, pp. 457–470. WB Saunders, Philadelphia
- Buchanan JW and Bücheler J (1995) Vertebral scale system to measure canine heart size in radiographs. *Journal of American Veterinary Medical Association* **206**(2), 194–199
- Chapman PS, Boag AK, Guitian J and Boswood A (2004) *Angiostrongylus vasorum* infection in 23 dogs (1999–2002). *Journal of Small Animal Practice* **45**, 435–440
- Chetboul V, Carlos C, Blot S *et al.* (2004) Tissue Doppler assessment of diastolic and systolic alterations of radial and longitudinal left ventricular motions in Golden Retrievers during the preclinical phase of cardiomyopathy associated with muscular dystrophy. *American Journal of Veterinary Research* **65**, 1335–1341
- Connolly DJ and Boswood A (2003) Dynamic obstruction of the left ventricular outflow tract in four young dogs. *Journal of Small Animal Practice* **44**, 319–325
- Dennis R, Kirberger RM, Wrigley RH and Barr F (2001) *Handbook of Small Animal Radiological Differential Diagnosis*. WB Saunders, Philadelphia
- Dukes-McEwan J, Borgarelli M, Tidholm A, Vollmar AC and Häggström J (2003) Guidelines for the diagnosis of canine idiopathic dilated cardiomyopathy. The ESCV Taskforce for canine dilated cardiomyopathy. *Journal of Veterinary Cardiology* **5**(2), 7–19
- Dunning D, Monnet E, Orton EC and Salman MD (1998) Analysis of prognostic indicators for dogs with pericardial effusion: 46 cases (1985–1996). *Journal of American Veterinary Medical Association* **212**, 1276–1280
- Ferasin L, Sturgess CP, Cannon MJ *et al.* (2003) Feline idiopathic cardiomyopathy: a retrospective study of 106 cats (1994–2001). *Journal of Feline Medicine and Surgery* **5**, 151–159
- Foale RD, White RA, Harley R and Herrtage ME (2003) Left ventricular myxosarcoma in a dog. *Journal of Small Animal Practice* **44**, 503–507
- Fox PR, Liu SK and Maron BJ (1995) Echocardiographic assessment of spontaneously occurring feline hypertrophic cardiomyopathy. An animal model of human disease. *Circulation* **92**, 2645–2651
- Fox PR, Maron BJ, Basso C, Liu SK and Thiene G (2000) Spontaneously occurring arrhythmogenic right ventricular cardiomyopathy in the domestic cat: a new animal model similar to the human disease. *Circulation* **102**, 1863–1870
- Fox PR, Moise NS, Evans HE and Bishop SP (1999) Cardiovascular anatomy. In: *Textbook of Canine and Feline Cardiology: Principles and Clinical Practice, 2nd edn*, ed. PR Fox, D Sisson and NS Moise, pp. 13–24. WB Saunders, Philadelphia
- Gavaghan BJ, Kittleson MD, Fisher KJ, Kass PH and Gavaghan MA (1999) Quantification of left ventricular diastolic wall motion by Doppler tissue imaging in healthy cats and cats with cardiomyopathy. *American Journal of Veterinary Research* **60**, 1478–1486
- Gidlewski J and Patrie JP (2003) Percardiocentesis and principles of echocardiographic imaging in the patient with cardiac neoplasia. *Clinical Techniques in Small Animal Practice* **18**, 131–134
- Haggstrom J, Kvarn C and Pedersen HD (2005) Acquired valvular heart disease. In: *Textbook of Veterinary Internal Medicine, 6th edn*, ed. SJ Ettinger and EC Feldman, pp. 1022–1039. Elsevier, St. Louis
- Hansson K, Haggstrom J, Kvarn C and Lord P (2002) Left atrial root indices using two-dimensional and M-mode echocardiography in cavalier King Charles spaniels with and without left atrial enlargement. *Veterinary Radiology and Ultrasound* **6**, 568–575
- Hansson K, Haggstrom J, Kvarn C and Lord P (2005) Interobserver variability of vertebral heart size measurements in dogs with normal and enlarged hearts. *Veterinary Radiology and Ultrasound* **46**, 122–130
- Hayward NJ, Baines SJ, Baines EA and Herrtage ME (2004) The radiographic appearance of the pulmonary vasculature in the cat. *Veterinary Radiology and Ultrasound* **45**, 501–504
- Johnson L, Boon J and Orton EC (1999) Clinical characteristics of 53 dogs with Doppler-derived evidence of pulmonary hypertension: 1992–1996. *Journal of Veterinary Internal Medicine* **13**, 440–447
- Kittleson MD (1998) Radiography of the cardiovascular system. In: *Small Animal Cardiovascular Medicine*, ed. MD Kittleson and RD Kienle, pp. 47–71. Mosby, St. Louis
- Koffas H, Dukes-McEwan J, Corcoran BM *et al.* (2006) Pulsed tissue Doppler imaging in normal cats and cats with hypertrophic cardiomyopathy. *Journal of Veterinary Internal Medicine* **20**, 65–77
- Lamb CR (2000) Ability to visualise the cardiac silhouette in animals with pleural fluid: the pericardial fat stripe. *Veterinary Radiology and Ultrasound* **41**, 519–520
- Lamb CR, Wikeley H, Boswood A and Pfeiffer DU (2001) Use of breed-specific ranges for the vertebral heart scale as an aid to the radiographic diagnosis of cardiac disease in dogs. *Veterinary Record* **148**, 707–711
- Less RD, Bright JM and Orton EC (2000) Intrapericardial cyst causing cardiac tamponade in a cat. *Journal of American Animal Hospital Association* **36**, 115–119
- Litster AL and Buchanan JW (2000) Vertebral scale system to measure heart size in radiographs of the cats. *Journal of American Veterinary Medical Association* **216**, 210–214
- Lord PF and Suter P (1999) Radiology. In: *Textbook of Canine and Feline Cardiology: Principles and Clinical Practice, 2nd edn*, ed. PR Fox, D Sisson and NS Moise, pp. 107–129. WB Saunders, Philadelphia
- MacGregor JM, Faria ML, Moore AS *et al.* (2005) Cardiac lymphoma and pericardial effusion in dogs: 12 cases (1994–2004). *Journal of American Veterinary Medical Association* **227**, 1449–1453
- Machida N, Hoshi K, Kobayashi M, Katsuda S and Yamane Y (2003) Cardiac myxoma of the tricuspid valve in a dog. *Journal of Comparative Pathology* **129**, 320–324
- Machida N, Kobayashi M, Tanaka R, Katsuda S and Mitsumori K (2003) Primary malignant mixed mesenchymal tumour of the heart in a dog. *Journal of Comparative Pathology* **128**, 71–74
- Mellanby RJ, Villiers E and Herrtage ME (2002) Canine pleural and mediastinal effusions: a retrospective study of 81 cases. *Journal of Small Animal Practice* **43**, 447–451
- Merlo M, Bo S and Ratto A (2002) Primary right atrium haemangiosarcoma in a cat. *Journal of Feline Medicine and Surgery* **4**, 123–125
- Olsen LH, Martinussen T and Pedersen HD (2003) Early echocardiographic predictors of myxomatous mitral valve disease in dachshunds. *Veterinary Record* **10**, 293–297
- Owens JM (1977) Pericardial effusion in the cat. *Veterinary Clinics of North America* **7**, 373–383
- Peterson PB, Miller MW, Hansen EK and Henry GA (2003) Septic pericarditis, aortic endarteritis and osteomyelitis in a dog. *Journal of American Animal Hospital Association* **39**, 528–532
- Reed JR, Thomas WP and Suter PF (1983) Pneumopericardigraphy in the normal dog. *Veterinary Radiology* **24**, 112–119
- Richardson P, McKenna W, Brntow M *et al.* (1996) Report of the 1995 World Health Organization/International Society and Federation of Cardiology Task Force on the Definition and Classification of cardiomyopathies. *Circulation* **93**, 841–842
- Ruehl WW and Thrall DE (1981) The effect of dorsal versus ventral recumbency on the radiographic appearance of the canine thorax. *Veterinary Radiology* **22**, 10–16
- Santilli RA and Bussadori C (1998) Doppler echocardiographic study of left ventricular diastole in non-anaesthetized healthy cats. *The Veterinary Journal* **156**, 203–215
- Schober KE, Luis Fuentes V and Bonagura JD (2003) Comparison between invasive haemodynamic measurements and non-invasive assessment of left ventricular diastolic function by use of Doppler echocardiography in healthy anaesthetized cats. *American Journal of Veterinary Research* **64**, 93–103
- Schwarz T, Willis R, Summerfield NJ and Doust R (2005) Aneurysmal dilatation of the right aortic in two dogs. *Journal of the American Veterinary Medical Association* **226**, 1512–1515
- Simpson DJ, Hunt GB, Church DB and Beck JA (1999) Benign masses in the pericardium of two dogs. *Australian Veterinary Journal* **77**, 225–229
- Sisson D, Kvarn C and Darke P (1999) Acquired valvular heart disease in dogs and cats. In: *Textbook of Canine and Feline Cardiology: Principles and Clinical Practice, 2nd edn*, ed. PR Fox, D Sisson and NS Moise, pp. 536–565. WB Saunders, Philadelphia
- Sisson D and Thomas WP (1999) Pericardial disease and cardiac tumors. In: *Textbook of Canine and Feline Cardiology: Principles and Clinical Practice, 2nd edn*, ed. PR Fox, D Sisson and NS Moise, pp. 679–701. WB Saunders, Philadelphia
- Suter PF (1981) The radiographic diagnosis of canine and feline heart disease. *Continuing Education* **3**, 441–454
- Suter PF (1984) *Thoracic Radiograph, A Text Atlas of Thoracic Diseases of the Dog and Cat*. Peter F. Suter, Wettswil, Switzerland
- Thomas WP, Reed JR, Bauer TG and Breznock EM (1984) Constrictive pericardial disease in the dog. *Journal of American Veterinary Medical Association* **184**, 546–553
- van den Broek AHM and Darke PGG (1987) Cardiac measurements on thoracic radiographs of cats. *Journal of Small Animal Practice* **28**, 125–135
- Van der Gaag I and Van der Luer RJT (1977) Eight cases of pericardial defects in the dog. *Veterinary Pathology* **14**, 14–18
- Venco L, Kramer L, Sola LB and Moccia A (2001) Primary cardiac rhabdomyosarcoma in a cat. *Journal of American Animal Hospital Association* **37**, 159–163
- Ware WA and Hopper DL (1999) Cardiac tumours in dogs: 1982–1995. *Journal of Veterinary Internal Medicine* **13**, 95–103
- Zoia A, Hughes D and Connolly DJ (2004) Pericardial effusion and cardiac tamponade in a cat with extranodal lymphoma. *Journal of Small Animal Practice* **45**, 467–471

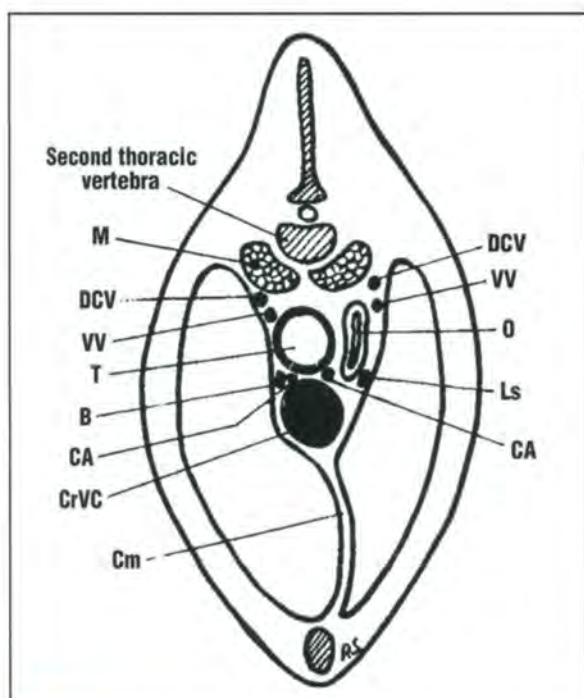
The mediastinum

Elizabeth Baines

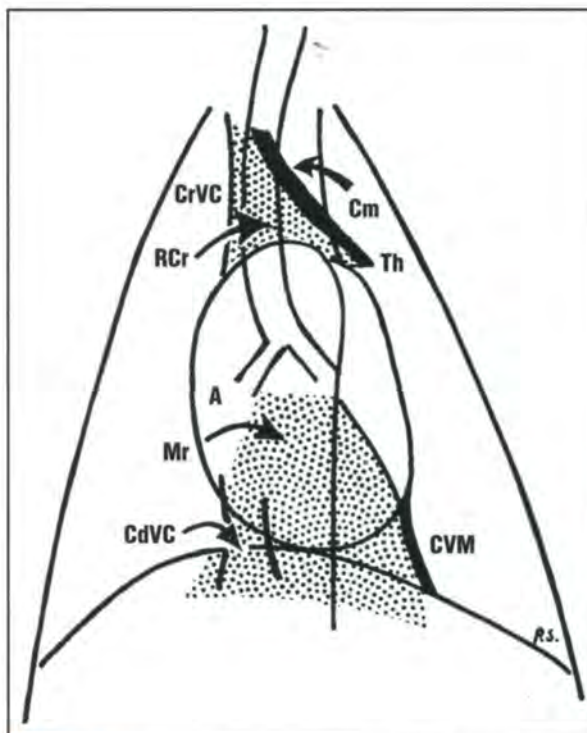
Radiographic anatomy

The mediastinum is the space between the left and right pleural cavities and encloses all the midline structures of the thorax (Figures 8.1 and 8.2). Its lateral limits are the mediastinal pleurae, which are reflections of the parietal pleurae as they leave the thoracic inlet and diaphragm. The mediastinum is continuous cranially with the fascial planes of the neck via the thoracic inlet and caudally with the retroperitoneal space through the aortic hiatus.

Structures within the mediastinum include the heart and great vessels, trachea, oesophagus, thoracic duct, nerves, lymph nodes and thymus. All mediastinal structures, with the exception of the



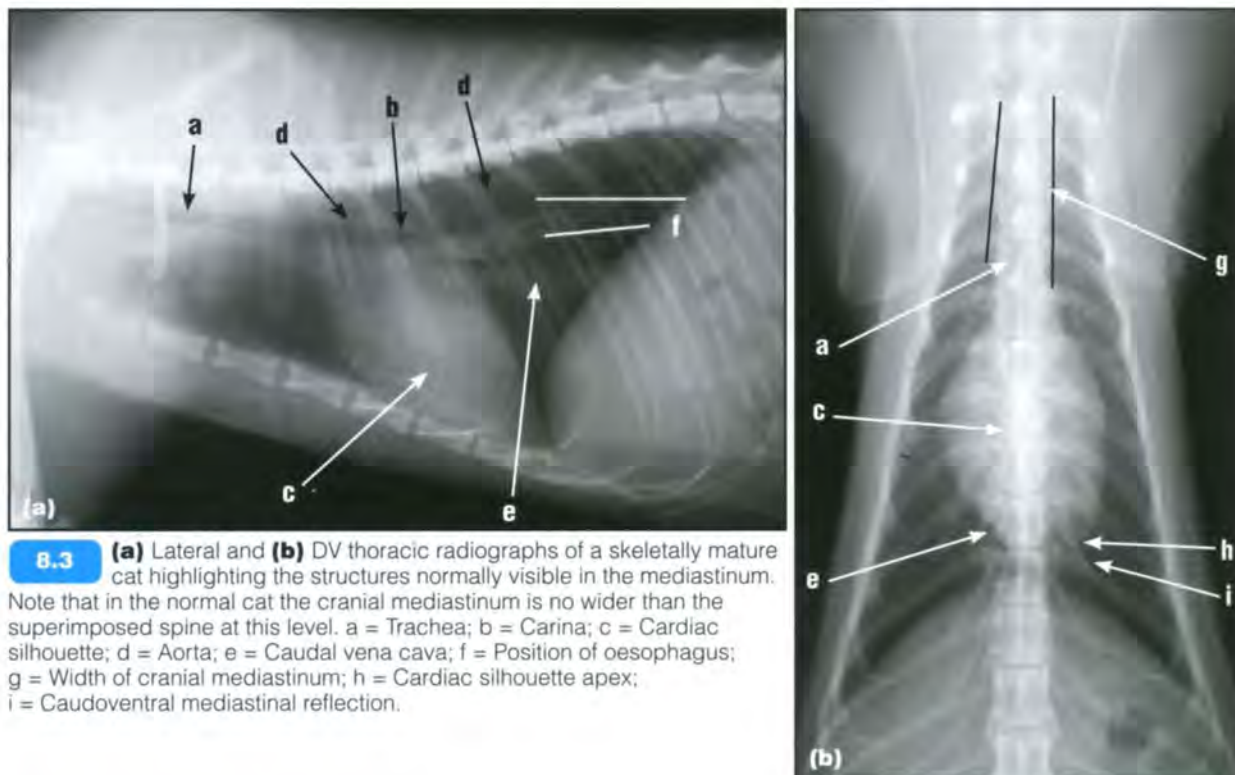
8.1 Transverse diagram of the mediastinum at the level of the second thoracic vertebra, showing the close association between the various soft tissue opacity structures in the cranial mediastinum. B = Brachiocephalic artery; CA = Right and left carotid arteries; Cm = Cranial mediastinum; CrVC = Cranial vena cava; DCV = Right deep cranial vertebral vein and left deep cranial vertebral vein; Ls = Left subclavian artery; M = Longus colli muscle; O = Oesophagus; T = Trachea; VV = Right and left vertebral veins. (Adapted from Suter (1984) with permission)



8.2 DV view of the thorax, showing the position of the cranial, middle and caudal parts of the mediastinum, including the position of the thymus. A = Accessory lobe of the right lung (seen as a dotted area); CdVC = Caudal vena cava; Cm = Cranial mediastinum; CrVC = Cranial vena cava; CVM = Caudoventral mediastinal reflection; Mr = Mediastinal recess, which accommodates the accessory lobe of the right lung; RCr = Right cranial lung lobe (seen as a dotted area); Th = Position of vestigial thymus. (Adapted from Suter (1984) with permission)

air-filled trachea and the lumen of the oesophagus, if air-filled, are of soft tissue opacity and so the normal mediastinum appears as a fairly homogenous soft tissue opacity with little contrast between adjacent structures (Figure 8.3). Even if large amounts of fat are deposited in the mediastinum, this is not usually sufficient to outline mediastinal soft tissue organs due to the low-contrast radiographic technique used for the thorax.

The ventral margin of the mediastinum is contiguous with the dorsal surface of the sternum. Radiographically there is often a band of soft tissue opacity dorsal to the sternum, which is a composite



8.3 (a) Lateral and (b) DV thoracic radiographs of a skeletally mature cat highlighting the structures normally visible in the mediastinum. Note that in the normal cat the cranial mediastinum is no wider than the superimposed spine at this level. a = Trachea; b = Carina; c = Cardiac silhouette; d = Aorta; e = Caudal vena cava; f = Position of oesophagus; g = Width of cranial mediastinum; h = Cardiac silhouette apex; i = Caudoventral mediastinal reflection.

shadow of the transverse thoracic muscle, internal thoracic artery and vein, sternal lymph nodes and other structures. Often a large retrosternal fat deposit is located at the level of, and caudal to, the xiphoid process. This often highlights the cardiac apex due to its opacity. The structures of the ventral floor of the mediastinum should not be confused with pleural or mediastinal effusion.

The mediastinum may be considered as being divided into three transverse sections by the heart: cranial, middle (containing the heart) and caudal parts; it is divided into dorsal and ventral parts by a dorsal plane at the level of the carina (see Figure 8.2).

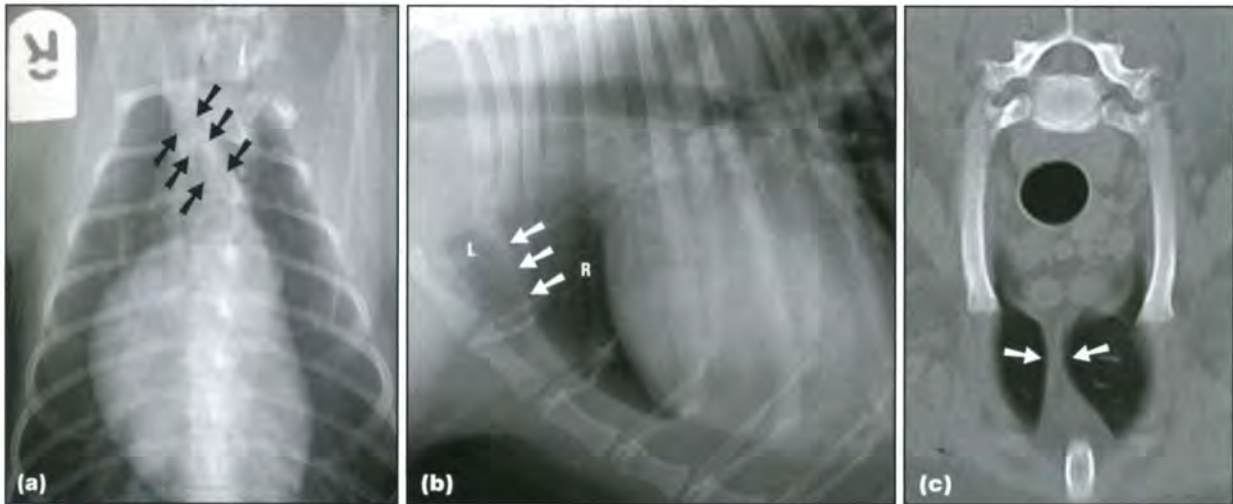
Three major mediastinal reflections are present:

- Cranioventral:
 - Represents the displacement of the cranioventral part of the mediastinum by the right cranial lung lobe (see Figures 8.1, 8.2 and 8.4)
 - Contains the internal thoracic arteries, veins and lymphatics
 - Ventrodorsal (VD) view (dogs): thin curvilinear opacity on the left of the vertebral column
 - Lateral view (dogs): curvilinear soft tissue opacity running from the level of the first rib to the sternum.
- Caudoventral:
 - Created by the accessory lobe, extending across the midline and pushing the mediastinum to the left (see Figure 8.2)
 - Not seen in lateral views
 - Seen better on the VD than the dorsoventral (DV) view, but is not consistently visible (Figure 8.5)

- Appears as a fine band of soft tissue opacity running between the left side of the diaphragm and the apex of the heart
- Has previously been mistakenly referred to as the cardiophrenic/sternopericardiac ligament. This structure is not radiographically visible (see also Figure 8.16).
- Plica venae cavae (see also Figure 8.16):
 - Surrounds the caudal vena cava (CdVC)
 - Not visible radiographically as an individual structure.

As the mediastinum is a difficult area to examine clinically, diagnostic imaging plays an important role in the detection and investigation of mediastinal abnormalities. Survey radiography is the imaging modality of choice for initial screening of the mediastinum, which should be assessed on two orthogonal views of the thorax. The lateral view allows examination of many of the normally visible structures, but does not allow assessment of mediastinal shift (see below). The DV or VD view allows full assessment of the position of the mediastinum and is more sensitive for the presence of mediastinal fluid and for definitive diagnosis of a mediastinal mass. The VD view allows a more complete assessment of the caudal mediastinum than the DV view, as the heart drops away from the diaphragm slightly, increasing the space available for the caudal mediastinum.

Optimal radiographic quality is vital; particular care must be taken to ensure that the thoracic limbs are extended cranially to avoid superimposition of the triceps muscle mass on the cranioventral thorax, mimicking the appearance of a cranioventral mediastinal mass on a lateral view.



8.4 (a) DV radiograph of a mature dog showing the cranioventral part of the mediastinum (arrowed). The animal is slightly rotated, which accentuates this structure. (b) Close-up of a right lateral radiograph of a 2-year-old dog showing the cranioventral mediastinum (arrowed) as a thin line of soft tissue opacity between the right cranial lobe (R) and the left cranial lobe (L). (c) Transverse CT image obtained at the level of the first rib and viewed on a wide window (window width 2000 HU, window level -500 HU). The cranioventral mediastinum is clearly seen between the left and right cranial lobes (arrowed).



8.5 (a) Close-up of a VD radiograph of the caudal lung fields of a skeletally mature normal dog. The caudoventral mediastinal reflection is seen as a narrow band of soft tissue opacity (arrowed) separating the accessory lobe (A) from the left caudal lobe (L). (b) Transverse CT image obtained at the level of the accessory lobe (window width 2000 HU, window level -500 HU). The caudoventral mediastinal reflection is clearly delineated (arrowed). The extension of the accessory lobe across the midline can be appreciated (A).

The width of the cranial mediastinum

In dogs, the maximum width of the cranial mediastinum on a VD/DV view should be less than twice the width of the vertebral column at this level.

In cats, the cranial mediastinum should be no wider than the width of the superimposed thoracic spine on a VD/DV view.

According to the body condition of the animal, the mediastinum may contain a variable amount of fat. Obese or brachycephalic breeds have larger fat deposits and this will cause widening of the mediastinum on the DV/VD view (may be greater than twice the width of the vertebral column). This can be difficult to differentiate from a true cranial mediastinal mass (Figure 8.6). Ultrasonography often assists in the differentiation (see below).



8.6 DV thoracic radiograph of an 8-year-old Bulldog bitch. The cranial mediastinum is within normal limits for this breed (arrowed).

Radiographic visualization of structures

Some mediastinal structures are readily visible on all thoracic radiographs (Figure 8.7). Many of the mediastinal structures are not normally visible, which may be because:

- They are too small to cause sufficient differential attenuation of the primary beam
- The radiographic low-contrast technique for the thorax does not allow mediastinal fat to outline these structures sufficiently
- They are in contact with other structures of the same opacity and so undergo border effacement.

Normally visible

Trachea, including its bifurcation and the origins of the bronchi
 Heart within the pericardium
 Aorta
 CrVC (usually seen better on the VD than the DV view due to shifting of the heart when the animal is in dorsal recumbency)
 Thymus in young animals
 Oesophagus (sometimes but not always seen; visible particularly on left lateral views and also if it contains air or fluid; rarely seen on the VD/DV view in a normal animal)

Not normally visible

CrVC (however, note that the CrVC forms the ventral border of the cranial mediastinum on a lateral view)
 Brachiocephalic trunk
 Left subclavian artery
 Azygos vein
 Main pulmonary artery
 Distal parts of the pulmonary veins
 Vagus nerve
 Recurrent laryngeal and phrenic nerves
 Thoracic duct
 Tracheobronchial, mediastinal and cranial sternal lymph nodes

8.7 Mediastinal structures normally visible and not normally visible on survey radiographs.

Most of these structures, with the exception of the azygos vein, the main pulmonary vessels and the tracheobronchial lymph nodes, lie within the cranial mediastinum and silhouette with one another (border obliteration or effacement). In the normal animal the tracheobronchial lymph nodes and the main pulmonary vessels silhouette with the heart base, and the azygos vein silhouettes with the aorta and ventral longitudinal ligaments of the vertebrae.

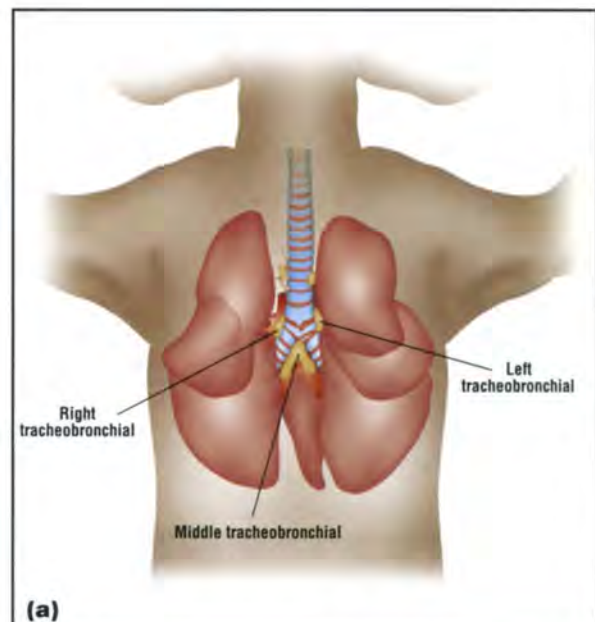
Lymph nodes

The cranial sternal (also known as sternal, retrosternal or presternal) lymph nodes are usually paired but some variation exists. These nodes lie just dorsal to the sternum, at the level of the second sternebra. Note that the sternal lymph nodes receive efferent lymphatics from the thoracic wall and abdominal cavity. If these nodes are enlarged then abdominal disease should be considered.

The cranial mediastinal lymph nodes vary in number. These nodes lie in the cranial mediastinum adjacent to the cranial vena cava (CrVC), brachiocephalic trunk, left subclavian artery and trachea.

The bronchial lymph nodes are divided into pulmonary and tracheobronchial groups. The pulmonary nodes are often absent. The middle tracheobronchial lymph node is the largest of the group and forms a V shape lying between the mainstem bronchi at the heart base, caudodorsal to the carina. The apex fits neatly into the angle formed by the tracheal bifurcation (Figure 8.8a). The right and left tracheobronchial lymph nodes lie on the lateral side of their respective bronchus. They sit immediately cranial to the carina, the right just ventral to, and the left just dorsal to the trachea (Figure 8.8a).

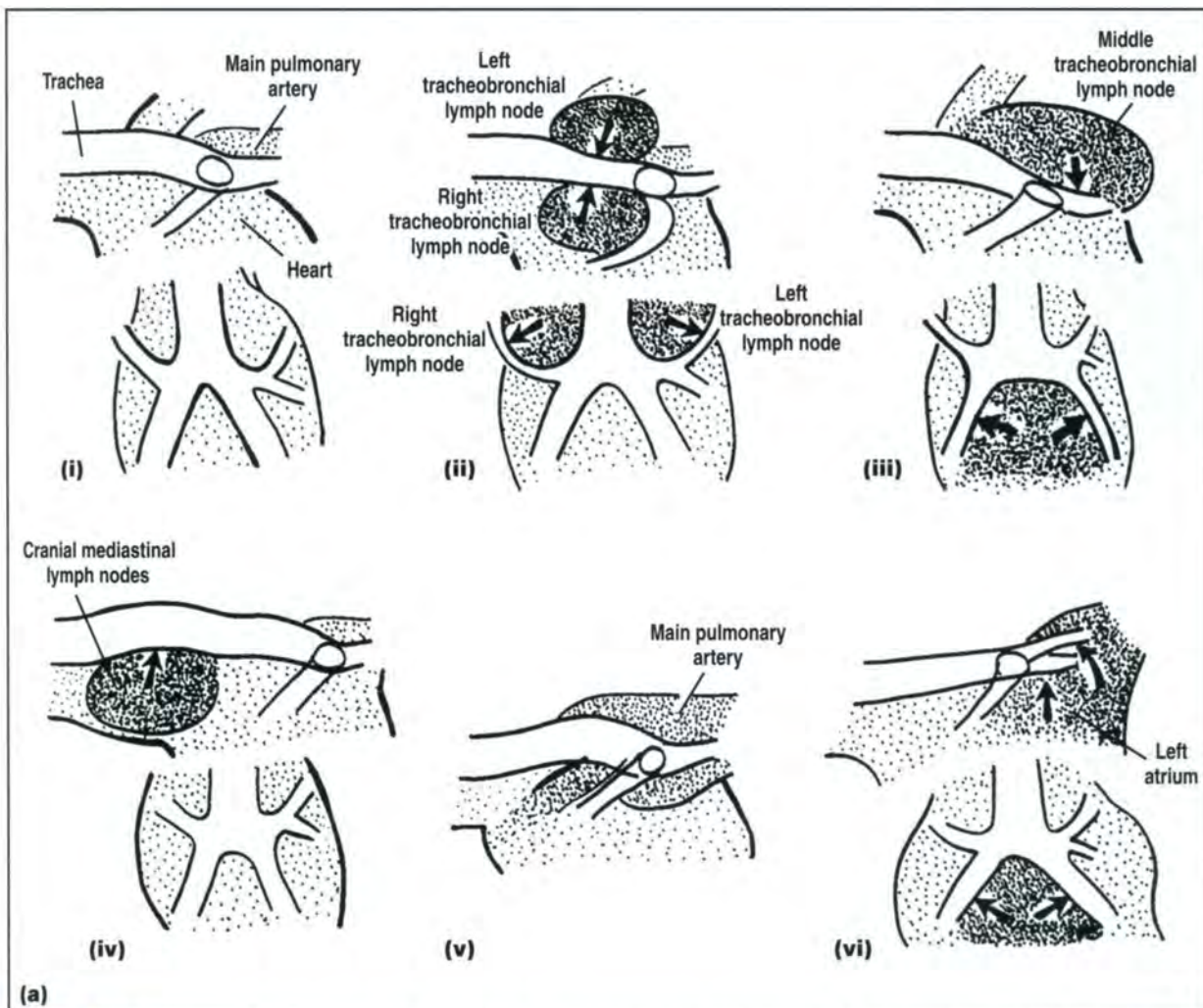
Specific radiographic features are seen when these lymph nodes are enlarged (Figure 8.9). Mineralization of the lymph nodes may be seen as a sequel to fungal disease (Figure 8.8b):



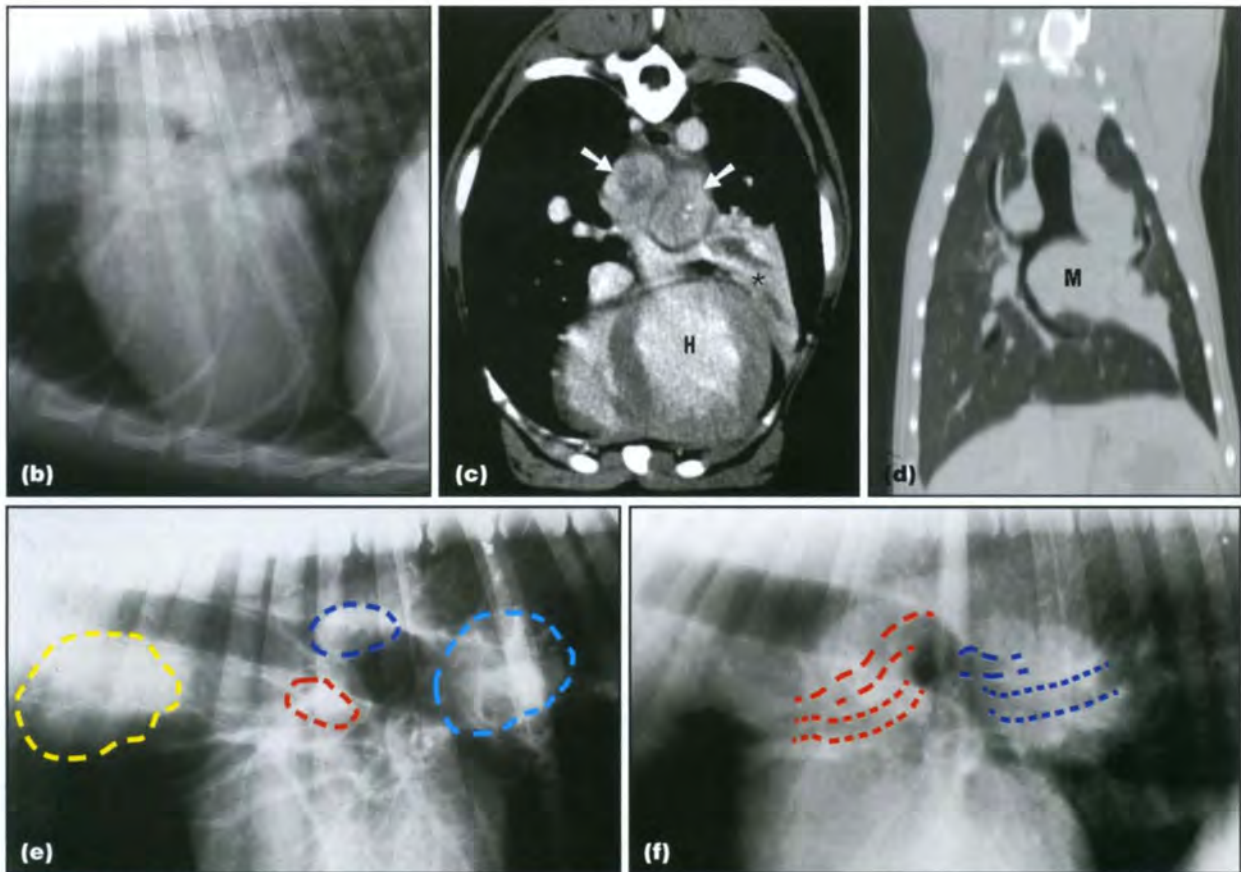
8.8 (a) Dorsal view of the tracheal bifurcation in the dog. The location of the tracheobronchial lymph nodes is shown. (b) Lateral radiograph of a spayed 8-year-old Labrador Retriever bitch with chronic systemic coccidioidomycosis. Many small pulmonary, hilar and cranial mediastinal lymph nodes (some arrowed) are faintly mineralized in this dog.

Lymph nodes	Radiographic features when enlarged
Tracheobronchial (Figure 8.10)	All mildly increased in size: hazy increase in perihilar opacity Middle: ventral depression of mainstem bronchi on lateral view, splaying or spreading of the caudal lobar bronchi on the VD/DV view Right and left: increased ventral depression of the trachea at the carina on the lateral view, caudal displacement of the left and right cranial lobar bronchi on the DV/VD view
Sternal (Figure 8.11)	Soft tissue opacity with broad base dorsal to the second sternebra, creating an extrapleural sign
Cranial mediastinal (Figure 8.12)	Widened cranial mediastinum on the VD/DV, difficult to perceive on the lateral view

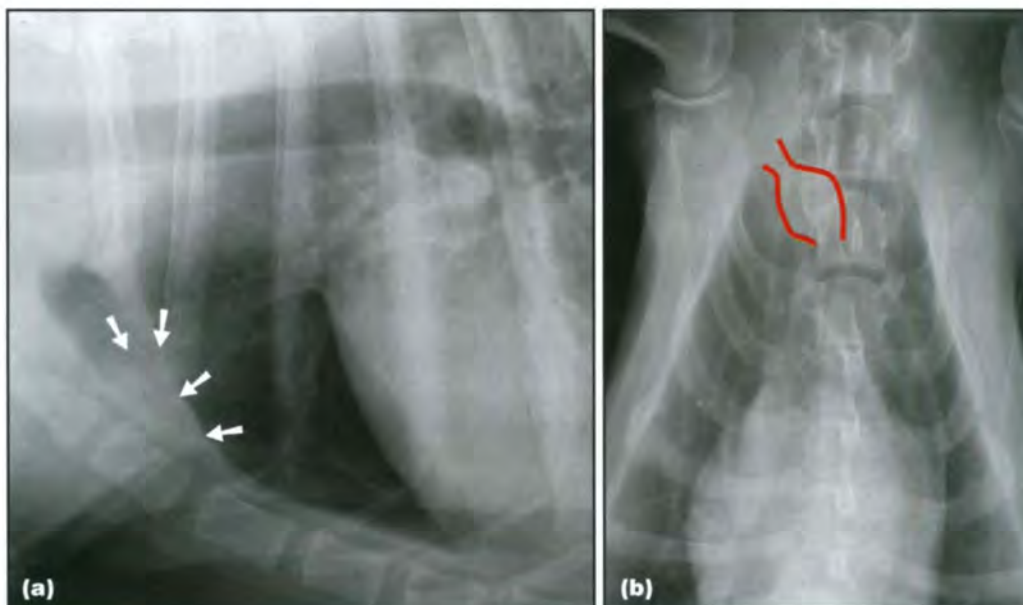
8.9 Radiographic features of enlarged mediastinal lymph nodes.



8.10 (a) There are several important differentials for increased perihilar opacity. (i) The normal perihilar structures are seen on lateral and DV views. Note that the angle between the caudal mainstem bronchi can vary with breed and centring of the X-ray beam. Note that the angle between the caudal mainstem bronchi can vary with breed and centring of the X-ray beam. (ii) The mass effect created by simultaneous enlargement of the left and right tracheobronchial lymph nodes is demonstrated. Both nodes can accentuate the ventral deflection of the trachea at the carina. The left and right nodes can be separated by looking for the adjacent bronchus. The left bronchus bifurcates immediately ventral to the carina. (iii) The mass effect created by an enlarged middle tracheobronchial lymph node. Note that the caudal lobar bronchi are separated on the DV view and pushed ventrally on the lateral view. (iv) The mass effect created by the cranial mediastinal lymph nodes. If these nodes are large enough they can elevate the trachea. Note that heart base tumours are often located in this region and can produce a similar effect. (v) Enlarged pulmonary arteries (and sometimes veins) can sometimes be mistaken for enlarged lymph nodes. This is a diagram of enlargement of the main pulmonary artery in dirofilariasis. (vi) Left atrial enlargement can be easily distinguished from middle tracheobronchial node enlargement. Both separate the caudal mainstem bronchi on a VD/DV view, but on the lateral view the bronchi are depressed ventrally with node enlargement and dorsally (especially the left) with left atrial enlargement. (a, Reproduced from Suter (1984) with permission) (continues)



8.10 (continued) **(b)** Enlarged perihilar (right, left and middle tracheobronchial) lymph nodes in a 3-year-old male neutered crossbred dog with systemic fungal disease. Note the ventral depression of the trachea and caudal lobar bronchi. **(c)** Transverse CT image (soft tissue window). The enlarged middle tracheobronchial lymph node (arrowed) is identified dorsal to the heart (H). A consolidated region of the caudal part of the left cranial lung lobe is identified adjacent to the nodes (*). **(d)** Dorsal CT reconstruction (lung window). The middle tracheobronchial lymph node (M) is identified displacing the caudal lobar bronchi laterally. **(e)** Close-up of a lateral thoracic radiograph of a dog with multicentric lymphoma. The middle (turquoise), right (red) and left (blue) tracheobronchial and cranial mediastinal lymph nodes (yellow) are moderately enlarged. **(f)** Close-up of a lateral thoracic radiograph of a 5-year-old Cocker Spaniel with multicentric lymphoma, demonstrating ventral deviation and split of cranial (red) and caudal (blue) lobar bronchi. Ventral lobar bronchial deviation is an important feature in hilar opacities to differentiate left atrial enlargement (dorsal bronchial displacement) from lymphadenopathy.



8.11 **(a)** Lateral and **(b)** VD images of a 6-year-old Australian Cattle Dog with mildly enlarged sternal lymph nodes (arrowed in (a), red lines in (b)) secondary to abdominal neoplasia.



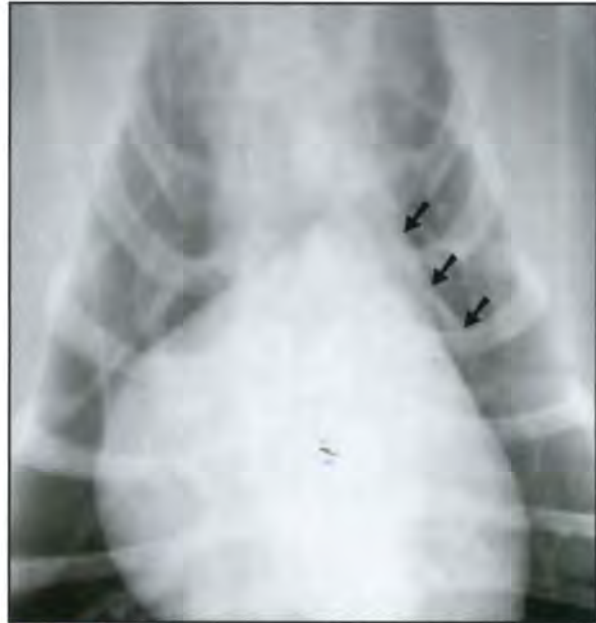
8.12 Close-up of a VD radiograph of the cranial thorax in an 8-year-old Border Collie. The widening of the cranial mediastinum (arrowed) was due to enlarged cranial mediastinal lymph nodes.

Juvenile mediastinum

In the juvenile animal the thymus may be visible due to its relatively large size. In the cat this is best seen on the lateral view as a crescent-shaped opacity, paralleling the cranial border of the heart in the cranioventral thorax (Figure 8.13). In the dog it can be best seen on the DV view as a triangular opacity, extending from the midline towards the left side, the so-called thymic sail (Figure 8.14). It may be occasionally seen cranial to the cardiac silhouette on the lateral view.

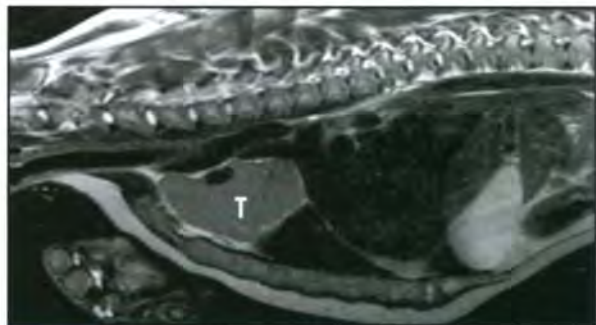


8.13 Lateral view of the thorax of a 5-month-old female Domestic Shorthair cat. The thymus is seen as a faint triangular soft tissue opacity (arrowed) cranial to the heart. It was not visible on the DV view.



8.14 DV thoracic radiograph of a 1-year-old Boxer bitch, showing a small thymic sail (arrowed) just cranial to the heart and to the left of the midline.

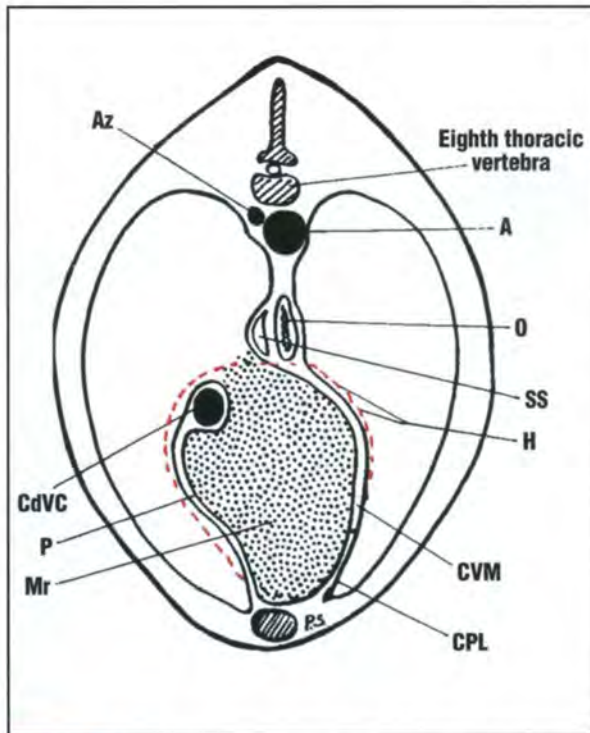
The thymus (Figure 8.15) reaches its maximum size at 4 months old, and then progressively undergoes involution until it is no longer visible at about 1 year of age. Occasionally, a thymic remnant may be seen in older animals as a narrow radiopaque line in the position of the previous thymus.



8.15 Sagittal plane T2-weighted MRI scan of the thorax of a 3-month-old Italian Spinone bitch, demonstrating the thymus as a hyperintense mass (T) cranial to the heart.

Sussdorf's space

Sussdorf's space refers to a region in the caudal mediastinum in humans, which is mentioned in some canine anatomy and radiology texts as being ventral to the aorta, to the right of the distal oesophagus (Figure 8.16). It derives embryologically from a remnant of the omental bursa becoming trapped within the thorax as the diaphragm develops. In humans it is also known as the *cavum mediastini serosum*, the persisting pneumatoenteric recess or the *infracardiac bursa*, and may be a potential space for herniation of abdominal organs.



8.16 Transverse diagram of the mediastinum at the level of the eighth thoracic vertebra and demonstrating the location of the plica venae cavae and Sussdorf's space. (A = Aorta; Az = Azygos vein; CdVC = Caudal vena cava; CPL = The true cardiophrenic ligament is located ventrally; CVM = Caudoventral mediastinum; H = Outline of position of the heart; Mr = Mediastinal recess; O = Oesophagus; P = Plica venae cavae; SS = Sussdorf's space. (Reproduced from Suter (1984) with permission)

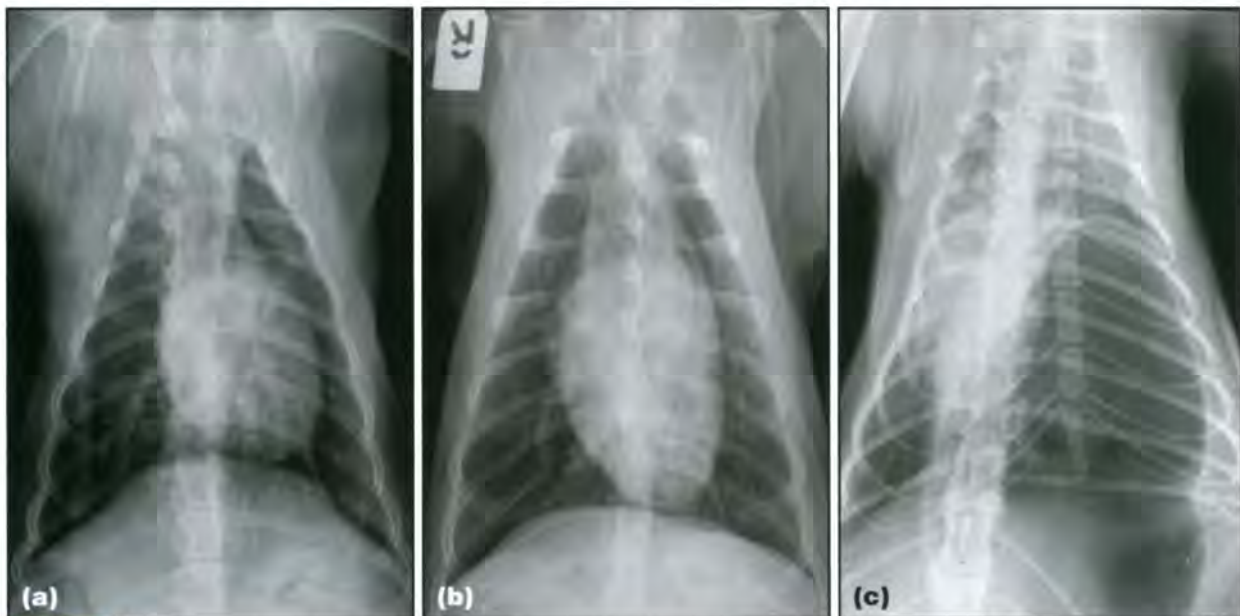
Interpretive principles

Mediastinal shift

This term does not usually relate to mediastinal disease but rather gives valuable information on disease processes on either side of the mediastinum. The mediastinum is a mainly midline structure, so displacement or shift to one side or the other, seen on the DV/VD view, is a strong indicator of *change in the volume of one hemithorax*. This is an important radiographic sign to recognize. For example, identification of mediastinal shift can be very important in correct diagnosis and prompt treatment of potentially life-threatening diseases, such as diaphragmatic hernia. Mediastinal shift is recognized by a change in the position of the heart, trachea, aortic arch and CdVC, and by asymmetry between the sizes of the two hemithoraces. It may persist after the active disease process has resolved, as a result of adhesions or lobar collapse.

Mediastinal shift can not be evaluated on a lateral radiograph. However, it must be noted that changes secondary to the shift may be seen on the lateral view. For example, the cardiac silhouette may appear to be elevated from the sternum due to collapse of the underlying lung lobe and mediastinal shift towards that side (see also Figure 13.13, p. 330).

Care must be taken to ensure that the VD or DV radiograph is correctly positioned and free from rotation before assessment is made of the position of the mediastinum, as rotation of the animal will falsely suggest mediastinal shift (Figure 8.17). If the apex of the heart has moved in the *same direction* as the sternum then any apparent mediastinal shift



8.17 (a) VD view of a mature dog with moderate rotation of the thorax. Note that the cardiac silhouette has moved in the *same* direction as the sternum. Mediastinal shift is unlikely to be present. (b) A straight VD view. Note that the cardiac silhouette is now in a normal position and no mediastinal shift is present. The previous displacement of the cardiac silhouette was simply due to rotation. (c) DV thoracic radiograph of an 8-year-old neutered male Oriental cat with a unilateral tension pneumothorax, showing contralateral mediastinal shift. Although the radiograph is poorly positioned with marked rotation, the apex of the heart has rotated in the *opposite* direction to the sternum, allowing confirmation of the mediastinal shift.

may be an effect of rotation. If the apex of the heart is moved away from the sternum, then true mediastinal shift must be present. Where there is doubt, a straight radiograph should be obtained.

The presence or absence of mediastinal shift can help differentiate between pathological and physiological processes; for example, an increase in opacity of the right middle lung lobe with ipsilateral mediastinal shift suggests lobar collapse, whereas an increase in opacity of the right middle lung lobe without mediastinal shift suggests lobar consolidation or a mass.

The direction of the mediastinal shift should be noted. In general:

- Unilateral decrease in volume causes shift towards that side (ipsilateral shift) (Figure 8.18a)
- Unilateral increase in volume causes shift away from that side (contralateral shift) (Figure 8.18b)
- Presence of an intrathoracic mass causes shift away from that side (contralateral shift) (Figure 8.18c).

Causes of mediastinal shift include:

- Unilateral lung collapse (concomitant signs should be looked for: increased opacity of the lung, cranial displacement of the diaphragm on affected side, etc.)
- Pleural disease with pleural adhesions
- Unilateral pleural effusion
- Unilateral pneumothorax
- Unilateral lobar overinflation due to unilateral pulmonary emphysema or compensatory hyperinflation
- Large single or multiple pulmonary masses
- Unilateral diaphragmatic hernia/rupture
- Deformities of the thoracic wall or spine, such as scoliosis or pectus excavatum.

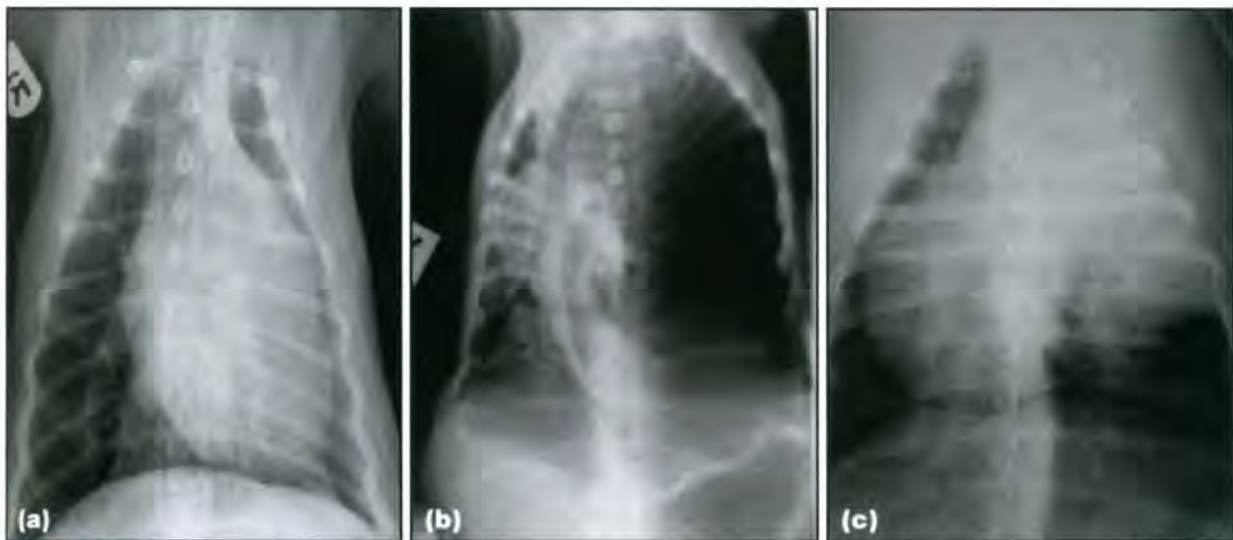
Abnormal visualization of mediastinal structures

It is unusual to see all the mediastinal structures as they are mostly of soft tissue opacity and hence silhouette positively (or border efface) with each other. If usually non-visible mediastinal structures are clearly definable, this must be due to the presence of a contrasting substance between them. There may be increased visibility of the cranial mediastinal structures on a lateral view in extremely obese animals, but on the DV/VD view, little more can be seen due to the thickness of the tissue at this point. The most common clinical situation in which mediastinal structures become visible is when gas highlights the serosal or outer surfaces, indicating pneumomediastinum (see below). A rare but concerning scenario is the presence of an infiltrating metal opacity outlining the serosal surfaces of mediastinal structures, suggesting extravasation of a previously administered contrast medium agent.

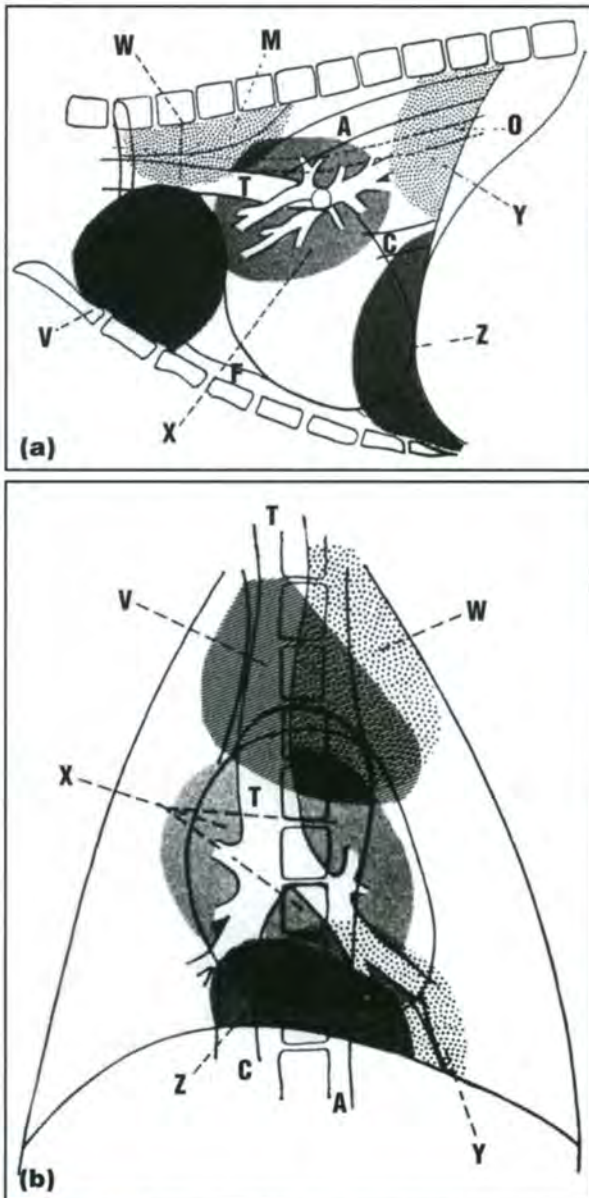
Mediastinal masses

It is important to distinguish a true mediastinal mass from a normal anatomical variant. Dogs with a wide shallow thoracic conformation, such as brachycephalic breeds, often have a wide mediastinum (see Figure 8.6). Obese small-breed dogs will have increased fat deposits in the mediastinum, again mimicking a mediastinal mass lesion, often accompanied by clinical signs that further support this diagnosis, such as dyspnoea and exercise intolerance.

Mediastinal masses may be located anywhere within the mediastinum, depending on their aetiology and tissue of origin. Mediastinal masses have been divided into five main locations (Figure 8.19). As with other parts of the body, location may suggest the organ or tissue of origin. For example, a perihilar mass is likely to be due to either enlargement of the



8.18 (a) VD thoracic radiograph of an anaesthetized neutered male 6-year-old mixed breed dog, showing ipsilateral mediastinal shift due to lung atelectasis. The cardiac silhouette has moved towards the left due to diminished left lung volume. (b) DV thoracic radiograph of a puppy with congenital lobar emphysema (see also Chapter 12). The trachea and cardiac silhouette are markedly shifted into the right hemithorax due to the presence of the emphysematous lobe on the left side. (c) DV thoracic radiograph of a dog with a left cranial lobar pulmonary mass. Note the mediastinal shift seen as a movement of the cardiac silhouette towards the right, away from the mass.



8.19 (a) Lateral and (b) DV diagrams of the thorax illustrating the five main locations of mediastinal masses. A = Descending thoracic aorta; C = Caudal vena cava; F = Fat in ventral mediastinum; M = Shadow of intrathoracic part of longus colli muscle; O = Oesophagus; T = Trachea; V = Cranioventral masses; W = Craniodorsal masses; X = Hilar and perihilar masses; Y = Caudodorsal masses; Z = Caudovernal masses. (Reproduced from Suter (1984) with permission)

tracheobronchial lymph nodes or a mass at the heart base. Often masses can be so large at presentation that their origin is difficult to determine.

Assessment of displacement of other intrathoracic structures is useful to determine the origin of such masses. The majority of masses are of soft tissue opacity, thus not permitting further differentiation on the basis of radiological appearance, but occasionally masses may be mineralized (e.g. teratoma) or of fat opacity (e.g. mediastinal lipoma). Ultrasonography can be very useful in further assessment of these lesions, either using the heart or liver as an acoustic window, or, if the mass is large enough, by a direct transthoracic technique.

Occasionally, it is difficult to decide whether a mass near the midline originates from the mediastinum or from a lung lobe adjacent to the mediastinum. This can be a challenging distinction to make. Factors that may assist in differentiation are shown in Figure 8.20 (see also below and Figure 8.27).

- The DV or VD view may provide an immediate answer as to whether or not the mass is in the midline
- Extrapleural sign (see Chapter 13) may be seen with mediastinal mass
- A mediastinal mass will usually be equal in size and similar in appearance on both left and right lateral views whereas a pulmonary mass may change with altered magnification and inflation of the surrounding lung
- Displacement and effacement of mediastinal structures suggests a mediastinal origin, but may occur if a pulmonary mass is large enough and close enough to the midline
- Ultrasonography may be useful in evaluation of motion of the mass with lung movement if a suitable window can be obtained (see Chapter 2)

8.20 Factors that may help in distinguishing a mediastinal mass from a lung mass adjacent to the mediastinum.

Mediastinal effusion

Mediastinal fluid results in further effacement of the contents of the mediastinum, and generalized mediastinal widening will usually be present. Reverse fissures may occasionally be visible on the DV/VD view. These are seen as smooth triangular soft tissue opacity projections, extending caudolaterally from the midline (Figure 8.21). Fluid may move freely between the pleural and mediastinal spaces if the mediastinal fenestrations remain perforate.



8.21 A 9-year-old neutered male Labrador Retriever with a mediastinal and pleural effusion. The arrows demarcate a triangular 'reverse fissure', likely to represent mediastinal fluid.

Free fluid versus loculated fluid and mass

Loculated fluid, such as may occur with mediastinitis, can result in a focal widening of the mediastinum and can appear similar to a mass lesion. Ultrasonography is very useful in determining the cause of a focal thickening/widening of the mediastinum. Positional radiography may displace free fluid and aid in this distinction (see also Chapter 13).

Alternative imaging of the mediastinum

Due to the limitations of radiographic assessment of the mediastinum it is important to realize the role of alternative imaging techniques in investigation of this region.

Transthoracic ultrasonography of the normal mediastinum is generally unrewarding due to the presence of air-filled lung between the thoracic wall and the mediastinum. However, many structures within the normal mediastinum can be identified using ultrasonography when a pleural effusion is present (see Chapter 13). In animals with mediastinal disease, ultrasonography is very useful in differentiating mediastinal fluid from a mass, and in determining the nature and extent of a mass. Ultrasonography also permits obtaining an ultrasound-guided fine-needle aspiration (FNA) or tissue biopsy. The cranial mediastinum can be accessed via parasternal, intercostal or thoracic inlet windows, the middle mediastinum via the cardiac notch and the caudal mediastinum either parasternally or via a transhepatic approach. Transoesophageal ultrasonography has been used in the dog to examine the heart base and great vessels, but this technique requires general anaesthesia and expensive equipment and is not widely available (see Chapter 2).

Computed tomography (CT) (Figure 8.22) and magnetic resonance imaging (MRI) are very useful for examining the mediastinum in both dogs and cats.

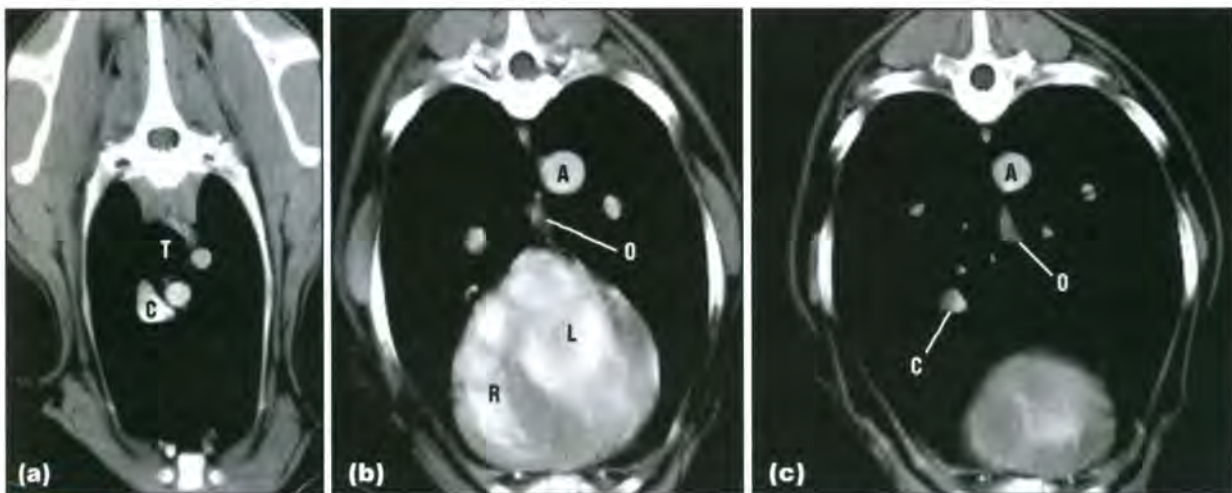
Both allow evaluation of the mediastinum without superimposition from other structures and have better contrast resolution than standard radiography, allowing distinction between solid, fatty, cystic, calcified and vascular structures. CT images of the mediastinum should usually be viewed using a soft tissue window; intravenous contrast medium administration (CT angiography) is particularly helpful in distinguishing mediastinal vessels from masses.

Diseases**Pneumomediastinum**

Pneumomediastinum is the presence of free gas (usually air) within the mediastinum. It always results from another disease process and the key to investigating and treating the condition lies in identifying the aetiology. When pneumomediastinum occurs alone there are usually no associated clinical signs, and with time the condition spontaneously resolves. However, pneumomediastinum may be accompanied by pneumothorax, subcutaneous emphysema and/or pneumoretroperitoneum. Clinical signs may then reflect dyspnoea or tachypnoea, secondary to the pneumothorax or discomfort, secondary to the subcutaneous emphysema. Rarely, a large-volume pneumomediastinum may compress the CrVC and CdVC and azygos vein, leading to diminished venous return and circulatory collapse.

An important rule of thumb is that if pneumomediastinum and pneumothorax are present simultaneously, then the pneumomediastinum may have led to the pneumothorax, but that the converse cannot be true. Pneumothorax does not lead to pneumomediastinum as the mediastinum is collapsed by the gas in the pleural space.

There are many possible causes of pneumomediastinum and these are listed in Figure 8.23.



8.22 Transverse CT images obtained from a normal dog with a soft tissue algorithm and viewed with a soft tissue window (window width 300 HU, window level 40 HU) at three different levels in the thorax. All images were taken after the administration of intravenous non-ionic iodinated contrast media. **(a)** At the level of T2. The cranial vena cava (C) and trachea (T) are marked. **(b)** At the level of the heart base. The aorta (A), oesophagus (O) and contrast within the left ventricle (L) and right ventricle (R) are seen. **(c)** At the level of the ninth thoracic vertebra. The aorta (A), oesophagus (O) and caudal vena cava (C) are seen. The other hyperattenuating structures within the lung fields (seen as small round structures) are the pulmonary arteries and veins beginning to fill with contrast medium.

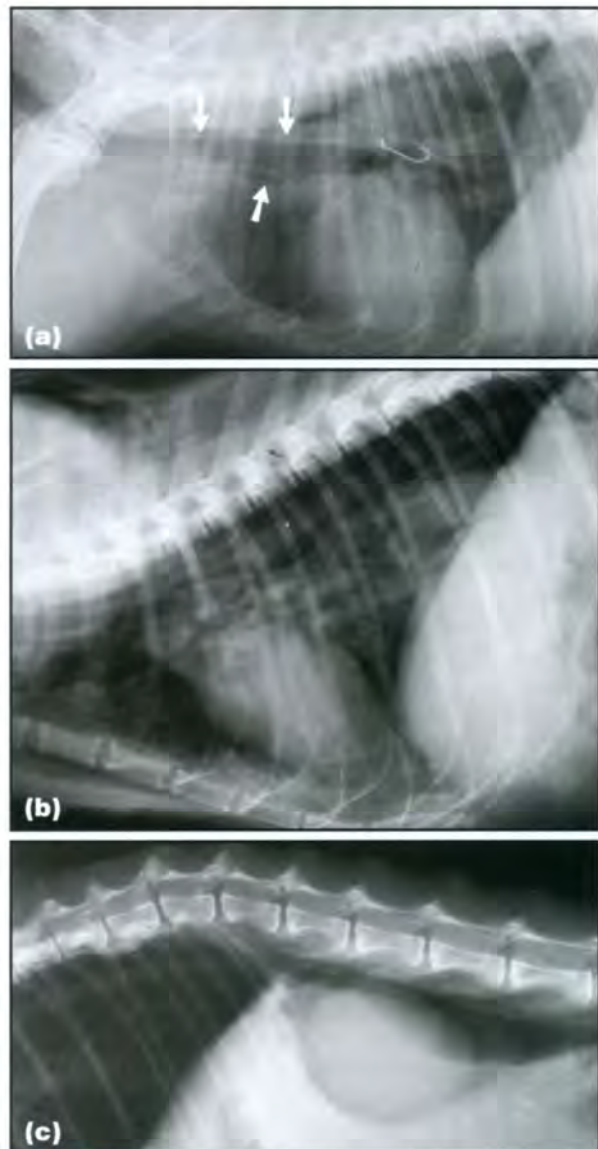
Cause	Comments
Thoracic, tracheal, oesophageal and cervical injury	Blunt thoracic trauma resulting in bronchial or alveolar rupture Perforating injury to skin or neck (e.g. puncture wounds, pharyngeal stick injuries) Iatrogenic cervical or tracheal injury (e.g. jugular venepuncture, transtracheal washing, tracheostomy) Tracheal rupture (e.g. secondary to overinflation of endotracheal tube cuff) Oesophageal rupture (e.g. foreign body, bite wound, iatrogenic)
Spontaneous	Following severe cough, respiratory disease (such as paraquat toxicity), pulmonary emphysema, etc.
Lung lobe torsion causing bronchial rupture	Rare
Idiopathic	No cause identified

8.23 Causes of pneumomediastinum.

Radiography

Radiography is essential in the diagnosis of pneumomediastinum. It allows assessment of the extent of the condition, shows associated lesions and complications, may identify the cause and allows assessment of the resolution or progression of the condition. Radiological appearance is similar in all cases (Figure 8.24):

- Increased radiolucency of the mediastinum with dissecting, infiltrating, linear radiolucencies delineating the outer surfaces of different mediastinal structures, greatly increasing visualization of these structures, such as the aorta, oesophagus and cranial mediastinal vessels
- Ventral border of *longus colli* muscles can be seen inserting on the ventral border of the sixth thoracic vertebra
- Both the luminal and the serosal surfaces of the trachea can be seen
- Extensive subcutaneous emphysema may also be present, making radiological interpretation more challenging, due to the superimposition of linear and reticulated gas shadows
- Radiographs of the neck or abdomen may demonstrate the causative lesion or extension of free gas into the retroperitoneal space
- Pneumoretroperitoneum originating from pneumomediastinum is incidental but should be differentiated from abdominal hollow viscus rupture, which is a surgical emergency (see Figure 8.24c)
- Oesophageal perforation will lead to mediastinal fluid accumulation so the presence or absence of this should be carefully assessed
- Pneumomediastinum can progress to pneumothorax if the volume is large enough (although the converse is not true) and this can hinder diagnosis.



8.24 (a) A 5-year-old mixed breed dog with a perforating oesophageal foreign body (a fish hook). A subtle pneumomediastinum is visible as small amounts of gas delineating the outer surface of the cranial intrathoracic trachea (arrowed). This is an extremely important radiographic finding. (b) Lateral thoracic radiograph of an 8-year-old neutered female Domestic Shorthair cat with pneumomediastinum, pneumothorax, extensive subcutaneous emphysema and pulmonary contusions after a road traffic accident. A ruptured trachea was identified on endoscopic examination. (c) Close-up of a lateral radiograph of an emaciated 12-year-old Domestic Shorthair cat with extension of pneumomediastinum to pneumoretroperitoneum. The thoracic and abdominal aorta and kidneys are highlighted by free gas. Minimal trauma to the aortic hilus allows gas tracking into the retroperitoneal space. This is an incidental finding but it should be differentiated from free abdominal gas originating from ruptured abdominal organs.

Contrast studies: If oesophageal or tracheal perforation is suspected, administration of 5–10 ml of a non-ionic iodinated contrast medium, such as iohexol, may identify the site of perforation. Lateral and DV/VD radiographs should be taken immediately and 5–10 minutes after administration to allow time for extravasation of the contrast medium.

Other imaging modalities

Due to the presence of free gas, ultrasonography is not useful. Advanced imaging techniques, such as CT or MRI, are rarely needed to make the diagnosis, although they may assist in identifying the cause (Figures 8.25 and 8.26).



8.25 Transverse CT image (lung window) from a neutered male 10-year-old Domestic Shorthair cat at the level of the heart. A small volume pneumomediastinum (M) and pneumothorax are present. Gas is also tracking along the peribronchial and perivascular sheaths. The cat had a CT scan for nasal neoplasia but the pneumomediastinum arose due to a presumed bronchial tear from anaesthetic ventilation (barotrauma).



8.26 CT image at the level of the first cervical vertebra of a male 3-year-old Labrador Retriever, which presented with a pneumomediastinum. A hyperattenuating structure was identified in the left ventrolateral perilaryngeal tissues surrounded by soft tissue swelling (window width 300 HU, window level 50 HU). During exploratory surgery this structure was found to be a stick.

Masses

Mediastinal masses can occur anywhere within the mediastinum, with the most common sites being cranioventral and perihilar. Clinical signs depend on the size and position of the mass. Patients with cranial mediastinal masses usually present with signs of dyspnoea, coughing and exercise intolerance. Occasionally gagging, vomiting or regurgitation may be present secondary either to oesophageal compression or mega-oesophagus due to paraneoplastic myasthenia gravis with thymoma.

Horner's syndrome, vocalization changes and laryngeal paralysis may result from peripheral nerve entrapment.

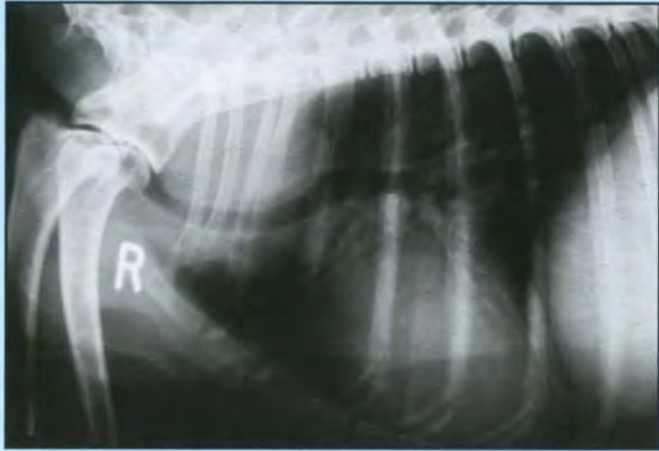
Mediastinal masses may also compress vascular or lymphatic structures. This may lead to head, neck and possibly forelimb swelling if the CrVC is involved, or ascites if the CdVC is involved.

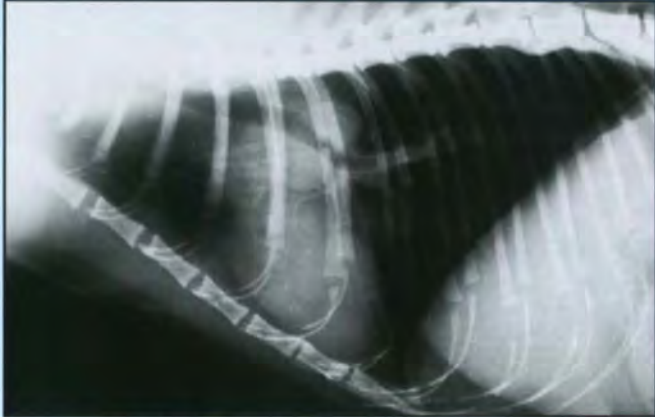
Causes of masses within the mediastinum and their main radiological signs are listed in Figure 8.27.

Radiography

Radiological appearance is similar in all cases, but depends on the position and size of the mass (see Figure 8.27):

- When small, the mass may silhouette with other mediastinal tissues and so only be visible as a subtle widening of the appropriate region of the mediastinum
- As the mass enlarges, displacement of nearby or associated structures should become evident. There is commonly border obliteration between a cranial mediastinal mass and the cardiac silhouette, which can make it difficult to assess the heart. However, large masses will push the heart caudally and displace the trachea. Location of the carina caudal to the sixth intercostal space on a lateral view is a sign of cardiac displacement, rather than enlargement (Figure 8.28a)
- The DV view is the most useful view to differentiate a mediastinal mass from a mass in the cranial lung lobes (see Figures 8.20 and 8.28ab)
- Small fat or soft tissue opacity lesions with an eggshell-like mineralization are occasionally seen in the mediastinum of cats. These are foci of nodular fat necrosis and of no clinical significance (Figure 8.28c)
- Mediastinal and/or pleural fluid are commonly present in association with mediastinal masses, resulting in further border effacement of intrathoracic structures. With large cranial mediastinal masses combined with pleural effusion, the mass and the cardiac silhouette are often completely obliterated by fluid. However, if caudal displacement of the carina is present (caudal to the sixth intercostal space), a diagnosis of cranial mediastinal mass can still be made
- Additional positional views, such as standing lateral or erect DV/VD views, using a horizontal beam may be useful to differentiate a mass from fluid (see also Chapter 13)

Causes	Radiological signs	Additional information	Image
Craniodorsal			
<p>Oesophageal diseases Tumours of neural or neuroendocrine origin Paravertebral or vertebral tumours Aortic aneurysm Exceptional location of chemodectoma or thymoma</p>	<p>Trachea depressed ventrally and to the right Silhouette sign with aorta Can be very difficult to see unless mineralized or very large</p>	<p>Oesophageal abnormalities should be looked for Vertebral abnormalities including, ventral new bone formation and a widened intervertebral foramen should be looked for</p>	 <p data-bbox="1393 762 1944 790">Craniodorsal oesophageal mass in a 10-year-old male Border Collie.</p>
Cranioventral			
<p>(Rule out obesity) Lymphoma Thymic lesions (thymoma, thymic lymphosarcoma, thymic branchial cyst, thymic haematoma (has been reported secondary to anticoagulant toxicity in juvenile dogs), thymic hyperplasia, thymic amyloidosis) Cranial sternal lymph node enlargement Mediastinal cysts (most common location) Ectopic thyroid and parathyroid tumours Chemodectoma Pericardial cyst Mediastinal haemorrhage</p>	<p>Trachea elevated \pm compressed Increase in soft tissue opacity in cranioventral thorax with loss of radiolucent space cranial to heart Widening of cranial mediastinum Caudal displacement of heart and carina Caudal displacement \pm compression of cranial lung lobes</p>	<p>Paraneoplastic disease may occur in association with thymoma; megaesophagus secondary to myasthenia gravis in dogs; exfoliative dermatitis in cats</p>	 <p data-bbox="1393 1324 2004 1351">An 11-year-old neutered male Domestic Shorthair cat with a large thymoma.</p>

Causes	Radiological signs	Additional information	Image
Perihilar			
<p>Chemodectoma or other heart base tumour Perihilar lymphadenopathy (lymphosarcoma, metastatic disease, fungal disease, tuberculosis, nocardiosis, actinomycosis) Vascular or cardiac enlargement mimicking a mass (pulmonary artery, aorta, atrial mass) Bronchogenic cysts Oesophageal foreign body</p>	<p>Increased perihilar opacity, often poorly defined Peripheral displacement of heart base structures Accentuated ventroflexion of distal trachea Impingement and displacement of carina and principal bronchi ± lung lobe collapse if complete Bronchial obstruction Often widened caudal mainstem bronchi on DV/VD (see Figure 8.10)</p>	<p>Enlarged lymph nodes elsewhere may support lymphadenomegaly as the cause of the perihilar mass effect</p>	 <p>Enlarged perihilar lymph nodes in a 5-year-old Domestic Shorthair cat with mycobacterial disease.</p>
Caudodorsal			
<p>Oesophageal lesions Neural tumours Hiatal hernia Peritoneopericardial diaphragmatic hernia (PPDH) Migrating foreign bodies Diaphragmatic lesions (abscess, mass, haematoma)</p>	<p>Widening of caudal mediastinum Displacement of oesophagus or impingement on lumen Silhouette sign with diaphragm</p>		 <p>A paraspinal sarcoma in an 8-year-old Rottweiler bitch. The lesion was destructive and entered the spinal canal.</p>

8.27 (continued) Mediastinal masses: sites, causes and main radiological signs. (continues)

Causes	Radiological signs	Additional information	Image
Caudoventral			
Hernias (PPDH, hiatal less common) Traumatic rupture Pericardial cyst Diaphragmatic mass lesions (abscess, mass, haematoma)	Displacement or impingement of the CdVC Border obliteration or effacement with caudal border heart \pm diaphragm	Diaphragmatic hernia and rupture – the abdomen and diaphragm should be closely examined	 <p data-bbox="1384 871 2040 919">A ventrally located diaphragmatic rupture in a neutered male 5-year-old mixed breed dog.</p>
Any mediastinal location			
Abscess Granuloma (including secondary to migrating foreign body) Haematoma Primary mediastinal tumours (e.g. haemangiosarcoma, fibrosarcoma, histiocytic sarcoma, lipoma, squamous cell carcinoma, etc.) Pleural tumours Bronchial tumours	Displacement of adjacent structures (depending on location)		

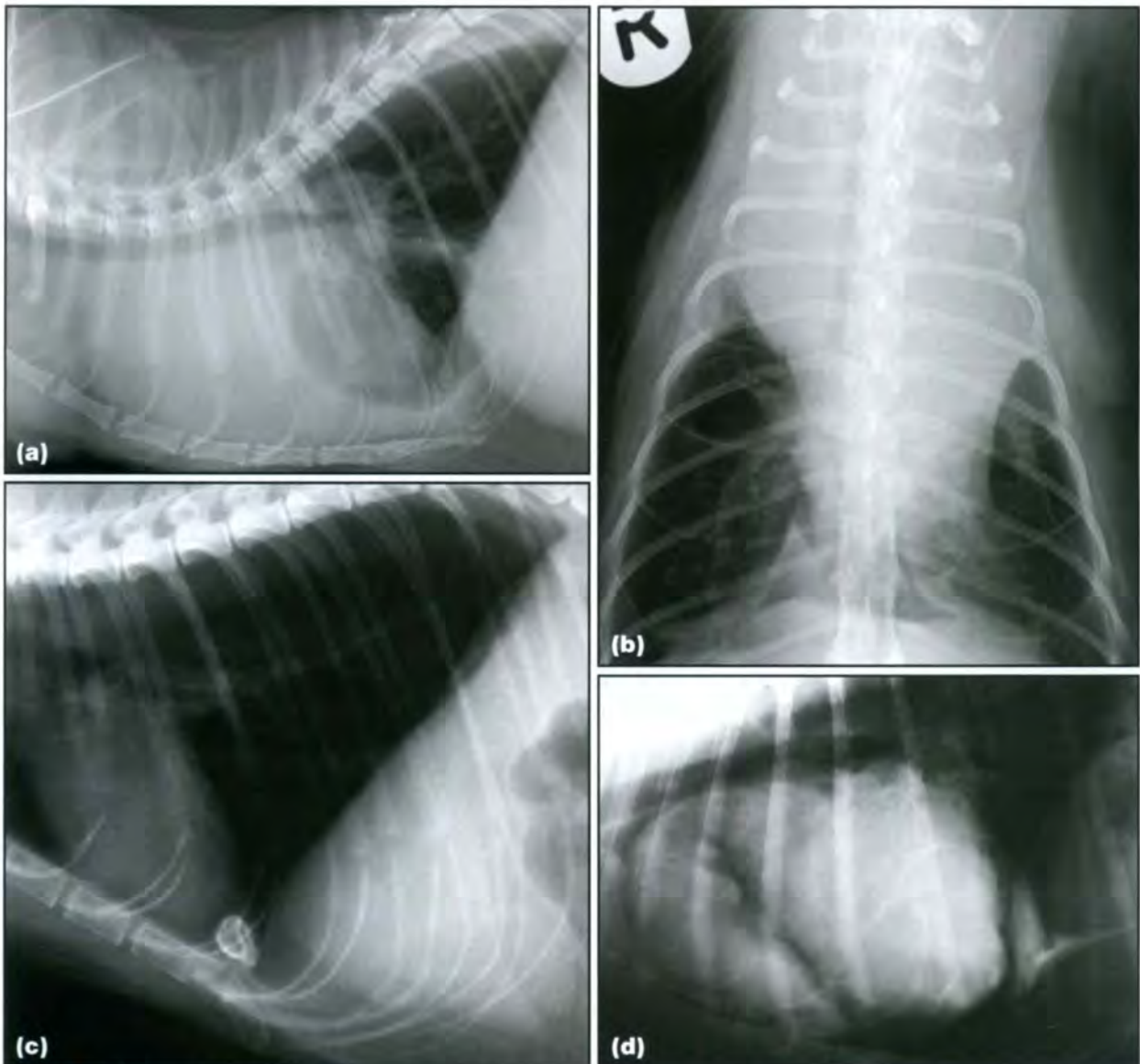
8.27 (continued) Mediastinal masses: sites, causes and main radiological signs.

- The accessory lobe sits in a pleural reflection that can become filled with fluid in pleural effusion. This can make it difficult to differentiate caudal mediastinal masses from loculated pleural fluid or accessory lobe or diaphragmatic masses
- Mediastinal haemorrhage can lead to haematoma formation with mass effect. Its margins can be somewhat moulded to the mediastinal border, which helps to distinguish it from other mediastinal masses (Figure 8.28d)
- Additional pathology, such as megaesophagus (may suggest thymoma with paraneoplastic myasthenia gravis) or abdominal lymphadenopathy and hepatosplenomegaly (may suggest lymphoma), should be looked for.

Further imaging techniques, such as contrast studies, ultrasonography and CT, may be required to try to identify the site of the lesion.

Contrast studies:

- Oesophagography may identify involvement or displacement of the oesophagus.
- Angiography may be useful to delineate masses or identify vascular invasion, malformation or involvement.
- Positive-contrast peritoneography may be performed to investigate cases of suspected PPDH or diaphragmatic rupture or hernia.



8.28 (a) Lateral and (b) DV thoracic views of a 3-year-old Siamese cat with thymic lymphosarcoma. The hilar lymph nodes are enlarged and a small volume pleural effusion is also present. The origin of the mass is clearly mediastinal on the DV view as it is located in the midline and displaces both left and right cranial lung lobes caudally and abaxially. The carina is displaced to the seventh intercostal space, indicating caudal cardiac displacement. (c) Lateral thoracic radiograph of a Himalayan cat with nodular fat necrosis in the retrosternal fat deposit in the caudoventral mediastinum. The eggshell-like mineralization is a typical feature of these incidental lesions that are more commonly seen in the peritoneal space. (d) Lateral thoracic radiograph of a dog that was involved in a road traffic accident, causing mediastinal haematoma formation and pneumothorax. The mediastinal haematoma can be seen as an irregular soft tissue mass filling out the cranial and caudoventral mediastinum. The trachea is deviated dorsally by the haematoma.

These procedures have now been largely superseded by ultrasonography.

Ultrasonography

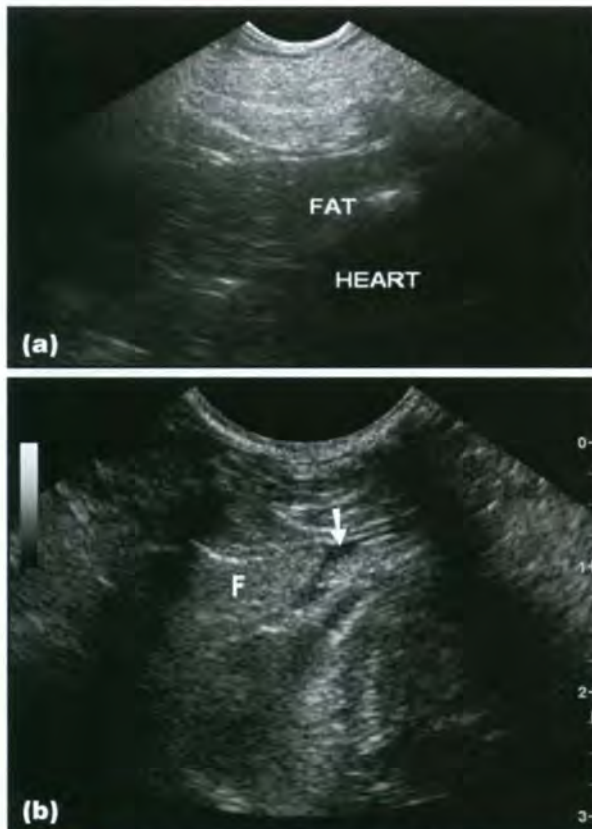
Ultrasonography is invaluable in assessing mediastinal masses, particularly those located in a cranioventral position where a suitable transthoracic acoustic window can be accessed. The caudal mediastinum is harder to image with ultrasonography, but a subcostal, or parasternal, approach may be successful. Assessment can be made of the echogenicity and margination of the mass, and any involvement of the other mediastinal structures. Mediastinal origin of a mass may be confirmed by identifying movement of the right and left lung lobes over the static mass.

Ultrasonography allows guided FNA or biopsy techniques to be performed for cytological diagnosis, and hence appropriate treatment to be instigated. It is essential to obtain a coagulation profile before performing a biopsy. It should be remembered that the mass may represent a large mediastinal blood clot in a coagulopathic animal.

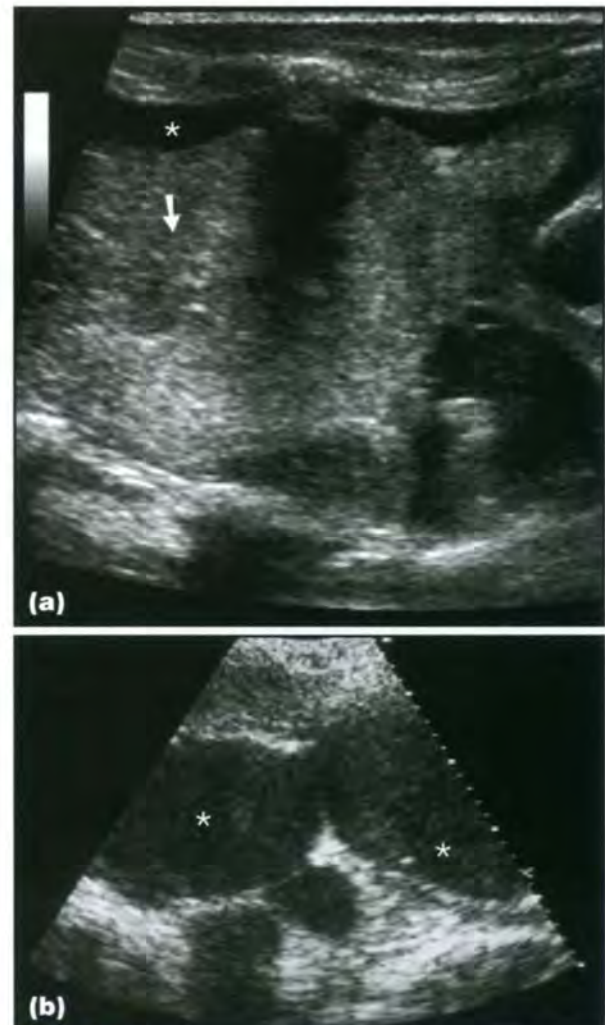
Ultrasonography is also particularly helpful in distinguishing cranial mediastinal fat or fluid from a true mass:

- Fat has a characteristic hyperechoic and hyperattenuating appearance and usually surrounds but does not displace vessels (Figure 8.29)
- Effusion will usually be anechoic (see below)
- Masses vary in appearance but are often hypoechoic compared to fat, displace mediastinal vessels, may have central vasculature identified with colour Doppler and may be accompanied by effusion (Figure 8.30).

It is not possible to confirm definitively the cause or origin of a mediastinal mass using ultrasonography; many masses appear identical on ultrasound scans.



8.29 The appearance of mediastinal fat on ultrasonography. **(a)** Dorsal image of the cranial mediastinum of a 6-year-old Cocker Spaniel in obese body condition. The hypoechoic cardiac chambers are labelled (heart). Cranial to the heart and distal to the thickened, hyperechoic thoracic wall is a large amount of homogenous tissue with a coarse echotexture, representing mediastinal fat. **(b)** Dorsal view of the cranial thorax of a 9-year-old neutered Maltese. There is hyperechoic tissue (F) with a triangular shape present cranial to the heart, the tip is surrounded by a very small amount of pleural effusion (arrowed). Mediastinal fat was suspected and confirmed by fine-needle aspirates. (Courtesy of G. Seiler)



8.30 **(a)** Dorsal image of the cranial thorax of a spayed female 10-year-old Domestic Shorthair cat. A large heterogenous mass (arrowed) is seen cranial to the heart in the cranial mediastinum. The mass is surrounded by bilateral pleural effusion (★). Carcinoma with haemorrhage was diagnosed on biopsy of this mass. (Courtesy of G. Seiler) **(b)** Cranial mediastinum of a neutered 5-year-old Flat-Coated Retriever bitch with a round cell sarcoma. A lobulated mass is identified (★). Enlarged mediastinal lymph nodes are also present.

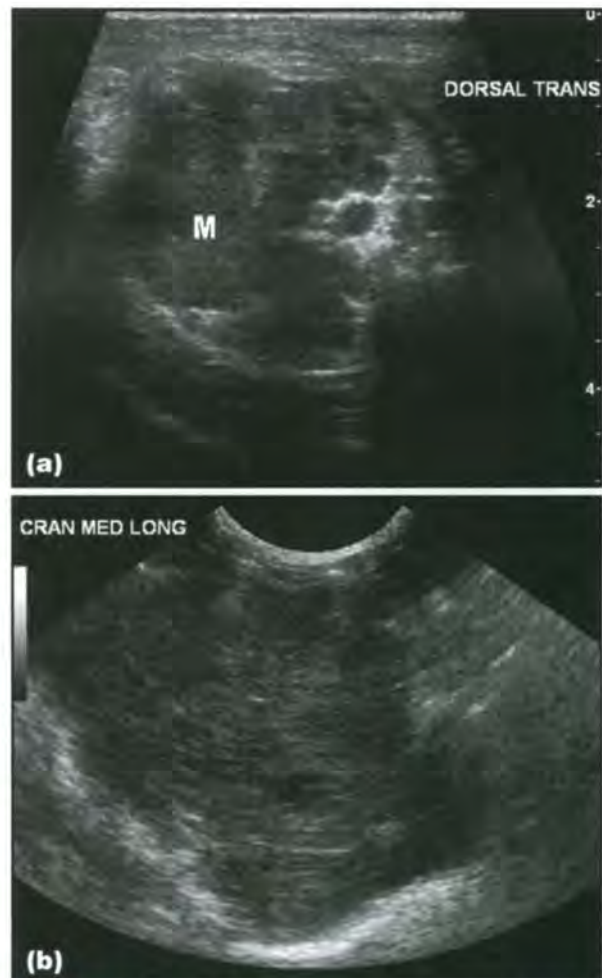
Biopsy remains the gold standard; however, certain ultrasonographic features may be useful in narrowing the differential list:

- Mediastinal lymph node enlargement and lymphoma:
 - Lymphoma may be represented by a number of enlarged nodes or a focal mass, often thymic in origin
 - Cranial mediastinal and presternal lymph nodes are usually easily identified as hypoechoic nodular masses surrounding the mediastinal vessels (Figure 8.31). They may occasionally be cystic or heterogenous
 - Multicentric lymphoma is also the most common cause of caudal mediastinal mass lesions. This region is harder to interrogate ultrasonographically
 - Certain ultrasonographic features may be more suspicious for malignant neoplasia rather than reactive nodal change. These require further investigation in animals but include abnormal size and shape, abnormal (non-hilar) angioarchitecture, altered echogenicity of the hilus and evidence of nodal necrosis. Contrast harmonic ultrasonography shows potential for the evaluation of malignant nodes
 - FNA often provides confirmation of the diagnosis, without the need for biopsy.
- Thymoma:
 - Ultrasonographic appearance may vary, and may look identical to thymic lymphoma (Figure 8.32)
 - Large thymomas are often echogenic with small to large cystic regions
 - Small thymomas may mimic abnormal lymph nodes
 - On occasion, thymomas may invade the CrVC.
- Oesophageal lesions: rarely, it is possible to identify an oesophageal mass lesion ultrasonographically (see Chapter 9). This is facilitated by the presence of pleural effusion, and a transhepatic route usually provides the best acoustic window



8.31 Dorsal view of the cranial thorax of a neutered male 5-year-old Domestic Shorthair cat. The cranial mediastinum is hyperechoic (fat) but several hypoechoic nodular structures are seen within it, representing enlarged cranial mediastinal lymph nodes (arrowed). There is a thin layer of pleural effusion present along the thoracic wall; small pockets of fluid may also be present within the mediastinum. (Courtesy of G. Seiler)

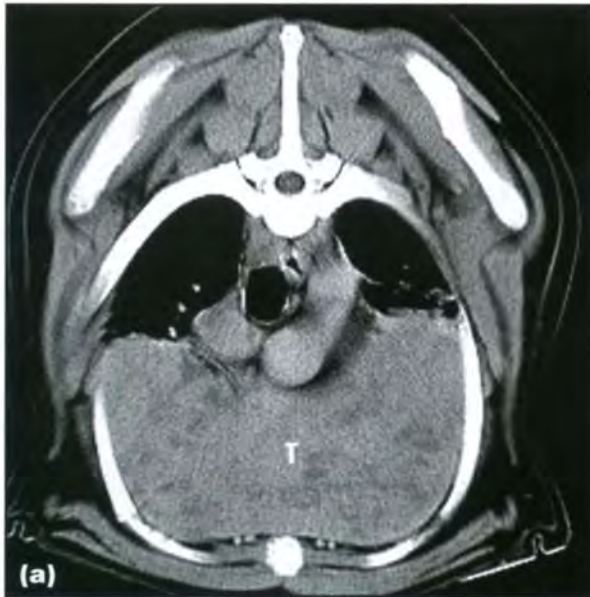
- Mediastinal cyst (see below)
- Mediastinal haematoma:
 - Varies greatly in appearance over time since haemorrhage occurred
 - A simple haematoma is avascular and usually shows ultrasonographic resolution with time
 - The presence of central vasculature within the mass suggests the presence of an underlying haemorrhagic lesion, i.e. the mass is not purely a large haematoma
 - Often co-existing effusion is present.



8.32 (a) Transverse left intercostal view, dorsal is to the right. A large, hypoechoic, lobulated mass occupies the cranioventral thorax (M). The mediastinal vessels are seen as round hypoechoic structures in the dorsal mediastinum and are partially surrounded by the mass. Ultrasound-guided biopsy of the mass led to the diagnosis of thymoma. (b) Dorsal view of the cranial mediastinum. The cranial mediastinum is filled by a hypoechoic, lobulated mass which was subsequently diagnosed as thymoma. (Courtesy of G. Seiler)

Computed tomography

CT is very useful in the diagnosis and evaluation of mediastinal masses (Figure 8.33). It provides further information on a radiographically identified mass and can also allow identification of a mass not seen or only suspected on standard radiographs. CT potentially allows distinction between tumours, abscesses, cysts and haematomas.



8.33 (a) CT image at the level of the fifth intercostal space of a spayed 7-year-old Labrador Retriever bitch with a thymoma (T) (window width 300 HU, window level 50 HU). (b) Post-contrast CT image at the level of the fifth intercostal space of a neutered male 5-year-old crossbreed with a thymoma (T) (window width 300 HU, window level 50 HU). Pleural effusion (P) is also present.

Biopsy remains the gold standard and CT-guided biopsy (Figure 8.34) may be performed in masses that are not amenable to biopsy under ultrasound guidance. CT is also extremely useful to guide surgical intervention or radiation therapy.

Intravenous contrast medium should be administered, unless there is a clinical contraindication. Pre- and post-contrast techniques allow assessment of the margins and vascularity of the lesion and the association between the mass and the vessels within the mediastinum, allowing differentiation between masses that are locally invasive and those which are merely space-occupying.



8.34 CT image at the level of the seventh intercostal space of a spayed 2-year-old Dogue de Bordeaux bitch with lymphoma, undergoing CT-guided biopsy of this lesion (window width 2000 HU, window level -500 HU). The needle (N) is shown within the skin and from this position is advanced further into the mass (see also Chapter 3).

CT angiography with a rapid injection pump will allow assessment of both arterial supply and venous drainage and facilitate surgical planning.

Tumour staging may be carried out, with assessment of local lymphadenopathy.

Scintigraphy

Scintigraphy using sodium ^{99m}Tc -pertechnetate or iodine-123 can be used to identify neoplastic ectopic thyroid tissue. Radionuclide uptake in the mass is indicative of thyroïdal origin of the tissue (Figure 8.35).



8.35 Right lateral (shown on left) and ventral (shown on right) images of the head, neck and cranial thorax of a 12-year-old hyperthyroid Domestic Shorthair cat, obtained 20 minutes after intravenous injection of sodium ^{99m}Tc -pertechnetate. Thoracic radiographs obtained prior to the study revealed an ill defined cranial mediastinal mass. On the scintigraphic images there is a focus of uptake associated with the right thyroid lobe, much higher in intensity than the salivary glands. The left thyroid lobe is not visible. A second intense focus of uptake is seen in the thorax, corresponding to the lesion seen on radiographs. Final diagnosis was hyperthyroidism with ectopic hyperfunctioning thyroïdal tissue in the cranial mediastinum. (Courtesy of F. Morandi)

Larger and more intense masses are more likely to be malignant (ectopic thyroid carcinoma or metastatic thyroid carcinoma infiltrating cranial mediastinal lymph nodes). Smaller and less intense masses may also represent hyperfunctioning ectopic thyroid tissue (especially in hyperthyroid animals or animals that have previously undergone thyroidectomy). Evaluation of the scintigram in light of the animal's history and hormonal status is mandatory; a biopsy sample is needed for definitive characterization of benign *versus* malignant disease.

Scintigraphy performed with indium-111 labelled white blood cells may be used to identify occult abscesses.

Cysts

A variety of mediastinal cysts may occur in cats and less frequently in dogs. These include cysts of pleural, bronchial, thymic, lymphatic, bronchogenic and neoplastic origin. Mediastinal cysts are often benign incidental findings, though compressive effects may be present. It should also be noted that occasionally cyst rupture may lead to chronic mediastinitis.

Idiopathic mediastinal cysts are commonly seen in older cats. These are usually solitary mass lesions in the cranioventral mediastinum and are benign and asymptomatic, unless very large. The contents are usually of low cellularity and aspiration is usually unnecessary.

In dogs, large fluid-filled cystic structures are occasionally identified in the caudal mediastinum. The exact origin of these cysts cannot always be determined, but paraoesophageal abscessation, cystic lung tumours or parasitic cysts should be considered.

Radiography

Findings are as for other mediastinal masses.

- A cranioventral location is most common.
- Small idiopathic mediastinal cysts in cats may appear as faint, barely visible soft tissue opacities on a lateral view cranial to the heart (Figure 8.36a).

Ultrasonography

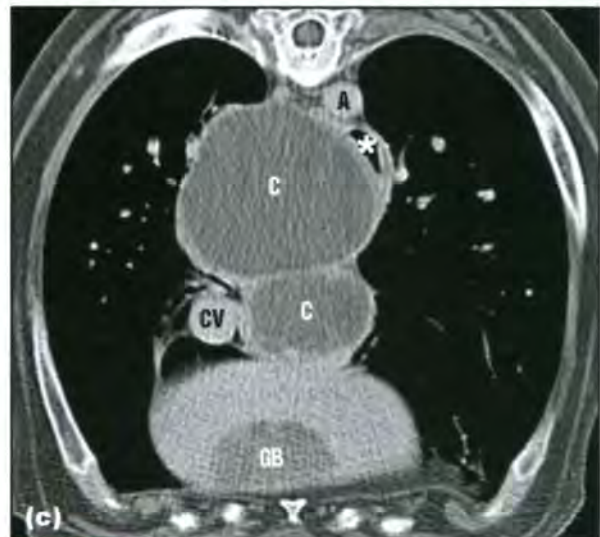
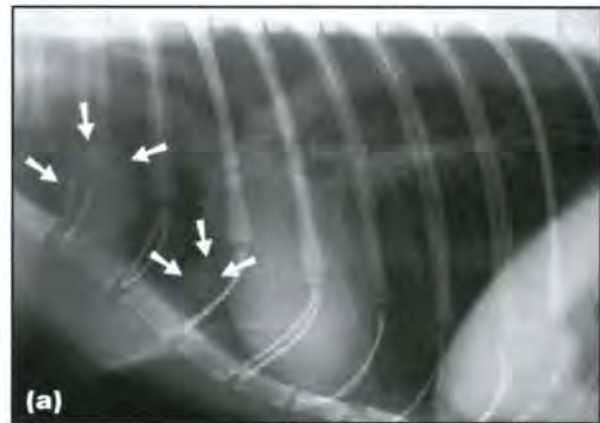
Findings are diagnostic for a cystic lesion (see Figure 8.36b):

- Thin-walled anechoic structure(s)
- Complex cysts may have a more echogenic fluid content
- Beware of cysts associated with neoplasia (such as cystic thymoma).

Computed tomography

Findings are diagnostic for cystic lesions (see Figure 8.36c):

- Thin-walled fluid-filled structure
- Contrast-enhancing rim
- CT-guided aspiration can be performed.



8.36 (a) Left lateral thoracic radiograph of a 12-year-old Siamese cat with two small cranial mediastinal cysts (arrowed). (b) Dorsal view of the cranial thorax (cranial to the heart) of a spayed female 12-year-old Domestic Shorthair cat. On radiographs a round soft tissue opacity was seen cranial to the cardiac silhouette. Ultrasonographically an anechoic fluid-filled structure separated into two cavities by a thin septum was found and a mediastinal cyst was diagnosed. (Courtesy of G. Seiler) (c) CT image of the caudal mediastinum of an 11-year-old St Bernard with two large fluid-filled cystic structures (C) in the caudal mediastinum wedged between the caudal vena cava (CV), oesophagus (★) and aorta (A). Final diagnosis was cystic adenocarcinoma arising from the accessory lung lobe. GB = Gallbladder.

Effusion

Mediastinal effusion or fluid is uncommon. Effusions include pus, lymph, blood, chyle, transudate and modified transudate.

In chylopleuritis, effusion from the thoracic duct will initially be limited to the mediastinum, but the fluid has usually entered the pleural space by the time the animal shows clinical signs.

Haemomediastinum may result from trauma. This may occur due to bleeding from one of the great vessels (usually rapidly fatal) or the haemorrhage may extend into the mediastinum from trauma to the neck. Other causes of mediastinal haemorrhage include coagulopathy, neoplastic erosion of vessels and, rarely, rapid involution of the thymus (which is usually fatal).

Oesophageal perforation results in mediastinitis, and initially small volumes of fluid may distribute evenly throughout the mediastinum.

Some neoplastic masses may produce a modified transudate.

Radiography

A DV view is the most useful:

- Reverse fissures are visible at the heart base
- Some widening of both the cranial mediastinum and the caudoventral mediastinal reflection is seen.

On the lateral view, the apex of the heart and the cranioventral mediastinal reflection may be obscured, but changes may be minimal.

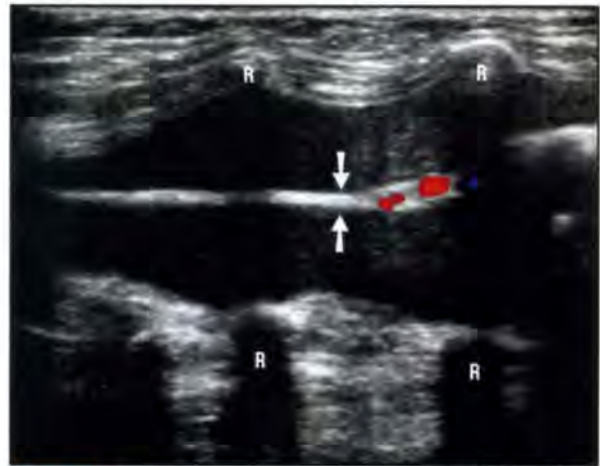
Ultrasonography

Ultrasonography has limited use in the presence of small volumes of fluid due to the difficulty in locating a suitable acoustic window. It may be useful to guide sampling techniques. It can be difficult to differentiate pleural and mediastinal fluid just on the basis of ultrasonography. However, this distinction is easier in the cranial thorax where more typical appearances are identified:

- Fluid in the pleural space of the cranial thorax is visualized as two discrete pockets separated by the narrow mediastinal pleura (Figure 8.37)
- Cranial mediastinal fluid causes a widened mediastinum and the mediastinal vessels are separated from fat by irregularly shaped fluid pockets.

Computed tomography

CT is much more sensitive for small volumes of mediastinal fluid and also allows identification of pocketed fluid. CT numbers can be measured, which may provide useful additional information about the nature of the fluid, particularly if a sample is unobtainable. Altering the position of the animal (e.g. sternal *versus* dorsal recumbency) and repeating a CT sequence will assist in displacing fluid, allowing better evaluation of co-existing lesions.



8.37 Dorsal view of the ventral aspect of the cranial mediastinum of a 3-year-old cat with a moderate pleural effusion. The entire width of the cat is included in the image. Note the ribs (R) on the left and right. The cranial mediastinum is seen as a narrow echogenic band (between arrows) between the left and right pleural spaces which are filled with an anechoic effusion. Note the small blood vessels identified within the mediastinum with colour Doppler.

Mediastinitis

Mediastinitis implies infection or inflammation in the mediastinum and results in thickening of the mediastinal pleurae and exudate production. It can develop from a primary disease process, such as chronic fungal (*Histoplasma* or *Cryptococcus* species) or bacterial (including *Actinomyces* and *Nocardia* species) granulomatous mediastinitis. Spirocercosis has also been associated with mediastinitis (see Chapter 9).

Mediastinitis may also occur secondary to perforation of the trachea or oesophagus, or as an extension of an infectious or inflammatory process from the cervical soft tissue, pericardium, pulmonary parenchyma or pleural space. The most common cause is oesophageal perforation.

Clinical features may include tachypnoea, dyspnoea, pain, cough, regurgitation, voice change (secondary to recurrent laryngeal nerve involvement) and head and neck swelling.

Radiography

- Widening and perhaps increase in opacity of the mediastinum may be seen, particularly on the DV/VD view.
- If the inflammation is focal then discrete thickenings or mass lesions may be seen, which must then be differentiated from neoplastic mediastinal masses.
- Pneumomediastinum may be present if the mediastinitis is secondary to tracheal or oesophageal perforation.

Contrast studies: If oesophageal perforation is suspected then oral administration of a small volume (5–10 ml) of non-ionic water-soluble iodine-containing

contrast medium, such as iohexol, may identify the site. Both lateral and DV/VD views should be taken to look for evidence of extravasation of the contrast medium. If no extravasation is seen on initial films then repeat films should be taken 5–10 minutes later to look for slow leakage.

In cases of chronic oesophageal perforation, the original perforation may have closed and no contrast leakage will be evident.

Ultrasonography

The usefulness of ultrasonography depends on the site and extent of the mediastinitis and whether or not any fluid or pleural thickening is loculated or focal. Appearance of mediastinitis includes:

- Gross thickening and increased echogenicity of the mediastinal pleurae, and small to moderate amounts of echogenic fluid
- Enlarged lymph nodes and free gas may also be identified.

Computed tomography

As with mediastinal fluid, CT is very sensitive to small volumes of exudate or subtle thickening of the mediastinum. Small volumes of mediastinal gas are easily seen when present. Contrast-enhanced CT images should show areas of inflammation or necrotic areas to allow the extent of the disease to be assessed.

Mediastinal oedema

Mediastinal oedema may accompany any condition that produces oedema elsewhere. It is often overlooked due to the concurrent presence of mediastinal effusion, but may be more readily recognized now that CT and MRI are more commonly used to evaluate the mediastinum.

References and further reading

- Henninger W and Gutmannsbauer B (1998) CT-anatomy of the canine mediastinum. Oral presentation at EAVDI Annual Conference, Sweden. *Veterinary Radiology and Ultrasound* **40**, 191
- Prather AB, Berry CA and Thrall DE (2005) Use of radiography in combination with computed tomography for the assessment of non-cardiac thoracic disease in the dog and cat. *Veterinary Radiology and Ultrasound* **46**, 114–122
- Reichle JK and Wisner ER (2000) Non-cardiac thoracic ultrasound in 75 feline and canine patients. *Veterinary Radiology and Ultrasound* **41**, 154–162
- Samii VF, Biller DS and Koblik PD (1998) Normal cross-sectional anatomy of the feline thorax and abdomen: comparison computed tomography and cadaver anatomy. *Veterinary Radiology and Ultrasound* **39**, 504–511
- Smallwood JE and George TF (1993) Anatomic atlas for computed tomography in the mesocephalic dog: thorax and cranial abdomen. *Veterinary Radiology and Ultrasound* **34**, 65–84
- Suter P (1984) *Thoracic Radiography*. Peter F. Suter, Wettswil, Switzerland
- Thrall DE (2002) The mediastinum. In: *Textbook of Veterinary Diagnostic Radiology, 4th edn*, ed. DE Thrall, pp. 376–389. WB Saunders, Philadelphia
- Yoon J, Feeney DA, Cronk DE, Anderson KL and Ziegler LE (2004) Computed tomographic evaluation of canine and feline mediastinal masses in 14 patients. *Veterinary Radiology and Ultrasound* **45**, 542–546
- Zekas LJ and Adams WM (2002) Cranial mediastinal cysts in nine cats. *Veterinary Radiology and Ultrasound* **43**, 413–418

The oesophagus

Wencke M. Wagner

Radiographic anatomy

The oesophagus is a tubular structure connecting the pharynx to the stomach, and is bound at each end by a sphincter. The cranial sphincter is composed of the paired thyropharyngeal and cricopharyngeal muscles. The caudal sphincter is complex and comprises the following:

- Focal thickening of the muscular part of the oesophageal wall
- Interdigitating gastric rugal folds
- A sling formed by the deep oblique smooth muscle of the lesser gastric curvature and the right diaphragmatic crus
- The acute angle of entrance into the gastro-oesophageal junction
- Positive intra-abdominal pressure compressing the intra-abdominal section of the oesophagus.

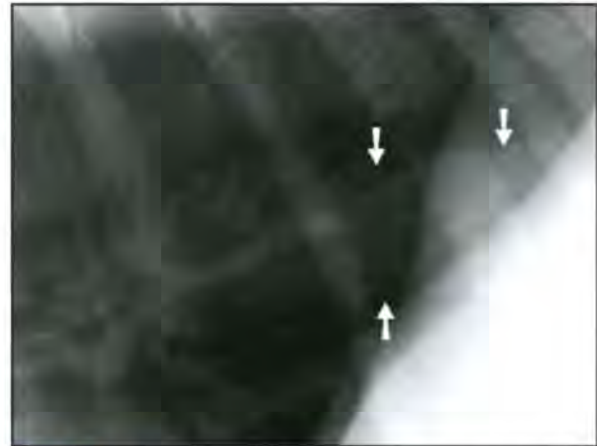
The oesophageal wall is composed of four layers: mucosa, submucosa, muscularis and serosa. The muscularis is a striated muscle in the dog, but in the cat the caudal third is a smooth muscle with the overlying mucosa having characteristic herringbone-like folds.

Thoracic (including the stomach area) and cervical (including the pharyngeal area) radiographs should be obtained in all animals suspected of having oesophageal disease. The oesophagus is located in the dorsal mediastinum, slightly to the left of the midline. It is rarely visible on survey radiographs, although occasionally a portion of it may be visible on the left lateral view as a poorly defined, tubular, faint soft tissue opacity between the heart base and the diaphragm (Figure 9.1).

The oesophagus may become visible in animals with pneumomediastinum. It may also be seen in emaciated animals with a deep, narrow thoracic conformation.

Small amounts of oesophageal air may be recognized in normal animals, secondary to aerophagia, dyspnoea, excitement or sedation. Air tends to accumulate at four sites in the oesophagus:

- As a triangular gas opacity in the most proximal cervical oesophagus
- Cranial to the first rib
- Between the first rib and the heart, dorsal to or superimposed on the trachea



9.1 Left lateral view of the dorsocaudal thorax of a 9-year-old Rottweiler bitch. Note the faintly visible tubular soft tissue opacity of the oesophagus (arrowed). This can be a normal finding on left lateral radiographs, particularly in deep-chested dogs.

- Caudal to the heart, between the aorta and the caudal vena cava (CdVC).

General anaesthesia may cause marked generalized dilation of the normal oesophagus, mimicking megaesophagus. Further studies may be warranted in animals with clinical signs of oesophageal disease and oesophageal air visible on survey radiographs.

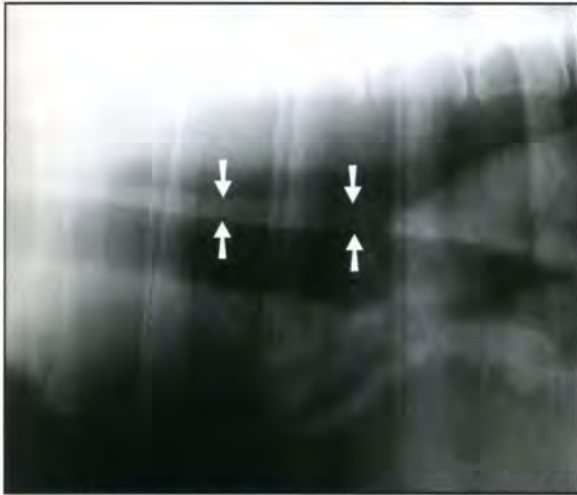
The absence of abnormal oesophageal findings on survey radiographs does not preclude the presence of oesophageal disease. Secondary signs of oesophageal disease should be looked for. These include:

- Pneumomediastinum
- Ventral displacement of trachea
- Tracheal stripe sign
- Mediastinitis
- Pleural effusion
- Aspiration pneumonia
- Hypertrophic osteopathy.

Interpretive principles

Tracheal stripe sign

The tracheal stripe sign (Figure 9.2) is also known as the tracheal band or tracheo-oesophageal stripe sign. The draping of the ventral wall of the



9.2 Right lateral view of the dorsocranial thorax of an 8-year-old male Dalmatian. Note the summation of the dorsal tracheal wall and draping of the ventral wall of the oesophagus, resulting in a soft tissue stripe called the tracheal stripe sign (arrowed), indicative of gas in the oesophagus.

oesophagus over the dorsal tracheal wall results in border effacement of the two walls. The tracheal stripe sign indicates oesophageal luminal air. Care should be taken not to confuse a tracheal stripe sign with a pneumomediastinum, where mediastinal gas may surround the external surface of the oesophagus (see Chapter 8).

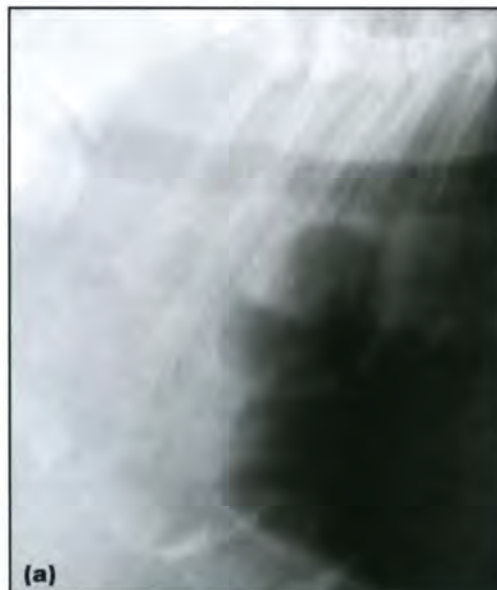
Redundant oesophagus

This is an occasional incidental finding. It is usually identified as a ventral, but occasionally lateral, deviation of the oesophagus in the thoracic inlet area in mainly young brachycephalic breeds, especially English Bulldogs (Figure 9.3) and Shar Peis. It has also been described in the cat.

Contrast radiography

The technique for oesophagography and the choice of contrast media are described in Chapter 1.

9.3 Right lateral view of the cranial thorax of a 6-year-old male English Bulldog. **(a)** Note the tortuous path (gas opacity) of the oesophagus in the thoracic inlet area. It represents a redundant oesophagus and is an incidental finding in this breed. **(b)** A small amount of contrast medium helps visualize the ventral deviation of the oesophagus.



The different muscular anatomy of the canine and feline oesophagus creates specific appearances following contrast medium administration. The canine oesophagus has a longitudinal linear pattern on positive contrast studies (Figure 9.4). In the cat the smooth muscle of the terminal third of the oesophagus creates a striated herringbone appearance (Figure 9.5).



9.4 Normal oesophagram of a mature dog. Note the longitudinal linear pattern of barium trapped between the mucosal folds.



9.5 Normal oesophagram of a mature cat. The cranial section of the thoracic oesophagus has the same longitudinal contrast medium pattern as that of the dog (see Figure 9.4); however, the caudal section of the thoracic oesophagus consists of smooth muscle, which throws the mucosa into a characteristic striated herringbone appearance.

It is important to understand normal oesophageal function. Contrast medium usually proceeds rapidly through the oesophagus. Primary peristalsis is generated in the pharynx and carries a bolus aborally to the lower oesophageal sphincter. If primary peristalsis fails to propel the bolus to the stomach, then a secondary peristaltic wave is quickly generated by intraluminal distension and complete transport of the bolus to the stomach occurs. Transit time of the bolus is longer in cats than in the dog.

Diseases

Megaesophagus

Megaesophagus is strictly a descriptive term and simply indicates dilatation of parts (segmental) of or the entire (generalized) oesophagus. The condition may be congenital (uncommon) or acquired (common). The greatest challenge is to determine the cause.

A familial predisposition for congenital megaesophagus has been suggested in the Irish Setter, Great Dane, German Shepherd Dog (Figure 9.6), Labrador Retriever, Chinese Shar Pei, Newfoundland, Miniature Schnauzer and Wirehaired Fox Terrier. Congenital segmental oesophageal dysfunction has been reported in Shar Peis and Newfoundland Retrievers. German Shepherd Dogs, Golden Retrievers and Irish Setters have been reported to have an increased risk for developing acquired megaesophagus. Congenital megaesophagus in cats is rare, but Siamese cats may be predisposed.

The underlying cause of acquired megaesophagus is often unidentified (idiopathic), although it may be secondary to one of many possible causes (Figure 9.7). Early diagnosis and elimination of predisposing diseases are essential for successful management because prolonged dysfunction can cause irreversible distension. Adult-onset idiopathic megaesophagus is associated with a poor to grave prognosis. The prognosis for cats with megaesophagus is guarded.

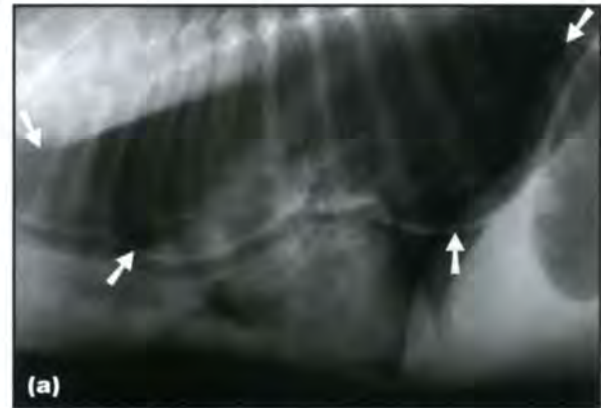
Animals with megaesophagus usually present with regurgitation or may occasionally be asymptomatic. In congenital cases, signs are usually first noticed after weaning.

It is important to note that many animals without oesophageal disease will appear to have a gas-filled, dilated oesophagus on survey radiographs as a result of aerophagia, sedation, general anaesthesia or oesophageal intubation (accidental or oesophageal stethoscope, endoscopy). Care should be taken not to confuse this incidental finding with a genuine megaesophagus. Repeat radiographs should be undertaken in the conscious patient, and a contrast study might be indicated if confusion remains.

Radiography

Findings include:

- Generalized or focal oesophageal dilatation (gas/ingesta)
- Tracheal stripe sign



9.6 Right lateral view of the thorax of a 3-month-old German Shepherd Dog bitch with congenital megaesophagus. **(a)** The survey radiograph illustrates that a markedly gas-distended oesophagus can easily be missed. Several hallmark features for megaesophagus can be detected with close scrutiny: thin soft tissue lines representing the oesophageal wall (arrowed) and ventral depression of the trachea and the cardiac silhouette. Note also the gas-distended stomach. **(b)** Follow-up thoracic radiograph 1 month later. Autocontrast is present within the megaesophagus due to the presence of soaked kibble. Food had accumulated secondarily to the severe loss of oesophageal peristalsis.

Neuromuscular disease

Idiopathic
Myaesthesia gravis
Systemic lupus erythematosus
Polymyositis/myopathy
Glycogen storage disease (type 2)
Dermatomyositis
Distemper virus
Tetanus

Oesophageal obstruction

Neoplasia
Foreign body
Stricture
Vascular ring anomaly

Toxicity

Lead
Organophosphate

9.7 Causes of acquired secondary megaesophagus. (continues)

Other
Hypoadrenocorticism
Hiatal hernia
Gastric dilatation–volvulus syndrome
Oesophagitis
Thymoma

9.7 (continued) Causes of acquired secondary megaesophagus.

- Sharp interface between oesophagus and longus colli muscles
- Rightward and ventral displacement of trachea
- May depress heart base (giving the impression of a small cardiac silhouette)
- Thin, converging soft tissue stripes, representing oesophageal walls, may be the only visible sign in a gas-distended oesophagus. Close scrutiny is required as this sign may be easily overlooked (Figure 9.8)



9.8 VD thoracic radiograph of a 4-year-old Boerboel bitch with an acquired megaesophagus. Note the reduced radiopacity of the dilated craniodorsal and caudodorsal mediastinum due to the gas-filled megaesophagus. It is indented on the left by the aorta and the right by the azygos vein (white arrows). The soft tissue stripes, representing the oesophageal wall, converge at the oesophageal hiatus (black arrows).

- Increased amount of gas in stomach or persistent gaseous gastric distension in the absence of torsion or pyloric obstruction
- Aspiration pneumonia is a common complication.

Contrast studies: These are required if the oesophagus is not identified on survey radiographs. Contrast medium defines the degree of oesophageal dilatation, the lack of function, the extent of involvement and structural abnormalities and helps evaluate the lower oesophageal sphincter region (Figure 9.9). Barium mixed with food ('barium burger') usually provides the best depiction of oesophageal abnormalities. In mild cases the oesophagus is marginally to slightly widened, allowing some pooling of barium (regular tube-like or irregular in outline).

There is a risk of aspiration pneumonia.



9.9 Right lateral view of the thorax of a 3-month-old Irish Setter puppy with congenital megaesophagus. Oral contrast medium mixed with a small amount of soft food has been used to distend the oesophagus. This procedure was used to rule out a vascular ring anomaly. The risks of aspiration should be considered before undertaking this procedure.

Fluoroscopy with contrast medium

This is indicated for early, mild or segmented disease and oesophageal motility evaluation. In early disease, the oesophagus is not dilated but rather has a decreased propulsive ability.

Scintigraphy

This is useful to identify those animals with subtle oesophageal motility abnormalities and consistent clinical signs but with no identifiable abnormality on routine diagnostic imaging. ^{99m}Techneium sulphur colloid is generally used.

Oesophagitis

Oesophagitis can be caused by gastro-oesophageal reflux (GER), trauma, foreign bodies, ingestion of caustic substances, structural abnormalities (hiatal hernia, neoplasm) and chronic vomiting. It has been demonstrated to be a risk factor for the development of megaesophagus in dogs. Oral dry administration of tablets (particularly of tetracycline or doxycycline) has been associated with development of oesophagitis in cats.

The presence of GER does not necessarily lead to oesophagitis and may be seen in normal patients. Reflux oesophagitis occurs when acidic gastric content remains within the oesophageal lumen for a prolonged period and fails to be neutralized by bicarbonate. Intra-abdominal surgery (such as ovariohysterectomy), old age and no or prolonged fasting (approaching 24 hours) before anaesthesia are associated with a higher risk of developing reflux oesophagitis.

Once oesophagitis has developed, a vicious cycle can ensue whereby inflammation decreases the tone of the lower oesophageal sphincter, predisposing to GER and further exacerbating inflammation. This may eventually lead to the development of an oesophageal stricture.

The prognosis of patients with uncomplicated oesophagitis tends to be good.

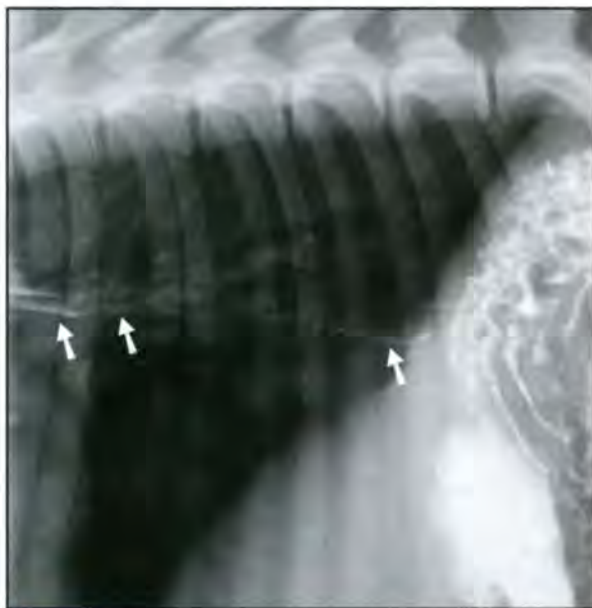
Radiography

This is usually normal. Findings may include generalized or focal oesophageal dilatation (air/ingesta/fluid). Underlying causes (such as hernias, neoplasia or foreign bodies) may be identified.

Contrast studies: These are usually necessary for diagnosis. Findings include:

- Generalized or focal oesophageal dilatation
- Thickened oesophageal wall
- Irregularities of oesophageal mucosa, prominent mucosal striation and prolonged retention of contrast material (Figure 9.10)
- Signs of ulceration, perforation and stricture formation
- Changes are often most evident in the terminal oesophagus.

Contrast studies may sometimes be normal.



9.10 Right lateral view of the dorsocaudal thorax of a 3-month-old Samoyed 1 hour after oral contrast medium was administered. Note the prolonged retention of contrast medium in the terminal oesophagus and irregular outline of the oesophageal wall (arrowed) consistent with oesophagitis.

Fluoroscopy with contrast medium

This is indicated to rule out oesophageal spasticity, GER and anomalies predisposing to the latter. It is more accurate than static contrast studies in the diagnosis of GER.

Oesophageal stricture

Oesophageal strictures are most commonly intraluminal acquired lesions and may occur secondary to trauma or severe inflammation. Typical scenarios include stricture formation (Figure 9.11) secondary to an oesophageal foreign body or reflux oesophagitis under anaesthesia. Strictures due to congenital or extraluminal disease are rare. Examples include perioesophageal fibrosis due to mediastinitis or external compression due to a perioesophageal mass (Figure 9.12). Degrees of oesophageal strictures (and hence prognosis) vary greatly, ranging from a minor reduction in oesophageal diameter with reduced distensibility, to near total closure of the oesophageal lumen. There may be a gradual progression of clinical signs as the stricture worsens.



9.11 Close-up of a right lateral oesophagram of a mature cat with an iatrogenic mid-thoracic oesophageal stricture. It extends over three intercostal spaces. The oesophagus can only distend up to rib width in this area. Note also the pooling of contrast medium cranial to the stricture.



9.12 Oesophagram of a 4-year-old Boerboel bitch with a craniodorsal mediastinal abscess. The resulting large perioesophageal mass (M) produced ventral deviation of the trachea and oesophagus. It also resulted in a perioesophageal stricture, illustrated by the thinned and deviated oesophageal column of contrast medium (arrowed), outlining the ventral extent of the mass.

Patients with severe oesophagitis at the site of stricture, those with long strictures and those with dense, thick mature accumulations of fibrous connective tissue at the stricture site have a more guarded prognosis.

Radiography

This is usually normal. Prestenotic oesophageal dilatation (gas/ingesta) may be seen.

Contrast studies: Positive contrast studies (barium burger) are often needed to confirm the diagnosis of stricture. They are useful in assessing the number, location and length of strictures and the diameter of the narrowed segment. Persistent luminal narrowing on sequential radiographs differentiates the stricture from oesophageal spasm. Prestenotic oesophageal dilatation may be evident. Normal longitudinal striations tend to converge and/or become irregular at the site of injury to the mucosa.

Fluoroscopy with contrast medium

This enables optimal evaluation of the length of strictures and maximal diameter of the narrowed segment, and the assessment of motility.

Ultrasonography

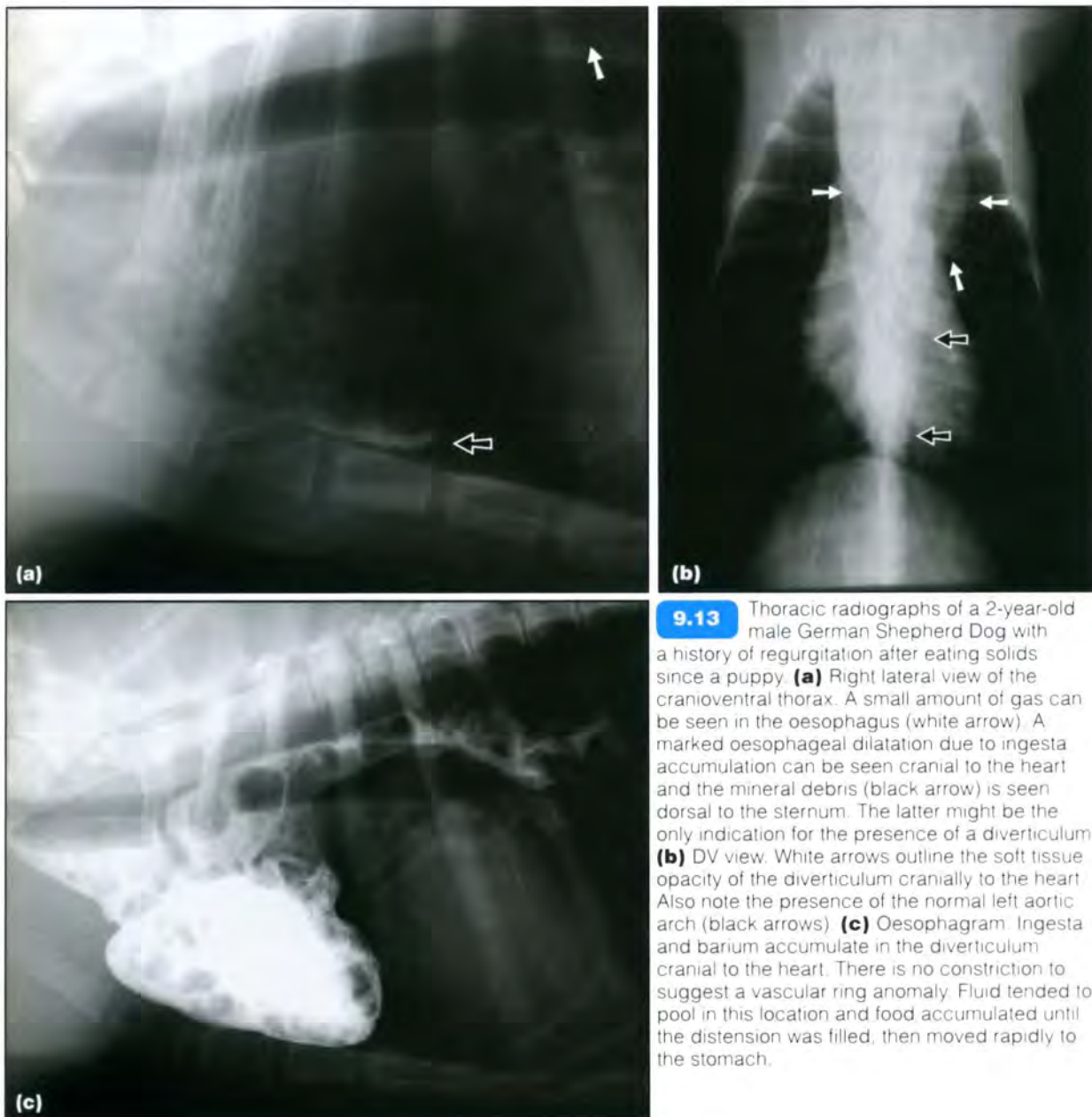
This modality is useful in diagnosing compressive strictures caused by an extramural mass. Fine-needle aspiration (FNA) may be performed under ultrasound guidance.

Oesophageal diverticulum

Oesophageal diverticula are rare pouch-like sacculations of the oesophageal wall that may be congenital (Figure 9.13) or acquired. Congenital diverticula occur most often in medium-sized to small-breed dogs. Clinical signs of diverticula are related to the underlying oesophageal disease or to local food stasis and inflammation.

Two types of acquired diverticula may occur:

- Pulsion diverticula result from conditions of increased intraluminal pressure, secondary to



9.13 Thoracic radiographs of a 2-year-old male German Shepherd Dog with a history of regurgitation after eating solids since a puppy. **(a)** Right lateral view of the cranioventral thorax. A small amount of gas can be seen in the oesophagus (white arrow). A marked oesophageal dilatation due to ingesta accumulation can be seen cranial to the heart and the mineral debris (black arrow) is seen dorsal to the sternum. The latter might be the only indication for the presence of a diverticulum. **(b)** DV view. White arrows outline the soft tissue opacity of the diverticulum cranially to the heart. Also note the presence of the normal left aortic arch (black arrows). **(c)** Oesophagram. Ingesta and barium accumulate in the diverticulum cranial to the heart. There is no constriction to suggest a vascular ring anomaly. Fluid tended to pool in this location and food accumulated until the distension was filled, then moved rapidly to the stomach.

obstruction (stricture or foreign body) or altered motility. The oesophageal wall thins and weakens and bulges out under increased intraluminal pressure

- Traction diverticula result from traction on the oesophageal wall, secondary to perioesophageal inflammation, fibrosis and adhesions. These are often small and insignificant.

The accumulation of ingesta within the diverticulum leads to oesophagitis, mechanical obstruction (seen with large diverticula) and disturbed oesophageal motility. Severe cases with mucosal ulceration may eventually perforate, resulting in mediastinitis.

Diverticula should not be confused with a normal redundant oesophagus. Extending the patient's neck should result in the disappearance of a 'false diverticulum'.

Radiography

This is usually normal. Findings may include:

- Pouch-like sacculations of oesophagus (gas/ingesta)
- Ingesta more commonly collects in pulsion than in traction diverticula.

Contrast studies: Findings include:

- Contrast medium within pouch-like sacculations of oesophagus
- Large multiloculated diverticula may only partially fill with contrast medium
- Pulsion diverticula usually have rounded or multilobed borders, thin wall and neck similar in size to the diverticulum itself
- Traction diverticula usually have triangular shape with wide base at the oesophagus, thick wall and tip pointing to the area of adhesion.

Oesophageal neoplasia

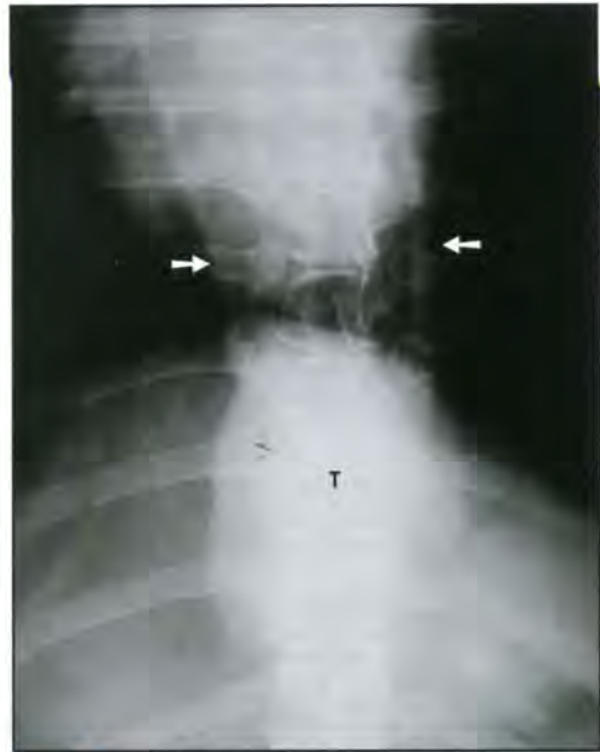
Fibrosarcoma and osteosarcoma developing from malignant transformation of *Spirocerca lupi* granulomas (see below) are the most common malignant oesophageal neoplasms in dogs. Other oesophageal neoplasms are extremely rare and constitute less than 0.5% of all cancers in the dog and cat. These may be of primary oesophageal, perioesophageal (lymph nodes, thyroid, thymus and heart base; see Chapter 8) or metastatic (thyroid, pulmonary and gastric carcinomas) origin.

Primary neoplasms include leiomyoma, leiomyosarcoma (Figure 9.14), carcinoma and chondrosarcoma in the dog, with squamous cell carcinoma being the most common in the cat. Leiomyomas show a slow growth rate and lack of invasiveness, and on occasion may only be recognized at necropsy.

Radiography

Radiographic findings include:

- Oesophageal dilatation or evidence of a perioesophageal lesion displacing the oesophagus



9.14 VD view of the caudal thorax of an 11-year-old Boxer bitch diagnosed with an oesophageal leiomyosarcoma. Note the relatively well defined, slightly irregular soft tissue opacity in the terminal oesophagus area (T) and the gas-dilated oesophagus cranial to it (arrowed).

- Mineralization of oesophageal mass (rare; differentials such as mineralization of a radiolucent foreign body, dystrophic mineralization, accumulation of mineralized food material, coating of abnormal mucosa by radiopaque oral medication should also be considered)
- Soft tissue 'stripe' between the descending aorta and the CdVC or midline soft tissue opacity bulge on the dorsoventral (DV)/ventrodorsal (VD) view
- Aspiration pneumonia and thoracic metastasis should be checked for.

Contrast studies: A positive or negative (pneumo-oesophagram) contrast medium may be employed. An intraluminal mass/filling defect and/or obstruction with contrast medium pooling cranially will be demonstrated.

Ultrasonography

This may give additional information. Ultrasonographic access should be attempted via the thoracic inlet, intercostal spaces or transdiaphragmatic route, depending on the radiographic location of the mass. Ultrasound-guided FNA can also be considered.

Computed tomography

This is recommended when surgery is contemplated. It is the most sensitive diagnostic imaging tool for pulmonary metastasis and also allows evaluation of regional lymph nodes.

Oesophageal foreign body

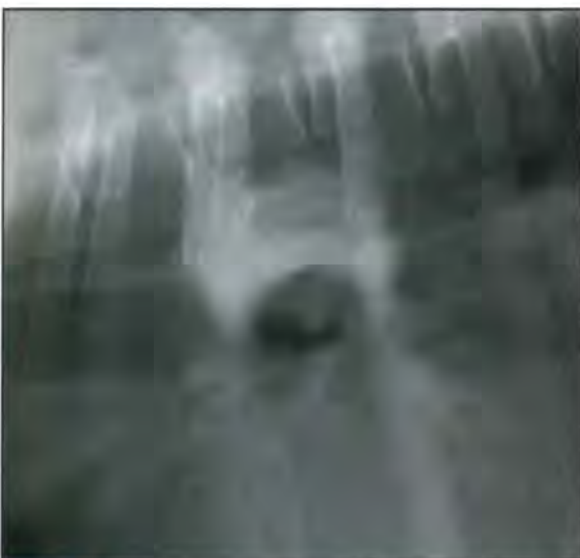
Foreign bodies are common in the dog, particularly in young dogs (up to 2–3 years) and terrier breeds. They are unusual in the cat. Retained oesophageal foreign bodies may cause partial or complete mechanical obstruction, accentuated by muscle spasms and tissue oedema around the foreign body. They most commonly lodge at the thoracic inlet, at the base of the heart or at the oesophageal hiatus. Thoracic (including the stomach area) and cervical (including the pharyngeal area) radiographs should be obtained.

Complications, such as aspiration pneumonia or oesophageal perforation (with secondary pneumomediastinum, pneumothorax, mediastinitis, pleural effusion, pleuritis, tracheo-oesophageal fistula), and underlying pathology should be ruled out. The longer the foreign body has been lodged, the greater the chance for perforation and the greater the risk of rupture during oesophageal retrieval. Sharp foreign bodies also have an increased risk of perforation.

Radiography

Findings may include:

- Radiopaque foreign body (Figure 9.15)
- Radiolucent foreign body may require contrast medium administration for diagnosis (Figure 9.16)
- Mild oesophageal dilatation (gas/ingesta) cranial to obstruction
- Small areas of gas accumulation around foreign body
- Displacement of surrounding organs, especially ventral and rightward displacement of the trachea
- Signs of complications (aspiration pneumonia, perforation and secondary pleuritis, mediastinitis or fistulae).



9.15 Right lateral view of the mid dorsal thorax of a mature dog. The trabeculated appearance of the structure at the heart base is consistent with a bony foreign body. Note also the small amount of cranial oesophageal air, causing a tracheal stripe sign.



9.16 Right lateral oesophagram of an immature dog. Note the multiple filling defects in the oesophagus caused by radiolucent foreign bodies.

Contrast studies: It is important to use non-ionic organic iodide, low-osmolar water-soluble agents (such as iohexol) if oesophageal perforation is suspected. Findings include:

- Filling defect (see Figure 9.15)
- Oesophageal dilatation cranial to the obstruction.

Contrast studies are useful to differentiate between partial and complete obstruction.

Fluoroscopy

This may be used to guide retrieval of the foreign body. It is an effective method of guiding treatment and complications are uncommon.

Vascular ring anomaly

Vascular ring anomalies are congenital malformations of the major arteries of the heart that entrap the intrathoracic oesophagus and cause oesophageal obstruction (see also Chapter 7). The condition is likely to be heritable in German Shepherd Dogs, Irish Setters and Greyhounds. Vascular ring anomalies are uncommon in the cat. There are several described vascular ring anomalies of which the persistent right aortic arch (PRAA) is by far the most common (95% of cases). Other less common vascular anomalies include persistent right or left subclavian arteries, double aortic arch (may cause dyspnoea), persistent right aorta, left aortic arch and right ligamentum arteriosum, and aberrant intercostal arteries. Frequently, additional cardiac or vascular anomalies (such as persistent left cranial vena cava, CrVC) are present but may not be of clinical significance.

Certain clinical signs are similar in all vascular ring anomalies. Most animals present as thin and stunted with a history of regurgitation of solid foods at the time of weaning. Rarely, the ductus arteriosus may remain patent in PRAA (corresponding radiographic signs of patent ductus arteriosus (PDA) should be looked for; see Chapter 7) and can be auscultated with its characteristic machinery or continuous murmur. Patients with double aortic arch anomalies may be dyspnoeic due to concomitant entrapment of the trachea.

The prognosis is variable as the oesophageal dilatation and hypomotility are not fully reversible. In general, patients with generalized megaesophagus or dilatation caudal to the heart have a poor prognosis, and contrast medium administration may be necessary to evaluate this. The earlier the condition is corrected, the better the prognosis.

Radiography

Radiographic findings include:

- Oesophageal dilatation or pulsion diverticulum (air/ingesta) cranial to stricture with abrupt tapering at about the fourth intercostal space to the sixth rib (Figure 9.17)
- Ventral deviation of trachea
- Moderate or marked focal leftward curvature of the trachea near the cranial border of the heart in DV/VD radiographs is a reliable sign of PRAA in young dogs with consistent clinical signs (Figure 9.18). Oesophagography is not necessary to confirm the diagnosis
- Moderate or marked focal narrowing of the trachea
- If a well defined normal left descending aortic margin is visible on the VD/DV view, one of the less common vascular ring anomalies should be considered
- Tracheal stenosis and malformation of tracheal rings are suggestive of double aortic arch anomaly
- Aspiration pneumonia is a common complication of a vascular ring anomaly
- Fibrous bands within the oesophagus may mimic vascular ring anomalies but angiography or oesophagoscopy will confirm the diagnosis.



9.17 Right lateral view of the thorax of a 6-week-old Great Dane bitch (slightly rotated). The oesophagus is markedly gas distended with a constriction at the fourth rib visible as a thin soft tissue band. Note also the accumulation of mineral debris and ingesta in the cranial oesophageal diverticulum and the markedly gas distended caudal oesophagus. There is also gas in the stomach. Findings are consistent with a vascular ring anomaly.



9.18 DV view of the cranial thorax of a 5-week-old Boerboel bitch with a history of regurgitating solids. Note the moderate focal leftward curvature of the trachea near the cranial border of the heart (arrowed) consistent with a vascular ring anomaly. This sign is reportedly present in 100% of PRAA cases. The focal narrowing of the trachea is present in 74% of DV/VD radiographs of dogs with this condition.

Contrast studies: Contrast medium (barium burger) is recommended for complete evaluation prior to surgery and for prognostic purposes. It confirms the location of the oesophageal obstruction and the severity of oesophageal distension. The right lateral view demonstrates a curved filling defect associated with PRAA (Figure 9.19).



9.19 Oesophagram of an 8-week-old Staffordshire Bull Terrier in right lateral recumbency. Note the prominent linear filling defect at the level of the fourth intercostal space as well as the cranially dilated oesophagus consistent with a vascular ring anomaly.

Fluoroscopy with contrast medium

This is useful to evaluate focal or generalized oesophageal motility disturbances and therefore useful as a prognostic indicator.

Selective angiography

This is occasionally performed for definitive confirmation of the type and location of the vascular anomaly prior to surgery. It should be considered if there is suspicion of an atypical vascular ring anomaly or PDA with PRAA.

Ultrasonography

This is advised in cases of PDA. It is also useful to exclude other congenital cardiac abnormalities.

Spirocercosis

The nematode *Spirocerca lupi* may lead to the development of oesophageal granulomas and neoplasms. The condition is common in endemic areas (most tropical and subtropical countries) but otherwise very rare. Although any breed can be affected, the condition is seen more commonly in large-breed dogs. Infections in cats are seldom reported. Eggs containing first-stage infective larvae are eaten by coprophagous dung beetles. Dogs then ingest the beetle or a paratenic host and the larvae penetrate the gastric wall, migrate through arteries and finally reach the thoracic aorta in about 3 weeks. After 10–12 weeks in the aorta the larvae migrate to the oesophagus and it is here that the adult develops within nodules in the oesophageal wall. With time, a granuloma forms and is typically situated in the terminal oesophageal wall. In atypical cases, it may be hilar and smaller. Granulomas may undergo neoplastic transformation to fibrosarcomas/osteosarcomas in 26–41% of cases. Animals typically present with regurgitation (or less commonly vomiting) or an oesophageal mass may be identified as an incidental finding.

Complications can occur due to perforation of the oesophagus (mediastinitis, pleuritis, mediastinal haematoma, aberrant migration with abscess formation) or rupture of the aortic aneurysm (acute haemothorax). Parotid salivary gland hypertrophy with hypersalivation may also occur.

Radiography

Radiographic findings include:

- Midline soft tissue opacity bulge in caudal thorax on DV/VD view (Figure 9.20). This view is often extremely useful
- Ill defined soft tissue opacity in the terminal oesophagus on the lateral view (Figure 9.21a)
- Rarely, the mass may be in an atypical location such as the cranial or mid-thoracic oesophagus
- Ventral displacement of the CdVC
- Oesophageal dilatation (gas/ingesta) cranial to the granuloma
- Spondylitis of last thoracic vertebrae (pathognomonic)
- ‘Pseudospondylosis’ (more lamellar spondylosis, extending to midventral vertebral bodies)
- Mineralized foci within granuloma (trapped mineralized ingesta or metaplasia into osteosarcoma)
- Metastasis to lungs
- Aortic aneurysm



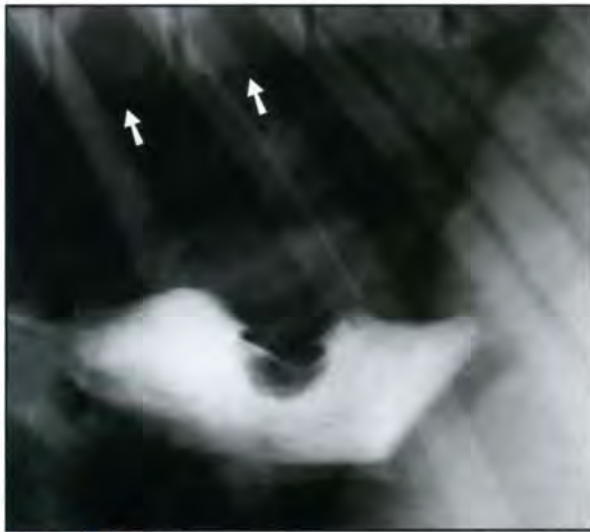
9.20 DV view of the terminal oesophagus in a mature dog. In cases of suspected *Spirocerca lupi* infection, it is always essential to follow the left outline of the aorta (white arrows). A second bulge in this area (black arrows) is consistent with an oesophageal *S. lupi* granuloma and/or aortic aneurysm secondary to *S. lupi* infection.



9.21 Right lateral view of the dorsocaudal thorax of a 4-year-old Labrador Retriever bitch. **(a)** Survey radiograph. An ill defined faint soft tissue opacity can be seen in area of the terminal oesophagus (G). Note the slightly irregular outline of the dorsal aortic arch consistent with aortic aneurysm (arrowed). **(b)** Pneumo-oesophagram, resulting in an air-dilated oesophagus, highlighting the oesophageal *S. lupi* granuloma (G).

- Hypertrophic osteopathy
- Periosteal reaction on ribs
- Signs of complications.

Contrast studies: A positive-contrast oesophagram (barium burger is best) or pneumo-oesophagram (Figure 9.21b) is used. A mural filling defect (often dorsally) is demonstrated (Figure 9.22).



9.22 Oesophagram showing a small dorsal oesophageal wall filling defect consistent with a *S. lupi* granuloma. Note also the thoracic spondylitis (arrowed), considered to be pathognomonic for *S. lupi* infection. Caudally there is also spondylosis deformans.

Computed tomography

Computed tomography (CT) is recommended when surgery is contemplated for mass resection. It is the most sensitive tool for detection of thoracic metastasis. CT is excellent for early detection of focal aortic mineralization (Figure 9.23) and early spondylitis,



9.23 Transverse CT image obtained immediately caudal to the carina of an 8-year-old neutered male Dalmatian (window level -215 HU, window width 1996 HU (lung window)). A *S. lupi* granuloma is visible in the oesophagus (arrowed). The mineralization within is indicative of malignant transformation (osteosarcoma or fibrosarcoma). Note also the small amount of gas within the remaining oesophagus dorsal to the mass. The aorta (A) also contained a very small amount of mineralization. The heart (H) is also identified.

and therefore extremely helpful in detection of extra-oesophageal disease. It is best performed with the patient in sternal recumbency, with inflation of the oesophagus with air via the endotracheal tube.

Ultrasonography

This will allow visualization of hypertrophic parotid salivary glands. An attempt can be made to scan the *S. lupi* granuloma using the liver as an acoustic window, via a diaphragmatic approach (Figure 9.24). Ultrasonography may also be useful to investigate mediastinal complications.



9.24 (a) Sagittal ultrasound image of a normal oesophagus crossing the diaphragm from the thoracic cavity into the abdomen in a 6-month-old mixed breed dog with a small amount of pleural effusion (P). The oesophagus is shown by the arrowheads. The liver (L) is seen in the near field. (b) Transverse ultrasound image of the terminal oesophagus of a 7-year-old male Staffordshire Bull Terrier using the liver (L) as acoustic window. Compare the 5 x 4 cm bilobed medium echogenicity of the *S. lupi* granuloma (callipers) to the normal oesophagus shown in (a). The arrow points to the ventral oesophageal wall.

Gastro-oesophageal intussusception

Gastro-oesophageal intussusception is a rare condition and results from invagination of the stomach, with or without other abdominal viscera (spleen, duodenum, pancreas and omentum), into the caudal oesophageal lumen.

Predisposing factors include megaesophagus, congenital oesophageal abnormalities, incompetency of the lower oesophageal sphincter and chronic vomiting. It has been reported to be more common in younger dogs (<3 months). The highest prevalence has been reported in German Shepherd Dogs, or large-breed dogs in general.

The clinical signs include regurgitation, vomiting and distress. Rapid deterioration occurs should a large portion of the stomach prolapse into the oesophagus. This constitutes a surgical emergency with mortality rates in excess of 95%.

Occasionally, gastro-oesophageal intussusception may be an intermittent problem.

Radiography

Radiographic findings include:

- Well demarcated soft tissue opacity or heterogenous mass within the terminal oesophagus (Figure 9.25)
- Gastric rugae extending into the mass
- Oesophageal dilatation (gas) cranial to the mass

- The gastric silhouette may be absent from the cranial abdomen, or when gas-distended, its lumen may reveal a defined communication with the mass.

Contrast studies: These are contraindicated if surgery is contemplated. Findings include:

- Abrupt cessation of the passage of barium in the oesophagus (Figure 9.26)
- Oesophageal dilatation cranial to the mass
- Gastric rugae within the oesophageal lumen are highlighted
- Contrast medium may outline transverse folds between the dilated oesophageal lumen and the intruded stomach.

Fluoroscopy with contrast medium

This may be useful to demonstrate the intermittent form; however, this cannot be excluded by a negative study.

Hiatal hernia

For information on hiatal hernias, see Chapter 14.



9.25 Thoracic radiographs of an 8.5-year-old German Shepherd Dog previously diagnosed with idiopathic megaesophagus and now presented with rapid deterioration. **(a)** Right lateral view. A well defined soft tissue opacity can be seen in the oesophagus with a markedly gas-distended oesophagus (arrowed) cranially. In addition, the lack of a cranial abdominal gastric silhouette, ventral displacement of the trachea and the cardiac silhouette are consistent with a gastro-oesophageal intussusception. On occasion rugal folds will be seen entering the caudal oesophagus and further assist with the diagnosis. **(b)** DV view. Rightward displacement of the trachea can be seen. Arrows indicate the gastro-oesophageal intussusception.



9.26 Oesophagram of a 3-month-old male Shar Pei. Note the abrupt cessation of the contrast medium passage, a large soft tissue opacity in the oesophagus and the absence of the gastric silhouette in the cranial abdomen, which are consistent with a gastro-oesophageal intussusception.

References and further reading

- Buchanan JW (2004) Tracheal signs and associated vascular anomalies in dogs with persistent right aortic arch. *Journal of Veterinary Internal Medicine* **18(4)**, 510–514
- Dvir E, Kirberger RM and Malleczek D (2001) Radiographic and computed tomographic changes and clinical presentation of spirocercosis in the dog. *Veterinary Radiology and Ultrasound* **42(2)**, 119–129
- Mears EA and Jenkins CC (1997) Canine and feline megaesophagus. *The Compendium of Continuing Education for the Private Practitioner* **19(3)**, 313–325
- Sellon RK and Willard MD (2003) Esophagitis and esophageal strictures. *Veterinary Clinics of North America: Small Animal Practice* **33**, 945–967
- Stickle RL and Love NE (1989) Radiographic diagnosis of esophageal diseases in dogs and cats. *Seminars in Veterinary Medicine and Surgery (Small Animal)* **4(3)**, 179–187
- Westfall DS, Twedt DC, Steyn PF, Oberhauser EB and VanCleave JW (2001) Evaluation of esophageal transit of tablets and capsules in 30 cats. *Journal of Veterinary Internal Medicine* **15(5)**, 467–470
-

The trachea

Nicolette Hayward, Tobias Schwarz and Chick Weisse

Radiographic anatomy

The trachea is a semi-rigid air-filled tube that connects the larynx with the bronchial system. The trachea ends caudally with a crest, called the *carina*, which divides and channels the airflow into the two mainstem bronchi. In a normal dog and cat the carina should be located at the level of the fourth or fifth intercostal space (Figure 10.1).



10.1 Lateral radiograph of a normal canine thorax. Note the divergence of the trachea from the thoracic vertebra, and narrowing of the most caudal part of the trachea. The trachea ends with the carina at the level of the fifth intercostal space (arrowhead).

The tracheal wall consists of C-shaped cartilages, interconnecting tracheal ligaments and respiratory mucosa. Dorsally the open cartilages are connected by the trachealis muscle and connective tissue.

- The tracheal wall is only distinguishable from neighbouring cervical and mediastinal soft tissue if air is present in the oesophagus, giving the 'tracheal stripe sign' (see Chapter 9), or if the tracheal cartilages are mineralized.
- In cross section the canine and feline trachea is slightly wider than it is high.
- The oesophagus is dorsally adjacent to the cranial cervical trachea and continues along the left dorsolateral aspect of the mid cervical to cranial thoracic trachea, where it courses again to the dorsal aspect of the tracheal bifurcation.

- The lateral view is most useful for assessment of the trachea, although the dorsoventral (DV) or ventrodorsal (VD) view is useful to assess lateral displacement.
- Radiographs should be made with the head in a neutral position to avoid artefacts.
- Separate radiographs should also be taken of the cervical and thoracic tracheal segments as exposure and positioning requirements differ.
- Contrast studies have been used in the diagnosis of tracheal disease, such as tracheal rupture and tracheal masses. However, tracheobronchoscopy has largely superseded this technique, as the aspiration of contrast media can exacerbate respiratory problems.

Interpretive principles

Tracheal size, shape and opacity

The normal tracheal diameter is variable between breeds. The ratio of tracheal diameter to thoracic inlet diameter has been used as an objective way to assess lumen size (Figures 10.2 and 10.3).

- The tracheal lumen should be smoothly outlined. In Dachshunds and other chondrodystrophic breeds, the tracheal lumen can be irregularly outlined. This is of no clinical significance.
- Mild to moderate cartilage mineralization is a normal feature in skeletally mature dogs and cats. Marked cartilage mineralization can frequently be seen in giant-breed and chondrodystrophic dogs as an incidental finding.
- Conditions that promote metastatic calcification (e.g. hyperadrenocorticism) can affect the trachea along with other soft tissues.
- In the normal dog and cat, the luminal diameter does not alter significantly between inspiration and expiration.

Dog breeds	Normal tracheal diameter:thoracic inlet ratio
Meso- and longicephalic	0.21 ± 0.03
Bulldogs	0.11 ± 0.03
Other brachycephalic	0.16 ± 0.03

10.2 Normal tracheal diameter:thoracic inlet ratio for different dog breeds.



10.3 Lateral radiograph of a normal canine thorax with annotations for the calculation of the tracheal diameter:thoracic inlet ratio. The thoracic inlet distance (black arrow) is measured from the ventral aspect of the vertebral column at the midpoint of the most cranial rib to the dorsal surface of the manubrium at its point of minimal thickness. The tracheal diameter (white arrow) is measured between the internal surfaces of the tracheal wall oriented perpendicularly to the tracheal long axis at the point where the thoracic inlet line crosses the midpoint of the tracheal lumen.

A local reduction of the radiographic cervical tracheal luminal gas shadow always represents a true anatomical reduction of the tracheal lumen. The cervical trachea is completely surrounded by soft tissue; therefore, changes in the relative position of some of the adjacent structures (oesophagus, longus colli muscle) do not change the X-ray beam attenuation over the trachea. However, the thoracic portion of the trachea is surrounded by air-filled lung. Superimposing soft tissue lesions at this level could therefore be confused with tracheal pathology.

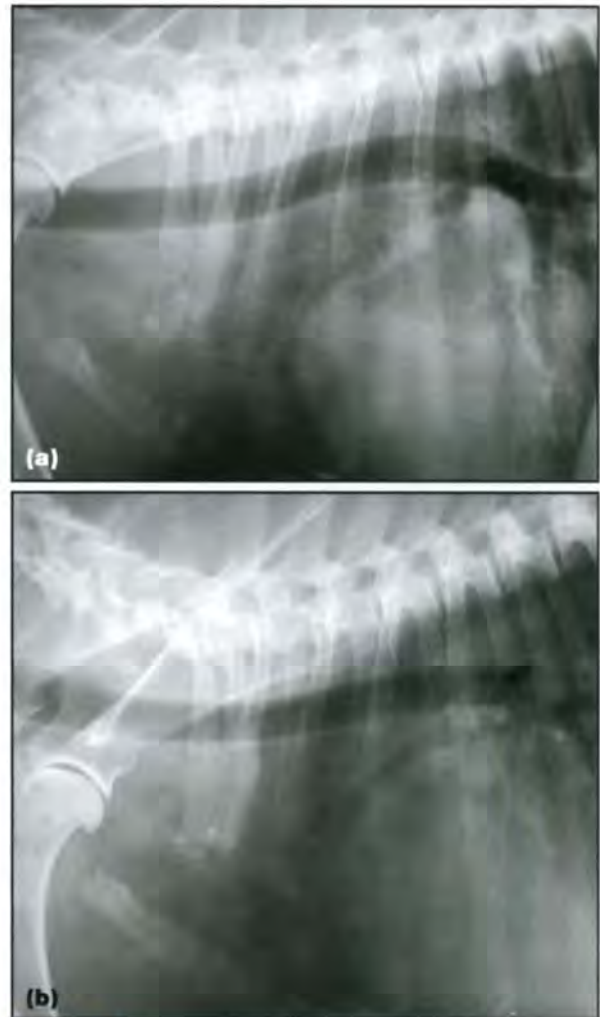
Tracheal location

On a lateral radiograph the course of the trachea is roughly parallel to the cervical spine.

- The trachea forms an angle with the thoracic spine that varies with body type (approximate range of 10–20 degrees).
- The most caudal part of the trachea often narrows in the DV view and angles ventrally before bifurcating into mainstem bronchi on the lateral view.
- The trachea is a relatively rigid tube that does not collapse in length and, at least not normally, in diameter.

- Cervical flexion shortens the distance between the larynx and the carina and therefore results in some tracheal deviation, usually seen at the thoracic inlet (Figure 10.4).
- Any space-occupying lesion along the normal tracheal course will also result in deviation rather than collapse of the tracheal lumen. Tracheal deviation should therefore always be assessed in context to avoid misinterpretation.

In the DV or VD view, the trachea is superimposed on the vertebrae and sternbrae, although it may deviate slightly to the right at the thoracic inlet and in the cranial mediastinum, especially in small barrel-chested breeds and obese animals.



10.4 (a) Lateral tracheal radiograph of a 12-year-old Labrador Retriever (with dilated cardiomyopathy) with flexed neck position, resulting in dorsal deviation of the distal trachea. (b) Repeated lateral radiograph with the neck in a neutral position. Note lack of kinking of the caudal trachea.

Incidental tracheal narrowing

The lumen of the caudal cervical trachea frequently appears narrowed with a dorsally concave tracheal border in dogs without contributable respiratory signs. This phenomenon is often referred to as 'pseudo-collapse' (Figure 10.5). This is a misnomer because:

- This condition is always caused by a true reduction in the tracheal lumen, but probably not marked enough to cause clinical signs
- A relatively wide dorsal trachealis muscle allows partial invagination of extratracheal structures into the tracheal lumen (sometimes referred to as 'redundant tracheal membrane')
- Rotation of the tracheal cross-sectional plane in relation to the axial plane of the neck exacerbates the radiographic effect
- Extension of the head and neck promotes compression and narrowing of the lumen.



10.5 (a) Lateral cervical radiograph of a 7-year-old Labrador Retriever with no signs of respiratory disease. Notice the narrowed tracheal lumen caused by the ventrally deviated dorsal tracheal wall. (b) CT image obtained immediately after radiography with similar recumbence and without chemical constraint. The cross-sectional area of the trachea at the level of the sixth cervical vertebra is reduced due to the invagination of the dorsal trachealis muscle into the lumen. Notice also the slight rotation of the tracheal height axis in relation to the dorsoventral axis of the body. This obliquity accentuates the luminal narrowing on the lateral radiograph.

Dynamic changes with inspiration and expiration

The tracheal luminal diameter should not alter markedly between inspiration and expiration. Dynamic variation in the tracheal lumen is increased by:

- Softening of the tracheal rings
- Flaring of the tracheal rings
- Obstruction to airflow
- Respiratory effort.

Pharyngeal, laryngeal and intrathoracic conditions can all influence tracheal dynamics and therefore these areas should also be assessed radiographically. The phase of respiration is important in the diagnosis of tracheal collapse and thus radiographs should be made in both inspiration and expiration, including both the cervical trachea and the thoracic trachea.

Echotracheography

The cervical trachea can be identified ultrasonographically in both sagittal and transverse planes. However, the presence of aerated lung in the thorax impairs the usefulness of intrathoracic tracheal ultrasonography. Ultrasonography has been used to identify tracheal collapse in the cervical region, where the trachea may be seen as a crescent shape during collapse. However, radiography and fluoroscopy remain more sensitive indicators of this condition.

Tracheal computed tomography

Indications and limitations

Tracheal computed tomography (CT) is a useful technique to investigate:

- Collapse
- Rupture
- Obstruction
- Mass lesion
- Placement of a stent.

Advantages of tracheal CT compared with other modalities include:

- Cross-sectional evaluation of the entire tracheal length
- Real-time evaluation during the respiratory cycle.

The technique is limited by the anaesthetic requirements.

- Intubation can either be difficult to achieve or render the study non-diagnostic.
- Dynamic studies are preferentially performed in conscious animals, which is only possible in very compliant patients.

A very useful application of tracheal CT is for the follow-up examination of dogs with intraluminal stent treatment for tracheal collapse. This is because it allows differentiation of intraluminal fluid accumulation from excessive granulation tissue, which is otherwise a difficult task (Figure 10.6).



10.6 CT image of the cranial thorax of a 4-year-old Yorkshire Terrier with an acute episode of respiratory distress 2 years after intraluminal stent placement for tracheal collapse. Radiographic evaluation revealed increased opacity of the stented tracheal lumen and in the right caudal thorax. The CT image reveals the presence of gravity-dependent tracheal fluid (meniscus-shaped fluid-gas interface), but no evidence of obstructive granulation or other tissue, and partially consolidated cranial lung lobes. Final diagnosis was a diaphragmatic hernia and pneumonia for which the dog was successfully treated. Notice the mild streak artefacts emanating from the metallic stent, which do not prevent diagnosis.

Technique

The animal should be placed in lateral or ventral recumbency, preferably using short-term injection anaesthesia. A helical CT scan of the entire tracheal length should be performed, with a 2–3 mm slice width and a pitch of 2.

Diseases

Tracheal diseases can be categorized according to morphological and/or dynamic origin, and by intraluminal, mural or extrinsic (external to wall) conditions as listed in Figure 10.7.

Tracheal hypoplasia

Tracheal hypoplasia is a congenital narrowing of the trachea by at least 50% of the cross-sectional lumen, affecting the entire length of the trachea. The tracheal rings are almost complete with a negligible dorsal muscle.

- There is an increased incidence of the condition in English Bulldogs and English Mastiffs, but tracheal hypoplasia has also been described in the Labrador Retriever, German Shepherd Dog, Weimaraner and Basset Hound.
- The condition is rarely seen in the cat.
- Tracheal hypoplasia is one component of the canine brachycephalic airway obstruction complex, which includes stenotic nares, elongated soft palate and everted laryngeal sacs.

Morphological, intraluminal and intramural disorders

- Tracheitis
- Tracheal oedema, inhalational injury
- Tracheal stenosis:
 - generalized – hypoplastic trachea
 - localized – segmental stenosis, scarring
- Tracheal foreign body
- Tracheal neoplasm
- Endotracheal granuloma – parasites, infection
- Tracheal trauma – bite wounds, laceration

Dynamic disorders – tracheal collapse syndrome

- Lower cervical – inspiratory
- Intrathoracic – expiratory
- Generalized – inspiratory/expiratory

Extrinsic disorders

- Cervical mass – thyroid gland, abscess
- Cranial mediastinal mass – lymphoma, thymoma, abscess
- Enlargement of the cardiac silhouette
- Craniodorsal mass (rare) – soft tissue sarcoma, vertebral body tumour
- Megaoesophagus and oesophageal foreign body
- Perihilar mass – lymphoma, granuloma

10.7 Important tracheal diseases.

- Concurrent congenital abnormalities, such as megaoesophagus and pulmonic and aortic stenosis, have also been identified.
- The condition can be diagnosed at an early age, and affected animals may present with stridor, dyspnoea, reduced exercise tolerance and coughing. Excitement exacerbates the condition, which is often progressive during the day. Recurrent respiratory infections may lead to bronchopneumonia.

Dogs and cats with mucopolysaccharidosis VII, a rare genetic lysosomal storage disease causing dysfunctional bone and cartilage formation, can have a similar narrowing of the internal tracheal diameter with thickened misshapen tracheal cartilages.

Imaging findings

- Radiographically, the trachea appears uniformly narrowed (Figure 10.8) compared with the variation of luminal size along the length of the trachea seen with tracheal collapse.
- Wall thickening (Figure 10.9) may be identified, which can be a result of chronic inflammation or genetic malformation.
- Tracheal growth may be retarded in some animals, which later have a period of compensation, thus the diagnosis should be made with caution in young animals.

The smallest ratio of trachea:thoracic inlet in Bulldogs with no clinical signs of respiratory disease has been established as 0.09 (see Figure 10.2).



10.8 Lateral view of the thorax of a 1-year-old terrier with tracheal hypoplasia. Note the uniform narrowing along the length of the trachea. The tracheal diameter:thoracic inlet ratio was 0.11. (Courtesy of the Animal Health Trust)



10.9 CT image of the trachea at the level of the sixth cervical vertebra of a Beagle cross dog with mucopolysaccharidosis VII. Notice the thickened and overlapping tracheal cartilages, resulting in a reduced lumen.

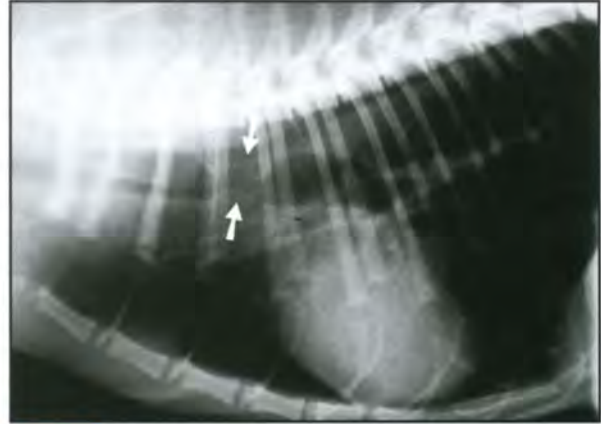
Tracheal stenosis

Tracheal stenosis is a rare condition and occurs as a result of bite wounds, prolonged intubation or tracheal surgery, although segmental tracheal stenosis may occur congenitally. It may be asymptomatic, despite a reduction of up to 80% in the size of the tracheal lumen in cross section. However, in severe cases, stenosis may result in exertional dyspnoea, wheezing and coughing, with the potential for cyanosis, syncope or asphyxiation.

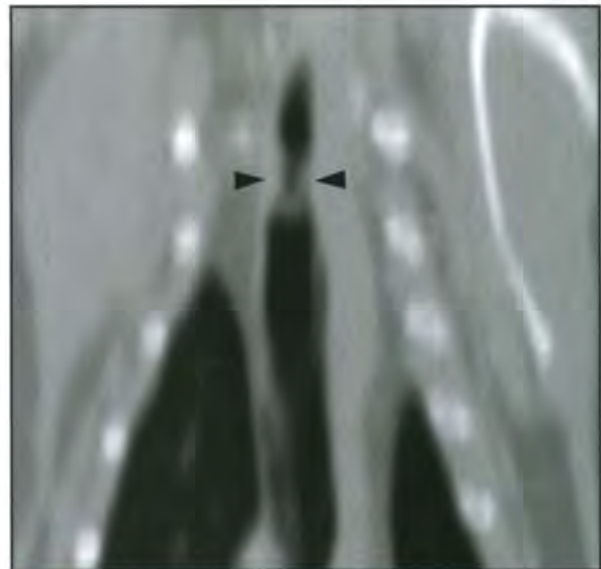
Imaging findings

- Readily recognizable radiographically as a focal narrowing in the trachea (Figure 10.10).

- May be variable in the number of tracheal rings involved.
- Loss of cartilage tissue results in soft tissue proliferation, which may be seen as an irregular margin of the stenosed region.
- CT can be very helpful for determining the exact location and extent of stenosis (Figure 10.11).



10.10 Lateral thoracic radiograph of a 4-year-old Domestic Shorthair cat with tracheal stenosis (arrowed). Note the marked dilatation of the segments of trachea cranial and caudal to the lesion as well as the hyperinflated lung fields.



10.11 Dorsally reconstructed tracheal CT image of a 13-year-old Domestic Shorthair cat with a 3-week history of increased respiratory effort. Notice the stenotic lumen and thickened wall of the trachea at the level of the first intercostal space (arrowheads). A granuloma was surgically resected.

Interventional radiology procedures

Intraluminal tracheal stent placement can allow alleviation of airway obstruction. The technique is discussed in Chapter 6.

Tracheal collapse

Tracheal collapse is a progressive, degenerative disease of the tracheal cartilage rings, predominantly affecting middle-aged to older small- and toy-breed dogs.

- Hypocellularity and decreased glycosaminoglycan and calcium content result in subsequent dynamic tracheal collapse during respiration.
- Elongation of the dorsal trachealis muscle and elastic dorsal tracheal membrane, and flaring of the tracheal rings, results in a flattening of the trachea into a crescent shape.
- Tracheal collapse may be: inspiratory, involving the cervical region; expiratory, involving the intrathoracic region; or mixed, where the entire trachea may be involved.
- The location and degree of collapse are variable and a mild degree of tracheal collapse is quite commonly seen in older small and toy breeds, often without clinical signs.
- Collapse may extend to the bronchi.

Clinical signs range from a mild, intermittent 'honking' cough to severe respiratory distress and cyanosis.

- Coughing can be elicited by tracheal compression and may be exacerbated by excitement, such as pulling against a collar, or drinking cold water.
- Tracheal collapse may be associated with tracheobronchitis, laryngeal oedema, emphysema, hepatomegaly, left heart failure and cor pulmonale.
- A presumably genetic condition has been observed by one of the authors [TS] in Golden Retrievers from a breeding colony where total tracheal collapse occurred after minimal pulling against the collar.
- Bronchoscopy is very useful in the diagnosis of tracheal collapse and a scoring system has been developed, which serves as a gold standard (Figure 10.12).

Grade	Degree of tracheal collapse
1 – mild	25%
2 – moderate	50%
3 – severe	75%
4 – total	100%

10.12 Bronchoscopic grading of tracheal collapse.

Cervical tracheal collapse can also occur as a consequence of laryngeal or nasopharyngeal airway obstruction in dogs or cats (laryngeal paralysis, masses, laryngitis, nasopharyngeal polyps).

- Increased inspiratory effort creates sufficient negative intratracheal pressure to collapse the tracheal lumen.
- This is particularly typical for cats, where degenerative cartilage ring disorders have only been described in mucopolysaccharidosis.

It is therefore important to look for an upper respiratory tract obstruction in any cat with tracheal collapse.

Imaging findings

Radiography, fluoroscopy and CT are all used in the diagnosis of clinically significant tracheal collapse.

- The lateral view is most useful in demonstrating the tracheal lumen.
- DV radiographs may demonstrate a fusiform widening of the trachea in areas which are narrowed from the lateral view, although superimposition of the spine may reduce visualization of this effect.
- The craniocaudal tangential view (Figure 10.13) of the thoracic inlet may be used to demonstrate tracheal collapse, but is difficult to perform. A crescentic appearance of the trachea is seen when tracheal collapse is present.



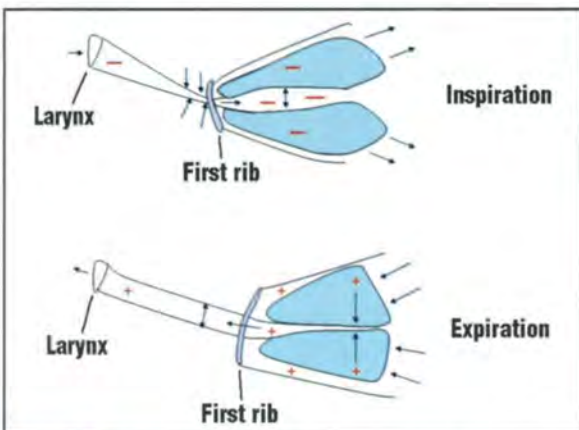
10.13 (a) Positioning of a dog for the tangential craniocaudal view of the trachea at the thoracic inlet. The central ray (yellow line) is directed at the ventral aspect of the thoracic inlet. Due to the obliquity of the beam only a parallel grid with grid lines oriented parallel to the long axis of the table, or a table top technique without a grid, can be used to obtain this view. This view requires manual restraint and should therefore only be taken if absolutely essential. (Courtesy of I. Schwarz)
 (b) Tangential rostricaudal radiograph of a 1-year-old Akita with a normal trachea. Notice the circular radiolucent tracheal lumen. (Courtesy of D. Rodriguez) (continues) ▶



10.13 (continued) **(c)** Tangential rostrorocaudal radiograph of a 4-year-old Pomeranian with tracheal collapse. The residual cross-sectional lumen of the collapsed trachea can be seen as a crescent-shaped gas opacity in the thoracic inlet (arrowheads). (Courtesy of D. Rodriguez)

- Fluoroscopy is particularly useful to demonstrate dynamic changes in phase with respiration at the cost of reduced image detail.

Inspiratory and expiratory lateral radiographs should be taken to demonstrate both cervical and intrathoracic collapse. Timing of exposure can be challenging as affected animals often suffer from shallow breathing. Figure 10.14 demonstrates the effect of respiration phase on the radiographic appearance of the collapsing trachea.



10.14 Diagram illustrating the dependence of tracheal collapse on phase of respiration. During inspiration a slightly positive pressure surrounds the cervical trachea as long as air moves towards the thorax. This positive pressure collapses the cervical trachea if it lacks sufficient stability. In the thoracic area, the pressure surrounding the trachea is lower than the pressure within the trachea, which results in tracheal distension. During expiration, the thoracic pressure exceeds the intratracheal pressure. This reduces the diameter of the thoracic trachea as long as air flows towards the larynx. However, the cervical trachea is distended due to the luminal pressure exceeding the outside pressure. (Adapted from Suter (1984) with permission)

- An inspiratory study demonstrates collapse of the cervical segment and dilatation of the thoracic segment.
- Expiratory views show collapse of the thoracic segment and a normal appearance of the cervical segment (Figure 10.15). In marked expiration or coughing, the tracheal lumen may become completely occluded (Figure 10.16).
- The ventral wall of the trachea usually remains straight, whilst the dorsal border is blurred or irregular due to uneven flaring of the tracheal rings and/or inflammatory mucosal changes (Figure 10.17).
- Radiography of the larynx, pharynx and nose can be helpful to rule out upper airway obstruction as a cause of cervical tracheal collapse, particularly in cats (Figure 10.18).



10.15 **(a)** Lateral radiograph centred on the thoracic inlet of a 15-year-old Miniature Poodle showing partial collapse of the extrathoracic portion and a distended intrathoracic portion of the trachea during inspiration. Notice also the radiolucent lung fields and mainstem bronchi. **(b)** Lateral radiograph demonstrating partial collapse of the intrathoracic portion and normal diameter of the cervical portion of the trachea during expiration. Notice the more opaque caudodorsal lung field and collapsed mainstem bronchi.



10.16 **(a)** Lateral cervicothoracic radiograph of a 16-year-old Chihuahua with complete collapse of the cervical and thoracic portion of the trachea. There is no distinguishable radiolucent lumen visible. (continues)



10.16 (continued) **(b)** CT image of the caudal cervical trachea of a 7-year-old Papillon with chronic inspiratory dyspnoea. The image was acquired during natural inspiration. The tracheal lumen is completely collapsed, the tracheal cartilage is flattened and the dorsal trachealis muscle is stretched.



10.17 Lateral cervicothoracic radiograph of a 16-year-old Chihuahua with extensive cervical and thoracic tracheal collapse. Notice the straight ventral and undulating dorsal aspect of the collapsing tracheal wall.



10.18 Lateral cervical radiograph of a 6-year-old Domestic Shorthair cat with chronic inspiratory stridor. Notice the marked collapse of the caudal cervical trachea. A congenital deformation in the cranial end of the trachea with significant luminal obstruction was found on autopsy. (Reproduced from Hendricks and O'Brien (1985) with permission from the *Journal of the American Veterinary Medical Association*)

Interventional radiological procedures

Intraluminal tracheal stent placement is a valid technique in the treatment of tracheal collapse in selected cases (for further information see Chapter 6).

Tracheal laceration and avulsion

Tracheal lacerations or avulsions are rare but serious conditions most commonly associated with trauma,

such as road traffic accidents and bite injuries, or following overzealous intubation (most commonly seen in cats).

- Tracheal laceration and avulsion may occur as a result of wound dehiscence following tracheal surgery, e.g. for a tracheal neoplasm, or more rarely following neoplastic tracheal wall invasion.
- Tracheal avulsion has specifically been reported as a rare consequence of neck hyperextension during trauma.
- Clinical signs include dyspnoea, of variable severity depending on the size of the lesion, subcutaneous emphysema, pneumomediastinum and possibly pneumothorax. However, clinical signs are often delayed and may be related to subsequent stenosis.

Imaging findings

- The tracheal wall lesion itself may not be directly visible, with secondary features being more readily identifiable (Figure 10.19).



10.19 Lateral cervicothoracic radiograph of a 7-month-old Domestic Shorthair cat suffering from a tracheal intubation injury caused during a routine spay procedure. The laceration site is not directly visible but the secondary subcutaneous emphysema and pneumomediastinum are. The tracheal wall is highlighted by gas on both sides.

- The shape of the trachea may be altered with irregularity of the walls and/or lumen.
- A pneumomediastinum is commonly identified and this may be relatively localized or generalized. This pneumomediastinum may occasionally extend to a pneumothorax and pneumoperitoneum or pneumoretroperitoneum.
- A 'pseudotrachea' may be identified radiographically, seen as a ballooned area of the trachea, where a complete rupture has occurred. Tracheal rings are not present in this section. Local mediastinal structures only focally distend with air, giving the false impression of an intact tracheal wall (Figure 10.20).



10.20 Lateral thoracic radiograph of a 4-year-old Domestic Shorthair cat with complete tracheal rupture due to a road traffic accident. Notice the absence of tracheal rings within the ballooned radiolucent area extending from the second to fourth intercostal space. This gas bubble contained in local mediastinal structures is sometimes referred to as a pseudotrachea. (Courtesy of E. Friend)

Tracheal masses

Endotracheal masses include neoplasms, granulomas, polyps and haematomas. Local haematomas may also occur with rodenticide toxicity, although diffuse narrowing of the trachea is more common in this condition.

- Tracheal masses are rare and often not identifiable if small or surrounded by exudates. They may be focal and polypoid, or sessile and plaque-like.
- Tracheal granulomas can occur as a result of infection (parasitic, fungal or bacterial) or following tracheotomy. Inflammatory masses include lymphoplasmacytic infiltration and lymphoid hyperplasia.
- Tracheal neoplasia (Figure 10.21) is rare in dogs and cats. Tumours may also invade the trachea extramurally, e.g. thyroid carcinoma, lung neoplasm, aortic body tumour and oesophageal tumour, although this is not a common finding.

Dogs	
Osteochondroma	Adenocarcinoma
Chondrosarcoma	Other carcinomas
Mast cell tumour	Osteosarcoma
Leiomyoma	Chondroma
Cats	
Lymphoma	Adenocarcinoma
Squamous cell carcinoma	Other carcinomas

10.21 Most common canine and feline tracheal neoplasms.

Clinical signs depend on the degree of obstruction. The condition can be asymptomatic until it is quite advanced, as up to half the airway may be compromised without the appearance of clinical signs. However, close examination may reveal a slow inspiratory phase of respiration, followed by a more rapid expiratory phase. Progressively, stridor and rattles, paroxysmal coughing, gagging, dyspnoea and dysphonia may occur.

Imaging findings

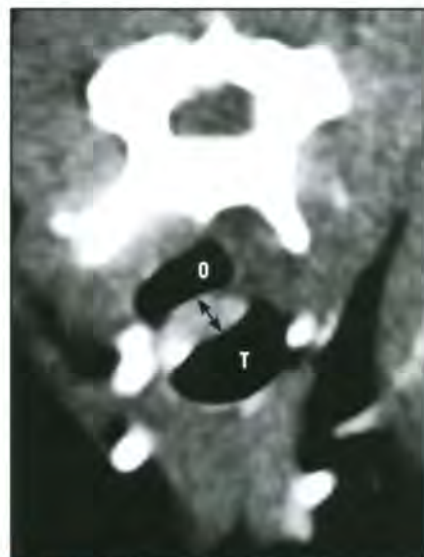
Radiography is relatively sensitive but non-specific for the diagnosis of tracheal masses.

- The main radiographic finding is a local obstruction of the radiolucent tracheal lumen by a lesion of soft tissue opacity (Figure 10.22).
- Underinflation of the lung may be seen with cervical tracheal obstruction.
- Intrathoracic obstruction may result in air trapping, seen as a hyperlucent lung field and caudal displacement of the diaphragm.

Contrast-enhanced CT allows assessment of the exact location and extent of tracheal masses (Figure 10.23).



10.22 Lateral cervical radiograph of a 7-year-old Rottweiler with chronic upper respiratory distress. There is a soft tissue and mineral opaque mass arising from the ventral aspect of the tracheal wall, inhibiting further passage of the endotracheal tube. An oesophageal tube can be seen dorsally. Final diagnosis was a tracheal chondrosarcoma.



10.23 Contrast-enhanced CT image at the level of the sixth cervical vertebra of a 10-year-old Domestic Shorthair cat with chronic inspiratory dyspnoea. There is a contrast-enhancing (bright) soft tissue mass (arrowed) arising from the dorsal wall of the trachea (T) adjacent to the gas-distended oesophagus (O). Final diagnosis was a tracheal lymphoma. Tracheal resection and chemotherapy maintained this cat in remission for almost 2 years.

Interventional tracheal radiology

Intraluminal tracheal stent placement can allow alleviation of airway obstruction caused by tracheal masses that are not readily accessible via surgery, or when surgery is declined, or not indicated. The technique is discussed in Chapter 6.

Foreign material in the trachea

The ease with which foreign bodies in the trachea can be seen depends upon the opacity, location, size and view used.

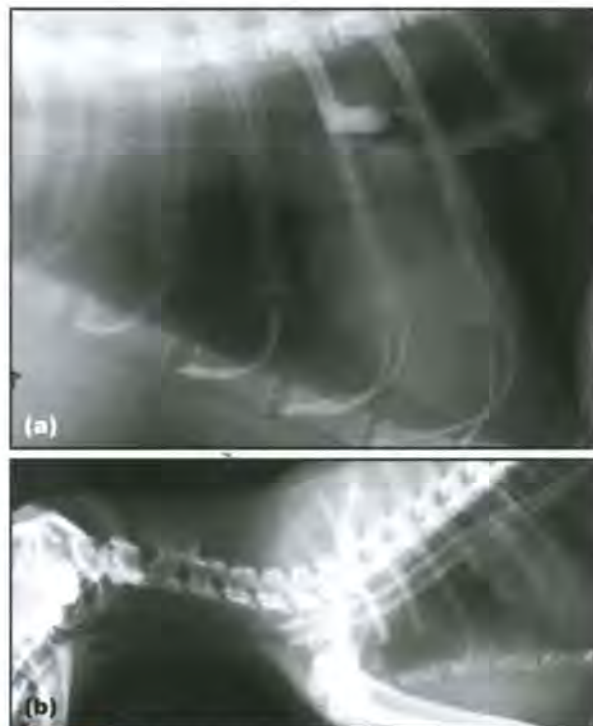
- Tracheobronchial secretions and superimposition of skeletal structures may impair visualization of the foreign body.
- Inhaled foreign bodies are most commonly found in young animals, with larger types, such as teeth and small stones, lodging at the tracheal bifurcation, and smaller foreign bodies, such as grass awns, passing into the bronchi.
- The left caudal lobe bronchus is the most common site as this lobe continues in a straight line on from the trachea.
- Small foreign bodies may be coughed out, unless they are barbed or pointed, or are surrounded by mucus, which may adhere them to the tracheal wall.

Clinically, animals with tracheal foreign bodies are more likely to present with dyspnoea and respiratory noise, whilst animals with bronchial foreign bodies more commonly produce a cough of sudden onset. The latter are most commonly working dogs. Haemoptysis may be seen. Chronic cases of plant awn inhalation may progress to abscessation, with perforation of the bronchus and the development of pneumonia, pyothorax and infection of distant sites (see Chapter 14). The variable consequences of partial or complete airway obstruction are discussed further in Chapter 11. In cats, the prominent ossified clavicles can be superimposed on the tracheal lumen and should not be confused with a tracheal foreign body.

Imaging findings

At least two radiographic views should be taken to localize tracheal foreign bodies.

- Radiopaque foreign bodies, such as stones, bones, teeth and marbles, are easily seen (Figure 10.24a).
- Plastic or organic foreign bodies are less visible, although the non-anatomical shape may help in identification.
- An endotracheal tube that has been bitten through and dislodged during anaesthetic recovery can easily be seen radiographically (Figure 10.24b) and removed endoscopically.
- Mucus surrounding the foreign body may be seen as a focal increase in soft tissue opacity.
- Fluid in the tracheal lumen is not radiographically visible since it does not create clear margins. However, aspirated barium liquid is frequently seen after oesophagography studies due to its mineral opacity. Small amounts are of no clinical consequence.



10.24 (a) Lateral thoracic radiograph of a 5-year-old Domestic Shorthair cat with a radiopaque foreign body in the caudal trachea. (Courtesy of E. Friend) (b) Lateral radiograph of a cat with a severed endotracheal tube in the thoracic trachea.

Interventional radiological procedures

Interventional radiological techniques are useful for retrieval of foreign bodies in the trachea and mainstem bronchi. In small patients where surgical or endoscopic intervention could severely compromise airway patency, interventional radiological techniques are particularly valuable. These techniques are described in Chapter 6.

Tracheitis

This condition may occur as a result of viral, bacterial or parasitic infection, or from non-infectious causes, such as prolonged barking, collapsing trachea or chronic cardiac disease.

- Irritation by gas, dust or allergy may result in tracheitis, and severe cases may be associated with bronchitis or bronchopneumonia.
- Exudate, necrosis and mucosal proliferation, as well as contraction of the trachealis muscle, may result in narrowing of the tracheal wall.
- Clinically, a dry, sometimes paroxysmal, cough is seen and may be associated with discomfort or rarely dyspnoea. The animal is otherwise healthy in uncomplicated cases of tracheobronchitis.

Imaging findings

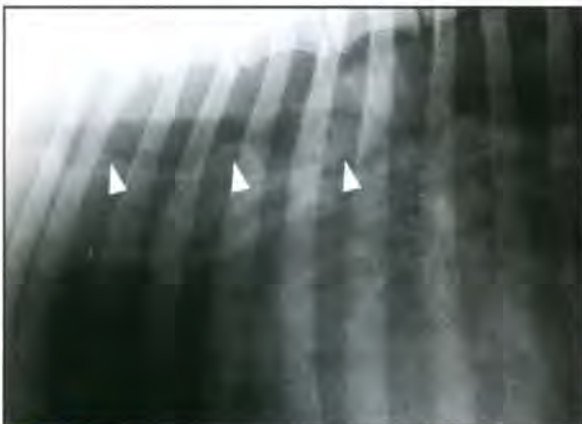
Tracheitis is often radiographically unremarkable unless it is severe or complicated by tracheal collapse, cardiac or pulmonary disease. Acute severe tracheobronchitis may result in marked luminal narrowing and may mimic tracheal hypoplasia.

***Oslerus osleri* infection**

This parasitic infection (previously known as *Filaroides osleri*) is relatively rare nowadays and is usually identified in dogs less than 2 years old, in particular in kennelled dogs, such as Greyhounds.

- Direct transmission from dog to dog is possible, including from dam to pup through faeces and saliva.
- Clinical signs include a mild to paroxysmal, hacking and often unproductive cough, which may end in retching, and is unresponsive to antibiotics.
- The trachea is sensitive to palpation and, unless a secondary infection is present, a normal body temperature is found.
- Wheezing, dyspnoea and weight loss may be seen in more advanced cases, although there may be no clinical signs.
- Bronchoscopy is the method of choice for diagnosis, where granulomas, papules or nodules may be identified.

Imaging findings: The trachea may appear radiographically normal. In severe cases, diffuse tracheal wall thickening, an indistinct mucosal surface or soft tissue nodules (Figure 10.25) may be seen protruding into the distal third of the tracheal lumen or bronchi.



10.25 Lateral radiograph of a 5-year-old Lurcher with several nodules (arrowheads) in the caudal thoracic trachea representing *Oslerus osleri* granulomas. (Courtesy of A. Holloway)

Tracheal haemorrhage

Tracheal haemorrhage can occur locally secondary to injury from external or internal trauma, particularly during intubation accidents, or more commonly, diffusely as a result of generalized bleeding disorders in dogs and cats. In particular, rodenticide intoxication can lead to diffuse thickening of the tracheal wall with submucosal haemorrhagic infiltrate and is often associated with other sites of haemorrhage, particularly in the mediastinum and lungs.

Imaging findings

- Marked widespread thickening of all aspects of the tracheal wall with a reduction in luminal diameter.

- Often associated with a widened mediastinum.
- Often associated with patchy areas of alveolar lung opacity in multiple lung lobes (Figure 10.26).



10.26 (a) Lateral thoracic radiograph of a 3-year-old Labrador Retriever with rodenticide toxicity (warfarin) causing submucosal tracheal and pulmonary haemorrhage. Notice the marked tracheal narrowing and increased opacity in the midcaudal lung field. (b) DV thoracic radiograph. There is marked cranial mediastinal widening and increased opacity in the left caudal lung lobe as a result of haemorrhage.

Extrinsic conditions affecting tracheal position and opacity

A variety of conditions of neighbouring organs can affect the radiographic position and opacity of the trachea. In most cases these do not result in clinical tracheal disease. Marked extrinsic tracheal compression may become clinically apparent.

Enlarged cardiac silhouette

Cardiac enlargement involving the heart base and marked pericardial effusion can cause dorsal deviation of the thoracic trachea.

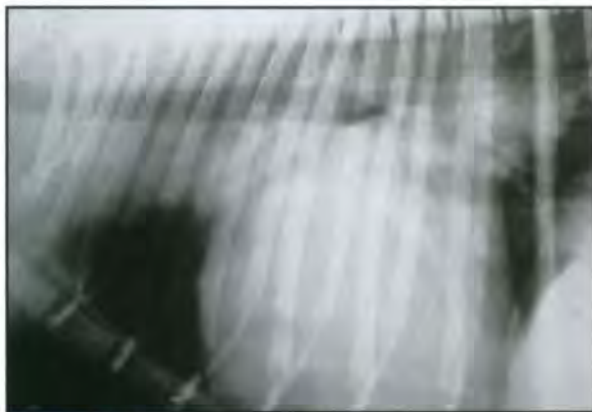
- Unless the cardiac enlargement is focal, such as with heart base tumours, the entire trachea is

typically dorsally deviated without being bent. This feature distinguishes most cardiac diseases from many other conditions that do bend the trachea.

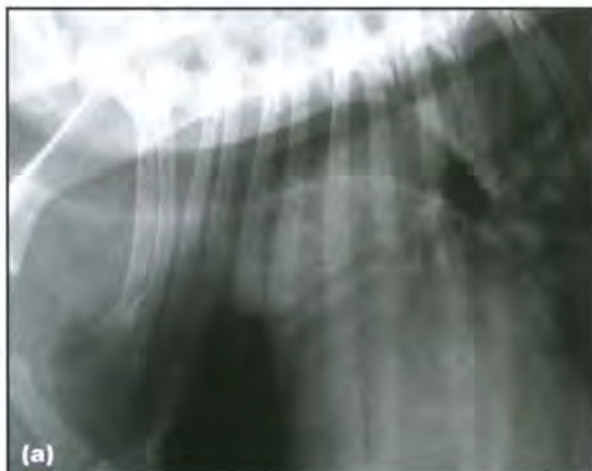
- In the presence of a pleural effusion with effacement of the cardiac borders, the course of the trachea may be the only remaining feature that is indicative of a cardiogenic or non-cardiogenic origin of the effusion.

Imaging findings:

- Dorsal deviation of the thoracic trachea with a straight course parallel to the thoracic spine (Figure 10.27).
- Heart base masses can cause focal dorsal and lateral deviation (Figure 10.28).
- In pulmonic stenosis, the dilated post-stenotic main pulmonary artery segment can protrude dorsally from the cranial heart base and superimpose on the ventral aspect of the caudal thoracic tracheal lumen. Based on its characteristic appearance, a term that has been coined to describe this feature is the 'hat sign',



10.27 Lateral thoracic radiograph of a dog with mitral valve endocardiosis and resulting cardiomegaly. Notice the straight course of the thoracic trachea, parallel to the thoracic spine, due to the enlarged cardiac silhouette.



10.28 (a) Lateral thoracic radiograph of a 10-year-old Cavalier King Charles Spaniel with a heart base tumour. Notice the focal marked dorsal tracheal deviation pivoting over the cranial cardiac silhouette. (continues) ▶



10.28 (b) (continued) Reconstructed dorsal plane thoracic CT image demonstrating the lateral deviation and partial compression of the caudal thoracic trachea as well as the left cranial lung lobe.

which is relatively specific for pulmonic stenosis. However, only a minority of dogs with pulmonic stenosis demonstrate a 'hat sign'. This is also an example of how an external soft tissue lesion can create the false impression of luminal narrowing of the thoracic trachea (Figure 10.29, see also Figure 7.56a, p. 116).



10.29 Lateral thoracic radiograph of an 8-month-old West Highland White Terrier with pulmonic stenosis. The protruding dilated main pulmonary artery segment is superimposed on the ventral aspect of the caudal thoracic tracheal lumen, creating the impression of a hat (i.e. the 'hat sign').

Persistent right aortic arch

A persistent right aortic arch (PRAA) is the most common vascular ring anomaly in dogs, where the aortic arch is formed by the right instead of the left aortic branch. The trachea and oesophagus are trapped between the right-sided aortic arch and left-sided ductus arteriosus. Deviation and focal compression of the thoracic trachea occur due to entrapment. Additional vascular anomalies are common (see also Chapters 7 and 9).

Imaging findings:

- Moderate to marked focal leftward tracheal deviation near the cranial cardiac border on VD/DV radiographs (Figure 10.30) is invariably seen.
- Focal tracheal narrowing near cranial cardiac border is commonly seen.
- Additional ventral tracheal deviation near the cranial cardiac border on lateral radiographs is occasionally seen.



10.30 VD thoracic radiograph of a dog with a PRAA. Notice the leftward deviation of the caudal thoracic trachea (arrowhead) caused by entrapment between the right aortic arch and the left-sided ductus arteriosus. This radiographic sign is relatively specific for PRAA and has been described as a hallmark for this condition. (Courtesy of J. Buchanan)

Cranial mediastinal masses and pleural effusion

The most commonly seen mediastinal masses in dogs and cats arise from lymphatic, thymic, thyroid or neuroendocrine tissue (see Chapter 8).

- If large enough, mediastinal masses can cause local dorsal tracheal deviation.
- Neuroendocrine and vertebral tumours can deviate the trachea ventrally.
- Perihilar lymphadenopathy will create focal deviation of the caudal trachea, as do heart base masses.
- A gas-distended oesophagus can highlight the tracheal walls but otherwise usually does not affect tracheal appearance.
- Marked pleural effusion can induce dorsal deviation of the trachea.

Imaging findings:

- Local dorsal tracheal deviation with pivotal point at the carina or cranial mediastinum. With perihilar lymphadenopathy, the caudal trachea can be dorsally or ventrally deviated, depending on the specific lymph node involved (Figure 10.31ab).

- Displacement of the carina caudal to the sixth intercostal space (Figure 10.31c).
- Occasionally, ventral tracheal deviation with craniodorsal mediastinal masses is seen (Figure 10.31d).
- Straight dorsal tracheal deviation on lateral radiographs with pleural effusion (Figure 10.32).



10.31 (a) Lateral thoracic radiograph of a 15-year-old Domestic Shorthair cat with a mediastinal carcinoma occurring 2 years after successful radiation treatment of a thymoma. Notice the dorsal tracheal deviation pivoting at the level of the fourth rib. There is also visible cranial lung lobe atelectasis (air bronchograms) and pleural effusion. (b) Lateral thoracic radiograph of a dog with perihilar lymphadenopathy causing ventral deviation and compression of the caudal thoracic trachea. (c) Lateral thoracic radiograph of an 11-year-old Domestic Shorthair cat with a large thymoma causing dorsal tracheal deviation and caudal displacement of the carina (eighth intercostal space). The heart is located at the caudodorsal aspect of the mass. The caudal displacement of the carina is pathognomonic for a cranial mediastinal mass. (continues)



10.31 (continued) **(d)** Lateral thoracic radiograph of a 2-year-old Irish Setter with a neuroendocrine tumour in the cranial mediastinum causing ventral deviation of the cranial thoracic trachea.



10.32 Cranial close-up of a lateral thoracic radiograph of a dog with pleural effusion. The trachea is straight but parallel to the thoracic spine, a common feature in pleural effusion.



10.33 **(a)** Lateral cervical radiograph of a 2-month-old Weimaraner with canine strangles. There is severe submandibular and retropharyngeal lymphadenopathy, the latter causing marked ventral deviation of the larynx and cranial trachea. **(b)** Lateral cervical radiograph of a 10-year-old Doberman with a mineralized thyroid tumour causing marked dorsal deviation of the cranial trachea.

Retropharyngeal and thyroid masses

The thyroid lobes are laterally or dorsolaterally adjacent to the first five to eight tracheal rings.

- Thyroid enlargement can cause ventral or dorsal tracheal deviation.
- Retropharyngeal masses (lymphadenopathy, foreign body abscessation) usually cause laryngeal displacement but if extensive can also affect the proximal trachea.
- In dogs thyroid neoplasia is usually a space-occupying lesion that frequently deviates the trachea.
- In cats thyroid neoplasia remains small and rarely causes a mass effect on the trachea.

Imaging findings:

- Marked ventral and lateral deviation of the cranial cervical trachea (Figure 10.33a).
- Less commonly dorsal tracheal deviation.
- Occasionally mineralization of mass (Figure 10.33b).

References and further reading

- Berkwitz L and Berzon JL (1985) Thoracic trauma. Newer concepts. *Veterinary Clinics of North America: Small Animal Practice* **15**, 1031–1039
- Carlisle CH, Biery DN and Thrall DE (1991) Tracheal and laryngeal tumours in the dog and cat: Literature review and 13 additional patients. *Veterinary Radiology* **32**, 229–235
- Coyne BE and Fingland RB (1992) Hypoplasia of the trachea in dogs: 103 cases (1974–1990). *Journal of the American Veterinary Medical Association* **201**, 768–772
- Dennis R, Kirberger RM, Wrigley RH and Barr FJ (2001) Lower respiratory tract. In: *Small Animal Radiological Differential Diagnosis*, ed. R Dennis *et al.*, pp. 103–108. WB Saunders, London
- Ettinger SJ and Kantrowitz B (2005) Diseases of the trachea. In: *Textbook of Veterinary Internal Medicine, 6th edn*, ed. SJ Ettinger and EC Feldman, pp. 1217–1231. Elsevier, St Louis
- Harvey CE and Fink EA (1982) Tracheal diameter: Analysis of radiographic measurements in brachycephalic and non-brachycephalic dogs. *Journal of the American Animal Hospital Association* **18**, 570–576
- Hendricks JC and O'Brien JA (1985) Tracheal collapse in a cat. *Journal of the American Veterinary Medical Association* **187**, 418–419
- Jakubiak MJ, Siedlecki CT, Zenger E, *et al.* (2005) Laryngeal, laryngotracheal, and tracheal masses in cats: 27 cases (1998–2003). *Journal of the American Animal Hospital Association* **41**, 310–316
- Johnson LR and McKiernan BC (1995) Diagnosis and medical management of tracheal collapse. *Seminars in Veterinary Medicine and Surgery (Small Animal)* **10**, 101–108
- Kneller SK (2002) The larynx, pharynx and trachea. In: *Textbook of Veterinary Diagnostic Radiology, 4th edn*, ed. Thrall DE, pp. 323–329. WB Saunders, Philadelphia

- Luis Fuentes V (1998) Tracheobronchial disease. In: *BSAVA Manual of Small Animal Cardiorespiratory Medicine and Surgery*, ed. V Luis Fuentes and S Swift, pp. 213–217. BSAVA Publications, Cheltenham
- O'Brien JA, Buchanan JW and Kelly DE (1966) Tracheal collapse in the dog. *Journal of the American Veterinary Radiology Society* **7**, 12–20
- Rudorf H, Herrtage ME and White RA (1997) Use of ultrasonography in the diagnosis of tracheal collapse. *Journal of Small Animal Practice* **11**, 513–518
- Stann SE, and Bauer TG (1985) Respiratory tract tumors. *Veterinary Clinics of North America: Small Animal Practice* **15**, 535–536
- Suter PF (1984) Diseases of the nasal cavity, larynx and trachea. In: *Thoracic Radiography. A Text Atlas of Thoracic Diseases of the Dog and Cat*, pp. 237–250. Peter F Suter, Wettswil, Switzerland
- Suter PS, Colgrove DJ and Ewing GO (1972) Congenital hypoplasia of the canine trachea. *Journal of the American Animal Hospital Association* **8**, 120–127
- White RAS and Williams JM (1994) Tracheal collapse in the dog – is there really a role for surgery? – a survey of 100 cases. *Journal of Small Animal Practice* **35**, 191–196
- White RN, and Milner HR (1995) Intrathoracic tracheal avulsion in three cats. *Journal of Small Animal Practice* **35**, 191–196
-

The bronchial tree

Panagiotis Mantis, Victoria Johnson and Federica Morandi

Radiographic anatomy

The bronchial tree begins at the termination of the trachea with its division into the right and left principal (or mainstem) bronchi. The principal bronchi are short and each divides into lobar bronchi (also known as secondary bronchi); these supply the various lobes of the lung and are named according to the lobe they supply (Figures 11.1 and 11.2).

The right principal bronchus divides into four lobar bronchi, one for each lobe of the right lung: cranial, middle, caudal and accessory. The left principal bronchus divides into two lobar bronchi: cranial and caudal. The cranial secondary bronchus then divides to supply the cranial and caudal segments of the left cranial lung lobe. The left caudal secondary bronchus supplies the left caudal lung lobe.

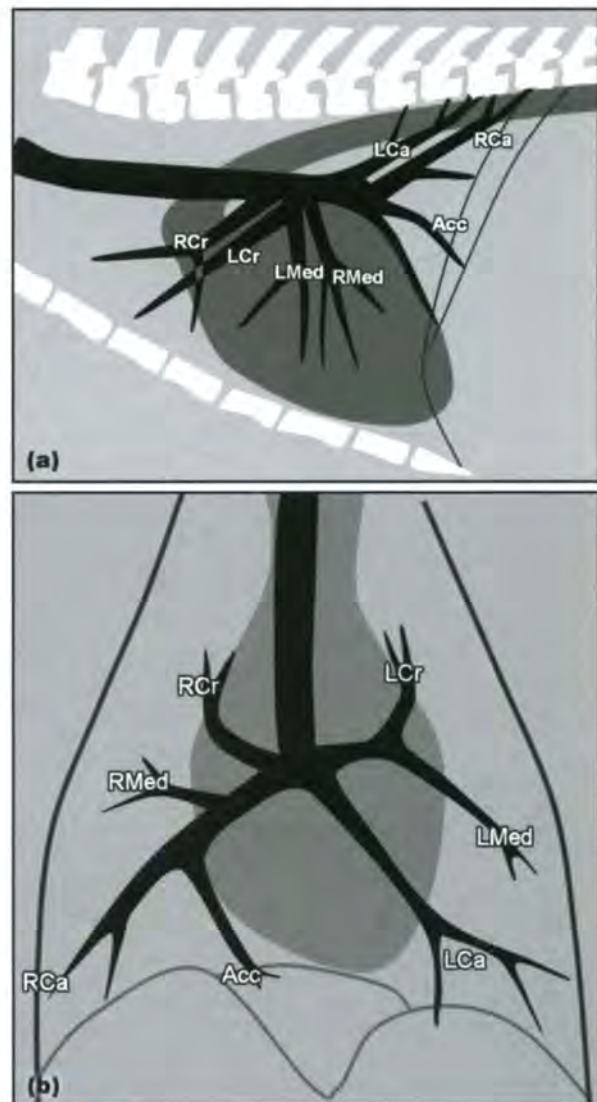
Within each lobe the lobar bronchi subdivide further into segmental bronchi (sometimes referred to as tertiary bronchi). The segmental bronchi with the lung tissue they ventilate are called *bronchopulmonary segments*. Each bronchopulmonary segment is independent. Adjacent bronchopulmonary segments normally communicate with each other in the dog through the interalveolar pores of Kohn and channels of Lambert (see also Chapter 12). The segmental bronchi branch into smaller generations of bronchi until the formation of the respiratory bronchioles, alveolar ducts, alveolar sacs and pulmonary alveoli. The number of generations depends on the size of the animal and is difficult to measure.

The bronchial walls are formed by hyaline cartilage rings and spiral bands of smooth muscle. Bronchioles are commonly less than 1 mm in diameter and have no cartilaginous support.

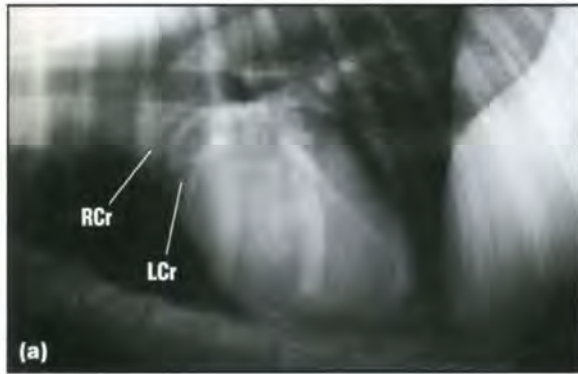
Bronchi and the surrounding tissue, up to the level of the respiratory bronchioles, receive their blood supply from the bronchial artery, which, although variable in origin, is commonly a continuation of the broncho-oesophageal artery. Venous return is via the pulmonary circulation.

On radiographs the bronchi are usually poorly seen unless they have a thickened or calcified wall. Only the larger bronchi in the hilar region can normally be identified on survey radiographs. The location of a bronchus is between the pulmonary artery and the vein with the artery being dorsal (or cranial) in lateral views and lateral in dorsoventral (DV) or ventrodorsal (VD) views. Bronchial arteries are not seen on radiographs. The space between the paired pulmonary artery and

vein on a radiograph does not necessarily represent the bronchial lumen. Bronchi should gradually taper towards the periphery.



11.1 Approximate location of the normal lobar bronchi in **(a)** a right lateral view and **(b)** a VD view. The normal lobar bronchi are labelled: Acc = Accessory lobe; LCa = Left caudal lobe; LCr = Cranial segment of the left cranial lobe; LMed = Caudal segment of the left cranial lobe; RCa = Right caudal lobe; RCr = Right cranial lobe; RMed = Right middle lobe.



11.2 (a) Left lateral view of a normal canine thorax. The larger bronchi and the mineralized bronchi can be seen. The right and left cranial lobar bronchi are marked (RCr, LCr); compare this with Figure 11.1a. The space between the paired pulmonary arteries and veins does not necessarily represent the bronchus. (b) Close-up of a right lateral thoracic radiograph in a normal dog. The cranial lobar pulmonary artery (A) and vein (V) are seen accompanying a cranial lobar bronchus (between the arrows). The bronchus is seen due to faint mineralization of its wall. (c) DV radiograph of a normal dog showing the trachea branching at the carina. The right and left caudal mainstem bronchi are shown by arrowheads. Compare this radiograph with Figure 11.1b. It is often possible to follow all the main divisions of the bronchial tree on a good quality DV/VD radiograph.

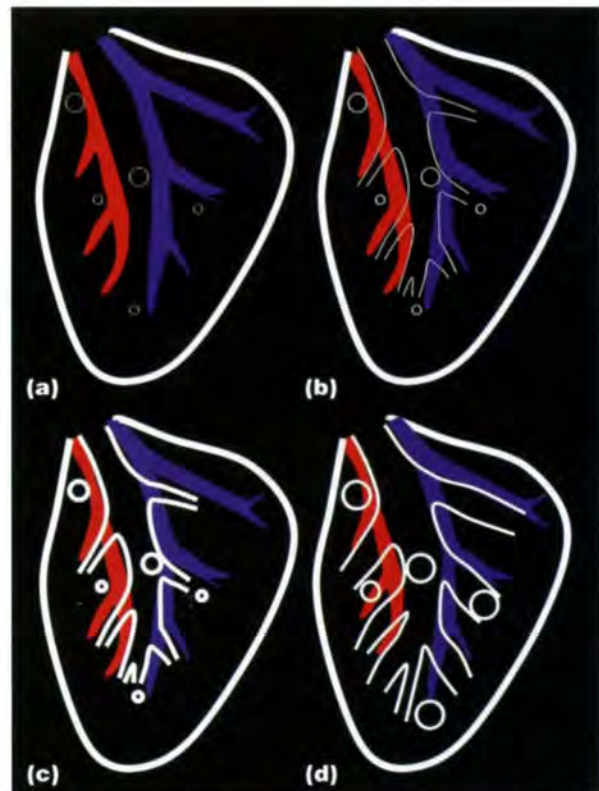
Interpretive principles

Radiographic signs of bronchial disease

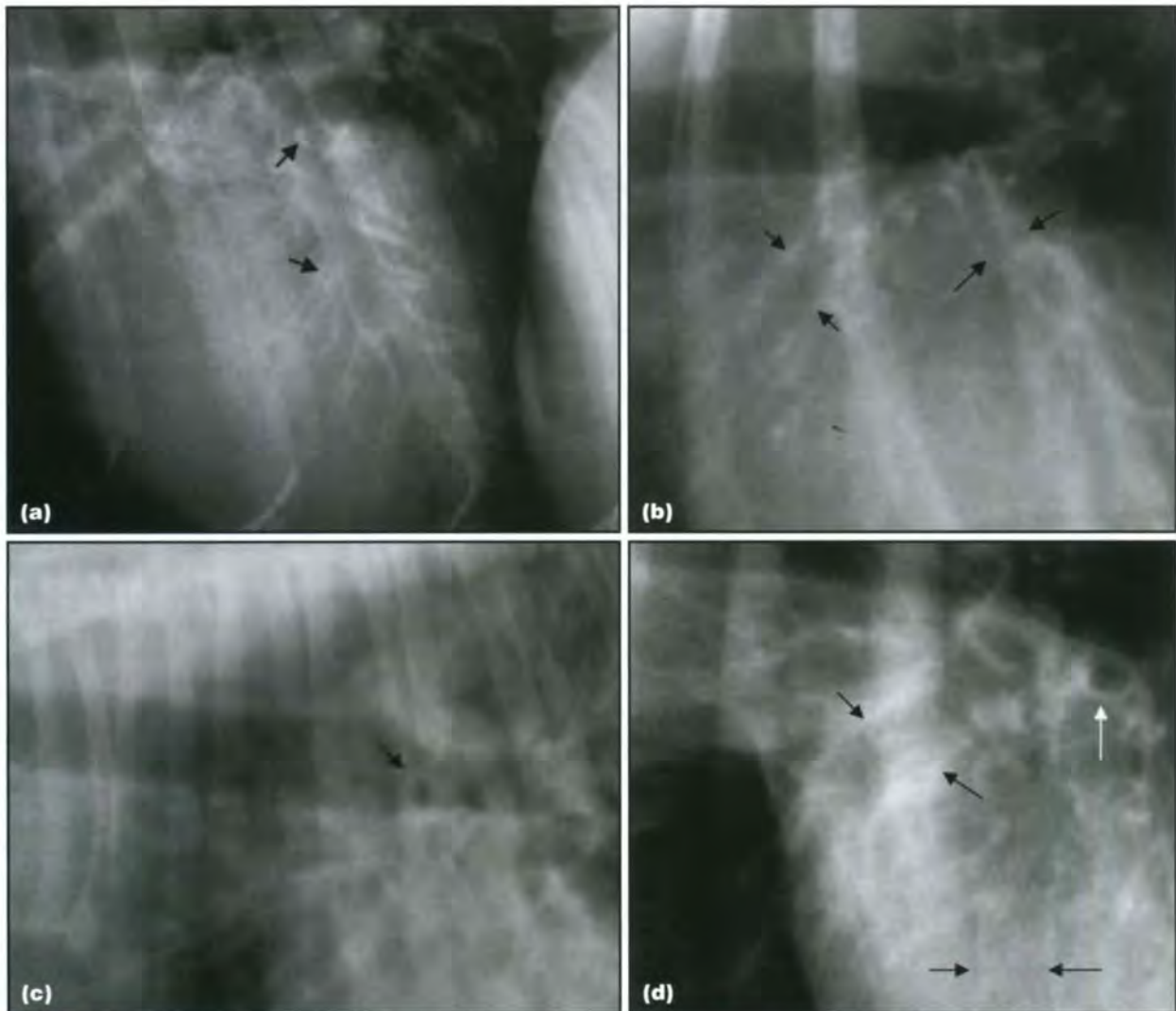
It is important to note that the severity of the clinical signs in bronchial disease does not always correlate with the radiographic signs. In many dogs with clinical bronchitis the thoracic radiographs may appear normal.

When radiographic changes are present, bronchial disease is identified by increased visibility of the bronchial walls. It is first important to distinguish the reason for increased visibility. Mineralization of the bronchial wall is usually an incidental finding and is discussed in further detail below. Other reasons for increased visualization are usually pathological and may be secondary to bronchial thickening, mucosal thickening or peribronchial infiltration. These changes may be accompanied by alteration in the size and shape of the bronchial lumen.

It is possible to distinguish between normal bronchi, mineralized bronchi, thickened bronchi and those with shape changes on radiographs (Figures 11.3, 11.4 and 11.5). When bronchial walls are thickened they appear as 'doughnuts' when viewed end-on or as 'tramlines' when viewed laterally. This is also referred to as a *bronchial pattern* (see also Chapter 12).



11.3 Radiographic variations in the appearance of the bronchial walls. (a) Normal dog. The bronchial walls may not be visible when viewed side-on but they may be seen end-on. (b) Bronchial mineralization. Can be a normal feature in skeletally mature dogs. Thin 'tramlines' and 'rings' may be seen. (c) Bronchial wall thickening. Thick 'tramlines' and 'doughnuts' will be seen. (d) Bronchiectasis. The bronchial diameter is increased and the bronchi do not taper normally. 'Doughnuts' and 'tramlines' will also be seen.



11.4 Bronchial patterns. **(a)** Close-up of a thickened bronchus on a right lateral thoracic radiograph in a Border Collie with severe chronic bronchitis. The wall is extremely thickened and prominent, resulting in the appearance of 'tramlines'. Thick 'doughnuts' are also seen (arrowed). Note that many dogs with chronic bronchitis show much milder or even no radiographic changes. **(b)** Bronchial mineralization (arrowed), which is an age-related change. **(c)** Multiple thickened bronchi (arrowed). **(d)** Bronchiectasis. Multiple dilated bronchi, which do not display tapering towards the periphery, seen in longitudinal section (black arrows) and end-on (white arrow).

Thin mineralized 'rings' and 'tramlines'

Age-related change
 Chondrodystrophoid breeds
 (Less commonly: metastatic mineralization, such as hyperadrenocorticism, renal secondary hyperparathyroidism)

Thick soft tissue opacity 'doughnuts' and 'tramlines'

Bronchitis (allergic, parasitic, bacterial, viral, irritant, etc.)
 Bronchopneumonia
 Bronchiectasis (if size and shape changes also seen)

Peribronchial cuffing

Oedema
 Bronchopneumonia
 Pulmonary infiltrates with eosinophils (PIE)

11.5 Bronchial patterns.

Changes in size and shape (e.g. saccular, cylindrical shape when viewed in long axis) of the bronchial lumen, followed by loss of the normal tapering of the bronchial lumen towards the periphery indicate the presence of *bronchiectasis*.

When changes in the interstitial opacity occur around a bronchial structure then '*peribronchial cuffing*' may be seen. This has a similar appearance to a bronchial pattern but the pathological changes constitute a cellular infiltrate in the interstitium rather than the bronchial wall. An unstructured interstitial pattern may also be present.

Bronchial and peribronchial mineralization

Mineralization of the bronchial walls along the bronchial tree makes smaller bronchi more readily identifiable. This mineralization is a common and clinically insignificant finding in older animals but can also be seen in younger animals, especially in

chondrodystrophoid breeds of dog. It results in the bronchial walls appearing as fine linear shadows when viewed laterally or as fine distinct circles when viewed end-on. These *thin* mineralized 'rings' and 'tramlines' should be differentiated from the thicker soft tissue opacities seen in bronchial disease (Figure 12.26, p. 254).

Bronchial mineralization may also be seen in systemic pathological conditions, such as hyperadrenocorticism and renal secondary hyperparathyroidism (Figure 12.27, p. 254).

In cats calcification of the peribronchial mucus glands may occur without clinical signs. These are seen as small multifocal mineralized opacities, and may be difficult to distinguish from the rare condition broncholithiasis (see Diseases, below).

Bronchial obstruction

Bronchial obstruction can be produced by a variety of mechanisms (Figure 11.6). The same classification system can be applied to tracheal obstruction (see Chapter 10).

Morphological obstruction is a structural obstruction of the bronchus and may be further classified as intraluminal, intramural or extramural, depending on the origin of the obstruction. Morphological obstructions may be complete or incomplete depending on their size and location. Rarely a morphological obstruction (especially a foreign body) can create a 'check valve' effect where air is permitted to pass the obstruction during inspiration when the bronchial lumen is wider, but not during expiration when the lumen is narrower.

This results in peripheral air trapping and overinflation. This change may not be apparent on inspiratory radiographs but will be identified as a hyperlucent region of lung on expiratory films.

Functional obstructions occur when the bronchi constrict with resultant air trapping. This may occur in asthma or allergic bronchitis and is discussed further below (see Feline chronic lower airway disease).

Dynamic obstructions occur when there is loss of the normal recoil or rigidity of the bronchial walls, resulting in flattening or collapse during forcible expiration or coughing. This condition often accompanies tracheal collapse and is discussed in more detail below (see Bronchial collapse).

The radiographic features of bronchial obstruction depend on the location and degree of the obstruction, the effectiveness of collateral ventilation and the chronicity of the condition (see Figure 11.6).

Bronchography

Bronchography has been used in the past to outline the bronchial tree (see Figure 1.19, p. 12) and therefore allow for further investigation of bronchial disease. It was considered especially useful for the evaluation of chronic obstructive airway disease, chronic bronchitis, bronchial spasm, bronchiectasis (Figure 11.7), bronchial stenosis or compression, bronchogenic neoplasms (see Figure 12.49, p. 265), bronchial cysts and in the identification of radiolucent bronchial foreign material. The contrast medium agent most commonly used was an aqueous suspension of propyl iodine.

Type of obstruction	Aetiology	Description	Radiographic features
Morphological	Intraluminal: foreign body, mucus plug, viscid exudates, mucosal polyp, neoplasia, iatrogenic endotracheal tube temporary obstruction Intramural: oedema, haemorrhage, infectious or inflammatory mucosal proliferation Extramural: enlarged left atrium, mediastinal or perihilar mass (lymph nodes, abscess, granuloma, oesophageal foreign body, aortic body tumour) or intrapulmonary mass (neoplasia, abscess, granuloma)	Complete: an intraluminal, intramural or extramural physical obstruction causing atelectasis or collateral air drift Incomplete: an intraluminal, intramural or extramural obstruction which may cause air trapping	Complete with absence of collateral ventilation: atelectasis with increased lobar opacity and loss of volume (mediastinal shift towards affected side); with air bronchograms if small airway is blocked; without air bronchograms if major airway is blocked Complete with collateral ventilation maintained: normal radiographs or hyperlucency and volume gain in affected lobe Incomplete: radiographs may be normal Incomplete with 'check valve' effect: air trapping with hyperlucency and volume gain in affected lobe. May only be recognized on expiratory radiographs
Functional	Asthma Allergic bronchitis Hypoxia	Reactive bronchial constriction of small airways causing air trapping	Normal radiographs or hyperlucency of all or part of the lung and volume gain
Dynamic	Bronchial collapse (cartilage degeneration) Chronic inflammatory change	Reduced rigidity of main bronchi and loss of stability of walls of small bronchi, resulting in expiratory bronchial airway collapse ± peripheral air trapping	Mainstem bronchial collapse: narrowed bronchi on expiration, no lung changes Peripheral small airway collapse: normal radiographs or regions of uneven or increased inflation with focal hyperlucencies and focal opacities

11.6 Causes of bronchial obstruction.



11.7 Bronchography of the left lung of a dog with bronchiectasis. Note the lack of tapering of the bronchial tree and budding of the smaller bronchi. This technique is now obsolete. (Courtesy of the University of Pennsylvania)

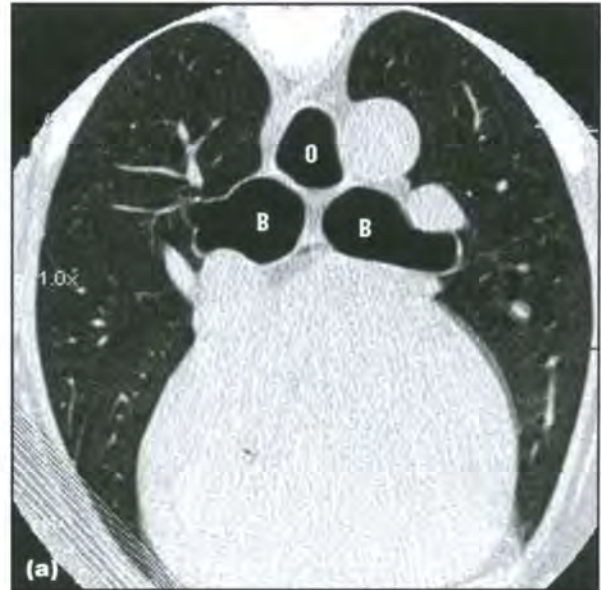
Although the procedure was relatively simple it was not well tolerated by the patient and only one lung at a time could be assessed bronchographically. Fibre-optic bronchoscopy and bronchial computed tomography (CT) are less invasive and have completely replaced this technique.

Bronchial computed tomography

Bronchi and bronchioles are readily visible and easily assessed on thoracic CT examinations in both the dog and cat. The correct choice of algorithm and image display is essential. A standard axial or spiral lung protocol is usually employed throughout the thorax, followed by a high-resolution series (thin slice width, high kV and mA, and high spatial frequency reconstruction algorithms) through the areas of interest. As for lung CT, it is important to obtain images without respiratory motion (see also Chapter 3). A lung window should always be used when examining the lung parenchyma. Small focal lung lesions will not be visualized in a soft tissue window.

The bronchi are seen as thin-walled branching structures with well demarcated, smooth, hyperattenuating inner and outer walls (Figure 11.8). They are generally accompanied by a pulmonary artery and vein. Usually, the artery lies closer and follows the course of the bronchus more rigidly than the vein. The bronchi and larger bronchioles are easily visible, but the smaller bronchioles become increasingly difficult to identify towards the periphery of the lung. They may not be definitively identified within 1 cm of the periphery of the lung margin. Attempts have been made to characterize normal bronchial wall thickness and cross-sectional areas in the dog. In human thoracic CT, well established bronchial measurements and ratios are used to assess wall thickening and bronchiectasis.

CT provides many advantages over standard thoracic radiographs in the evaluation of the smaller airways. Bronchial rupture may be confirmed and localized. Intraluminal material such as foreign bodies and mucus plugs are easily identified. CT achieves visualization of tiny bronchioles that cannot



11.8 (a) Transverse CT image obtained from a normal dog with a high-resolution lung algorithm and displayed with a lung window. The image was obtained just caudal to the carina. The mainstem bronchi are marked with a B and sit dorsal to the heart. Note the thin smooth hyperattenuating walls. The oesophagus (O) is air filled. (b) Transverse CT image obtained more caudally at the level of the cranial liver. Many small branches of the bronchial tree are clearly seen; one bronchus is marked (arrowed).

be accessed by bronchoscopy and also has the advantage that intravenous contrast medium can be administered to aid in the differentiation of neoplastic and inflammatory intraluminal masses from foreign material. Bronchiectasis, whilst sometimes difficult to evaluate radiographically, can be definitively identified with lung CT (Figure 11.9). Different types of bronchiectasis may be distinguished on CT images, such as traction bronchiectasis seen in conditions of interstitial fibrosis (see Chapter 12). Dynamic CT studies may be used in the evaluation of bronchial collapse in dynamic airway disease just as for the trachea (see Chapter 10).

CT is helpful in the differentiation of peribronchial infiltrates and peribronchial masses from true bronchial masses and also provides valuable information



11.9 Transverse CT image (lung window) obtained with a high-resolution lung algorithm from the caudal lung lobes of a 5-year-old Rottweiler with severe bronchitis and bronchiectasis, consistent with primary ciliary dyskinesia. Compare the bronchi to those seen in Figure 11.8a, which was obtained from the same region of the lungs. Markedly thickened bronchial walls are seen. Many bronchi are enlarged, have lost their normal round shape and are peripherally distended, consistent with bronchiectasis.

for presurgical planning (see Figures 12.38, p. 260 and 12.61a, p. 270). Multiplanar reconstructions may be particularly useful. CT-guided biopsy can be used for further evaluation of bronchial and peribronchial mass lesions. This is a useful and relatively safe procedure when minimal aerated lung is penetrated to obtain a tissue sample. CT is also useful for staging neoplastic bronchial disease, as the bronchial and tracheobronchial lymph nodes can be visually assessed for evidence of metastatic disease (see Chapter 8).

A rapidly developing technique in the human medical field is the use of multidetector CT to obtain non-invasive 'virtual bronchoscopy' images. The images produced closely resemble those seen with fiberoptic bronchoscopy. Although it is widely considered that this technique will not replace standard fiberoptic bronchoscopy, it has value in certain clinical situations and may be used to direct more invasive procedures.

Bronchial ultrasonography

The presence of aerated lung surrounding bronchial structures means that they are inaccessible to ultrasonographic examination. However, bronchi are occasionally seen on an ultrasound examination when the surrounding lung lobe is collapsed or consolidated, eliminating the air content, thus providing an acoustic window for the evaluation of intrapulmonary structures including the bronchi. When fluid is present within the bronchial lumen they are referred to as 'fluid bronchograms' (see Chapter 12). It is also possible to identify bronchiectasis in this situation.

Diseases

Canine chronic bronchitis

Chronic bronchitis is an inflammatory disease of the airways. Animals usually present with a history of *chronic harsh cough* (more than 2 months) and exercise intolerance. Typically middle-aged to older small-breed dogs are predisposed, but the disease is also common in large breeds. Tracheal sensitivity may be present on clinical examination and inspiratory crackles and expiratory wheezes may be identified on auscultation. Heart rate is usually normal to low and a pronounced sinus arrhythmia may be present.

Diagnosis of chronic bronchitis in the dog and cat is usually one of exclusion. Other conditions such as infectious airway disease, structural airway disease (collapse, bronchiectasis) and neoplasia must be ruled out.

The condition is never completely cured but can be controlled by a combination of medical therapy, weight loss and environmental changes (reduced smoke, pollutants, heat, etc.). When poorly controlled, bronchitis may result in irreversible bronchiectasis and even pulmonary hypertension (secondary to chronic hypoxia and/or vascular remodelling).

Radiography

Radiographic findings include:

- Presence of a bronchial pattern (see Figures 11.3c and 11.4a)
- Increase in the non-vascular linear markings and peribronchial infiltration (peribronchial cuffing)
- Thickened bronchial walls and increased numbers of visible bronchial walls are reportedly the most reliable evidence of canine chronic bronchitis on radiographs
- Bronchi containing exudate may appear as solid structures and may be confused with vessels or even nodules when seen end-on
- There may be right-sided cardiomegaly in dogs with chronic airway disease that develop pulmonary hypertension and/or cor pulmonale.

It should be noted that radiographic changes may not be present. Normal thoracic radiographs do not rule out chronic bronchitis.

Computed tomography

CT findings include:

- Increased visibility of the bronchial markings
- Thickened bronchial walls. Attempts have been made to characterize the bronchial wall thickness, but currently it remains a subjective evaluation.

Canine acute bronchitis

Thoracic radiographs in cases of acute bronchitis are indicated mainly to rule out other diseases or complications, especially if clinical signs are severe or prolonged. Many animals with acute bronchitis show no radiographic changes. Acute bronchitis may appear as a bronchial pattern irrespective of the cause and radiographic findings are similar to those seen in canine chronic bronchitis (see above).

Feline chronic lower airway disease

Feline chronic lower airway disease encompasses a multitude of small airway diseases in the cat including *feline asthma*. Inflammation of the airways leads to a reversible obstruction to airflow (functional obstruction) and hence air trapping. The obstruction is due to a combination of bronchoconstriction, bronchial wall oedema and submucosal gland hypertrophy.

Clinical signs vary from chronic coughing and wheezing to severe respiratory distress. The condition can affect cats of any age with Siamese appearing to have an increased incidence. Hyper-responsive airways and reversible airflow obstruction lead to a reduced airway diameter and increased airway resistance. The condition can be extremely severe in presentation and care should be taken when handling dyspnoeic cats.

Radiography

Radiographs may be normal. It should be noted that the severity of the radiographic signs may not correlate with the clinical signs. Findings include:

- Classically *peribronchial cuffing* is identified, although a variety of bronchial, interstitial and alveolar lung patterns (Figure 11.10) may be observed
- Excessive mucus production and accumulation in the bronchial lumen may give the impression of pulmonary nodules if seen end-on
- Obstruction of larger airways can cause alveolar infiltrates, consolidation or atelectasis
- In particular, *right middle lung lobe collapse* (Figure 11.11) is a common sequel to severe feline chronic lower airway disease
- Evidence of *air trapping* and *hyperinflation* (Figure 11.12; see also Figures 12.16, p. 250 and 12.70, p. 276) may be seen: flattened diaphragm and hyperlucent lungs (variable depending on the lung pattern present)
- Severe coughing may produce rib fractures in the cat and on occasion multiple fractures at differing stages of healing may be identified (see Figure 12.70, p. 276).



11.10 Close-up of a lateral thoracic radiograph of an 8-year-old Domestic Shorthair cat with prominent bronchial thickening. 'Doughnuts' (arrowed) are visible throughout the lung fields.



11.12 Close-ups of (a) lateral and (b) VD thoracic radiographs from a 15-month-old Domestic Shorthair cat with chronic lower airway disease. The bronchi are thickened throughout the lung fields and in areas where they are filled with mucus they resemble pulmonary nodules when seen end-on (especially visible in the caudoventral lung fields on the lateral view and the right caudal lung fields on the VD view). The lungs are hyperinflated as shown by the flattened diaphragm on both views and ribs that are more widely spaced than normal.



11.11 VD view of a Siamese cat with chronic lower airway disease. The right middle lung lobe is consolidated and is seen as a triangular soft tissue opacity on the right side adjacent to the cardiac silhouette (arrowed).

Computed tomography

CT findings include:

- Thickened bronchial walls with increased attenuation (Figure 11.13)
- Nodular non-enhancing hyperattenuating areas representing mucus-filled bronchi
- Hyperattenuating lung fields in areas of lung consolidation or atelectasis.
- Generally hypoattenuating lung fields in cats with hyperinflated lungs (see Figure 12.72, p. 276).



11.13 Transverse CT image (lung window) of the lung of an 8-year-old Domestic Shorthair cat with markedly thickened bronchial walls visible throughout the lung fields.

Bronchiectasis

The word bronchiectasis was derived from the Greek words 'bronchos' meaning bronchus and 'ectasis' meaning extension. Bronchiectasis is irreversible *bronchial dilatation* often with accumulation of pulmonary secretions. It can be focal or disseminated and it is uncommon in dogs and rare in cats. In cats, a predisposition for older males has been described.

It can occur as a sequel to long-standing infectious or inflammatory pulmonary disease, secondary to airway obstruction or smoke inhalation, as a complication to radiation-induced pneumonitis or in association with primary ciliary dyskinesia. Also, it has been noted that halothane dilates airways by blocking baseline vagal tone.

Bronchial secretions accumulate in the dilated bronchi and predispose the patient to recurrent airway and pulmonary infections.

Dogs with bronchiectasis are commonly presented with a history of chronic productive coughing and recurring pneumonia that initially responds to antibiotics.

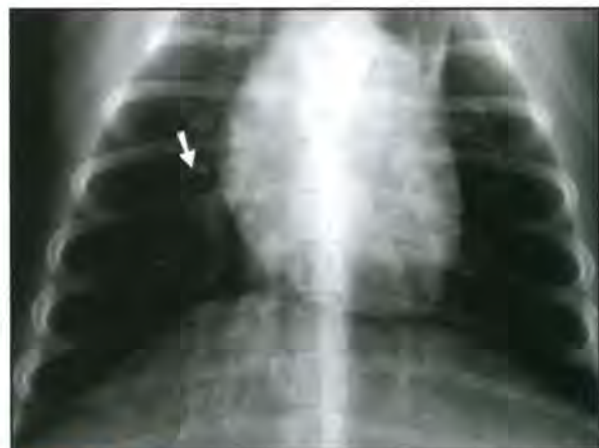
Radiography

Changes may be localized or generalized (see also Figures 12.71, p. 276 and 12.110, p. 299):

- Widening and unevenness of the bronchial lumen (Figure 11.14). This may be *saccular* or (more commonly) *cylindrical* (also known as tubular)

- dilatation. *Cystic* and *varicose* forms have also been described but are rarely identified. Saccular bronchiectases have round drop-like saccules filled with secretions at the end of normal bronchi (Figure 11.15). Cylindrical bronchiectases are dilated bronchi with a fairly even lumen and little diameter change as they subdivide. Each bronchus is club-like and occluded distally
- There may be thickened bronchial walls
- The dilated bronchial lumen may be visualized further into the periphery than normal, e.g. in the ventral areas of the lung fields
- Bronchi filled with secretions/exudate may appear as nodular opacities when seen end-on
- In saccular bronchiectasis many of the bronchi distal to the saccular dilatations are obliterated or filled with an exudate. Occasionally, after secondary infection, the saccules may form localized abscesses
- Often multiple regions of lung consolidation due to accompanying pneumonia
- Development of bronchogenic cysts secondary to bronchiectasis has been described in the dog.

Thoracic radiography may not be sensitive for the diagnosis of bronchiectasis in cats.



11.14 Close-up of a DV thoracic radiograph from a 7-year-old Fox Terrier. The markedly dilated bronchi are visible in longitudinal section and end-on (arrowed).



11.15 Close-up of a lateral thoracic radiograph from an 8-year-old mixed breed dog with saccular bronchiectasis. The bronchi are dilated and filled (partially or fully) with secretions (arrowed) and should not be confused with pulmonary nodules.

Computed tomography

CT findings include:

- Dilated airways: 'tramline' and 'ring'/'doughnut' appearance of the bronchi that are significantly wider than the adjacent vessels
- Clusters of dilated bronchi in more severely affected areas
- Dilated medium-sized bronchi may extend almost to the pleura
- Thickening of the bronchial walls (see Figure 11.9) and obstruction of airways (e.g. from mucus plugs)
- There may be lung consolidation.

In humans a CT classification system exists for different types of bronchiectasis.

Primary ciliary dyskinesia

Primary ciliary dyskinesia (PCD), also known as *immotile cilia syndrome*, is a diverse group of inherited structural and functional abnormalities of the respiratory and other cilia, which results in recurrent respiratory tract infections in the dog. More specifically, PCD is an inherited defect in microtubule formation, affecting cilia of the respiratory and urogenital tract and the auditory canal.

Typically PCD is diagnosed in young purebred animals with a reported higher incidence in the Bichon Frise. The condition may be seen in mixed breed dogs and also in cats.

There is a relatively high prevalence of a respiratory disease and the phenotype is almost identical to PCD in humans. The respiratory manifestations include chronic rhinitis, bronchitis and severe pneumonia with or without bronchiectasis. Affected animals are presented with recurrent chronic nasal discharge, productive cough, respiratory distress and exercise intolerance. Additional findings are infertility, hydrocephalus and loss of hearing.

Assessment of deficient mucociliary transport is initially performed with nuclear scintigraphy. Transmission electron microscopy of nasal or bronchial respiratory epithelium or seminal samples provides confirmation of the diagnosis.

Radiography

There are variable findings including bronchitis and pneumonia with or without bronchiectasis (Figure 11.16).

Computed tomography

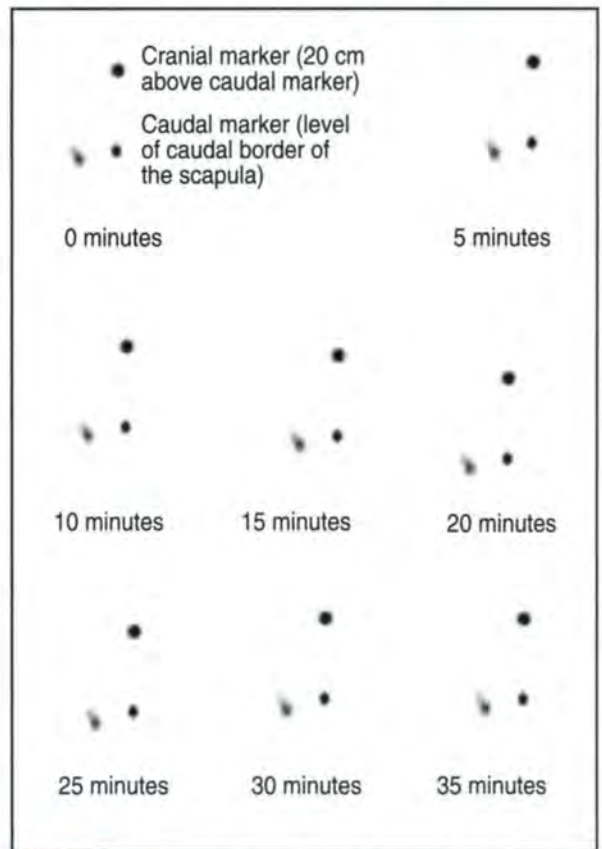
Feline PCD has been reported in a 2.5-year-old cat with morphological alterations in the ultrastructure of oviductal cilia. CT findings were consistent with early lesions of bronchiectasis. Foci of pleural thickening and interstitial enlargement were also observed.

Scintigraphy

To perform a scintigraphic study (see Chapter 5) a droplet of ^{99m}Tc-MAA is deposited in the distal aspect of the trachea. The diagnosis is confirmed by the absence of movement of the radiopharmaceutical droplet throughout the scintigraphic study (Figure 11.17). It should be noted that droplet movement *always* indicates normal ciliary function (i.e. no false-negatives). Findings include:



11.16 Close-up of a right lateral radiograph of a 5-year-old Rottweiler (same dog as in Figure 11.9) with bronchiectasis and ventral bronchopneumonia (seen over the diaphragm) consistent with PCD.



11.17 Mucociliary radionuclide scan of a 1-year-old Golden Retriever with PCD and a history of recurrent pneumonia. The two static foci of radioactivity to the right of each image represent external markers positioned at the caudal border of the scapula and 20 cm cranial to it. The images are dorsal views obtained at 0, 5, 10, 15, 20, 25, 30 and 35 minutes after deposition of a small droplet of ^{99m}Tc-MAA just cranial to the carina. The radioactive droplet is at the level of the caudal external marker in the top left image (time 0) and remains at the same location throughout the duration of the study, indicating lack of mucociliary function.

- False-positives (no droplet movement) may occur if the droplet is deposited in an ulcerated area of the trachea, in an area of thick mucus or inside the endotracheal tube

- Occasionally the droplet may move initially, then come to a stop; this happens most commonly because the droplet comes in contact with the end of the endotracheal tube or because it encounters an area of exudate, mucus or ulceration.

Kartagener's syndrome

Kartagener's syndrome is an uncommon congenital condition that has been reported in several breeds of dogs. It can be considered as a subset of PCD and is characterized by PCD with situs inversus, rhinosinusitis and bronchiectasis.

Bronchial collapse

Bronchial collapse may occur concurrently with tracheal collapse (see Chapter 10). Usually animals are presented with a history of chronic non-productive cough or respiratory difficulty. The condition is more common in dogs (especially small and toy breeds) than in cats. The disease is caused by progressive bronchial cartilage degeneration and results in a dynamic bronchial obstruction. Changes may occur in the mainstem bronchi and/or the more peripheral smaller airways. The remainder of this discussion refers to mainstem bronchial collapse. The gold standard for diagnosis of this condition is fiberoptic bronchoscopy. However, radiographic and fluoroscopic examination provide a preliminary two-dimensional (2D) evaluation and dynamic CT may provide a non-invasive screening alternative to bronchoscopy.

Radiography

Radiographic findings include:

- *Narrowed lumen* of principal or lobar bronchi near the carina. This may be demonstrated better on a lateral thoracic radiograph taken during expiration
- Lung fields are usually normal.

Fluoroscopic and bronchoscopic examination are usually required for evaluation of intrathoracic airway collapse and the mainstem bronchi.

Fluoroscopy

This provides dynamic evaluation of bronchial lumen changes and associated tracheal collapse. The patient can remain conscious for evaluation and can also be assessed during an induced cough. It is surpassed by fiberoptic bronchoscopy as fluoroscopy remains a 2D study.

Computed tomography

This allows identification of the narrowed or collapsed bronchus. Other causes of narrowing such as external compression or intraluminal material can be excluded. Dynamic CT may be used for real-time assessment of collapse.

Bronchial foreign body

A variety of foreign bodies may be inhaled, for example plant awns, toys, pebbles, bones, peanuts, dental calculus and even teeth.

The foreign body may cause complete or incomplete morphological bronchial obstruction and hence a wide spectrum of radiographic changes (see Figures 1.19, p. 12, 6.5, p. 85 and 11.7). Smooth

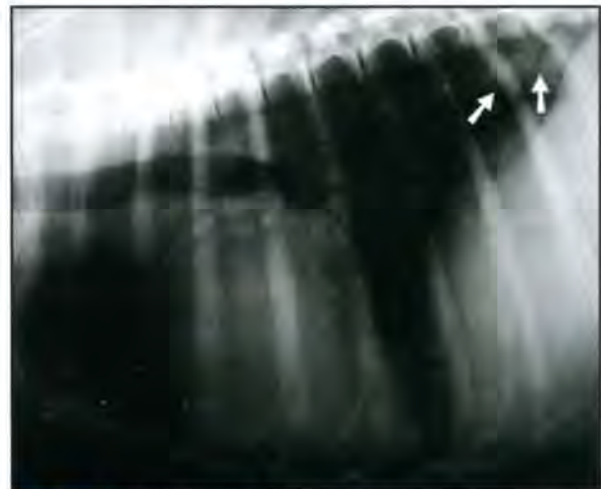
foreign bodies (metal, marbles, pebbles) do not cause irritation, but usually cause obstruction. These do not usually pass beyond the carina. Irritant foreign bodies (such as seeds or grass awns with rough surfaces) may cause intense focal bronchial irritation with or without obstruction.

Bronchial foreign bodies should be considered in animals with an acute onset progressing to chronic cough. Animals with laryngeal paralysis are more likely to aspirate material. Eventually pneumonia, bronchiectasis and even pulmonary abscessation may result. Identification of the underlying cause can be a diagnostic challenge.

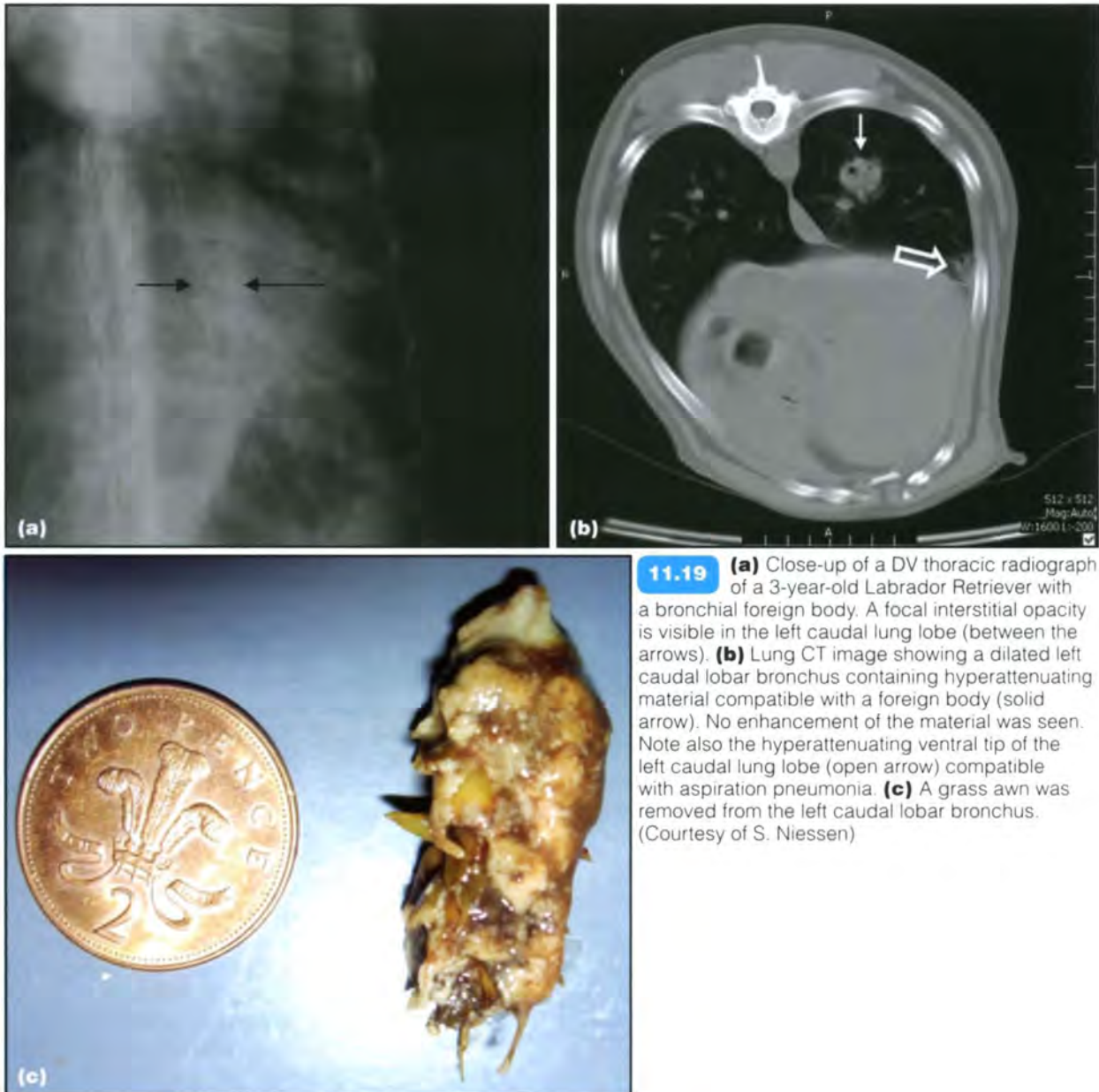
Radiography

The foreign body will be visible if it is radiopaque. No radiographic changes may be seen in the early stages if the foreign body is radiolucent and collateral ventilation is maintained.

- Complete blockage of a mainstem bronchus with loss of collateral ventilation causes lobar atelectasis and a resultant increase in opacity and a mediastinal shift towards the affected lobe. Pleural effusion may be seen around the collapsed lobe.
- Complete blockage of a smaller bronchus with collateral ventilation maintained may cause no radiographic changes or focal consolidations due to infection, and trapped secretions, especially along a bronchus (Figure 11.18), may be identified.
- Incomplete obstruction with 'check valve' effect appears as a hyperlucency and volume gain (mediastinal shift away from the lesion). It is important to acquire both end-expiratory and end-inspiratory radiographs to aid diagnosis.
- An irritant non-obstructing foreign body causes a focal interstitial opacity with central radiolucency and increased bronchial pattern (Figure 11.19), resulting from focal pneumonia. Over time more severe pneumonia, bronchiectasis and lung abscessation are seen.



11.18 Right lateral thoracic radiograph of a 4-year-old Golden Retriever with a grass awn in the right caudal lobar bronchus. Note the focal interstitial alveolar infiltrate in the tip of the caudodorsal lung fields (arrowed).



11.19 (a) Close-up of a DV thoracic radiograph of a 3-year-old Labrador Retriever with a bronchial foreign body. A focal interstitial opacity is visible in the left caudal lung lobe (between the arrows). (b) Lung CT image showing a dilated left caudal lobar bronchus containing hyperattenuating material compatible with a foreign body (solid arrow). No enhancement of the material was seen. Note also the hyperattenuating ventral tip of the left caudal lung lobe (open arrow) compatible with aspiration pneumonia. (c) A grass awn was removed from the left caudal lobar bronchus. (Courtesy of S. Niessen)

Hypertrophic osteopathy associated with a bronchial foreign body has been reported in a dog.

It should be noted that migrating grass awns may initially present as a *spontaneous pneumothorax* and later as a paralumbar abscess or draining tract with adjacent spondylitis.

Computed tomography

CT is more sensitive than radiography in the detection of bronchial foreign bodies (see Figure 11.19). Secondary pulmonary changes, bronchiectasis and pleural effusion may also be seen and their severity assessed more accurately.

Bronchial neoplasia

Bronchial tumours are a type of primary pulmonary tumour. Primary pulmonary tumours are uncommon

in dogs and cats. Most primary lung tumours arising from the bronchial epithelium are carcinomas. Cytology and histopathology can provide the definitive diagnosis. Bronchoalveolar carcinoma, for example, has the unique characteristic of extension along the airways and alveolar septa with occasional projections into the alveolar lumen.

The clinical signs of animals with bronchial tumours vary. Chronic cough unresponsive to antibiotics, exercise intolerance, tachypnoea and overt respiratory distress may be seen in dogs. Cats may be presented with signs including anorexia, weight loss, lethargy, tachypnoea, dyspnoea and non-productive cough.

Regional lymph nodes, the pleura and other organs should be assessed for metastatic disease. CT is particularly useful in this respect and should be considered when surgical resection is contemplated.

Radiography

Radiographic findings include:

- Canine bronchoalveolar carcinoma (Figure 11.20; see also Figures 12.23, p. 253, 12.40, p. 261, 12.68, p. 274). A varied radiographic appearance has been reported. Solitary nodules, multiple non-circumscribed interstitial nodules, diffuse opacities or alveolar consolidation may be seen
- Feline bronchoalveolar carcinoma. Three main patterns have been described: mixed bronchoalveolar pattern, ill defined alveolar mass and mass with cavitation. All cats have a co-existing bronchial pattern. Cavitation is common, suggesting a tendency for the tumour to form necrotic centres. Mineralization should increase the degree of suspicion for neoplasia. Beware: neoplasia may mimic severe feline chronic lower airway disease.



11.20 Lateral radiograph of an 8-year-old mixed breed dog with a chronic cough and weight loss. There is a focal alveolar pattern surrounding one of the bronchi (arrowed). The bronchus itself has an irregular outline. The final diagnosis was bronchoalveolar carcinoma.

Enlarged hilar lymph nodes may also be identified; these are suggestive of metastatic disease. Pleural effusion may be seen and pleural metastases have been reported.

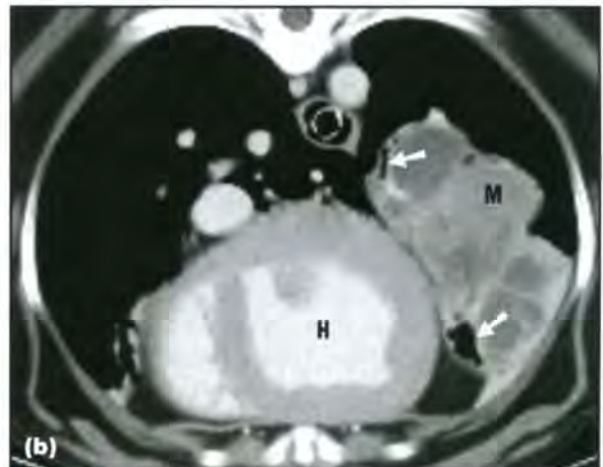
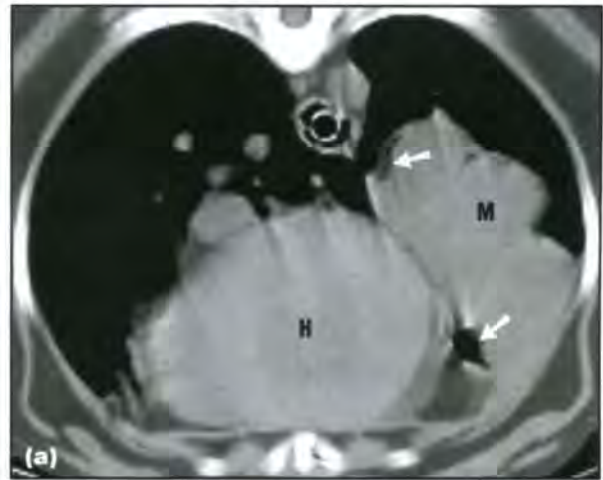
Computed tomography

This is more sensitive than radiography for the detection of small lesions. It allows excellent assessment of the location and course of the tumour, the presence of tissue within the bronchial lumen, cavitation and necrosis, mineralization, etc.

The CT appearance of bronchial neoplasms (Figure 11.21) is variable. CT-guided biopsy may be performed. CT is extremely useful for surgical planning. It may detect enlarged regional lymph nodes suggestive of metastasis and thus assist with tumour staging.

Magnetic resonance imaging

The use of thoracic magnetic resonance imaging (MRI) is experimental in lung cancer diagnosis and treatment in humans. It has the potential to provide



11.21 Transverse CT images (soft tissue window) from an 8-year-old Beagle with a bronchoalveolar carcinoma. (a) before and (b) after intravenous contrast medium administration. Both images were acquired at the level of the heart (H). A large mass (M) is seen in the left lung and is compressing and distorting a bronchus (arrowed). (b) Contrast medium administration reveals multiple non-enhancing cystic or necrotic regions.

more accurate information on tumour extension/margins before surgical resection.

Bronchial rupture

Bronchial rupture is uncommon; tracheal rupture is more common. Usually the rupture occurs within 1–4 cm of the tracheal bifurcation. The most common causes are:

- Blunt trauma to the neck and/or thorax
- Chronic cough
- Venepuncture resulting in bronchial rupture and resultant fatal tension pneumothorax has been reported in a kitten. The aetiology was considered most likely to be occlusion of the upper airways (either directly or due to laryngospasm) plus pressure on the chest or alternatively due to stretching and twisting of the bronchial tree
- Traumatic avulsion of the left principal bronchus has also been reported in a cat
- Foreign body.

Bronchial rupture will usually result in pneumomediastinum and/or pneumothorax (less common), depending on the location and orientation of the tear. Free gas commonly tracks under the bronchial serosa into the mediastinum.

Radiography

Radiographic findings include:

- Pneumomediastinum, pneumothorax or tension pneumothorax
- In cases of tracheal rupture, tracheal discontinuity may be identified on survey radiographs; bronchoscopy is more helpful for identification of bronchial rupture.

Computed tomography

Tracheobronchoscopy is usually employed in this situation, but CT may be useful if this technique has failed to identify the location of the rupture. CT is able to localize small peribronchial gas pockets suggestive of bronchial rupture (see Figure 8.25, p. 189).

Bronchiolitis obliterans with organizing pneumonia

Bronchiolitis obliterans with organizing pneumonia (BOOP) is a rare inflammatory condition in the cat and dog and is a multifactorial disease. The characteristic pathohistological finding is granulated tissue plugs within the lumen of small airways, which extend into the alveolar ducts and alveoli. Definitive diagnosis relies on lung biopsy. In humans BOOP may be secondary to a usual interstitial pneumonia. A few case reports exist in dogs, and CT and open or keyhole lung biopsy have been used successfully for diagnosis.

Radiography

Radiographically various combinations of bronchial, interstitial and alveolar patterns may be seen. One case report in the dog describes a diffuse interstitial pattern in all lung fields. Commonly patchy areas of alveolar pattern and bronchial wall thickening are seen. The radiographic changes are non-specific.

Computed tomography

CT has been reported as a sensitive technique for this condition. One canine case report describes bilateral asymmetrical areas of air space consolidation and bronchial dilatation.

Bronchial microlithiasis

Miliary broncholitis is a rare sequel to inflammatory bronchial disease reported in cats. Inspissated mucopurulent plugs with calcified concretions are found throughout the bronchi. It can lead to obstructive resorption atelectasis and compensatory emphysema.

Radiography

Radiographic findings include:

- Small mineralized opacities scattered throughout the lung fields contained within the bronchi (Figure 11.22)



11.22 Close-up of a lateral thoracic radiograph of a cat. Multiple mineralized opacities are visible throughout the lung fields consistent with bronchial microlithiasis.

- Atelectasis of obstructed lobes/areas possible
- Compensatory hyperinflation and emphysema.

Broncho-oesophageal fistula

Broncho-oesophageal fistulae may be congenital or acquired. The latter may occur secondary to trauma or an oesophageal or bronchial foreign body. The result of the condition is usually a recurring aspiration pneumonia and hence cough. Definitive diagnosis is by oesophagography (see Chapters 1 and 9), although the fistula may occasionally be recognized on endoscopic examination.

Radiography

Radiographic findings include:

- Recurrent focal pneumonia
- Occasionally gas distension of the oesophagus.

Congenital bronchial anomalies

Congenital bronchial anomalies are uncommon but have been reported in the dog and cat.

Bronchial cartilage dysplasia, causing congenital lobar bullous emphysema, has been reported in dogs. Lung hyperlucency, mediastinal shift and flattening of the diaphragm are identified radiographically (see Chapter 12).

Bronchial dysgenesis has been reported in a cat. Thoracic radiographs showed hyperinflation of the right lung and atelectasis or agenesis of the left lung. Bronchial dysgenesis was identified in all but the right caudal lung lobe.

References and further reading

- Allan GS and Howlett CR (1973) Miliary broncholitis in a cat. *Journal of the American Veterinary Medical Association* **162**(3), 214–216
- Corcoran BM, Foster DJ and Fuentes VL (1995) Feline asthma syndrome: a retrospective study of the clinical presentation in 29 cats. *Journal of Small Animal Practice* **36**(11), 481–488
- Corcoran BM, Fuentes VL and Clarke CJ (1992) Chronic tracheobronchial syndrome in eight dogs. *Veterinary Record* **130**(22), 485–487
- Corcoran BM, Thoday KL, Henfrey JL, *et al.* (1991) Pulmonary infiltration with eosinophils in 14 dogs. *Journal of Small Animal Practice* **32**, 494–502
- Douglas SW (1974) The interpretation of canine bronchograms. *Journal of the American Veterinary Radiological Society* **15**, 18–23
- Edwards DF, Patton CS and Kennedy JR (1992) Primary ciliary dyskinesia in the dog. *Problems in Veterinary Medicine* **4**(2), 291–319

- Hawkins EC, Basseches J, Berry CR, *et al.* (2003) Demographic, clinical, and radiographic features of bronchiectasis in dogs: 316 cases (1988–2000). *Journal of the American Veterinary Medical Association* **223**(11), 1628–1635
- LaRue MJ, Garlick DS, Lamb CR and O'Callaghan MW (1990) Bronchial dysgenesis and lobar emphysema in an adult cat. *Journal of the American Veterinary Medical Association* **197**(7), 886–888
- Losonsky JM, Thrall DE and Prestwood AK (1983) Radiographic evaluation of pulmonary abnormalities after *Aelurostrongylus abstrusus* inoculation in cats. *American Journal of Veterinary Research* **44**(3), 478–482
- Mantis P, Lamb CR and Boswood A (1998) Assessment of the accuracy of thoracic radiography in the diagnosis of canine chronic bronchitis. *Journal of Small Animal Practice* **39**(11), 518–520
- Moise NS, Wiedenkeller D, Yeager AE, *et al.* (1989) Clinical, radiographic, and bronchial cytologic features of cats with bronchial disease: 65 cases (1980–1986). *Journal of the American Veterinary Medical Association* **194**(10), 1467–1473
- Moon M (1992) Pulmonary infiltrates with eosinophilia. *Journal of Small Animal Practice* **33**, 19–23
- Myer CW (1980) Radiography review: the vascular and bronchial patterns of pulmonary disease. *Veterinary Radiology* **21**(4), 156–160
- Myer CW and Burt JK (1973) Bronchiectasis in the dog: Its radiographic appearance. *Journal of the American Veterinary Radiological Society* **14**, 3–12
- Norris CR and Samii VF (2000) Clinical, radiographic, and pathologic features of bronchiectasis in cats: 12 cases (1987–1999). *Journal of the American Veterinary Medical Association* **216**(4), 530–534
- Webbon PM and Clarke KW (1977) Bronchography in normal dogs. *Journal of Small Animal Practice* **18**(5), 327–332
-

The lung parenchyma

Wilfried Mai, Robert O'Brien, Peter Scrivani, Yael Porat-Mosenco, Emma Tobin, Gabriela Seiler, Fraser McConnell, Tobias Schwarz and Allison Zwingenberger

Radiographic anatomy

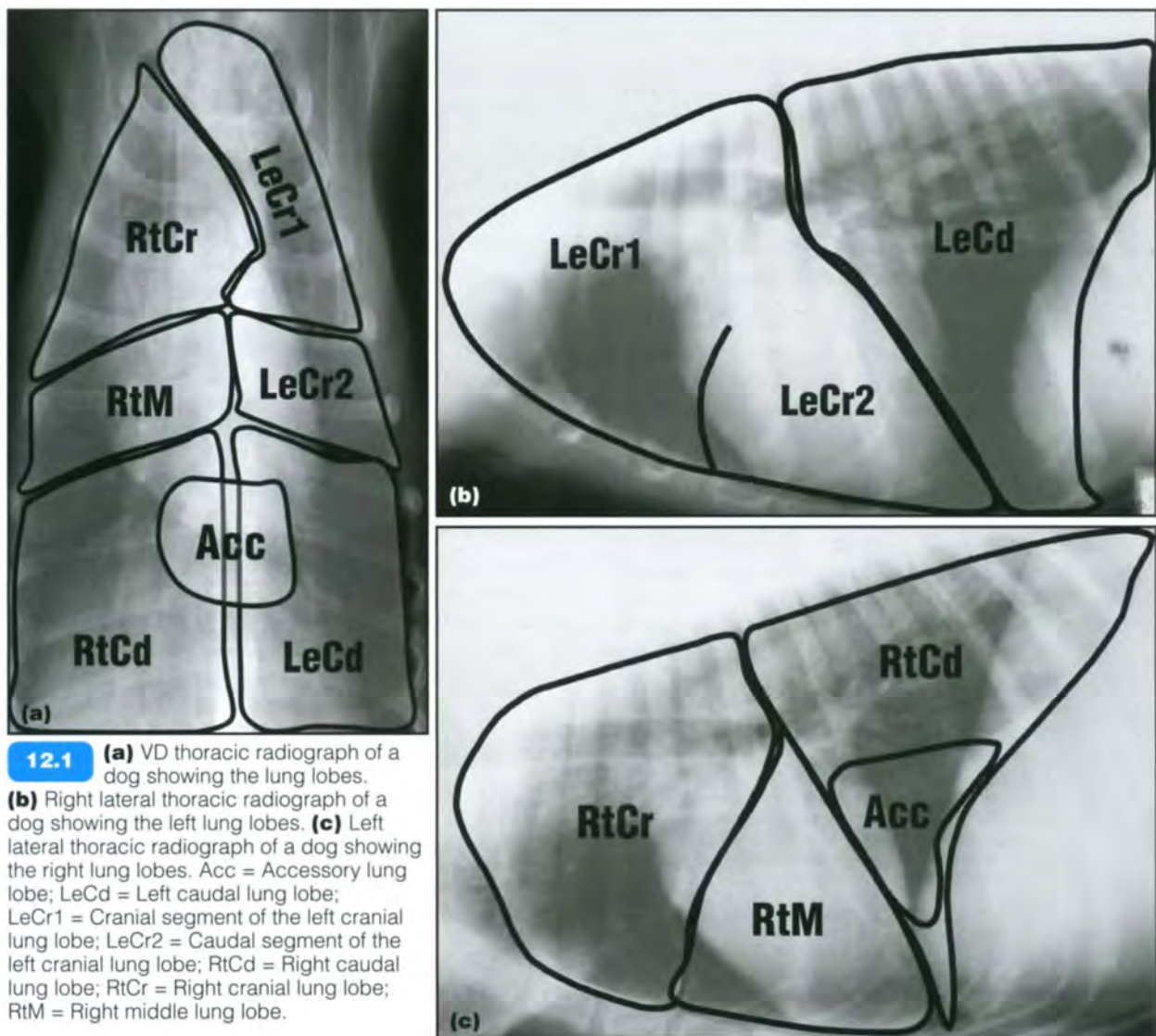
Normal aspect of the lungs

Lobar anatomy

Dogs and cats have two lungs, which are not symmetrical in terms of size and lobation. The lobar anatomy is based on the bronchial division.

- The left lung consists of two lobes (Figure 12.1ab):

- Left cranial lung lobe, further divided into a cranial segment and a caudal segment
- Left caudal lung lobe.
- The right lung consists of four lobes (Figure 12.1ac):
 - Right cranial lung lobe
 - Right middle lung lobe
 - Right caudal lung lobe
 - Accessory lung lobe.



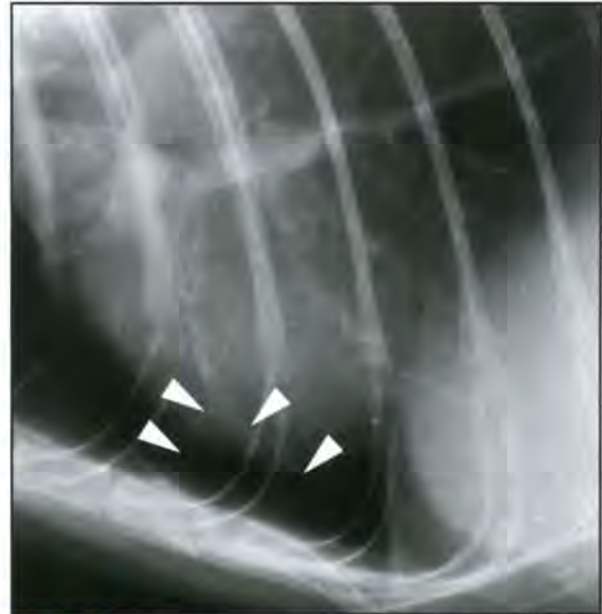
The overall volume of the right lung is 25% larger than that of the left lung. When the lungs are well inflated, the cranial part of the left cranial lung lobe extends cranially beyond the level of the first ribs and into the right hemithorax. It can be visible on a lateral view, creating a relative lucent area cranial to the first pair of ribs, which is separated from the right cranial lung lobe by a band of soft tissue opacity (cranioventral mediastinal reflection) (see Figures 12.1a and 12.2).



12.2 Close-up of a lateral thoracic radiograph at the level of the first ribs of a dog. The cranial tip of the left cranial lung lobe (black arrows) is seen as a round lucency in the pleural cupula, cranial to the first pair of ribs. It is separated from the remainder of the lung by a soft tissue opaque band, which represents a mediastinal fold (white arrow).

At full inspiration, the right middle lung lobe can expand ventral to the cardiac silhouette. The relatively lucent space between the heart and the sternum, visible on a lateral view, should not be confused with a pneumothorax (Figure 12.3). With incomplete inspiration, the right cranial and middle lung lobes leave a small triangular area free for the right ventricle cranioventrally, termed the cardiac notch, usually at the fourth to fifth intercostal space. This lung-free area is used as a right parasternal window in echocardiography.

In normal animals, the exact margins between the lung lobes are usually not visible due to the fact that the different lobes have a similar opacity and silhouette with each other. Nevertheless, it is useful to know the normal location of pleural fissures as this is where pleural fissure lines and lobar signs will be found in diseased animals:



12.3 Lateral thoracic radiograph of a Domestic Shorthair cat with a relatively radiolucent area ventral to the cardiac silhouette. The visible bronchovascular structures (arrowheads) indicate that this is inflated lung and not pleural free gas.

- On the left side, the cranial segment of the left cranial lung lobe shares limits with two lobes (see Figure 12.1b):
 - Ventrally, with the caudal segment of the left cranial lung lobe; the fissure between the two being located at the level of the fourth intercostal space
 - Dorsally, with the left caudal lung lobe; the fissure between the two being located at the level of the sixth to seventh intercostal space.
- On the right side, the right cranial lung lobe shares limits with two lobes (see Figure 12.1c):
 - Ventrally, with the right middle lung lobe; the fissure between the two being located at the level of the fourth to fifth intercostal space
 - Dorsally, with the right caudal lung lobe; the fissure between the two being located at the level of the sixth to seventh intercostal space.

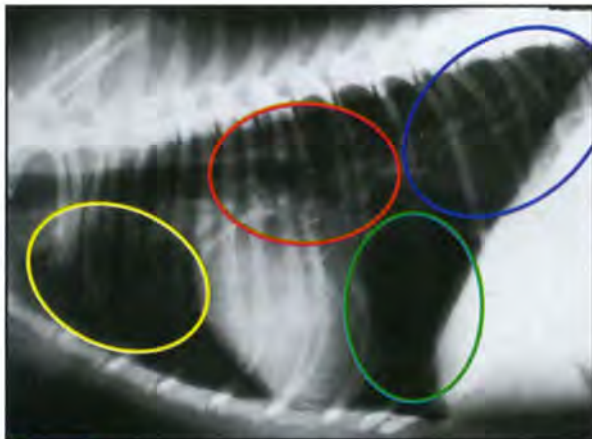
Lung lesions should be described according to their lobar anatomical location if:

- The specific lobe can be determined
- The lesion distribution follows the lobar anatomy.

Topographical description

Topographical terms are often used to describe a lung area without designating it to a specific lobe. Commonly used terms are (Figure 12.4):

- Cranioventral (outdated synonym: precardial)
- Caudoventral (outdated synonym: postcardial)
- Caudodorsal
- Midventral (to describe the midventral thoracic area, the term 'superimposed on the cardiac silhouette' is frequently used)
- Perihilar (synonyms: hilar, central)
- Peripheral.



12.4 Lateral thoracic radiograph of a dog with superimposed lung fields. Caudodorsal = Blue; Caudoventral = Green; Cranioventral = Yellow; Perihilar = Red.

This terminology can be used in conjunction with the term *lung field* or *zone*, and provides a means to localize a lung lesion accurately where a specific lobe cannot be designated; for example, *caudodorsal lung opacification* based on a single lateral radiograph, instead of *an opacification in one or both of the caudal lung lobes*. These terms are also used to more accurately describe the localization of a lung lesion which does not strictly follow the lobar anatomy in distribution; for example, *perihilar lung opacity* in pulmonary oedema, instead of *an opacification in the craniomedial aspect of both caudal and accessory, and caudodorsomedial aspect of both cranial lung lobes*. The lobar anatomical description is preferred if applicable.

Lung opacity

The normal lung opacity is the result of the summation of:

- Gas opacity within the alveoli, bronchioles and bronchi
- Soft tissue opacity of the blood vessels, lung interstitium, bronchial and alveolar walls
- Superimposing soft tissue opacities (e.g. thoracic wall, mediastinum).

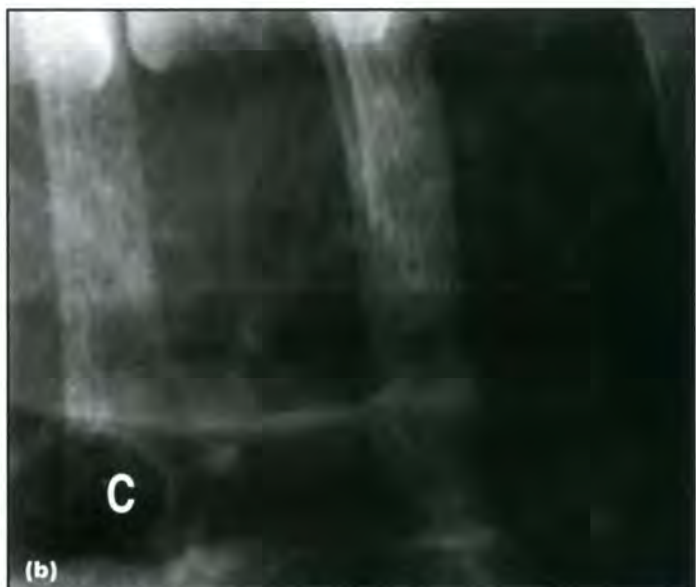
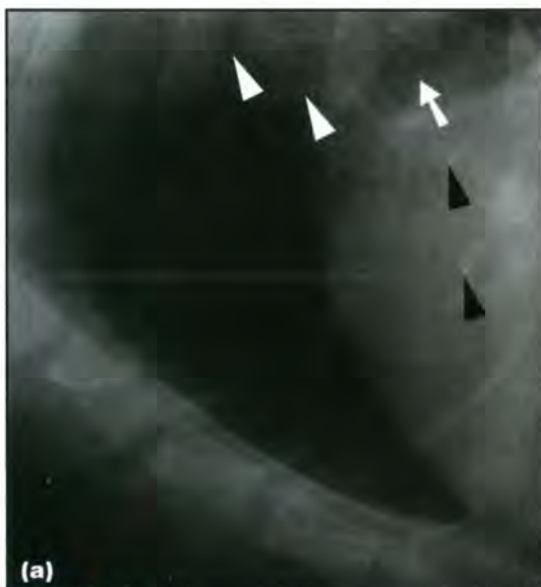
Due to the large proportion of air-filled spaces in the lungs, the normal lung is very lucent (Figure 12.5a). Dogs and cats have very little interstitial lung tissue and no lobular septations (classified as type II lung), which therefore contribute only minimally to the overall lung opacity. A fine reticular background on normal lung tissue, as occasionally seen radiographically, is the result of small vascular and interstitial structures (Figure 12.5b).

The pulmonary vessels can be seen within the parenchyma due to the contrast provided by the surrounding pulmonary gas (Figure 12.5a). Other structures that may be seen in a normal canine lung are the walls of the airways to the level of the primary and secondary divisions of the bronchi; they appear as thin parallel soft tissue or mineralized lines that branch into the periphery (Figure 12.5).

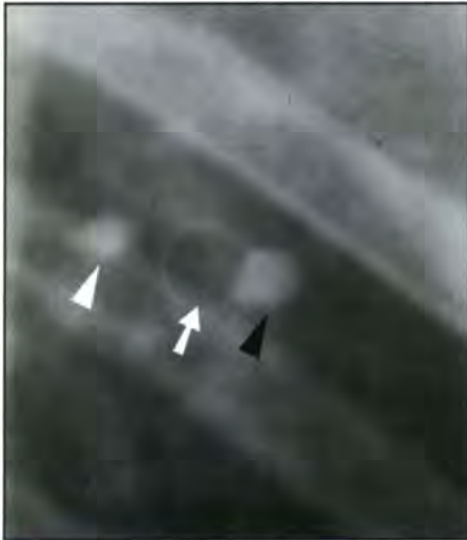
Lung vessels

The lungs contain two distinct vascular systems:

- A functional vascular system:
 - The pulmonary arteries carrying oxygen-deprived blood
 - The pulmonary veins carrying oxygen-rich blood.



12.5 (a) Cranioventral close-up of a lateral thoracic radiograph of a 6-year-old Briard. The lungs appear almost as lucent (dark) as the air outside of the patient (lower left corner). Air does not attenuate the X-ray beam, and inflated lung mainly consists of air. Visible pulmonary structures include lung vessels in side-on (white arrowheads) or end-on (black arrowheads) orientation, and mineralized bronchial walls (arrowed). (b) Close-up of a lateral radiograph of normal lung tissue caudodorsal to the carina (C). First- to third-order vascular branches and mineralized bronchi are easily distinguishable. A reticular (mesh-like) pattern of increased opacities is seen dorsally, created by small vessels and interstitium. The superimposed descending aorta contributes an additional homogenous increase in opacity to the upper half of the image.



12.6 Close-up of a VD thoracic radiograph of the left caudal lung field of a dog. A triad of artery (black arrowhead), bronchus (arrowed) and vein (white arrowhead) can be seen (viewed end-on) with the vein at a small distance from the bronchus.

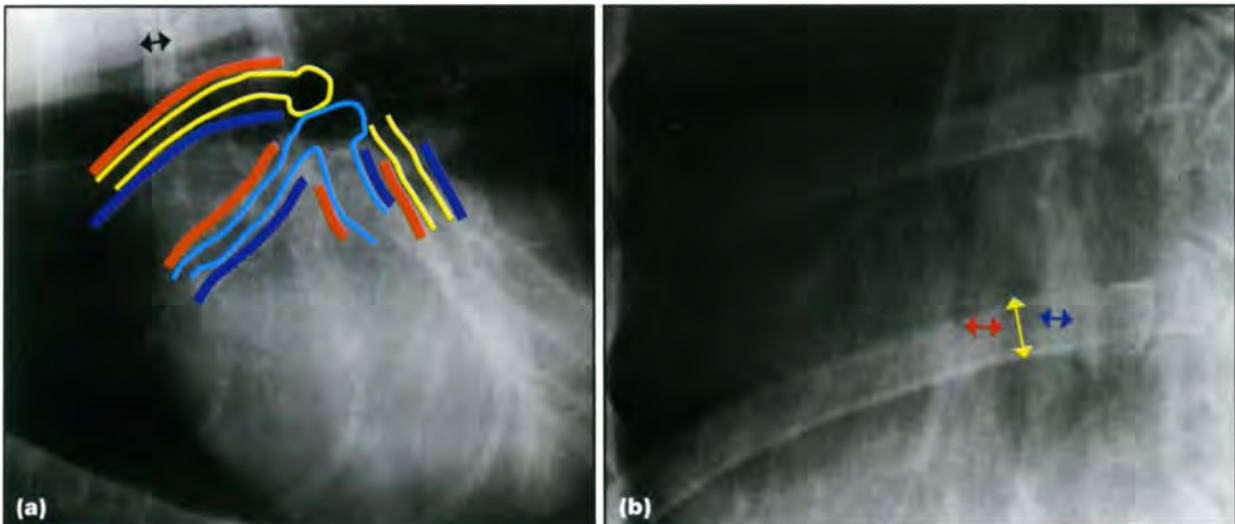
- A nutritional blood supply: the bronchial arteries coming from the aorta, a minor contributor to the pulmonary circulation (1% of the cardiac output).

Only the functional vascular system is radiographically visible. The major pulmonary arteries and veins are the most prominent radiopaque structures within the normal lungs. They are larger at the hilus and then branch and taper progressively towards the periphery. They appear as band-like soft tissue opacities when viewed along their long axis, and as nodule-like opacities when viewed end-on (see Figure 12.5a).

In dogs and cats, the pulmonary arteries are directly adjacent to the bronchial tree along their entire course, whereas the veins separate from the bronchus at the segmental level (bronchoarterial lung type). This means that small pulmonary veins may be seen at some distance from the corresponding bronchus, and that the distance between the arteries and corresponding veins does not exactly represent the bronchial diameter (Figure 12.6). The pulmonary arteries and veins can be differentiated based on their relationship to the mainstem bronchi (Figures 12.7 and 12.8).

Lung lobes	Radiographic view for pulmonary vessel identification	Vessels	Location in reference to corresponding bronchus	Maximal normal vessel diameter in relation to rib
Cranial	Lateral view only (left lateral view best)	Arteries	Dorsal to bronchus	Vascular diameter at intersection of fourth rib should not exceed width of fourth rib at dorsal third
		Veins	Ventral to bronchus	
Caudal	DV or VD view only (DV view best)	Arteries	Lateral to bronchus	Width of ninth rib at point of intersection
		Veins	Medial to bronchus	

12.7 Normal canine and feline pulmonary vessel location and size.



12.8 (a) Normal left lateral thoracic radiograph of a 5-year-old Bull Mastiff with annotations for: the main bronchus for the right cranial and middle lung lobes (yellow); the main bronchus for the cranial and caudal segments of the left cranial lung lobe (light blue); the associated pulmonary arteries (orange); and the associated pulmonary veins (blue). Notice the more dorsal location of the origin of the right stem bronchus compared with the left one, which is used as a landmark. The two most cranially oriented bronchi are accompanied dorsally by the artery, and ventrally by the vein. Maximal normal diameter of the cranial lung lobe vessels should not exceed the width of the proximal third of the fourth rib (arrowed). **(b)** Close-up of a DV thoracic radiograph of the right caudal thorax in a dog. The artery (red arrow) and vein (blue arrow) of the right caudal lung lobe are smaller than the width of the ninth rib where they intersect (yellow arrow).

The cranial lung lobe arteries and veins can only be differentiated on a lateral view. A left lateral view is better because there is less superimposition of left and right bronchovascular structures. On a left lateral view, the left and right cranial and middle pulmonary vessels are arranged in the following order in an anti-clockwise direction (Figure 12.8a):

- Right cranial lobe (most craniodorsal)
- Cranial segment of the left cranial lobe
- Caudal segment of the left cranial lobe
- Right middle lobe (most caudoventral).

The right cranial lobe bronchovascular structures can also be located ventral to those of the cranial segment of the left cranial lung lobe on this view. The left cranial lung lobe can be recognized as such because of the short common lobar bronchus, which divides into the cranial and caudal segmental bronchi. Caudal lung lobe arteries and veins can only be differentiated on a dorsoventral (DV) or ventrodorsal (VD) view. A DV view is better because the dorsal part of the caudal lungs is more ventilated than on a VD view (Figure 12.8b). It can be difficult to measure the feline caudal pulmonary arteries and veins on the DV view.

The pulmonary functional circulation is a low pressure system; both arteries and veins are thin-walled and easily distensible and collapsible by physiological or pathological processes. Pulmonary arteries and veins should be approximately the same size, but it is common to see arteries that are slightly larger than the veins in normal animals.

Normal variations

Lung opacity and aeration

Air does not attenuate the X-ray beam; therefore, a change in the amount of pulmonary air does not directly affect lung opacity. However, secondary effects associated with lung expansion and retraction

do affect the opacity of the lungs. With inspiration or lung inflation the expanding lungs:

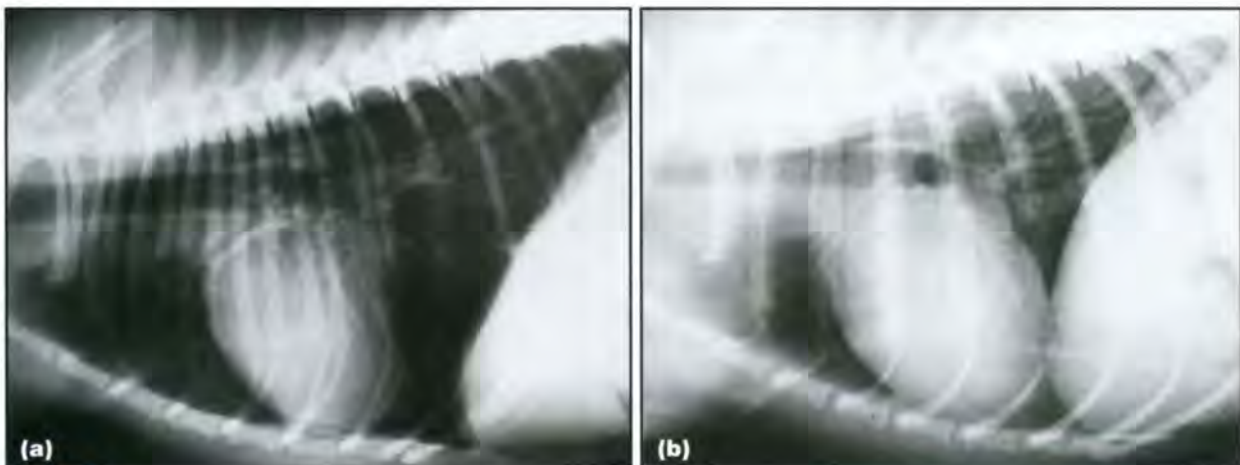
- Replace more opaque extrathoracic structures in the image
- Compress the heart and the easily collapsible pulmonary vessels. These fluctuations in intrapulmonary blood content are the main reason for respiration-related differences in lung opacity (Figure 12.9).

The opacity of the lung tissue cranial and caudal to the cardiac silhouette can differ under normal conditions. Large amounts of superimposing soft tissue cranially (shoulders, cranial mediastinum) can make the lungs appear more opaque in this location. Conversely, expiratory views may reveal more opaque caudal lung tissue. Due to the larger amount of lung tissue caudally, and the mobility of the diaphragm, respiratory changes have a higher net result on opacification in this location.

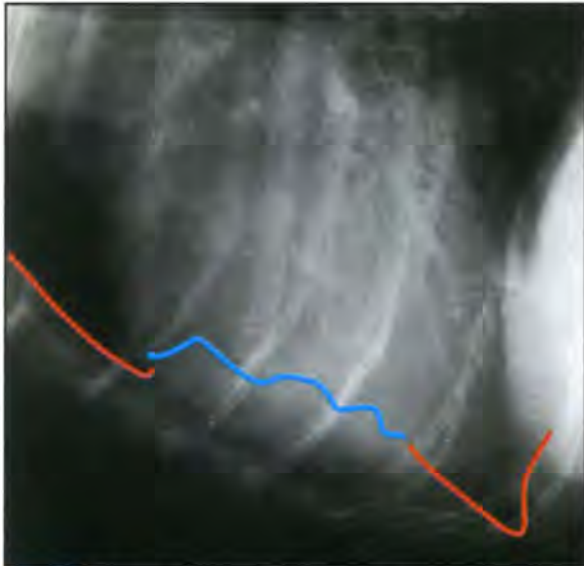
Lung tissue in the mid-thorax can be difficult to evaluate due to the superimposition of the cardiac silhouette. However, the ventral pleural margin can often be identified as a curtain-like structure over the ventral aspect of the cardiac silhouette, and can be used as a landmark (Figure 12.10).

Only a fraction of the normal lung capacity is needed in a normal dog and cat at rest. Consequently, the lungs are often not fully expanded and partial collapse occurs (Figure 12.10). Collapse occurs preferentially at the lung periphery and in the dependent part of the animal. Collapsed lung becomes a soft tissue opacity and radiographically visible if:

- A large enough area of lung has completely collapsed
- It has structural features, such as air bronchograms
- It is contrasted by surrounding aerated lung.



12.9 (a) Lateral thoracic radiograph of a normal dog obtained at peak inspiration. The lungs are expanded, separating the cardiac and diaphragmatic silhouettes and opening the lumbodiaphragmatic recess beyond the thirteenth thoracic vertebra. Cardiovascular structures appear relatively small. The net result is relatively radiolucent lung tissue. (b) Lateral thoracic radiograph obtained during the expiratory pause. Due to lung retraction, the cardiac and diaphragmatic silhouettes overlap, the lumbodiaphragmatic recess only extends to the twelfth thoracic vertebra, and the cardiovascular structures appear bigger. The resulting lung opacity is markedly increased, yet it is normal for this phase of respiration.



12.10 Ventral close-up of a lateral thoracic radiograph of a West Highland White Terrier with annotated ventral lung margins. Cranial and caudal lung margins (red lines) extend to the ventral thoracic boundaries. The mid section of the lung only extends to the level of the ventral aspect of the cardiac silhouette with a wavy margin (blue line). This is a sign of normal incomplete lung lobe inflation with or without peripheral lung collapse.

A large area of incomplete collapse may create only a generalized subtle increase in overall opacity, insufficient to outline the collapsed lung. Physiological lung collapse is a diagnostic problem because:

- Radiographically visible collapsed lung is difficult to distinguish from lung pathology
- Collapsed lung silhouettes with potential soft tissue lesions.

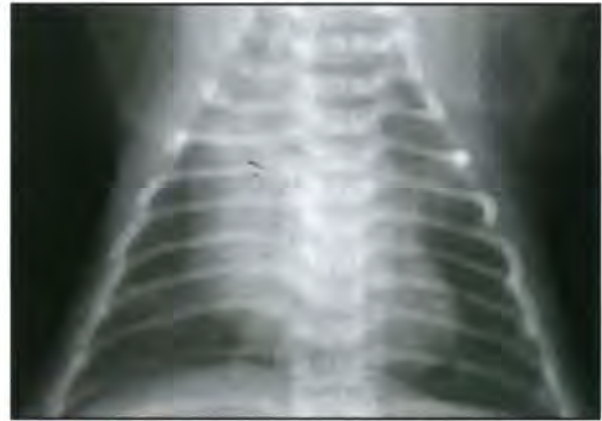
To minimize the effect of lung collapse it is therefore useful to obtain lateral radiographs in both left and right recumbency. On a right lateral view, the non-dependent left lung is more aerated and hence easier to interpret. On a left lateral view, the non-dependent right lung is more aerated and hence easier to interpret. This is not an all-or-nothing phenomenon but rather a gradual one. It would not be correct to assume that all radiolucent areas must belong to the non-dependent lung and all radiopaque areas to the dependent lung. However, by comparing both views it can usually be established whether a lung area with soft tissue opacity is more likely to be a dependency-related lung collapse (less opaque in non-dependent position) or a pathological lung lesion (equally or more opaque in non-dependent position). An additional DV/VD view can prove extremely helpful (lung opacity, mediastinal shift) to confirm or refute the radiographic diagnosis.

General anaesthesia promotes lung collapse. It is associated with prolonged recumbency and shallow breathing, and less lung tissue is needed for gas exchange (complete rest, ventilation with oxygen rather than air). Thoracic radiography should therefore be avoided during general anaesthesia and be scheduled before or after the procedure instead. Alternatively, the lungs can be inflated

and radiographed in a state of maximal expansion. Manual bag holding is necessary for this technique, which requires appropriate shielding of personnel.

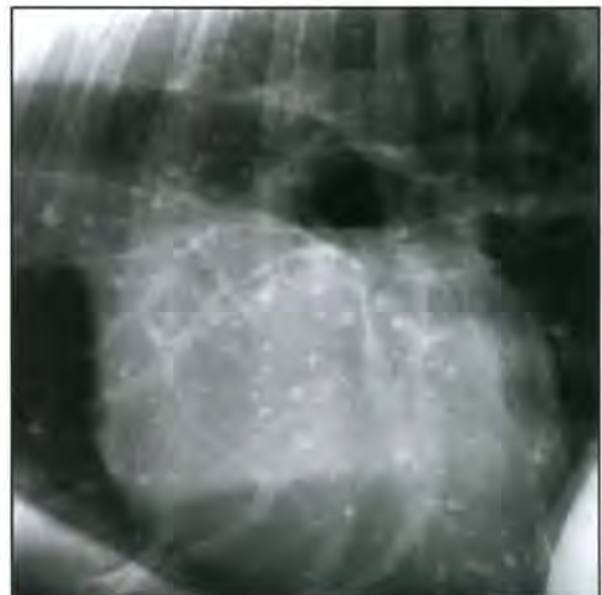
Age and breed variations

Puppies and kittens often have more opaque lungs than adults, which is probably due to an increased water content of the interstitial lung parenchyma and the presence of a thymus (Figure 12.11).



12.11 VD thoracic radiograph of a 4-month-old Abyssinian cat. The lung opacity is relatively high for the size of the animal but normal for its age and expiratory phase.

Linear (and much less commonly nodular) markings of interstitial origin increase the overall lung opacity in normal old dogs. This should not be misinterpreted as abnormal. Bronchial markings can be more prominent in older dogs and cats, without being associated with current bronchial disease. Heterotopic bone (also known as pulmonary osteomas, pneumoliths or pleural plaques) can form in the lungs and pleura of skeletally mature dogs, and be radiographically visible as small (1–4 mm) nodules of mineral opacity (Figure 12.12).



12.12 Close-up of a lateral thoracic radiograph of a 9-year-old English Springer Spaniel with heterotopic pulmonary bone formation, manifesting as round mineral opacities throughout the lungs. The opacities ranged in size from 1–3 mm.

They are particularly common in Collie breeds. They should not be mistaken for metastatic lung lesions. Similarly sized metastases would not be sufficiently opaque to be radiographically visible (with the rare exception of mineralized metastases and miliary lung lesions).

In some animals, thickening of the pleural surface allows the margins of the lobes to be seen, where the X-ray beam is tangential to the border between two lobes.

In chondrodystrophic dogs, early mineralization of the bronchial cartilages is common, and the bronchial walls therefore become clearly identified as parallel lines accompanying the vascular structures, or as ring-like structures when viewed end-on.

Species differences

Cranial lung expansion (cranial to the first ribs) is more pronounced in dogs. The feline lung commonly extends further caudally than the canine lung (at peak inspiration to the level of T12–13 in dogs, and L1–2 in cats).

In dogs, the dorsal lung margins are completely superimposed on the ventral aspect of the thoracolumbar spine. In cats, the caudodorsal lung margin is separated from the spine by the psoas minor muscle, which originates at the ventral surface of the last two thoracic vertebrae (the last thoracic vertebra in the dog) (Figure 12.13).

Body condition

Obese animals have large amounts of fat around and within the thoracic cavity, which leads to increased X-ray attenuation and generation of scatter radiation. The net result is an increased lung opacity (Figure 12.14) with poor visibility of the bronchovascular structures. Intrathoracic fat restricts full lung expansion during inspiration, which also contributes to the more opaque appearance of the lungs in these animals. These changes should not be mistaken for pathologically increased lung opacity.

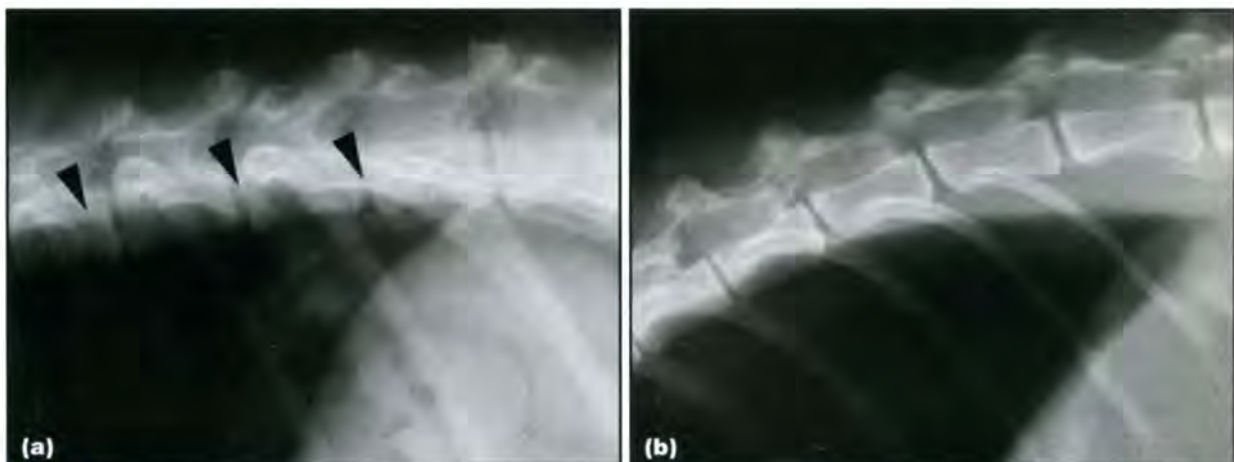


12.14 DV thoracic radiograph of an obese small-breed dog. Note the relatively high lung opacity due to the large amount of superimposing subcutaneous fat. Large amounts of fat are also accumulated in the cranial mediastinum and pericardium, which further restricts full lung expansion.

In lean dogs and cats, and in deep-chested dogs, the lungs tend to look very lucent. A close inspection with a highly luminescent light source should reveal normal bronchovascular structures and thereby differentiate this variation from a pneumothorax.

Interpretive principles

The lungs are one of the most difficult organs to assess radiographically because of:



12.13 (a) Close-up of a lateral radiograph of the caudodorsal lung margin of a 4-year-old Whippet at peak inspiration. The dorsal lung margins are superimposed on the thoracic vertebrae (arrowheads) and the lung expands to the level of the last thoracic vertebra. (b) Close-up of a lateral radiograph of the caudodorsal lung margin of an 18-year-old Domestic Shorthair cat at peak inspiration. The caudodorsal lung margin is separated from the spine by the psoas minor muscle. The lung expands to the level of the first lumbar intervertebral disc space. (Courtesy of C. Jarrett)

- Superimposition of other organ systems
- Wide range of normal anatomical and physiological variations
- Wide overlap of radiographic features of physiological and pathological processes
- Similar imaging features for different diseases
- Lack of confirmation by other non-invasive tests.

Radiologists have developed interpretive principles for the lungs, which are an adaptation of the classic Röntgen signs. These principles are constantly refined, challenged, changed and individualized, indicating that there is no perfect system to interpret the lungs radiographically. In the following paragraphs the classic interpretive principles to approach the lungs are discussed, and newer alternative ways of appraisal are provided. Regardless of the approach utilized, the final differential list for a given radiographic appearance should remain the same.

Alterations in lung opacity

The first and most important step in the correct identification of lung disease is the categorization as *abnormal*:

- Most diseases result in increased opacity of the lungs or regions of the lungs
- Increased lung opacity must be interpreted in the context of possible anatomical and physiological variations of normal lungs
- Pulmonary mineralization should be assessed in context with signalment and clinical history, and be differentiated from cardiac, cutaneous and other superimposed mineral-opaque lesions (see Interstitial mineralization).

Once normal variants have been ruled out, a system needs to be applied to help sort through the various differentials, which includes the following steps:

- Determination of location and extent of abnormality

- Correlation of lung opacity and volume changes with state of inflation
- Determination of the pulmonary pattern (for diffuse lesion) or lesion type (for focal lesion)
- Consideration of the species, age, breed and co-existing clinical signs.

Functional interpretation of abnormal lung volume and opacity

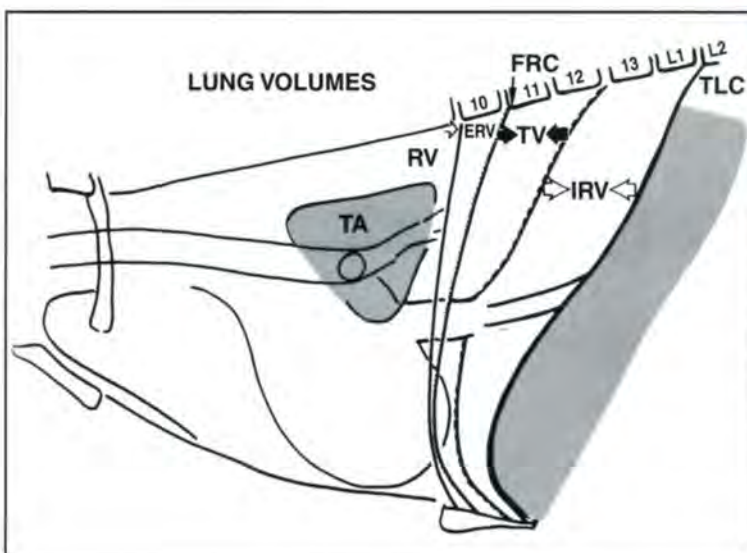
Lung volume and aeration can change dramatically in response to a wide range of extra- and intrathoracic forces, and not just pulmonary diseases (Figure 12.15). Changes in lung opacity should therefore also be correlated to changes in:

- Airway calibre
- Cardiovascular perfusion
- Shape and position of the rib cage and diaphragm.

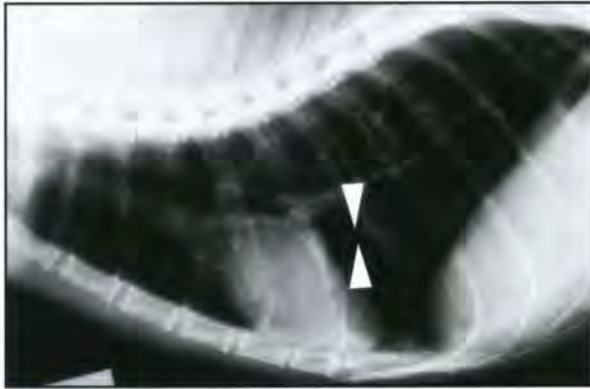
Hyperlucent lungs with increased volume

Possible causes include:

- Air trapping: one-way valve obstruction of upper or, more commonly, small lower airways. Air can enter the alveoli during inspiration but not leave it during expiration. Seen in patients with allergic small airway disease, emphysema and obstructive bronchial masses
- Perfusion deficits: reduced pulmonary perfusion decreases lung opacity and promotes hyperventilation. Seen in patients with right-to-left shunts, pulmonic stenosis, right heart failure, pulmonary thromboembolism and hypovolaemia
- Central nervous stimulation:
 - Stress, commonly seen in hyperthyroid cats, aggressive and feral animals, but also as a normal variant
 - Metabolic acidosis
 - Shock
 - Brainstem pathology (infarct, mass).



12.15 Lung volumes as they appear on a lateral thoracic radiograph of a dog. A normal expiratory radiograph is taken with the lung in functional residual capacity (FRC, small black arrow). At peak inspiration, the tidal volume (TV, between large black arrows) is added. With hyperinflation (stressed animal, air trapping), the inspiratory reserve volume (IRV, between large white arrows) is added and the lung reaches total lung capacity (TLC), deviating the diaphragm caudally. With forced expiration, the FRC may be reduced by the expiratory reserve volume (ERV) to reach the reserve volume (RV, small white arrow) of the lung. If the lung is compressed (mass, increased intrapleural pressure) it can become totally atelectatic (TA). (Reproduced from Suter (1984) with permission)



12.16 Inspiratory lateral thoracic radiograph of a cat with asthma. The lungs are hyperlucent and the pulmonary vessels and cardiac silhouette are small (vertebral heart score 7). The lung fields are enlarged. The diaphragmatic silhouette is deviated far caudally from the cardiac silhouette and appears flattened. The caudodorsal lung margins open the lumbodiaphragmatic recess and extend caudally to the level of L2. The barely visible caudal vena cava (between arrowheads) is small. The stomach is gas-distended (aerophagia). If the lungs remain hyperlucent and enlarged at expiration, air trapping is a likely cause, consistent with bronchiolar disease.

General radiographic features (Figure 12.16) include:

- Hyperlucent lung fields:
 - Lungs appear darker than normal
 - Pulmonary blood vessels appear small but are visible (as opposed to pneumothorax).
- Enlarged lung fields:
 - Caudal displacement of the diaphragm:
 - Opening of the costodiaphragmatic recess, resulting in a dome-shaped diaphragmatic silhouette (DV/VD view)
 - Opening of the lumbodiaphragmatic recess and flattening of diaphragmatic contour (lateral view)
 - Tenting: pronounced visibility of the diaphragmatic attachments to the thoracic wall.
 - Small cardiac silhouette and caudal vena cava
 - Pleural cupula with cranial lung fields extending cranial to first pair of ribs (in dogs)
 - Rib orientation horizontal to the spine on DV/VD view.
- Gas-distended stomach due to concurrent aerophagia.

Hyperopaque lungs with decreased volume

Possible causes include:

- Restrictive conditions:
 - Pulmonary: fibrosis, consolidation
 - Pleural and mediastinal: pleural adhesions, effusion or air, intrathoracic fat, large masses
 - Thoracic wall: diaphragmatic paralysis, hernias, rib cage deformities, trauma, masses
 - Abdominal distension and pain.

- Upper airway obstruction:
 - Laryngeal or pharyngeal obstruction: laryngeal paralysis and collapse, masses, laryngeal oedema, foreign bodies
 - Tracheal collapse.
- Increased frequency of respiration with reduced tidal volume (e.g. panting).

Radiographic features (Figure 12.17) may include:

- Increased lung opacity
- Smaller than normal intrathoracic volume at peak inspiration
- Abnormal diaphragmatic silhouette (see Chapter 14)
- Chest wall abnormalities (see Chapter 14)
- Intrathoracic space-occupying lesions (mass, fluid, gas)
- Abdominal distension
- Decreased air space of pharynx, larynx and trachea.



12.17 Inspiratory lateral thoracic radiograph of a 7-week-old kitten with pectus excavatum, a chest wall anomaly. The caudodorsal lung fields are increased in opacity due to the restricted chest wall expansion, prohibiting full lung inflation.

Lung patterns

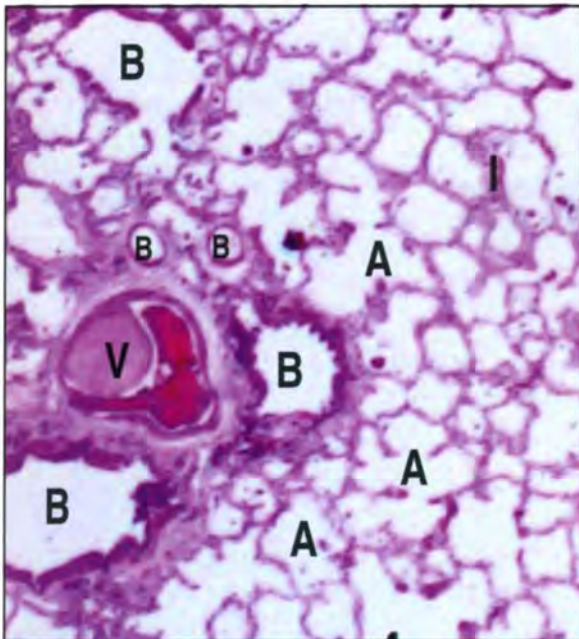
A radiographic pattern is a descriptive term to characterize a regionally or diffusely distributed disease. Lung patterns are an attempt to correlate imaging features of increased lung opacity with the morphological correlate of the lung (Figure 12.18):

- Alveolar airspace
- Bronchi
- Vessels
- Connective tissue (interstitium).

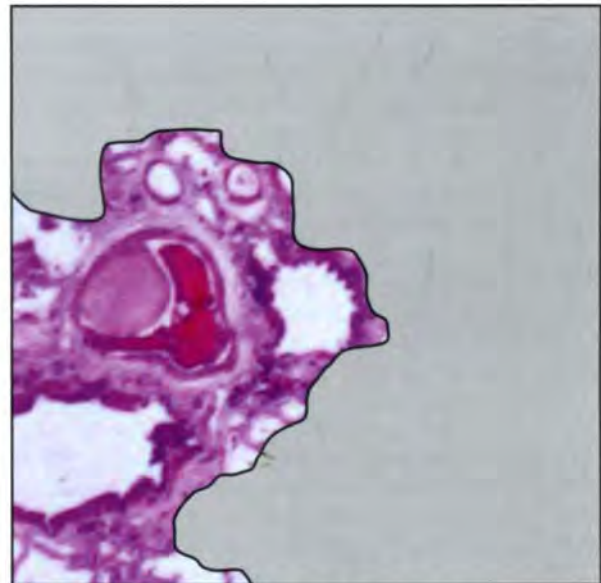
If only one component is pathologically altered, pattern recognition allows a relatively short list of differential diagnoses. In most lung diseases, more than one component is pathologically altered and a mixed pattern is evident radiographically. Usually one component is most affected and will be radiographically dominant; the predominating radiographic pattern should be treated as the most relevant.

Lung pattern recognition will not be a useful exercise if:

- Used to describe a focal lesion
- Anatomical and physiological alteration cannot be ruled out
- A mixed pattern with multiple equally contributing components is evident.



12.18 Histological image of a canine lung. For the purpose of radiographic evaluation the lungs can be interpreted as the sum of the vessels (V), bronchi (B), alveolar airspace (A) and pulmonary interstitium (I). H&E stain; original magnification x160.



12.19 Histological image of a canine lung demonstrating the concept of an alveolar lung pattern. The alveolar air has been replaced by more opaque structures (grey area) either due to airspace compression or filling. The encroached air-filled bronchi could create air bronchograms. H&E stain; original magnification x160.

Lung pattern recognition – questions you should ask yourself

Is there *abnormally* increased lung opacity over a wide area?
Which *one* of the main lung components predominantly contributes to this opacification?

The lung pattern approach is designed to explain why lung opacity is increased. If this question has already been answered, the pattern designation does not contribute to the diagnosis and should be avoided. For example, with a large soft tissue mass in a lung lobe, avoid the attribute *alveolar*.

Alveolar lung pattern

Classic radiographic features: Increased lung opacity contributed by the alveolar space occurs if:

- The alveoli are completely collapsed and void of any air
- The alveoli are filled with fluid or soft tissue material (Figure 12.19).

The features of the alveolar lung pattern do not translate into a direct visualization of the alveoli, but into a set of more abstract features (Figure 12.20):

- Homogenous soft tissue opacification
- Border obliteration with adjacent soft tissue structures or fluid
- Air bronchograms (see below) if bronchi are air-filled.



12.20 VD thoracic radiograph of a 1-year-old Bichon Frisé with pulmonary haemorrhage due to rodenticide intoxication. The right lung is homogeneously opacified to a similar degree as the soft tissue organs, such as the heart and liver. Several radiolucent bands can be seen within the opacified lung, representing air bronchograms (arrowheads). The cardiac silhouette is slightly shifted towards the right, indicating some loss of normal right lung volume. Both the cardiac silhouette and the right hemidiaphragm are partially obliterated by the lung (border obliteration sign). These are all classic features of the alveolar lung pattern. The left lung appears hyperinflated and hyperlucent, indicative of compensatory hyperinflation.

Air bronchogram: When a lung collapses or consolidates, a bronchus may remain gas-filled and open because the bronchial cartilage resists collapse, or the vast alveolar airspace fills up with fluid or exudates prior to the airways. In this situation, an air-filled bronchus surrounded by lung of soft tissue opacity may be visible radiographically, and is called an *air bronchogram* (see Figure 12.20). It indicates:

- Lung pathology. Air bronchograms cannot be created by superimposing opacities (e.g. pleural effusion, mediastinal mass)
- Alveolar lung pattern. Air bronchograms cannot be created by any other pattern.

Air bronchograms may not be seen in every case of alveolar lung disease, but their presence is pathognomonic for the alveolar lung pattern. Absence does not rule out alveolar lung pattern.

Margination:

- If the affected area is smaller than the lobe (Figure 12.21) there are indistinct margins (fluffy, resemblance to a cloud).
- If an entire lobe is affected (Figure 12.22) there is border obliteration with adjacent soft tissue structures (e.g. cardiac silhouette, diaphragm) or a lobar sign if the neighbouring lobe is aerated (see below).

The lobar sign: The border between two lung lobes becomes distinguishable if one is consolidated/



12.21 Lateral thoracic radiograph of a 5-year-old Labrador Retriever with traumatic chordae tendinae rupture and mitral valve regurgitation with secondary cardiogenic pulmonary oedema. There is increased lung opacity with the alveolar pattern in the perihilar lung region, with indistinct margination towards the lung areas with an interstitial pattern (caudal) and a normal appearance (ventral) in the lung periphery. The marked pulmonary oedema combined with the mild left atrial enlargement is consistent with the recent traumatic history. (Courtesy of P. Wotton)

collapsed and the other one normally aerated. This seemingly trivial feature is called a *lobar sign* (see Figure 12.22). However, it is a useful sign in that it is a pathognomonic feature of the alveolar lung pattern and differential to a fissure line in pleural effusion:

- Fissure line: two lucent lung lobes separated by an opaque band
- Lobar sign: directly adjacent opaque and lucent lung area.

Size of affected lung lobes: If a large enough area of the lung is affected by alveolar lung disease, the lung lobe size may change and allow distinction between collapsed and consolidated lung. This is best visualized on a DV/VD radiograph and assessed via the mediastinal shift:

- Consolidated lung may be normal or increased in size, and if enlarged may cause a shift of the mediastinal structures away from it (Figure 12.23)
- Collapsed lung will be decreased in size and may cause a shift of the mediastinal structures towards it (see Figure 12.22)



12.22 VD thoracic radiograph of a 6-year-old Briard with pneumonia. Only the right middle lung lobe is affected and shows the alveolar lung pattern. There is border obliteration with the cardiac silhouette, some air bronchograms, and distinct margination towards the normally aerated right cranial and caudal lung lobes (lobar sign). The cardiac shadow is completely confined to the right hemithorax, indicating mediastinal shift due to right middle lung lobe collapse. Compensatory hyperinflation of the left lung is present.



12.23 VD thoracic radiograph of an 8-year-old Cocker Spaniel with bronchoalveolar carcinoma. The mainly affected left lung is increased in opacity with an alveolar pattern and increased in volume, indicated by the deviation of the cardiac silhouette into the right hemithorax (arrowheads).

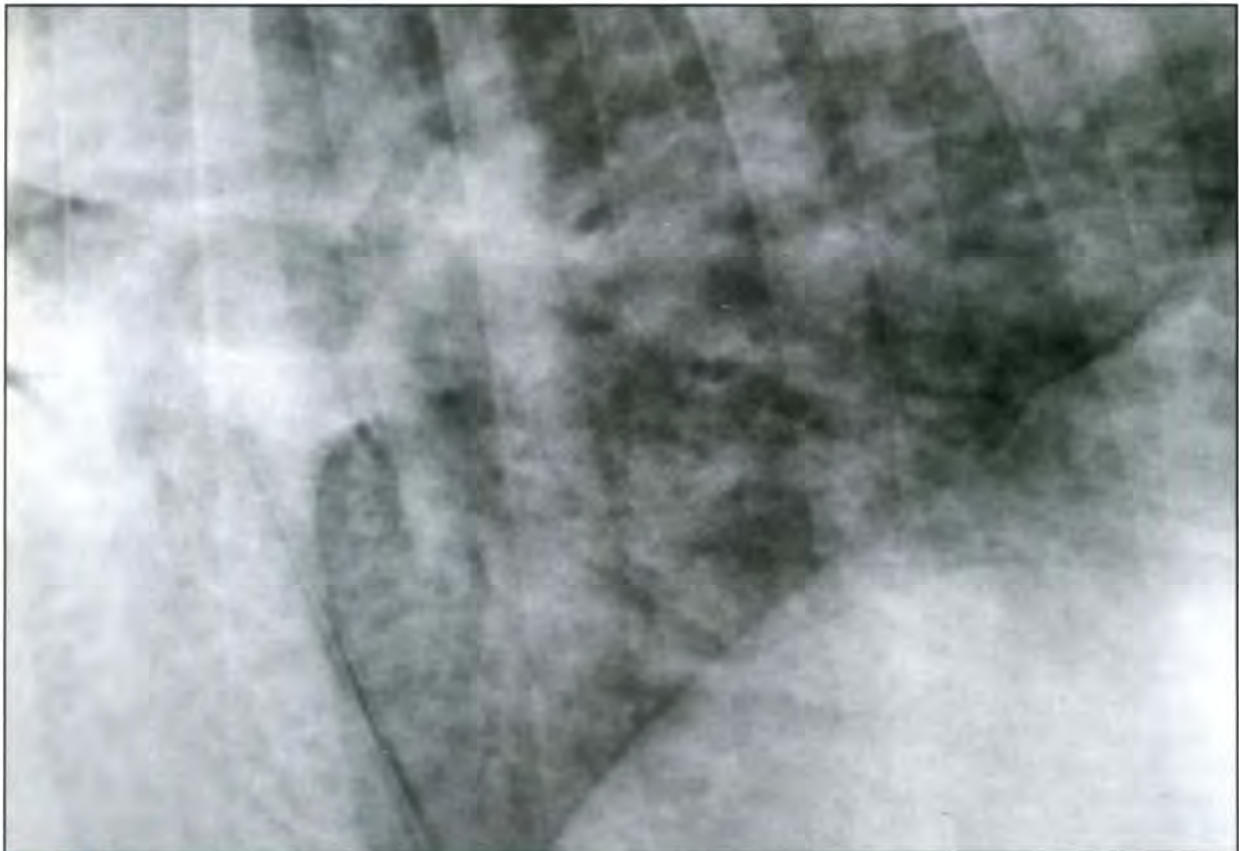
- Chronic collapse, especially in cats with right middle lung lobe collapse secondary to airway disease, may result in hyperinflation of adjacent lobes and resolution of the mediastinal shift.

Partial or non-consolidating alveolar lung pattern: In many situations, the alveolar airspace of an affected lung area is mostly, but not completely, collapsed or consolidated. The resulting radiographic pattern then consists of a heterogeneous soft tissue opacification with residual lucent spots (Figure 12.24). This is colloquially referred to as a 'salt-and-pepper' appearance. Residual lucent grape-like air spaces are occasionally referred to as *air alveolograms*. There may or may not be distinctive air bronchograms. There is usually no border obliteration or lobar sign. Partial alveolar pattern is arguably more common than complete lung consolidation.

Bronchial lung pattern

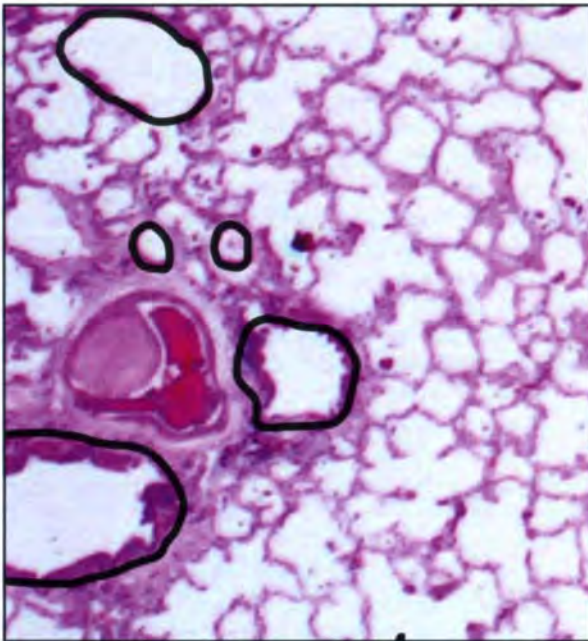
Increased lung opacity contributed by the bronchial tree can be caused by the following (see also Chapter 11):

- Thickening of many bronchial walls
- Excessive mineralization of many bronchial walls
- Enlargement of many deformed bronchi (bronchiectasis).



12.24 Caudodorsal close-up of a lateral thoracic radiograph of a 2-year-old Mastiff with vegetative endocarditis and secondary pneumonia and pulmonary oedema. There is generalized increased lung opacity, created by the partially obliterated alveolar airspace (partial alveolar pattern). Particularly in the more ventral lung fields, vessels are no longer distinguishable and air bronchograms begin to emerge; however, the opacity is still inhomogeneous due to residual air-filled alveoli (air alveolograms), giving the image a 'salt-and-pepper' appearance. Thin pleural fissure lines are visible superimposed over the caudal cardiac silhouette.

It should be noted that the changes include both the central and peripheral lung fields (Figure 12.25).



12.25 Histological image of a canine lung demonstrating the concept of the bronchial lung pattern. Bronchial walls (outlined ring structures) create an increased lung opacity by virtue of wall thickening or extensive wall mineralization. H&E stain; original magnification x160.

Classic radiographic features: Ring shadows (increased circular opacity with lucent centre, also known as 'doughnuts') represent end-on bronchi (Figure 12.26):

- Thin-walled: mineralized bronchi (Figure 12.27)
- Thick-walled: inflamed, infiltrated bronchi.

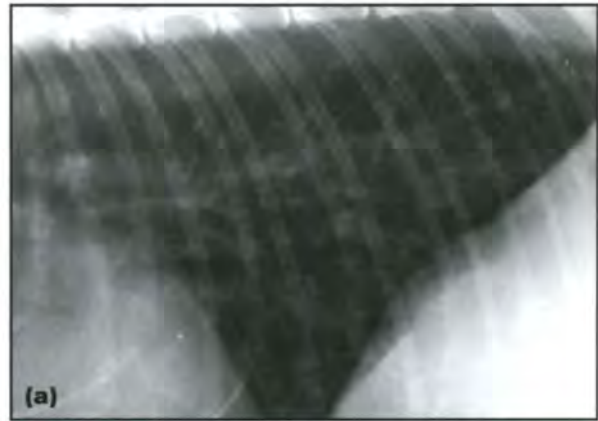
Tram lines (parallel lines of increased opacity) represent side-on bronchi:

- Thin walled: mineralized bronchi
- Thick walled: inflamed, infiltrated bronchi (usually not as prominent as ring shadows).

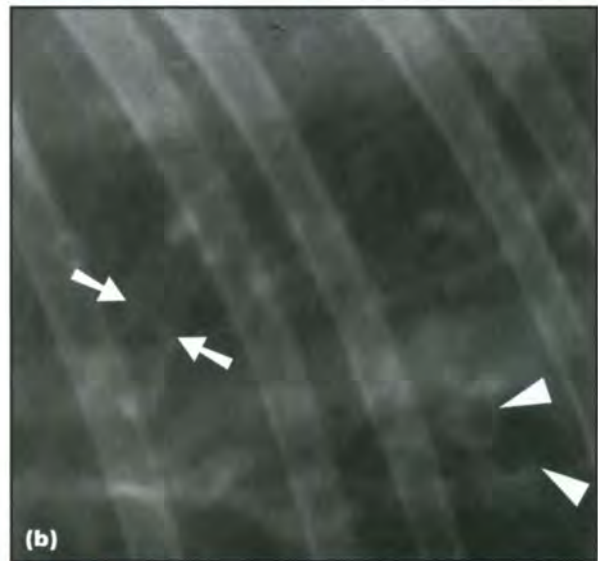
Many peripherally distended irregular bronchi may be seen (bronchiectasis) (see Chapter 11). Differentiation of the bronchial lung pattern from a normal variation can be challenging, because mild to moderate bronchial mineralization is a normal feature in skeletally mature dogs. Mild to moderate bronchial markings can frequently be seen in older cats without current clinical respiratory disease. It is unknown whether this is attributable to normal degeneration, or to current subclinical or previous disease.

Vascular lung pattern

Increased lung opacity contributed by the pulmonary vasculature (see also Chapter 7) can occur if:



(a)



(b)

12.26 (a) Caudodorsal close-up of a lateral thoracic radiograph of a 14-year-old Domestic Shorthair cat with asthma. There is an increased lung opacity, predominantly created by the bronchial structures (bronchial pattern). It can be difficult to differentiate normal vessels from abnormal bronchi. The presence of ring shadows ('doughnuts') indicates bronchial origin. **(b)** Further close-up reveals thickened bronchi in both long axis (tram lines, arrowed) and short axis (ring shadows, arrowhead).

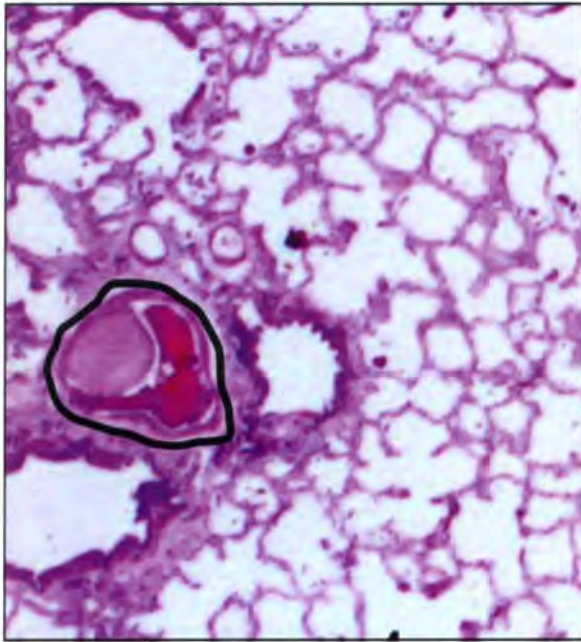


12.27 Close-up of a lateral thoracic radiograph of a 9-year-old Standard Poodle with hyperadrenocorticism, causing excessive widespread bronchial mineralization. Increased lung opacity results from the bronchi that are more opaque, but not thicker, than normal (bronchial pattern). (Reproduced from Schwarz *et al.* (2000) with permission from the *Journal of Small Animal Practice*)

- Many pulmonary arterial branches are distended or thickened
- Many pulmonary veins are distended
- Both pulmonary arteries and veins are distended (Figure 12.28).

Classic radiographic features: The lung fields are occupied by many vessels, which are increased in size (Figure 12.29):

- Round opaque shadows (end-on vessels)
- Thick band-like shadows (side-on vessels).



12.28 Histological image of a canine lung demonstrating the concept of a vascular lung pattern. Pulmonary vessels (outlined) create an increased lung opacity by virtue of wall thickening or distension. H&E stain; original magnification x160.



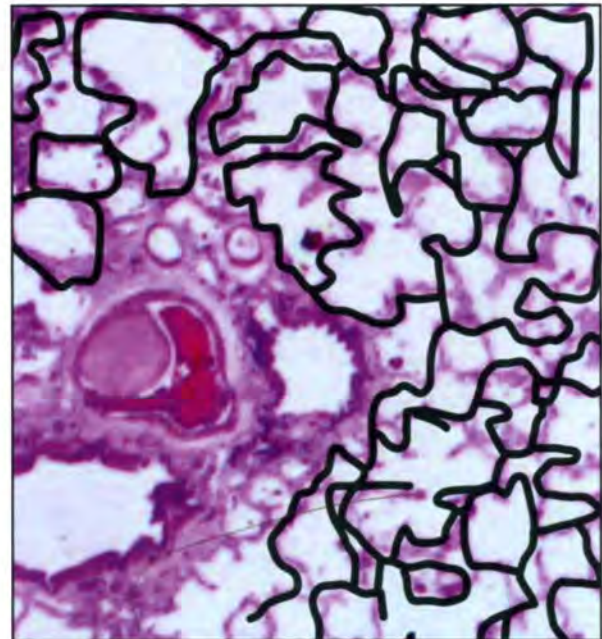
12.29 Caudodorsal close-up of a lateral thoracic radiograph of a 9-month-old German Shepherd Dog with a patent ductus arteriosus and left-to-right shunt, resulting in pulmonary hyperperfusion. There is increased lung opacity due to numerous distended pulmonary vessels (vascular pattern). A distinction between arteries and veins cannot be made in this region on this view. The left atrium is enlarged due to volume overload.

For further information on vessel identification (arteries *versus* veins, and which is the associated lung lobe) see Figures 12.7 and 12.8.

Interstitial lung pattern

Increased lung opacity contributed by the pulmonary interstitium can occur in two situations:

- Nodular interstitial pattern: caused by nodular lesions arising from the interstitium:
 - Metastatic neoplasia
 - Granulomatous disease
 - Primary miliary neoplasia.
- Unstructured to fine-structured interstitial pattern: a diffuse swelling of the interstitial space (Figure 12.30) due to:
 - Oedema (vascular leakage, lymphatic back-up)
 - Haemorrhage
 - Exudates
 - Excessive fibrocyte proliferation
 - Diffuse neoplastic infiltrate
 - Mineralization.



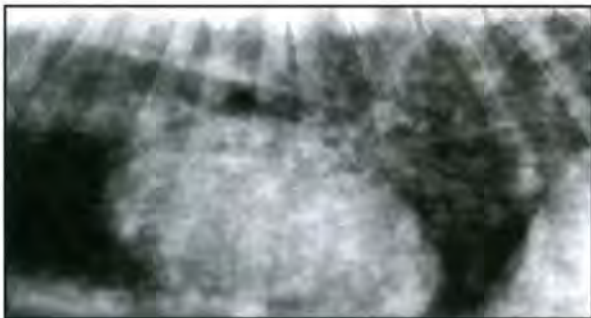
12.30 Histological image of a canine lung demonstrating the concept of an interstitial lung pattern. A thickened pulmonary interstitial space (outlined) creates an increased lung opacity. Since the alveolar airspace remains intact, small lung vessels will still be sufficiently outlined by air to be visible. The interstitium is the weakest contributor to lung opacification. If combined with other compartment disorders, which is often the case, other patterns are usually predominant. H&E stain; original magnification x160.

Nodular interstitial pattern:

Classic radiographic appearance: There are multiple nodules of soft tissue opacity throughout lung fields (Figures 12.31 and 12.32). The opacity correlates with nodule size and number.



12.31 VD thoracic radiograph of a 13-year-old Cocker Spaniel with ocular melanoma and metastatic lung disease. There is an increased lung opacity created by numerous pulmonary soft tissue nodules of various sizes (nodular pattern). In some parts, the nodular shadows coalesce.



Radiographic visibility of lung nodules is size-dependent. A minimal diameter of 3–5 mm is required for a single soft tissue nodule to be visible. Larger nodules are more opaque. Visibility depends on there being a large enough area of aerated lung tissue surrounding the lesion; visibility is poor in a small lung area superimposed on a large soft tissue structure (heart, liver) and nodules will be poorly visible or not visible if surrounded by collapsed/consolidated lung.

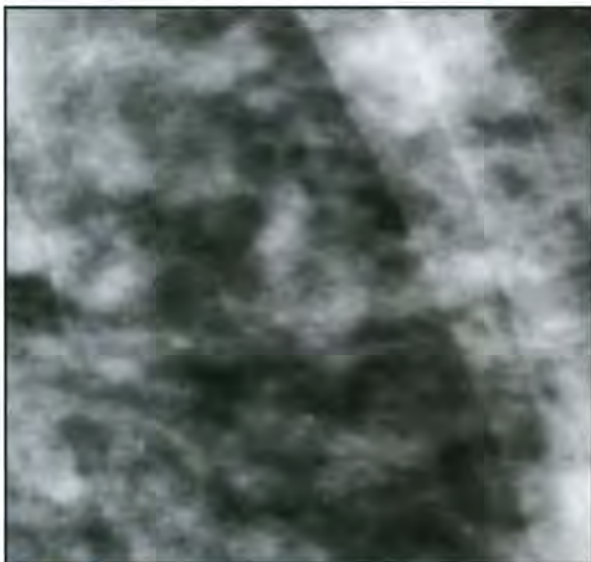
Superimposed body wall structures can mimic pulmonary nodules, e.g. costochondral junctions or nipples. They are often multiple with a regular distribution, and can often be identified on the orthogonal view.

Well visualized nodules smaller than 3 mm (Figure 12.33) may represent:

- Miliary lesions (very many small superimposed nodules)
- End-on vessels (more soft tissue superimposed)
- Mineralized nodules, such as pulmonary osteomas (more opaque tissue).



12.33 Caudodorsal close-up of a lateral thoracic radiograph of a dog with histoplasmosis. There is increased lung opacity created by numerous 2–4 mm mineralized nodules throughout the lungs (nodular pattern). The combination of small nodular size and high opacity would make these lesions unlikely candidates for metastatic neoplasia.



12.32 Lateral thoracic radiograph with a caudal close-up of a 9-year-old Golden Retriever with a heart base mass and miliary pulmonary metastases. There is increased lung opacity created by very many small soft tissue nodules (miliary nodular pattern) that superimpose on each other and coalesce. The close-up image demonstrates more clearly the nodular nature of the opacity.

End-on vessels and most small mineralized nodules are normal or incidental features, which need to be differentiated from soft tissue nodules. Pulmonary osteomas are often irregular in shape as well as being extremely opaque for their size.

Unstructured to fine-structured interstitial pattern:

Classic radiographic appearance: There is a mild to moderate increase in lung opacity (Figure 12.34). There may be a homogenous opacity (unstructured pattern) or a range of finely structured opacities (fine-structured pattern), including very small nodular structures, short linear or reticular opacities (web-like) or honeycombs. Small pulmonary blood vessels are still distinguishable.

The interstitial lung pattern is one of the most elusive radiographic features. It has become a fertile ground for speculation, imagination and prejudice among those who believe to know, and insecurity among those who do not. Recommendations and limitations for use of the interstitial lung pattern include:



12.34 Caudodorsal close-up of a lateral thoracic radiograph of a 3-year-old German Shepherd Dog with lymphoma. There is a mild increase in lung opacity, diffusely spread over the lung fields. This opacification is caused by interstitial infiltration of the lymphoma. Given the well inflated state, and appropriate exposure settings, such lung opacity can be classified as abnormal and other patterns can be ruled out based on appearance. The fact that small lung vessels are still visible is an indicator for the interstitial pattern.

- Should only be used in a well inflated lung
- Should only be used as a last resort when other patterns do not fit
- Subdivision into unstructured and fine-structured pattern is not helpful
- Silhouetting of small lung vessels with the lung excludes interstitial pattern and indicates alveolar pattern.

An interstitial component is part of many mixed patterns.

Mixed lung pattern

If multiple lung components contribute to lung opacification, a mixed pattern results (see Figures 12.21 and 12.35). Most lung diseases show a mixed pattern; the predominant pattern should be treated as the most relevant.



12.35 Caudodorsal close-up of an inspiratory lateral thoracic radiograph of an 8-year-old Siamese cat with asthma. There is increased lung opacity, created by numerous thickened bronchi and a superimposed veil of diffuse opacification. This can be called a *bronchointerstitial pattern*. The bronchial component is predominant, as well as more specific, and should be focused on for diagnosis, prognosis and treatment.

Alternative appraisal of the lung

This method emphasizes the macroscopic distribution of lesions (instead of the microscopic correlation in pattern diagnosis) as the most important Röntgen sign for refining the differential diagnosis. The following steps are undertaken:

1. Determination of lung opacity as normal or abnormal.
2. Determination of abnormal opacity as increased or decreased.
3. Assessment of the affected lung lobe size.
4. Assessment of the appearance of the opacity.
5. Assessment of the macroscopic lesion distribution.
6. Comparison of test results with patient information and establishment of:
 - Definitive radiographic diagnosis
 - Prioritized list of differential diagnoses of possible causes
 - Recommendations for additional testing, if necessary.

Assessment criteria

Lung opacity

Normal lung opacity: Normal lung opacity is mainly composed of air and blood vessels. Normal lungs appear mostly black (gas opacity) with bands of soft tissue opacity (pulmonary blood vessels). Other pulmonary structures (e.g. bronchial walls) should only minimally contribute to the overall opacity. There is a wide range of normal breed, age and physiological variation in lung opacity, and technically related differences.

Abnormal lung opacity:

- Decreased opacity of the lung – the lungs are more lucent than normal. The distribution of the lesion may be focal, multifocal or diffuse.
- Increased opacity of the lung – the lungs are more opaque than normal. The abnormal opacity may be described in relationship to lung lobe size, appearance and macroscopic distribution.

Lung lobe size

- Normal – the lung may be consolidated, filled with fluid or cells, or have a mass and generally indicates disease.
- Reduced – the lung is atelectatic, may be due to disease or not (e.g. technical complication). Atelectasis due to disease may result in the inability to expand the lung due to compression or bronchial obstruction.
- Enlarged – the lung may be consolidated, filled with fluid or cells, or have a mass and generally indicates disease.

Appearance of increased opacity of the lung

- Airspace – analogous to descriptions of unstructured interstitial and alveolar patterns. The terms interstitial (mild airspace) and alveolar (severe airspace) originally were thought to

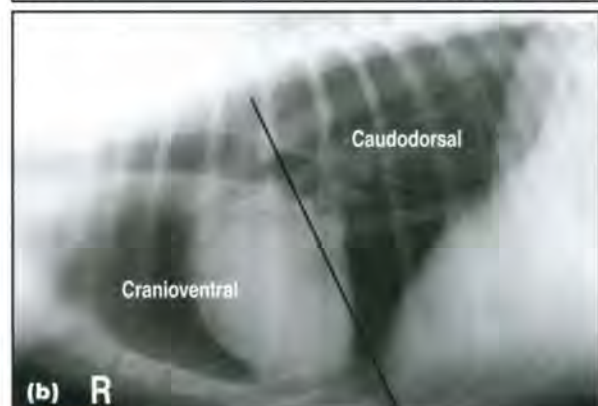
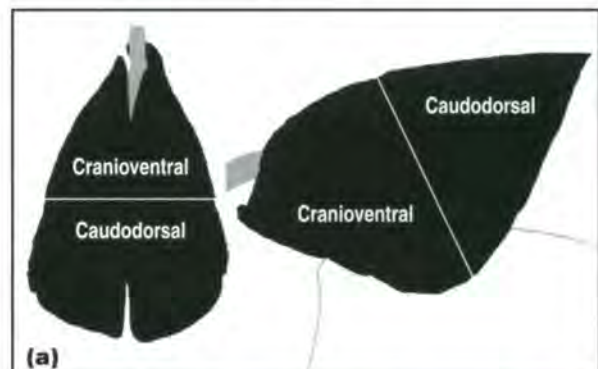
correspond to the microscopic distribution of disease. These terms might represent disease severity better than microscopic distribution.

- Airway – analogous to the previous description of bronchial and bronchointerstitial patterns.
- Nodule – may be small (miliary) or large, solid or cavitory, focal or multifocal, poorly or well defined.
- Mixed – indicates that there is a combination of patterns.

Macroscopic distribution of lung lesions

The entire region does not have to be involved to designate one of the following macroscopic distributions:

- Cranioventral – although other lung lobes may be involved (depending on the severity of the lesion), this area generally conforms to the region of the left cranial, right cranial and right middle lung lobes (Figure 12.36)
- Caudodorsal – although other lung lobes may be involved (depending on the severity of the lesion), this area generally conforms to the region of the left caudal, right caudal and accessory lung lobes (Figure 12.36)
- Diffuse – all parts of all lung lobes are abnormal
- Focal – a single lesion that usually is well defined but may be a poorly defined patch



12.36 (a) Cranioventral and caudodorsal lung fields. (b) Clinically normal right lateral thoracic radiograph of a dog. A line is drawn to indicate the approximate demarcation of the cranioventral and caudodorsal lung fields. Note that the cranioventral lung field extends to the most caudoventral aspect of the thorax, and is superimposed on the heart. This is important because the most common location for aspiration pneumonia is in the cranioventral lung field superimposed on the heart.

- Multifocal – more than one lesion is detected in one, multiple or all lung lobes. If all lung lobes are involved, then there is still some normal lung between the lesions (i.e. it is not diffuse). The lesions usually are discrete but, alternatively, may be poorly defined patches that have a random distribution
- Asymmetrical – one or more lesions that are usually, but not necessarily, patchy and poorly defined. There is usually left–right asymmetry, and the lesion does not conform to one of the other categories
- Lobar – one entire lung lobe is abnormal
- Mixed – a combination of the above distributions.

Common radiographic patterns of lung disease

The above Röntgen signs of opacity, size, appearance and macroscopic distribution may be combined to form radiographic patterns of disease. Evaluation of these patterns are tests for the diseases that may produce them. The results of the tests are either positive or negative, and they may be true or false. The more commonly encountered patterns are:

- Cranioventral air space pattern
- Consolidated lung lobe
- Caudodorsal-to-diffuse air space pattern
- Diffuse airway pattern
- Focal lung nodule (soft tissue)
- Multifocal lung nodule (soft tissue)
- Focal lung nodule (gas)
- Multifocal lung nodule (gas)
- Focal lung nodule (cavitary)
- Multifocal lung nodule (cavitary)
- Diffuse hyperlucent lung pattern
- Atelectasis
- Asymmetrical lung pattern
- Mixed lung pattern.

Cranioventral airspace pattern or consolidated lung lobe: Differential diagnoses include:

- Bronchopneumonia
- Aspiration pneumonia
- Haemorrhage
- Neoplasm
- Lung lobe torsion.

Caudodorsal-to-diffuse airspace pattern: Differential diagnoses include:

- Cardiogenic pulmonary oedema
- Non-cardiogenic pulmonary oedema:
 - Vasculitis
 - Inhaled toxin
 - Upper airway obstruction
 - Neurogenic
 - Near drowning
 - Fluid overload
 - Hypoproteinaemia
 - Disseminated intravascular coagulation
 - Acute respiratory distress syndrome.
- Immune-mediated lung disease
- Neoplasm (e.g. lymphoma).

Diffuse airway pattern: Differential diagnoses include:

- Bronchitis:
 - Allergic
 - Infectious: viral, bacterial, parasitic.
- Asthma
- Lymphatic spread of cancer (metastasis)
- Cardiogenic pulmonary oedema (mild).

Focal soft tissue nodule: Differential diagnoses include:

- Neoplasm (especially primary lung neoplasm)
- Abscess
- Granuloma
- Haematocele.

Multifocal soft tissue nodules: Differential diagnoses include:

- Neoplasm (especially metastasis)
- Abscesses
- Granulomatous disease
- Haematoceles
- Superimposed cutaneous nodules
- Pulmonary infiltrates with eosinophilia
- Ossifying pulmonary metaplasia.

Focal or multifocal lucent or cavitary nodules: Differential diagnoses include:

- Pneumatocele (bullae), traumatic or idiopathic
- Abscess
- Neoplasm.

Atelectasis: Differential diagnoses include:

- Technical complication:
 - Prolonged recumbent position
 - Anaesthesia-related
 - Incomplete inhalation.
- Disease:
 - Bronchial foreign body
 - Neoplasm
 - Asthma
 - Bronchopneumonia
 - Immaturity
 - Compression by pulmonary mass, pleural fluid, or body wall mass
 - Pulmonary thrombosis.

Diffuse hyperlucent lung pattern: Differential diagnoses include:

- Hypovolaemia
- Asthma
- Emphysema.

Asymmetrical lung pattern: Differential diagnoses include:

- Trauma
- Neoplasia
- Immune-mediated lung disease (e.g. pulmonary infiltrates with eosinophilia)
- Infectious
- Cardiogenic pulmonary oedema (cat).

Mixed lung pattern or distribution: See the differential diagnoses list for the patterns or distributions comprising the mixture. The pattern may be due to a single or multiple disease processes.

Prioritizing the differential diagnosis

Prioritization is an essential last step to establish a *meaningful* diagnosis. Hedging behind endless lists of differential diagnoses does not help the treatment and prognosis of the patient. A definitive diagnosis should be stated clearly whenever possible or when one disease is much more likely than others; for example, a cranioventral air space pattern in a coughing dog with megaesophagus and fever is most likely to be due to aspiration pneumonia. Other differentials can be thought of (e.g. coincidental pulmonary haemorrhage) but are no more common than chance, i.e. unrelated to the radiographic feature (e.g. patient could coincidentally also have a brain tumour).

In most circumstances, there are several likely diseases that could cause a similar radiographic pattern. In this situation, the list of possibilities should be kept reasonably short and be prioritized by incorporating knowledge of test accuracy and prior probability of disease, which is best estimated by knowing the patient's signalment (age, sex and breed), chief complaint and pertinent history or findings. This may be the most influential step in the process of making an accurate radiographic diagnosis.

In some circumstances, a very large number of diseases could create a similar radiographic pattern. In this situation a differential list would be very long and could not be prioritized, and is therefore not useful. It is then sufficient to say that pulmonary disease is present but the cause is not determined.

Diseases

Solid pulmonary masses

A pulmonary mass is a fluid, soft tissue or mineralized structure replacing, compressing or displacing the air-filled portion of the lung (Figure 12.37). The clinical implications rest on the assessment of whether the

- Metastatic disease
- Primary lung tumour
- Granuloma:
 - Mycotic (blastomycosis, coccidioidomycosis, histoplasmosis, cryptococcosis, aspergillosis)
 - Parasitic: heartworm (*Dirofilaria immitis*), lungworm (*Strongyloides*; *Filaroides hirthi* and *milksi*; *Paragonimus kellicotti*, *Aelurostrongylus abstrusus* in the cat), protozoa (*Toxoplasma gondii*)
 - Foreign body (grass awn, barium sulphate or mineral oil aspiration)
 - Eosinophilic
 - Bacterial (mycobacteria, *Nocardia*)
- Abscess
- Cyst
- Fluid-filled bulla
- Mucus-filled bronchus
- Haematoma

12.37 Differential diagnoses for a pulmonary nodule/mass.

mass is benign or malignant. It can be difficult to differentiate between various types of lung mass solely on imaging features; however, a prioritized differential diagnoses list can be created based on the imaging characteristics described below and other factors, such as:

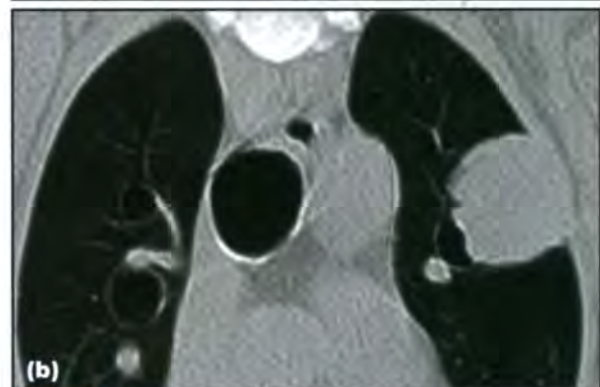
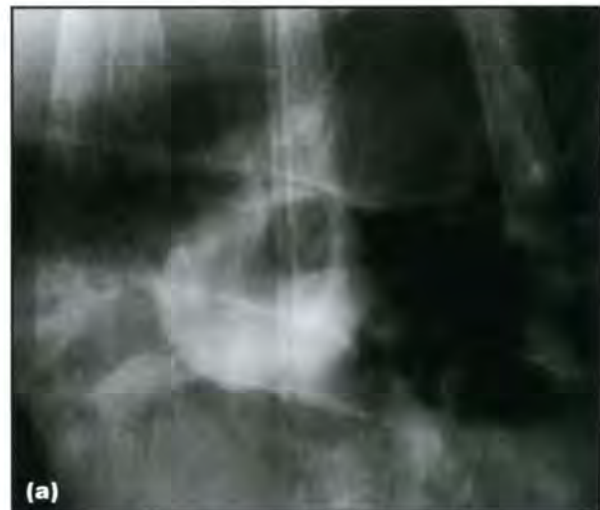
- Age
- Species and breed
- Geographical area where animal lives or has travelled to
- Additional diagnostic tests.

Cystic masses are discussed later in this chapter.

Radiography

Thoracic radiography is usually the initial examination. Radiographically, a pulmonary mass is evident as a discrete opacity, surrounded by (more) lucent lung. Most pulmonary masses are expansile and displace, rather than contain, major airway structures (Figure 12.38). Common features of such masses are:

- Bronchial deviation
- Absence of air bronchograms.



12.38 (a) Central close-up of a right lateral thoracic radiograph of a 12-year-old German Shepherd Dog with a pulmonary carcinoma. The mass slightly deviates the air-filled left cranial lung lobar bronchus but does not give rise to an air bronchogram. This indicates that the mass is of an expansile rather than infiltrative nature. (b) CT image confirms how the mass abuts but does not encroach into the bronchus. (Courtesy of L. Jarrett)

However, a minority of lung masses are infiltrative and can contain and occlude bronchi (Figure 12.39).

Both types of mass can result in bronchial obstruction and subsequent pulmonary atelectasis or secondary haemorrhage and infection, which can result in:

- A large area of alveolar lung disease with air bronchograms and a lobar sign
- Border obliteration between the mass and the adjacent secondary lung changes, making size assessment difficult.



12.39 (a) Close-up of a DV thoracic radiograph of a dog with a histiocytic sarcoma in the right middle lung lobe. The mass occupies a large portion of the lobe, giving rise to a lobar sign cranially and caudally, and contains air bronchograms. This is consistent with an infiltrative lesion encroaching on the airways. (b) Caudal close-up of a VD thoracic radiograph of a 12-year-old Domestic Shorthair cat with nasal and pulmonary lymphoma. Notice the increased opacity with an alveolar pattern (air bronchogram) supportive of an infiltrative process. Radiographically evident pulmonary involvement in feline lymphoma is extremely rare.

Features of the alveolar lung pattern can therefore in some circumstances be suggestive of, but are not indicative for, the assessment of the growth pattern of a mass.

Classic Röntgen signs:

- Size: lesion up to 3 cm is termed a *nodule*; lesion larger than 3 cm is termed a *mass*.
- Shape: usually round (equal growth in each direction) but other shapes are possible, especially at the lung margins.
- Opacity: usually soft tissue opacity. There may be a central lucency in cavitated lesions, and a mineralized centre may be seen due to dystrophic mineralization.
- Location: random. Some diseases extend from the mediastinal lymph nodes into the adjacent perihilar lung tissue (lymphomatoid granulomatosis).
- Number: solitary or multiple.

Neoplasia: Primary pulmonary neoplasia typically presents as a *solitary nodule* (Figure 12.40) or *mass* (see Figures 12.38a, 12.39a and 12.41). It may be accompanied by additional smaller lesions, representing metastatic disease from the primary neoplasia. Occasionally, concurrent cranial mediastinal or hilar lymphadenopathy and/or pleural effusion are radiographically visible.

A small solitary nodule is equally likely to be metastatic or primary neoplasia. The larger the nodule is, the more likely it is to be primary neoplasia. Pulmonary neoplasia can also manifest as *diffuse parenchymal disease*:



12.40 Left lateral thoracic radiograph of a 12-year-old mixed breed dog with primary bronchoalveolar carcinoma. A solitary nodule with soft tissue opacity is seen in the right middle lung lobe (arrowed).



12.41 VD thoracic radiograph of an 8-year-old Rottweiler with pulmonary adenocarcinoma. There is a mass with soft tissue opacity in the left caudal lung lobe. Note the border obliteration between the mass and the heart.

- Interstitial, peribronchial infiltration or a patchy alveolar pattern is possible (e.g. interstitial pattern in canine lymphoma; see Figure 12.34)
- May be caused by complications of the neoplastic disease, such as inflammation, infection or haemorrhage
- *Lobar consolidation* occurs if a lung lobe is gradually infiltrated or if the lobar bronchus is obstructed by the mass (Figure 12.42). Examples include:



12.42 VD thoracic radiograph of a 12-year-old Bichon Frisé with primary pulmonary carcinoma. The entire left cranial lung lobe is consolidated.

- Lymphomatoid granulomatosis (a rare primary pulmonary angiodescriptive neoplasm seen mainly in young to middle-aged dogs). The lung lobe typically has an *increased volume*, resulting in convex, bulging borders
- Bronchogenic carcinoma may also occlude a bronchus, causing atelectasis and thus *loss of volume* and concave margins.
- A lung tumour may become cavitated, and uncommonly is mineralized, although no correlation between radiographic pattern and histological type of disease has been found.

Species differences

Mineralization of lung tumours

- Cats: central mineralization of primary pulmonary neoplasia is common (Figure 12.43).
- Dogs: central mineralization is rare.

Pulmonary infiltration of lymphoma

- Cats: very rarely any radiographically evident lung lesion in lymphoma (see Figure 12.39b).
- Dogs: commonly causes a diffuse unstructured interstitial lung pattern (see Figure 12.34) but very rarely nodules or masses.

Pulmonary metastases

- Cats: often poorly marginated, irregularly shaped (see Figure 12.55).
- Dogs: usually well defined round nodules (see Figure 12.54).

Primary pulmonary neoplasia and digital metastasis in cats

The digits are a predilection site for metastases from feline primary pulmonary neoplasia. This has been reported in:

- Pulmonary adenocarcinoma
- Pulmonary squamous cell carcinoma
- Bronchogenic carcinoma.

Older cats are usually presented for digital swelling and lameness, and are free of respiratory signs. Occasionally, skeletal metastases of lung tumours in dogs occur in the axial skeleton and long bones proximal to the stifle and elbow, but have not been reported in the digits.

Primary digital neoplasia and pulmonary metastases in dogs

The most commonly diagnosed digital neoplasms in dogs are:

- Squamous cell carcinoma
- Subungular melanoma (Figure 12.44).

Melanoma has a high rate of lung metastases. Dogs or cats with digital swelling and lameness warrant screening for neoplastic lung disease.

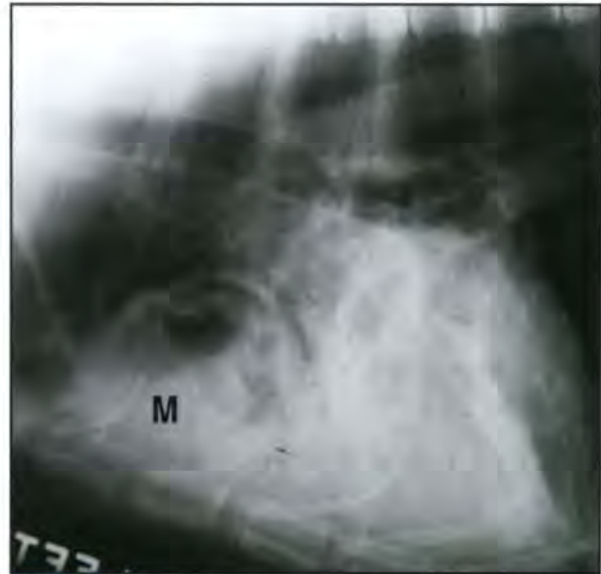


12.43 Craniodorsal close-up of a right lateral thoracic radiograph of a 10-year-old Domestic Shorthair cat with a primary lung lobe tumour in the left cranial lobe. There are multiple small mineralizations in the craniodorsal lung fields. A VD view confirmed their location within the left cranial lung lobe.



12.44 Close-up of a radiograph of the third phalanx of the fifth digit of the right manus of a 9-year-old Rottweiler with digital pain. Notice the soft tissue swelling and extensive osteolysis of P3 (histological diagnosis: subungular melanoma).

Abscesses: A pulmonary abscess typically has a thick wall with an irregular inner surface. It may be cavitory, if it contains gas, either due to gas-producing bacteria or due to connection with the airways (Figure 12.45). It may be surrounded by abnormal, consolidated lung, or may be well demarcated and surrounded by normal lung. Horizontal beam radiographs may demonstrate a fluid–gas interface. It is not commonly associated with pleural effusion.



12.45 Left lateral thoracic radiograph of a 1-year-old Great Dane with suppurative pneumonia. A cavitary mass (M) is seen in the right cranial lung lobe. The centrally present gas delineates a thick wall with an irregular inner surface. The caudally adjacent right middle lung lobe is increased in opacity with an alveolar pattern (air bronchograms, lobar sign), consistent with pneumonia.

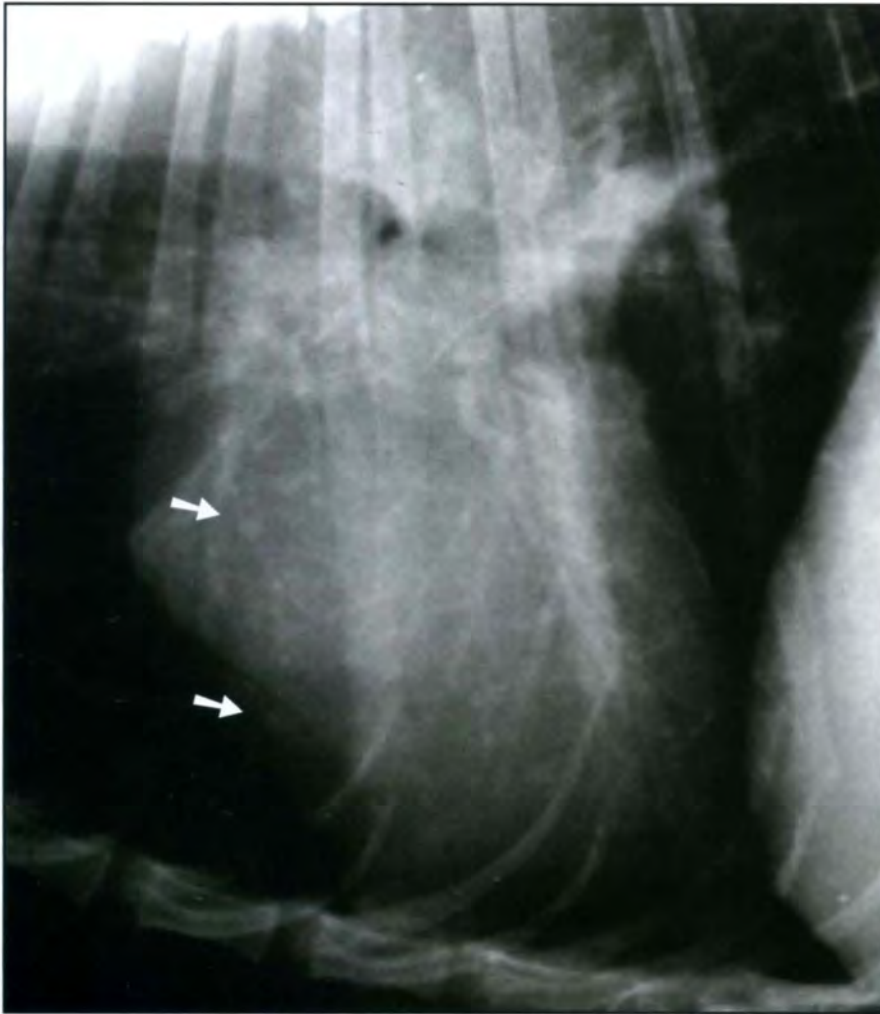
Granulomas:

- Nodules/confluent nodules/amorphous masses (see Figure 12.33).
- Poorly defined margins when active, more sharply margined when resolving.
- Often in association with hilar and/or mediastinal lymphadenopathy (Figure 12.46) and with a bronchointerstitial pulmonary pattern.
- May become cavitated (most common in *Paragonimus* fluke infection).
- May become mineralized (especially histoplasmosis granulomas) (see Figure 12.33).

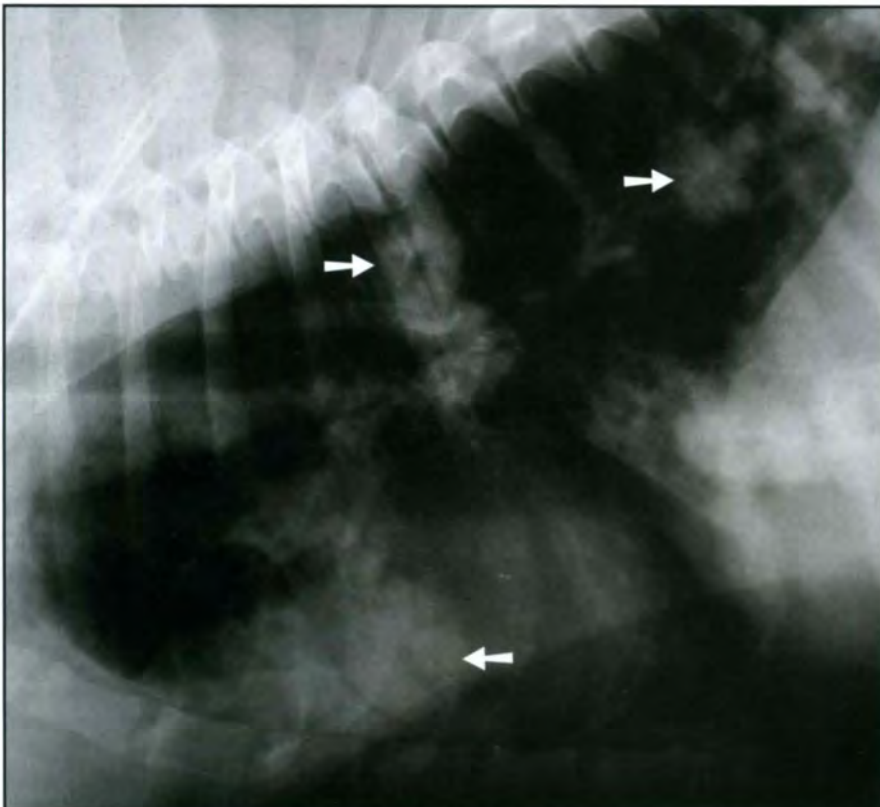
Foreign body granulomas differ from other granulomas in that there is an absence of hilar lymphadenopathy, and they are usually solitary and larger than most other granulomas. They may develop into an abscess, if secondarily infected.

Pulmonary infiltration with eosinophilia (PIE) can manifest with single or multiple pulmonary nodule(s)/mass(es) (also known as eosinophilic granulomas), varying in size from 2 to over 10 cm, in addition to more commonly seen peribronchial changes. Tracheobronchial lymphadenopathy is not a consistent feature of this disorder (Figure 12.47).

Haematomas: While pulmonary haemorrhage often presents as patchy areas of interstitial or alveolar disease, a haematoma may also appear as a round to oval, well circumscribed soft tissue opacity, and may contain air. A haematoma is typically associated with lung contusions and pneumothorax, and is suspected based on a history of trauma. It can be differentiated from other masses with follow-up radiographs, which show a decrease in its size within several days.



12.46 Ventral close-up of a lateral thoracic radiograph of a 3-year-old mixed breed dog with granulomatous fungal pneumonia. There are multiple small soft tissue nodules throughout the lungs (arrowed). There is also hilar lymphadenopathy, evident by the increased opacity dorsal to the heart base.



12.47 Lateral thoracic radiograph of a 6-year-old Rottweiler with pulmonary infiltration and eosinophilia. There is increased lung opacity with a mixed pattern of bronchial and alveolar disease. Note the nodular component (arrowed) caused by the formation of granulomas.



12.48 Close-up of a lateral oesophagram of a 14-year-old Boxer with a perihilar mass. Barium outlines the oesophageal mucosa cranial and caudal to the mass with a normal pattern (bolus at the gastro-oesophageal sphincter and position), making an oesophageal lesion unlikely. Final diagnosis was bronchial adenocarcinoma. (Courtesy of the University of Pennsylvania)



12.49 Close-up of a bronchogram of the left lung of an 8-year-old English Springer Spaniel with bronchial adenocarcinoma arising from the left mainstem bronchus. Survey radiographs showed a hilar soft tissue mass. The contrast study demonstrates the central filling defect resulting from the mass and residual patency, allowing filling of peripheral bronchi with contrast medium. Bronchography has been superseded by bronchoscopy and CT. (Courtesy of the University of Pennsylvania)

Neoplasia:

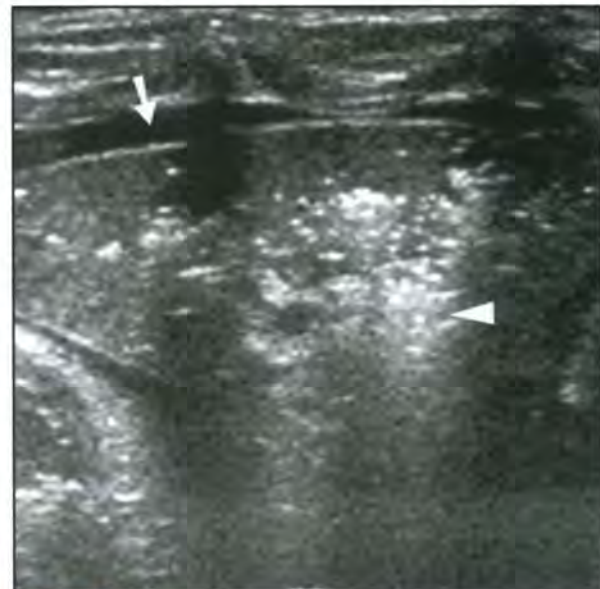
- Typically appears as a round, hypoechoic mass but can have a variable appearance, depending on the presence of central necrosis, cavitations and trapped gas (Figure 12.50).
- The deep margin of the mass is often smooth, in contrast with inflammatory lesions.
- It usually arises in the interstitium and displaces the surrounding lung tissue. As a result, no fluid-filled bronchi or normal branching vessels are seen within the mass. Inflammatory and infiltrative lesions may show fluid bronchograms and encroached vessels.
- A sterile abscess as a complication of tumour necrosis is indistinguishable from a septic abscess.

Contrast studies: These are not often indicated. An oesophagram (Figure 12.48) can be helpful in differentiating a pulmonary mass from an oesophageal lesion or a hiatal hernia. Bronchography (Figure 12.49) can outline a mass effect, lobar location and relation of a mass to the bronchial system. Bronchography has been superseded by less invasive techniques (e.g. computed tomography, CT).

Ultrasonography

A pulmonary mass is typically identified on thoracic radiographs. If there is not much aerated lung present between the mass and the thoracic wall, thoracic ultrasonography may be helpful to:

- Confirm pulmonary origin of an intrathoracic mass
- Differentiate between a soft tissue and a fluid-filled lesion
- Perform ultrasound-guided fine-needle aspiration for cytology.



12.50 Ultrasonographic thoracic linear transducer image of a 5-year-old Domestic Shorthair cat with a primary lung tumour. The affected lung lobe has lost its normal reflectivity and appears with the echogenicity of soft tissue. Residual amounts of trapped air are hyperechoic and cause dirty shadowing distally (arrowhead). Note also the small amount of anechoic pleural effusion (arrowed).

Abscesses:

- An abscess usually appears as a mass with a cavitated centre and thick walls with irregular internal margins (Figure 12.51).
- Contents may be anechoic, hypoechoic or echogenic, and often move with gravity to the dependent side. Internal septations are possible.
- May contain gas, in addition to the fluid, indicating communication with a bronchus or anaerobic infection.
- When an abscess is suspected, an underlying foreign body should be considered. Most foreign bodies will create a clean acoustic shadow within the mass.

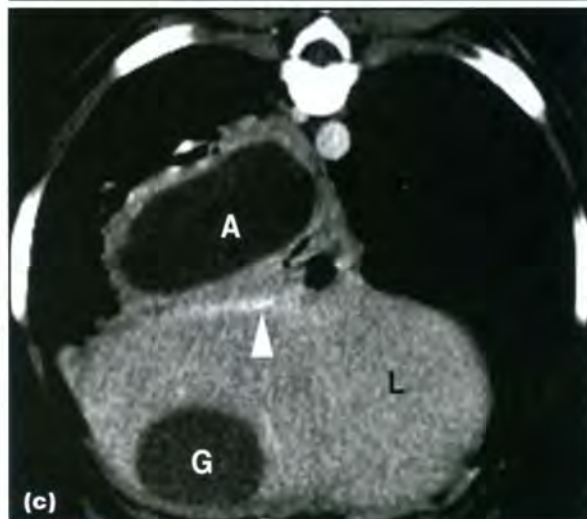
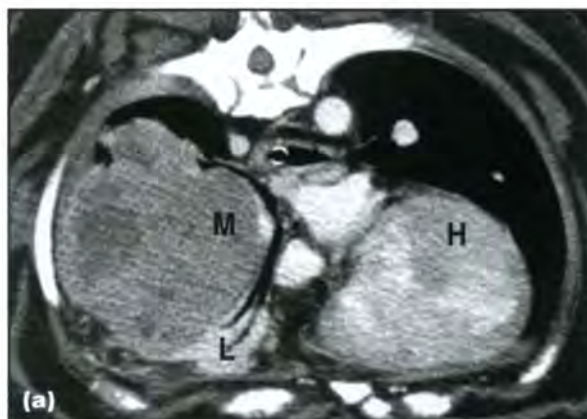


12.51 Ultrasonographic thoracic curvilinear transducer image of a 2-year-old Weimaraner with a lung abscess. Adjacent to the pleural lung margin, there is a round mass with a thick echoic capsule with irregular internal margins and a hypoechoic core. The hyperechoic area around the mass represents normal aerated lung.

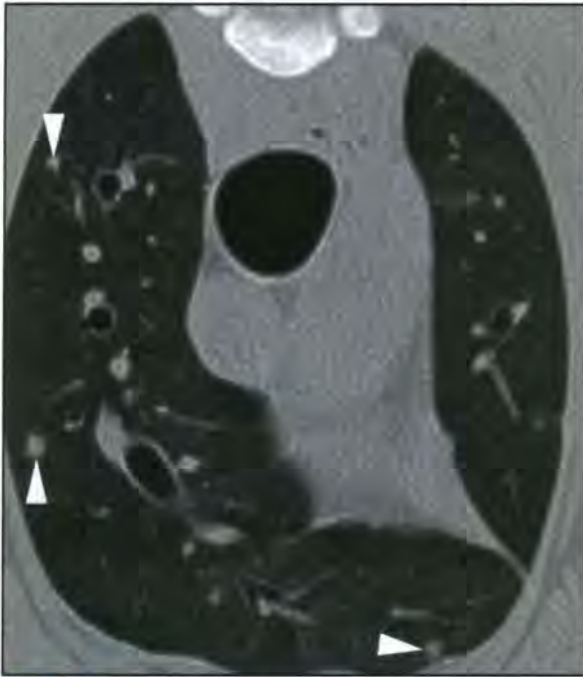
Computed tomography

CT is very helpful to confirm the pulmonary origin of a mass seen on radiographs and to determine accurately its extension and any involvement of the surrounding structures, especially when surgical resection is considered (see Figures 12.38b, 12.52 and 12.53). CT may be able to confirm the presence of a solid mass lesion which is not clearly evident on radiographs due to the superimposition of an adjacent alveolar infiltrate (representing secondary oedema, inflammation or tumour extension) on the mass. CT enables detection of smaller nodules than those identified radiographically and may reveal additional lesions, such as metastatic disease and lymphadenopathy.

CT can be very helpful to obtain a guided aspirate of a lesion, when the presence of aerated lung peripheral to the lesion prevents an ultrasound-guided biopsy (see Figure 3.7, p. 69). Pneumothorax and haemorrhage are common complications of this procedure, but they are rarely clinically evident or significant.



12.52 (a) Post-contrast CT image at a level immediately caudal to the carina of a 7-year-old Bulldog with a primary pulmonary carcinoma. A large soft tissue attenuating mass (M) is displacing the heart (H) and major vessels towards the left, and deviating and compressing the right middle lung lobe (L) and its bronchus. There is heterogenous mild enhancement of the mass with rim enhancement, and strong enhancement of the collapsed lung. (b) Ventrally viewed 3D reconstruction with the air-filled spaces in white. A large void in the right lung corresponds to the tumour and atelectatic lung tissue. (c) Post-contrast CT image of the caudal thorax of a 2-year-old English Cocker Spaniel with a lung abscess. There is a hypoattenuating mass in the right caudal lung lobe (A), with a thick, mildly enhancing capsule. The liver (L) and hypoattenuating gallbladder (G) are seen ventrally. Note the complete flattening of the contrast-enhanced caudal vena cava (arrowhead) due to compression by the mass.



12.53 High-resolution thoracic CT image at the level of the aortic arch of the same dog as in Figure 12.46 with granulomatous pneumonia. Note the soft tissue attenuating nodules in the peripheral lung (arrowheads). These can be differentiated from vessels by their larger size in the peripheral lung, and by evaluating contiguous images (vessels can be followed cranially and caudally).

Magnetic resonance imaging

Very few publications describe lung mass magnetic resonance imaging (MRI) in veterinary medicine. In human medicine, breath-hold techniques enable lung nodules of 5 mm to be detected. A three-dimensional (3D) gradient echo sequence with cardiac and respiratory gating is preferred for imaging lung parenchyma to minimize phase artefacts from cardiac motion (see Figure 4.4a, p. 73).

Metastatic lung disease

Radiography is the screening tool for metastatic lung disease in cases of known or suspected primary neoplasia anywhere in the body. Since radiography is such a simple, fast, non-invasive and inexpensive test, even screening of patients with a relatively low risk of neoplasia is still useful if other complex, time-consuming, invasive and expensive diagnostic tests or interventions are anticipated. Most pulmonary metastases manifest as lung nodules. These need to be differentiated from benign nodular lesions (granulomatous, incidental osteomas) and end-on vessels (see Nodular interstitial lung pattern and Solid pulmonary masses).

Radiography

Thoracic radiography has a relatively low sensitivity to pulmonary metastases. A pulmonary soft tissue nodule must be 3–5 mm in size to be visible. Nodules smaller than this may be visible if multiple nodules summate with each other, or if the nodule is mineralized. Pulmonary metastases rarely mineralize; however, a clearly visible nodule smaller than 3–5 mm is most

likely to represent an end-on vessel or an incidental mineralized nodule (heterotopic bone, granuloma).

Nodules are more detectable if surrounded by well inflated lucent lung, with maximal contrast between the lesion and the normal lung. Inspiratory, opposite lateral views are therefore essential, since on each view the lung on the dependent side is incompletely inflated, and metastases in that lung could be missed. It is not uncommon that nodules identified on one or both lateral films are not visible on VD/DV views. If a nodule is visible only on one view, this should not lead to dismissal of a lesion.

When a nodule is identified superimposed on the lung fields, an extrapulmonary location, such as the skin (mass, nipple, tick) or mediastinum, should be ruled out by evaluating an orthogonal view and by careful examination of the body wall of the patient. An extrapulmonary location should be suspected if a nodule or mass appears very opaque for its size. This is due to the increased contrast provided by the surrounding air outside the body. While identification of a nodule on two orthogonal views confirms the intrapulmonary location of a lesion with a high degree of certainty, it is often impossible to visualize a nodule on both views, even if real.

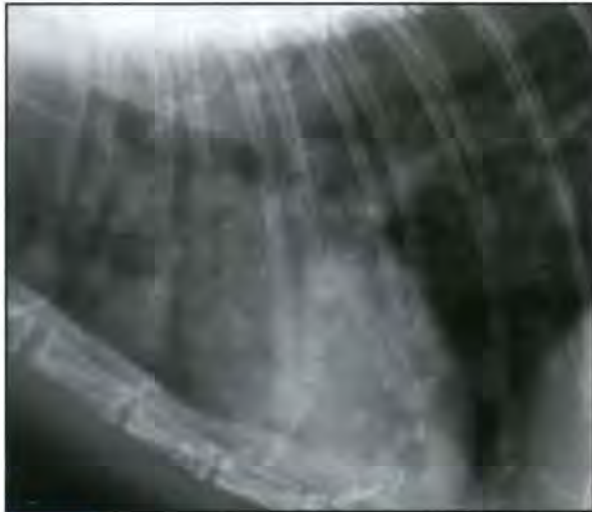
The most characteristic radiographic appearance of pulmonary metastatic disease is the presence of well defined soft tissue opacity nodules of variable size throughout the lung fields (see Figures 12.31 and 12.54).



12.54 Lateral thoracic radiograph of a 4-year-old Rottweiler with metastatic pulmonary disease from an unidentified primary neoplasia. Note the numerous, round, relatively well marginated nodules, with soft tissue opacity of variable size throughout the lungs.

Other manifestations of metastatic lung disease include:

- Ill defined nodules (particularly in cats) (Figure 12.55)
- Unstructured interstitial lung pattern (see Figure 12.34)
- Lung consolidation (coalescing nodules, infiltrative lesions) (see Figure 12.31)
- Miliary nodular pattern (a large number of small metastases of 2–3 mm in diameter spread throughout the lungs) (see Figure 12.32).



12.55 Close-up of a lateral thoracic radiograph of a 12-year-old Domestic Longhair cat with metastatic pulmonary neoplasia. Compared with the dog in Figure 12.54, the nodules are ill defined and not round. This is a relatively common appearance of metastatic nodules in cats.

Mesenchymal tumours, which spread primarily via the blood, tend to produce a low number of well defined metastases; whilst epithelial tumours, which spread primarily via the lymphatic system, often produce a large number of relatively small, ill defined nodules. However, this is only a general rule.

Radiographic patterns have been described for several tumour types:

- Haemangiosarcoma: most commonly, poorly defined small coalescing nodules (Figure 12.56). Less commonly, well circumscribed nodules or an alveolar infiltrate secondary to haemorrhage may be seen



12.56 Caudodorsal close-up of a lateral thoracic radiograph of a 10-year-old Papillon with pulmonary metastases from a splenic haemangiosarcoma. There are multiple poorly defined small coalescing nodules spread throughout the lungs.

- Transitional cell carcinoma: most commonly, diffuse interstitial pattern or nodular interstitial pattern
- Mammary gland neoplasia in dogs: well defined nodules/ill defined nodules/miliary nodules. Pulmonary alveolar septal metastases is a rare form of mammary tumour metastases described in dogs; the lungs are diffusely infiltrated by carcinoma, predominantly in the arteries and small capillaries of the alveolar septa. It results in a wide range of radiographic manifestations, but most commonly an unstructured interstitial pattern
- Mammary gland neoplasia in cats: ill defined nodules/diffuse pulmonary pattern; less commonly, well defined nodules.

Contrast studies are not indicated.

Ultrasonography

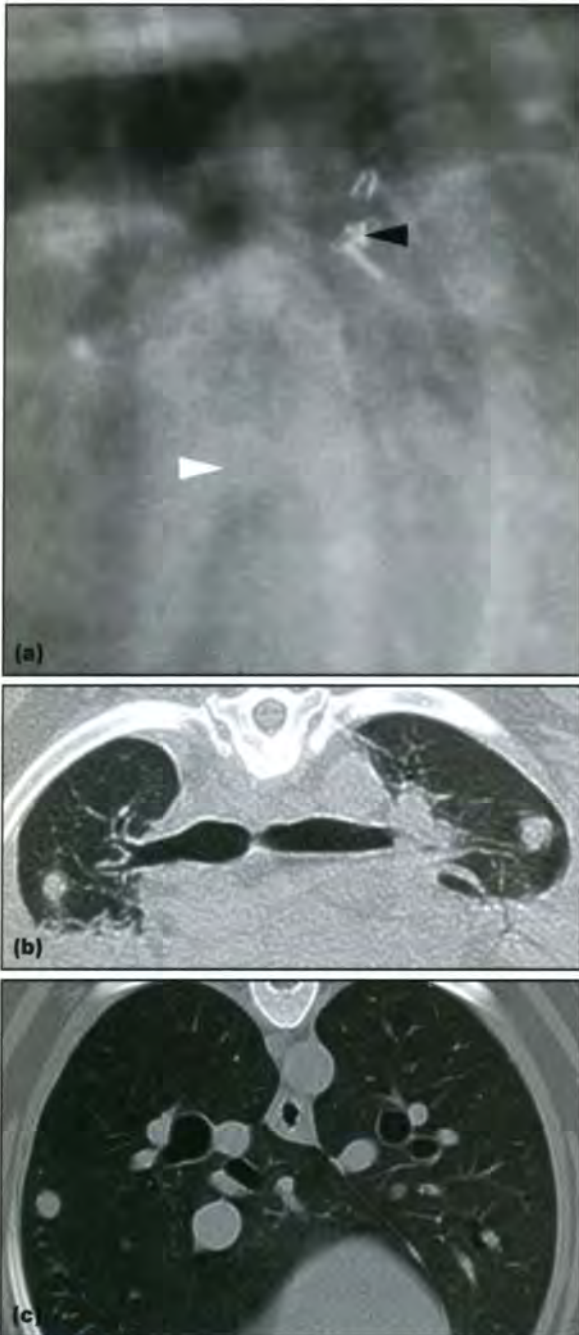
Similar to the findings described for pulmonary masses. It may be possible to image a peripheral metastatic nodule (Figure 12.57) and obtain an ultrasound-guided aspirate of the lesion.



12.57 Ultrasonographic thoracic curvilinear transducer image of a 9-year-old Boxer with a neuroendocrine heart base tumour and metastatic pulmonary disease. The peripheral metastatic nodule is round and hypoechoic with a small hyperechoic core, and smooth margins surrounded by hyperechoic aerated lung

Computed tomography

CT is the preferred imaging modality for pulmonary metastases in human medicine. It is more sensitive than radiography for the identification of pulmonary metastatic neoplasia. Nodules 3–6 mm in size may be seen with standard techniques, and those as small as 1–2 mm can be seen with high-resolution CT techniques (Figure 12.58; see also Figure 3.3, p. 67). CT also identifies a large number of nodules not seen with radiography.



12.58 (a) Central close-up of a right lateral thoracic radiograph of a 9-year-old mixed breed dog taken 3 months after removal of the right middle lung lobe with a pulmonary carcinoma. Notice the surgical staples (black arrowhead) and a faintly visible nodular opacity (white arrowhead). The opposite lateral film was unremarkable. (b) High-resolution thoracic CT image at the level of the tracheal bifurcation. There is a soft tissue nodule in each cranial lung lobe (6 mm right, 9 mm left diameter) and ventral recumbency-related atelectasis. (c) High-resolution thoracic CT image at the level of the accessory lung lobe of a 7-year-old mixed breed dog with anal sac adenocarcinoma and pulmonary metastases. Multiple nodules, 1–4 mm in size, are visible throughout the lungs. Nodules in the lung periphery are easily identified whereas more central lesions must be distinguished from normal lung vessels with slice-by-slice comparison. Such nodules appear similar to granulomatous soft tissue nodules (see Figure 12.53) and must be evaluated in conjunction with the clinical history and disease progression.

Ditzels – little things that *may* matter

The ability to visualize very small, previously unseen, lung lesions with CT poses new challenges for interpretation and prognosis. Such 1–2 mm, commonly seen, small nodules of unknown significance are called *ditzels* (presumably derived from 'ditzzy', indicating their confusing effect on the reader). There is a large variation in potential for malignancy in such lesions, and there is currently no reliable way to determine malignancy non-invasively and instantaneously.

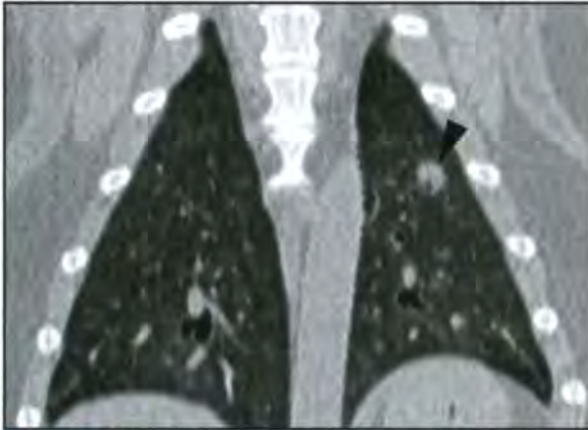
Procedural recommendations for ditzels include:

- Small mineralized lesions are unlikely to be metastatic neoplasia (Figure 12.59)
- Granulomatous lesions should be considered in patients living in areas where fungal diseases are endemic (see Figure 12.52)
- Primary disease and likelihood of neoplastic nodular metastasis should be considered (see Figures 12.58 and 12.60)
- Occult primary neoplasia elsewhere in the body should be searched for
- Follow-up CT should be performed to monitor progression of the lesion.

Metastases are more commonly located in the peripheral lung, in a subpleural location, making these lesions more difficult to detect radiographically, but easier to distinguish from vessels on a CT image. Nodules can be distinguished from vessels by the fact that they are not continuous with a vascular structure on adjacent slices (see Figure 12.58c). CT is able to document unusual spread of metastatic disease, such as peribronchial infiltrate (Figure 12.61a), parenchymal bands of increased opacity, subpleural interstitial thickening, subpleural lines, irregular perfusion and ground-glass opacity (Figure 12.61b).



12.59 High-resolution thoracic CT image at the level just caudal to the carina of a 9-year-old Labrador Retriever with a nasal adenocarcinoma. There are numerous 1 mm mineralized ditzels throughout the lungs. These are incidental osteomas and not neoplastic metastases. Nasal neoplasia rarely metastasizes to the lungs, and pulmonary metastases only very rarely mineralize.



12.60 Dorsal plane reconstruction of a high-resolution thoracic CT image of a 13-year-old West Highland White Terrier with idiopathic pulmonary fibrosis. There is a 4 mm soft tissue nodule, including a lucent bronchus, in the cranial aspect of the left lung (arrowhead). The fact that this nodule encroaches a bronchus makes it an unlikely candidate for metastasis. A follow-up investigation showed no progression of the lesion.



12.61 (a) High-resolution thoracic CT image at the level of the accessory lung lobe of an 11-year-old Bichon Frisé with an anaplastic carcinoma in its left cranial lung lobe, causing complete consolidation of that lobe (L) and deviation of the heart (H). There is distinct bronchial wall thickening in the left caudal lung lobe (compared with the right). Subsequent investigation confirmed a neoplastic peribronchial infiltrate. (b) Close-up of a CT image at the level of the accessory lung lobe of an 11-year-old Cairn Terrier with adrenal carcinoma and pulmonary carcinosis, with widespread infarction of pulmonary capillaries and tributary lung tissue. Notice the multiple, small, wedge-shaped, subpleural lesions with pleural retraction and ill defined parenchymal lesions consistent with infarct, and ventral areas of non-specific ground-glass opacity.

Scintigraphy

This is uncommonly used to identify metastatic lung disease and has not been shown to offer additional benefits, compared with radiography. It is a very useful technique to detect metastatic bone disease, secondary to pulmonary or other neoplasia.

Gas- or fluid-containing pulmonary lesions

Bullae and blebs

Bullae are gross air accumulations within the lung parenchyma formed by the loss or breakdown of the alveolar walls. Bullae may also be known as pneumatoceles, and the two terms may be used interchangeably. Some authors and medical texts consider pneumatocele a specific term for a large pulmonary bulla. The bulla wall is created by connective lung tissue and visceral pleura, and this defines the bulla type (Figure 12.62). Pulmonary bullae can also be classified according to their origin as:

- Congenital bullae: see Congenital lobar emphysema
- Traumatic bullae: the result of blunt thoracic trauma, causing a sudden rise in intrathoracic pressure. Air cannot be exhaled due to reflexive epiglottic closure (diving reflex), leading to lung laceration. Chronic lung diseases with frequent coughing can also weaken pulmonary parenchyma and lead to lung laceration
- Idiopathic bullae: found in combination with spontaneous pneumothorax, without known cause of gas accumulation.

Blebs are intrapleural gas accumulations, which arise when air escapes the pulmonary parenchyma and gets trapped between the visceral and parietal layers of the pleura (Figure 12.63):

- Often located at the lung apices
- Usually a sequel to parenchymal bullous disease of any origin
- More difficult to detect radiographically
- More prone to rupture and to create a pneumothorax.

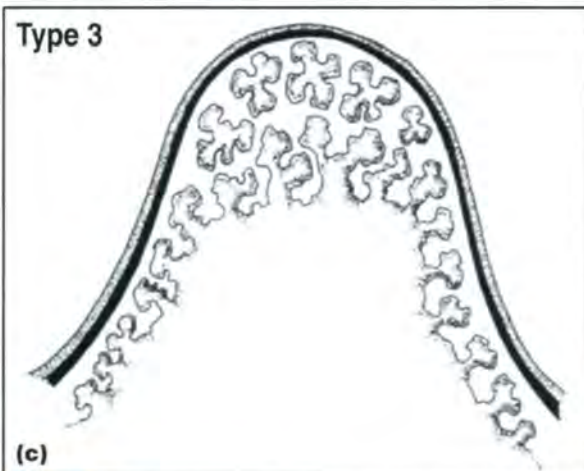
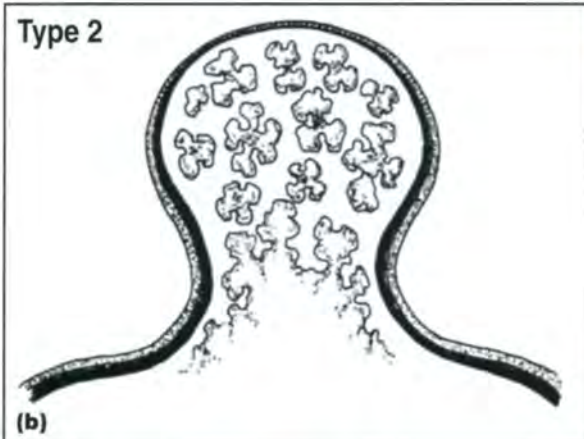
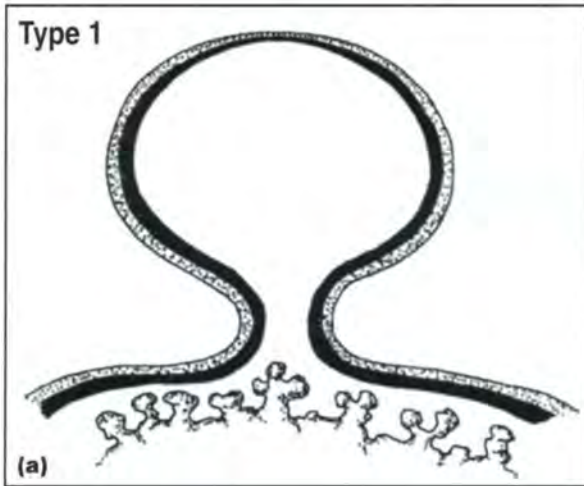
Cysts

Pulmonary cystic lesions are fluid- or air-filled lesions surrounded by a thin wall of respiratory epithelium. The histological composition of the cyst wall determines the cyst type:

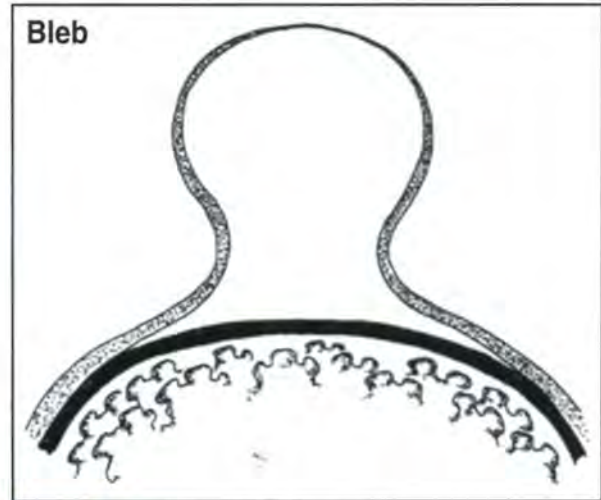
- *Pulmonary cysts* are formed from alveolar epithelium with no remnant of a bronchial wall on histopathology
- *Bronchogenic cysts* are dilated bronchioles or bronchi which have a bronchial wall remnant on histopathology.

Cavitating lung lesions

These are defined as soft tissue masses with a fluid- or gas-filled centre. They may develop from an apparently solid nodule or mass, as the centre



12.62 Different types of pulmonary bullae. The internal and external layers of the visceral pleura (marked as black and grey, respectively) are not dissected by bullae but can be herniated in different ways. **(a)** A *type 1 bulla* is a round gas accumulation within the herniated visceral pleura, with a small isthmus to the pulmonary parenchyma. They are usually found at the lung apices. These bullae macroscopically resemble blebs, except that blebs are usually not spherical. **(b)** A *type 2 bulla* arises from subpleural parenchyma and contains emphysematous lung tissue, connected to the pulmonary parenchyma with a wider neck. **(c)** A *type 3 bulla* is usually a large gas pocket with or without emphysematous lung tissue deep in the pulmonary parenchyma, with possibly a more broad-based deviation of the visceral pleura. (Reproduced from Lipscomb VJ *et al.* (2003) with permission from the *Journal of the American Animal Hospital Association*)



12.63 Pulmonary bleb. The internal and external layers of the visceral pleura (marked as black and grey, respectively) are dissected by a gas pocket that has escaped from the pulmonary parenchyma. (Reproduced from Lipscomb VJ *et al.* (2003) with permission from the *Journal of the American Animal Hospital Association*)

of the solid structure can liquefy due to a necrotic process. On occasions, a neoplasm may grow around a bronchus thus incorporating the bronchus into the mass; therefore, it is important to distinguish air within a bronchus within a mass from a cavitating lung lesion. Cavitating lung lesions are rare in cats and occur more commonly in dogs. The clinical signs vary with the underlying disease.

Radiography

Gas-filled pulmonary lesions: Gas-filled pulmonary lesions (i.e. blebs and bullae) are best visualized if surrounded by opaque lung tissue, which is best achieved with:

- An expiratory phase radiograph
- The dependent-side lung on laterally recumbent radiographs (both lateral films should be obtained).

Pneumothorax and bullae/blebs

A search for pulmonary bullae/blebs is a common procedure to identify the cause of a pneumothorax. Pneumothorax can hinder or promote visibility of a bulla, depending on the amount of free air, degree of collapse and location of the bulla. Pre- and post-thoracocentesis radiographs are recommended. CT is the modality of choice for the detection of leaking bullous lesions in pneumothorax.

Ruptured bullae/blebs have a tendency to collapse. Identified bullae/blebs are suggestive of the general cause of the pneumothorax (ruptured lung tissue) but the leaking collapsed bullae/blebs may not be visible.

Superficial blebs are more prone to rupture than deep parenchymal bullae. This should be weighted in the decision-making for conservative/surgical treatment of pneumothorax. It may not be safe to release a patient with a large bleb, despite successful drainage of the pneumothorax.

Typical radiographic features of bullae/blebs are:

- Radiolucent structure with an absent or barely perceptible wall (Figure 12.64a)
- Bullae are usually round and within the lung parenchyma
- Blebs are often ovoid and always peripheral (Figure 12.64b).

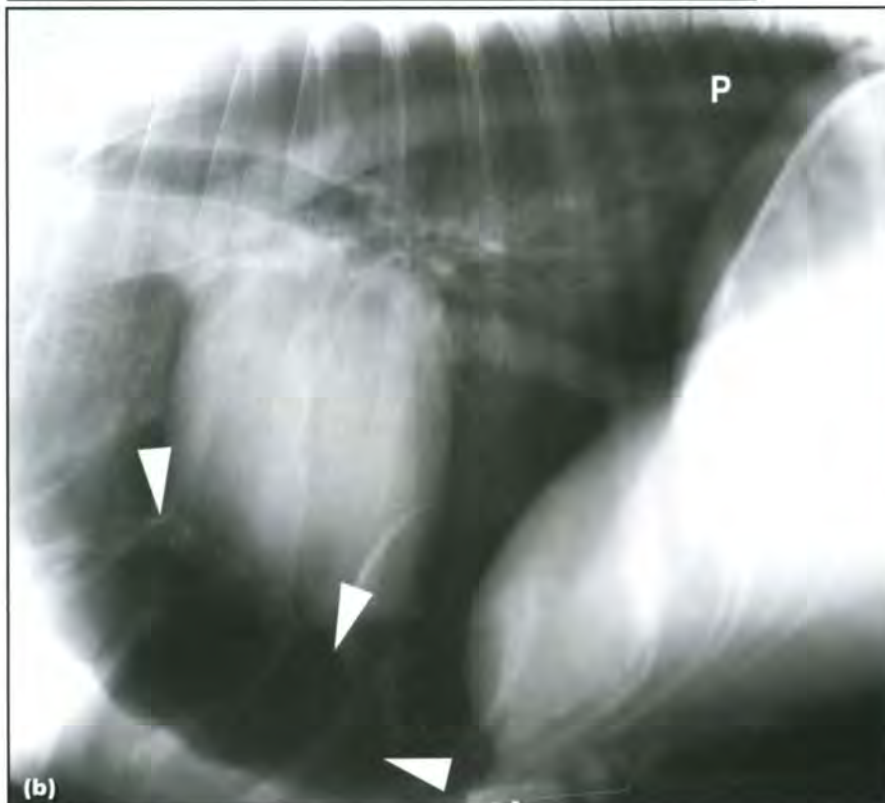
Secondarily infected or haemorrhagic bullae may appear as circular soft tissue opacities with areas of hyperlucency, and may mimic cavitating lung lesions or soft tissue masses (Figure 12.65). Horizontal beam radiography can help in outlining a fluid line in cysts or infected bullae.

Fluid-filled pulmonary lesions:

- Similar opacity to solid masses, hence difficult to differentiate.
- Fluid-filled cysts are often ovoid (see Figure 12.65); metastatic lung nodules are usually round.
- Follow-up radiographs may show reduction in size and/or gas accumulation (fluid drainage) and help differentiate fluid-filled pulmonary lesions from solid masses (equal or increased size).



12.64 (a) Close-up of a lateral thoracic radiograph of a 10-year-old Labrador Retriever. Notice the round radiolucency surrounded by a thin radiopaque wall (arrowed), superimposed on the cardiac silhouette. This bulla was an incidental finding. (b) Lateral thoracic radiograph of a 4-year-old Doberman with spontaneous pneumothorax. Notice the large amount of free pleural gas (P) and a large ovoid gas bubble contained by a thin soft tissue rim (arrowheads) in the cranioventral lung periphery, consistent with a bleb.

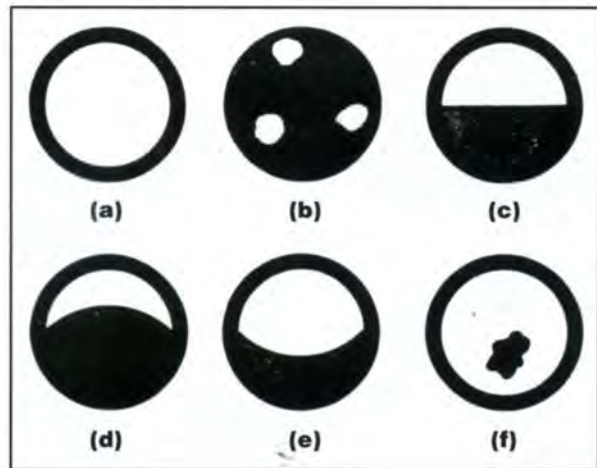




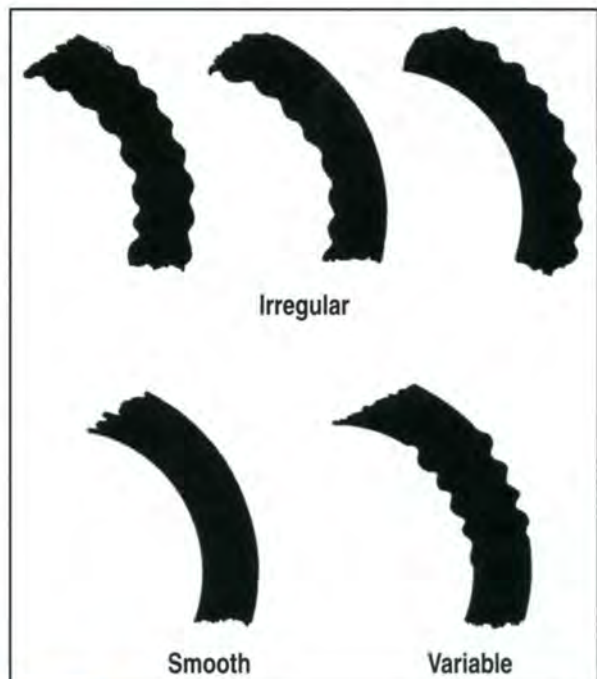
12.65 (a) Close-up of a lateral thoracic radiograph (vertical beam) of a dog that was involved in a road traffic accident 24 hours previously. A sternal luxation, pneumothorax and multiple ovoid pulmonary soft tissue masses (arrowheads) can be identified, which could be related to the trauma or an unrelated illness. (b) Close-up of the non-dependent hemithorax of a VD thoracic radiograph obtained with a horizontal beam. Beside the serial rib fractures (arrowheads) and free pleural gas (P) in the most elevated part of the thorax, two of the previously seen masses (M) are also visible with a straight fluid-gas interface and a thin smoothly outlined wall. These findings are most consistent with blood-filled bullae, haematocoeles.

Pulmonary lesions containing fluid and gas:

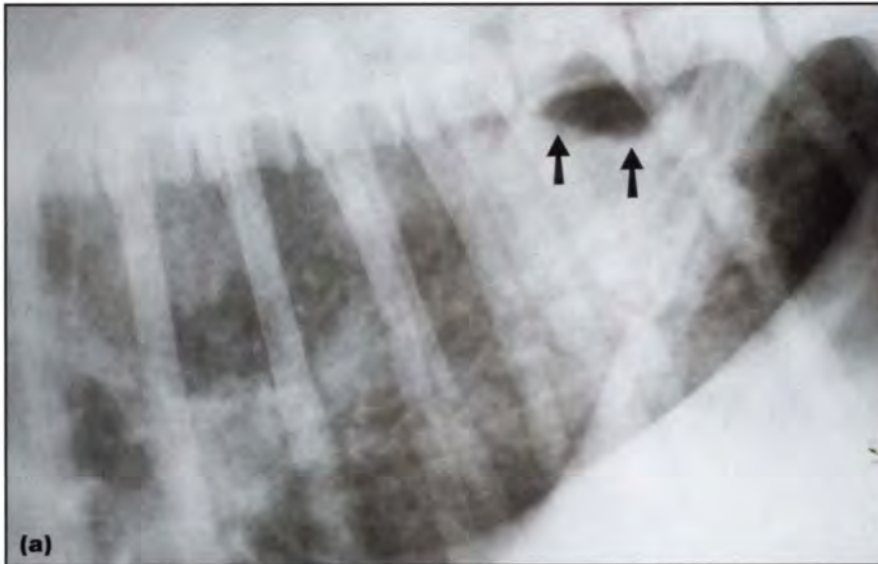
- Assessment of the location, number, size and shape of the gas lucency allows further characterization of the lesion (Figures 12.66 and 12.67).
- Cavitated abscesses are most likely to have thick irregular walls (see Figure 12.45) and less likely to have thin and smooth walls (Figure 12.68a).
- Cavitated neoplasia may contain amorphously shaped air bubbles (Figure 12.68b).
- Cavitated parasitic granulomas are commonly seen with paragonimiasis (Figure 12.68c).



12.66 Typification of gas- and fluid-containing lung lesions, according to gas location and fluid-gas interface. In vertical beam radiography (a) one large central gas lucency is more likely to indicate a cyst, large abscess or bulla. (b) Several small, irregularly shaped and distributed gas lucencies are more suggestive of neoplasia, foreign bodies or gas-producing bacteria. In horizontal beam radiography (c) low-viscosity fluid tends to create a straight interface with gas, whereas (d and e) high-viscosity fluid tends to create a convex or concave margin. (f) Gas within solid lesions creates no interface. (Adapted and reproduced from Silverman S *et al.* (1976) with permission from the *Journal of the American Veterinary Radiological Society*)



12.67 Typification of gas-containing lung lesions, according to their wall characteristics. The wall can be regular or irregular, on either or both sides, or have a mixture of both. Smooth-walled lesions are most likely to be bullae or cysts; whereas, irregular margins are a result of tissue necrosis and infection, and are commonly seen with abscesses and neoplasms (cavitating lesions). In lesions that contain fluid and gas, these features can only be applied to horizontal beam radiographs. (Adapted and reproduced from Silverman S *et al.* (1976) with permission from the *Journal of the American Veterinary Radiological Society*)



12.68 (a) Standing lateral horizontal beam radiograph of the caudal thorax of a 4-year-old Great Dane. The dog presented with extreme dyspnoea and coughing. A cavitating lung abscess can be seen with a horizontal fluid line (arrowed) separating the fluid from the gas. There is a marked alveolar lung pattern with a diffuse increase in soft tissue opacity of the lung fields. (b) Close-up of a DV thoracic radiograph of an 11-year-old mixed breed dog with a chronic productive cough. The caudal part of the left cranial lung lobe has a marked increase in soft tissue opacity with retraction of the lobe edge from the thoracic wall (arrowed). There is an irregular-shaped radiolucent area eccentrically positioned within the lung lobe (arrowheads), which represents a cavitated centre. This was confirmed to be bronchogenic carcinoma with central necrosis. (c) Lateral thoracic radiograph of a 6-year-old Domestic Shorthair cat with *Paragonimus kellicotti* fluke infection. Notice the multiple pulmonary soft tissue nodules containing irregular small central air bubbles. This is a classic radiographic feature of paragonimiasis in dogs and cats.



Other imaging techniques

- CT is a more sensitive diagnostic imaging modality for the detection of bullae and blebs (Figure 12.69).
- Ultrasonography and CT are sensitive techniques to characterize fluid-filled lesions (see Figures 12.51 and 12.52).
- Ultrasonography can only be used for peripheral lung lesions but offers easy guidance for fine-needle aspiration of solid and fluid-filled lesions.
- CT is indicated for deeper lesions with the option of CT-guided fine-needle aspiration.



12.69 **(a)** High-resolution thoracic CT image at the level of the accessory lung lobe of a 16-year-old Standard Poodle with numerous pulmonary bullae (★) throughout the lungs. Slice-by-slice image analysis is necessary to rule out bronchiectasis. These relatively small bullae would be difficult to identify radiographically. The interpretation of relevance of such small lesions can only be made in light of the clinical history of the patient. There is ventral hypostatic lung collapse. **(b)** High-resolution thoracic CT image at the level of the aortic arch of an 8-year-old Golden Retriever with spontaneous left-sided pneumothorax (P). CT enabled identification of a leaking type 1 bulla (★) in the left cranial lung lobe. A thoracocentesis drain can be seen in cross section adjacent to the collapsed left lung.

Pulmonary emphysema

Pulmonary emphysema is characterized by an abnormal increase in the size of the alveolar air spaces due to destruction of the alveolar walls. It may be associated with bronchiolar obstruction with a valve mechanism (dynamic collapse):

- Inspired air enters the pulmonary parenchyma but is unable to escape even with forced expiration (air trapping)
- Increased expiratory intra-alveolar pressure leads to laceration of the alveolar walls and bulla formation.

It is usually confined to the lung periphery. Clinically manifesting lung emphysema is rare in dogs and cats. It is important not to confuse air trapping with forced inspiration or pneumothorax.

Congenital lobar emphysema

This is a rarely reported congenital bronchial cartilage abnormality or bronchial plug in puppies, leading to dynamic airway collapse and air trapping (see Figure 8.18b, p. 185). Usually only one lung or lobe is affected, but there may be tension collapse of other lobes. It has been reported in Shih Tzu, Jack Russell Terrier, Basset Hound and Pekingese puppies. Single bullous lesions without widespread emphysema can also be congenital in origin.

Acquired pulmonary emphysema

Obstructive bronchiolar disease (chronic bronchitis, feline asthma, bronchial neoplasia, bronchial foreign body) can lead to dynamic airway collapse and air trapping. Chronic compensatory hyperinflation has been reported to cause lobar emphysema. Mild changes are commonly seen in cats with asthma; marked changes are rarely seen in dogs or cats. Changes are usually bilateral.

Radiography

Radiographs should be taken on both full inspiration and expiration. Emphysema is confirmed if there is no difference between inspiration and expiration in the position of the diaphragm or pulmonary radiolucency. A horizontal beam DV/VD view can be useful, as the dependent lung lobe does not collapse with lobar emphysema.

Signs of pulmonary hyperinflation on expiratory films (Figures 12.70 and 12.71) include:

- Hyperlucent, enlarged lung fields
- Scant but visible vascular markings
- Caudally displaced, flattened diaphragm
- Transverse rib position
- Chronic rib fractures.

With lobar emphysema there may be:

- Mediastinal shift and compression of the unaffected lung lobes
- Herniation of the affected lung lobes into the contralateral hemithorax
- No collapse of the affected lung in the dependent position on the lateral film.



12.70 (a) Expiratory lateral thoracic radiograph of a cat with asthma. Notice the small size of the cardiovascular structures, generalized bronchial lung pattern, large bulla and multiple non-union rib fractures. (b) Caudodorsal close-up of the same radiograph reveals hyperlucent peripheral lung fields, consistent with air trapping and emphysema.



12.71 Lateral thoracic radiograph of a 5-month-old Australian Cattle Dog with a history of chronic bronchopneumonia. Notice the multiple distended tortuous bronchi and gas pockets throughout the lungs, consistent with bronchiectasis and bullous emphysema.

Other imaging techniques

- CT to detect small emphysematous lung areas (Figure 12.72).
- Ventilation/perfusion lung scintigraphy to establish V/Q mismatch.
- Pulmonary angiography to establish lack of regional vasculature.



12.72 High-resolution thoracic CT image at the level of the accessory lung lobe of a 16-year-old cat with chronic lower airway disease. There are multiple soft tissue septae throughout the lungs, consistent with fibrotic changes, and focal areas of pulmonary hyperlucency consistent with emphysema (*).

Lung lobe torsion

Lung lobe torsion is an uncommon condition in small animals, but it is potentially life-threatening and requires surgical intervention in most cases.

Rotation of a lung lobe occurs around its axis, usually close to the hilus or rarely also in the middle of a lobe:

- This leads to twisting and occlusion of the bronchovascular structures
- Venous return and lymphatic drainage from the lung lobe are compromised, whereas arterial supply is preserved initially to some degree due to the stronger muscular arterial walls
- This leads to venous congestion, pulmonary oedema, sequestration of blood within the twisted lung lobe and eventually lung lobe necrosis
- Blood and fluid enter the alveoli and distal bronchi.

Air can be trapped within the twisted lung lobe due to incomplete bronchial obstruction with a one-way valve effect. Pulmonary emphysema can develop as a consequence of increased alveolar pressure, alveolar or bronchial tears; pneumothorax or pneumo-mediastinum can result from bronchial tears.

Decreased lymphatic drainage, as well as increased interstitial and hydrostatic pressure within the affected lung lobe, leads to production of pleural effusion.

- The effusion initially presents as a transudate.
- It later becomes haemorrhagic or suppurative.
- Necrosis or fibrosis in the later stages of the disease lead to a decrease in lung lobe volume.

Large-breed dogs with deep and narrow chests, particularly Afghan hounds, are predisposed. Small chondrodystrophic dogs with round chests, such as Pugs, have also been described with spontaneous lung lobe torsion. Small dogs and cats are more commonly reported to have an underlying condition, leading to the lung lobe torsion.

Underlying diseases are characterized by collapse of a lung lobe, which is also suspended in either pleural fluid or air, leading to increased lung lobe mobility. Pleural effusion, pneumothorax, trauma with compression of the thoracic cavity and partial collapse of a lung lobe, but also pneumonia and surgical manipulation, are described as predisposing conditions.

The most commonly affected lung lobes are:

- Right middle lung lobe (most common in deep-chested dogs)
- Left cranial lung lobe, the entire lobe or the cranial part (most common in small, chondrodystrophic breeds).

All other lung lobes can be affected, and more than one lung lobe can be affected. Mid-lobar torsions are possible. Recurring lung lobe torsion has been described, but is unusual.

Radiography

Pleural effusion is a consistent finding in patients with lung lobe torsion. The pleural effusion can be:

- Bilaterally symmetrical
- Asymmetrical
- Unilateral and centred around the affected lung lobe (Figure 12.73).

In most cases pleural effusion is the consequence rather than the cause of the lung lobe torsion, and therefore it may be absent very early on in the disease process. However, this very early stage is rarely observed.

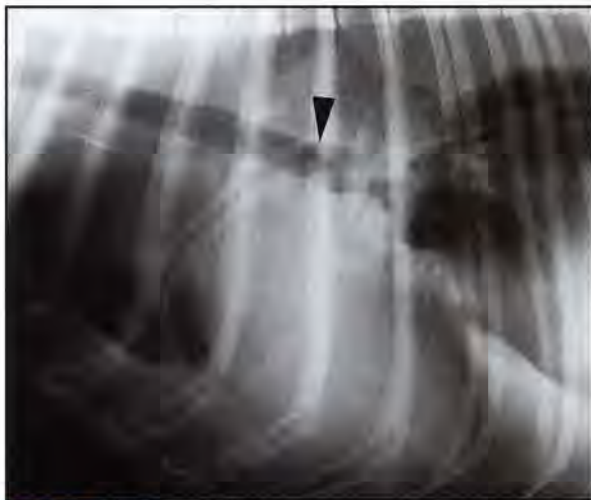
A mediastinal shift with displacement of the cardiac silhouette is sometimes present, usually away from the affected lung lobe, but can be towards a lung lobe with chronic torsion. The trachea can be dorsally deviated or have some degree of axial rotation at the level of the carina, caused by the abnormal position of the twisted lung lobe. This is best seen on a lateral radiograph (Figure 12.74).

Consolidation of the affected lung lobe is evident as an alveolar pattern with loss of visibility of the pulmonary vasculature; whereas, the unaffected lung lobes are relatively normal.

- The affected lobe is enlarged and has rounded borders due to congestion.
- Small air bronchograms or scattered gas lucencies throughout the affected lung lobe (air alveolograms, vesicular gas pattern) result in a foamy appearance of the lung.
- Gas bubbles can also be gathered in 'clusters' (Figure 12.75).



12.73 (a) VD thoracic radiograph of an 8-year-old Jack Russell Terrier with torsion of the right middle lung lobe. There is pleural effusion in the right cranial thorax, centred around the right middle and cranial lung lobes. The right middle lung lobe is rounded and contains some air with a vesicular pattern. The cardiac silhouette appears misshapen due to a previous pericardectomy. (b) Right lateral radiograph. There is increased lung opacity in the cranioventral thorax with air alveolograms cranially. The bronchus to the right middle lung lobe is very narrow close to the carina, and turns sharply cranially instead of caudoventrally (arrowheads), a sign consistent with lung lobe torsion.



12.74 Left lateral radiograph of a 6-year-old Borzoi with left cranial lung lobe torsion. There is moderate pleural effusion. The carina is axially rotated, resulting in dorsal displacement of the right cranial lobar bronchus (arrowhead); a bronchus to the left cranial lung lobe is not visible. The increased opacity dorsal to the carina represents the consolidated left cranial lung lobe.



12.75 DV thoracic radiograph of a 6-year-old Akita Inu with a left caudal lung lobe torsion. The left caudal lung lobe is enlarged, causing a mediastinal shift, and contains multiple small air bubbles (vesicular pattern).

Less commonly, the lung lobe is uniformly opacified without evidence of air bronchograms, as air bronchograms usually disappear after a few days, when the air is replaced by blood or fluid. In chronic cases there is a loss of volume in the twisted lung lobe.

The lobar bronchus to the affected lung lobe is visible only over a short distance and is blunted, narrowed or ends abruptly close to the carina.

- Air-filled bronchi running in an abnormal direction (inverted air bronchograms) indicate an abnormal position of a lung lobe (see Figure 12.73b).
- Vessels in an abnormal position are rarely observed due to the consolidation of the lung lobe.
- The adjacent aerated lung lobes are displaced towards the centre of the thorax, evident by a change in direction of the blood vessels and bronchi, as well as the pleural fissure lines.
- Rupture of a bronchus can lead to pneumomediastinum or pneumothorax.

The change in shape or orientation of the affected lung lobe is best seen after removal of the pleural fluid. In the presence of large amounts of pleural effusion, radiographs should be repeated after drainage of the pleural fluid. In addition, horizontal beam radiographs can provide valuable information by shifting the pleural fluid.

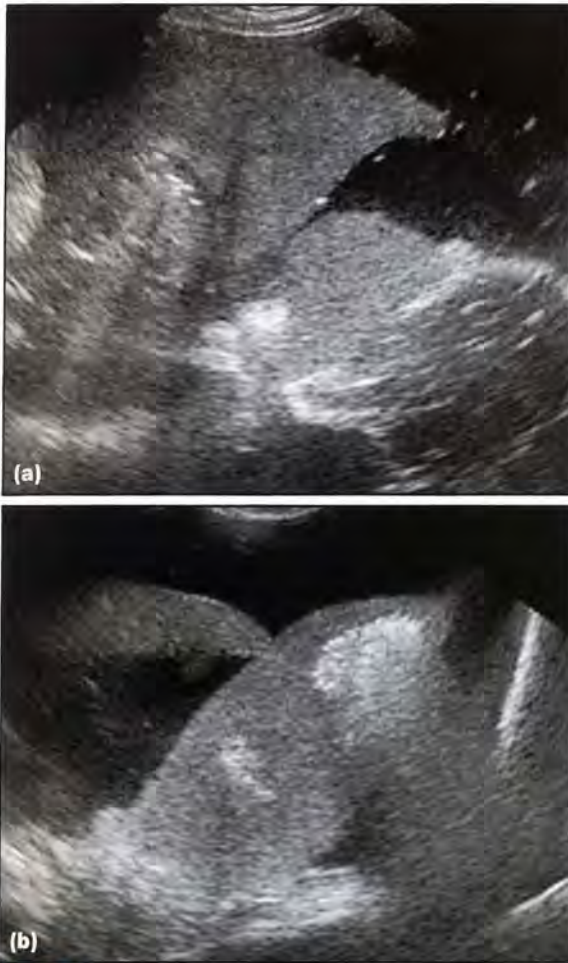
Contrast studies: Positive-contrast bronchograms using barium sulphate have been used to demonstrate the obstructed bronchus. This procedure has been superseded by other imaging modalities and is now obsolete (e.g. ultrasonography and CT).

Ultrasonography

This can be helpful in patients with inconclusive radiographic findings and may give additional information about the presence of a lung lobe torsion and/or underlying disease. Ultrasonography can be performed in the non-sedated patient in a standing position or in sternal recumbency, which is tolerated even by dyspnoeic patients.

Ultrasonographic findings include (Figure 12.76):

- Pleural effusion, particularly around the twisted and congested lung lobe. The pleural fluid can be anechoic to cellular, depending on the haemorrhagic component of the fluid
- Enlarged, consolidated lung lobe, which is either hypoechoic or isoechoic to parenchymatous tissues such as the liver ('hepatization') with rounded borders
- In chronic torsions, the lung lobe may be smaller and retracted towards the hilus
- Foci of gas trapped within the pulmonary parenchyma recognized as hyperechoic foci with reverberation artefacts. If a large amount of gas is trapped within the twisted lung lobe, the whole lobe is hyperechoic with many reverberation artefacts
- Linear hypoechoic structures without blood flow and with a hyperechoic wall, representing fluid-filled bronchi (fluid bronchograms)
- Abnormal course or shape of fluid bronchograms
- Abnormal position of the affected lung lobe, dorsal to the base of the heart, with the tip pointing up, or pointing cranially.



12.76 Thoracic curvilinear transducer ultrasound images of the same dog as in Figure 12.74. Left oblique (intercostal) view, craniodorsal is to the left. **(a)** There is marked anechoic pleural effusion and consolidation of both parts of the left cranial lung lobe with an abnormally dorsal location. **(b)** Slightly more caudal image showing the periphery of the twisted left cranial lung lobe. There are large pockets of trapped gas present within the lung lobe, seen as hyperechoic areas with distal reverberation artefacts.

Care should be taken to assess the thoracic cavity and especially the cranial mediastinum for associated problems, such as mediastinal lymphadenopathy or other mediastinal masses, which are obscured radiographically by the pleural effusion but may be an underlying problem, leading to the pleural effusion and consequent lung lobe torsion.

Doppler examination: Doppler (colour or power Doppler) examination can be very helpful to determine whether a consolidated lung lobe is twisted, or if it is filled with fluid or cellular infiltrates (pneumonia, neoplasia). In a lung lobe torsion, typical Doppler findings include:

- Absence of venous blood flow
- Absence of, or reduced, arterial blood flow.

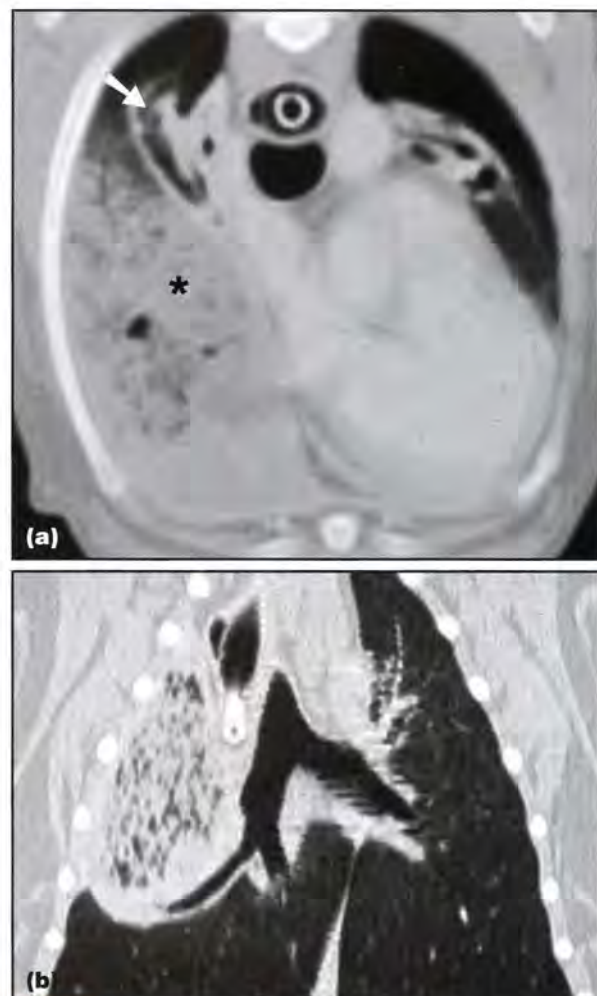
However, Doppler examination is hampered by artefacts produced by the motion of the lung lobe in the pleural effusion, due to the usually increased respiratory rate.

Computed tomography

This is the diagnostic method of choice, other than exploratory thoracotomy, for patients with unclear or inconclusive radiographic and ultrasonographic findings. It requires general anaesthesia, but is diagnostic in almost all cases of lung lobe torsion, and in addition allows screening for underlying diseases, such as lung or cranial mediastinal masses.

CT findings (Figure 12.77) are similar to radiographic findings; however, the position and patency of each bronchus can be better assessed:

- All bronchi should be followed from the carina into their respective lung lobes. This is best achieved on images reformatted in various planes, according to the position of the bronchus to be evaluated. The bronchus to a twisted lung lobe is blunted, ends abruptly or is narrowed considerably and changes its direction



12.77 **(a)** Thoracic CT image at the level of the aortic root of the same dog as in Figure 12.73. There is a mediastinal shift to the left and presence of free gas in the dorsal pleural spaces. The twisted right middle lung lobe is enlarged and partially consolidated with multiple gas pockets (*). The right cranial lung lobe is completely collapsed (arrowed) and dorsally displaced by the enlarged right middle lung lobe. **(b)** Dorsal plane reconstruction of a thoracic CT image at the level of the carina of a 2-year-old Pug with chronic torsion of the right cranial lung lobe. The right cranial lobar bronchus is tapering into the consolidated lobe with a vesicular pattern.

- In animals with chronic pleural effusion, it can be very difficult to differentiate a collapsed lung lobe from a twisted lung lobe, since both will have lost volume and collapsed lung lobes are also slightly dorsally rotated in the presence of large amounts of pleural effusion. It is helpful in these cases to scan the patient in dorsal and ventral or lateral recumbency to direct the pleural effusion away from the lung lobe. After ventilating the lungs for a few minutes, the lung lobe should be reassessed for degree of re-inflation, position and shape of the bronchus. Failure to inflate in the non-dependent position is a sign of lung lobe torsion or other bronchial obstruction
- An abnormal course of pulmonary vessels can also be seen; this is best visualized after intravenous administration of an iodinated contrast medium.

Lung herniation

Mediastinal lung herniation (a mediastinal shift caused by the lung) is commonly seen in dogs and cats with lung masses and unilateral hyperinflation or emphysematous changes. Affected lung lobes protrude into the contralateral hemithorax and deviate the mediastinal structures and heart away from midline. It is usually reversible if the increased lung volume can be reduced. In patients with lung removal or lobectomy or lung collapse, the remaining lung tissue will also occupy the vacant space in the contralateral hemithorax.

Cervical or thoracic wall herniation of the lung lobes is very rarely seen in dogs and cats. It can occur due

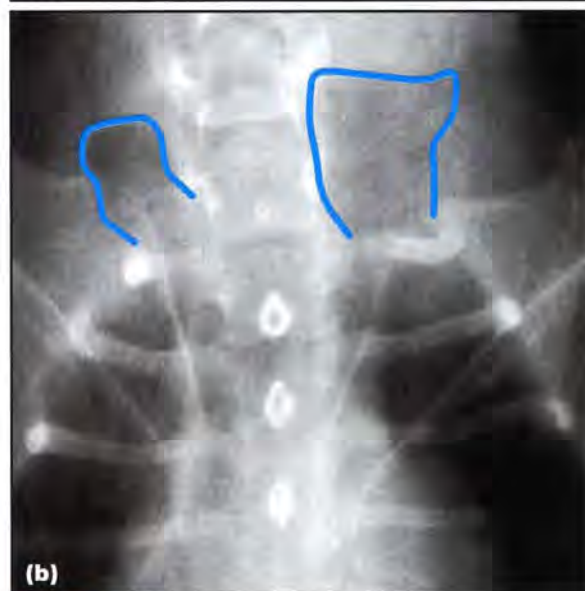
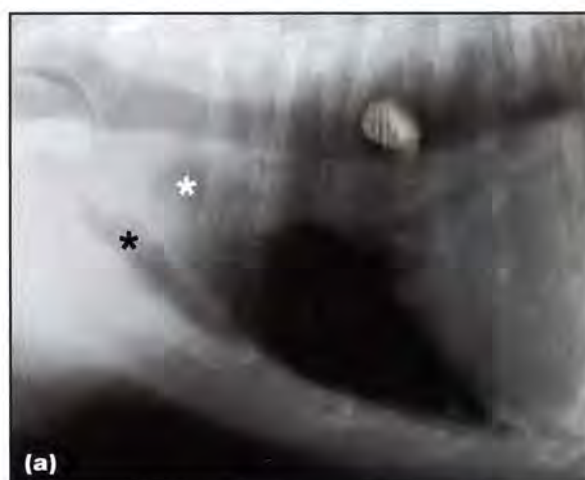
to interruption of the thoracic boundaries with sudden intrathoracic pressure changes, as a consequence of trauma and chronic coughing.

Imaging findings

- Mediastinal lung herniation (Figure 12.78): marked mediastinal shift with lung expansion into the contralateral hemithorax.
- Cervical or thoracic wall lung herniation (Figure 12.79):
 - Protrusion of a lung lobe outside the thoracic boundaries. Often dynamic appearance consistent with respiratory phase
 - Possible concurrent signs of thoracic trauma (e.g. rib fractures, pneumothorax).



12.78 High-resolution thoracic CT image at the level of the accessory lung lobe of an 11-year-old Domestic Shorthair cat with a primary lung lobe tumour, leading to bronchial obstruction and collapse of the left caudal lung lobe (L). The compensatory hyperinflation of the right lung leads to mediastinal herniation of the right caudal (R) and accessory (A) lung lobes into the left hemithorax.



12.79 (a) Expiratory lateral radiograph of a 9-year-old Yorkshire Terrier with intrathoracic tracheal collapse. There is mild narrowing of the intrathoracic trachea. Cranial to the thoracic inlet, there are two separated lung fields protruding into the caudal cervical area (*). Only the left cranial lung lobe normally protrudes cranial to the thoracic inlet, and usually not during expiration. (b) Expiratory VD fluoroscopic image of the thoracic inlet, demonstrating the cervical herniation of both cranial lobes (outlined). (continues)



12.79 (continued). **(c)** Inspiratory VD fluoroscopic view showing the cranial lung margins confined to the thoracic boundaries. This is cervical lung herniation, secondary to expiratory intrathoracic tracheal collapse and associated pressure changes.

Predominantly alveolar lung diseases and pneumonias

The term alveolar disease in this chapter is used for diseases in which an alveolar radiographic pattern is a predominant feature (see Alveolar lung pattern). Some types of pneumonia that do not produce a predominantly alveolar pattern are also included in this section.

Diagnosis of specific alveolar lung diseases is challenging because:

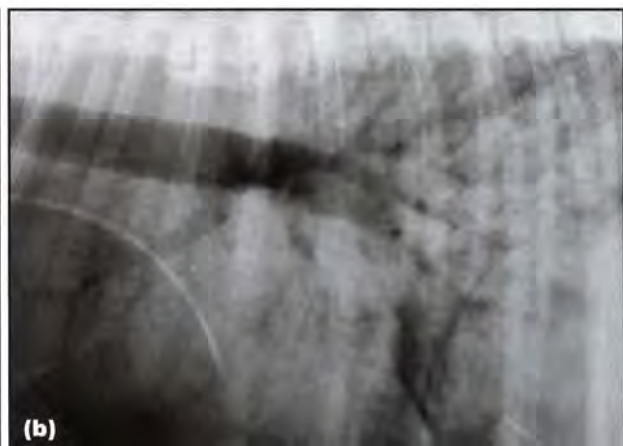
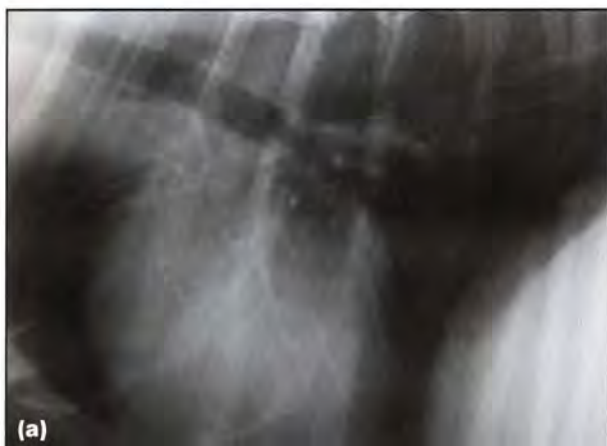
- Most alveolar diseases also affect other components of the lung, e.g. the interstitium and bronchi. Very few diseases affect only the alveolar spaces (e.g. pulmonary alveolar proteinosis)
- There is a wide overlap in radiographic changes seen with the different alveolar diseases.

A meaningful diagnostic approach to alveolar lung diseases therefore includes:

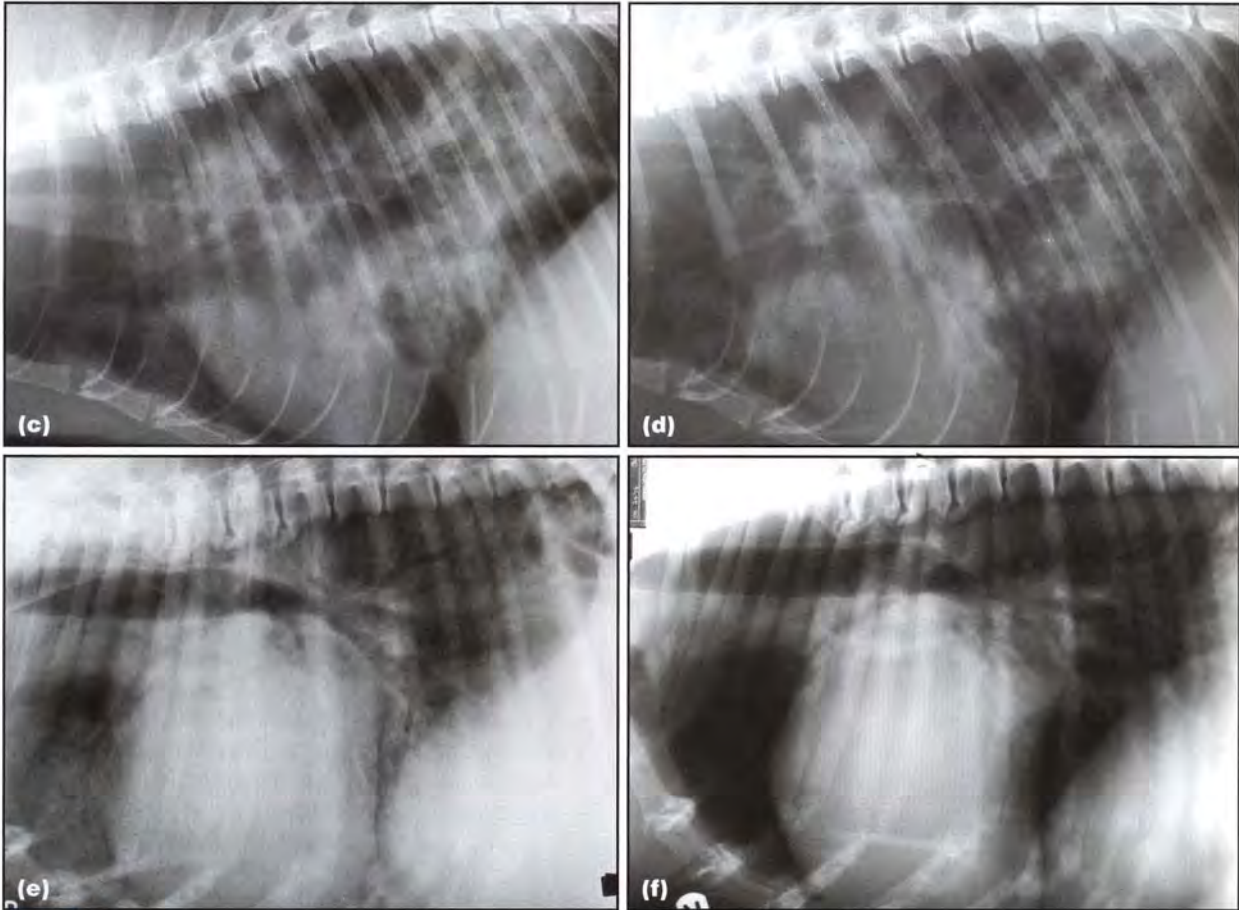
- Consideration of the history and results of other tests
- Temporal assessment of disease: different diseases may vary in speed of onset and resolution (Figures 12.80 and 12.81)
- Localization of pathology: different diseases often differ in preferential locations (Figure 12.82).

Disease	Onset within	Resolution following treatment within
Acute alveolar diseases:		
Oedema	Hours	Hours
Haemorrhage	Minutes	Days
Pneumonia	Hours to days	Days to weeks
Aspiration	Minutes	Days to weeks
Chronic alveolar diseases:		
Pneumonia	Days	Weeks to months
Granulomatous diseases	Weeks	Months to never
Neoplasia	Weeks	Weeks to never (depending on tumour type and treatment)

12.80 Onset and resolution of different alveolar lung diseases.



12.81 **(a)** Lateral thoracic radiograph of a Labrador Retriever with pancreatitis. The thorax is normal. **(b)** Lateral thoracic radiograph taken 48 hours later. Note the severe generalized alveolar pattern, which developed rapidly following aspiration of gastric fluid. (continues)



12.81 (c) Lateral thoracic radiograph of a 6-year-old Maine Coon cat presented with chronic coughing and dyspnoea. There are multifocal areas of ill defined soft tissue opacity in multiple lung lobes. The presumptive diagnosis was pneumonia, possibly granulomatous or atypical in origin. Open lung biopsy showed chronic inflammatory changes. (d) Lateral thoracic radiograph following treatment with antibiotics for 3 weeks. There is no change in the lung lesions. Histopathological examination postmortem confirmed diffuse pulmonary adenocarcinoma. (e) Lateral thoracic radiograph of an Irish Wolfhound with pulmonary oedema secondary to dilated cardiomyopathy. (f) Lateral thoracic radiograph taken 72 hours later following treatment with diuretics. Note the resolution of the oedema in contrast to the lack of progression seen in (c) and (d). (c, d Courtesy of Cambridge Veterinary School)

Disease	Preferential lung location
Bacterial pneumonia	Ventral lung areas Right middle lobe Both cranial lobes
<i>Pneumocystis carinii</i> infection	Caudal and middle lobes
Hypostatic atelectasis	Right middle lobe Lung periphery Dependent lung
Resorption atelectasis, secondary to bronchial obstruction (plugging) in feline asthma	Right middle lobe
Resorption atelectasis, secondary to chronic obstructive bronchial foreign body	Caudal lobes
Atelectasis, secondary to pleural effusion	Right middle lobe
Neoplasia	Caudal lobes
Contusion	Ipsilateral to trauma
Haemorrhage	Random Location of penetrating injury
Lung lobe torsion	Right middle lobe (deep-chested dogs) Left cranial lobe (barrel-chested dogs)

12.82 Preferential location of different alveolar lung diseases. (continues) ▶

Disease	Preferential lung location
Canine cardiogenic pulmonary oedema	Perihilar Symmetrical or slightly more in right caudal lobe
Canine non-cardiogenic pulmonary oedema	Caudodorsal aspect of caudal lobes (bilateral) Right caudal lobe often more affected
Feline pulmonary oedema	Random
Pulmonary emboli and infarcts	Lung periphery
Acute respiratory distress syndrome	Random
Metastatic neoplasia	Random
<i>Angiostrongylus vasorum</i> infection	Lung periphery

12.82 (continued) Preferential location of different alveolar lung diseases.

Atelectasis

The Greek word ατελεκτασία means non-expansion of a terminal space. As a medical term, atelectasis is defined as an acute or chronic collapse or airless state of the whole lung or parts of it, caused by congenital or acquired conditions. This broad definition is synonymous with collapse and both terms are used in this manual in this sense.

In the normal lung, surfactant maintains lung compliance and alveolar stability. The negative pleural pressure and surfactant prevent elastic recoil and lung lobe collapse. If either of these is missing then the lung may collapse. There are different types of atelectasis:

- Passive atelectasis (Figure 12.83 and 12.84):
 - Occurs if extra-alveolar pressure moderately increases
 - Condition is non-obstructive – if pressure normalizes, reinflation is possible
 - Mild to moderate loss of volume and recoil



12.83

DV thoracic radiograph of a Greyhound with a simple pneumothorax following trauma. There is passive collapse of all the lung lobes. Note how the collapsed lobes maintain their shape and collapse to a similar degree (arrowheads). There is an increase in opacity within the atelectatic lung due to reduced aeration.



(a)



(b)

12.84 **(a)** VD radiograph (vertical beam orientation) of a 13-year-old Domestic Shorthair cat obtained after being under general anaesthesia in left lateral recumbency for 20 minutes. The left cranial lung lobe is collapsed with mild cardiac shift towards the left. **(b)** Immediate repeat VD radiograph with the cat in right lateral recumbency (horizontal beam orientation). The non-dependent left lung is now well aerated; whereas, the dependent right middle and caudal lobes are atelectatic under the weight of the heart (hypostatic lung collapse).

- A common form is hypostatic collapse – the dependent lung portion collapses under the weight of the non-dependent structures (particularly the heart) if the full lung capacity is not used. This is a physiological process
- Examples include mild pleural effusion or pneumothorax and prolonged unchanged recumbency (especially if anaesthetized).
- Compression atelectasis (Figure 12.85):
 - Occurs if extra-alveolar pressure exceeds atmospheric pressure
 - Condition is non-obstructive – if pressure normalizes, reinflation is possible
 - Considerable loss of lung volume beyond recoil
 - Examples include tension pneumothorax, large pleural effusion and large thoracic masses.
- Resorption atelectasis (Figure 12.86 and 12.87):
 - Occurs if gas enters the alveoli at a slower rate than it is removed
 - May be either obstructive or non-obstructive
 - Non-obstructive form – oxygen replaces nitrogen as the predominant alveolar gas. Oxygen diffuses more readily into the bloodstream, leading to a reduction in alveolar volume. This is a physiological process
 - Obstructive form – resorption of alveolar gas following total bronchial obstruction
 - Examples include supplemented oxygen inhalation (non-obstructive), bronchial foreign bodies, masses and plugs (obstructive).
- Adhesive atelectasis:
 - Occurs due to lack or destruction of surfactant. Surfactant normally diminishes surface tension allowing alveoli to inflate
 - Condition is non-obstructive – major airways remain patent
 - Examples include congenital atelectasis, pneumonia and acute respiratory distress syndrome (ARDS).



12.85 Lateral thoracic radiograph of a skeletally immature dog with a tension pneumothorax as a result of a road traffic accident. The lung lobes are significantly reduced in size and are almost as opaque as other soft tissue structures, indicating compression atelectasis.



12.86 (a) High-resolution thoracic CT image at the level of the accessory lung lobe of an 8-year-old mixed breed dog in dorsal recumbency under general anaesthesia, with oxygen-supplemented ventilation performed for evaluation of potential metastatic lung disease. The dorsal lung regions are collapsed and cannot be assessed for metastases. The oesophagus is gas- and fluid-distended (*). (b) CT image at the same location from a repeat series obtained with the dog in sternal recumbency. The dorsal lung region is completely aerated again; however, the ventral tip of the right caudal lung lobe is now atelectatic. Oxygen supplementation promotes non-obstructive resorption atelectasis, particularly in the dependent lung regions (hypostatic component). Changes are quickly reversed with recumbency change, enabling diagnosis of atelectasis and assessment of the affected lung regions.

- Cicatrization atelectasis (Figure 12.88):
 - Occurs if fibrosis and scar formation of lung tissue reduces lung compliance
 - Condition is non-obstructive – major airways remain patent
 - Examples include idiopathic pulmonary fibrosis, chronic pneumonia and adhesive pleuritis.



12.87 VD thoracic radiograph of a cat with chronic bronchial disease. There is collapse of the right middle lung lobe (arrowhead), probably due to obstruction of the bronchus (plug formation) and resorption of air from the affected lobe, and a mild shift of the cardiac silhouette towards the right hemithorax. This is an example of obstructive resorption atelectasis, commonly seen in the right middle or cranial lobes in cats with bronchial disease.



12.88 Caudal close-up of a DV thoracic radiograph of an English Springer Spaniel following thoracocentesis (causing subcutaneous emphysema) for a chronic pyothorax. There is an iatrogenic pneumothorax, which highlights the pleural surface of the left caudal lung lobe. The lung has lost its normal shape and is rounded with increased opacity and thickening of the pleura (arrowheads). There is cicatrization atelectasis due to the thickened pleura preventing re-expansion of the lung.

The location and degree of lung collapse depend on many factors, including:

- Pleural surface area:lung volume ratio: lobes or lung areas with a relatively large surface area and small volume have a higher tendency to collapse, e.g. right middle lobe and lobe apices
- Collateral ventilation: a term used to describe aeration of the alveoli other than by direct airway connections. This is a major factor in preventing lobar collapse and allowing pulmonary reinflation after pneumonia. It also explains why a lobe may not collapse distal to a complete bronchial obstruction. Gas exchange occurs between lung segments via small pores and channels and airway anastomoses. A check-valve effect of pores of Kohn allows reinflation of collapsed lung areas during inspiration and prevents air escape during expiration. Collateral ventilation also promotes spread of infection throughout a lobe. Collateral ventilation is particularly effective with large pressure differences, e.g. during coughing
- It is ineffective with: small pressure differences; pulmonary exudates and secretions obliterating pores and alveoli; and a high pleural surface:lung volume ratio
- Gravitational effects: dependent lung areas always have a higher tendency to collapse. Non-physiological recumbency during medical procedures can put additional weight on the dependent lungs and promote collapse. Heart and mediastinal structures can exert pressure on the lungs
- Tidal volume: reduced activity, particularly under sedation/anaesthesia and during prolonged medical procedures, reduces the air space volume needed and promotes collapse
- Inhaled gases: oxygen supplementation promotes resorption atelectasis.

Why is the right middle lung lobe so prone to collapse with chronic respiratory disease?

It has a high pleural surface area:lung volume ratio, leading to less collateral ventilation. The opposite is true for the caudal lobes, which have a low pleural surface area:lung volume ratio, more collateral ventilation, and hence are unlikely to collapse.

Radiography and computed tomography: Findings include (see Figures 12.83 to 12.88):

- Affected lung volume is reduced
- Increased opacity with an alveolar pattern
- Affected lung is triangular in shape with a broad base and apex towards the periphery
- Mediastinal shift and cranial displacement of the ipsilateral diaphragmatic crus on the DV or VD view
- Unaffected lobes may hyperinflate to compensate (non-specific sign)
- Narrowing of the intercostal spaces on the affected side

- Displacement of interlobar fissures may be seen due to the displacement of lobes adjacent to the atelectatic lobe
- Thin parts of the lung lobes are preferentially affected. Atelectasis is most common in the right middle lung lobe, and the ventral and cranial parts of the lungs
- In cases of chronic pleural effusion, fibrosis of the lung and pleura may prevent lung re-expansion following drainage. The atelectatic lung remains reduced in size and in some cases rounded in shape
- Atelectasis of the right middle lobe is often present in cases of feline bronchial disease; other radiographic changes may also be present.

Ultrasonography: Only gas-free lung directly adjacent to the thoracic wall can be assessed ultrasonographically. Ultrasonography is, therefore, a good method for further investigation of lung that is radiographically collapsed or consolidated. Induction of hypostatic lung collapse is also useful to further investigate or allow ultrasound-guided fine-needle aspiration of a soft tissue lung lesion in the proximity of the lung margin.

The animal should be positioned with the affected lung in a dependent position for several minutes prior to scanning. The patient should be scanned before reinflation occurs, either from underneath the table (echocardiography table helpful) or immediately after turning the animal over so that the affected side is upper most.

Ultrasonographic findings include (see Figures 2.6 and 2.8, p. 22):

- Highly echogenic lung tissue
- Dispersed residual gas pockets
- Usually no fluid bronchograms
- Reduced volume of the affected lobe
- Sharp pointed or triangular margins are retained
- Gradual increase in reverberation in non-dependent position with physiological collapse; this does not occur with pathophysiological collapse, consolidation or mass.

Relevance of atelectasis in the diagnostic imaging work-up: Atelectasis is a very common phenomenon, which can occur within minutes of animal positioning during diagnostic imaging procedures. It is useful to be able to:

- Differentiate atelectasis from non-atelectatic alveolar lung diseases. The lobar shape and position, mediastinal and diaphragmatic shift should be evaluated. Lung volume is reduced in atelectasis, and normal or increased in non-collapsing alveolar diseases
- Differentiate between physiological and pathophysiological forms of atelectasis:
 - Progression and resolution of collapse: rapid onset and resolution in physiological collapse; chronic, non-reversible collapse in pathological forms of atelectasis

- Gravitational effects. Radiographs in opposite recumbency and/or with manual inflation should be obtained and assessed. Pathological collapse does not resolve in non-dependent position or inflated state
- Tidal volume and inhaled gases. The patient should be assessed/reassessed without general anaesthesia, sedation, prolonged recumbency or oxygen supplementation, which all promote physiological atelectasis.
- Avoid/reverse physiological atelectasis for radiographic/CT assessment of the relevant lung areas (see Figures 12.84 and 12.86):
 - Prolonged unchanged recumbency prior to anaesthesia/sedation should be avoided
 - If the animal is anaesthetized, it should be positioned in sternal recumbency as soon as possible following induction
 - DV or VD radiographic views should be taken prior to lateral views
 - The recumbency of patient can be reversed to assess affected lung areas
 - The lungs should be manually inflated.
- Promote hypostatic lung collapse for pulmonary ultrasonography (see above).

Pulmonary oedema

Pulmonary oedema is defined as a pathological extra-vascular fluid accumulation in the lungs, originating from the pulmonary vessels. Direct aspiration is treated as a separate entity in this manual. Oedema develops if interstitial fluid production exceeds the capacity of the pulmonary lymphatic drainage. Increased fluid accumulates initially within the interstitium and then extends into the alveolar spaces. There are four main mechanisms for its development:

- Permeability oedema:
 - Increased vascular permeability due to alveolar/capillary wall damage
 - High protein content of oedema fluid
 - Normal vascular pressure.
- Hydrostatic oedema:
 - Increased microvascular pressure
 - Low protein content of oedema fluid
 - Volume overload of pulmonary vascular bed:
 - Left heart disease
 - Left-to-right shunt
 - Anuric renal failure
 - Excessive intravenous fluid therapy (hyperhydration). Commonly seen in cats.
- Reduced capillary plasma oncotic pressure:
 - Due to severe hypoalbuminaemia (<10 g/l)
 - Low protein content of oedema fluid
 - Rarely leads to pulmonary oedema in dogs and cats
 - Contributing factor with intravenous fluid therapy (haemodilution).
- Reduced lymphatic drainage: most likely to be due to neoplasia; rarely leads to pulmonary oedema in dogs and cats.

In most diseases there is a combination of mechanisms, with permeability and hydrostatic

oedema as the most important factors (*mixed oedema*). Because of the clinical implications, pulmonary oedema is often classified as *cardiogenic* or *non-cardiogenic*.

Cardiogenic pulmonary oedema (congestive heart failure): Primarily hydrostatic oedema is seen. It is one of the pathological processes in left-sided heart failure. It occurs primarily as a result of increased vascular pressure due to backward left heart failure:

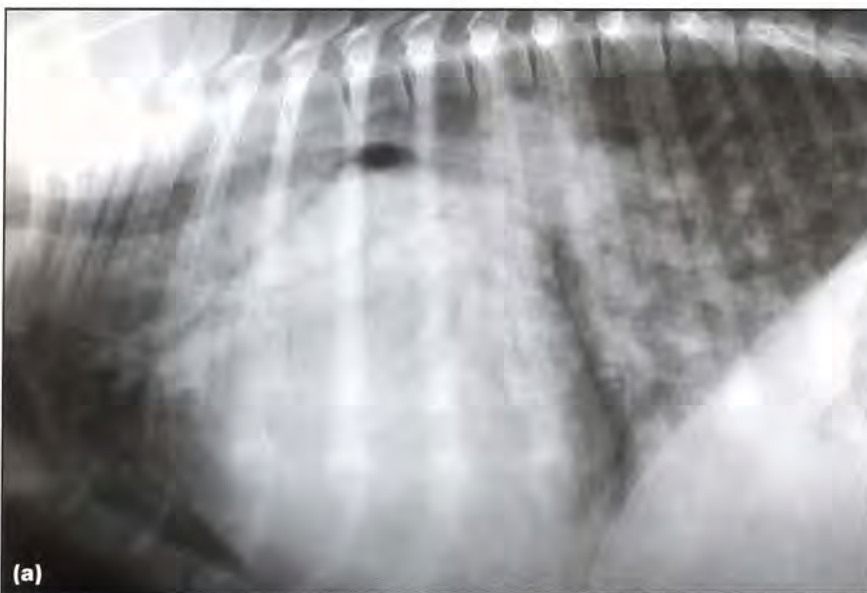
- With mitral regurgitation there is an increased volume of blood within the left ventricle and left atrium
- Elevated left atrial pressure causes increased pressure within the pulmonary veins
- This results in increased interstitial fluid production, which, if lymphatic drainage capacity is exceeded, leads to pulmonary oedema.

Aetiology includes:

- Mitral valve disease. Most common cause in small-breed dogs (myxomatous mitral valve degeneration)
- Cardiomyopathies. Common cause in large-breed dogs (dilated cardiomyopathy) and most common cause in cats (all forms)
- Left-to-right shunts (patent ductus arteriosus, ventricular septal defect)
- High-output states (hyperthyroidism, anaemia, etc.) (rare).

Cardiovascular diseases causing pressure overload (aortic stenosis, systemic hypertension) do not commonly induce left-sided heart failure.

Radiography: Findings with untreated hydrostatic pulmonary oedema (Figure 12.89; see also Figures 12.17, 12.21 and 12.81e) include:



12.89 (a) Lateral thoracic radiograph of a 4-month-old German Shepherd Dog puppy with a patent ductus arteriosus and congestive heart failure. Note the typical perihilar distribution of the pulmonary oedema, and enlargement of the pulmonary veins and arteries and cardiac silhouette. (Courtesy of Cambridge Veterinary School). (b) Lateral thoracic radiograph of a kitten with a patent ductus arteriosus and pulmonary oedema.



- Initially an unstructured interstitial pattern, progressing to an alveolar pattern
- Pulmonary vascular distension, particularly venous (not consistently seen)
- Left-sided cardiomegaly common in cardiogenic oedema
- Normal heart size in hyperhydration, some left heart diseases (bacterial endocarditis, chordae tendinae rupture, myocarditis), and traumatic chordae tendinae rupture and mitral valve prolapse (see Figure 12.21)
- Distended stomach from aerophagia if very dyspnoeic
- Right caudal lobe may be more severely affected than other lobes
- Individual lung lobes may be affected if their pulmonary vein is obstructed (e.g. with some cases of cor triatrium sinister and anomalous pulmonary venous drainage)
- Oedema is labile and may change distribution within the lungs with alteration in the animal's position.

Species differences

- In dogs, changes are centred on the perihilar region but extend to the periphery of the caudal lung lobes as severity increases. Ventral and peripheral areas are relatively spared, possibly due to greater lymphatic drainage than the hilar regions. The changes are often symmetrical.
- In cats, the location of expanding patchy alveolar lung areas is random.

Cardiogenic or hyperhydration-induced pulmonary oedema responds within a few hours to diuretic treatment (see Figures 12.81ef). Imaging findings include:

- Pulmonary vessels return to a normal size
- Resolution of the alveolar pattern
- Disappearance of the interstitial pattern, a sign of complete oedema resolution.

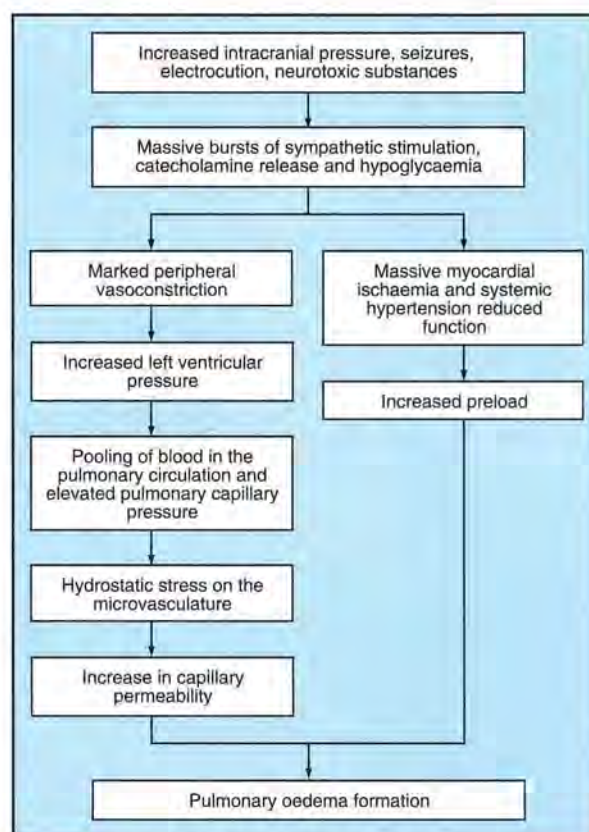
Resolution of lung opacity does not always correlate well with normalization of vascular size. The administration of a diuretic, such as furosemide, may reduce pulmonary venous size before lung pattern resolution occurs.

Other imaging techniques: Echocardiography may be used to identify the cause of the heart disease and assess cardiac function (see Figure 7.137, p. 158).

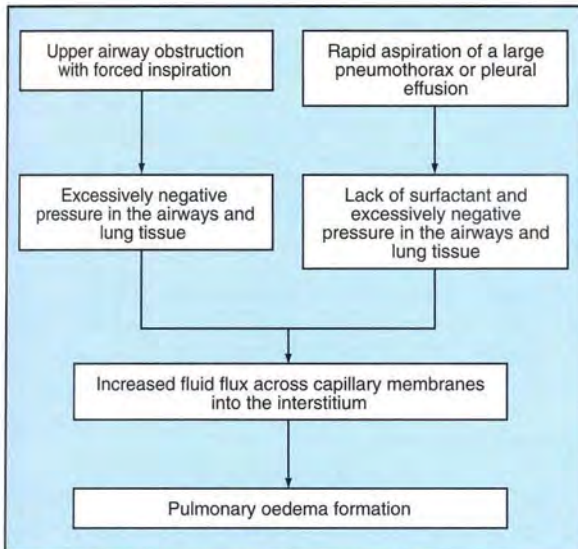
Non-cardiogenic pulmonary oedema: This is primarily a permeability oedema. It is uncommon in dogs and rare in cats. There are three main aetiological subtypes:

- Neurogenic pulmonary oedema (Figure 12.90):
 - Working dogs undertaking strenuous exercise are the most commonly affected. Male Swedish Drevlers are over-represented with familial trait

- Head injuries, other causes of raised intracranial pressure
- Seizures
- Electric cord bite injury, causing electrocution; most commonly seen in young dogs.
- Pulmonary oedema secondary to decreased interstitial tissue pressure (Figure 12.91):
 - Rare sequel to laryngeal paralysis or other forms of laryngeal obstruction or compression. Bulldogs over-represented due to the high incidence of upper airway disease
 - Re-expansion pulmonary oedema is a rare sequel to rapid pleural draining of fluid or air. Occurs within 1–2 hours of re-expansion and resolves over a few days.
- Pulmonary oedema due to direct toxic effects on the capillary endothelium and alveolar epithelium:
 - Severe viral or bacterial infection
 - Toxic inhalants: smoke, sulphur dioxide, toxic gases
 - Vascular toxins: snake venoms, endotoxins, kerosene; vasoactive substances: kinins, prostaglandins, allergens
 - ARDS, fat embolism, uraemia
 - Lung trauma
 - Aspiration of acidic gastric contents
 - Hyperosmolar effect of aspirated salt water or ionic iodinated contrast media.



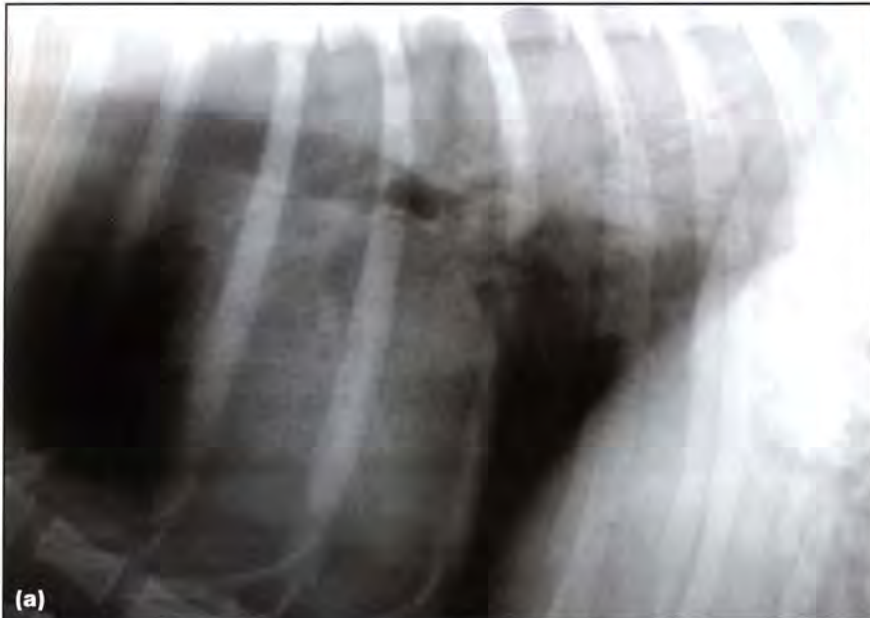
12.90 Suspected pathophysiology of neurogenic pulmonary oedema.



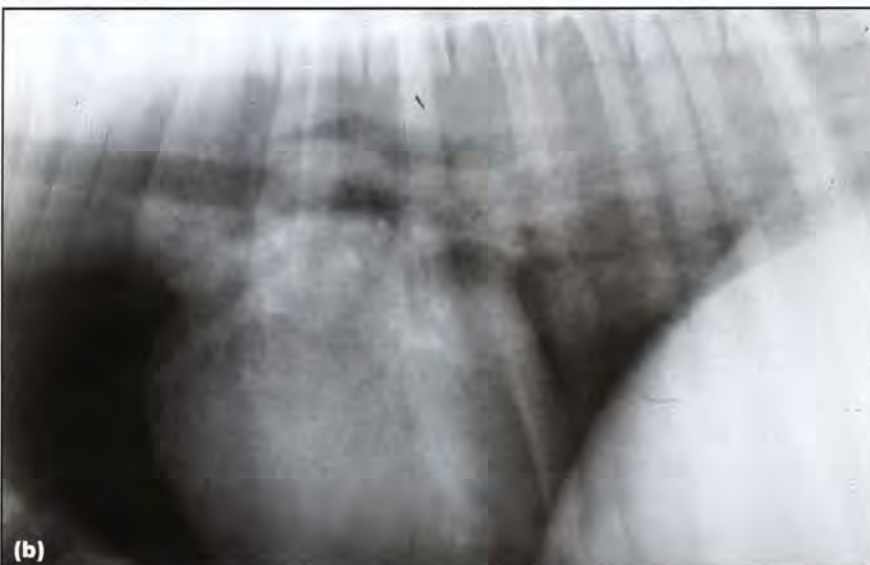
12.91 Pathophysiology of pulmonary oedema secondary to decreased interstitial tissue pressure.

Radiography: Radiographic findings include:

- Increased lung opacity with a predominantly alveolar pattern (Figure 12.92)
- May be an unstructured interstitial lung pattern in the mild/early form
- Distribution:
 - Caudodorsal lung fields
 - Additional perihilar location common, cranioventral rare
 - Diffuse in severe cases
 - Lung periphery in early/mild cases
 - Right lung usually more severely affected.
- Rarely, complete lobar opacification with air bronchograms (in contrast to pneumonia)
- In case of upper airway obstruction:
 - Dilated intrathoracic trachea
 - Scalloping of the intercostal spaces or small inspiratory volume
 - Direct evidence of upper airway obstruction.
- Gas-distended stomach (non-specific feature of dyspnoea).



12.92 (a) Lateral thoracic radiograph of a 4-year-old mixed breed dog with neurogenic pulmonary oedema, following electrocution due to biting an electrical cord. Notice the alveolar lung pattern in the caudodorsal lung fields, consistent with a non-cardiogenic form of pulmonary oedema.



(b) Lateral thoracic radiograph of a dog with a history of strangulation. There is increased opacity in the caudodorsal lung fields with an interstitial to alveolar pattern.

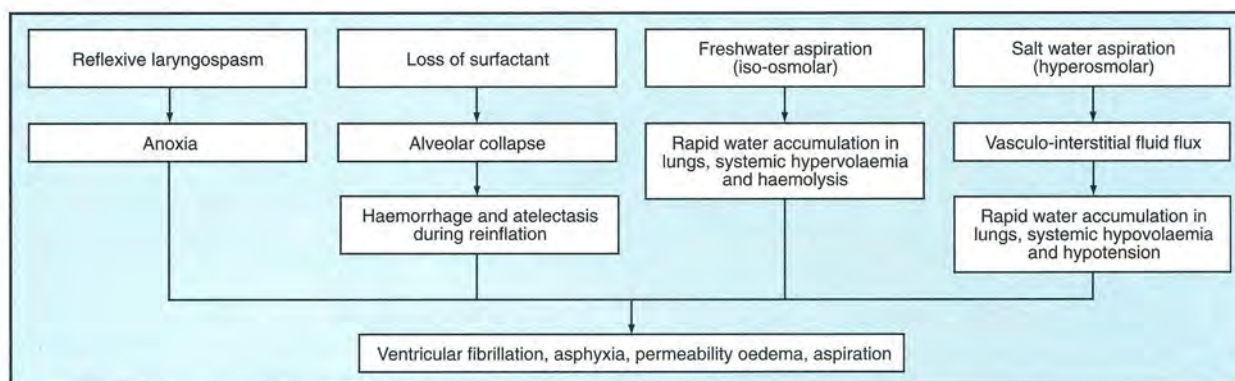
Other imaging techniques: Head CT or MRI may be useful in patients with neurological signs:

- MRI has superior soft tissue contrast (seizures, suspected mass)
- CT is superior for imaging head trauma (free gas, bone or metal fragments)
- Head CT is quicker than MRI and may be easier to accomplish with sedation only, in patients where general anaesthesia is contraindicated.

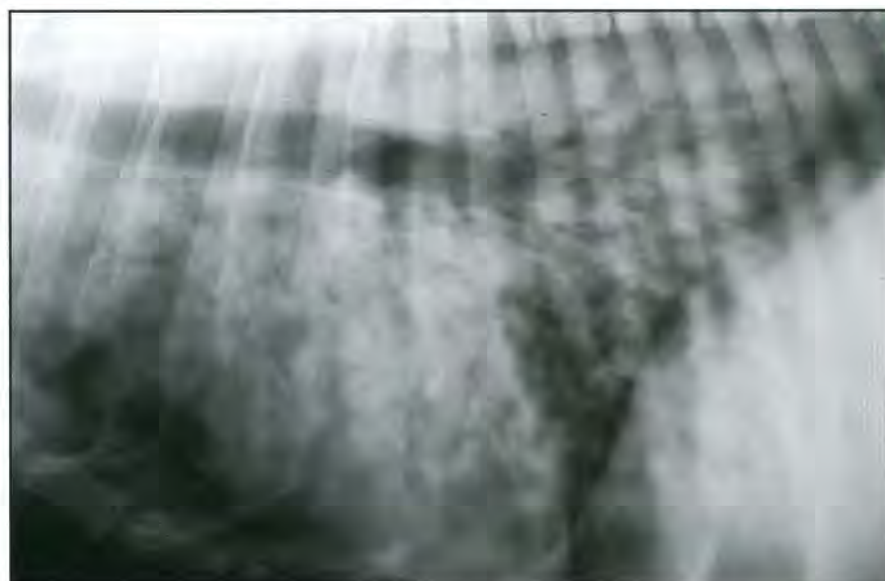
Respiratory CT may be used to differentiate pulmonary oedema from other alveolar diseases and identify upper airway obstructions. Laryngotracheal ultrasonography allows assessment of the upper airways. This technique does not require sedation or anaesthesia. It may show laryngeal paralysis or laryngeal masses/swelling; it is particularly useful in cases of laryngeal masses in cats and allows guided biopsy. Echocardiography may be used to rule out cardiogenic oedema.

Near drowning

Near drowning is defined as survival (at least temporarily) following asphyxia and/or aspiration whilst submerged in fluid, and usually comes with a history of submersion (Figure 12.93).



12.93 Pathophysiology of near drowning.



12.94 Lateral thoracic radiograph of a dog obtained 8 hours after a near drowning accident in a river. The dog was able to walk home and only became severely dyspnoeic several hours later. A diffuse patchy alveolar pattern and slight dyspnoea-related movement blur can be seen.

Radiography: Radiographic findings include:

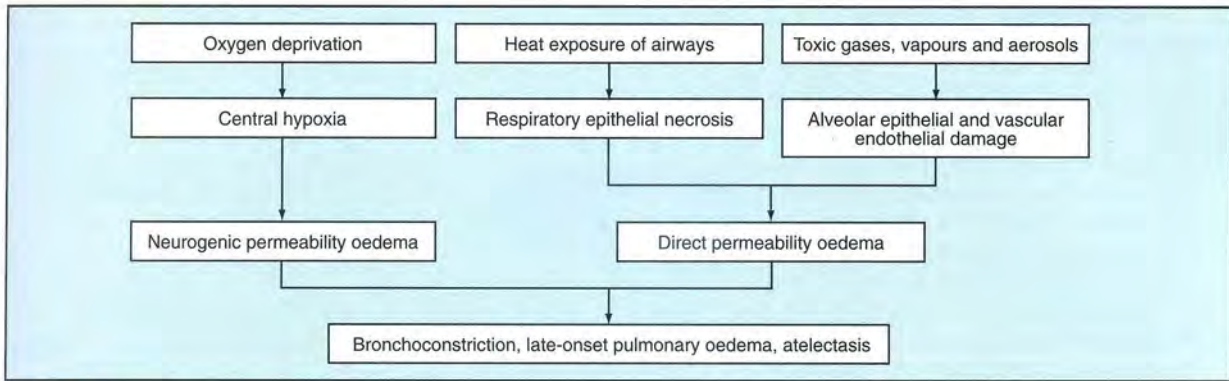
- Increased lung opacity, preferentially the caudal lobes (Figure 12.94)
- Diffuse interstitial pattern to complete consolidation
- Right lung often more severely affected
- *Sand bronchograms* possible with submersion in sandy-bottomed rivers.

Radiographic abnormalities commonly occur or worsen with the first 24 hours following submersion. If radiographic abnormalities do not clear within 48 hours, secondary pneumonia should be suspected.

Smoke inhalation

This diagnosis is based upon a history of exposure to fire or smoke (Figure 12.95). There is no breed, age or sex predisposition. There is a seasonal bias, with an increased incidence in the winter months. Smoke inhalation results in a variety of pulmonary abnormalities:

- Clinical signs include stupor, coma, respiratory distress, coughing, epistaxis, ataxia, weakness, ptyalism and ocular irritation
- Evidence of burns or smoke contamination of the skin



12.95 Pathophysiology of smoke inhalation.

- Most animals have evidence of respiratory disease on clinical examination with peak within 24 hours
- Cyanosis or hyperaemic mucous membranes may be present in some cases
- Secondary bronchopneumonia or ARDS is possible.

Radiography: There may be no radiographic abnormalities (in approximately 25% of reported cases). Radiographic changes (Figure 12.96) may not appear until 16–24 hours after the insult. A reduced luminal gas column is seen with laryngeal oedema.

In dogs, radiographic findings have a random distribution; an alveolar pattern is most common. In cats, there is a predilection for the cranial or middle lobes; there is usually a diffuse interstitial pattern or focal alveolar opacities.

Acute respiratory distress syndrome

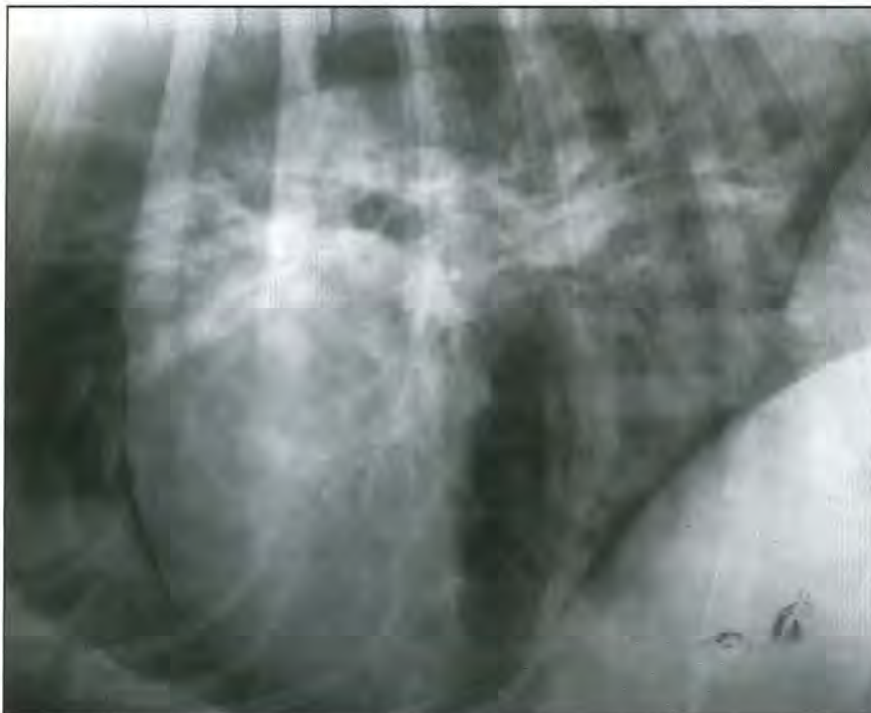
ARDS is a human term defined as acute fulminating respiratory failure, resulting from a variety of diseases,

leading to diffuse lung injury. It may also be called adult respiratory distress syndrome or shock lung.

ARDS is considered to be a subgroup of non-cardiogenic oedema. It is part of the systemic inflammatory response, leading to increased vascular permeability, pulmonary hypertension and airway constriction and obstruction. Inciting factors may be pulmonary (e.g. smoke inhalation, bacterial pneumonia) or non-pulmonary (e.g. endotoxaemia, pancreatitis, trauma, paraquat and other toxicities, fat embolism) in origin.

Histologically, ARDS is characterized by alveolar inflammation, oedema, haemorrhage, necrosis with formation of hyaline membranes or vascular congestion in conjunction with type 2 alveolar cell proliferation or interstitial fibrosis.

Clinical signs are acute onset of severe and progressive respiratory distress; in some cases signs are associated with an underlying cause (e.g. vomiting, evidence of trauma, etc.). Progressive tachypnoea and dyspnoea are seen in most animals with altered lung sounds.



12.96 Lateral thoracic radiograph of a 6-month-old German Shepherd Dog that was rescued from a fire. There is a patchy alveolar pattern, particularly in the caudodorsal lung fields, consistent with smoke inhalation.

The most common reported underlying causes in dogs are:

- Bacterial pneumonia (which may be secondary to smoke inhalation or parasitic pneumonia)
- Sepsis and aspiration pneumonia
- Ventilator-acquired pneumonia
- Lung lobe torsion
- Non-pulmonary causes: gastric torsion, splenic torsion, trauma, laryngeal obstruction, pancreatitis, parvovirus infection, uraemia, disseminated intravascular coagulation (DIC), snake venom, drug toxicity
- Hyperoxia due to high inspired oxygen concentration (may result in lung injury similar to ARDS).

ARDS is possibly more common in younger dogs; no sex predisposition has been reported. A familial form is suspected in young Dalmatians (<1 year old), some of which also have renal aplasia or hydrocephalus.

Radiography: Radiographic findings include:

- May be normal in initial 24 hours
- Diffuse interstitial ± alveolar lung pattern, affecting all lobes is most common (Figure 12.97). Increasing severity with time, with air bronchograms visible by 36 hours after onset of lung injury
- Opacities relatively slow to change due to high protein content of fluid within the alveoli
- Bilateral distribution

- Pneumothorax and pneumomediastinum may occur in later stages
- Radiographic signs associated with the underlying cause may be present
- In the familiar form, pneumomediastinum and gastro-oesophageal intussusceptions are seen in the late stages of the disease. Radiographic changes are mixed alveolar, interstitial and peribronchial patterns.

Other imaging techniques: Abdominal ultrasonography or CT may identify the source of the sepsis.

Uraemic pneumonitis (uraemic pneumonopathy)

Histopathological changes are similar to those of ARDS, and uraemic pneumonitis may be considered part of this syndrome. The high protein content of the oedema fluid suggests permeability oedema due to toxic lung damage. Other factors also are likely to play a role, e.g. reduced oncotic pressure and cardiovascular effects.

Clinical signs are related to severe renal disease (polyuria, polydipsia, anorexia, etc.) plus respiratory signs associated with oedema. Uraemic pneumonitis should be differentiated from other renal-induced respiratory diseases:

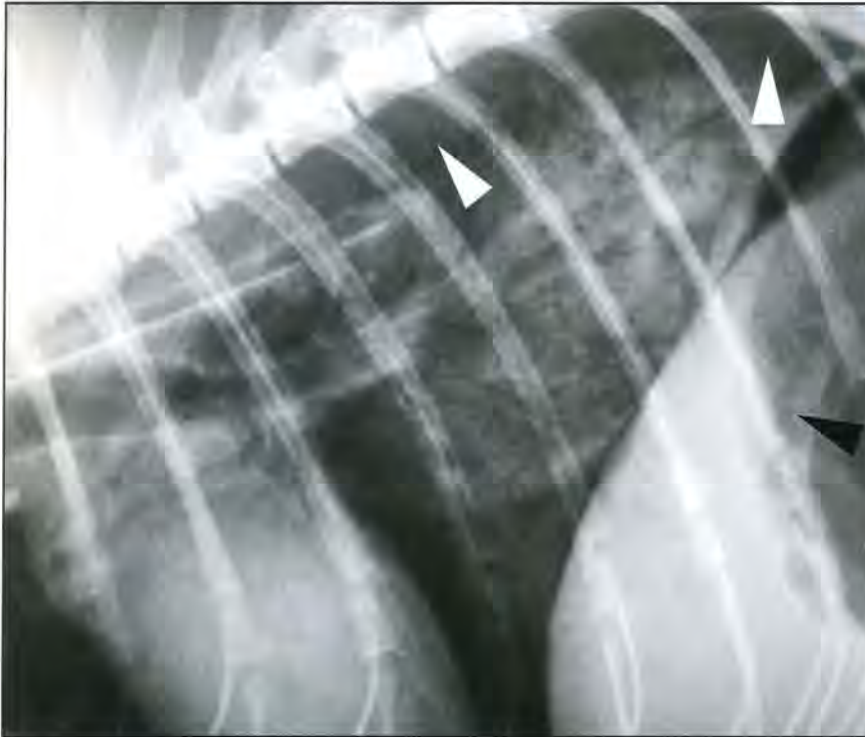
- Volume-overload pulmonary oedema
- Thromboembolic disease.

Radiography: Radiographic findings include:

- Pulmonary oedema within the caudodorsal lobes (Figure 12.98) may be associated with ARDS or non-cardiogenic oedema due to fluid overload



12.97 (a) VD thoracic radiograph of a 6-year-old Bernese Mountain Dog obtained 1 day after a road traffic accident, resulting in multiple pelvic fractures and hindlimb injuries. The thorax is normal. (b) A repeat radiograph obtained 4 days later. There is increased lung opacity, particularly in the left lung with a partial alveolar pattern. The dog had developed progressive systemic disease characterized by hyperthermia, immune-mediated haemolytic anaemia, erlichiosis, lymphadenopathy and metabolic acidosis. The dog was euthanized with a clinical diagnosis of ARDS.



12.98 Lateral thoracic radiograph of a 5-year-old Domestic Shorthair cat with terminal chronic renal failure. There is increased opacity with a partial alveolar pattern in the caudal lung lobes, aortic (white arrowheads) and gastric rugal (black arrowhead) mineralization, and gas distension (dyspnoea). The cat was euthanized and necropsy confirmed chronic renal failure with extensive metastatic mineralization and uraemic pneumonitis.

- Abdominal radiographs may show evidence of underlying renal disease
- In cases of renal secondary hyperparathyroidism, mineralization of the blood vessels and myocardium may be present. There may also be demineralization of the skeleton
- Chronic uraemia may lead to degeneration and calcification of connective tissue.

Other imaging techniques:

- Renal ultrasonography is indicated to identify structural renal changes.
- Nuclear medicine (scintigraphy) allows measurement of the glomerular filtration rate and quantification of the severity of the renal disease.
- If acute renal failure due to urinary tract obstruction or rupture is suspected, contrast radiographic studies are indicated.

Pulmonary vascular embolic events and lung infarction

Pulmonary arterial embolism can occur in dogs and cats due to:

- Thromboembolic disease
- Iatrogenic foreign material embolism and thrombosis, e.g. coil occlusion of a patent ductus arteriosus and accidentally dislodged coils into the pulmonary arteries, broken off intravascular catheter material
- Fat/bone marrow embolism due to trauma or bone marrow compressive surgery
- Septic emboli (vegetative endocarditis)
- Neoplastic vascular emboli
- High heartworm burden or broken off parts during attempted extraction.

Pulmonary venous embolism is uncommon in dogs and cats. Infarction is an uncommon sequel to embolic disease because:

- The lungs have an extensive collateral circulation
- Occlusion of central vessels results in ischaemia rather than infarction
- Infarcts typically occur in lung periphery.

Consequences of an infarction depend upon the size and the amount of lung affected:

- Small numbers of emboli may cause no clinical or radiographic changes (e.g. transient fat emboli seen during total hip replacement surgery)
- Large numbers of emboli can result in severe respiratory distress.

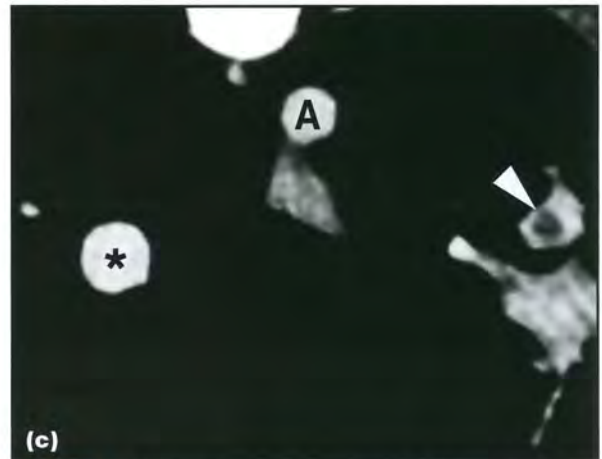
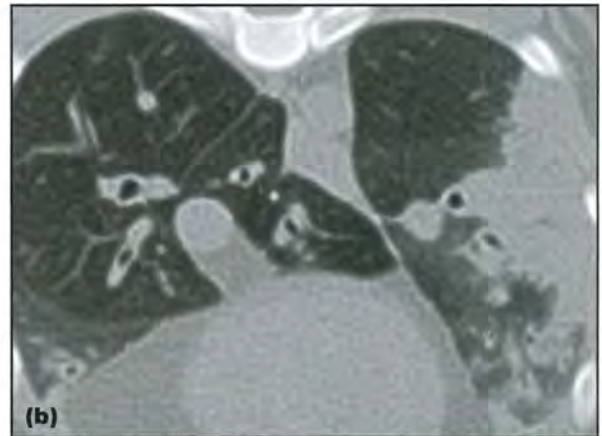
Infarction is reported more commonly in dogs than cats. Reported predisposing causes for infarction include amyloidosis, pancreatitis, immune-mediated haemolytic anaemia, hyperadrenocorticism, dirofilariasis, neoplasia (thromboembolism) and surgical intervention with bone marrow compression (fat embolism). Renal disease is the most commonly identified underlying cause. Clinical signs include acute onset dyspnoea. Septic emboli may lead to multiple abscessation or pneumonia. Neoplastic emboli may lead to atypical seeding of a metastatic tumour. For more information on pulmonary vascular embolic events and lung infarction, see Chapter 7.

Radiography: Lungs are radiographically normal in most cases. Findings may include (Figures 12.99, 12.100, 12.101 and 12.102):

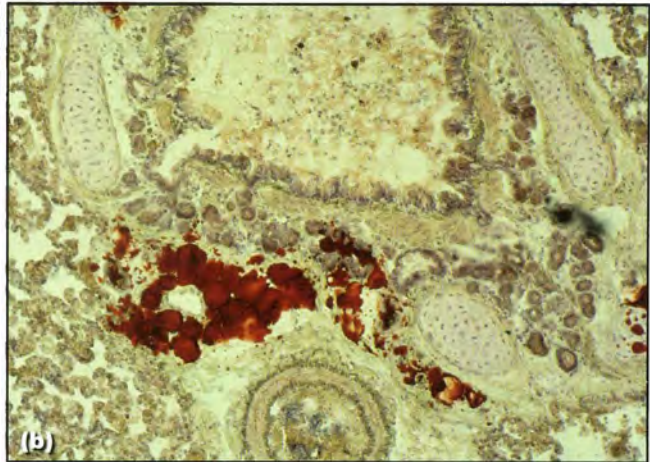
- Hyperlucent portion of the lung with attenuation of a vessel if pulmonary thromboembolism without infarction occurs
- Distribution:
 - Caudodorsal lung fields, especially at the costodiaphragmatic recess, most common
 - Focal area of peripheral alveolar or interstitial lung pattern with wedge shape (base towards hilus in large infarcts, apex towards hilus in small infarcts) is highly suggestive of infarction, but is rare. The increased opacity extends to the pleural surface. Rarely, in severe cases, may affect entire lobe
 - Small areas of alveolar disease affecting multiple lobes (right lung more than left, and caudal lobes more than cranial) are the most common radiographic abnormality seen.



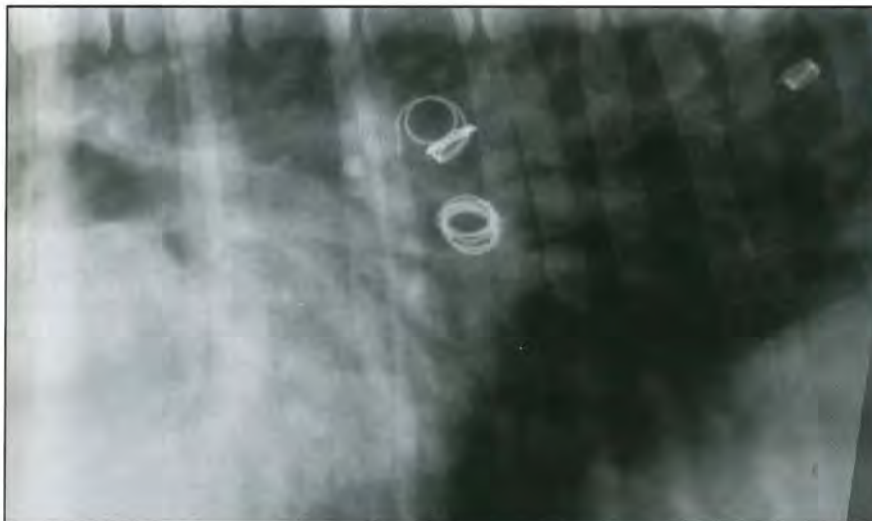
12.99 (a) VD thoracic radiograph of an 8-year-old Irish Setter with sudden onset of dyspnoea. The left caudal lung lobe appears hyperlucent and less vascularized than normal. (b) Close-up of the left caudal lung lobe. The lobar artery (between arrowheads) is distended and then disappears at the level of the ninth rib (*). These are classic, albeit rare, signs of pulmonary thromboembolism: a thrombus-distended pulmonary artery and tributary oligoemia.



12.100 (a) VD thoracic radiograph of a 6-year-old Domestic Shorthair cat with sudden onset of severe dyspnoea. There is increased opacity with a partial alveolar pattern in the left caudal lung lobe in the costodiaphragmatic recess. (b) Thoracic high-resolution CT image at the level of the accessory lung lobe demonstrates a wedge-shaped peripheral consolidation in the left caudal lung lobe consistent with an infarct. (c) Close-up of a pulmonary CT angiogram at the same level demonstrates contrast medium within the caudal vena cava (*) and aorta (A), and a large filling defect (dark core) in the left caudal lobar pulmonary artery (arrowhead), indicating an occlusive thrombus.



12.101 (a) Close-up of a VD thoracic radiograph of the right caudal lung lobe of a 1-year-old Domestic Shorthair cat, which had sustained sudden respiratory arrest when an intramedullary pin was advanced into the humerus for a fracture repair. The radiograph was obtained during the resuscitation attempts, which ultimately failed. There is increased lung opacity with an alveolar pattern in the right costodiaphragmatic recess. (b) Microscopic examination of the lungs confirmed a massive shower of occlusive fat emboli (red stained) throughout the pulmonary capillary bed and pulmonary fat embolism was established as the cause of death. Oil Red O with Mayer's haemulm stain; original magnification x220. (Reproduced from Schwarz *et al.* (2001) with permission from the *Journal of Small Animal Practice*)



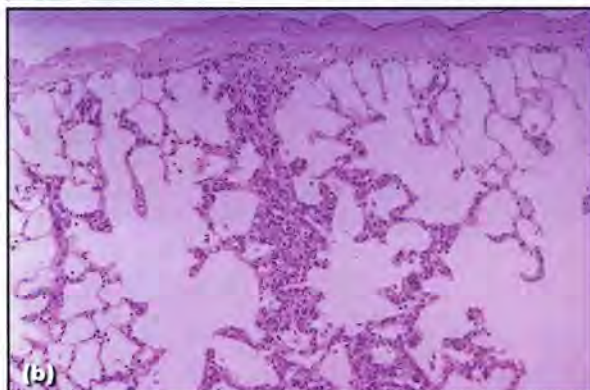
12.102 Caudal close-up of a lateral thoracic radiograph of a 4-year-old Labrador Retriever with a patent ductus arteriosus and left-to-right shunt, obtained during a coil embolization procedure. Three metallic coils can be seen dislodged in the caudal lung lobe arteries. Coils designed for human infants are commonly used in dogs, which typically have a wider duct. Due to the well developed collateral circulation, dislodged coils are usually of no clinical consequence. The duct was eventually successfully occluded.

- May see absence or attenuation of the pulmonary artery but may be obscured by the alveolar infiltrate
- Mild to moderate pleural fluid is often present
- Iatrogenically dislodged foreign bodies usually in caudal lobar arteries
- Cardiac changes uncommon but may include right ventricular or pulmonary artery enlargement
- In some cases, signs associated with the underlying disease are seen.

Contrast studies: Selective pulmonary arteriography may be used. Infarction shows failure of opacification or filling defects within the affected blood vessels. This technique requires general anaesthesia and ideally fluoroscopy or a rapid film changer.

Other imaging techniques:

- Echocardiography allows diagnosis of:
 - Main pulmonary artery thrombosis
 - Pulmonic valve insufficiency or tricuspid regurgitation, secondary to pulmonary hypertension (Doppler echocardiography)
 - Embolic showers during bone marrow compression surgery (e.g. total hip replacement) (monitoring device).
- CT (see Figures 12.61b, 12.100 and 12.103; see also Figure 7.159, p. 172):
 - High-resolution lung CT is used to identify pulmonary infarction and neoplastic subpleural infiltrate
 - CT angiography can identify vascular emboli.



12.103 (a) Thoracic high-resolution CT image at the level of the accessory lung lobe of an 8-year-old Hungarian Vizsla with pyrexia and carcinomatous infiltrate in a peripheral lymph node. A frond-like subpleural infiltrate is present in the dorsal aspect of both caudal lung lobes. (b) Microscopic examination of a corresponding lung area reveals a matching neoplastic capillary and interstitial subpleural infiltrate. Final diagnosis on necropsy was an adrenal carcinoma and pulmonary carcinosis. H&E stain; original magnification x160. (Reproduced from Johnson *et al.* (2004) with permission from the *Journal of Small Animal Practice*)

- Scintigraphic ventilation and perfusion scans (see Figures 5.7, p. 79, 7.160, p. 173 and 7.161, p. 173). A normal ventilation scan with a deficit in the perfusion scan is diagnostic for pulmonary thromboembolism.

Pulmonary haemorrhage

Most cases are associated with coagulopathies or trauma. Rodenticide poisoning (coumarin derivatives) is the most common cause of severe pulmonary haemorrhage; outdoor cats and dogs are at risk. Other causes include:

- DIC
- Trauma
- *Angiostrongylus* infection (dogs)
- Other coagulopathies
- Neoplasia (usually mass-related signs predominate).

Clinical signs include:

- Generalized blood loss (weakness, bruising, haematochezia, haematuria)
- Respiratory bleeding (cough, dyspnoea, haemoptysis)
- Upper airway obstruction.

Thoracic changes may include haemorrhage of the mediastinum, pleura and tracheobronchial airways.

Radiography: Radiographic findings include:

- Generalized patchy interstitial/alveolar pattern with random distribution (Figure 12.104; see also Figures 10.26, p. 223 and 12.20)
- Possible pleural or mediastinal haemorrhage
- Tracheal narrowing due to submucosal/mucosal haemorrhage or extratracheal haematoma with narrowing of tracheal lumen – often generalized.

The combination of tracheal narrowing with pleural and mediastinal fluid and lung changes is suggestive of anticoagulant toxicity. Thoracic changes due to coumarin toxicity should resolve within 1–5 days of starting therapy. Haemorrhage due to *Angiostrongylus vasorum* infection usually also has radiographic changes of parasitic pneumonia. The pattern is classically peripheral in distribution (see Figure 7.158, p. 170).

Pulmonary contusion and laceration

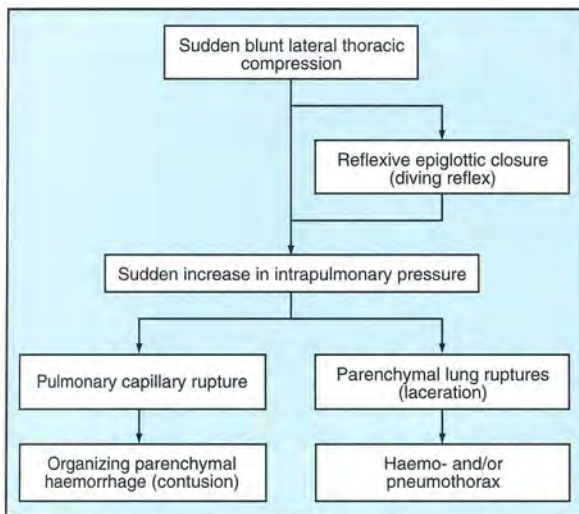
Blunt external thoracic trauma is the most common cause of traumatic lung changes in dogs and cats, commonly seen in road traffic accidents and high rise syndrome (Figure 12.105).

Blunt internal thoracic trauma (barotrauma) is a relatively common cause of lung laceration in cats; for example, following iatrogenic manual or automated hyperinflation of lungs during anaesthesia. It can cause pneumomediastinum, pneumo- or haemothorax, but does not cause widespread contusion.

Perforating lung injuries are uncommon in dogs or cats:



12.104 Lateral thoracic radiograph of a Labrador Retriever with coagulopathy due to warfarin toxicity. Note the tracheal narrowing, pleural fluid and partial alveolar lung pattern. This combination is highly suggestive of coumarin toxicity. (Courtesy of Cambridge Veterinary School)



12.105 Pathophysiology of blunt external thoracic trauma.

- External: bite, gunshot, stab wound; iatrogenic laceration during fine-needle lung aspiration or biopsy
- Internal: intubation injury, penetrating bronchial or oesophageal foreign body or instrument.

Perforating lung injuries can cause pneumo-mediastinum, pneumo- or haemothorax; there is usually a local area of pulmonary haemorrhage.

Radiography: Radiographic findings include:

- Contusion:
 - Consolidated lung lobe(s), usually ipsilateral to impact (Figure 12.106)
 - Patchy alveolar opacity in mild or resolving contusion
 - Rounded lung margins
 - Enlarged lobes, causing mediastinal shift.
- Rib fractures and chest wall swelling
- Traumatic gas- or blood-filled bullae (pneumato- and haematocoles)
- Free pleural or mediastinal gas or effusion.



12.106 DV thoracic radiograph of a Chihuahua following thoracic trauma. There are multiple right rib fractures. The right lung is consolidated and causes a cardiac shift towards the left. Lung contusion is usually adjacent to the site of blunt impact. (Courtesy of Cambridge Veterinary School)

Contrast studies: These should be used if necessary for confirmation of a suspected diaphragmatic hernia (in cases of trauma). Positive-contrast gastrointestinal studies or peritoneography may be used to identify loss of diaphragmatic integrity.

Other imaging techniques: Abdominal radiography should be carried out in cases of suspected trauma. Thoracic ultrasonography may be used to differentiate mediastinal fluid from mediastinal masses, and for evaluation of diaphragmatic integrity.

Pulmonary alveolar microlithiasis (pumice stone lung)

This is a rare condition with widespread mineralized concretion within the alveolar lumen reported in humans, dogs and other animals. It has never been

reported in cats. Inflammatory changes may or may not be present. The aetiology is unknown.

Despite its marked radiographic manifestation at an early stage, the clinical onset is insidious and progression is very slow. Cardiorespiratory signs range from completely absent or harsh lung sounds to pulmonary insufficiency and cor pulmonale. The term 'pumice stone lung' relates to the postmortem appearance of the lung, which is stone hard and requires a saw for sectioning.

Radiography: There is marked widespread micronodular mineralization in all lung lobes, tapering towards the lung periphery (Figure 12.107). There is slow progression of radiographic signs over time. Differential diagnoses should include:

- Incidental pulmonary osteomas and mineralized granulomas, which are fewer and bigger (2–4 mm)
- Bronchial microlithiasis is seen in cats. Concretions are intrabronchial, fewer and larger (2–4 mm) (see Chapter 11)
- Metastatic mineralization due to neoplastic, metabolic (Cushing's disease) or inflammatory conditions (uraemic pneumonitis) usually results in an interstitial lung pattern
- Incompletely resorbed barium aspiration is usually more localized (ventral, right middle and cranial lung lobes).



12.107 (a) A close-up of a lateral thoracic radiograph of a 10-year-old Labrador Retriever with pulmonary alveolar microlithiasis. The dog had harsh lung sounds but otherwise no cardiorespiratory abnormalities. Notice the widespread micronodular mineralization, which is most pronounced in the perihilar region. (b) Postmortem radiograph of the right lung. The lung was solidly mineralized and had to be sectioned with a saw. The reason for euthanasia in this dog was severe chronic coxofemoral and cubital arthritis not cardiorespiratory disease. (Reproduced from O'Neill *et al.* (2006) with permission from the *Irish Veterinary Journal*)

Pneumonia

Pneumonia is defined as inflammation of the alveolar parenchyma. The term pneumonia has been used to describe acute and exudative inflammation, and pneumonitis is used to describe chronic proliferative lesions. Regardless of the aetiology, the clinical signs and radiographic features of pneumonia are often similar. In this chapter pneumonias are classified first according to the initial site of involvement and the spread of infection, which can be documented radiographically. The characteristic radiographic findings caused by specific pathological agents are discussed following this classification.

- Bronchopneumonia – originates at the bronchoalveolar junction. Often acute in onset and infectious in origin. Usually cranioventral in distribution and due to an aerogenous origin. Bacterial causes are most common, often secondary to other lung insult, and result in suppurative pneumonia.
- Lobar pneumonia – the entire lobe is affected; usually due to fulminating bronchopneumonia, less commonly due to a tracheobronchial foreign body.
- Interstitial pneumonia – huge variety of causes and probably under-recognized. Predominantly interstitial pattern with viral infection and chronic inflammatory diseases.

Non-specific canine bacterial pneumonia: This is the most common cause of pneumonia and often develops as a secondary infection following primary lung insult (e.g. haemorrhage, viral infection). Bronchopneumonia is the most common pathology and is thought to be due to an aerogenous infection. The cranial and middle lung lobes are preferentially affected due to the inherent vulnerability of the bronchoalveolar junction and gravitational effects. In haematogenous infections, the caudal lung lobes may be more severely affected. Involvement of the entire lobe is often seen as extensive collateral ventilation allows rapid spread of infection (lobar pneumonia). Clinical signs are variable but often include:

- Soft cough with increased respiratory effort
- Anorexia and lethargy
- Pyrexia is variably present
- Clinical signs of an underlying cause, e.g. regurgitation, dysphagia.

Animals with impaired immune systems or mucociliary clearance (e.g. ciliary dyskinesia) are predisposed. Irish Wolfhounds and brachycephalic dogs are also predisposed.

Radiography: A three-view study is very useful to assess all lung areas and differentiate alveolar disease from collapse. The radiographs may be normal (or just have an interstitial pattern) in the early stages. Changes often start in the tip of the lobes. Findings include (see also Figures 11.15, p. 235, 11.16, p. 236 and 12.45):

- Alveolar pattern, often affecting the entire lobe (lobar pneumonia) (Figures 12.108 and 12.109)
- Ventral location is most common
- Patchy peribronchial areas in bronchopneumonia
- Predominately cranial and middle lobes affected
- Asymmetrical distribution is common
- Variable bronchial component but normally present (Figure 12.110)
- In bacterial pneumonia, secondary to haematogenous infection, may get generalized miliary or nodular pattern or septic infarction
- Small volume of pleural fluid or pleural thickening in severe cases
- After recovery, a mild bronchial pattern often remains
- Abscess formation with a cavitating lung lesion is occasionally seen
- If there is necrosis of the lung, may get spontaneous pneumothorax

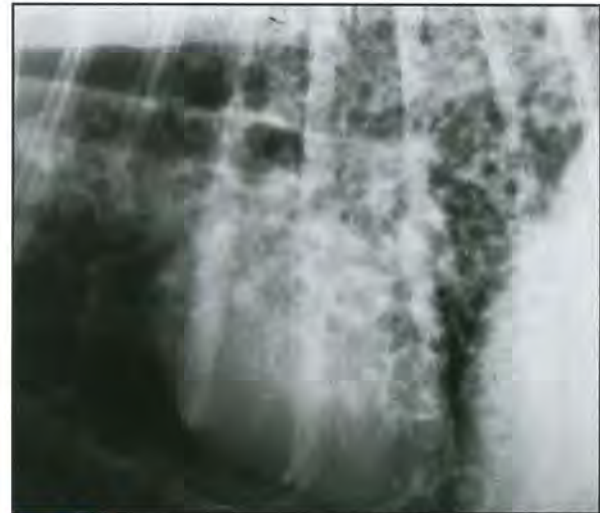
- Ciliary dyskinesia often results in bronchiectasis, and situs inversus may be seen (right-to-left transposition of thoracic and abdominal viscera).

Other imaging techniques: For ciliary dyskinesia other techniques include:

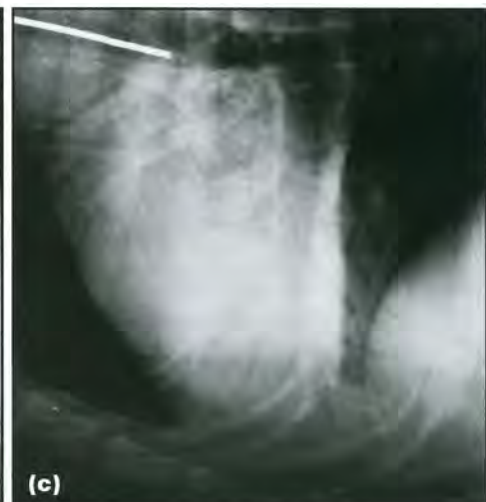
- Nasal radiography, CT and MRI to identify associated non-destructive rhinitis
- Brain CT/MRI to demonstrate associated hydrocephalus in some cases
- Scintigraphy to demonstrate lack of mucociliary clearance (see Figure 11.17, p. 236).



12.108 Lateral thoracic radiograph of a 1-year-old English Springer Spaniel with bronchopneumonia. Typical radiographic features include patchy areas of alveolar pattern and peribronchial infiltrate throughout the lungs. (Courtesy of Cambridge Veterinary School)



12.110 Lateral thoracic radiograph of a dog with bronchiectasis and associated bronchopneumonia. Notice the numerous widened, irregular, thick-walled bronchial ring shadows surrounded by lung tissue of increased opacity. The oesophagus is distended with gas.



12.109 **(a)** VD thoracic radiograph of a 6-year-old Briard with lobar pneumonia of the right middle lung lobe. There is an alveolar lung pattern with air bronchograms of the entire lobe with clear margination to neighbouring lobes (lobar sign). The heart is partially obliterated by the lobe (border obliteration sign) and mainly contained within the right hemithorax (cardiac shift), indicating a degree of collapse of the right middle lung lobe. **(b)** Right lateral thoracic radiograph. Due to the hypostatic collapse of the entire right lung, the opacification of the middle lobe is not distinguishable. **(c)** Left lateral thoracic radiograph. The now non-dependent right lung is fully aerated again, except for the middle lobe which is now visibly opacified. This is an indication of alveolar disease rather than just hypostatic lung collapse. Notice the DV orientation of the right middle bronchus, facilitating preferential aspiration in this lobe. The radiopaque marker in the trachea should be ignored as it was placed for an interventional procedure.

For lung consolidation (and abscessation) thoracic ultrasonography may be used. Findings include:

- Homogenous, mid to low echogenic lung (see also Figure 12.51)
- Often small areas of gas with reverberation artefacts
- The lung may be mildly, but not markedly, enlarged with rounded borders as seen with lung lobe torsion
- *Fluid bronchograms* may be seen (Figure 12.111): branching anechoic fluid-filled bronchus. Doppler ultrasonography helps differentiate fluid bronchograms from blood vessels
- Abscesses may be identified.



12.111 Dorsal plane thoracic ultrasound image of a 5-year-old Staffordshire Bull Terrier with pneumonia. The visible right caudal lung lobe is echogenic and contains two anechoic tubular structures, representing a pulmonary artery (black arrowhead, confirmed with Doppler ultrasonography) and a fluid-filled bronchus with hyperechoic walls (mineralized cartilage, white arrowheads). This is called a *fluid bronchogram* and is useful in the differentiation of altered lung tissue from masses or herniated abdominal organs (liver).

Aspirates can be obtained for culture and sensitivity. It should be noted that consolidated lung may mimic the appearance of the liver, especially when large fluid bronchograms are present. Care should be taken not to misdiagnose liver herniation.

CT (high-resolution, contrast-enhanced) may be used for the diagnosis of lung abscessation, interstitial pneumonia and differentiation from other lung diseases (Figure 12.112).

Non-specific feline pneumonia: Pneumonia occurs less commonly in cats than in dogs. Clinical signs include coughing, increased tracheal sensitivity, dyspnoea and tachypnoea. Coughing may be absent. Males are possibly predisposed. A variety of infectious agents have been recorded but the most common are *Pasteurella multocida*, *Escherichia coli*, *Klebsiella pneumoniae*, *Bordetella bronchiseptica*, *Salmonella* spp., and eugonic fermenter-4 infection.

Radiography: Radiographic findings include:

- May have a granular appearance in the early stages with peribronchial spread
- Bronchial pattern in combination with alveolar disease is most common



12.112 High-resolution thoracic CT image at the level cranial to the aortic arch of a 12-year-old Miniature Dachshund with severe respiratory distress of unclear aetiology after clinical and radiographic work-up. There is partial consolidation of the right cranial lung lobe with a ventral distribution, consistent with pneumonia. The dog improved after antibiotic treatment.

- Right middle and cranial lobes most commonly affected, often lobar signs
- Nodular pattern may be seen with toxoplasmosis, mycoplasmosis, cryptococcosis and eugonic fermenter-4 infection (Figure 12.113)
- *Pasteurella* infection often causes abscessation.



12.113 Lateral thoracic radiograph of a cat with polyarthritis. There are multiple ill defined areas of focal alveolar disease with a nodular appearance in places. Based on the clinical signs and radiographic changes, a granulomatous lung disease was suspected but neoplasia and pneumonia were differential diagnoses. A bronchoalveolar lavage showed chronic inflammatory changes. The lesions resolved following antibiotic therapy.

Aspiration and fistulous pneumonia: This is caused by pulmonary intake of large particles or fluid. Aspiration of small quantities of oral contents is common and does not cause problems if there are normal respiratory defence mechanisms. Barium is commonly aspirated if orally fed for alimentary

contrast studies; small to medium amounts are well tolerated by animals, but resorption by tributary lymph nodes can take months to years. See Lipid pneumonia (below) for details about oil or milk aspiration.

With defective mucociliary clearance, immunodeficiency or aspiration of large quantities of infective material, aspiration pneumonia may develop. Gastric contents cause chemical damage to the airways and resultant airway constriction and oedema. This may be followed by secondary bacterial infection and development of ARDS. Airway obstruction or constriction may occur.

Aspiration usually affects the cranial and ventral aspect of the lungs, unless the animal aspirated whilst anaesthetized or recumbent when any part of the lung may be affected. Aspiration is common with any condition causing megaesophagus and dysphagia, and is most commonly seen in the right middle lobe. Clinical signs include:

- Acute dyspnoea within 2 hours of aspiration; may be longer if particulate material, e.g. food
- Coughing, tachypnoea, wheezing and cyanosis.

Chronic tracheobronchial foreign bodies may lead to lobar pneumonia, due to occlusion of the bronchus and secondary bacterial infection (see Chapter 11):

- Caudal and middle lobes are most commonly affected
- Grass awns are the commonest inhaled foreign body in dogs, usually in summer/autumn
- Large-breed and working dogs predisposed
- Clinical signs of acute onset coughing after running in vegetation.

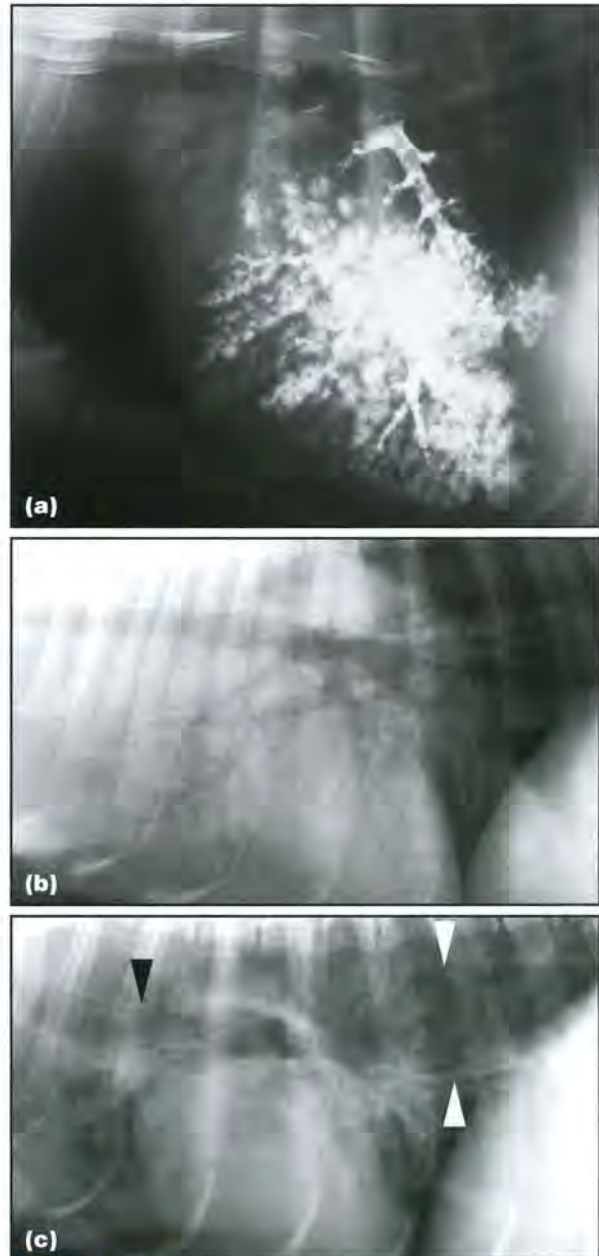
Broncho-oesophageal or bronchogastric fistulae are rare causes of pneumonia and are usually traumatic in origin (secondary to foreign body) but may be congenital. Clinical signs are of recurrent pneumonia and often associated with eating.

Radiography: Radiographs are normal in the initial stages but develop abnormalities within 12–36 hours. In cases of particulate aspiration, radiographic changes may take longer to appear and disappear. The dependent lung at the time of aspiration is predominantly affected. Cranioventral parts of the cranial and middle lobes are most commonly affected, often with lobar opacification (Figure 12.114). Signs of the underlying condition may be seen, especially with oesophageal disease.

A combination of aspiration pneumonia, megaesophagus and cranial mediastinal mass are commonly seen in thymoma and may be reversible if the tumour can be treated successfully.

Other imaging techniques:

- Barium contrast oesophagram (see also Chapter 9) to identify oesophageal diseases causing aspiration. Barium aspiration may further aggravate lung disease.
- Fluoroscopic barium contrast study to demonstrate the functional abnormalities of swallowing.



12.114 (a) Lateral thoracic radiograph of a 9-year-old Labrador Retriever obtained after a barium oesophagram had been performed. The oesophagus is normal, but barium was aspirated in the right middle and left caudal lung lobes. (b) Lateral thoracic radiograph of a German Shepherd Dog with severe aspiration pneumonia. Note the typical cranial and ventral distribution of alveolar opacity with air bronchograms. (c) Lateral thoracic radiograph of a Shih-Tzu with aspiration pneumonia and megaesophagus. Note the generalized dilatation of the oesophagus (between white arrowheads) and ventral deviation of the trachea (black arrowhead). There are multifocal areas with an alveolar pattern within the dependent lobes, most marked in the right middle lobe.

- Iodine-based oesophagram to investigate fistulous pneumonia.
- Thoracic CT for bronchial obstruction and bronchiectasis (see Figures 11.9, p. 233 and 11.19, p. 238).
- Head CT or MRI for suspected central nervous cause of reduced gag reflex.

Canine leptospiral pneumonia: Clinical signs relate to acute renal failure rather than pulmonary involvement.

Radiography: A mild to marked un- or fine-structured interstitial pattern is seen, most noticeable in the caudodorsal lung fields or disseminated patchy opacities (Figure 12.115). In severe cases there may be a generalized increase in opacity in all lobes.

Other imaging techniques: Renal ultrasonography may be used to demonstrate increased renal cortical echogenicity, subcapsular fluid and an echogenic medullary band.

Mycoplasmal pneumonia: *Mycoplasma* spp. are small bacteria that are part of the normal oral flora in dogs and cats. In the lungs, mycoplasmal bacteria are involved in lower airway and lung disease, along with other bacteria. Immunodeficient or

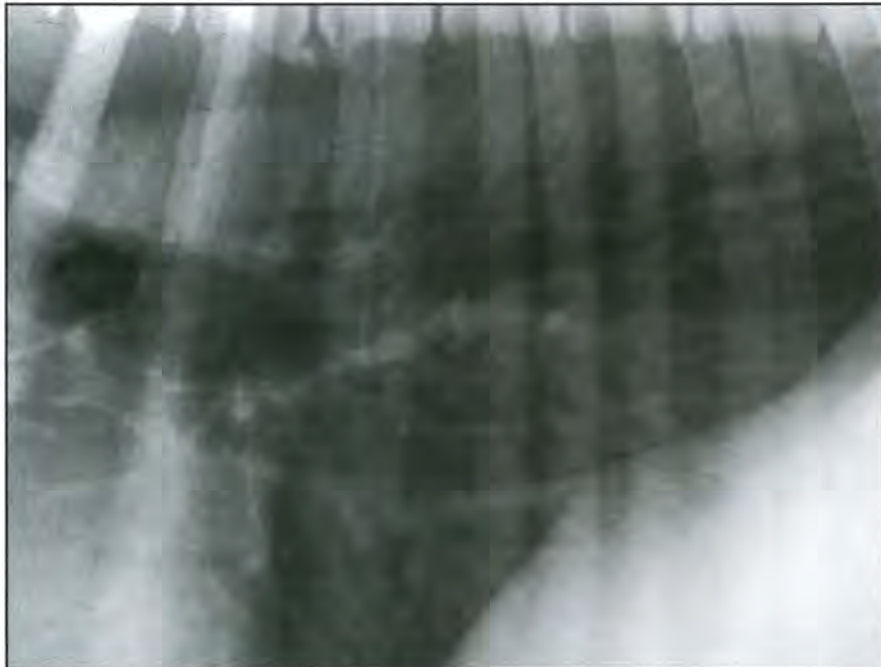
otherwise compromised animals are predisposed to mycoplasmal disease.

Radiography: A diffuse bronchointerstitial pattern is seen (Figure 12.116). An alveolar component is less common.

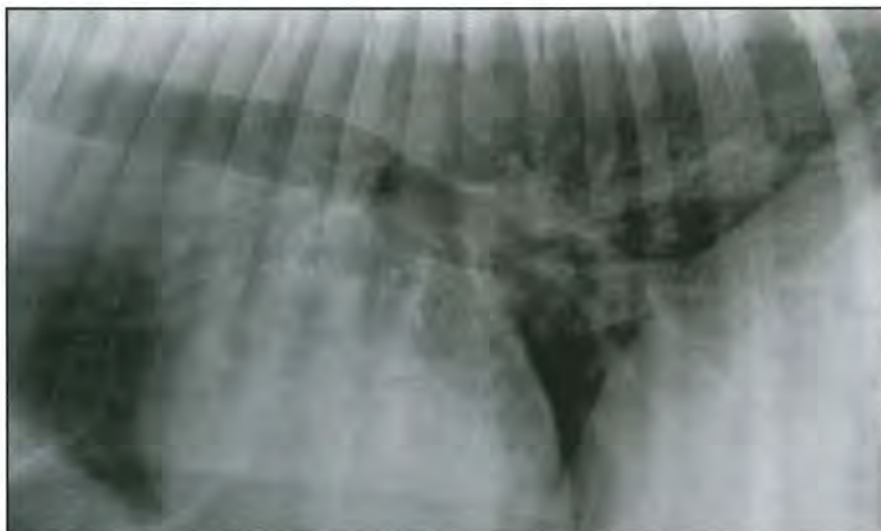
Viral pneumonia: Common pneumonia-inducing viruses include:

- Dogs: canine distemper virus, canine adenovirus 2, canine parainfluenza
- Cats: feline calicivirus.

Young, unvaccinated or immunocompromised animals are most commonly affected. Clinical signs include pyrexia, coughing and oculonasal discharge. Thoracic involvement with feline coronavirus infection (which causes feline infectious peritonitis) usually presents as pleural effusion rather than lung disease.



12.115 Caudodorsal close-up of a lateral thoracic radiograph of a dog with leptospiral pneumonia. There is a mild increase in lung opacity with a fine-structured interstitial pattern, typical of mild or early-phase leptospirosis.



12.116 Lateral thoracic radiograph of a 9-year-old mixed breed dog with mycoplasmal pneumonia. There is a diffuse bronchointerstitial lung pattern throughout the lungs.

Radiography: Radiographic findings (see also Figure 12.135) include:

- Radiographs may be normal
- Mild diffuse interstitial lung pattern, often in the caudodorsal lung fields (Figure 12.117)
- In severe cases, an alveolar lung pattern
- Peribronchial cuffing, if there is secondary bacterial infection; the radiographic signs resemble those seen with bacterial and aspiration pneumonia.

Fungal pneumonia: Dimorphic fungi have a relatively well defined geographical distribution due to their specific growth requirements (Figure 12.118). Species include:

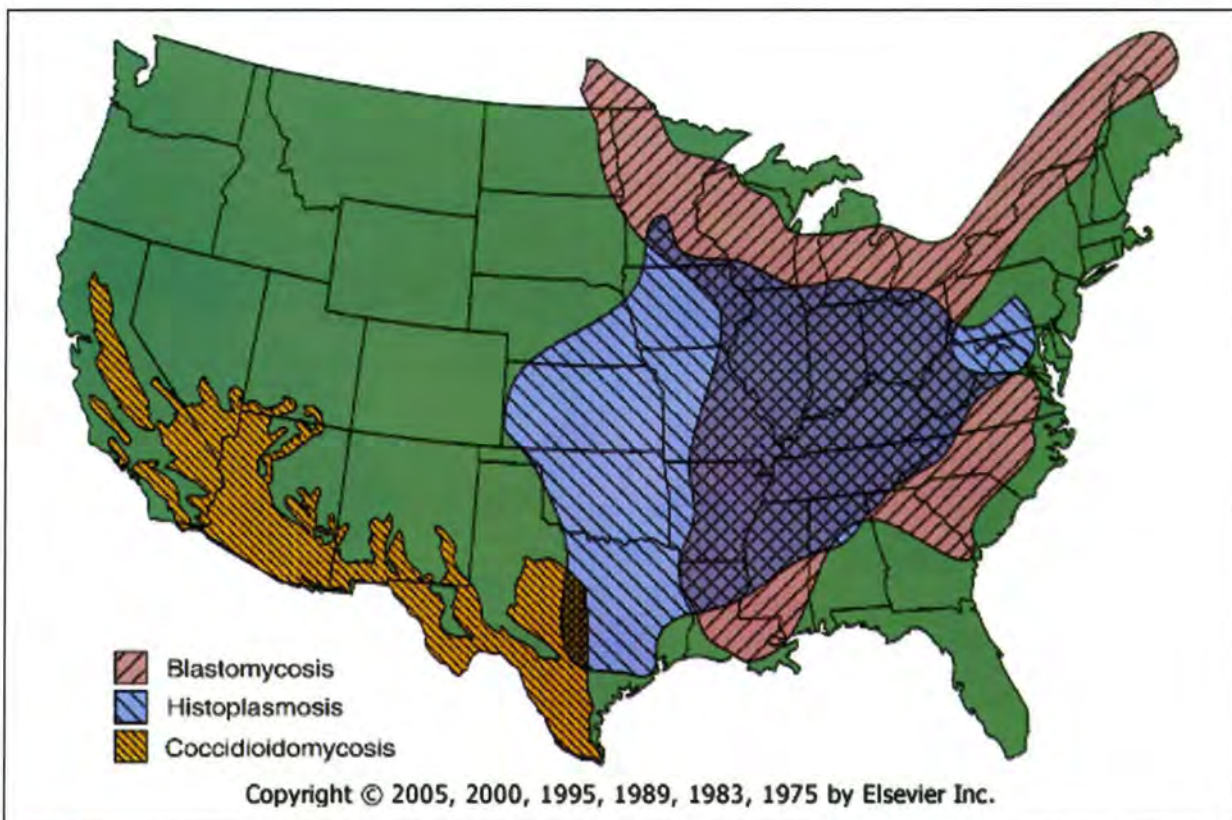
- *Histoplasma capsulatum*
- *Blastomyces dermatitidis*
- *Coccidioides immitis*.

Yeast species, e.g. *Cryptococcus neoformans*, have a worldwide distribution. Infection occurs due to inhalation of fungal particles in most cases. Dimorphic fungi convert from the mycelial to the parasitic phase at body temperature and can cause primary infection in the lungs and mediastinal lymph nodes. Failure of the immune system to contain infection can lead to disseminated disease.

Histoplasmosis: This is caused by *Histoplasma capsulatum*. It affects dogs and cats, most commonly less than 4 years old. In dogs there is usually



12.117 Lateral thoracic radiograph of a 7-month-old Chihuahua with canine distemper virus infection. There is a diffuse increase in lung opacity with an interstitial pattern, more pronounced caudodorsally. This feature is representative of an early viral stage of pneumonia. Bacterial secondary infection will add a patchy alveolar pattern with a random or ventral distribution. (Courtesy of the University of California Davis)



12.118 Major endemic areas for blastomyces, coccidioidomycosis and histoplasmosis in the USA. (Reproduced from Wolf and Troy (1989) with permission from the publisher)

gastrointestinal involvement; in cats there is usually pulmonary involvement. The fungus requires a humid environment and has a wide distribution throughout temperate and tropical regions of the world; in the USA it is found in the drainage system of the Ohio, Missouri and Mississippi rivers (midwestern states).

Clinical signs are often absent; they may include coughing, dyspnoea, weight loss, lethargy and fluctuating fever. Thoracic radiographic findings (see Figures 12.119 and 12.33) include:

- Active phase: diffuse interstitial lung pattern and/or areas of coalescing opacities
- Chronic/healed phase: numerous 2–4 mm soft tissue or mineralized nodules; tracheobronchial lymphadenopathy and mineralization
- Disseminated form: polyostotic aggressive bone lesions are the most obvious radiographic feature.



12.119 Lateral thoracic radiograph of a dog with chronic inactive histoplasmosis. There are numerous small mineralized nodules throughout the lung (calcified granulomas). The left tracheobronchial lymph node (dorsal to the carina) is moderately enlarged and also mineralized.

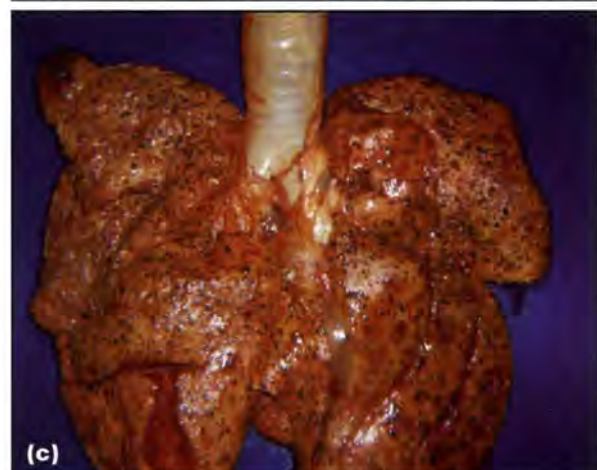
Blastomycosis: This is caused by *Blastomyces dermatitidis*. It is common in dogs and uncommon in cats; most often seen in animals less than 4 years old. It is endemic in southeastern and eastern parts of the USA and southeastern Canada.

Routes of infection and primary focus include:

- Direct skin inoculation
- Inhalation and primary pulmonary form
- Dissemination to abdomen, skeleton and central nervous system possible.

Clinical signs of primary pulmonary form include dyspnoea, tachypnoea, coughing, fever, anorexia and weight loss. Thoracic radiographic findings (Figure 12.120) include:

- Active phase:
 - Miliary or mixed patterns
 - Focal lung nodule/mass/consolidation
 - Pleural effusion
 - Tracheobronchial lymphadenopathy common.



12.120 (a) Lateral thoracic radiograph of a 3-year-old Golden Retriever with active pulmonary blastomycosis. There is alveolar disease cranioventrally and caudodorsally, numerous 2–4 mm soft tissue nodules throughout the lung, and a mild dorsal deviation of the caudal trachea and an associated soft tissue opacity (★) suggestive of mediastinal lymphadenopathy. (Courtesy of the University of California Davis) (b) Lateral thoracic radiograph of a dog with active diffuse pulmonary blastomycosis. There is a miliary pattern throughout the lungs created by many small soft tissue nodules. (c) Corresponding necropsy image with multiple small pulmonary granulomas. (Courtesy of the University of Pennsylvania)

- Chronic/healed phase: tracheobronchial lymphadenopathy possible; numerous non-mineralized nodules
- Disseminated form: polyostotic aggressive bone lesions are the most obvious radiographic feature.

Coccidioidomycosis: This is caused by *Coccidioides immitis*. It is common in dogs and rare in cats. The fungus requires semi-arid conditions and is endemic in southwest and western regions of the USA, and widespread in parts of Mexico, Central and South America.

Routes of infection and primary focus include:

- Direct skin inoculation (very rare)
- Inhalation and primary pulmonary form
- Dissemination to abdomen, skeleton and central nervous system possible.

The primary pulmonary form often has no clinical signs (subclinical and self-limiting). There may be a mild cough and fever, partial anorexia and weight loss. Thoracic radiographic findings (Figure 12.121; see also Figure 8.8b, p. 180) include:

- Active phase: interstitial lung pattern; tracheobronchial lymphadenopathy possible
- Chronic/healed phase: disseminated, ill defined soft tissue nodules; tracheobronchial lymphadenopathy is uncommon
- Disseminated form: polyostotic aggressive bone lesions are the most obvious radiographic feature.



12.121 (a) Lateral thoracic radiograph of a 2-year-old Rottweiler with pulmonary coccidioidomycosis. There is a diffuse pattern of poorly circumscribed nodules throughout the lungs and perihilar lymphadenopathy, causing caudal tracheal deviation. (b) Postmortem image of a lung section demonstrates disseminated fungal granulomas. (Courtesy of the University of California Davis)

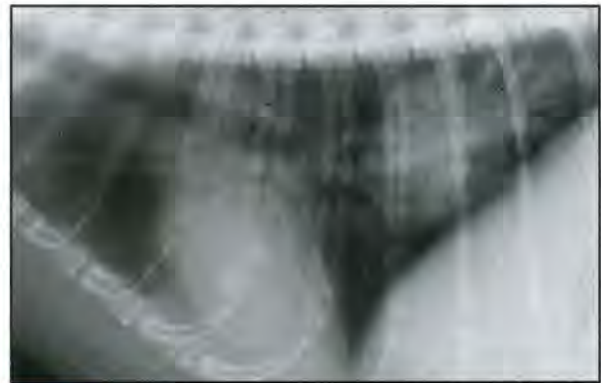
Cryptococcosis: This is caused by the yeast *Cryptococcus neoformans*. It is common in cats and uncommon in dogs. It has a worldwide distribution.

Routes of infection and primary focus include:

- Inhalation and primary nasal form in cats
- May extend to central nervous system and cause neurological disease
- Primary or secondary lung infection is possible.

Thoracic radiographic findings (Figure 12.122) include:

- Multiple nodules or small masses throughout the lungs
- Lung consolidation and pleural effusion possible.



12.122 Lateral thoracic radiograph of a 10-year-old Domestic Shorthair cat with pulmonary cryptococcosis. There is a large caudodorsal soft tissue mass (granuloma) and marked perihilar lymphadenopathy, causing tracheal deviation. (Courtesy of the University of California Davis)

Aspergillosis: This is caused by *Aspergillus* spp. It is common in dogs and rare in cats; the disseminated form is rare in both. German Shepherd Dog bitches are predisposed to the disseminated form. Aspergillosis has a worldwide distribution.

Routes of infection and primary focus include:

- Inhalation and primary nasal form with *Aspergillus fumigatus*; usually restricted to nose
- Inhalation and usually primary pulmonary form with *A. terreus* and *A. deflexus*; haematogenous spread to other organs possible.

There is a variety of non-specific clinical signs with disseminated aspergillosis, often including signs of spinal disease (discospondylitis). Thoracic radiographic findings include:

- Non-specific interstitial lung pattern
- Soft tissue nodules throughout the lungs
- Usually less important than other organ changes, such as discospondylitis.

Pneumocystosis: *Pneumocystis carinii* is a ubiquitous saprophytic fungus that is present within the alveoli in normal animals. Clinical signs are seen in immunocompromised dogs and include dyspnoea, weight loss and exercise intolerance. Young Cavalier King Charles Spaniels and Miniature Dachshunds are predisposed. Naturally occurring clinical disease in cats has not been reported, but it may be caused experimentally with infection and concurrent glucocorticoid therapy. Radiographic findings (Figure 12.123) include:



12.123 Lateral thoracic radiograph of a 1-year-old Cavalier King Charles Spaniel with *Pneumocystis carinii* infection. There is a generalized interstitial pattern with mild bronchial thickening. The generalized nature of the changes in a young dog is unusual but in combination with the breed is highly suggestive of pneumocystosis.

- Usually a generalized diffuse interstitial and peribronchial pattern, progressing to an alveolar lung pattern (most marked in the middle lobes), which is symmetrical
- May affect all lung lobes and be severe, but cranioventral lobes may be relatively spared
- Patchy distribution is less common
- Bronchiectasis, pneumothorax, cavitating lesions and emphysema have also been reported but are uncommon presentations.

Parasitic pneumonia:

Toxoplasmosis: *Toxoplasma gondii* is a protozoa with a worldwide distribution. Cats and other felidae are the only definitive host; they may also serve as intermediate hosts. Clinical toxoplasmosis occurs during the intermediate phase. Cats and dogs may be affected; cats are most commonly infected and have non-specific multiorgan signs. Respiratory involvement is common in acute disease.

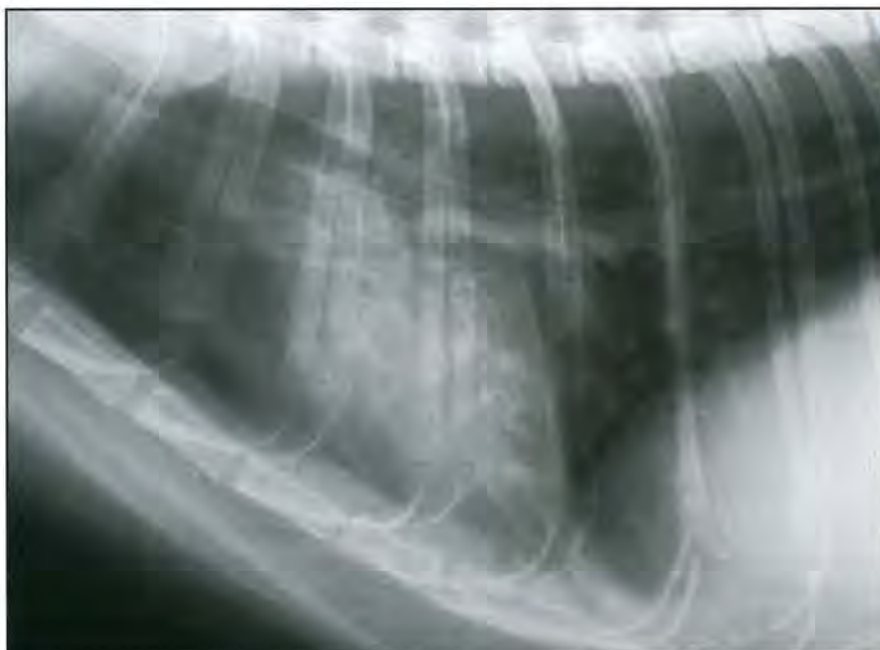
Thoracic radiographic findings (Figure 12.124) include:

- Diffuse interstitial and patchy alveolar infiltrate
- Random distribution of changes.

Heartworm disease: This is caused by *Dirofilaria immitis*, a filarial nematode that resides primarily in the pulmonary arteries (see also Chapter 7). It has a worldwide distribution in temperate and tropical climates, including most of the USA, Central and South America, Japan, Australia and southern Europe.

Clinical signs include exercise intolerance, weight loss, coughing, right-sided heart failure and dyspnoea in severe cases. It is a predisposing factor for pulmonary thromboembolism. Heartworm disease is common in dogs and less common in cats.

Radiographic findings (Figure 12.125; see also Figures 7.153, p. 167 and 7.154, p. 168) include:



12.124 Right lateral thoracic radiograph of a 10-year-old Domestic Shorthair cat with pulmonary toxoplasmosis. There are patchy areas of alveolar lung pattern in the mid-ventral lung fields. The opposite lateral film also revealed right middle lung lobe collapse.



12.125 Lateral thoracic radiograph of a dog with dirofilariosis. There is a widespread increase in lung opacity, caused by enlarged, tortuous pulmonary arteries, and oedematous and granulomatous reactive lung.

- Patchy to extensive alveolar pattern, most marked in the caudal lobes in severe cases
- Changes have a periarterial distribution
- Enlarged and tortuous arteries (caudal in most cases but also often in the cranial lobes) may be seen
- Right-sided heart enlargement
- Pulmonary granulomas present in some cases.

Echocardiography may demonstrate *D. immitis* worms within the right ventricle or main pulmonary artery in some cases (see Figures 7.156, p. 169 and 7.157, p. 169). The worms typically appear as thin, parallel linear echogenicities, or as an echogenic mass in severe cases. Signs of pulmonary hypertension with right ventricular hypertrophy may be seen.

Angiostrongylosis: (French heartworm disease): *Angiostrongylus vasorum* is a metastrongylid parasite of dogs and foxes (see also Chapter 7). The adult worm lives in the main pulmonary artery, the right side of the heart or the pulmonary arterioles. It is most commonly reported in the southern UK and southern Europe; it is rarely diagnosed in the USA.

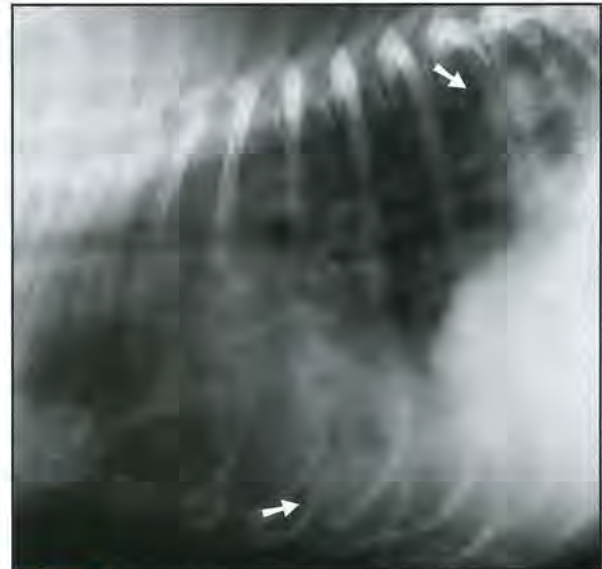
There are two main clinical syndromes:

- Respiratory disease due to an inflammatory response to the eggs and migrating larvae
- Haemorrhagic diathesis, possibly due to antigenic factors secreted by the parasite.

The disease is more common in young dogs, with Cavalier King Charles Spaniels and Staffordshire Bull Terriers possibly over-represented. Clinical signs include coughing, dyspnoea, ecchymotic haemorrhage, haemoptysis, haematomas, gastrointestinal bleeding, vomiting, diarrhoea and neurological disease.

Radiographic findings (Figure 12.126; see also Figure 7.158, p. 170) include:

- Diffuse bronchial and interstitial pattern initially (5 weeks after infection)
- Patchy alveolar pattern with peripheral distribution, preferentially affecting the caudodorsal lung lobes. Maximal changes 7–9 weeks after infection. May have lobar opacification. Bronchial component present in most cases



12.126 Lateral thoracic radiograph of a Staffordshire Bull Terrier with *Angiostrongylus vasorum* infection. Note the peripheral distribution of the pulmonary lesions (arrowed), which is commonly seen in angiostrongyloidosis.

- Small volume of pleural fluid in some cases
- Mild hazy interstitial pattern remains following treatment
- Cardiovascular changes are uncommon.

Paragonimiasis: This is caused by the lung fluke *Paragonimus kellicotti*. It is endemic around the Great Lakes, and in midwestern and southern parts of the USA. Transmission occurs via a crayfish as the intermediate host. Adult flukes reside in pulmonary cysts and cause lung pathology. Clinical signs may be absent; coughing, wheezing and acute dyspnoea with pneumothorax may be seen.

Radiographic findings (see Figure 12.68c) are relatively specific:

- Solitary or multiple ill defined nodular opacities
- Lesions are often cavitated and contain gas pockets
- Peribronchial or interstitial infiltrate.

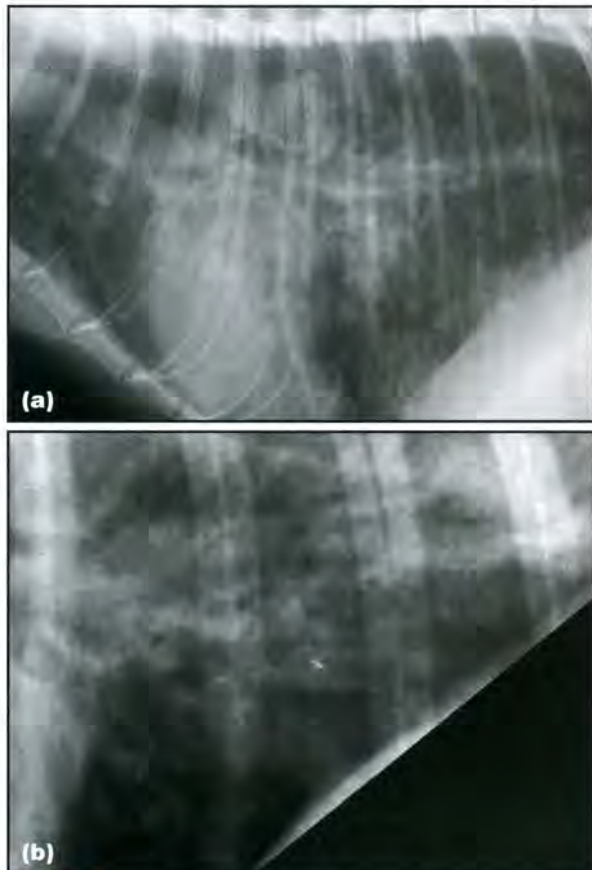
Verminous pneumonia: This is a collective term for pneumonia induced by worms residing in or migrating through the lower airways:

- *Capillaria aerophila* is a small lungworm that resides in the upper airways and bronchi of dogs and cats
- *Aelurostrongylus abstrusus* is a small lungworm in cats that resides in the bronchioli
- *Filaroides hirthi* is a small lungworm that resides in the terminal bronchioli and alveoli in dogs
- *Oslerus osleri* is a worm that resides in the trachea and major bronchi of dogs (see Chapter 10)
- *Crenosoma vulpis* is a worm that resides in the trachea, bronchi and bronchioli of dogs.

Clinical signs of lungworms may be absent or those of bronchopneumonia. *Toxocara canis*, *Ancylostoma caninum* and *Strongyloides stercoralis* are intestinal parasites in dogs that undergo pulmonary migration. With heavy infection, transient pulmonary signs are possible.

Radiographic findings (Figure 12.127; see also Figure 10.25, p. 223) include:

- Patchy bronchointerstitial and/or alveolar pattern
- Miliary or nodular pattern (*Filaroides hirthi*, *Aelurostrongylus abstrusus*)
- Tracheobronchial abnormalities (*Oslerus osleri*).



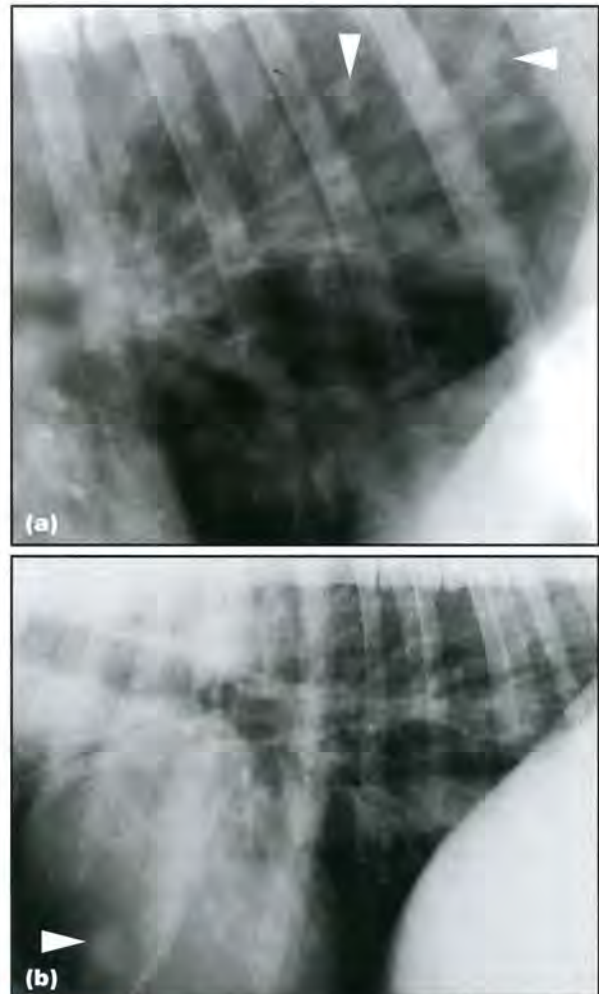
12.127 **(a)** Lateral thoracic radiograph of a 7-month-old Domestic Shorthair cat with an *Aelurostrongylus abstrusus* infection in the small airways. There is a bronchointerstitial infiltrate with peribronchial thickening throughout the lungs. **(b)** Caudodorsal close-up of a lateral radiograph of a 2-year-old Cavalier King Charles Spaniel with a *Filaroides hirthi* infection. There is a bronchointerstitial lung pattern with marked bronchial thickening.

Allergic pneumonia:

Pulmonary infiltrate with eosinophilia: Pulmonary infiltrate with eosinophilia (PIE; eosinophilic bronchopneumonopathy) is a manifestation of immunological hypersensitivity. The underlying cause cannot be found in most cases. It usually occurs in young adult or middle-aged dogs. Siberian Huskies and Alaskan Malamutes are possibly predisposed. The main clinical sign is coughing, but signs may include dyspnoea, exercise intolerance and nasal discharge.

Radiographic findings include:

- Bronchointerstitial pattern in most cases, with or without bronchiectasis (Figure 12.128; see also Figure 12.47)
- Less commonly, nodules and pulmonary masses are seen
- Patchy alveolar pattern and lobar consolidation in severe cases
- Distribution is similar to bronchopneumonia, but it is often diffuse and has a tendency to affect the caudodorsal lobes.



12.128 **(a)** Caudodorsal close-up of a lateral thoracic radiograph of a 2-year-old Boxer with PIE. There is a bronchointerstitial lung pattern with bronchial mineralization and thickening, and small areas of peribronchial infiltrate (arrowheads). **(b)** Lateral thoracic radiograph of a 2-year-old Boxer with chronic coughing and eosinophilia. There is a bronchointerstitial pattern with mineralized and thickened bronchi throughout the lungs, and two ovoid soft tissue nodules (one is visible on this view, arrowhead). The differential diagnoses includes PIE with lung granulomas, as well as neoplastic and fungal disease.

Pulmonary alveolar proteinosis: This is a pathological accumulation of surfactant proteins and phospholipids. It is suspected to be a primary condition or to occur secondarily to exposure to inhaled allergens. Clinical signs include progressive exercise intolerance,

increased respiratory sounds and coughing. It has only been reported in two young small to medium-sized dogs.

Radiographic findings include:

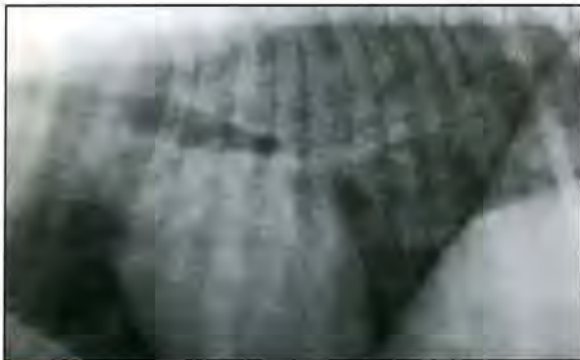
- Patchy alveolar pattern, most marked in the caudal lobes but affecting all lungs lobes
- Fine diffuse unstructured interstitial pattern, more common in humans and also reported in a dog.

Other non-infectious pneumonia:

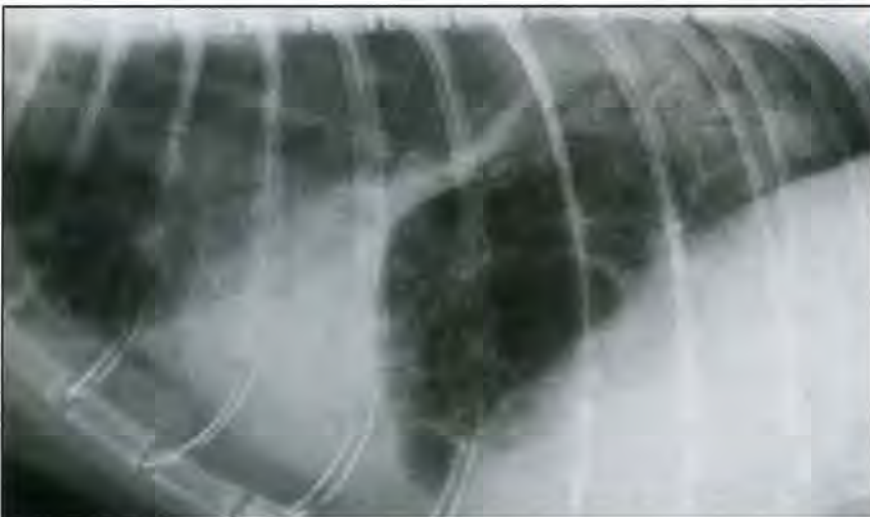
Inhalation pneumonia: This is caused by intake of noxious gases, fumes, aerosols and vapours. It is rare in dogs and cats. Smoke inhalation is a specific form of inhalation pneumonia (see above). Usually, it is a result of inhalation of non-infectious toxic substances, such as acute inhalation of carpet cleaner or chronic exposure to silicate dusts. Silicate pneumoconiosis is a rare disease in dogs exposed to silicate dusts, resulting in chronic coughing.

Radiographic findings include:

- Predominantly interstitial or bronchointerstitial pattern (Figure 12.129)
- Perihilar lymphadenopathy with silicosis
- Smoke inhalation (see above).



12.129 Lateral thoracic radiograph of a 6-month-old Afghan Hound that developed acute dyspnoea after being doused in chlorinated carpet cleaner. There is a diffuse interstitial to alveolar pattern throughout the lungs. The preferential caudodorsal distribution is a hallmark of inhalation pneumonitis.



12.130 Lateral thoracic radiograph of a cat with exogenous lipid pneumonia. The cat had been medicated with liquid paraffin for constipation. Note the right middle lung lobe collapse, caudodorsal alveolar opacity and bronchiectasis, and cavitating lesions throughout the ventral lungs. The generalized interstitial pattern could be related to lipid transport without removal by pulmonary macrophages.

Lipid pneumonia (lipoid pneumonia): Exogenous lipid pneumonia is most commonly reported in cats. It is due to oil aspiration following forced oral oil administration (e.g. liquid paraffin for constipation or hairballs) or aspiration of milk. The severity of the lung changes depends upon the type and amount of oil aspirated:

- Most vegetable oils are reportedly non-irritant
- Animal and some vegetable oils are hydrolysed by pulmonary lipases and invoke an acute inflammatory response and necrosis
- Mineral oils act as foreign bodies and provoke a granulomatous reaction
- Macrophages transport lipids throughout the lungs, where they can persist for years.

There is no coughing reflex with mineral oil aspiration. There may be a varying degree of respiratory compromise, and the animal may be febrile, anorexic and depressed. *Endogenous lipid pneumonia* is seen occasionally in cats and rarely in dogs. The pathogenesis is uncertain:

- Stressor on alveolar membrane: airway obstruction, toxic inhalants or disturbed lipid metabolism
- Pulmonary cell wall breakdown and alveolar type II cell proliferation
- Overproduction of cholesterol-containing surfactant that is phagocytosed but not removed by macrophages.

Radiographic findings include:

- Diffuse interstitial lung pattern in mild cases or as a late change (can persist for several years)
- Poorly circumscribed alveolar opacities in severe cases (Figure 12.130)
- Consolidation peripheral to a bronchial obstruction (endogenous form)
- Cavitated lung lesions with granulation (mineral oil aspiration)
- Changes are chronic and do not resolve with standard antimicrobial treatment.

Thoracic mycobacterial and other granulomatous diseases

Mycobacterial infection of the thorax is more common in dogs than in cats. Pulmonary tuberculosis is normally acquired as an aerogenous infection. The incidence of fungal infection is related to geography; it is very rare in the UK and USA, and most parts of western and central Europe. Clinical signs are variable but there is often weight loss, chronic coughing and dyspnoea if there is a large volume of pleural fluid.

Radiography: Radiographic findings include:

- Multiple patchy areas of ill defined soft tissue opacity (see Figure 12.46)
- Usually multiple lobes are affected and there is an asymmetrical distribution
- Primary foci often occur initially within the dorsal aspect of the lobes
- Spread of infection follows the bronchial tree
- May appear nodular but nodules are poorly margined
- *Actinomyces*, *Nocardia* and mycobacterial infections often have similar radiographic findings, with intrathoracic lymphadenopathy, pleural fluid (may be localized) and nodules, pulmonary masses or lobar consolidation. Multiple nodules are more common in mycobacterial and *Nocardia* infections. Nodules or masses may cavitate
- Mineralization of the lymph nodes or granulomas in some cases of mycobacterial infection
- Periosteal reaction on the ribs and sternebrae may be seen in cases of *Actinomyces* infection.

Other imaging techniques: Ultrasonography allows identification of enlarged sternal lymph nodes and guided fine-needle aspiration. In addition, CT allows complete assessment of the thorax (see Figures 3.7, p. 69 and 12.53).

Pulmonary neoplasia

Neoplastic causes of the alveolar pattern may be due to extension of the tumour into the alveoli, bronchial obstruction or inflammatory reaction to the tumour. An alveolar pattern may be seen with both primary and, less commonly, secondary pulmonary neoplasia.

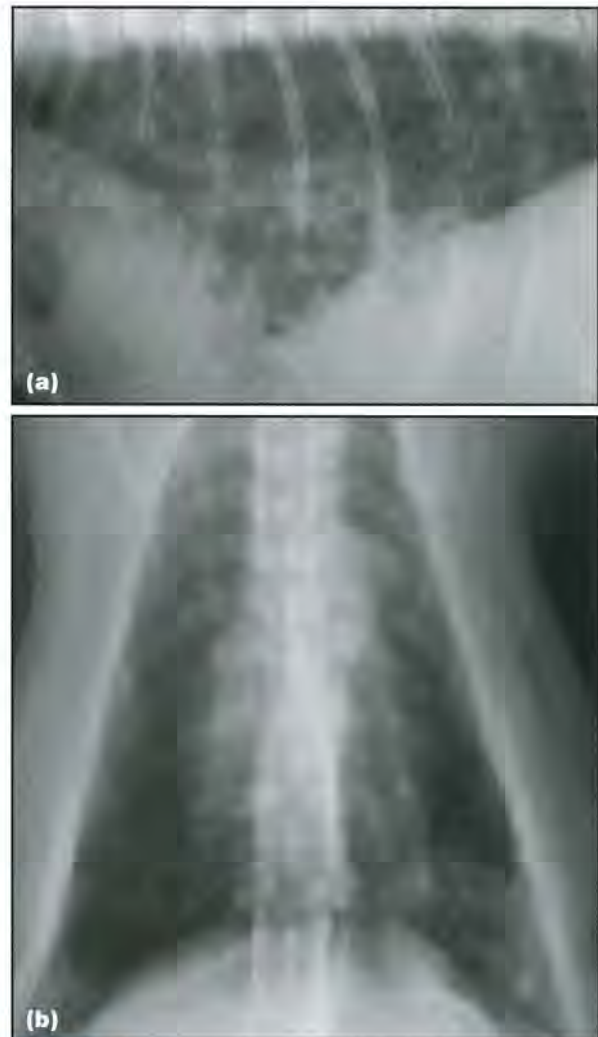
Neoplastic alveolar disease is chronic and does not resolve with standard antimicrobial treatment (see Figure 12.81cd). The lack of short-term temporal evolution helps differentiate it from the more common acute alveolar diseases.

Primary lung tumours frequently cause lobar consolidation either due to obstruction of a bronchus or direct invasion of the lobe, but usually affect single lobes. Air bronchograms are uncommon, in contrast to acute alveolar disease, as the bronchi are often filled by tumour tissue or displaced by it. Lymphoma and some bronchoalveolar tumours grow around the airways, so may result in air bronchograms.

In cats, generalized or multifocal alveolar disease may be seen with primary and metastatic tumours. Neoplasia should be suspected if there is enlargement of an affected lobe, particularly in older animals.

Radiography: Radiographic findings (see Figures 12.23, 12.38 to 12.43, 12.48, 12.49 and 12.68b) include:

- Primary lung tumours are most common in the caudal lobes
- Feline bronchoalveolar carcinoma results in a mixed bronchoalveolar pattern (Figure 12.131a), ill defined alveolar masses and cavitated masses (Figure 12.131b). These are seen in combination with: bronchiectasis or other bronchial abnormalities; an interstitial component of lung opacity; and possibly a generalized or focal mass
- Metastatic neoplasia in cats may cause focal consolidation or patchy alveolar opacities (often mammary or other carcinoma) (see Figure 12.55)
- Pulmonary collapse (rather than consolidation) can occur with a hilar mass obstructing the lobar bronchus and secondary resorption atelectasis (Figure 12.132)



12.131 (a) Lateral thoracic radiograph of a 12-year-old Domestic Shorthair cat with a bronchoalveolar carcinoma. There is a mixed bronchoalveolar pattern and bronchiectasis present throughout all lung lobes. (b) DV thoracic radiograph of a 10-year-old Domestic Shorthair cat with a bronchoalveolar carcinoma. There is a generalized bronchointerstitial pattern throughout the lungs and a cavitated mass in the left caudal lobe. (Courtesy of E. Ballegeer)



12.132 DV thoracic radiograph of a cat with a pulmonary carcinoma. The left caudal lung lobe has a soft tissue opacity and is partially collapsed (cardiac and diaphragmatic shift, arrowed). This is most likely to be the result of bronchial obstruction and peripheral resorption atelectasis.

- Diffuse metastatic carcinoma is a very rare cause of the diffuse interstitial/alveolar pattern in dogs
- Multicentric lymphoma may occasionally give rise to an alveolar pattern (multiple lobes and patchy or diffuse pattern) but usually in association with lymphadenopathy, with or without pleural fluid (see Figure 12.39b)
- A small amount of pleural effusion is commonly associated with pulmonary neoplasia (Figure 12.133):
 - Usually caused by the prevention of normal lymphatic lung drainage
 - May contain malignant cells (*malignant effusion*)
 - May be most marked around lesion.

Other imaging techniques: Ultrasonography is useful in pulmonary neoplasia both to identify and to characterize the lesion, as well as to sample it for definitive diagnosis (see Figure 12.50):

- Neoplastic masses may have a wide variety of appearances but are often solid and homogenous
- An increase in lobar size and rounding of lobar borders will usually be seen
- Doppler ultrasonography is useful to identify vascularity within a mass
- Neoplastic masses may be more likely to have smooth regular margins at their junction with the normal lung, in comparison with non-neoplastic consolidation where the junction may be irregularly margined
- Gas or mineralized foci may be seen within the mass. Necrotic centres may also be identified as more hypo- or anechoic regions.



12.133 DV thoracic radiograph of a cat with unilateral pleural effusion. There is preferential collapse of the left cranial lung lobe with accumulation of fluid around the collapsed lobe (arrowed). This is suggestive of pathology within the left cranial lobe. Ultrasound-guided fine-needle aspiration of the affected lung confirmed lymphoma.

CT and MRI may both allow identification of pulmonary masses (see Figures 3.6, p. 69, 4.4, p. 73, 12.38 and 12.52). CT is preferred as it is faster and allows better assessment of the airways; it also allows assessment of the tracheobronchial lymph nodes.

Predominantly interstitial lung diseases

The pulmonary interstitium consists of the subse-rosal lung capsule and a network of fibroblasts, collagen and elastic fibres covering the alveolar membranes, airways and vessels. Dogs and cats lack interstitial septae between the lung lobes. The interstitium has a trophic and immunoprotective function, provides a mechanical framework for the alveoli, airways and vessels, and is responsible for the elastic recoil of the lung. Diseases that affect the interstitium often change the pulmonary compliance (see Figure 12.15):

- Destruction of the elastic fibre network results in an abnormally *high* compliance, e.g. emphysema, causing distended air spaces on inspiration and expiration
- Interstitial proliferation results in an abnormally *low* compliance, e.g. interstitial fibrosis, resulting in incompletely distended air spaces on inspiration.

The major types of pulmonary interstitial disease are:

- Fluid accumulation causing interstitial oedema
- Infiltration with inflammatory or neoplastic cells
- Chronic conditions causing collagen deposition, fibrosis and mineralization.

All of these conditions cause thickening of the alveolar walls and peribronchial tissues, which results in an overall increased opacity of the lungs and blurring of the fine vascular structures (see Interpretive principles, above). Primarily interstitial lung diseases may be localized or diffuse, with systemic diseases often associated with diffuse pulmonary involvement. Interstitial disease can progress to an alveolar pattern if the alveoli become fluid-filled, such as in acute interstitial pneumonia or secondary pneumonia, or if the alveolar walls become markedly thickened and the alveolar sac is compressed. However, identification of an interstitial pattern can help to determine the nature of the disease process. The interstitial pulmonary pattern is a common and often non-specific radiographic sign.

The interstitial pattern must first be differentiated from age-associated changes and physiological causes, such as hypoinflation and obesity. Once the pattern is determined to be significant, a list of differential diagnoses can be formulated. An interstitial pattern is a stage in many disease processes, and the temporal aspect has to be considered in the radiographic interpretation.

All of these remarks refer to the *unstructured* or *fine-structured interstitial pattern*. The nodular pattern, which is also a form of interstitial pattern, is discussed above (see Solid pulmonary masses).

Interstitial oedema

Under normal conditions, there is fluid flux from the pulmonary capillaries through small gaps between the endothelial cells into the interstitium, and drainage from the interstitial space by lymphatic vessels (see also Pulmonary oedema, above). Increased interstitial fluid production (oedema) occurs due to one or more of the following:

- Increased microvascular hydrostatic pressure
- Reduced capillary oncotic pressure
- Increased vascular permeability
- Reduced lymphatic drainage.

The pulmonary lymphatics can increase their drainage capacity 3–10 fold in an acute situation to prevent oedema from occurring. If this flow is exceeded fluid starts to accumulate, initially in the interstitial tissues surrounding the vessels and lymphatics. The largest amount of fluid tends to gather around the pulmonary arteries.

The interstitial space can expand up to twice its normal volume. When the pressure in the expanded interstitial space rises to a similar pressure to the alveolar interstitium, forward flow decreases and the alveolar interstitium starts to expand, causing alveolar wall thickening. Eventually, the alveolar walls cannot withstand the pressure and gaps or ruptures form in

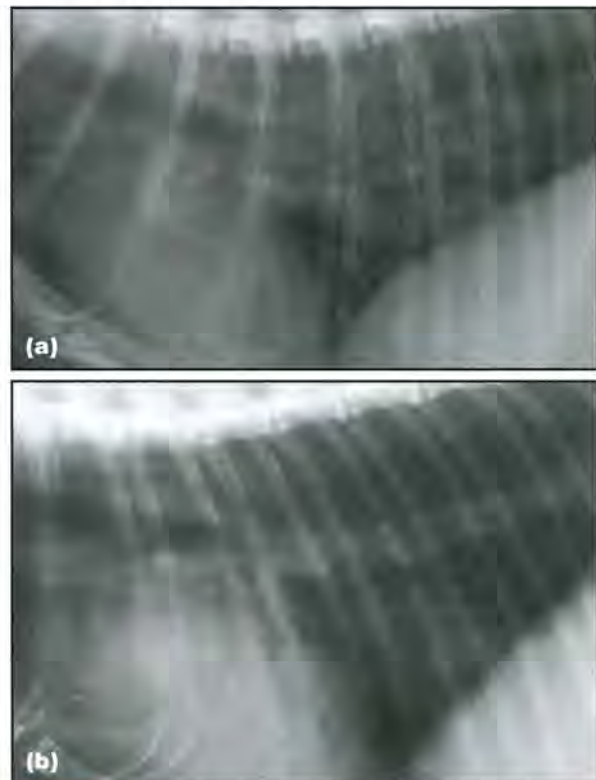
the alveolar epithelium. Filling of the alveoli with fluid is the alveolar stage of pulmonary oedema.

Radiography: Interstitial oedema can be recognized radiographically only if no alveolar opacities are superimposed, and should be expected in the:

- Early stage of developing pulmonary oedema
- Late stage in the resolution of pulmonary oedema
- Less affected area of an oedematous lung.

Radiographic features may include:

- Mild increase in lung opacity (see Figure 12.92b)
- First- and second-branch pulmonary vessels are still visible, but the edges become indistinct and the bronchi may become more prominent
- A 'ground-glass' pattern – fine, granular soft tissue opacity
- Generally homogenous, may become patchy as it progresses to alveolar oedema
- Interstitial pulmonary pattern in the perihilar region or right caudal lung lobe (dogs and cats) (Figure 12.134)
- Diffuse or peripheral patchy interstitial to alveolar pattern (cats)
- Rapid progression or resolution of disease on repeat radiographs.



12.134 **(a)** Lateral thoracic radiograph of a cat with hypertrophic cardiomyopathy and cardiogenic interstitial pulmonary oedema. There is cardiomegaly, pulmonary vascular distension, a small amount of pleural effusion and a diffuse interstitial pattern throughout the lungs, most pronounced in the perihilar region. **(b)** Repeat radiograph 12 hours after initiation of diuretic treatment reveals persistent cardiomegaly, normal sized pulmonary vessels, resolution of the pleural effusion and lung opacification. Prompt resolution of radiographic signs after diuresis is a hallmark of cardiogenic pulmonary oedema.

Additional radiographic findings may help to determine the cause of interstitial oedema and are outlined in the Pulmonary oedema section (above).

Interstitial pneumonia

Interstitial pneumonia (see also above) is caused by infiltration of inflammatory cells into the alveolar walls (sparing the airways) or by toxic exposure. The original inflammatory or toxic insult may arise from the bloodstream or may be carried by aerosol, resulting in acute damage to the alveolar membranes. A number of different aetiologies (viral, bacterial, parasitic, fungal, toxic) may result in pneumonia manifesting as an interstitial pattern.

Interstitial pneumonias are divided into acute and chronic, with some degree of overlap, and may present at either stage:

- Acute pneumonia is often caused by infectious agents and is self-limiting. It does not always cause a radiographic interstitial pattern
- Chronic interstitial pneumonia begins with an acute phase, followed by an ongoing idiopathic or toxic inflammatory process. The final stage is development of fibrosis. Infectious causes of interstitial pneumonia do not usually lead to significant or progressive fibrosis.

Radiography: Radiographic findings (see also Figures 12.115 to 12.117 and 12.129) include:

- Diffuse increase in opacity with poor definition of vessels and bronchi (Figure 12.135)
- Unstructured or fine-structured interstitial pattern
- Occasionally, an alveolar pattern in the acute phase
- Often begins in the lung periphery
- Less uniform than with interstitial oedema
- Tracheal distension with increased respiratory effort

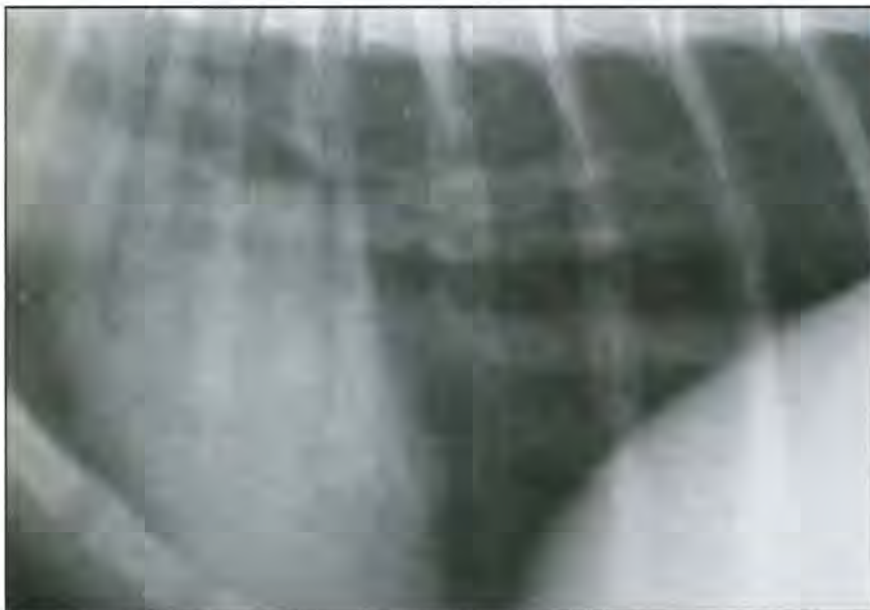
- Acute viral interstitial pneumonia, such as with distemper virus infection, is often complicated by secondary bacterial infection by the time of radiography, resulting in a mixed interstitial to alveolar or bronchial pattern
- Caudodorsal or peribronchial distribution of the interstitial pattern may indicate an inhaled agent or toxin (toxic gases or vapours).

Interstitial fibrosis

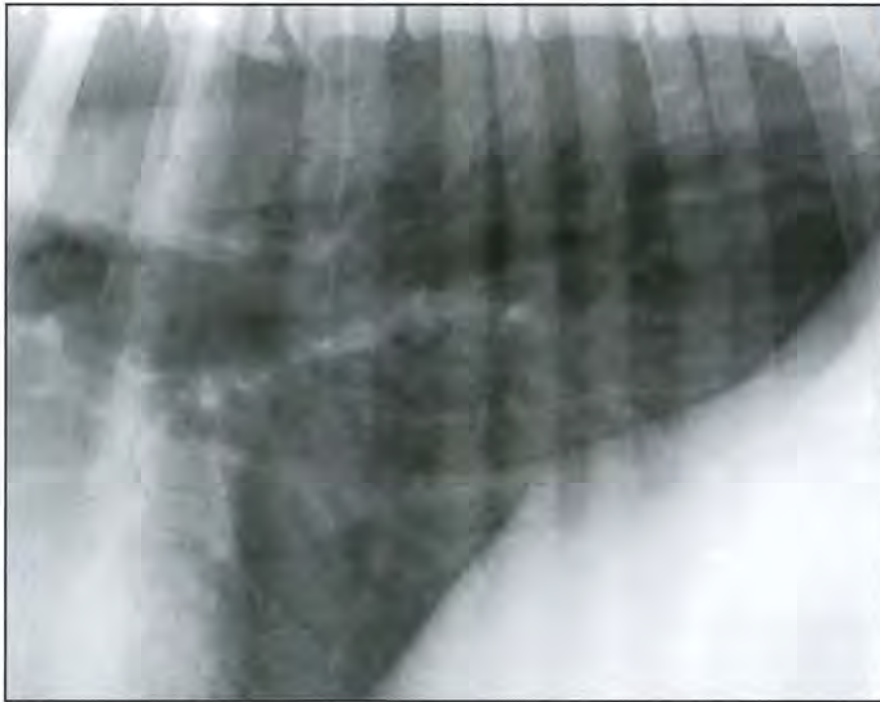
Interstitial fibrosis is the end-stage of a variety of pulmonary diseases with irreversible alterations to the collagen-supporting structures of the interstitium. The original insult may be infectious, inflammatory or idiopathic in nature and often cannot be determined when the animal is presented. Acute infectious pneumonias and cardiogenic pulmonary oedema usually do not result in chronic fibrosis. Pulmonary fibrosis can occur focally, or secondarily to an abscess, infarction or trauma but this is usually insufficient to cause respiratory compromise. Consequences of pulmonary fibrosis are a decrease in functioning lung tissue, compliance and tidal volume.

Radiography: Radiographic findings include:

- Diffuse un- or fine-structured interstitial pattern (Figure 12.136)
- In severe cases of decreased lung compliance, the thoracic volume may be small and the trachea enlarged on inspiratory radiographs:
 - Lumbodiaphragmatic recess at the tenth thoracic vertebra
 - Overlap of the diaphragmatic and cardiac silhouettes
 - Minimal change between the inspiratory and expiratory radiographs.
- Stable radiographic appearance or gradual progression over time
- Pleural fissure lines due to pleural fibrosis.



12.135 Lateral thoracic radiograph of a kitten with acute interstitial pneumonia secondary to feline leukaemia virus infection. The fine vascular structures are blurred yet still visible, and there is an overall increase in lung opacity. Acute viral pneumonia typically presents with radiographically normal lungs or an interstitial lung pattern, as in this case.



12.136 Caudodorsal close-up of a lateral thoracic radiograph of a 5-year-old German Shepherd Dog with marked dyspnoea. There is a fine-structured interstitial pattern throughout the caudodorsal lung fields. The histological diagnosis was pulmonary fibrosis of unknown aetiology.

Idiopathic pulmonary fibrosis: Idiopathic pulmonary fibrosis (IPF) is a chronic progressive fibrosis of the lung interstitium in older terrier breed dogs. It is particularly common in West Highland White and Cairn Terriers. It shares many features with a similarly named condition in humans; a similar but not identical condition has recently been reported in cats.

Affected animals suffer from progressive exercise intolerance, coughing and dyspnoea, and have marked inspiratory crackles on auscultation.

Radiography: Findings in canine IPF (Figure 12.137) include:



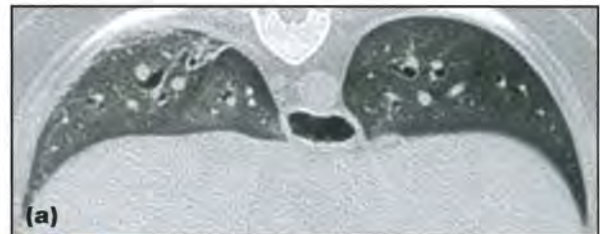
12.137 Lateral thoracic radiograph of a 14-year-old West Highland White Terrier with idiopathic pulmonary fibrosis. Notice the general increase in lung opacity with an interstitial pattern, partial tracheal collapse and dyspnoea-related gas distension of the stomach (aerophagia). There is mild right cardiac and marked hepatic (not included in image) enlargement, features commonly seen in terrier breed dogs with idiopathic pulmonary fibrosis.

- Diffuse interstitial infiltrate in all lung lobes
- Right heart enlargement
- Hepatomegaly of unclear origin. Hepatic congestion due to right heart failure is usually *not* present
- Often concurrent partial tracheal collapse.

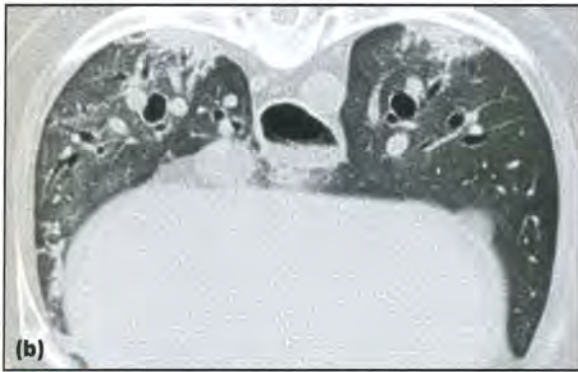
Radiographic signs are non-specific and all differential diagnoses for the interstitial lung pattern apply. The age and breed of the patient should be considered when making the diagnosis, which often requires ruling out other lung diseases (i.e. diagnosis of exclusion). Feline IPF is seen radiographically as patchy interstitial lung opacities.

High-resolution lung computed tomography: Findings of canine IPF (Figure 12.138) include:

- Ground-glass opacity of some or all lung lobes
- Parenchymal bands of lung consolidation
- Subpleural and peribronchial consolidations
- Mild traction bronchiectasis.



12.138 (a) High-resolution lung CT image at the level of the caudal thorax of a 12-year-old West Highland White Terrier with idiopathic pulmonary fibrosis. There is a mild generalized increase in lung opacity (ground-glass opacity) and a small subpleural fibrotic infiltrate in the right caudal lung lobe. The oesophagus is mildly distended with gas. (continues) ▶



12.138 (continued) **(b)** On a slightly more cranial image, there is a hyperattenuating infiltrate in the dorsal portions of both caudal lung lobes and subpleural bands. Patches of ground-glass attenuation are present in the right lung. These changes are consistent with fibrosis.

CT findings of feline IPF (Figure 12.139) include:

- Ground-glass opacity of some or all lung lobes
- Subpleural consolidations
- Parenchymal bands.



12.139 High-resolution lung CT image at the level of the caudal thorax of an 11-year-old obese Domestic Shorthair cat with fibrotic lung changes. Notice the ground-glass opacity of the lung, a small subpleural consolidation (curved arrow) and bands of soft tissue originating from the pleural surface (straight arrow).

Radiation-induced lung fibrosis: Radiation damage to the lung from accidental exposure is rare. However, with radiation therapy for thoracic wall neoplasia and prolonged fluoroscopic and interventional procedures becoming more common, radiation damage to focal areas of the lung may be encountered.

Radiation damage depends on the dose and irradiated volume. Clinical signs are to be expected if more than 25% of both lungs are exposed. The lung is one of the most sensitive tissues with late response to radiation:

- After a latent period of 1–6 months, acute pneumonitis develops, causing interstitial oedema, inflammation and capillary congestion
- Chronic inflammation leads to pulmonary fibrosis 2–24 months after exposure to radiation. These changes are permanent and static.

Radiation pneumonitis may cause clinical signs, such as respiratory distress, decreased exercise tolerance and coughing. These should improve as the inflammatory phase subsides. Radiographic changes are visible 2–3 weeks before the onset of clinical signs.

Radiography: Radiographs are initially normal. At 1–2 months an alveolar pattern is seen (acute pneumonitis) (Figure 12.140). In later stages (2–24 months following exposure) there is:

- Diffuse interstitial pattern (whole body exposure)
- Focal homogenous interstitial or alveolar pattern near the site of the radiation therapy or imaging
- Bronchiectasis
- Cicatrization atelectasis (scar formation) with chronic fibrosis.



12.140 **(a)** Lateral port film of a 9-year-old Domestic Longhair cat for radiation treatment planning with cobalt photons for a non-resectable interscapular fibrosarcoma. The beam field includes the very dorsal aspect of the caudal lung fields. **(b)** Lateral thoracic radiograph obtained 1 month after completion of radiation therapy demonstrates a sharply delineated alveolar opacity of the exposed lung, consistent with acute radiation pneumonitis. **(c)** Caudodorsal close-up of a lateral thoracic radiograph obtained 6 months following radiation. The affected area is now slightly reduced in size and of a mixed interstitial-alveolar pattern. These findings are consistent with radiation-induced chronic lung fibrosis and will remain permanent. (Courtesy of D. Thrall)

Dipyridylum derivate intoxication: Dipyridylum derivatives (paraquat, diquat, morfamquat) are used as desiccant and defoliant herbicides. Paraquat is one of the most commonly used herbicides worldwide and is highly toxic to animals and humans. It reacts with oxygen to form oxygen free radicals, which are extremely damaging to the lungs. Contamination is usually via oral ingestion, and vascular distribution with particular affinity to the lungs. The underlying mechanism of disease damage to the alveolar epithelial cells is necrosis and oedema, and subsequent inflammation and fibrosis of the alveolar septal walls. The clinical course is progressive respiratory and renal failure.

Radiography: Radiographic findings depend on the stage of disease (see Interstitial fibrosis):

- Acutely there may be no radiographic change
- Progressive diffuse interstitial pattern
- Cicatrization atelectasis (scar formation)
- Pleural fibrosis causes fissure lines
- Pneumomediastinum.

Interstitial neoplastic infiltrate

In dogs and cats primary lung neoplasia and metastatic neoplasia can both cause diffuse interstitial patterns. Metastatic diffuse neoplasia is more common than primary diffuse neoplasia, and more common in cats than in dogs. Secondary oedema, infection, infarction, fibrosis and necrosis may accompany neoplastic disease and complicate radiographic diagnosis.

Multicentric lymphoma: This is the most common canine interstitial lung tumour; it rarely affects the lungs of cats. It usually also affects other non-thoracic organs (multicentric). The neoplastic cells accumulate in the interstitium and lymphatic system. The presence of a pulmonary lymphoma infiltrate does not correlate with survival or remission. In dogs with multicentric lymphoma there is thoracic involvement (lymphadenopathy and/or pulmonary infiltrate) in approximately 70% of cases. Thoracic radiographs are indicated in staging lymphoma.

Alveolar septal metastases: These are common with anaplastic mammary carcinoma and less common with salivary or pulmonary carcinoma or transitional cell carcinoma of the urinary bladder. Metastatic spread to the interstitium of the lung occurs via the lymphatic system and microvasculature. Neoplastic cells infiltrate the alveolar septal walls causing thickening, and may also cause thrombosis of small vessels.

Diffuse primary bronchoalveolar carcinoma: This is an uncommon primary lung neoplasia, which spreads along the airways and alveolar interstitium (see also Alveolar diseases).

Haemangiosarcoma: Metastases in the pulmonary capillaries can cause a diffuse fine-structured interstitial pattern.

Radiography:

Multicentric lymphoma: Radiographic findings include:

- Diffuse un- or fine-structured interstitial pattern most common (Figure 12.141a; see also Figures 12.34 and 12.39b). This is often described as reticular, honeycomb or micronodular
- Most apparent in the caudodorsal and perihilar lung fields
- Bronchial wall thickening (neoplastic lymphatic infiltrate)
- The pulmonary vessels are generally well seen despite the interstitial pattern
- May develop within days and regress similarly quickly with chemotherapy
- Very rarely, a nodular pattern or large masses can occur
- Additional common findings are pleural effusion, lymphadenopathy of the tracheobronchial, cranial mediastinal and sternal lymph nodes, and mediastinal widening.



12.141 (a) VD thoracic radiograph of a dog with systemic lymphosarcoma and a diffuse fine-structured interstitial infiltrate. (b) High-resolution CT image at the level caudal to the carina demonstrating a diffuse ground-glass opacity throughout the lungs.

An interstitial pattern with lymphadenopathy is very suggestive of lymphoma, with the other main differential diagnosis being fungal pneumonia. Differential diagnoses of other rapidly appearing interstitial infiltrates are:

- Oedema
- Infection
- Haemorrhage due to trauma or DIC
- Metastatic disease.

Alveolar septal metastases and bronchoalveolar carcinoma: Radiographic findings are not specific (see Figure 12.131) but may include:

- Diffuse interstitial disease with occasional alveolar infiltrates or ill defined nodules
- Hyperlucent lung areas (regional embolic oligoemia)
- Peribronchial cuffing (filling of lymphatic system with tumour cells)
- Pleural thickening
- Mild pleural effusion
- Sternal lymphadenopathy.

Computed tomography:

Multicentric lymphoma: Radiographic diagnosis is usually sufficient. CT may be performed for other reasons and typical features should be recognized:

- Ground-glass opacity (see Figure 12.141b), which may be more prominent in the caudal lung lobes
- Enlarged sternal, cranial mediastinal and tracheobronchial lymph nodes.

Alveolar septal metastases: CT provides exceptional detail of the lung tissue and vasculature, and is very useful for diagnosis and staging of radiographically occult neoplastic disease. Imaging findings in dogs may include:

- Normal pleura
- Subpleural zone:
 - Subpleural lines (see Figure 12.103) due to an interstitial infiltrate and fibrosis
 - Subpleural wedge-shaped interstitial thickening (base parallel to the pleura) caused by neoplastic infiltration and fibrosis
 - Patches of ground-glass opacity caused by tumour cells, necrosis and haemorrhage
 - Subpleural emphysema due to small airway obstruction caused by fibrosis
 - Mosaic perfusion: patchy hyperattenuating and hypoattenuating areas with small pulmonary arteries due to altered perfusion patterns, secondary to neoplastic embolization
 - Distortion of architecture
 - Small nodules
 - Areas of consolidation.
- Peribronchial zone:
 - Peribronchovascular interstitial thickening due to tumour nodules or atelectasis
 - Small nodules
 - Areas of consolidation.

Interstitial mineralization

Mineralization of the pulmonary parenchyma may be dystrophic, metastatic or idiopathic. Calcium and other minerals are concentrated in the mitochondria of the cell or in the vesicles in the extracellular space. Minerals are deposited as non-crystalline calcium phosphate (dystrophic), calcium carbonate salts (metastatic) or hydroxyapatite crystals (dystrophic and metastatic).

Dystrophic mineralization: This occurs with damaged or necrotic lung tissue in dogs with normal serum calcium, and with diseases of calcium metabolism, secondary to parasitic or fungal granulomas (histoplasmosis), abscessation, neoplasia or metabolic disease (hyperadrenocorticism). Diffuse inflammatory lesions that result in fibrosis, such as chronic uraemia, can also have a component of mineralization. Heterotopic bone (pulmonary osteoma) is considered a form of dystrophic mineralization. Small islands of bone matrix are deposited in the pulmonary parenchyma and mineralize. This is commonly seen in older dogs as an incidental finding. Bronchial walls commonly mineralize in dogs, but rarely do so in cats. Osteosarcomas occasionally form osteoid pulmonary metastases.

Hyperadrenocorticism (Cushing's disease): This causes dystrophic mineralization of the soft tissues, including the skin, stomach, arteries, skeletal muscles and kidneys. Cortisol alters glucose production in the liver, and this has catabolic effects. Proteins formed in relation to these processes are altered, and may result in increased calcium binding to the organic matrix. The lungs are one of the most frequently mineralized tissues at the microscopic level; macroscopic radiographically evident mineralization is rare. Serum calcium levels are generally within normal limits.

If the degree of mineralization is severe, dogs may experience significant respiratory distress and be oxygen-dependent. This hypoxaemia may be due to impaired gas diffusion across the mineralized alveolar walls.

Metastatic mineralization: This is caused by altered serum calcium and phosphorus levels with deposition of minerals in the normal tissues. Causes of hypercalcaemia include primary and secondary hyperparathyroidism, hypervitaminosis D, lymphosarcoma, cholecalciferol rodenticide toxicity and disseminated bone cancer, such as multiple myeloma. Tumours (e.g. anal gland carcinomas) can also produce a parathormone-like hormone, which causes hypercalcaemia as a paraneoplastic syndrome. Most instances of metastatic mineralization in the lung are visible only at the microscopic level.

Idiopathic and iatrogenic mineralization: This includes pulmonary alveolar and bronchiolar micro-lithiasis (idiopathic) and mineralization secondary to barium aspiration (iatrogenic).

Radiography: Interstitial lung mineralization can manifest as:

- Normal appearing lung
- Small nodular mineralization (heterotopic bone) (see Figure 12.33)
- Central or peripheral mineralization of masses (see Figures 12.43 and 12.142a)
- Unstructured interstitial lung pattern with or without mineralized appearance (Figure 12.142b)
- Diffuse marked mineralization (alveolar microlithiasis, barium resorption) (see Figures 12.107 and 12.114a).

Hyperadrenocorticism: Radiographic findings in dogs with Cushing's disease are often mild and can be partially caused by artefacts. The obesity of cushingoid dogs means that a high kV setting is required to obtain the radiographs; a high kV reduces image contrast (scatter, high penetration, Compton-related low image contrast). Low image contrast can mimic an interstitial lung pattern. Body condition should, therefore, be taken into account when diagnosing interstitial disease.

Common radiographic findings (see Figures 12.27 and 12.142b) include:

- Mineralization difficult to see radiographically and usually causes an unstructured interstitial pattern

- Marked bronchial mineralization, most pronounced in the caudodorsal lung fields due to an increased volume of lung in that area
- May progress to an alveolar pattern with air bronchograms
- Interstitial pattern does not resolve with diuresis (as opposed to oedema).

Computed tomography: CT is very sensitive to changes in density, and is more sensitive than radiographs at diagnosing pulmonary mineralization (see Figure 12.59). The Hounsfield units (HU) can be measured and compared with the normal values for soft tissue and mineral to determine the presence of mineralization. Soft tissue is usually 30–60 HU, and mineralized tissue is greater. CT is also useful in patients with hyperadrenocorticism to identify pituitary or adrenal masses.

Scintigraphy: Pulmonary mineralization can be diagnosed using nuclear scintigraphy. ^{99m}Techetium-methylene diphosphonate can be injected intravenously, as for a bone scan. At the 2-hour time point, the pulmonary parenchyma will show an increased uptake of radiopharmaceutical due to binding with the hydroxyapatite crystals in the interstitium, which



12.142 **(a)** Left caudal close-up of a VD thoracic radiograph of a 5-year-old Irish Setter with heartworm disease and an associated calcified pulmonary haematoma. Notice the distended left lobar artery (A) and the eggshell-like mineralization of the haematoma. **(b)** Caudodorsal close-up of a lateral thoracic radiograph of a 5-year-old Dachshund with Cushing's disease. Diffuse interstitial and bronchial mineralization has resulted in a bronchointerstitial pattern. The bronchi and pulmonary parenchyma have a subtle mineral opacity. In most cases, interstitial mineralization is not marked enough to cause a mineral radiopacity, and the interstitial opacity is often mistaken for interstitial oedema. A persistent interstitial lung pattern, despite diuretic treatment in hyperadrenocorticoid dogs, should prompt consideration of mineralization and fibrosis as differential diagnoses.

are similar to those in bone (Figure 12.143). This may be a useful technique if the dog has a mild interstitial pattern and it is unclear whether it is due to pulmonary oedema or diffuse mineralization.



12.143 Dorsal thoracic scintigram of a dog obtained approximately 2 hours after intravenous injection of a bone-binding diphosphonate compound. Notice the diffuse radiopharmaceutical uptake in the lungs compared with the photopenic abdomen. Differential diagnoses for this uptake include Cushing's disease, heterotopic bone formation, diffuse pulmonary metastases and recently performed lung scintigraphy.

References and further reading

- Adams WM and Dubielzig R (1978) Diffuse pulmonary alveolar septal metastases from mammary carcinoma in the dog. *Journal of the American Veterinary Radiology Society* **19**, 161–167
- Anderson GI (1987) Pulmonary cavity lesions in the dog. *Journal of the American Animal Hospital Association* **23**, 89–94
- Au JJ, Weisman DL, Stefanacci JD and Palmisano MP (2006) Use of computed tomography for evaluation of lung lesions associated with a spontaneous pneumothorax in dogs: 12 cases (1999–2002). *Journal of the American Veterinary Medical Association* **228**, 733–737
- Ballegeer EA, Forrest LJ and Stepien RL (2002) Radiographic appearance of bronchoalveolar carcinoma in nine cats. *Veterinary Radiology and Ultrasound* **43**, 267–271
- Bair FJ, Gibbs C and Brown PJ (1986) The radiological features of primary lung tumours in the dog: a review of thirty-six cases. *Journal of Small Animal Practice* **27**, 493–505
- Barthez PY, Hornof WJ, Theon AP, Craychee TJ and Morgan JP (1994) Receiver operating characteristic curve analysis of the performance of various radiographic protocols when screening dogs for pulmonary metastases. *Journal of the American Veterinary Medical Association* **204**, 237–240
- Baumann D and Flückiger M (2001) Radiographic findings in the thorax of dogs with leptospiral infection. *Veterinary Radiology and Ultrasound* **42**, 305–307
- Berry C, Galloway A, Thrall DE and Carlisle C (1993) Thoracic radiographic features of anticoagulant rodenticide toxicity in fourteen dogs. *Veterinary Radiology and Ultrasound* **34**, 391–396
- Berry CR, Hawkins EC, Hurley KJ and Monce K (2000) Frequency of pulmonary mineralization and hypoxemia in 21 dogs with pituitary-dependent hyperadrenocorticism. *Journal of Veterinary Internal Medicine* **14**, 151–156
- Berry CR, Moore PF, Thomas WP, Sisson D and Koblik PD (1990) Pulmonary lymphomatoid granulomatosis in seven dogs (1976–1987). *Journal of Veterinary Internal Medicine* **4**, 157–166
- Boag AK, Lamb CR, Chapman PS and Boswood A (2004) Radiographic findings in 16 dogs infected with *Angiostrongylus vasorum*. *Veterinary Record* **154**, 426–430
- Brownlee L and Sellon RK (2001) Diagnosis of naturally occurring toxoplasmosis by bronchoalveolar lavage in a cat. *Journal of the American Animal Hospital Association* **37**, 251–255
- Burk RL, Joseph R and Baer K (1990) Systemic aspergillosis in a cat. *Veterinary Radiology and Ultrasound* **31**, 26–28
- Carpenter DH, Macintire DK and Tyler JW (2001) Acute lung injury and acute respiratory distress syndrome. *Compendium on Continuing Education for the Practicing Veterinarian* **23**, 712–725
- Chandler JC and Lappin M (2002) Mycoplasmal respiratory infections in small animals: 17 cases (1988–1999). *Journal of the American Animal Hospital Association* **38**, 111–119
- Clercx C, Reichler I, McEntee K *et al.* (2003) Rhinitis/bronchopneumonia syndrome in Irish Wolfhounds. *Journal of Veterinary Internal Medicine* **17**, 843–849
- Cohn LA, Norris CR, Hawkins C *et al.* (2004) Identification and characterization of an idiopathic pulmonary fibrosis-like condition in cats. *Journal of Veterinary Internal Medicine* **18**, 632–641
- Coleman MG, Warman CGA and Robson MC (2005) Dynamic cervical lung hernia in a dog with chronic airway disease. *Journal of Veterinary Internal Medicine* **19**, 103–105
- Confer AW, Qualls CW Jr, MacWilliams PS and Root CR (1983) Four cases of pulmonary nodular eosinophilic granulomatosis in dogs. *Cornell Veterinarian* **73**, 141–151
- Corcoran BM, Cobb M, Martin MWS *et al.* (1999) Chronic pulmonary disease in West Highland white terriers. *Veterinary Record* **144**, 611–616
- Cornell KK and Waters DJ (1998) The cat is not a small dog: ten issues in feline oncology. *Kleintierpraxis* **43**, 17–24
- D'Anjou MA, Tidwell AS and Hecht S (2005) Radiographic diagnosis of lung lobe torsion. *Veterinary Radiology and Ultrasound* **46**, 478–484
- Drobatz KJ, Walker LM and Hendricks JC (1999) Smoke exposure in dogs: 27 cases (1988–1997). *Journal of the American Veterinary Medical Association* **215**, 1306–1311
- Drobatz KJ, Walker LM and Hendricks JC (1999) Smoke exposure in cats: 22 cases (1986–1997). *Journal of the American Veterinary Medical Association* **215**, 1312–1316
- Drolet R, Kenefick KB, Hakomaki MR and Ward GE (1986) Isolation of group eugonic fermenter-4 bacteria from a cat with multifocal suppurative pneumonia. *Journal of the American Veterinary Medical Association* **189**, 311–312
- Egenvall A, Hansson K, Sateri H, Lord PF and Jonsson L (2003) Pulmonary oedema in Swedish hunting dogs. *Journal of Small Animal Practice* **44**, 209–217
- Fitzgerald SD, Wolf DC and Carlton WW (1991) Eight cases of canine lymphomatoid granulomatosis. *Veterinary Pathology* **28**, 241–245
- Flückiger MA and Gomez JA (1984) Radiographic findings in dogs with spontaneous pulmonary thrombosis or embolism. *Veterinary Radiology* **25**, 124–131
- Forrest LJ and Graybush CA (1998) Radiographic patterns of pulmonary metastasis in 25 cats. *Veterinary Radiology and Ultrasound* **39**, 4–8
- Foster SF, Martin P, Allan GS, Barrs VR and Malik R (2004) Lower respiratory tract infections in cats: 21 cases (1995–2000). *Journal of Feline Medicine and Surgery* **6**, 167–180
- Foster SF, Martin P, Davis W, Allan GS, Mitchell DH and Malik R (1999) Chronic pneumonia caused by *Mycobacterium thermoresistibile* in a cat. *Journal of Small Animal Practice* **40**, 453–464
- Godshalk CP (1994) Common pitfalls in radiographic interpretation of the thorax. *Compendium on Continuing Education for the Practicing Veterinarian* **16**, 731–739
- Gottfried SD, Popovitch CA, Goldschmidt MH and Schelling C (2000) Metastatic digital carcinoma in the cat: a retrospective study of 36 cats (1992–1998). *Journal of the American Animal Hospital Association* **36**, 501–509
- Hahn KA and McEntee MF (1997) Primary lung tumors in cats: 86 cases (1979–1994). *Journal of the American Veterinary Medical Association* **211**, 1257–1260
- Hayward NJ, Baines SJ, Baines EA and Herrtage ME (2004) The radiographic appearance of the pulmonary vasculature in the cat. *Veterinary Radiology and Ultrasound* **45**, 501–504
- Herrtage ME and Clarke DD (1985) Congenital lobar emphysema in two dogs. *Journal of Small Animal Practice* **26**, 453–464
- Hoover JP, Henry GA and Panciera RJ (1992) Bronchial cartilage dysplasia with multifocal lobar bullous emphysema and lung lobe torsions. *Journal of the American Veterinary Medical Association* **201**, 599–602
- Hudson JA, Montgomery RD, Powers RD and Brawner WR (1994) Presumed mineral oil aspiration and cavity lung lesion in a dog. *Veterinary Radiology and Ultrasound* **35**, 277–281
- Jarvinen AK, Saario E, Andresen E *et al.* (1995) Lung injury leading to respiratory distress syndrome in young Dalmatian dogs. *Journal of Veterinary Internal Medicine* **9**, 162–168
- Jefferies AR, Dunn JK and Dennis R (1987) Pulmonary alveolar proteinosis (phospholipoproteinosis) in a dog. *Journal of Small Animal Practice* **28**, 203–214
- Jerram RM, Guyer CL, Braniecki A, Read WK and Hobson HP (1998) Endogenous lipid (cholesterol) pneumonia associated with bronchogenic carcinoma in a cat. *Journal of the American Animal Hospital Association* **34**, 275–280

- Johnson VS, Corcoran BM, Wotton PR, Schwarz T and Sullivan M (2005) Thoracic high-resolution computed tomographic findings in dogs with canine idiopathic pulmonary fibrosis. *Journal of Small Animal Practice* **46**, 381–388
- Johnson VS, Ramsey IK, Thompson H *et al.* (2004) Thoracic high-resolution computed tomography in the diagnosis of metastatic carcinoma. *Journal of Small Animal Practice* **45**, 134–143
- Jones DJ, Norris CR, Samii VF and Griffey SM (2000) Endogenous lipid pneumonia in cats: 24 cases (1985–1998). *Journal of the American Veterinary Medical Association* **216**, 1437–1440
- Kerr LY (1989) Pulmonary edema secondary to upper airway obstruction in the dog: a review of nine cases. *Journal of the American Animal Hospital Association* **25**, 207–212
- King L (2003) *Textbook of Respiratory Disease in Dogs and Cats*. WB Saunders, Philadelphia
- Kirberger RM and Lobetti RG (1998) Radiographic aspects of *Pneumocystis carinii* pneumonia in the miniature Dachshund. *Veterinary Radiology and Ultrasound* **39**, 313–317
- Kramek BA, Caywood DD and O'Brien TD (1985) Bullous emphysema and recurrent pneumothorax in the dog. *Journal of the American Veterinary Medical Association* **186**, 971–974
- LaRue MJ, Garlick DS, Lamb CR and O'Callaghan MW (1990) Bronchial dysgenesis and lobar emphysema in an adult cat. *Journal of the American Veterinary Medical Association* **197**, 886–888
- Lipscomb VJ, Hardie RJ and Dubielzig RR (2003) Spontaneous pneumothorax caused by pulmonary blebs and bullae in 12 dogs. *Journal of the American Animal Hospital Association* **39**, 435–444
- Liu SK, Suter PF and Ettinger S (1969) Pulmonary alveolar microlithiasis with ruptured chordae tendineae in mitral and tricuspid valves in a dog. *Journal of the American Veterinary Medical Association* **155**, 1692–1703
- Lord PF (1975) Neurogenic pulmonary edema in the dog. *Journal of the American Animal Hospital Association* **11**, 778–783
- Lord PF (1976) Alveolar lung diseases in small animals and their radiographic diagnosis. *Journal of Small Animal Practice* **17**, 283–303
- Lord PF and Gomez JA (1985) Lung lobe collapse. Pathophysiology and radiologic significance. *Veterinary Radiology* **26**, 187–195
- Marino DJ and Jaggy A (1993) Nocardiosis. A literature review with selected case reports in two dogs. *Journal of Veterinary Internal Medicine* **7**, 4–11
- Matros L, Riedesel EA and Myers RK (1994) Silicate pneumoconiosis in a dog: case report and current concepts of pathogenesis. *Journal of the American Animal Hospital Association* **30**, 375–381
- McEntee MC, Page RL, Cline JM and Thrall DE (1992) Radiation pneumonitis in 3 dogs. *Veterinary Radiology and Ultrasound* **33**, 190–197
- Moise NS, Wiedenkeller D, Yeager AE, Blue JT and Scarlett J (1989) Clinical, radiographic, and bronchial cytologic features of cats with bronchial disease: 65 cases (1980–1986). *Journal of the American Veterinary Medical Association* **194**, 1467–1473
- Moon M (1992) Pulmonary infiltrate with eosinophilia. *Journal of Small Animal Practice* **33**, 19–23
- Moon ML, Greenlee PG and Burk RL (1986) Uremic pneumonitis-like syndrome in ten dogs. *Journal of the American Animal Hospital Association* **22**, 687–691
- Munden RF and Hess KR (2001) 'Ditzels' on chest CT: survey of the members of the Society of Thoracic Radiology. *American Journal of Roentgenology* **176**, 1363–1369
- Myer W (1980) Radiography review: the interstitial pattern of pulmonary disease. *Veterinary Radiology* **21**, 18–23
- Neath PJ, Brockman DJ and King LG (2000) Lung lobe torsion in dogs: 22 cases (1981–1999). *Journal of the American Veterinary Medical Association* **217**, 1041–1044
- Nemanic S, London CA and Wisner ER (2006) Comparison of thoracic radiographs and single breath-hold helical CT for detection of pulmonary nodules in dogs with metastatic neoplasia. *Journal of Veterinary Internal Medicine* **20**, 508–515
- Nykamp SG, Scrivani PV and Dykes NL (2002) Radiographic signs of pulmonary disease: an alternative approach. *Compendium on Continuing Education for the Practicing Veterinarian* **24**, 25–35
- Olsson S-E (1957) On tuberculosis in the dog. A study with special reference to X-ray diagnosis. *Cornell Veterinarian* **47**, 193–219
- O'Neill RG, Schwarz T, Thompson H, Sullivan M and Argyle DJ (2006) Pulmonary alveolar microlithiasis: undoubtedly underdiagnosed. *The Irish Veterinary Journal* **59**, 627–632
- O'Sullivan SP (1989) Paraquat poisoning in the dog. *Journal of Small Animal Practice* **30**, 361–364
- Parent C, King LG, Walker LM and Van Winkle TJ (1996) Clinical and clinicopathologic findings in dogs with acute respiratory distress syndrome: 19 cases (1985–1993). *Journal of the American Veterinary Medical Association* **208**, 1419–1427
- Phillips S, Barr S, Dykes N *et al.* (2000) Bronchiolitis obliterans with organizing pneumonia in a dog. *Journal of Veterinary Internal Medicine* **14**, 204–207
- Radlinsky MG, Homco LD and Blount WC (1998) Ultrasonographic diagnosis – radiolucent pulmonary foreign body. *Veterinary Radiology and Ultrasound* **39**, 150–153
- Reif JS and Rhodes WH (1966) The lungs of aged dogs: a radiographic-morphologic correlation. *Journal of the American Veterinary Radiological Society* **7**, 5–11
- Rooney MB, Lanz O and Monnet E (2001) Spontaneous lung lobe torsion in two pugs. *Journal of the American Animal Hospital Association* **37**, 128–130
- Schwarz T, Crawford PE, Owen MR, Störk CK and Thompson H (2001) Fatal pulmonary fat embolism during humeral fracture repair in a cat. *Journal of Small Animal Practice* **42**, 195–198
- Schwarz T, Störk CK, Mellor D and Sullivan M (2000) Osteopenia and other radiographic signs in canine hyperadrenocorticism. *Journal of Small Animal Practice* **41**, 491–495
- Scott-Moncrieff JG, Elliott GS, Radovsky A and Blevins WE (1989) Pulmonary squamous cell carcinoma with multiple digital metastases in a cat. *Journal of Small Animal Practice* **30**, 696–699
- Silverman S, Poulos PW and Suter PF (1976) Cavitary pulmonary lesions in animals. *Journal of the American Veterinary Radiological Society* **17**, 134–146
- Silverstein D, Greene C, Gregory C, Lucas S and Quandt J (2000) Pulmonary alveolar proteinosis in a dog. *Journal of Veterinary Internal Medicine* **14**, 546–551
- Spencer CP, Ackerman N and Burt JK (1981) The canine lateral thoracic radiograph. *Veterinary Radiology* **22**, 262–266
- Stampley AR and Waldron DR (1993) Reexpansion pulmonary edema after surgery to repair a diaphragmatic hernia in a cat. *Journal of the American Veterinary Medical Association* **203**, 1699–1701
- Starrak GS, Berry CR, Page RL, Johnson JL and Thrall DE (1997) Correlation between thoracic radiographic changes and remission/survival duration in 270 dogs with lymphosarcoma. *Veterinary Radiology and Ultrasound* **38**, 411–418
- Suter PF (1984) Chapter 1 – Normal radiographic anatomy and radiographic examination. Chapter 11 – Lower airway and pulmonary parenchymal diseases. In: *Thoracic Radiography: A Text Atlas of Thoracic Diseases of the Dog and Cat*, ed. PF Suter, pp. 1–45, 517–682. Peter F Suter, Wettswil, Switzerland
- Suter PF and Lord PF (1974) Radiographic differentiation of disseminated pulmonary parenchymal diseases in dogs and cats. *Veterinary Clinics of North America: Small Animal Practice* **4**, 687–710
- Thrall DE and Losonsky JM (1976) A method for evaluating canine pulmonary circulatory dynamics from survey radiographs. *Journal of the American Animal Hospital Association* **12**, 457–462
- Tiemessen I (1989) Thoracic metastases of canine mammary gland tumors. A radiographic study. *Veterinary Radiology* **30**, 249–252
- Weaver AD (1982) Severe traumatic pneumothorax and lung prolapse in a Jack Russell bitch. *Veterinary Record* **111**, 505
- Wolf AM and Troy GC (1989) Deep mycotic diseases. In: *Textbook of Veterinary Internal Medicine – Diseases of the Dog and Cat, Volume 1, 3rd edn*, ed. S.J Ettinger, pp. 341–372. WB Saunders, Philadelphia
- Woodring JH and Reed JC (1996) Types and mechanisms of pulmonary atelectasis. *Journal of Thoracic Imaging* **11**, 92–108

The pleural space

Mairi Frame and Alison King

Radiographic anatomy

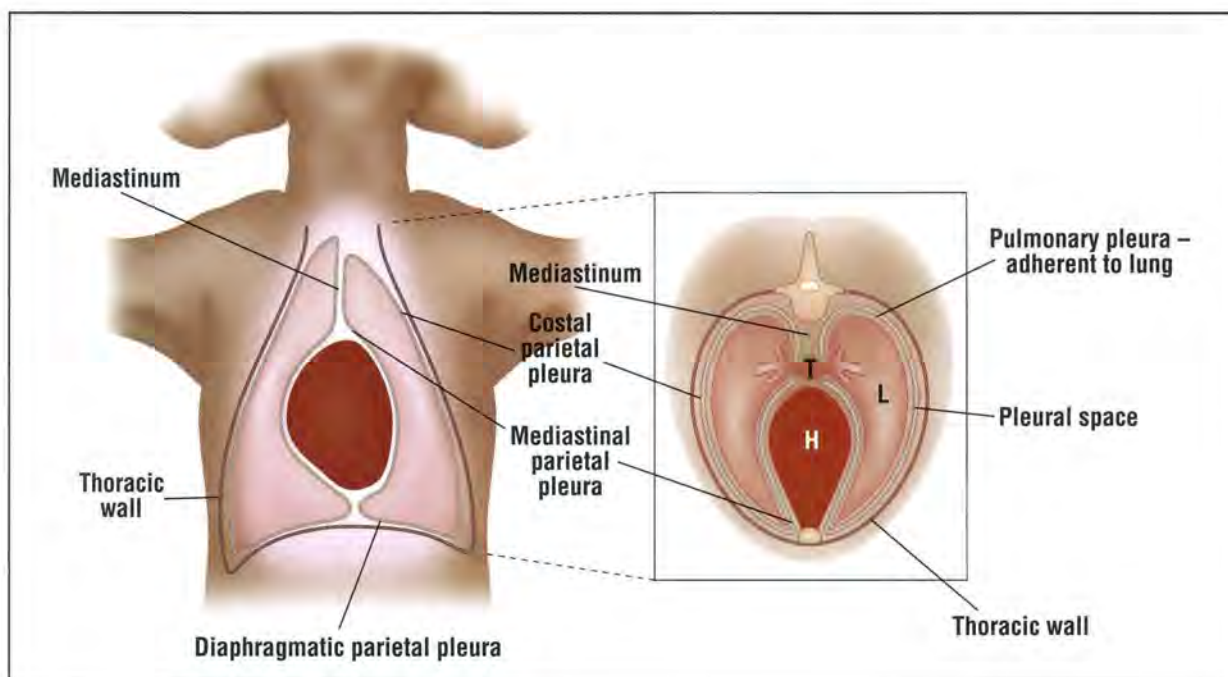
The pleural membrane consists of a single layer of flattened mesothelial cells that overlie a connective tissue layer containing blood vessels and lymphatics. There are two types of pleura: *parietal* and *visceral*.

The *parietal* pleura line the inner surface of the wall of the thorax and the diaphragm, enveloping the central thoracic structures including the heart, great vessels and oesophagus to form the mediastinum (Figure 13.1). They can be divided into costal, diaphragmatic and mediastinal parietal pleura. The parietal pleura tend to curve slightly inward as they cross each rib and to curve slightly outward in the intercostal space. They form a closed cavity on each side that communicates with the contralateral pleural cavity via fenestrations in the mediastinum. These fenestrations are absent in some animals. The pleural space is not continuous with the mediastinum.

The *visceral* pleura cover the lung surface and form the interlobar fissures, merging at the hilus with the mediastinal pleura to form the pulmonary ligaments (Figure 13.1).

The parietal and visceral pleura are separated by the *pleural space*, which is a potential space of normally less than 1 mm in thickness. The pleural space contains a small quantity of fluid (approximately 2–3 ml) as a lubricant to minimize friction during respiration. The surface tension of the pleural fluid holds the lung against the thoracic wall. Negative pressure within the pleural space keeps the lungs inflated against their natural tendency to collapse through elastic recoil, and allows the lung to remain partially expanded even after complete expiration. Negative pressure also plays an important role in maintaining expansion of the small airways, which are not supported by cartilage, during inspiration. There is a continuous high turnover of pleural fluid in normal and diseased states. In humans 5–10 litres of fluid pass through the pleural space in 24 hours.

The parietal pleura are supplied by the systemic circulation via the intercostal and regional arteries; the visceral pleura are supplied and drained by the pulmonary circulation in the dog and cat, which results in an overall movement of pleural fluid between the



13.1 Dorsal plane view of the pleural layers. Note the continuity of the costal, mediastinal and diaphragmatic parts of the parietal pleura (outermost grey line). Inset: Transverse plane view. Note that the pleural space (between the grey lines) is not continuous with the mediastinum. H = Heart; L = Lungs; T = Trachea.

parietal and visceral pleura. The lymphatic vessels of the visceral and diaphragmatic pleura drain the pleural cavity. The pleural fluid moves through the capillaries of the parietal pleura into the pleural space where it is absorbed by the capillaries of the visceral pleura and by lymphatics. Visceral pleural lymphatics play an important role in the circulation of pleural fluid. The lymphatics also provide the only means for proteins, red blood cells and particulate matter to return to the vascular system.

In the cat there is thought to be an anatomical variation in visceral pleural drainage that is incompletely understood. Conflicting information is reported in the literature. The clinical significance of this variation is in the tendency of some cats to develop pleural effusion secondary to left heart failure.

As a general rule, the pleura is too thin to be visible on the thoracic radiograph of a normal dog or cat. However, there are circumstances when the normal pleura may be seen as thin pleural lines:

- Occasionally the X-ray beam traverses the patient exactly parallel to a pleural fissure and is absorbed sufficiently to create a visible line. This is radiographically indistinguishable from mild pleural thickening
- A sharp line is often seen on the left side of a ventrodorsal (VD) or dorsoventral (DV) view, running from near the apex of the heart to the diaphragm. This line has been (falsely) called the cardiophrenic ligament. It is actually a fold of mediastinal pleura lying between the accessory and left caudal lobes. A more correct radiographic descriptive term is the caudoventral mediastinal reflection (see Figure 8.5, p. 179)
- Thickening or calcification of the pleura may occur in older animals, making those membranes that lie parallel to the X-ray beam visible radiographically.

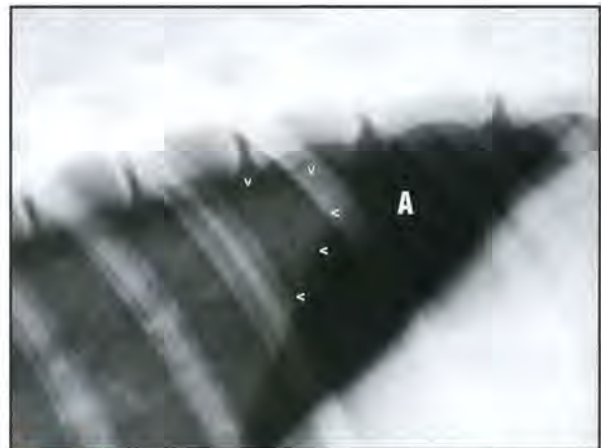
Interpretive principles

Increased or decreased opacity of the pleural space

The pleural space becomes radiographically visible only when distended with gas, fluid, fibrin or cellular material. When distended with fluid, fibrin or cellular material, it will be visible as an area of increased radiopacity. When distended with gas, the pleural space will be seen as an area of decreased opacity outlining the lung lobes (Figure 13.2). Pleural gas is differentiated from air-filled lung tissue by its lack of vascular or bronchial markings (an intensive light source may be required).

Elevation of the cardiac silhouette

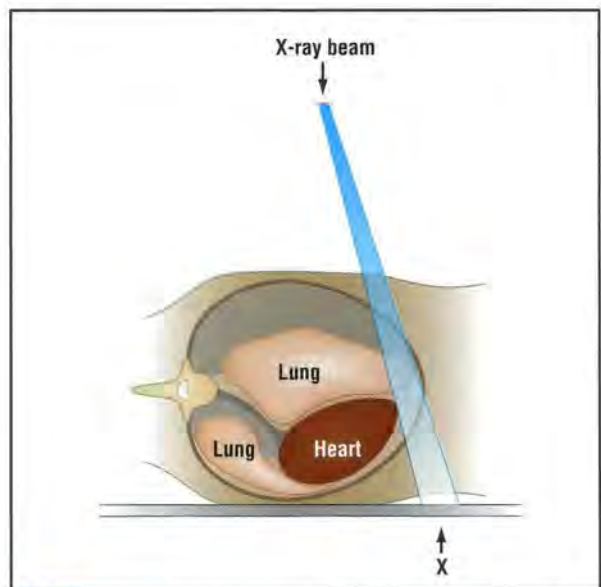
Elevation of the cardiac silhouette from the sternum on the lateral radiograph is a common radiographic feature of pneumothorax in the dog and cat. It may also be seen with pleural effusion, particularly in the cat. The term is misleading as the cardiac silhouette is not really elevated, but rather falls away from the sternum. This phenomenon can be explained by loss



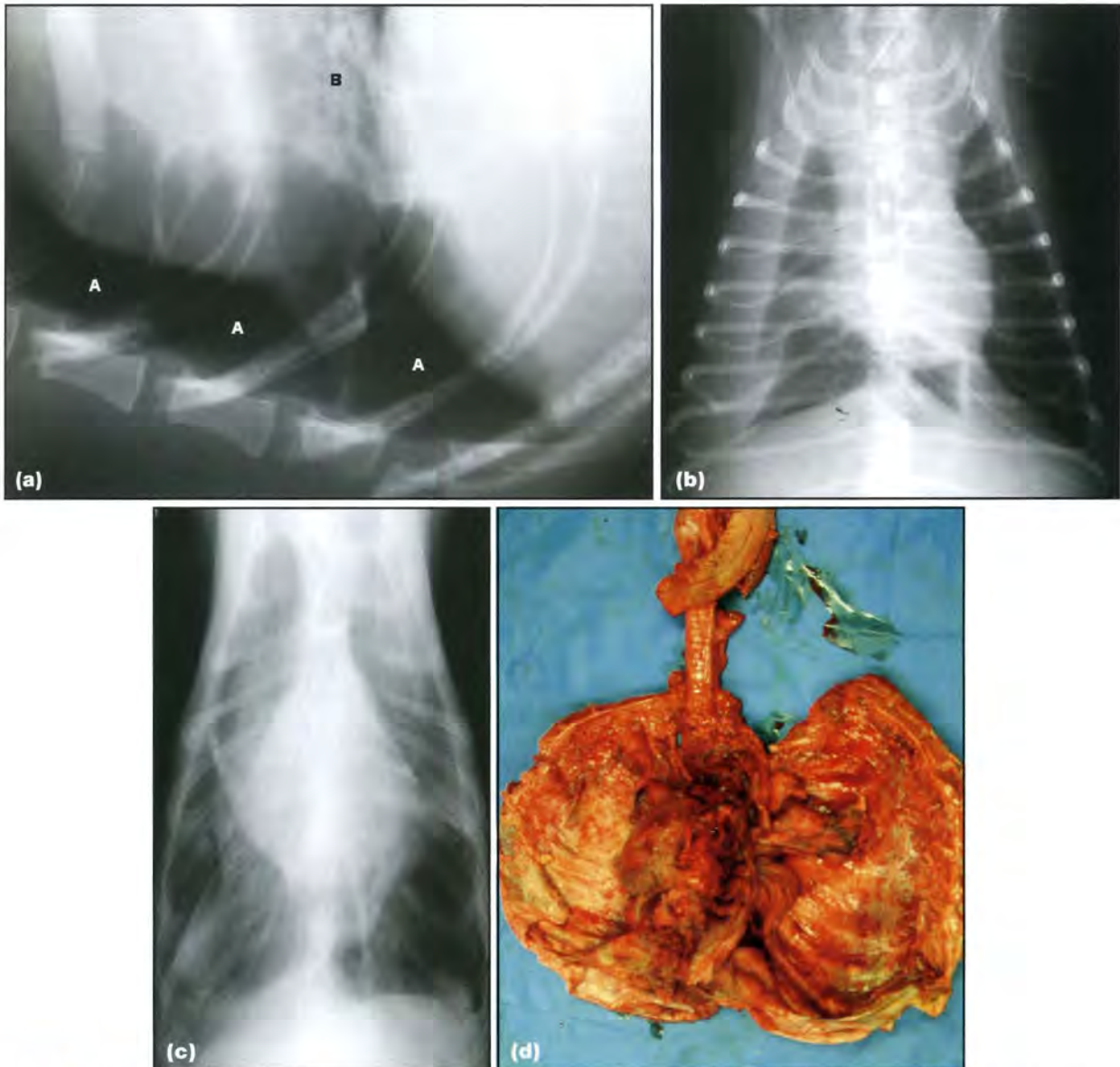
13.2 Close-up of a lateral radiograph of the caudodorsal part of the thorax of a 2-year-old Labrador Retriever bitch with pneumothorax, showing retraction of the lung margins from the thoracic wall and diaphragm (arrowheads). The lung tissue is increased in opacity but vascular markings can still be seen. Note the lack of lung markings in the area occupied by the gas (A).

of the air-filled lung supporting the heart in its normal anatomical position within the thorax (Figure 13.3). The heart moves towards the dependent side of the thorax, creating a gap between the cardiac apex and the sternum.

When air is present in the pleural space, the gap between the heart and the sternum is seen as a radiolucent (dark) area without lung markings (Figure 13.4a). This radiographic feature may not always be evident if an animal with a unilateral pneumothorax is positioned with the affected side uppermost.



13.3 Altered cardiac position in lateral radiographs with pneumothorax. This phenomenon can be explained by loss of the air-filled lung supporting the heart in its normal anatomical position within the thorax. Where pneumothorax is present on the dependent side, the lack of supportive lung tissue allows the heart to move towards the dependent thoracic wall. The space thus created between the cardiac apex and the sternum is highlighted by the X-ray beam causing the heart to appear elevated from the sternum by distance X.



13.4 (a) Close-up of a lateral view of the thorax of a 1-year-old male Whippet with traumatic pneumothorax showing apparent elevation of the cardiac shadow from the sternum. The space between the apex of the heart and the sternum is occupied by free pleural gas (A). Note the absence of lung markings in this area. Patchy opacification (B) of the lung overlying the cardiac shadow is likely to represent contusion. (b) VD thoracic radiograph of a 4-year-old Chihuahua with recent onset of right-sided chyloous effusion. Notice the reduced size but normal shape of the right lung with sharp lung margins. (c) VD radiograph of a 3-year-old Afghan Hound with chronic bilateral chylothorax, which was drained prior to radiography. Notice the interlobar fissure lines and rounded lung margins, indicating chronicity and scarring of the visceral pleura. The irregular margins of the cardiac silhouette are related to a previous pericardectomy. (d) Corresponding postmortem photograph of the opened thorax of the same dog in (c), viewed ventrally. The lungs and heart are collapsed in the centre of the image and are covered in multiple layers of fibrous adhesions. There are marked fibrinous changes on the parietal pleura consistent with fibrinous pleuritis.

When fluid is present in the pleural space, the gap between the heart and the sternum will be of soft tissue opacity. The cardiac silhouette will be obscured to a variable degree since the fluid surrounding it is of the same opacity. Therefore, elevation of the cardiac silhouette (\pm trachea) secondary to pleural effusion may give a false impression of cardiomegaly.

Other causes of apparent cardiac elevation on the lateral radiograph, which should be differentiated from pleural abnormalities, include mediastinal fat, hypovolaemia, pulmonary emphysema and overinflation.

Lung lobes and lobar margins in pleural disease

Uniform lung lobe collapse

When air or fluid is introduced into the pleural space, the normal negative pressure is lost and so the lung lobes withdraw from the chest wall. The lung lobes have an inherent elasticity that causes them to collapse uniformly, retaining their shape (see Figures 13.4b and 12.83, p. 283). The narrower parts of the lung and the smaller lobes are more susceptible to the altered intrapleural pressure and therefore tend to collapse first.

The right middle and left cranial lobes have a greater surface area to volume ratio and so are more compliant, i.e. more likely to collapse (see also Chapter 12).

Uneven or asymmetrical lung lobe collapse

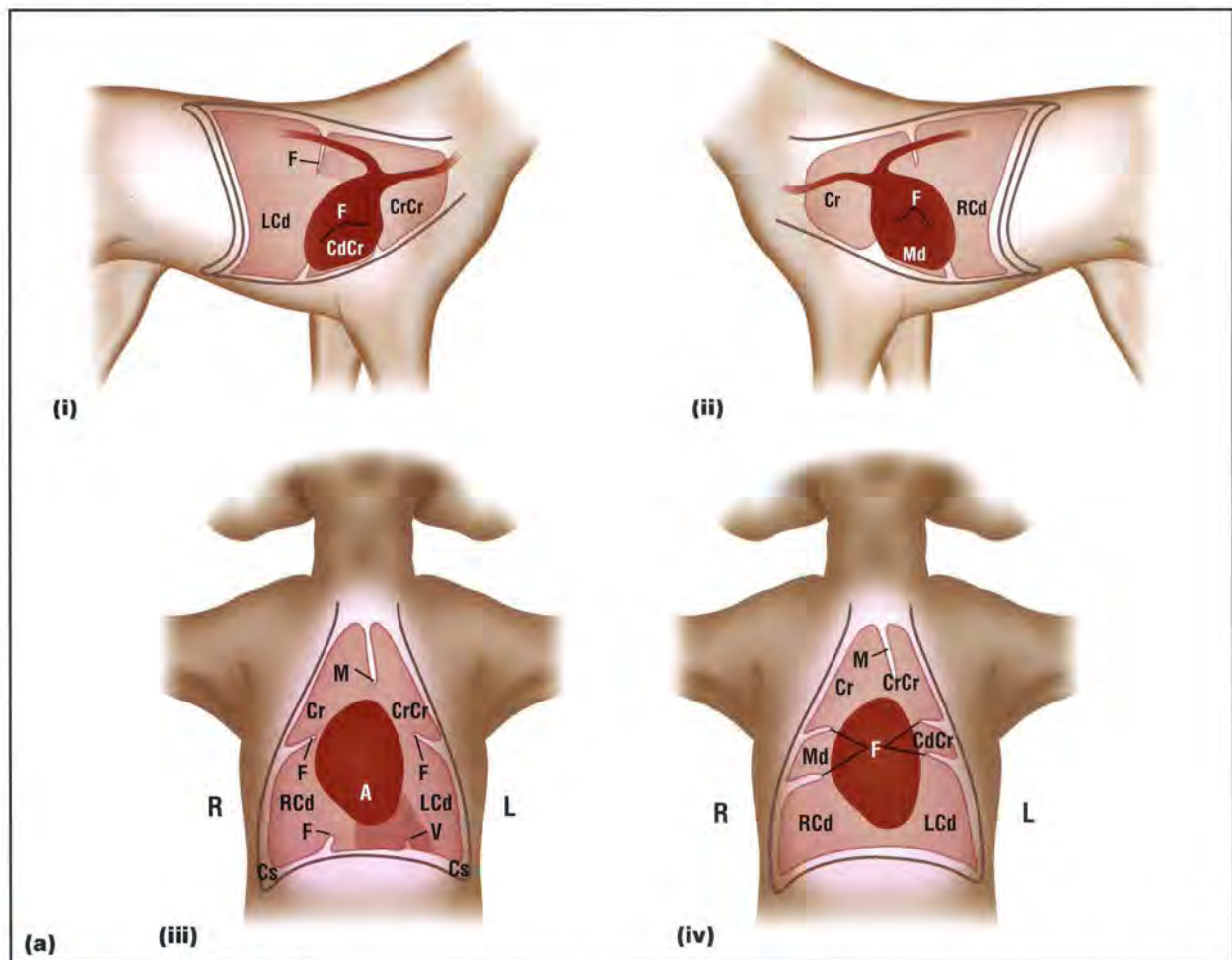
This may be a sign of underlying pulmonary disease. For example, a contused or pneumonic lung lobe will tend to collapse more readily than a normally inflated lung. If the pleura become thickened or the lung loses its elasticity, the normal triangular shape of the lung lobes may be lost, giving a rounded appearance to their margin. This can also occur where a pleural effusion has been present for some time or where the nature of the effusion causes an inflammatory reaction in the underlying pleura or lung (see Figures 13.4cd and 12.88, p. 285). *Rounding or scalloping* of lobar margins is often a feature of so-called 'reactive' effusions (e.g. pus or chyle). It may sometimes be seen in the absence of an effusion where chronic pleural scarring or fibrosis has developed, secondary to severe inflammatory lung disease. Sometimes this

is a difficult distinction to make as an effusion may develop secondarily around a diseased lung lobe (see Chapter 12).

Interlobar fissures and pleural lines

The division between two adjacent lung lobes is called an interlobar fissure. An interlobar fissure can be seen on a radiograph only under certain circumstances: it must be thickened or filled with fluid or other material, must contrast sharply with air (lung) on each side of it and must lie parallel to the X-ray beam. Fissures lying obliquely or 'en face' to the X-ray beam do not attenuate the beam enough to be detected.

When two adjacent lobes are minimally separated at a fissure a *pleural line* is seen. These fine lines either curve towards the heart from the thoracic wall or radiate from the hilus. They are distinguished from other radiodense lines by their location, orientation and the absence of branching. Knowledge of the normal location of the interlobar fissures is helpful in identifying these pleural lines (Figure 13.5).



13.5 (a) Location of the interlobar fissures. Since only fluid-filled fissures that are tangential to the X-ray beam are visible, the volume of fluid and the position of the patient will determine the fissures that are seen. (i) Fissures of the lateral aspect of the left lung (looking medial to lateral) are more likely to be seen when the patient is in left recumbency. (ii) Fissures of the lateral aspect of the right lung (looking medial to lateral) are more likely to be seen when the patient is in right recumbency. (iii) Fissures on the dorsal aspect of the lungs are more likely to be seen when the patient is in dorsal recumbency. (iv) Fissures on the ventral aspect of the lungs are more likely to be seen when the patient is in ventral recumbency. A = Accessory lobe; CdCr = Caudal part of the left cranial lobe; Cr = Right cranial lobe; CrCr = Cranial part of the left cranial lobe; Cs = Costodiaphragmatic recess; F = Interlobar fissure; LcD = Left caudal lobe; M = Mediastinal reflection; Md = Right middle lobe; Rcd = Right caudal lobe; V = Caudoventral mediastinal reflection between the left caudal lobe and the accessory lobe (pleural fluid may accumulate adjacent to this reflection). (continues) ▶



13.5 (continued) **(b)** DV thoracic radiograph from a dog with a moderate amount of pleural effusion. A thin radiopaque pleural line is indicated by the arrows.

Larger amounts of pleural fluid more widely separate the lung lobes and highlight the interlobar fissures. These are seen as elongated wedges or triangular opacities, extending from the thoracic wall towards the hilus (Figure 13.6).



13.6 DV thoracic radiograph of a mixed breed dog with a moderate pleural effusion. A wedge-shaped interlobar fissure is shown by the arrows.

The pleural surface must create a sharp interface with air (lung) on each side of it, if it is to be seen. If pleural fluid borders one or two lung lobes with soft tissue opacity, there will be border obliteration between the lung and fluid, and neither of them can be distinguished. If a lung lobe of soft tissue opacity borders a normally aerated lung lobe, the interface between the lobes is highlighted and is called a *lobar sign* (see Figure 12.22, p. 252). This is a sign of alveolar lung disease and should be differentiated from a fissure line indicating pleural disease, where a line or band of soft tissue opacity is seen separating two aerated lung lobes.

Pleural fluid and its distribution

Free *versus* trapped or encapsulated fluid

Since fluid is denser than lung tissue, it always moves towards the dependent part of the thorax and the lung floats on top. The exception to this rule is fluid which is encapsulated, trapped or loculated, often as a result of an inflammatory process. Trapped fluid can be difficult to differentiate radiographically from extrapleural masses. Ultrasonographic assessment can be very helpful in such circumstances.

Patient position

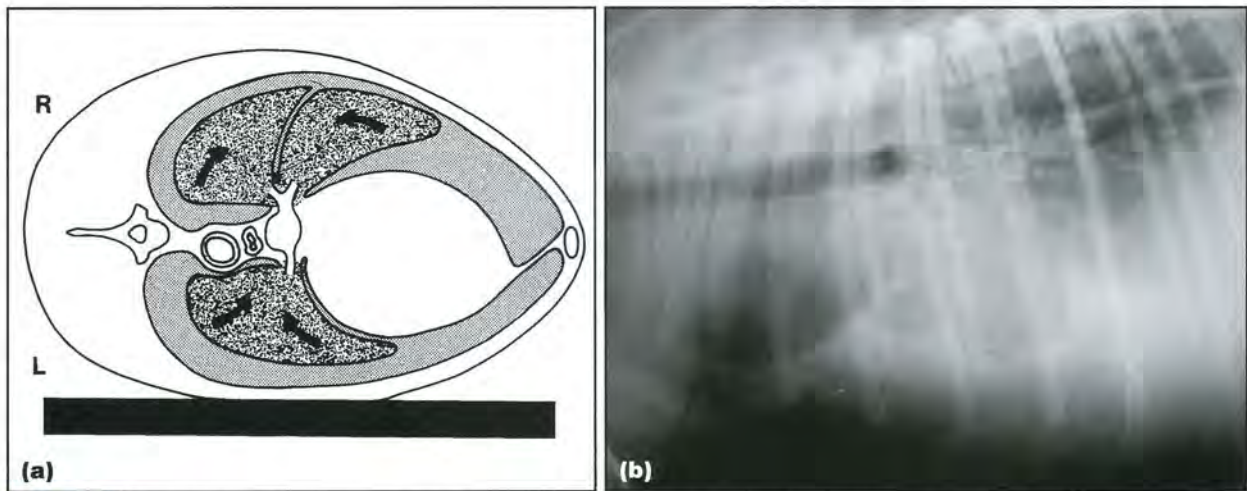
The distribution of pleural fluid changes with patient position. With the animal in lateral recumbency, fluid tends to accumulate in the dorsal and ventral part of both hemithoraces, creating border obliteration with the heart and diaphragm and retraction of the ventral lung margins with interlobar fissures in the non-dependent lung (Figure 13.7).

With the animal in dorsal recumbency, fluid will tend to accumulate dorsally in the lumbodiaphragmatic recess and so the heart will usually be visible on the VD view, which can be of diagnostic importance. (It should be noted that there is an increased risk to the patient associated with dorsal recumbency, so this view should only be obtained if it is safe for the patient.) Small amounts of fluid in this location will not be seen radiographically due to the overlying heart, mediastinum, sternum and spine (Figure 13.8ab).

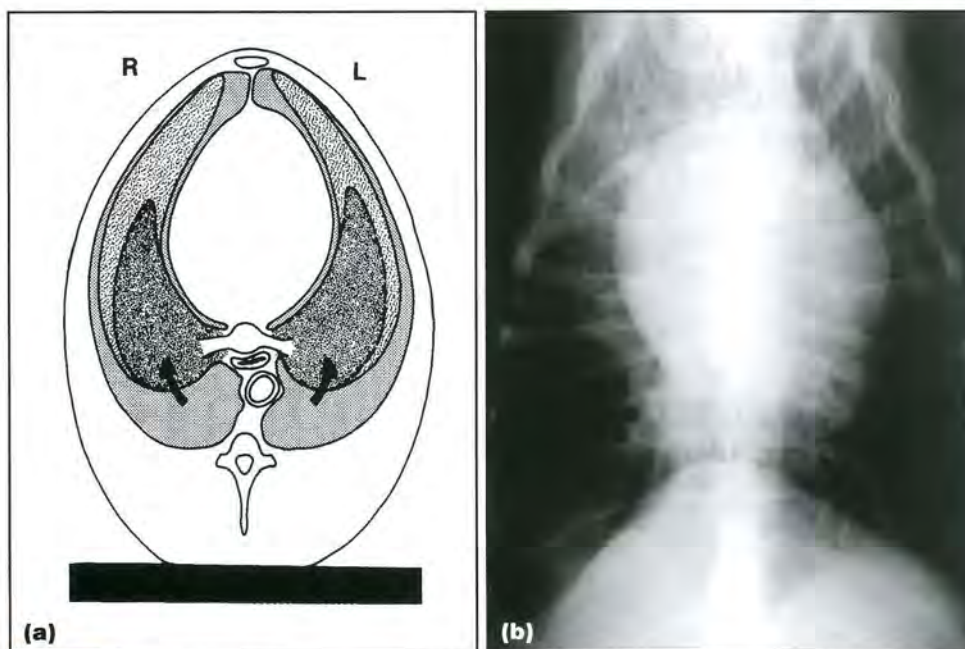
In ventral recumbency, the fluid will accumulate ventrally, surrounding the heart and obscuring it from view on the DV radiograph. The fluid level within the thorax is higher in ventral recumbency than in dorsal recumbency because the ventral part of the thorax is narrower. Thus, the opacity on the radiograph will be greater on the DV view (Figure 13.8cd).

Volume of effusion

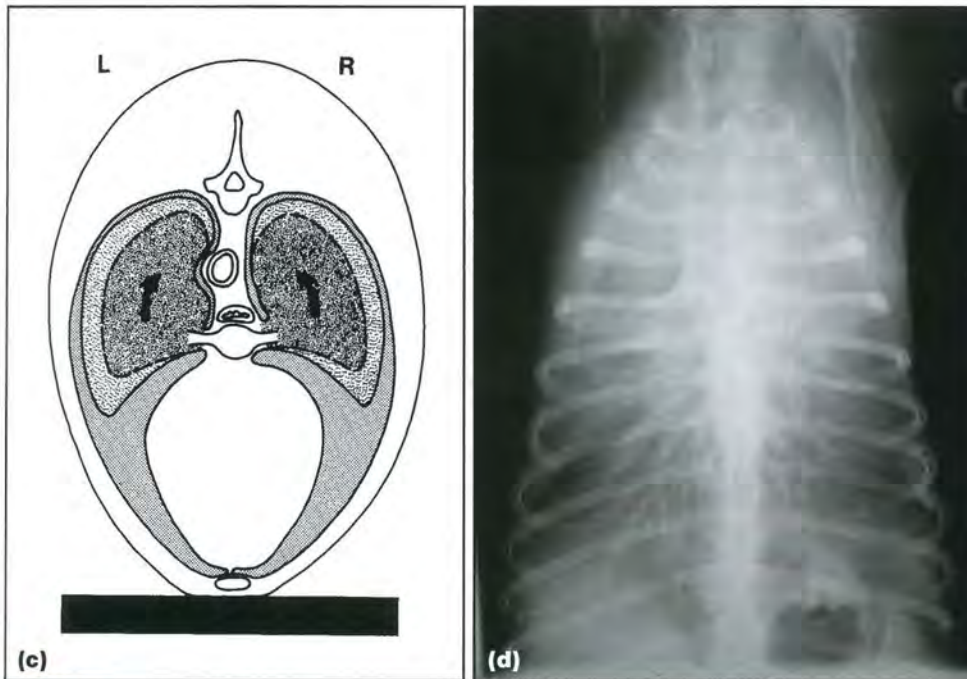
The radiographic appearance of different volumes of pleural effusion are shown in Figures 13.9 and 13.10. The elasticity of the lung tissue is such that the smaller lobes and the thinner parts of the lung lobes are more likely to collapse under the pressure of fluid in the pleural cavity. Thus, the first place for fluid to be seen in the lateral view is usually along the sternum (Figure 13.9) where the thin ventral edges of the lung retract easily. In this position, a coating of fluid over the most dependent part of the lung causes only a slight increase in opacity and may be difficult to detect.



13.7 (a) Fluid distribution in lateral recumbency (shaded area). Fluid in the non-dependent hemithorax is suspended by the cranial mediastinum, producing a soft tissue opacity dorsal to the sternum and causing retraction of the ventral lung margins. The ventral cardiac margin and apex, and the dome of the diaphragm are obscured. Fluid in the lower costodiaphragmatic recess between the lung and the thoracic wall is not visible (perpendicular to beam) but contributes to an increased opacity throughout the thorax. Interlobar fissures are visible. The lungs retract in the direction of the arrows. (Reproduced from Suter (1984) with permission) (b) Lateral thoracic radiograph of a dog with a large amount of pleural effusion. Notice the obliteration of the cardiac silhouette, scalloping of the ventral lung margins and interlobar fissure lines.



13.8 (a) Fluid distribution in dorsal recumbency (shaded area). Fluid collects dorsally, obscuring the descending aorta, and in the costodiaphragmatic angles, causing blunting of the lung margins. The diaphragmatic crura may be obscured but the dome remains visible. Lungs float upwards and pivot medially at the hilus to lie adjacent to the heart; therefore, the cardiac shadow remains visible. Fluid accumulates between the lungs and the lateral thoracic wall, and in the mediastinal reflection between the left caudal and accessory lobes. The cranial mediastinum remains visible as the cranial thorax is at a higher level than the caudal thorax. Fluid pools dorsally over a larger area than when the animal is in ventral recumbency, so fluid depth and consequent overall opacity are less than on the DV view. The lungs retract in the direction of the arrows. (Reproduced from Suter (1984) with permission) (b) VD thoracic radiograph of a 9-year-old Doberman with dilated cardiomyopathy and a small amount of cardiogenic pleural effusion. The enlarged cardiac silhouette is clearly visible and a small fissure line can be seen in the right cranial thorax, enabling a diagnosis of cardiac disease and cardiogenic effusion in this patient. The majority of the fluid is pooling in the lumbodiaphragmatic recess where it does not influence visibility of other thoracic organs. (continues)



13.8 (continued) **(c)** Fluid distribution in ventral recumbency (shaded area). Fluid pools ventrally. The lungs float upwards and pivot laterally about the hilus resulting in medial fluid accumulation, causing the mediastinum to appear widened and the cardiac shadow and diaphragm to be obscured. Little fluid accumulates laterally between the lung margins and thoracic walls. The thoracic cavity is narrower ventrally than dorsally, so when the animal is in sternal recumbency, fluid rises to a higher level making overall opacity greater than in a VD view. Interlobar fissures are visible. The lungs retract in the direction of the arrows. (Reproduced from Suter (1984) with permission) **(d)** DV thoracic radiograph. The cardiac silhouette is completely obliterated by the surrounding pleural fluid, multiple pleural fissure lines are visible and diagnosis of heart disease is not possible. Even mild pleural effusion can completely obliterate the cardiac silhouette in the DV view. If tolerated by the patient, a VD view is advantageous in the presence of pleural effusion.



13.9 Lateral radiograph of a 7-year-old Domestic Shorthair cat with a small volume of pleural effusion. An effusion of soft tissue opacity surrounds and effaces the ventral aspect of the cardiac silhouette. Falciform fat is seen ventrally within the abdomen.

As the amount of effusion increases, retraction and separation of the lung lobes from the thoracic wall become evident in all views (Figure 13.10). With mild to moderate effusions, the amount of retraction of the lung lobes seen on the DV or VD view does not

reflect the true extent of the pleural effusion. This is because the fluid accumulates with gravity beneath the lungs and only the fluid lying between the lung and the thoracic wall is struck tangentially by the X-ray beam.

Volume of effusion	General comments	Lateral view	Ventrodorsal view	Dorsoventral view
Small	<p>Lateral view is preferable to VD/DV views to identify small volumes of effusion</p> <p>Expiratory views are preferable as lung volume is less so the fluid volume is relatively greater and distributed over a smaller area.</p>	<p>Soft tissue opacity dorsal to sternum causing mild retraction of lung</p> <p>Ventral margins of the cardiac shadow and diaphragm obscured</p> <p>Interlobar fissures visible as linear opacities</p>	<p>Very small volumes concealed by mediastinum</p> <p>Soft tissue opacity between the lung and lateral thoracic walls, causing mild retraction of the lung</p> <p>Rounded lung margins at costophrenic angles</p> <p>Interlobar fissures visible even with small volume of fluid</p>	<p>Mediastinum conceals small volumes or may appear slightly widened</p> <p>Cardiac shadow and dome of diaphragm become hazy and partially obscured</p> <p>Fissure adjacent to the accessory lobe may be visible but others are less likely to be seen</p>
Moderate	<p>Interlobar fissures appear as wedge-shaped opacities extending towards the hilus</p> <p>As the volume increases they become easier to identify and a larger number become visible, even on DV views</p> <p>The effusion begins to compress the lungs more and produces an increased opacity throughout the lung fields</p>	<p>Overall increased opacity throughout thorax (fluid in lower costomediastinal recess)</p> <p>Moderate retraction of the lung margins from the sternum</p> <p>Ventral two-thirds of the cardiac shadow and diaphragmatic line obscured</p> <p>Prominent interlobar fissures</p>	<p>Moderate retraction of the lung margins from the lateral thoracic walls but lobes retain their normal shape</p> <p>Increased area of soft tissue opacity between the lung margins and the lateral thoracic walls</p> <p>Prominent interlobar fissures</p> <p>Widened and rounded costophrenic recesses</p> <p>Left border of descending aorta obscured</p> <p>Cardiac shadow and diaphragmatic line less well visualized</p> <p>Cranial mediastinum remains visible</p>	<p>Mediastinum widened</p> <p>Cardiac shadow and dome of the diaphragm completely obscured</p> <p>Moderate retraction of the lung margins from the lateral thoracic walls</p> <p>Narrow area of soft tissue opacity between the lung margins and the lateral thoracic walls</p> <p>Peripheral areas of interlobar fissures become visible</p>
Large	<p>Thoracic cavity may appear expanded or barrel-shaped, especially in cats</p> <p>Diaphragm may be flattened on all views causing caudal displacement of the liver (must be differentiated from primary hepatomegaly)</p> <p>Interlobar fissures extend to the hilus and separate lobes, producing a leaf-like arrangement</p> <p>Progressive compression of the lung eventually results in collapse. Smaller lobes (right middle then left and right cranial, then accessory) and peripheral areas of larger lobes are the most compliant, so collapse first. Caudal lobes usually remain inflated. Air bronchograms may be associated with complete collapse</p> <p>Cardiac shadow and diaphragm remain visible longer on VD than on DV and lateral views</p>	<p>Marked retraction of the lung towards the hilus</p> <p>Lungs float in the fluid causing dorsal displacement of the trachea and pulmonary hilus</p> <p>Cranial lobes may be completely collapsed and caudally displaced</p>	<p>Widened mediastinum</p> <p>Lung lobes separated but retain normal shape</p> <p>Cardiac shadow and diaphragm obscured</p> <p>Descending aorta obscured</p>	<p>Marked retraction of the lung margins from the lateral thoracic walls</p> <p>Lung lobes separated</p> <p>Cardiac shadow and thoracic side of the diaphragmatic line obscured</p>

13.10 Radiographic appearance of different volumes of pleural effusion.

With massive amounts of pleural fluid the lung lobes are markedly retracted toward the hilus, and some intrapulmonary details are obscured by atelectasis (lung collapse) and the opacity of the fluid. The smaller cranial lobes and right middle lobe are the most severely affected and may disappear from view

when they collapse, due to the overlying fluid opacity.

Unilateral versus bilateral

Most pleural effusions in dogs and cats are bilateral. Unilateral or uneven bilateral effusions can result from:

- Closure of the mediastinal fenestrations, which can be congenital or secondary to a neoplastic or reactive effusion (e.g. pyothorax (Figure 13.11; see also Figure 14.15b, p. 349), chylothorax, haemothorax)
- The presence of trapped or encapsulated fluid
- Fluid accumulation adjacent to a collapsed lung lobe as a result of reduced intrapleural pressure.



13.11 VD thoracic radiograph of a cat with a left-sided unilateral pleural effusion due to pyothorax. The ipsilateral lung is completely collapsed and there is compensatory hyperinflation of the contralateral lung.

Unilateral effusion is easiest to identify on VD and DV views. Large volumes may collapse the ipsilateral lung and displace the mediastinum towards the contralateral side. Unilateral effusions are more difficult to identify on lateral views. Increased soft tissue opacity dorsal to the sternum and retracted lung margins are only visible when the animal is positioned with the fluid in the non-dependent hemithorax. Fluid in the dependent hemithorax results in soft tissue opacity superimposed over the inflated upper lung, which may mimic a uniform pulmonary infiltrate.

Freely moveable bilateral effusion results in the lung on the dependent side always being more collapsed than the lung on the non-dependent side, as fluid moves across the mediastinum with repositioning.

Uneven bilateral effusion will produce asymmetrical changes on DV or VD views, reflecting the volume of fluid present in each hemithorax.

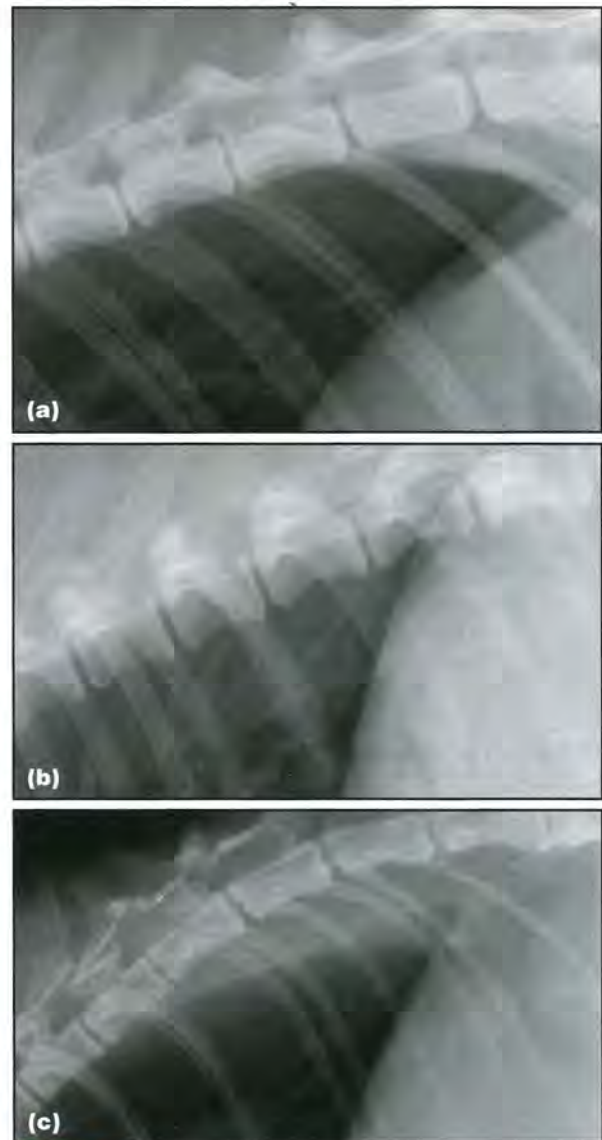
Pseudoeffusion

Mediastinal fat can elevate the cardiac shadow, outline the ventral margins of the lung lobes and cause them to appear rounded on the lateral view, mimicking the presence of an effusion. This normal feature can be differentiated from an effusion since the cardiac shadow is not obscured by the fat opacity.

The ventral lung margins in dogs with deep narrow chests, mimicking the presence of a small-volume

effusion. The chest conformation of certain breeds, notably the Dachshund, may mimic the presence of a small pleural effusion on a VD or DV view, due to the curvature of the ribs and costal cartilages (see Figure 14.24, p. 353).

In the cat, the lung fields do not extend to fill the angle between the spine and the diaphragm (the lumbodiaphragmatic recess) on a lateral radiograph, as they do in the dog. The presence of the psoas minor muscle in this region gives rise to a narrow triangle of soft tissue opacity between the caudal margin of the lung and the vertebral column, which should not be misinterpreted as pleural fluid (Figure 13.12; see also Figure 12.13, p. 248).



13.12 (a) Normal radiographic appearance of the lumbodiaphragmatic recess of the cat. The psoas minor muscles have a more cranial origin in this species and are responsible for the soft tissue opacity in this region. (b) Normal radiographic appearance of the lumbodiaphragmatic recess of the dog. Note that the lung fields extend up to and even slightly dorsal to the spine, in contrast to the cat. (c) A cat with a moderate volume of pleural effusion. The caudodorsal tips of the lung lobes are retracted and rounded. Compare this with the normal appearance in (a).

Cranial mediastinal mass or pleural effusion?

Pleural effusion must be differentiated from thoracic masses, especially if elevation of the trachea and pulmonary hilus are present:

- Small volumes of fluid are unable to deviate the trachea dorsally in the absence of a mass, and even large volumes are unable to compress or distort the trachea or displace the carina caudally
- With marked pleural effusion, the trachea can obtain an orientation which is straight but parallel to the spine (see Figure 10.32, p. 226). This should be considered if cardiac size is assessed solely on tracheal position
- The heart and trachea should move with gravity, so non-gravitational movement suggests the presence of a mass
- Horizontal beam radiography may be useful to visualize areas of the thorax concealed by fluid on standard views
- Ultrasonography is extremely useful to differentiate between masses and effusion (see Chapter 8).

Lung mass and pleural effusion

Many lung masses are accompanied by pleural effusion and it can be difficult at times to diagnose and characterize the mass in this situation. Decubitus or positional radiography can be helpful to separate the mass from small amounts of free pleural fluid (Figure 13.13). Ultrasonography is useful in these cases.

Pleural gas and its distribution

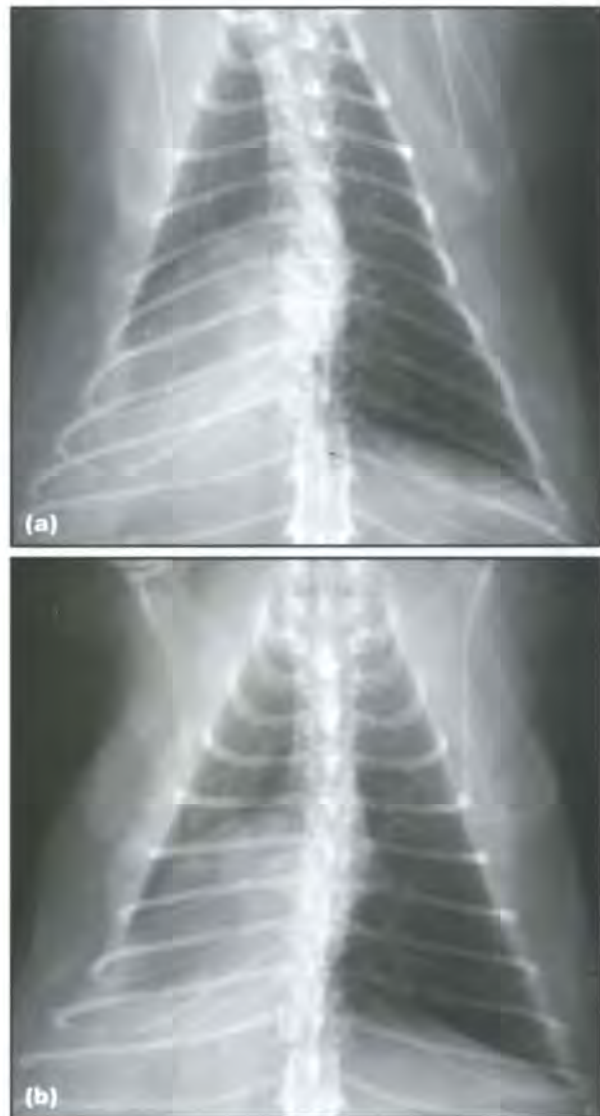
Pleural gas rises to the highest point of the thorax; thus, it is commonly seen surrounding the caudal and caudodorsal lung lobe margins on DV and lateral views (see Figure 13.2). Small to moderate pneumothorax is often not visible in routine VD views since the air accumulates in the midline, where it is obscured by the overlying mediastinal structures. Special radiographic views may be necessary to identify small volumes of pleural gas (see below).

Pseudopneumothorax

Conditions which may be mistaken for pneumothorax are summarized in Figure 13.14.

The most common of these is the presence of skin folds. On a DV or VD radiograph, folds of skin running parallel with the long axis of the patient may create a sharp air-tissue interface, which is projected over the periphery of the lung field (Figure 13.15; see also Figure 14.8b, p. 345). These folds can be distinguished from a true pneumothorax as they can often be traced beyond the thoracic margins, a lung pattern is usually detectable within the radiolucent regions (using an intense light source), and the direction of the curvature of the lines is different from true interlobar fissures.

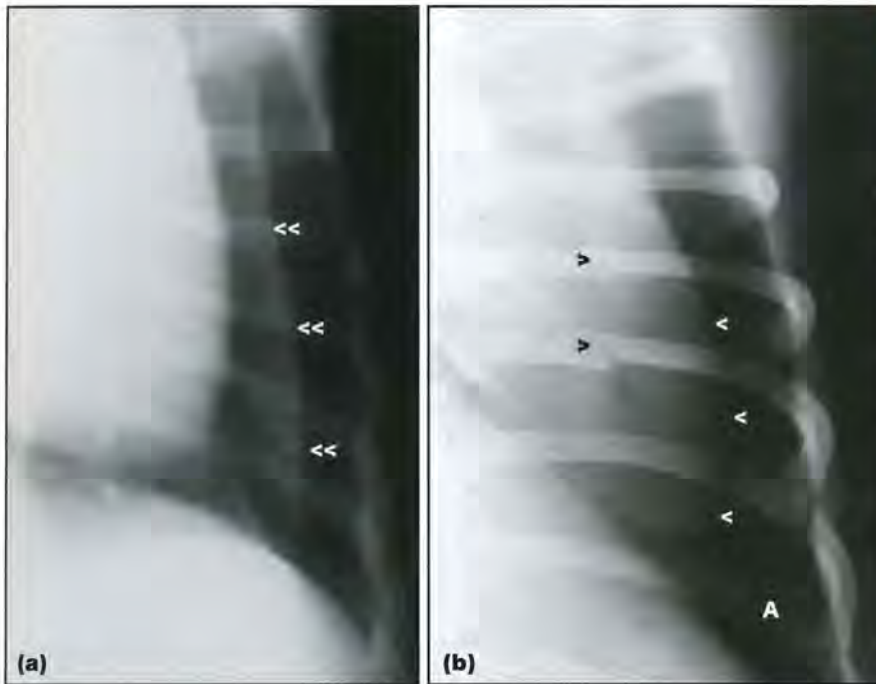
Conditions causing hyperlucency of the lung fields must also be differentiated from pneumothorax. These include emaciation, emphysema, overinflation associated with asthma or bronchial disease, and hypovascularity of the lung field due to hypovolaemia or conditions such as tetralogy of Fallot. Faint vascular markings will usually be seen extending up to the



13.13 (a) VD thoracic radiograph of an 8-year-old Siamese cat with a bronchial carcinoma causing lobar resorption atelectasis. There is right caudal lung lobe collapse indicated by ipsilateral cardiac shift and border obliteration between the heart, lung, diaphragm and potential pleural effusion. (b) VD radiograph with the cat in the same position but the table and X-ray tube tilted 25 degrees towards the cat's head, allowing free fluid to move cranially within the thorax. The soft tissue opacity in the caudal thorax is reduced and there is an overall increased opacity in the cranial thorax. This relatively simple and well tolerated manoeuvre helped to diagnose the presence of pleural effusion.

Superimposed skin folds
 Overpenetration (overexposure) of thoracic radiographs
 Underperfusion of pulmonary vasculature (shock) or thromboembolism
 Compensatory hyperinflation of lungs in animals under stress
 Pulmonary emphysema or bullae
 Pneumomediastinum
 Subcutaneous emphysema
 Incarceration and gaseous dilatation of prolapsed stomach or intestine

13.14 Radiographic differential diagnosis of pneumothorax. (Adapted and reproduced from Suter (1984) with permission).



13.15 (a) VD thoracic radiograph of a 3-year-old mixed breed dog showing a skin fold (double white arrowheads), mimicking pneumothorax. Pulmonary vascular markings were visible lateral to the skin fold when viewed with a bright light. (b) DV thoracic radiograph of a 7-month-old male Boxer with traumatic pneumothorax. The single white arrowheads outline the curved edge of a collapsed lung lobe, which is surrounded by free pleural gas (A). The black arrowheads show two rib fractures.

thoracic wall in these conditions, and there will be no thin line to mark the edge of a collapsed lung lobe. An intense light source may be required to identify the lung markings in overexposed areas.

Thoracic size and shape

In the presence of massive pleural effusion or tension pneumothorax, the thoracic width can be seen to increase markedly. The ribs and costal cartilages lie at right angles to the spine and the intercostal spaces are widened. The extent of these changes is often best appreciated when pre- and post-drainage films are compared. Also, the diaphragm can be flattened or even curved concavely (see Figure 14.14, p. 348).

Special radiographic views for pleural disease

It is important to note that patient safety is paramount. Good quality radiographs may be difficult to obtain in dyspnoeic animals. Consideration should be given when positioning these animals to avoid precipitating a crisis. In particular, dorsal recumbency may be contraindicated in animals with large volume effusions or respiratory compromise. Drainage of an effusion or pneumothorax prior to radiography may therefore be advisable.

There are many techniques that can be employed to assess pleural disease better. These include altering patient position, beam angulation and making use of different respiratory phases. Radiation safety must be carefully considered when obtaining horizontal beam views or when holding a patient in different body positions.

Radiographic technique will often require adjustment where pleural disease is suspected. Exposure values based simply on measurements of patient thickness will result in underexposure in the presence of pleural effusion, and overexposure in patients with pneumothorax.

Diseases

Pleural effusion

Pleural effusion is the accumulation of any type of fluid in the pleural space. Small volumes may be tolerated without primary clinical signs, as may larger volumes if they have accumulated slowly. Cats may not demonstrate clinical signs unless stressed or near death. Clinical examination may reveal tachypnoea and dyspnoea. Large volume effusions may result in a barrel-shaped thorax, muffled or absent heart sounds, loss of a palpable apical beat, reduced respiratory sounds, especially ventrally, and dull sounds on percussion. Additional clinical findings will depend on the cause of the effusion.

Indications for radiography in animals with pleural effusion include:

- Confirmation of the presence of effusion
- Identification of small-volume effusions not revealed on clinical examination
- Identification of the primary cause of the effusion
- Identification of fluid pocketing.

It should be noted that it is important to stabilize the patient before obtaining radiographs. This may include thoracocentesis.

Causes of effusion

Hydrothorax: This is the accumulation of aqueous fluids and is associated with the presence of a transudate or modified transudate. A *true transudate* results only from hypoproteinaemia (serum albumin below 15 g/l), secondary to protein-losing enteropathies and nephropathies, chronic hepatic disease or severe malnutrition. Even a true transudate causes pleural irritation and so will become modified with time.

A *modified transudate* is a transudate that becomes altered by the presence of non-inflammatory cells. This may result from:

- Systemic hypertension, secondary to right-sided heart failure (see Chapter 7). Left-sided failure in dogs does not usually result in pleural effusion, unless there is concurrent right failure, when it will be accompanied by hepatic congestion and peritoneal effusion. In cats, pleural effusion is less common with right failure, but can occur with left failure due to variations in the visceral pleural drainage (see Radiographic anatomy above)
- Reduced pleural lymphatic or venous drainage (e.g. due to cranial mediastinal masses)
- Protein leakage from chronic diaphragmatic hernias, especially with liver strangulation
- Increased pleural hydrostatic pressure due to conditions causing lung lobe collapse or preventing re-inflation.

Exudates are inflammatory effusions and are often associated with disease of the pleural surfaces. An exudate may be sterile or septic. *Sterile exudates* may arise secondary to:

- Pneumonia
- Pulmonary or pleural neoplasia
- Exudative pleuritis (feline infectious peritonitis, FIP)
- Autoimmune disorders (e.g. systemic lupus erythematosus, SLE; rheumatoid arthritis; immune-mediated haemolytic anaemia)
- Pulmonary granulomatous disorders.

Pyothorax: Thoracic empyema or pyothorax is a septic exudate, which may result from contamination by a large range of agents. The most common agents are *Pasteurella multocida*, *Bacteroides* and *Fusobacterium* in cats, and *Nocardia* and *Actinomyces* in dogs. Entry may be gained by:

- Direct trauma (cat bites, penetrating injuries)
- Foreign material (sticks, grass awns) migrating from the skin surface, oesophagus or respiratory tract (often encountered in hunting dogs)
- Haematogenous or lymphatic spread from distant septic focus
- Rupture of mediastinal structures (e.g. oesophagus)
- Direct extension from a lung lesion (abscess, pneumonia)
- Iatrogenically (surgery, thoracocentesis).

Haemothorax: This is the accumulation of blood in the pleural space and can result from:

- Erosion or rupture of thoracic vessels due to trauma, neoplasia, inflammation, aneurysm (e.g. *Spirocerca lupi*) or iatrogenically (surgery, thoracocentesis)
- Rupture of an intrathoracic mass (e.g. haemangiosarcoma)
- Clotting abnormalities: congenital (von Willebrand's disease) or acquired (anticoagulant rodenticides)

- Pulmonary infarcts
- Lung lobe torsion
- Thymic involution in young dogs.

Chylothorax: This is the accumulation of chyle in the pleural space resulting from:

- Heart disease (such as cardiomyopathy, pericardial effusion or tricuspid dysplasia)
- Heartworm
- Cranial mediastinal mass
- Cranial vena cava thrombosis
- Fungal granulomas
- Congenital or traumatic lesions of the thoracic duct (rare)
- Idiopathic chylothorax (the majority of cases).

Pseudochole: This contains lipid breakdown products from malignant or exfoliated pleural cells, and accumulation in the thorax may be associated with:

- Any longstanding effusion
- Feline cardiomyopathies
- Low-grade pleural infections
- Intrathoracic neoplasia.

Abdominal conditions: Pleural effusion may also occur secondary to *abdominal* conditions:

- Abdominal fluid may be transported across the diaphragm via the lymphatic drainage, resulting in a concurrent pleural effusion of the same type
- Transport of pancreatic enzymes in animals with pancreatitis may result in a thoracic exudate
- *Bile thorax* may occur from transdiaphragmatic transport of bile in animals with extrahepatic biliary tract rupture and bile peritonitis. Alternatively, it may result from penetrating injuries, creating a direct tract between the biliary system and thoracic cavity through the diaphragm
- *Urothorax* may occur in cats with ureteral and diaphragmatic trauma due to the mobility of the kidneys, allowing prolapse through a diaphragmatic tear.

Radiography

General pleural effusion: Radiographic findings include:

- Soft tissue opacity present within the pleural cavity
- Interlobar fissures visible in consistent locations on each view (see Figure 13.5)
- Lung margins retract towards the hilus
- Normal lung retracts evenly so fluid should be uniformly distributed, although dependent portions will collapse most
- In acute or non-reactive effusions the lung margins remain sharp (see Figures 13.4b and 13.16)



13.16 Lateral thoracic radiograph of a dog with a moderate volume of pleural effusion. Note that the lung margins remain sharp, consistent with an acute non-reactive effusion.

- Increased opacity throughout the lung fields, secondary to compression and overlying effusion
- Minimum volume identified radiographically is typically 50 ml in a small dog or cat and 100 ml in a medium-sized dog. Radiographs usually underestimate the volume present, as not all of the fluid is visualized in each view
- Fluid types cannot be distinguished by opacity
- Fluid is indistinguishable from adjacent soft tissue masses, lung lesions, adhesions, etc.
- Diaphragm can usually still be located by the presence of fat on the abdominal side, unless peritoneal effusion is also present.

The primary cause of the effusion (e.g. cardiac enlargement, mediastinal mass) should be sought. The VD view is often better than the DV view in cases of pleural effusion as it enables better visualization of the cardiac silhouette and cranial mediastinal masses. The DV view is always safer in a dyspnoeic patient and is better for assessing caudal lobar pulmonary vessels. Secondary changes (e.g. lung collapse, lung lobe torsion) should not be overlooked. Beware of anatomical or conformational differences that can mimic effusion (see Interpretive principles).

Chronic or reactive pleural effusion: Pleural thickening or pleuritis will result from chronic pleural effusion of any type, but will occur more rapidly in association with reactive (pyothorax, chylothorax, haemothorax) rather than non-reactive effusions. Reactive effusions may lead to the formation of fibrous adhesions and trapping or encapsulation of fluid (see below).

Radiographic findings include:

- Lung margins become irregular, rounded, undulating or scalloped (see Figures 13.4c and 13.17)
- Uneven retraction of the lung lobes
- Lung collapse with smaller lobes and peripheral portions of larger lobes being most susceptible
- *Trapped* fluid is restricted by fibrous adhesions; therefore, is unequally and abnormally distributed but moves with gravity
- *Encapsulated* fluid is completely confined by fibrous material, so its position and shape remain constant and are no longer altered by gravity.



13.17 Lateral thoracic radiograph of a 13-year-old dog with a chronic chylothorax. Note the rounded edges of the retracted lung lobes in contrast to the sharp margins shown in Figure 13.16. This dog also has several pulmonary osteomas seen as small irregular mineralized opacities.

Thoracocentesis

Drainage may be indicated to:

- Relieve respiratory compromise
- Obtain a fluid sample to aid identification of cause
- Allow radiographic assessment of intrathoracic structures previously obscured by fluid.

Radiography during drainage or lavage is indicated to assess drain placement. Drainage should be avoided or undertaken with care in animals with bleeding disorders or herniated abdominal contents. Radiography following drainage is useful to:

- Identify primary cause or secondary changes
- Identify incomplete drainage or fluid pocketing
- Identify recurrence of effusion
- Identify restricted lung re-expansion, indicating the presence of adhesions.

Lung collapse resulting from the effusion may be identified immediately after drainage but should resolve, allowing differentiation from underlying lung disease.

Other radiographic techniques: Other techniques may be useful to visualize areas concealed by the fluid on standard views and differentiate mobile fluid from static soft tissue masses, fibrous adhesions or non-mobile fluid accumulations:

- Decubitus view (see Chapter 1) is the most reliable method for identifying small volumes (5–50 ml in the dog) and assessing changes in volume over time
- Different patient positions will alter the distribution of fluid and may be useful to identify co-existing pathology:
 - Dorsal recumbency with beam directed laterally will move fluid away from ventral areas
 - Animal held upright and beam directed ventrodorsally moves fluid from cranial areas to identify cranial mediastinal lesions. It is important to consider safety implications associated with manual restraint
 - It is often sufficient to use a moderate table tilt to move free pleural fluid in desired locations (see Figure 13.13).
- Negative- and positive-contrast pleurography have been used in the past to evaluate pleural lesions but have been superseded by computed tomography (CT), magnetic resonance imaging (MRI) and ultrasonography
- Standard radiographic lymphangiography may be used to evaluate the thoracic duct, although more recently, CT lymphangiography and MRI evaluation have also shown potential.

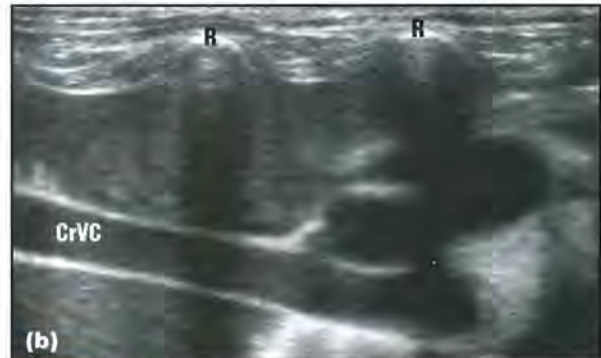
Ultrasonography

Ultrasonography is useful to investigate the primary cause, e.g. assess cardiac function, evaluate pleural membranes, identify cranial mediastinal masses, diaphragmatic defects and lung lobe torsion. It is also useful for evaluating secondary changes, e.g. lung atelectasis, fibrin tags indicating chronicity, etc.

Ultrasonography can be used to locate small volumes or areas of trapped fluid, and to guide therapeutic drain placement or diagnostic fine-needle aspiration of the fluid. Multiple windows may be required to identify small volumes of effusion (it may be useful to scan from the dependent side). Large volumes may be found through most intercostal windows.

Pleural effusion greatly improves the ability of the ultrasonographer to visualize intrathoracic structures, such as mediastinal fat, vessels, lymph nodes, the oesophagus and occasionally the trachea and mainstem bronchi. Echogenicity of the effusion varies with the type; for example, exudates, haemorrhage and carcinomatosis are more likely to be echogenic (Figure 13.18).

Chronic effusions may lead to fibrin formation, seen as linear echogenic strands. Fluid in the pleural space of the cranial thorax is visualized as two discrete pockets separated by the mediastinum (Figure 13.19). This differs from cranial mediastinal fluid, where the mediastinum is widened and the mediastinal vessels are separated from fat by irregularly shaped fluid pockets.



13.18 (a) Ultrasonographic image obtained via an intercostal window in an 8-year-old dog with a large-volume pleural effusion. The effusion was a transudate and is seen as completely anechoic. Echoic, collapsed normal lung can be identified surrounded by the effusion. (b) Ultrasonographic image obtained in long axis across the cranial thorax of a 1-year-old cat. Rib shadows (R) are seen in the foreground and the cranial vena cava (CrVC) is seen as two echotic stripes with an anechoic lumen, running from left to right across the image. An echogenic effusion is present in both the left and right pleural spaces, surrounding the CrVC. This was in association with FIP.



13.19 Thoracic ultrasonographic image of a 3-year-old Siamese cat with a marked volume of slightly echotic pleural effusion. The image has been obtained with a linear transducer placed in a dorsal plane across several ribs at the level of the costochondral junctions. The ventrocranial mediastinum is seen as a narrow hyperechoic horizontal band surrounded by the pleural effusion in the left and right pleural spaces. The ribs (R) are seen in the foreground.

Computed tomography

CT is useful to identify underlying or concomitant lesions, such as masses, lung lobe torsion or diaphragmatic defects. The patient's body position can be altered (sternal *versus* dorsal recumbency) during the scan to redistribute the fluid (taking care with patient safety).

Contrast medium administration and soft tissue algorithms are required for all studies. High-resolution lung algorithms may be useful to evaluate the pulmonary parenchyma. CT lymphangiography can be used for assessment of the thoracic duct and branches in animals with chylothorax.

Pleuritis, fibrosing pleuritis and pleural masses

Pleuritis is inflammation of the pleura, resulting in thickening of the pleural membranes. In cats, the most common cause is FIP, where the non-effusive form causes a focal pyogranulomatous pleuritis. Pleuritis can also occur in dogs and cats due to:

- An extension of lung disease (fibrinous bronchopneumonia, pleuropneumonia) or neoplasia
- Irritation from material in the pleural space, including bile, pancreatic enzymes and asbestos-type material
- Systemic conditions, such as septicaemia
- In association with a chronic pleural effusion of any type.

If the pleuritis leads to the production of an exudate (e.g. effusive FIP in cats, suppurative processes, neoplasia) then pleural effusion will result. Pleural thickening may also arise due to focal pleural haemorrhage associated with trauma. Pleural thickening may remain in animals even once causative factors have been removed.

Fibrosing pleuritis refers to fibrous strand or adhesion formation between pleural surfaces and may occur in pyothorax, chylothorax, haemothorax, FIP and mycobacterial disease. 'Pleural peel' is a thick fibrous layer produced by the organization of fibrin deposits in the pleural space. It can adhere to the pleura and extend into the lung parenchyma, reducing lung volume and restricting lung movement. It can even cause the affected area to adhere to the thoracic wall. Progression results in the lobes becoming enshrouded in fibrin, leading to chronic underinflation (see Figure 13.4d). The volume of fluid associated with fibrosing pleuritis may be small and trapped or encapsulated (Figure 13.20), although it can become severe and bilateral.

Pleural masses can take the form of herniated abdominal viscera, granulomatous lesions, haematomas, pleural adhesions, pleural peel or neoplasia. Mesothelioma is the only primary neoplasm of the pleura. It does not present as a mass lesion but rather is disseminated and usually results in a large-volume pleural effusion. Diagnosis can be extremely challenging. Metastatic lung neoplasia (carcinoma) may also involve the pleura. Effusion is more commonly associated with pleural masses than lung or extrapleural masses (see also Chapter 14).

Radiography

- Pleuritis results in thickening and irregularity of the pleura, producing linear opacities where tangential to the beam. This is best visualized at



13.20 DV thoracic radiograph of a cat with pyothorax and abscess formation. An area of encapsulated fluid (F) is present in the right caudal thorax.

sites of interlobar fissures (see Figure 13.5) but if severe, may be observed around entire lung margin

- Differentiate from pleural thickening and calcification in older animals
- Differentiate from small-volume pleural effusion. (Horizontal beam radiography may differentiate mobile fluid from static pleural lines. Moderate fluid volume results in wedge rather than linear opacities)
- The presence of adhesions may be suggested by tent- or U-shaped opacities
- Restricted areas of lung will be reduced in size, increased in opacity and will not inflate further despite repositioning animal
- May be minimal difference between the lung volume in inspiratory and expiratory views
- Following drainage, affected areas of lung may fail to re-expand and retain a rounded outline with a radiopaque margin, an appearance known as cortication. These areas may appear similar to hilar masses and must be differentiated from pulmonary neoplasia (primary or secondary), lung lobe torsion and hilar lymphadenopathy
- Intrapleural pressure around the lung lobes that remain collapsed will be reduced following drainage, therefore encouraging reformation of the effusion.

Pleural masses are usually associated with pleural effusion, so drainage is required for visualization but a mass may be suspected in the presence of:

- Non-gravitational displacement of the cardiac shadow or other thoracic structures
- Uneven lung compression
- Soft tissue opacity not conforming to the linear or triangular shape of the pleural space (often spindle-shaped)
- Soft tissue opacity that maintains its shape and position despite moving the patient, although this must be differentiated from trapped or encapsulated fluid.

Ultrasonography

This is useful to confirm pleural thickening and can differentiate between parietal and visceral pleura involvement:

- Mild pleural fibrosis appears as smooth thickening of the pleura
- If the pleura are irregularly thickened or gnarly and echogenic, an inflammatory or neoplastic change should be considered
- Pleural fluid is usually present in active pleuritis and in neoplastic disease
- Aspiration of fluid or a pleural mass may contribute to diagnosis
- Pleural masses may be identified (Figure 13.21)
- It may be challenging to differentiate a pleural mass from a lung mass. A useful trick is to watch the motion of the mass with the animal's breathing. A lung mass will move with the lung; a pleural mass will remain stationary whilst the lung moves around it. Holding a dog's nostrils and mouth closed for a few seconds and then releasing may be useful to encourage the dog to take a deep inspiration, thereby enabling the motion of the lung and mass to be assessed. This should only be attempted if the animal is clinically stable.



13.21 Ultrasonographic image showing multiple irregular pleural masses (M) in a 2-year-old Labrador Retriever with a large volume of haemorrhagic pleural effusion. The masses are cauliflower-like and surrounded by the effusion. The final diagnosis was a rare neoplasm, telangiectatic osteosarcoma.

Pneumothorax

Pneumothorax is the accumulation of gas within the pleural space and may develop in a variety of ways (Figure 13.22). Clinical signs of pneumothorax may be subtle or dramatic and progress from rapid

Traumatic

Open:

- Gun shot
- Bite
- Stab wound
- Injury secondary to road accident

Closed:

- **Blunt external trauma**
- **Subpleural bleb, secondary to trauma (goes on to rupture)** iatrogenic due to thoracocentesis, transthoracic aspiration or biopsy, or pericardiocentesis
- Extension from pneumomediastinum
- Gas from the abdomen, if a diaphragmatic hernia is present

Spontaneous

Primary:

- Lungs are normal
- Occurs in deep-chested breeds of dog, usually middle-aged

Secondary:

- Lungs are diseased
- Examples include emphysema, neoplasia, pneumonia, pulmonary abscessation, parasites (*Oslerus osleri*, *Dirofilaria immitis*, paragonimiasis), migrating foreign bodies, asthma

13.22 Causes of pneumothorax. Common causes are shown in **bold**.

shallow breathing to open-mouthed panting. If the air accumulates slowly, the early signs of respiratory difficulty may only be present on inspiration. Small amounts of pneumothorax are often difficult to detect clinically. Radiographic detection is valuable to pinpoint an underlying condition.

Types of pneumothorax

Pneumothorax may be generally classed as traumatic or spontaneous.

Traumatic: This may be classed as open or closed:

- **Open:** the chest wall has been breached. Gas from the external environment enters the pleural space
- **Closed:** the thoracic wall is not compromised. Gas from within the animal enters the pleural space.

Closed traumatic is the most common type of pneumothorax (Figure 13.23). This usually occurs secondary to blunt external trauma, such as a road traffic accident. A bronchus or area of lung tissue ruptures when the sudden blow to the thorax increases intrathoracic pressure against a closed glottis. Another possibility is that internal shearing forces may create a subpleural bleb (see Chapter 12) that goes on to rupture.

Open traumatic pneumothorax occurs due to thoracic wall injuries. Typical examples include gun shot, bite or stab wounds or injury secondary to road accidents. Air rapidly enters the pleural space through the wound during inspiration, and pleural and atmospheric pressures equilibrate.



13.23 Lateral thoracic radiograph of an 8-year-old Rottweiler with a traumatic closed pneumothorax after being hit by a car. A moderate-volume pneumothorax is present. Gas lucency with no lung markings is present ventral to the cardiac silhouette and surrounds the caudodorsal lung lobe tips.

There are also some less common causes of traumatic pneumothorax. Air may be introduced iatrogenically into the pleural space during thoracocentesis or pericardiocentesis. Pneumothorax can occur as a complication of pneumomediastinum, but the converse is not true (see Chapter 8). Air may enter the pleural space from the abdomen if a diaphragmatic rupture and free abdominal gas are present.

Spontaneous: This refers to a pneumothorax occurring where no traumatic or iatrogenic cause can be identified. It is thought to result from the rupture of blebs or bullae (see Chapter 12), and may be considered *primary*, where the lungs are normal, or *secondary*, where underlying lung pathology is present.

Primary spontaneous pneumothorax most commonly occurs in large deep-chested breeds. Hounds, and Siberian Huskies in particular, are over-represented. There is no sex predilection but middle-aged dogs are more commonly affected. Secondary spontaneous pneumothorax is more common and underlying lung diseases include emphysema, neoplasia, pneumonia, pulmonary abscess, parasites (including *Dirofilaria*, paragonomiasis), migrating plant foreign bodies and asthma (several reports in cats). Pleural adhesions arising from chronic inflammation may also tear, resulting in pneumothorax.

Tension: If the pleural gas pressure exceeds the atmospheric pressure, a tension pneumothorax is present. This occurs when a one-way valve effect exists between the source of air and the pleural space. Air enters the pleural space with inspiration but does not exit with expiration, and positive pressure rapidly develops within the pleural space. The pressure rises with each breath, thus the condition rapidly becomes life-threatening. The lung and vessels collapse and a fatal decrease in ventilation and cardiac output result. The animal's thorax may be clinically observed to expand as the condition progresses.

Liquidopneumothorax: This is also called hydropneumothorax, and refers to the presence of fluid and gas within the pleural cavity. This condition can arise secondary to trauma (where the fluid is blood) or more often as a complication of pulmonary abscessation or oesophageal perforation (where the fluid is pus). Liquidopneumothorax can create bizarre radiographic patterns, due to the simultaneous presence of border obliteration and hyperlucency. If the presence of gas can be identified, confirming a liquidopneumothorax, this shortens the list of differential diagnoses for pleural effusion.

Radiography

General pneumothorax: Radiographic findings include:

- Lung margins retracted from the thoracic wall, diaphragm and spine
- Sharply demarcated collapsed lung lobes outlined by gas (see Figure 13.15b)
- Increased opacity of collapsed lobe(s)
- No lung markings visible peripheral to the collapsed lung lobe(s) (see Figures 13.2 and 13.15b)
- Cardiac silhouette may be separated from the sternum by gas lucency (see Figures 13.4a and 13.23)
- Pneumothorax is most commonly bilateral, either due to a bilateral entrance of gas or movement across the mediastinum.

The underlying causes should be sought; although, a causal bleb or bulla is often not identified on radiographs. Uneven collapse of the lung lobes may point towards concurrent pulmonary disease, e.g. contused lung may collapse while normal lung remains inflated. There may be additional findings of skeletal trauma, pulmonary contusion, pneumomediastinum, subcutaneous emphysema, etc.

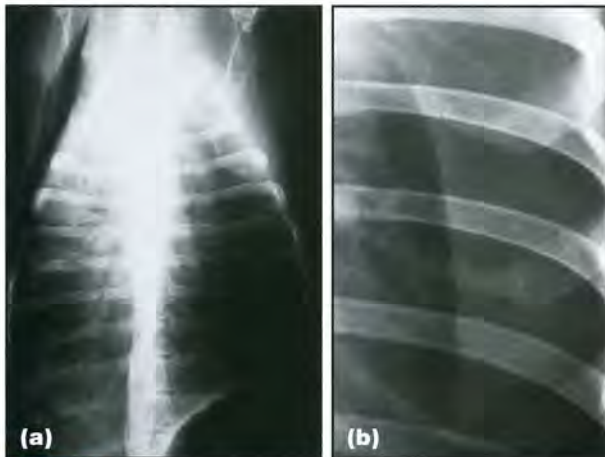
Tension pneumothorax: Radiographic features of pneumothorax are seen, in addition to (Figure 13.24):

- Progression (worsening) of radiographic changes over a short time
- Severe lung lobe collapse/compression
- Markedly radiopaque lung fields
- Flattened diaphragm
- Overdistension of the thorax with widened intercostal spaces
- Ribs and costal cartilages perpendicular to the spine
- Mediastinal shift away from a *unilateral* tension pneumothorax (uncommon).



13.24 Lateral thoracic view of a 6-year-old Standard Poodle with tension pneumothorax. The cardiac shadow is markedly elevated from the sternum and the normal lung markings are absent. Note the extreme distension of the thorax with maximal opening of the lumbodiaphragmatic recess and the relative overexposure of the thoracic structures due to the replacement of lung tissue with free pleural gas. The margins of the severely collapsed lung lobes cannot be clearly outlined.

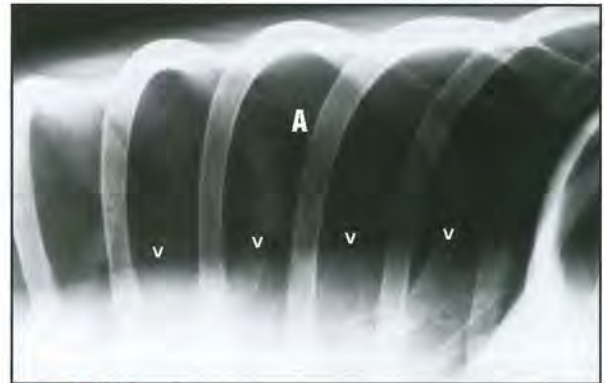
Liquidopneumothorax: In this condition there are radiographic features of pleural effusion and pneumothorax (Figure 13.25):



13.25 (a) DV thoracic radiograph of a 9-year-old German Shorthaired Pointer that was involved in a road traffic accident. The cardiac silhouette is completely obscured, indicating pleural effusion, yet the overall opacity is decreased rather than increased, particularly peripherally. (b) Close-up of (a) showing the left hemithorax viewed with an intense light source, reveals a lung margin separated from the rib cage by a gradient of peripheral free lucent gas and central free opaque fluid, consistent with a liquidopneumothorax. (c) Lateral thoracic radiograph of a 2-year-old Domestic Shorthair cat with liquidopneumothorax. The cardiac shadow is partly obscured by free pleural fluid (B) and appears elevated from the sternum. Between the cardiac apex and the sternum is a pocket of pleural gas (A). Pleural gas also surrounds the caudodorsal margin of the collapsed lung. The margin of the lung (arrowheads) is more sharply defined than expected because the pleura are thickened. Note the normal triangular psoas minor muscle (C), with soft tissue opacity; seen in the cat between the lumbodiaphragmatic recess and the spine.

- Cardiac shadow is often obscured
- Lung margins retracted from the thoracic wall
- Peripheral hyperlucent thoracic cavity
- Appearance depends on the amount and relationship of free gas and fluid
- Decubitus or standing views show fluid and gas in the pleural space
- Horizontal fluid–gas interface present on horizontal beam views.

Other techniques: Occasionally, it is difficult to identify small-volume pneumothorax on survey radiographs. When standard vertical views are used, the DV view may be preferable to a VD view. Generally, the decubitus view (Figure 13.26) increases the likelihood of detecting a small amount of pleural gas. One study showed *detection* was best on decubitus VD and vertical beam left lateral views, but the *amount of gas* was shown best on a vertical beam right lateral view.



13.26 Lateral decubitus VD radiograph of the non-dependent hemithorax of a 2-year-old mixed breed dog with pneumothorax, showing the lung lobe margins retracted from the thoracic wall (arrowheads) and free pleural gas (A).

End-expiratory radiographs are also useful as the lungs appear more radiopaque, the costo-diaphragmatic angles are blunted, and the relative amount of pleural gas is greater compared with the reduced lung volume.

Computed tomography

This is useful to demonstrate small quantities of pleural gas, pleural effusion or pockets of trapped pleural fluid, which may be difficult to visualize radiographically. It is more sensitive for detecting bullae or blebs underlying spontaneous pneumothorax, and may help to guide surgical intervention.

Ultrasonography

Radiographs easily surpass ultrasonography in the diagnosis of pneumothorax. However, ultrasonography may be useful to assess gas in the pleural space, especially following ultrasound-guided interventional techniques (such as fine-needle aspiration).

Free gas has an almost identical appearance to gas within the lung (reverberation artefact) and as such is difficult to detect. However, on close observation the gliding movement of the normal lung will not be identified and the gas will be static. Previously identified lung lesions will no longer be seen once pleural gas is present.

Sometimes fluid and gas may be present (e.g. if haemorrhage and pneumothorax have occurred secondary to lung aspirate or biopsy sample). The fluid accumulates ventrally and the gas dorsally. In this situation a so-called 'curtain sign' may be seen in transverse images of the thorax. This refers to the repetitive ventral to dorsal motion of the fluid–gas interface with respiration, which has been compared to the lowering of a curtain.

References and further reading

- Au JJ, Weisman DL, Stefanacci JD and Palmisano MP (2006) Use of computed tomography for evaluation of lung lesions associated with spontaneous pneumothorax in dogs: 12 cases (1999–2002). *Journal of the American Veterinary Medical Association* **228**, 733–737
- Forrester SD, Troy GC and Fossum TW (1988) Pleural effusions: pathophysiology and diagnostic considerations. *Compendium on Continuing Education for the Practicing Veterinarian* **10**(2), 121–136
- Lord PF, Suter PF, Chan KF, Appleford M and Root CR (1972) Pleural, extrapleural and pulmonary lesions: a radiographic approach to diagnosis. *Journal of the American Veterinary Radiology Society* **13**, 4–17
- Puerto DA, Brockman DJ, Lindquist C and Drobatz K (2002) Surgical and nonsurgical management of and selected risk factors for spontaneous pneumothorax in dogs: 64 cases (1986–1999). *Journal of the American Veterinary Medical Association* **220**, 1670–1674
- Suter PF (1984) Pleural abnormalities. In: *Thoracic Radiography: A Text Atlas of Thoracic Diseases of the Dog and Cat*, ed. PF Suter, pp. 683–734. Peter F. Suter, Wettwil, Switzerland
- Suter PF and Gomez JA (1981) Pleural diseases. In: *Diseases of the Thorax – Radiographic Diagnosis*, pp. 18–22. Venture Press, Davis, California

The thoracic boundaries

Francisco Llabrés-Díaz, Audrey Petite, Jimmy Saunders
and Tobias Schwarz

Radiographic anatomy

The boundaries of the canine and feline thoracic cavity consist of the thoracic skeleton, the cranial and caudal thoracic apertures and the covering soft tissue structures. The rib cage is covered by thoracic, pectoral, spinal and other musculature, subcutaneous fat and skin, and serves as an attachment for the thoracic extremities.

Cranial thoracic aperture

The cranial thoracic aperture (also known as the thoracic inlet) is a small passage for the trachea, oesophagus, vessels and nerves. It is enclosed by the deep fascia as well as the pectoral, scalenius and longus colli muscles. Radiographically, it is synonymous with the area between the first pair of ribs.

The right pleural cupula normally extends to the level of the first rib in the dog (both cupula extend to this level in cats; see Figure 12.1, p. 242). The left pleural cupula extends slightly further cranially in full inspiration in the dog (see Figures 12.1c, p. 242 and 12.2, p. 243).

The thoracic inlet serves as a reference for radiographic tracheal diameter measurements (see Figure 10.3, p. 214) and a tangential radiographic view into the inlet can be used for assessment of tracheal collapse (see Figure 10.13, p. 218). Occasionally, it is used as an ultrasonographic approach for the cranial mediastinum.

Thoracic skeleton

The thoracic skeleton consists of the ribs, sternum and thoracic spine.

Ribs

Dogs and cats normally have 13 pairs of ribs, which have the following characteristics:

- Flat surface in dogs, cylindrical in cats
- Contour:
 - Evenly curved (barrel-chested dog breeds, cylindrical-shaped feline thorax)
 - Angled (wedge- or flat-chested dog breeds)
 - S-shaped ('cottage loaf' chest in Basset Hounds and Dachshunds).
- Consist of a large bony dorsal and small cartilaginous ventral portion (costal cartilage)
- The dorsal extremity of the rib consists of a head, neck and tubercle
- Two synovial joints between the rib and the spine:
 - Costovertebral joint between the rib head and the costal vertebral facet (hinge joint)
 - Costotransverse joint between the tubercle and the transverse process of the vertebra (sliding joint).
- Costochondral junction between the osseous and cartilaginous part of the rib
- Synovial sternocostal joints for the first eight to nine ribs (sternal ribs), remaining ribs fused by connective tissue to each other and the last sternal rib to form the costal arch (asternal or false ribs)
- Last one (dogs) or two (cats) pair(s) of ribs not connected to the costal arch (floating ribs).

Sternum

The sternum consists of a series of eight bones that form the floor of the thorax. The most cranial sternebra is called the manubrium, and the most caudal sternebra is the xiphoid process. The xiphoid cartilage prolongs the xiphoid process caudally. The individual sternebrae are joined by intersternbral cartilage. The first nine ribs articulate with the sternum through the costal cartilages.

Dogs have a curved sternum, which is square in cross section; cats have a cylindrical straight sternum with a flat xiphoid process. The sternum rotates outward in inspiration with the anchor point at the manubrium. The respiratory excursion is higher in cats (3–5 degrees) than in dogs (1 degree in the German Shepherd Dog).

Thoracic spine

Dogs and cats usually have 13 thoracic vertebrae, which articulate cranially with a corresponding rib pair. The cranial nine thoracic vertebrae share the following features:

- Short bodies with flattened extremities
- Flat articular facets
- Closely fitting vertebral arches
- Long spinous processes with converging orientation. Eleventh, or occasionally tenth, thoracic vertebra is closest to dorsoventral orientation (anticlinal vertebra)
- Small transverse process bearing the costal facets for articulation with the ribs

- At the caudal thoracic spine, the mamillary and accessory processes emerge from the transverse process and diverge in opposite directions (Figure 14.1)
- Species and breed differences:
 - Vertebral body shape in cats is more cylindrical than in dogs
 - Spinal arrangement is physiologically more flexible in cats (curving)
 - Brachycephalic dog breeds have very short vertebral bodies.



14.1 Lateral view of a canine thoracic spine (ribs removed) where two bony processes arise from the transverse process. The mamillary process (*) diverts craniodorsally and eventually merges with the cranial articular process of T11, whereas the accessory process (#) projects caudally.

Caudal thoracic aperture and diaphragm

The diaphragm is a dome-shaped musculotendinous organ that attaches to the costal arch and covers the caudal thoracic aperture. It develops from six embryogenic segments into two muscular masses, the crura diaphragmatica, and a central collagenous tendon. The normal adult diaphragm has three openings:

- Dorsal aortic hiatus (for aorta, azygos vein and thoracic duct)
- Central oesophageal hiatus
- Dextroventral caval foramen (for caudal vena cava, CdVC).

The diaphragm is normally only radiographically visible as an interface between the air-filled lungs and the combined soft tissue opacity of the diaphragm and liver. In obese dogs and most cats, the ventral diaphragm is visible in lateral radiographs as a narrow, soft tissue band between the falciform and retrosternal fat (or caudoventral lung margins) (Figure 14.2). The dorsal portion of the crura diaphragmatica attaches to the ventral surfaces of the third and fourth lumbar vertebrae. At this junction the diaphragm forms the lumbodiaphragmatic recess.

The diaphragmatic silhouette has a variable appearance on the different radiographic views (see Figures 1.27, p. 17 and 1.29, p. 18):

- On the lateral view, the tendinous dome is projected cranioventrally and the two crura are projected caudodorsally
- On the ventrodorsal (VD) view, the tendinous dome is projected most cranially with the peak of the dome slightly to the right of midline. Both crura are positioned laterally



14.2 Lateral thoracic radiograph of a normal 8-year-old Domestic Shorthair cat. The diaphragm is visible in its ventral portion (arrowed), outlined by the aerated lungs and retrosternal fat cranially, and falciform fat caudally.

- On the dorsoventral (DV) view, only the dome is radiographically visible
- The right crus is positioned cranially to the left crus in right lateral recumbency, and *vice versa* in left lateral recumbency. This is due to the weight of the abdominal organs pushing more on the dependent crus
- The right crus can be easily identified radiographically because the CdVC enters the thoracic cavity via the caval foramen through the right crus
- The left crus is often underlined by the gas-filled fundus of the stomach
- In right lateral recumbency, the two diaphragmatic crura tend to run parallel; whereas they are usually converging ventrally in left lateral recumbency.

The diaphragm forms several recesses where it attaches to the thoracic wall: the dorsal, ventral, right and left costodiaphragmatic recesses. The right and left costodiaphragmatic recesses are located at the same level on both sides (see Figure 1.27, p. 17). On DV/VD views, the point where the projection of the caudal mediastinum joins the shadow of the diaphragm also forms an angle, referred to as the cardiaphragmatic angle (see Figure 1.29, p. 18).

Conventional radiography displays the diaphragmatic position only at the precise moment of the exposure. Fluoroscopy allows dynamic assessment of the diaphragm during inspiration and expiration.

Functional aspects of the thoracic boundaries

The thoracic boundaries are constructed to protect the thoracic viscera, yet allow the respiratory expansion of the lungs. During inspiration the diaphragm contracts, resulting in a flattening of its contour. There is opening of the lumbodiaphragmatic and costodiaphragmatic

recesses. The diaphragm is the main contributor to inspiratory chest expansion. Contraction of the inspiratory muscles contributes to chest expansion via:

- Outward rotation of the ribs
- Slight ventral angulation of the sternum
- First rib pair is fixated by scalenius muscles and thereby acts as an anchor point for rib cage movement.

During expiration there is passive relaxation of diaphragm, resulting in its dome-shaped cranial contour, and relaxation of the inspiratory muscles. Expiration can be enhanced by contraction of the expiratory thoracic and abdominal musculature. There are slight differences in the functional anatomy of the rib cage in dogs and cats, which are outlined in Figure 14.3.

Interpretive principles

Thoracic skeleton

Ribs

The ribs are often overlooked or not carefully scrutinized during thoracic radiographic assessment. Their small individual size and abundant number, combined with low-contrast chest radiographic technique, makes them blend in with other thoracic structures. To avoid distraction from other thoracic organs, it is useful to evaluate the ribs with the radiograph in a non-standard orientation (see Figure

1.21, p. 14). Assessment of the ribs should be based on the classic Röntgen signs.

Number, location and symmetry: It is important to count the ribs when assessing them. If there are rib abnormalities, it is important to know which particular rib is affected:

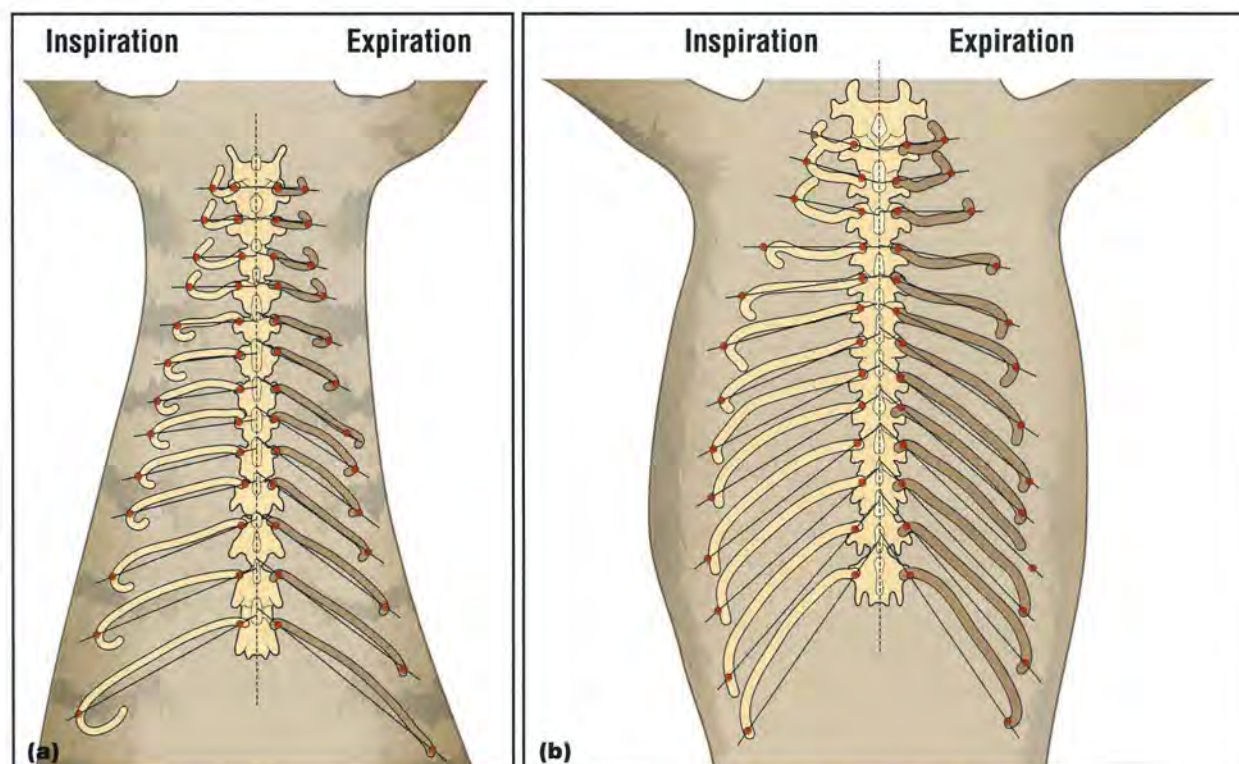
- Monostotic rib lesions are suggestive of primary rib neoplasia, osteomyelitis or focal trauma
- Polyostotic rib lesions are suggestive of trauma, osteochondromatosis, osteomyelitis (bite wounds, migrating foreign body), or underlying metastatic or metabolic disease.

Asymmetry of rib spacing can be an indicator of:

- Thoracic and spinal deformities
- Local trauma or previous surgery
- Unilateral pneumothorax
- Unilateral hyper- or hypoinflation
- Oblique radiographic technique (artefactual).

Shape and opacity:

- Osteolysis (Figure 14.4):
 - Irreversible destruction of bone by aggressive disease
 - Active destruction of the rib cortex and/or medulla
 - Punctate lucencies in bone marrow tumour (multiple myeloma or lymphoma)
 - May lead to pathological fracture
 - Tangential radiographs helpful in subtle lesions.



14.3

The (a) feline and (b) canine rib cage in inspiration (left) and expiration (right). The feline thorax has a truncated cone shape with near-parallel oriented ribs, allowing maximal respiratory excursion but offering less stability. The canine thorax is barrel-shaped. The fan-shaped array of ribs allows less respiratory excursion but offers more stability. (Redrawn after Vollmerhaus B *et al.* (1999) with permission from *Tierärztliche Praxis K*)



14.4 Close-up of a DV thoracic radiograph of an 8-year-old Boxer with a primary osteosarcoma in the distal third of the left tenth rib. There is an expansile predominantly osteolytic rib lesion (arrowhead) and adjacent external and internal (extrapleural) soft tissue swelling (arrowed).

- Osteopenia (see Figures 14.5 and 14.43):
 - Benign, reversible process
 - Predominant mineral resorption due to: local disuse (Wolff's law), leading to detached rib fragments; or generalized disturbance of calcium homeostasis, commonly seen with hyperparathyroidism and hyperadrenocorticism
 - May lead to pathological fractures.
- Periosteal reaction (Figure 14.6):
 - A reparative or proliferative process of bone
 - Active and/or proliferative processes have more irregular margins
 - Inactive and/or benign processes have smoother margins
 - The nature of the periosteal reaction plus other features (e.g. osteolysis) will indicate whether the process is aggressive or benign.
- Sclerosis and osteopetrosis (Figure 14.7):
 - Increased radiopacity without alteration in shape due to internally laid down bone
 - Sclerosis is a local phenomenon in response to applied stress (Wolff's law) and is rarely seen in ribs
 - Osteopetrosis (myelosclerosis) is a generalized condition with defective bone resorption (bone dysplasia). It can be associated with diseases affecting the bone marrow (feline leukaemia virus, pyruvate kinase deficiency or other genetic defects). It affects the entire skeleton but ribs are among the most evidently affected bones. Affected ribs have a marbled opaque appearance.



14.5 Lateral thoracic spinal radiograph of a 13-year-old Jack Russell Terrier with chronic hyperadrenocorticism. All visible vertebrae and ribs are relatively osteolucent. The ribs are almost not visible and the vertebral margins stand out against the more demineralized medullary cavity. Obesity contributes to the low image contrast.



14.6 Close-up of the left thoracic wall from a DV radiograph of a 9-year-old Burmese cat with a primary rib osteosarcoma. Notice the marked irregular new bone formation, primarily on the external thoracic wall. (Courtesy of the Animal Health Trust)

Other indicators of rib pathology include:

- Adjacent soft tissue swelling
- Extrapleural sign (see Figures 14.4 and 14.35c). This sign is characterized by a locally concave peripheral lung margin and signifies the presence of a mass originating from the pleura, chest wall or ventral mediastinum (sternal lymphadenopathy).

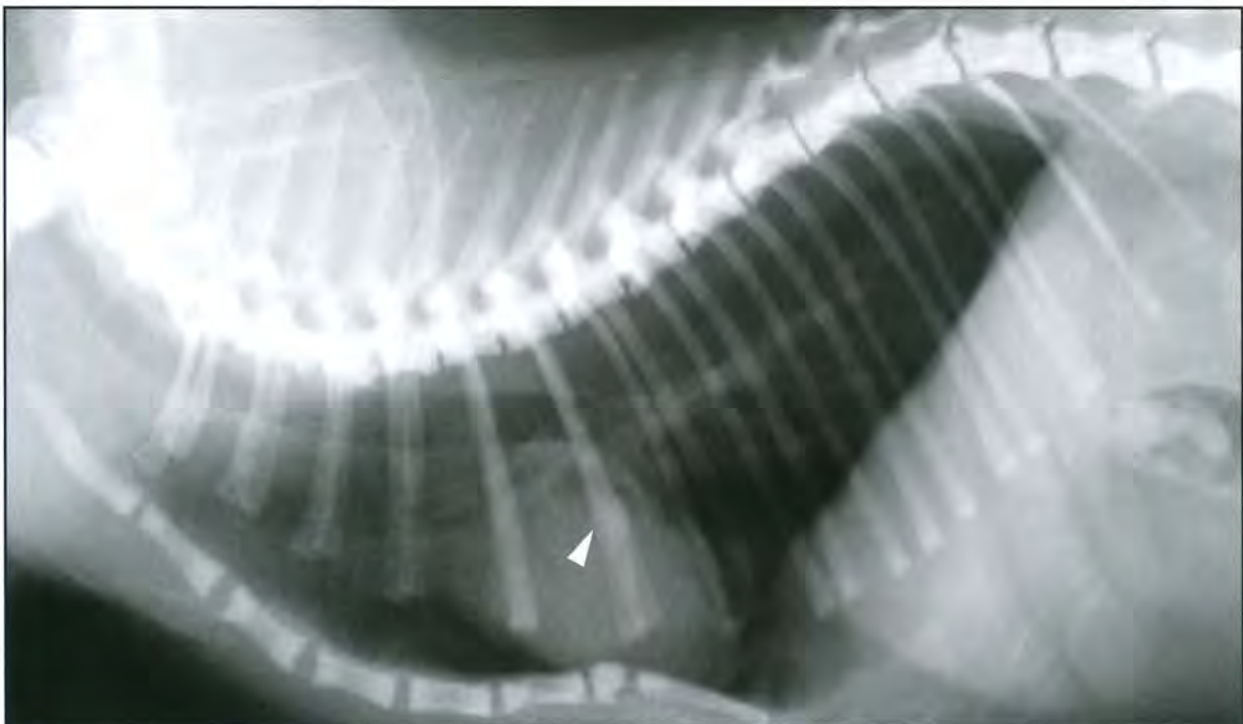
Soft tissues of the thoracic wall

The soft tissue mantle of the rib cage should be thin and even. Skin folds are common in many dog breeds, and are particularly prominent in Shar Peis (Figure 14.8). They can cast a disturbing pattern of lucencies and opacities over the entire thorax. Skin folds should be differentiated from intrathoracic pathology; skin folds extend beyond the thoracic margins. They can give rise to a false appearance of pneumothorax (pseudopneumothorax) (see Chapter 13).

Subcutaneous emphysema is a common sequel to neck and chest wall injuries (Figure 14.9) and displays a pattern of dispersed lucencies over the thorax, which could be misinterpreted as lung pathology. Two views and careful examination of the soft tissues with an intense light source will aid in differentiation:

- Usually extends beyond the chest wall margin
- Can be localized to skin via an orthogonal view.

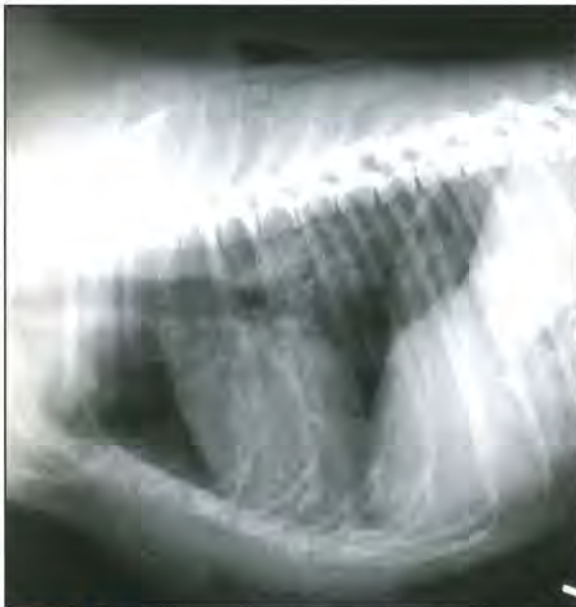
A wet haircoat and subcutaneous oedema create a mottled or streaky (hair) opacity superimposed on the thorax. Ultrasound coupling gel can also give rise to confusing patterns and should be thoroughly wiped off before radiography.



14.7 Lateral thoracic radiograph of a 7-month-old Domestic Shorthair cat that presented with spontaneous bilateral patellar fractures. There is increased medullary opacity of all visible bones consistent with osteopetrosis. Smooth callus from an old healed rib fracture (arrowhead) can be seen. The exact cause of the disease could not be established, but the multiple pathological fractures and age of the cat suggest a genetic disorder.



14.8 (a) Lateral thoracic radiograph of a Shar Pei. The extremely folded skin can create a bizarre pattern of opaque and lucent stripes. Notice how the folds extend beyond the ventral and dorsal margins of the thoracic cavity. (b) Close-up of a DV radiograph of the left caudal thorax of a dog. There is a very lucent area in the caudolateral thorax, separated from normal lung tissue by a sharp line. The line extends cranially beyond the thoracic cavity (arrowheads) indicating that this is a skin fold. A close inspection with an intense light source should be undertaken to rule out pneumothorax.



14.9 Lateral thoracic radiograph of a 5-year-old mixed breed dog that sustained bite injuries from another dog. Notice the finely dispersed gas bubbles over the ventral thorax and subcutaneous gas pockets dorsally.

Lipomas, nipples and other soft tissue masses should be recognized radiographically. If palpable, it can be useful to mark masses with barium or a radiopaque marker, to account for their contributing radiopacity to the radiographic image.

Spine

For proper radiographic assessment of the thoracic spine it is important to:

- Position the animal in an extended position, preferably under general anaesthesia
- Ensure straight positioning by use of positioning devices (foam wedges, trough):

- Sternum overlaps spine on a VD radiograph
- Dorsal arches of rib pairs superimpose on a lateral radiograph.
- Obtain a VD view rather than a DV radiograph (to avoid magnification).

Assessment of the spine relevant to thoracic diseases should include:

- Counting the number of vertebrae
- Relative position, size, shape and opacity of thoracic vertebrae and spine as a whole:
 - Rule out fractures and aggressive bone lesions
 - Relate to rib abnormalities
 - Rule out scoliosis, lordosis and kyphosis.
- Assessment of the intervertebral disc spaces for size and margination.

Sternum

The sternum is best evaluated on the lateral view (see Figure 1.23, p. 15) because of superimposition over the spine on straight VD/DV views. Oblique views can be helpful if sternal abnormalities are suspected. Normal degenerative ageing features include:

- Formation of ventral or dorsal bony spurs, bridging between sternebrae
- Mineralization of sternal cartilages and sternal–costal junctions.

Diaphragmatic silhouette

Several parameters should be taken into consideration when assessing the diaphragm radiographically:

- Position
- Shape and symmetry
- Integrity and contour.

Numerous technical and patient-related factors have a great influence on the appearance of the diaphragmatic silhouette. These should be ruled out before diaphragmatic disease is diagnosed, and include:

- Location of the central ray and beam direction. The diaphragm appears different on radiographs centred over the abdomen
- Visceral distension, obesity, state and depth of respiration
- Recumbency of animal
- Breed-specific chest conformation.

Diaphragmatic displacement

Diaphragmatic displacement is usually caused by thoracic or abdominal volume increase or reduction. Intrinsic diaphragmatic diseases, causing phrenic laxity, are rare. The position of the diaphragm can be subjectively assessed evaluating:

- The distance between the diaphragmatic dome and the cardiac silhouette
- The orientation of the CdVC and cardiodiaphragmatic angle

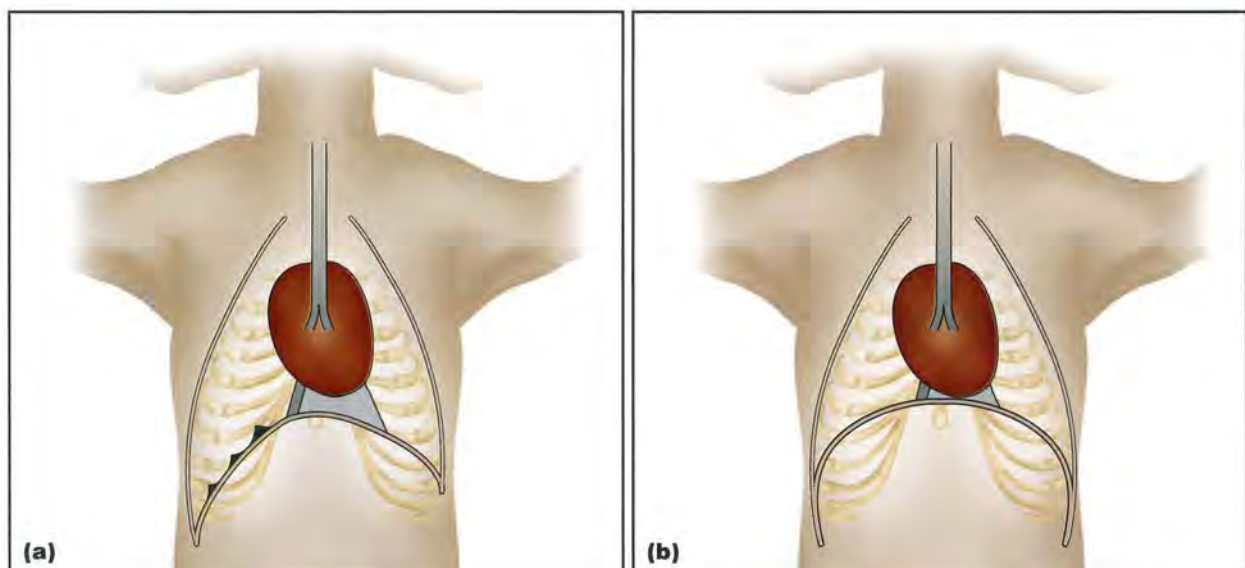
- The caudal extent and angle of the costodiaphragmatic and lombodiaphragmatic recesses.

Unilateral displacement: DV or VD radiographs are best to assess alterations from the physiological asymmetry of the diaphragm (Figures 14.10, 14.11 and 14.12):

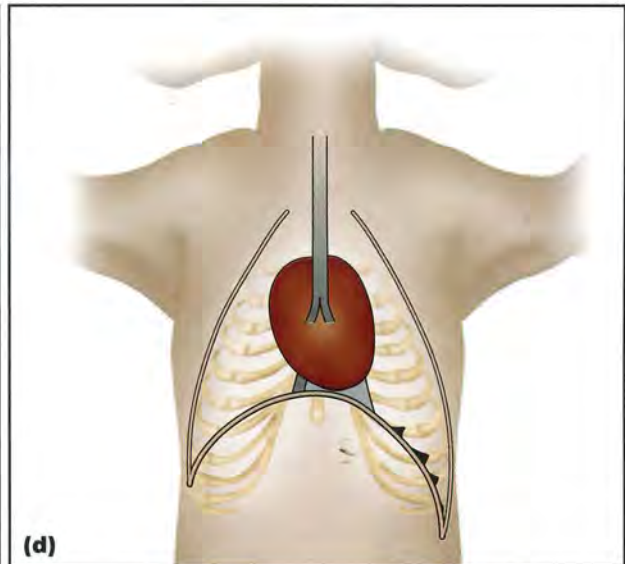
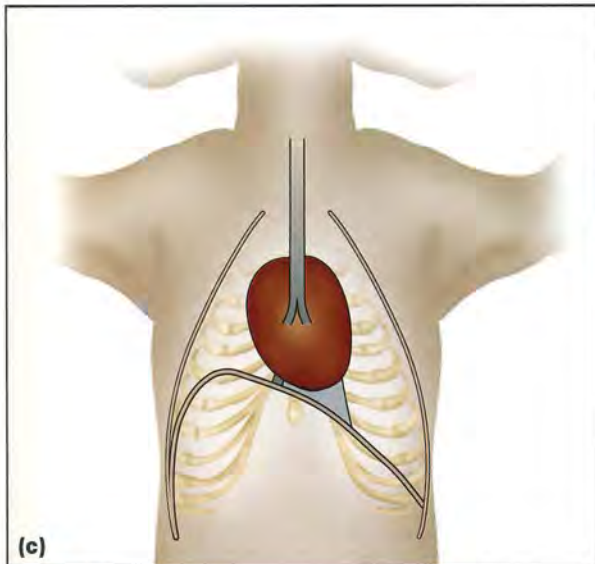
- A raised right hemidiaphragm or a depressed left hemidiaphragm will accentuate the asymmetry
- A depressed right hemidiaphragm or a raised left hemidiaphragm will decrease the degree of asymmetry
- The costodiaphragmatic recesses will move cranially or caudally with the raised or depressed hemidiaphragm accordingly, both sides being then at a different level of rib number
- A marked asymmetry of the diaphragm without asymmetry of the costodiaphragmatic angles is usually of no clinical significance.

Abnormally raised hemidiaphragm	
Collapsed caudal lung lobe Previous lung lobectomy Unilateral pleural adhesions, secondary to pleural scars, dry pleuritis or abscesses Cranial abdominal mass, such as haematoma, abscess or neoplasm of the liver or spleen Eventration (thinning and weakening of one hemidiaphragm with absence or atrophy of the muscles)	Unilateral phrenic nerve paralysis Severe thoracic wall trauma Scoliosis Sternal malformations Diaphragmatic hernias Diaphragmatic tumours
Abnormally depressed hemidiaphragm	
Unilateral incomplete bronchial obstruction ('check valve' obstruction) Bullous or lobar emphysema and cysts Unilateral pneumothorax	Unilateral pleural effusion Extrapleural mass Intrathoracic mass

14.10 Principal causes of unilateral diaphragmatic displacement.



14.11 Unilateral diaphragmatic displacement. (a) A depressed right hemidiaphragm and (b) a raised left hemidiaphragm, lead to an increased symmetry of the diaphragmatic shadow. (Adapted from Suter (1984) with permission) (continues)



14.11 (continued) Unilateral diaphragmatic displacement. **(c)** A raised right hemidiaphragm or **(d)** a depressed left hemidiaphragm, lead to an increased asymmetry of the diaphragmatic shadow. Note the different levels of the costodiaphragmatic angles between the right and the left side saw tooth-like diaphragmatic surface: tenting of the diaphragmatic rib cage insertion (forceful diaphragmatic contraction). (Adapted from Suter (1984) with permission)



14.12 DV thoracic radiograph of a 3-year-old Bengal cat with an old healed chest wall injury from a road traffic accident. Marked asymmetry of the diaphragm is present due to the abnormal thoracic wall conformation. This is a clinically non-significant finding as the costophrenic angles are at the same level and no respiratory signs were present.

If a change in asymmetry of the diaphragm is suspected on the DV view, it should be confirmed by obtaining a VD view and *vice versa*. An increased asymmetry on the VD/DV views often corresponds to a marked disparity in the level of the two crura on the lateral view. Inspiratory as well as expiratory radiographs may help in confirming the asymmetry/disparity of level between the two crura.

Associated radiographic signs, such as thoracic wall integrity, pleural effusion or thickening, mediastinal shift and alterations in lung lobe volumes, should be assessed to identify a potential underlying thoracic aetiology.

Bilateral displacement: Bilateral displacement of the diaphragm is more difficult to diagnose as the normal shape of the diaphragm is maintained (Figures 14.13, 14.14 and 14.15):

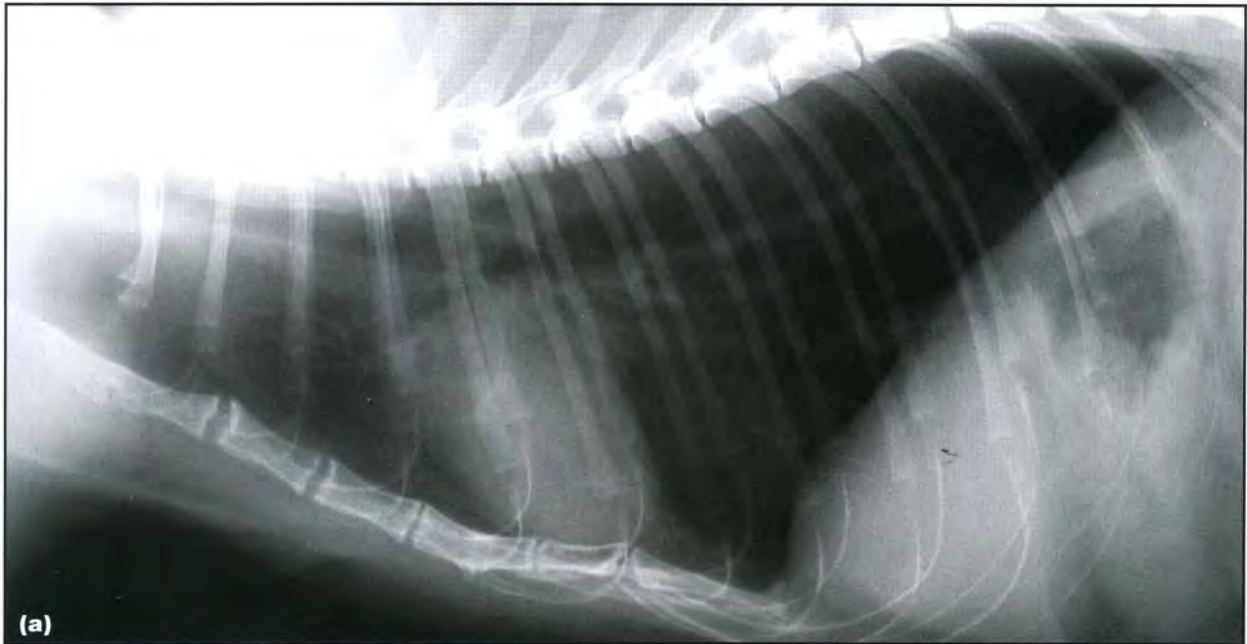
Abnormally raised diaphragm

- Excess food or gas in the stomach
- Bilateral lung lobe collapse
- Pulmonary fibrosis with cicatrization
- Severe pain
- Bilateral pleural adhesions
- Obesity
- Ascites
- Carcinomatosis
- Advanced pregnancy or pyometra
- Hepatomegaly or splenomegaly
- Large abdominal mass (abscess or neoplasm)
- Bilateral phrenic nerve paralysis

Abnormally depressed diaphragm

- Deep inspiration or forced manual inflation
- Emphysema
- Obstructive airway disease
- Diffuse pulmonary hyperinflation, secondary to shock or acidosis
- Chronic bronchial disease (bronchitis or asthma)
- Large intrathoracic mass
- Large pleural effusion
- Large closed pneumothorax or tension pneumothorax
- Emaciation
- Decreased volume of abdominal organs secondary to large body wall hernia or rupture

14.13 Principal causes of bilateral diaphragmatic displacement.

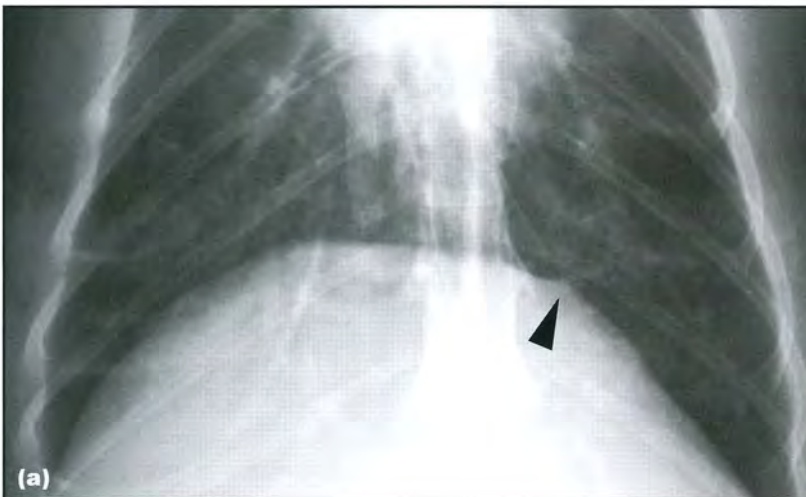


(a)



(b)

14.14 **(a)** Lateral thoracic radiograph of a 3-year-old Domestic Shorthair cat with inspiratory hyperpnoea. The lungs are maximally extended, resulting in caudal deviation and flattening of the diaphragm, and extension of the cranial lung margins beyond the thoracic inlet. **(b)** DV thoracic radiograph of a 2-year-old Domestic Shorthair cat with left pyothorax and right compensatory hyperpnoea. The diaphragmatic silhouette (arrowhead) is displaced and bent caudally by the increased intrathoracic pressure. Recognition of the diaphragmatic silhouette helps to rule out a diaphragmatic rupture with abdominal organ prolapse.



(a)

14.15 **(a)** Close-up of an inspiratory VD radiograph of the diaphragmatic silhouette of a 14-year-old hyperpnoeic Domestic Shorthair cat with asthma. Notice the subtle tent-shaped margins of the diaphragm (arrowhead) due to maximal phrenic contraction and pulling at the costal arch insertion. (continues) ▶



14.15 (continued) **(b)** VD thoracic radiograph of an 8-year-old Cairn Terrier with severe inspiratory dyspnoea. For an inspiratory radiograph the diaphragmatic dome is not flat enough, yet its irregular contour, tenting and rib spacing suggest increased respiratory effort against some obstructive force. **(c)** Lateral neck radiograph demonstrates a large laryngeal mass, diagnosed as a lymphoma.



- Repeated exposures at various stages of the respiratory cycle or continuous fluoroscopy may be necessary to assess the dynamics of the diaphragm in relation to respiration
- In animals with radiographic signs of increased inspiratory effort yet an incompletely contracted diaphragm, an upper airway obstruction impeding respiratory flow and full lung inflation should be considered.

Interrupted outline and changes in diaphragmatic contour

The diaphragmatic silhouette should be assessed on at least two orthogonal views. Radiographic change or interruption of the diaphragmatic contour (see Figures 14.4 and 14.16) can be due to:

- The presence of soft tissue opacity cranial to the diaphragm (border obliteration)
- Interruption of the diaphragm with herniation of abdominal organs into the thorax
- Diaphragmatic masses.

Tenting of the diaphragm refers to small triangular protrusions with their base at the diaphragm and their peaks toward the lungs. This is frequently seen in cats, due to visualization of the diaphragmatic attachments to the costal arch ribs during deep inspiration. It can be a manifestation of pleural adhesion (inspiration and expiration).

If gas opacities outline both sides of the diaphragm, free peritoneal and/or retroperitoneal gas must be present (see Figure 14.49). The following should be considered:

Intrinsic diaphragmatic masses protruding into the thorax

Abscess
Cyst
Neoplasm
Granuloma
Eventration

Diaphragmatic hernias

True diaphragmatic hernia
Hiatal hernias
Peritoneopericardial diaphragmatic hernia

Diaphragmatic rupture

Border obliteration by a thoracic soft tissue opacity

Pleural effusion
Pulmonary mass
Pleural mass
Oesophageal mass
Caudal mediastinal mass

14.16 Principal causes of change of outline or interrupted contour of the diaphragm.

- Pneumoretroperitoneum as an extension of pneumomediastinum/pneumothorax
- Recent laparotomy or other gas-introducing procedure
- Abdominal hollow viscus organ rupture
- Gastrointestinal ulceration with rupture
- Body wall laceration
- Gas-producing organisms.

Diseases of the thoracic skeleton

Congenital and developmental abnormalities

Congenital abnormalities of the thoracic skeleton are a relatively common phenomenon, particularly in dogs, and are often incidental. Rib, spinal and sternal abnormalities are often combined and should be assessed together. It is important to recognize these changes so as not to mistakenly diagnose pulmonary pathology due to superimposition.

Abnormal number of ribs

This is usually an incidental finding, which is only relevant if the ribs are used as a surgical landmark. Supernumerous or subnumerous ribs are usually associated with transitional vertebrae at the cervicothoracic or thoracolumbar junction. Fusion of the first and second ribs is occasionally seen in chondrodystrophic dog breeds. Rib duplication is rare.

Radiography: The abnormal number and shape of ribs are easily recognizable (Figure 14.17).

Metaphyseal developmental disorders of ribs

Metaphyseal osteopathy: Metaphyseal osteopathy (hypertrophic osteodystrophy) is an osteomalacic disease in young growing dogs of unknown aetiology.



14.17 Close-up of a lateral radiograph of the thoracic inlet of a Soft-Coated Wheaten Terrier with a ventrally fused left first thoracic and supernumerous seventh cervical rib. This is an incidental finding.

It primarily affects metaphyses of the long bones but can also affect the ribs, which may be swollen and painful. The condition is usually self-limiting. Radiographic findings include abnormal radiolucent lines in all rib metaphyses. These are seen better on long bone metaphyses.

Rickets: This is caused by vitamin D deficiency; it is rare in dogs and cats in the developed world. It can result in a *rickettic rosary*, a chain of palpable swellings along the costochondral junctions. Radiographic findings include widening and radiolucency of the metaphyseal side of the physis. Rickets may result in bony deformity.

Sternal abnormalities

Variation in the size and number of sternbrae, and in the shape of the manubrium and xiphoid process, is common and is usually incidental. Cats commonly have a ventrally deviated xiphoid process, which can be painful.

Sternal dysraphism is the failure of the left and right cartilaginous sternal precursors to fuse. It leads to a ventral defect that is only closed by thoracic fascia and pleura. In the absence of diaphragmatic defects, sternal dysraphism has no adverse respiratory or circulatory consequences.

The absence, splitting or malformation of the xiphoid cartilage has been associated with peritoneopericardial diaphragmatic hernia, which can be a useful radiographic feature in distinguishing this condition from other pericardial diseases.

Radiography: Radiographic findings include:

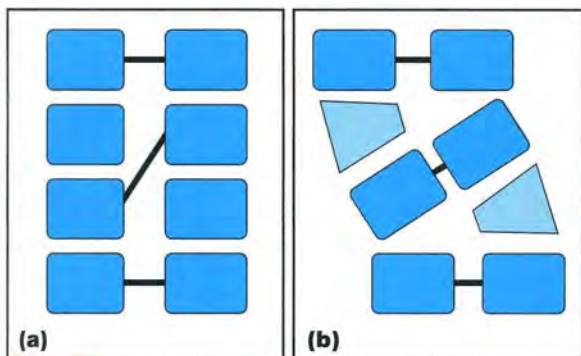
- Abnormal number and shape of sternbrae (Figure 14.18) is easily recognizable
- Ventrally deviated xiphoid process in cats
- Split sternum or xiphoid process is seen on VD/DV or oblique views with dysraphism.



14.18 Close-up of a lateral thoracic radiograph of the cranial sternum of a 2-year-old Labrador Retriever without trauma history. The manubrium is kinked, most likely due to an embryogenic fusion anomaly. This is an incidental finding.

Spinal abnormalities

Hemivertebrae: This is a congenital malformation due to hemimetameric displacement or lack of vascularization of somites (Figure 14.19). It can result in spinal curvature. It is very common in screw-tailed dog breeds, where it is usually an incidental finding.

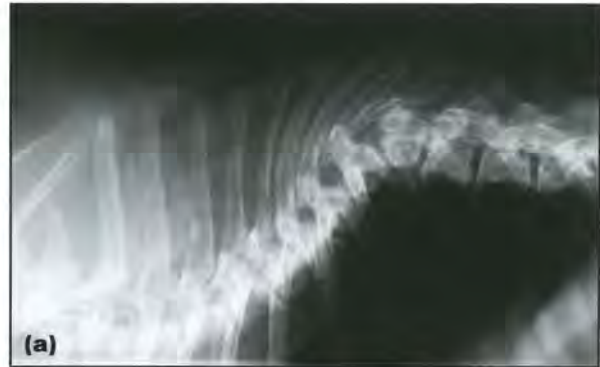


14.19 Hemivertebra formation. **(a)** Normally, paired mesodermal segments, called somites, merge and form a cartilaginous precursor of the vertebral body (upper and lower pair). **(b)** If a mismatch in the fusion pattern occurs (hemimetameric displacement), unmatched somites will form wedge-shaped hemivertebrae, resulting in a spinal curvature deformity.

Radiographic findings include:

- Curved thoracic spine (scoliosis and kyphosis most common) (Figure 14.20)
- Associated abnormal number and spacing of ribs (Figure 14.21).

Other spinal disorders: Transitional vertebrae (super- or subnumerous thoracic vertebrae) are only clinically relevant if used as surgical landmarks. Spondylosis deformans is very commonly seen in the ventral aspect of the thoracic spine of dogs and cats, and is of no clinical significance. If bone formation



(a)

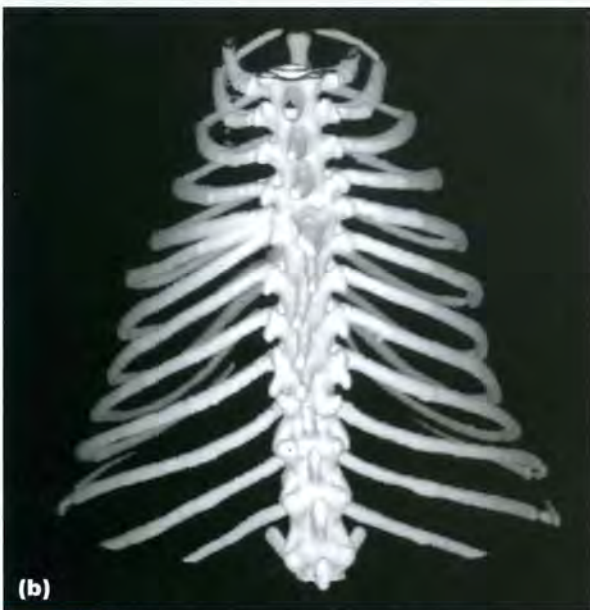


(b)

14.20 **(a)** Lateral thoracic spinal radiograph of an 8-year-old Bulldog with hemivertebra formation of the eighth thoracic vertebra, resulting in marked kyphosis. **(b)** The corresponding VD radiograph shows the additional scoliosis and associated abnormal rib spacing. Hemivertebra formation in the mid-thoracic spine is almost ubiquitous in Bulldog-type breeds and is usually of no clinical significance. Severe cases may lead to spinal cord compression.

over at least four contiguous vertebrae is present, the condition is called disseminated skeletal hyperostosis (DISH), but does not cause thoracic disease. This term is derived from human medicine and its use in animals is controversial.

There is a widespread misconception that intervertebral disc degeneration and prolapse does not occur in the mid-thoracic spine. However, in cats and some dog breeds, such as the German Shepherd Dog, mid-thoracic degenerative disc disease with spinal cord compression is not uncommon.



14.21 (a) Lateral thoracic radiograph of a 12-year-old Domestic Shorthair cat with a thymoma. There is uneven spacing of the mid-thoracic ribs. (b) 3D reconstruction from a CT scan demonstrates scoliosis and fusion of the origin of the right fifth and sixth ribs and missing left sixth rib due to hemivertebra formation.

Radiographic findings are shown in Figures 14.22 and 14.23 (see also Figure 1.23, p. 15):

- Identification of transitional vertebrae requires an entire spinal radiographic series
- Spondylosis deformans is characterized by smooth ventral and lateral bone spurs, bridging adjacent endplates
- DISH is characterized by abundant smooth or irregular new bone formation, along the ventral and lateral aspects of at least four subsequent vertebral bodies
- Intervertebral disc degeneration is characterized by a narrowed intervertebral disc space, foramen and articular facet space, and mineralized disc material protruding into the vertebral canal (protrusion or extrusion). Detailed description is beyond the scope of this book (see *BSAVA Manual of Canine and Feline Neurology*).



14.22 Lateral thoracolumbar spinal radiograph of a skeletally mature Boxer with bony spur formation on the endplates (spondylosis deformans) and exuberant new bone formation along multiple vertebral bodies (disseminated skeletal hyperostosis). Despite the sometimes dramatic appearance, neither condition usually has any clinical significance.



14.23 (a) Lateral thoracic myelogram of a 12-year-old German Shepherd Dog with chronic aggravating hindlimb weakness. There is marked dorsal deviation and thinning of the subarachnoid contrast medium column at the T6–7 intervertebral disc space. (b) Sagittal gross image at postmortem. The T6–7 intervertebral disc was degenerated and protruded. The spinal cord (removed) was markedly compressed and atrophied by the disc and dorsal longitudinal ligament proliferation. The mid-thoracic spine should not be discounted if spinal cord abnormalities are clinically confined to the T3–L3 spinal cord segment. (Courtesy of L. Jarrett)

Altered ribcage conformation

Chondrodysplasias: These are congenital skeletal deformities, resulting from abnormal cartilage development. They cause proportionate (all bones affected) or disproportionate (affecting primarily facial bones and/or appendicular skeleton) dwarfism. They are often inherited and selectively bred for in many breeds of dogs, e.g. disproportionate dwarfism in Dachshunds and Basset Hounds gives rise to the unusual ‘cottage loaf’ chest conformation.

Congenital hypothyroidism causes disproportionate dwarfism as a result of arrested thyroid activity. Mucopolysaccharidosis is a group of genetic connective tissue disorders in dogs and cats, which result in generalized skeletal deformities.

Radiographic findings include:

- Chondrodystrophic breed chest conformation on VD/DV view: inward deviation of the ventral rib component and soft tissue opaque chest wall (Figure 14.24)
- Congenital hypothyroidism: delayed physal closure and shortened, often kyphotic vertebrae (Figure 14.25)
- Mucopolysaccharidosis:
 - Oar-shaped ribs
 - Endplate sclerosis, widened and fused vertebrae
 - Degenerative joint disease and spondylosis
 - Often pectus excavatum (see below).



14.24 VD thoracic radiograph of a normal 9-year-old Basset Hound. A soft tissue opaque rim separates the right lateral lung margin from the ribs. This is due to the S-shaped rib anatomy in this chondrodystrophic breed.



14.25 Lateral thoracic spinal radiograph of a skeletally mature dog with congenital hypothyroidism. The vertebrae are stunted and have irregular epiphyses.

Pectus excavatum: Pectus excavatum (funnel chest) is a congenital or developmental abnormality, with a variable decrease in the thoracic dorsoventral diameter due to inward deviation of the sternum,

especially in its middle portion. It can affect normal respiratory physiology in severe cases. Canine brachycephalic breeds are more commonly affected and concurrent congenital malformations have been reported (hypoplastic trachea, ventricular septal defect, peritoneopericardial diaphragmatic hernia and mucopolysaccharidosis).

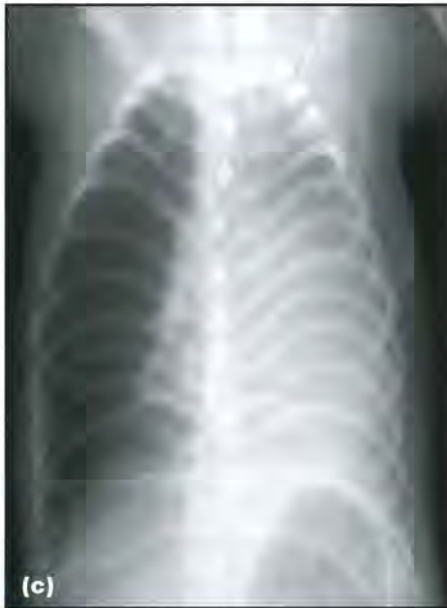
Pectus excavatum should be differentiated from physiological respiratory excursion of the sternum, which is relatively high in cats (3–5 degrees). With severe inspiratory dyspnoea due to upper airway obstruction, the sternum rotates inward to its maximal range and can mimic mild pectus excavatum. It should also be differentiated from flail sternum (bilateral rib cartilage fractures, see below) by taking radiographs at peak inspiration and expiration.

Radiographic findings (see Figures 14.26 and 12.17, p. 250) include:

- S-shaped ventral aspect of the ribs/costal cartilages with the ribs extending ventral to the sternum, which is superimposed on the cardiac silhouette (lateral radiograph)
- Static appearance in inspiratory and expiratory views
- Lateral displacement of the cardiac silhouette, usually towards the left (VD/DV view).



14.26 (a) Close up of a lateral thoracic radiograph of a 4-month-old Golden Retriever with mild pectus excavatum and an atrial septal defect. Notice the dorsal deviation of the caudal sternbrae, causing an extrapleural sign. Rib cage anomalies are commonly associated with other congenital defects. (b) Lateral thoracic radiograph of a 7-year-old Pekingese with severe pectus excavatum. (continues) ▶



14.26 (continued) (c) VD view showing the associated left-sided deviation of the heart.

Some radiographic indices have been proposed to assess the severity of the condition/need for surgical intervention:

- **Fronto-sagittal index:** ratio between the width of the chest at the tenth thoracic vertebra and the distance between the centre of the ventral surface of the tenth thoracic vertebral body and the nearest point on the sternum. Moderate cases have a ratio of 2–3. More than 3 is seen in severe cases
- **Vertebral index:** ratio between the distance from the centre of the dorsal surface of the tenth thoracic vertebral body to the nearest point on the sternum, and the dorsoventral diameter of the vertebral body at the same level. Moderate cases have a ratio of 6.00–8.99. Less than 6 indicates a severe case
- The vertebral index better differentiates normal from abnormal chest conformation, but there is still some overlap between the groups and diagnosis should not be based solely on indices.

Flat pup syndrome: Flat pup syndrome (swimmers, turtle pup) is presumably a congenital condition in dogs, similar to pectus excavatum (decreased dorsoventral thoracic diameter), but without inward rotation of the sternum. ‘Swimmer puppies’ have flattened chests and move dragging themselves by paddling their limbs laterally and caudally. Being kept on smooth floors and being overweight are believed to be contributing factors. Both chondrodystrophic and non-chondrodystrophic breeds can be affected. Radiographs show that the chest is flattened dorsoventrally, with no inward deviation of the sternum.

Pectus carinatum: Pectus carinatum (pigeon or keeled chest) is a rare congenital or developmental abnormality, with an increase in the dorsoventral

diameter of the thoracic cavity due to the outward deviation of the cranial sternebrae, together with an inward deviation of the most caudal sternebrae. It is usually incidental. There is a possible relationship with congenital cardiac abnormalities. Radiographs show an increased dorsoventral dimension of the rib cage due to caudal displacement of the sternum.

Barrel chest: This is an acquired condition where a maximally dilated chest is found, with a marked outward position of all ribs and the sternum. An underlying condition should be identified and could include:

- Marked pleural effusion or pneumothorax
- Large intrathoracic masses
- Pulmonary emphysema or hyperpnoea.

Barrel chest is a breed-specific feature in some brachycephalic dog breeds (e.g. Bulldog, Boston Terrier). Radiographic findings include:

- Rounded chest conformation with wide equal rib spacing in inspiration and expiration
- Radiographic features of an underlying condition, causing chest distension.

Fractures of the thoracic skeleton

Rib fractures

Most rib fractures are of *traumatic* origin. However, particularly in outdoor cats or stray animals, a traumatic history is not always known. Traumatic fractures are usually transverse, oblique or segmental, and are often multiple and sequential. Displaced fragments can cause penetrating injuries, and open or closed pneumothorax. With a known history of trauma, rib fractures should be taken as an indicator of potential adjacent lung trauma. Radiographic signs of lung contusion may only become visible 6 hours after the injury; serial radiographs are useful to monitor pulmonary disease in such cases.

Rib fractures and thoracic wall bruising can be very painful and impair proper ventilation, leading to hypoxaemia. Non-displaced rib fractures are most commonly treated conservatively (analgesia and rest), whereas internally displaced rib fractures need surgical reduction and stabilization.

Flail chest is associated with the presence of three or more sequential segmental rib fractures or five or more single rib fractures.

- Causes paradoxical movement of the affected portion of the thoracic wall (inward on inspiration, outward on expiration).
- Worsens hypoxaemia and contusion to the underlying lung parenchyma.
- Requires surgical stabilization.

Flail sternum is a specific form of flail chest, which can occur with multiple bilateral rib cartilage fractures and paradoxical respiratory movement of the sternum.

Pathological or stress rib fractures are not uncommon and can be associated with conditions that weaken the bone structure, or as a result of chronic hyperinflation and cough. Features of pathological fractures include:

- Usually chronic malunion or non-union fracture
- More common in females and cats
- Often multiple
- Preferential caudal and dorsal location (serratus dorsalis cranialis muscle insertion)
- Often coincident with hiatal hernia
- Occasionally occur as a greenstick fracture
- Usually not painful.

Without traumatic history, rib fractures should be considered as an indicator for underlying osteopenic, osteolytic or respiratory conditions. Possible underlying diseases of pathological or stress fractures are:

- Chronic feline renal disease or other causes of hyperparathyroidism
- Rib neoplasia (fracture consistent with lesion location)
- Feline asthma, chronic canine bronchial disease
- Lobar emphysema.

Because of the constant movement of the thoracic bellows, ribs have a poor healing tendency and

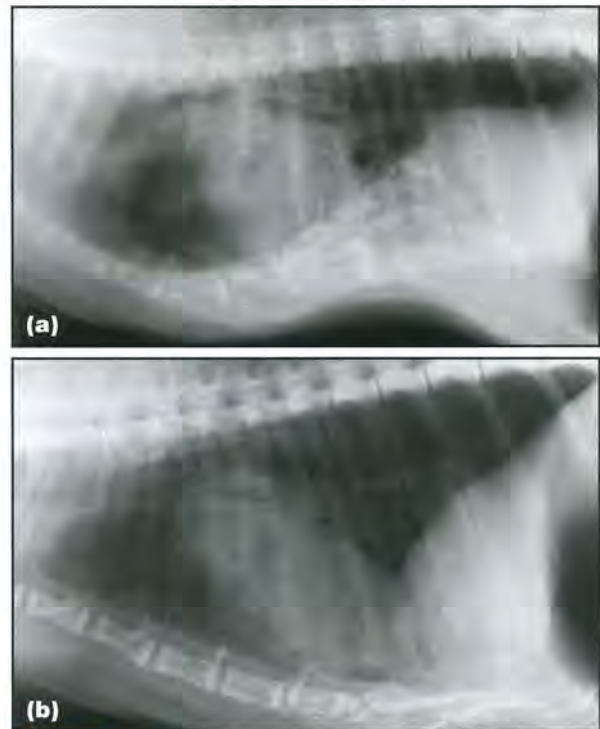
non-union or malunion fractures are commonly seen. The age of a fracture should be considered when relating it to the history and current complaint of the patient.

Radiography: Radiographic findings include:

- Interruption of the cortical margins/radiolucent line traversing the rib
- Focal increase in radiopacity at the site where the fracture ends overlap
- Altered direction and spacing of the ribs
- Flail chest: inspiratory inward displacement of fracture segments of three or more adjacent ribs (Figure 14.27)
- Flail sternum: inspiratory inward displacement of the sternum, expiratory outward rotation (Figure 14.28)
- Traumatic fractures, usually ipsilateral to the impact site
- Fractures due to metabolic or respiratory conditions, often serial and caudally and dorsally located
- The fracture margin should be sharp in recent traumatic fractures and remodelled in chronic fractures. Unsharp fracture margins without remodelling suggest a recent pathological fracture due an osteolytic process.



14.27 Close-up of a DV thoracic radiograph of a 7-year-old Golden Retriever with multiple segmental rib fractures as a result of a road traffic accident. There is also adjacent lung consolidation consistent with contusion. Flail chest causes paradoxical respiratory movement and requires surgical stabilization.



14.28 (a) Lateral inspiratory thoracic radiograph of an 11-year-old Domestic Shorthair cat with dyspnoea and a suspected trauma history. There is a marked dorsal deviation of the sternum, resembling a pectus excavatum malformation. (b) Repeat expiratory radiograph reveals a normal sternal position. This is consistent with a flail sternum caused by multiple bilateral fractures of the ventral rib cartilages. Due to the incomplete mineralization of those cartilages, the fractures are not radiographically visible. (Courtesy of the University of Pennsylvania)

Orthogonal views should always be taken in cases of suspected/known thoracic trauma (Figure 14.29). Multiple views should help to detect:

- Non-displaced fractures
- Lesions of the costal cartilage or junction, or the very proximal aspect of the rib
- Costosternal luxations.

Findings with chronic fractures may include:

- Normal callus formation: smooth bony proliferation that diminishes over time, small static residual changes

- Non-union: 'elephant foot'-like, enlarged, sclerotic fracture ends (Figure 14.30)
- Malunion: abnormal angulation, often with a large callus.

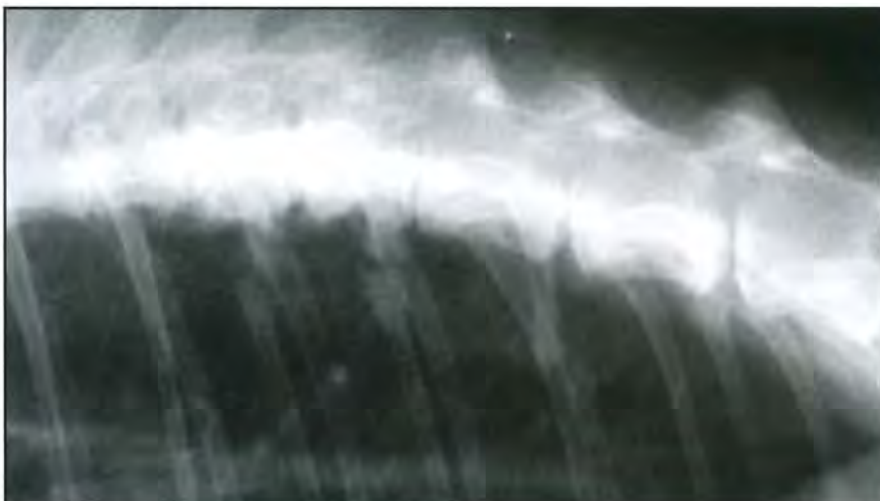
Sternal fractures and dislocation

Malalignment of sternebrae, with or without prior trauma, is frequently observed and is insignificant unless accompanied by intra- and extrathoracic soft tissue swelling or clinical signs.

Radiography: There is usually obvious dislocation (Figure 14.31). Malposition of the xiphoid process in cats is usually not traumatic.



14.29 (a) Close-up of a lateral thoracic radiograph of a 7-year-old German Shepherd Dog that was involved in a road traffic accident. There is dorsocaudal lung opacification, a small pneumothorax and several rib fractures which are difficult to see. (b) The corresponding DV radiograph demonstrates more clearly a series of six rib fractures. Orthogonal views can be very helpful in identifying rib fractures.



14.30 Close-up of a lateral thoracic radiograph of a 10-year-old Domestic Shorthair cat with chronic inspiratory dyspnoea due to a nasal adenocarcinoma. Notice the serial fractures in the proximal aspect of three ribs with round widened margins (non-union). The history and fracture location (serratus dorsalis cranialis muscle insertion) are most consistent with stress fractures, secondary to chronic hyperinflation.



14.31 Close-up of a lateral thoracic radiograph of a 10-year-old Labrador Retriever with an old untreated dislocation of the fourth intersternbral joint. The sternum is more likely to dislocate than to fracture on blunt force trauma. This is usually of no clinical significance, although some instability might be palpable.

Spinal fractures and dislocations

Spinal fractures and dislocations usually occur at junctions between major segments (cervical, thoracic, lumbar, sacral and coccygeal), are often compressive and can be a sequel to underlying osteolysis (pathological fracture). In the context of thoracic trauma, the spine should be carefully examined for evidence of fractures because radiographic features are often subtle; this requires two orthogonal views, and may change prognosis and treatment options.

Radiography: Radiographic findings include:

- Epiphyseal slip fracture in young animals with often minimal displacement (Figure 14.32)
- Compression fracture: shortening of the vertebral body.

Computed tomography: Computed tomography (CT) is a sensitive and specific tool used to assess the instability of spinal fractures (Figure 14.33).



(a)

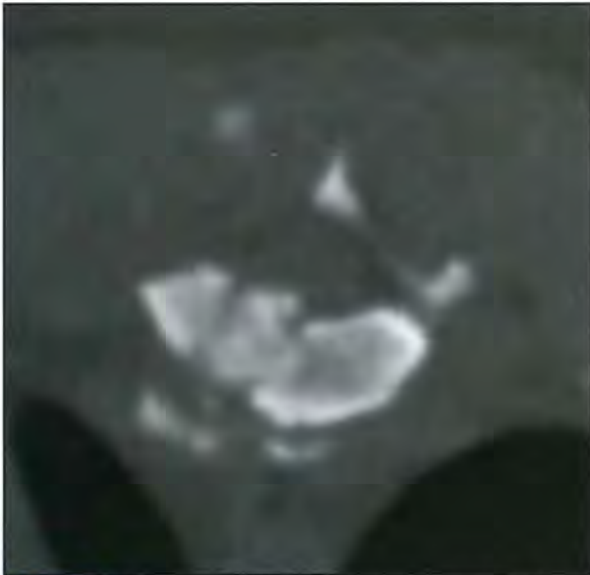


(c)



(b)

14.32 (a) Close-up of a thoracic spinal radiograph of a 4-month-old English Springer Spaniel, which was involved in a road traffic accident. There is a minimally displaced physeal fracture of the caudal endplate of the eleventh thoracic vertebra, which is barely recognizable (arrowhead). (b) Postmortem specimen radiograph clearly demonstrates the fracture and displacement. A diligent fracture search is indicated if spinal trauma is suspected. The muscular bracing often prevents large displacement of fracture elements. (c) DV postmortem specimen thoracic spinal radiograph of a 2-year-old paraplegic Irish Terrier, which was involved in a road traffic accident. There is complete luxation of the T5-6 intervertebral and right vertebrocostal joint, a fracture of T6 and complete shearing of the spinal cord. Thoracic spinal dislocation is unusual in dogs and cats, and most likely to be related to strong bending forces associated with a blunt force trauma.



14.33 CT image of the twelfth thoracic vertebra of a 1-year-old Pug, which was involved in a road traffic accident. There is a comminuted compression fracture involving the ventral, middle and dorsal compartment of this vertebra with compression of the spinal cord.

Benign mass lesions

Osteochondroma

This is a skeletal dysplasia (a form of hamartoma) associated with expansile bony lesions, which usually arises from the osteochondral junction of bones. The lesion usually stops growing at the time of skeletal maturity. Aetiological theories include:

- Herniation of part of a physis
- Proliferative response to stress at the physal margin
- Biochemical disorder, allowing redirection of physal growth
- Periosteum regaining its perichondral potential due to an unknown factor.

It is potentially a hereditary condition. In rare cases malignant transformation may occur. Commonly affected areas are the costochondral rib junctions; less frequently, the metaphyses of the long bones and vertebrae may be involved. Small rib lesions are common in dogs, but rare in cats. The condition can affect multiple sites simultaneously (multiple cartilaginous exostoses).

Clinical signs are usually related to lameness or paresis/paralysis in the case of spinal cord compression.

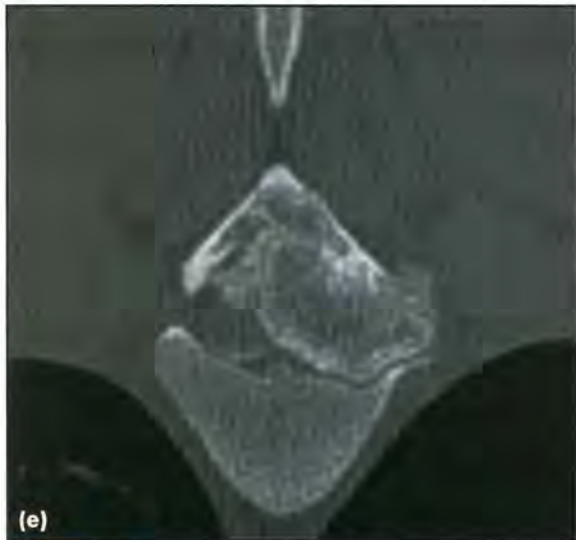
Radiography: There is one or more bone mass of variable opacity and margination (Figure 14.34):

- Often cauliflower or soapy bubble-like
- Active lesion irregular in opacity and poorly margined
- Inactive lesions are homogeneously opaque and smoothly margined.



14.34 The different facets of osteochondromatosis.

(a) Most commonly encountered as a polyostotic small irregular mineralization at the costochondral junction, which may give rise to an extrapleural sign (arrowhead), as in this 12-year-old Golden Retriever. **(b)** Occasionally, a single costochondral osteochondroma is present, as in this 4-year-old Shetland Sheepdog. **(c)** Other areas of the ribs can be affected, as in this dog with multiple cartilaginous exostoses in the ribs and appendicular skeleton. (continues) ▶



14.34 (continued) The different facets of osteochondromatosis. **(d)** Other bones, such as the sternum, can give rise to osteochondromatosis, as in this 3-year-old Domestic Shorthair cat. **(e)** If osteochondromas occur in the thoracic spine, such as seen on this CT image of the sixth thoracic vertebra in a 2-year-old Great Dane, they can cause significant spinal cord compression. Osteochondromas are osteoproliferative lesions with variable margination. In contrast to most malignant bone tumours they are not osteolytic, but may cause pressure atrophy of adjacent bones.

Differentiation of osteochondroma from malignant neoplasia and healed rib fracture is based on the typical location at the costochondral junction of several ribs.

Other imaging techniques: CT or magnetic resonance imaging (MRI) may be used to assess spinal cord compression of vertebral osteochondroma.

Aneurysmal bone cyst

This is a rare benign non-neoplastic condition seen in different bones, including the ribs. The presumed aetiology is that an original insult disrupts, but does not interrupt, bone marrow vasculature. A large arteriovenous fistula then forms, distending the cortex.

Radiography: Radiographic findings include:

- Large expansile osteolytic rib lesion with eggshell-like rim
- Monostotic
- Cannot always be differentiated from malignant neoplasia and osteochondroma.

Neoplasia

Rib and chest wall tumours

Primary rib tumours are relatively rare in dogs and very rare in cats; there is no known sex or breed predisposition, and they are also seen in young animals. Osteosarcoma and chondrosarcoma are the most common; fibrosarcoma, haemangiosarcoma and benign neoplasms (osteoma, chondroma) are seen less frequently. Primary tumours are often located in the distal third of the rib (costochondral junction). They tend to metastasize to the lungs and other organs. Primary rib tumours are rare compared with appendicular primary bone tumours. Clinical signs are associated with the enlargement of the mass:

- Fixed firm chest wall mass in some cases
- Can expand predominantly intrathoracically without a visible external mass
- Dyspnoea, cough due to lung compression and/or haemothorax
- Front limb lameness if impeding on shoulder joint or brachial plexus.

Metastatic, bone marrow and invading soft tissue neoplasia in ribs have certain features:

- Metastatic rib tumours are usually small and located in the proximal or middle portion of the rib
- Multiple myeloma frequently affect the ribs along with the vertebrae and other bones, where changes are more easily recognizable
- Primary bone lymphoma or bone involvement in multicentric lymphoma is rare in dogs and cats. Young animals can be affected. Primary bone lymphoma can preferentially affect the metaphyses in growing bones
- The most common soft tissue mass of the chest wall is fibrosarcoma, which is particularly common in cats. Fibrosarcomas can usually be distinguished from diffuse processes, such as cellulitis or haemorrhage, by their focal distribution and their propensity to grow toward the thoracic cavity. They can be difficult to differentiate from primary rib tumours. There is often polyostotic involvement in soft tissue tumours
- Pleural neoplasia (mesothelioma) can affect multiple ribs and be difficult to differentiate from other types of neoplasia.

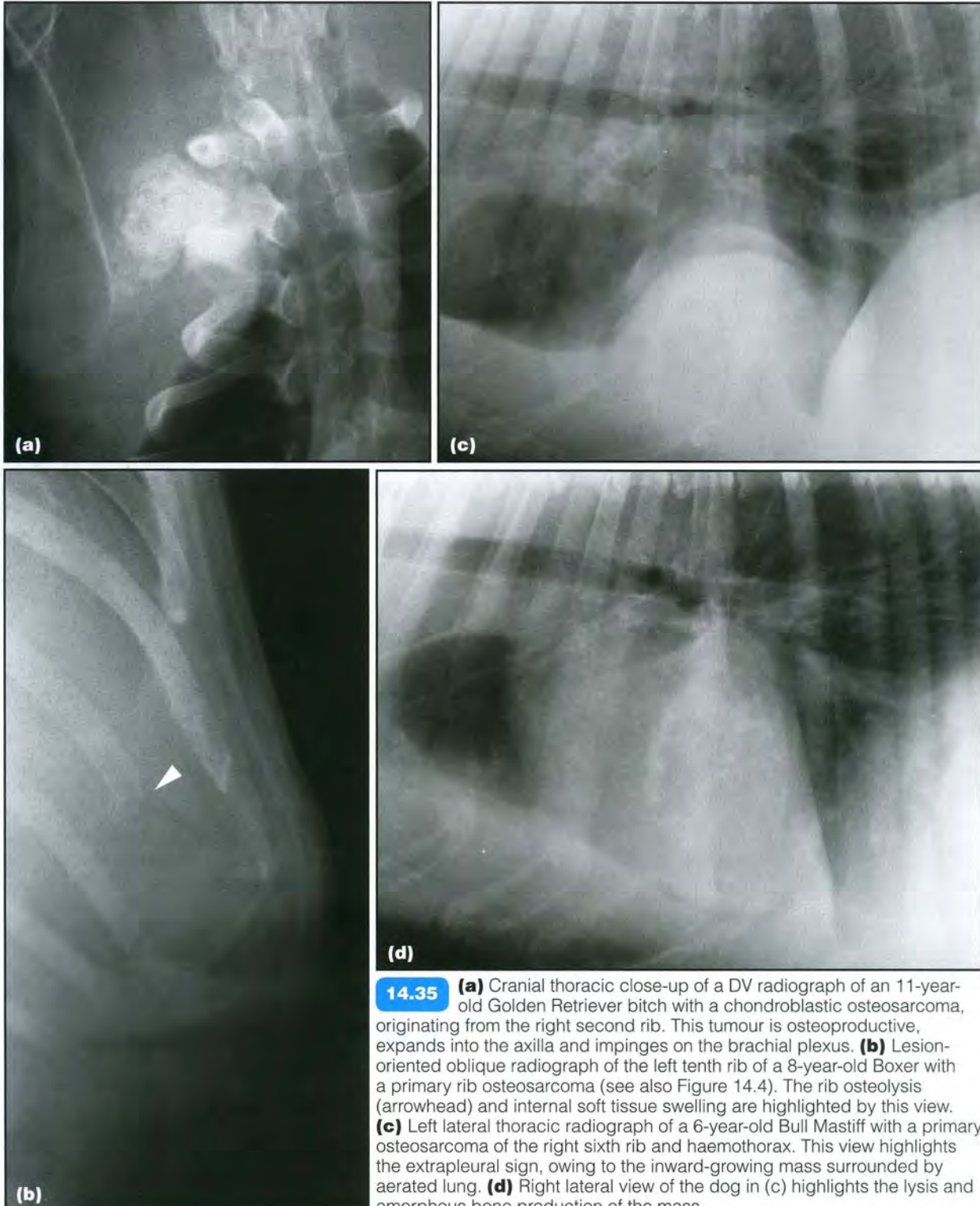
Lipoma and liposarcoma may arise from the thoracic wall. Benign lipomas are extremely common in the subcutaneous layers of the thoracic wall, and are characterized as soft, moveable slow-growing masses. Occasionally, a benign mass arises from the internal thoracic wall and causes a mass effect on internal thoracic organs. Infiltrative lipomas

and liposarcomas can also infiltrate the inter- and intramuscular layers of the thoracic wall.

Radiography: Tangential and opposite lateral radiographs are often helpful. Osteolysis is seen (Figure 14.35) but can be subtle to detect. There may be an irregular to sunburst periosteal reaction and amorphous new bone. Fractures may be present, with unsharp margins (pathological fracture). The extrapleural sign (focal inward deviation of the pleural

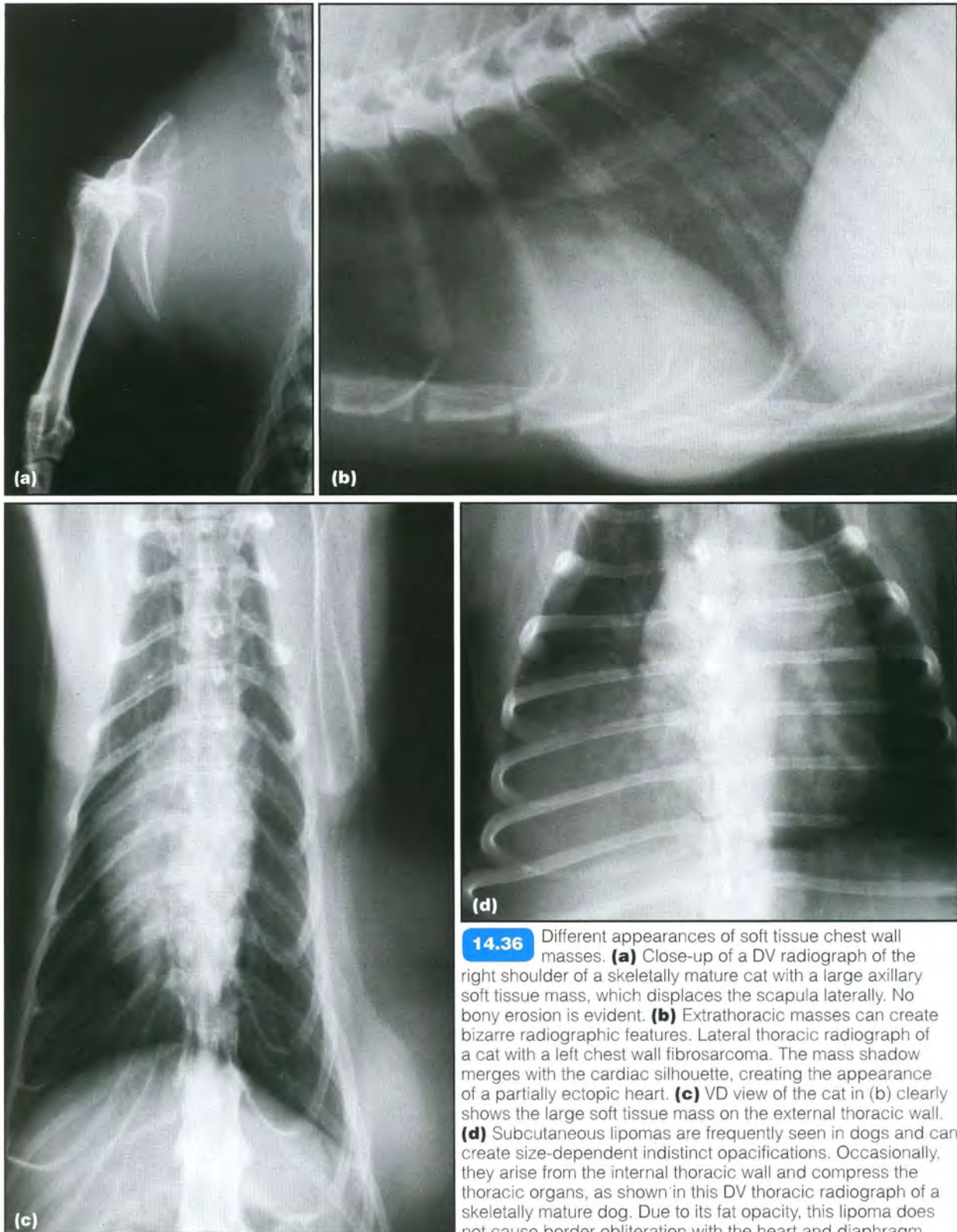
and pulmonary structures) may be seen. There may be displacement of adjacent ribs.

- Primary rib tumours:
 - Monostotic
 - Preferentially distal third of the rib (costochondral junction)
 - Displaced adjacent ribs, which are otherwise normal
 - Often very large intrathoracic component.



14.35 (a) Cranial thoracic close-up of a DV radiograph of an 11-year-old Golden Retriever bitch with a chondroblastic osteosarcoma, originating from the right second rib. This tumour is osteoproliferative, expands into the axilla and impinges on the brachial plexus. (b) Lesion-oriented oblique radiograph of the left tenth rib of a 8-year-old Boxer with a primary rib osteosarcoma (see also Figure 14.4). The rib osteolysis (arrowhead) and internal soft tissue swelling are highlighted by this view. (c) Left lateral thoracic radiograph of a 6-year-old Bull Mastiff with a primary osteosarcoma of the right sixth rib and haemothorax. This view highlights the extrapleural sign, owing to the inward-growing mass surrounded by aerated lung. (d) Right lateral view of the dog in (c) highlights the lysis and amorphous bone production of the mass.

- Metastatic rib tumours:
 - Often polyostotic, but randomly oriented
 - Preferentially middle and proximal third of the rib
 - Often small at time of detection.
- Soft tissue tumour invading the ribs (Figure 14.36):
 - Soft tissue mass with variable external component
 - Osteolysis, periosteal reaction, fractures of multiple adjacent ribs
 - Any part of the rib can be affected
 - Mesothelioma: abundant pleural effusion, no external chest wall mass, periosteal reaction on several ribs possible.



14.36 Different appearances of soft tissue chest wall masses. **(a)** Close-up of a DV radiograph of the right shoulder of a skeletally mature cat with a large axillary soft tissue mass, which displaces the scapula laterally. No bony erosion is evident. **(b)** Extrathoracic masses can create bizarre radiographic features. Lateral thoracic radiograph of a cat with a left chest wall fibrosarcoma. The mass shadow merges with the cardiac silhouette, creating the appearance of a partially ectopic heart. **(c)** VD view of the cat in (b) clearly shows the large soft tissue mass on the external thoracic wall. **(d)** Subcutaneous lipomas are frequently seen in dogs and can create size-dependent indistinct opacifications. Occasionally, they arise from the internal thoracic wall and compress the thoracic organs, as shown in this DV thoracic radiograph of a skeletally mature dog. Due to its fat opacity, this lipoma does not cause border obliteration with the heart and diaphragm.

- Multiple myeloma and lymphoma:
 - Multiple myeloma: multiple punctate lucencies without periosteal reaction or sclerosis; pathological fractures are uncommon
 - Lymphoma: irregular periosteal reaction and punctate or diffuse lysis in metaphyseal area; pathological fractures are uncommon.
- Lipoma and liposarcoma:
 - Fat opacity in lipoma lesions, which distinguishes them from soft tissue masses
 - Liposarcoma may have fat and/or soft tissue opacity
 - Can be difficult to differentiate from obesity-related fat deposition
 - External masses should be marked for radiography to explain opacity changes.

Other imaging techniques: Ultrasonography is helpful to differentiate a mass lesion from pleural effusion, lung and other internal thoracic structures, and to characterize the nature and extent of the lesion. Assessment can be made of the mass movement in relation to respiration:

- Chest wall mass moves with the rib cage
- Lung mass moves with pulmonary excursion
- Smooth convex mass displaces the normal pleura–lung interface inwards.

Most neoplasms have a mixed echogenic appearance (Figure 14.37a), often with central hypoechoic (necrosis, haemorrhage) regions. Hyperechoic foci with shadowing (soft tissue mineralization) may be identified. The margins may or may not be discernible. The echogenicity of the mass should always be compared with the adjacent normal tissue. This can be useful in identifying a lipoma, which is uniformly hyperechoic compared with the surrounding tissue (Figure 14.37b). A liposarcoma is more echogenic and less organized than a lipoma.

Ultrasonography is rarely tissue- or cell-specific but is very useful in guiding a needle into a mass for aspiration or biopsy. CT and MRI can be very helpful to assess:

- Tumour extent for surgical resection and radiation treatment planning (see Figures 14.38 and 4.1, p. 71)
- Involvement of other thoracic organs
- Detection of lung metastases.

Bone scintigraphy may be used for detection of subtle active lesions, or assessment of the number and location of skeletal metastases (Figure 14.39).

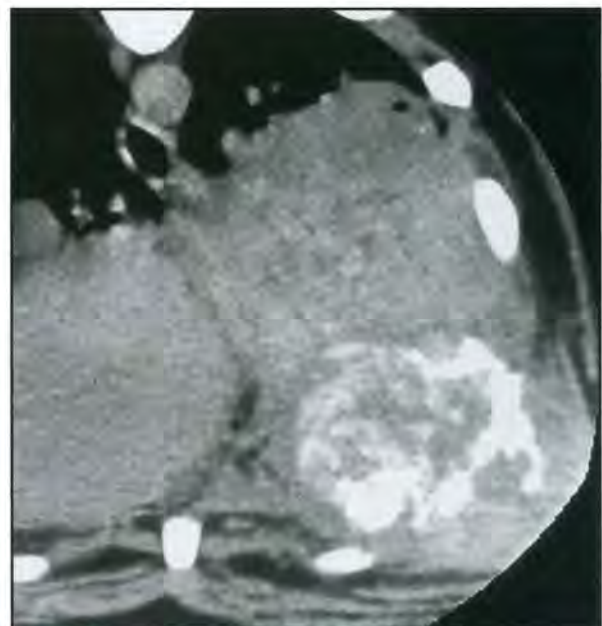
Sternal neoplasia

Primary or secondary neoplasia of the sternum is rare and should be differentiated from osteomyelitis.

Radiography: A combination of osteolytic and irregular osteoproliferative lesions is seen. Masses may grow into the thorax and reach a large size.



14.37 (a) Ultrasonographic image of the chest wall of a dog with cutaneous haemangiosarcoma. Notice the mixed echogenic appearance of the mass, containing cystic hypoechoic content consistent with central necrosis or haemorrhage. (b) In comparison, this ultrasonographic chest wall image of a dog with a lipoma has a much more homogenous hyperechoic appearance.



14.38 Thoracic CT image at the level caudal to the carina of a 21-month-old Rottweiler with a large primary chondrosarcoma of the left sixth rib and haemothorax.



14.39 Lateral scintigram of the cranial thoracic skeleton of a 16-year-old mixed breed dog with a primary osteosarcoma of one of its caudal most ribs, obtained approximately 2 hours after intravenous injection of a bone-binding diphosphonate compound. The primary tumour is not included in the scan but numerous focal areas of intense bone tracer localization, consistent with costal, sternal and spinal metastases can be seen. (Courtesy of F. Morandi)

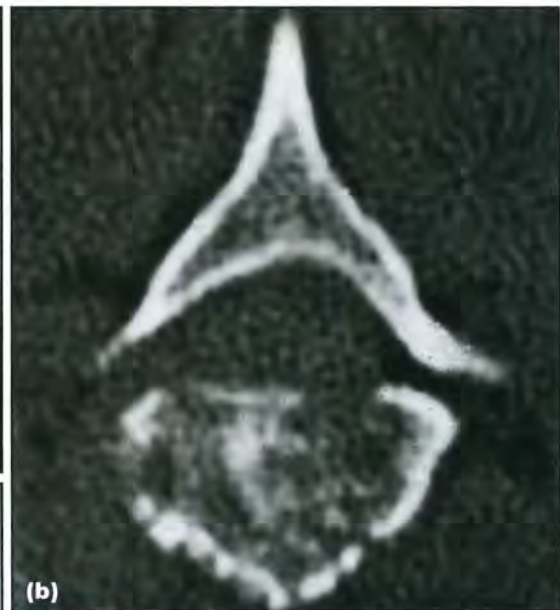
Spinal neoplasia

Primary or secondary neoplasia can occur in the vertebrae, surrounding soft tissues, meninges and spinal cord. The most common vertebral tumours include osteosarcoma, chondrosarcoma, fibrosarcoma and haemangiosarcoma. Paravertebral neoplasms include neuroendocrine tumours and soft tissue sarcomas. Diffuse neoplasms, such as multiple myeloma and lymphoma, also occur. Lymphoma is the most common spinal tumour in the cat. The thoracic spine is a common location for spinal neoplasia.

Radiography: Radiographic findings include:

- Vertebral tumours (Figure 14.40):
 - Monostotic (primary) or randomly polyostotic (secondary)
 - Usually very subtle osteolysis with or without periosteal reaction
 - Occasionally, osteosclerotic appearance
 - Pathological compression fracture is common
 - Perivertebral soft tissue mass extension into the thorax is possible.
- Paravertebral neoplasms:
 - Large soft tissue mass in the dorsal mediastinum (see Figures 14.41 and 10.31d, p. 226)
 - Periosteal reaction along several vertebrae is possible.

Detailed discussion of other spinal neoplasms is beyond the scope of this manual.



14.40 **(a)** Lateral myelogram of a 7-year-old Border Collie with a primary bone tumour of the second thoracic vertebra (T2). There is very subtle osteolysis in the vertebral body and the ventral myelographic contrast medium column is elevated. Radiography has a poor sensitivity to detect bony lysis. **(b)** The corresponding CT image demonstrates the extensive lysis and spinal cord compression. **(c)** Lateral radiograph of the caudal thoracic spine of a 6-year-old mixed breed dog with vertebral neoplasia of the ninth thoracic vertebra. The vertebra is mildly osteosclerotic compared with its neighbours, an unusual manifestation of a spinal tumour. (continues) ▶



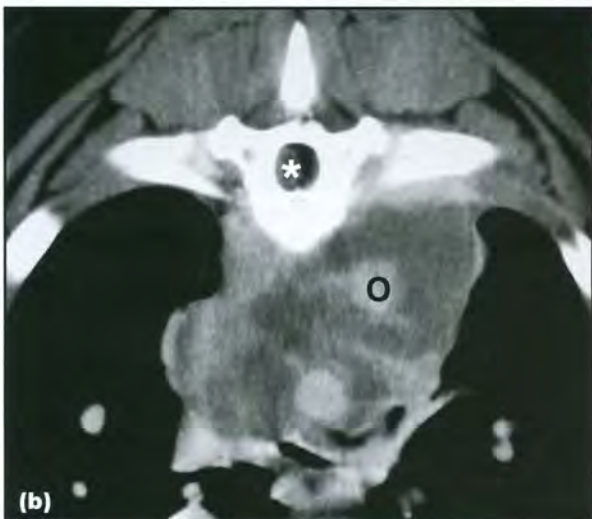
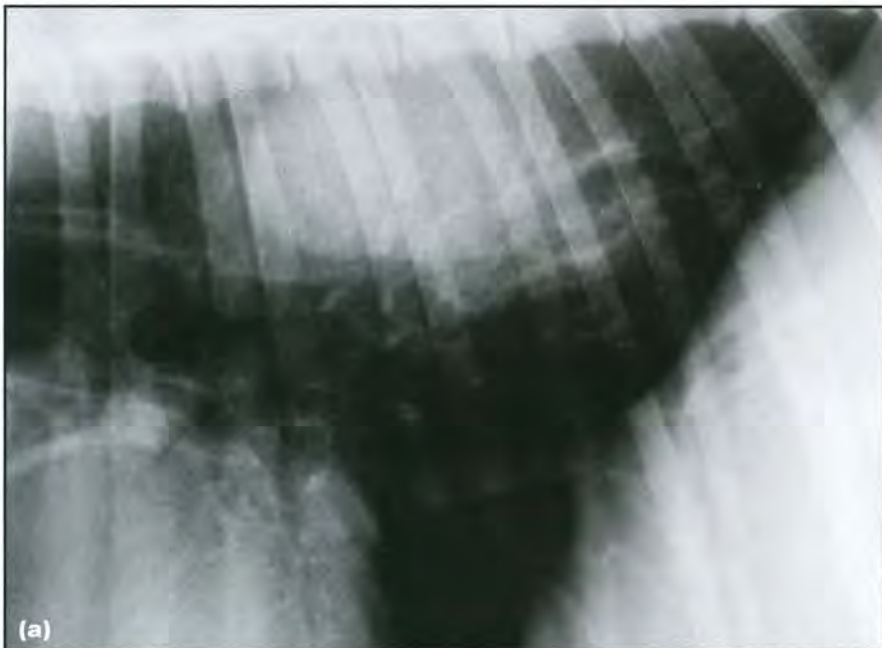
14.40 (continued) **(d)** Lateral thoracic radiograph of a 10-year-old Labrador Retriever with multiple myeloma. Notice the numerous punched-out osteolucencies in multiple vertebral bodies, a classic radiographic feature of this neoplasm.

Osteomyelitis, metabolic and reactive changes

Ribs and chest wall

Osteomyelitis and abscessation: Infections of the thoracic wall result from foreign bodies, lacerations, bite wounds or surgical wound contamination. Migrating foreign bodies, such as grass awns, penetrating via the skin, or a wooden skewer, penetrating via the gastrointestinal tract, can cause inflammatory disease, an abscess/granuloma, a fistulous tract in the thoracic wall region or even lead to pleural effusion. Inhaled grass awns often migrate towards the epaxial musculature of the cranial lumbar spine, causing local abscessation and spondylitis. Fungal or parasitic (hepatozoonosis) osteomyelitis and cellulitis occur in endemic areas. These lesions are often very painful, more so than neoplasia.

Metabolic diseases: Nutritional or renal hyperparathyroidism causes marked demineralization and



14.41 **(a)** Lateral thoracic radiograph of a 3-year-old Labrador Retriever with a caudodorsal mediastinal mass that was diagnosed as a paraganglioma. **(b)** The corresponding post-contrast CT image at the level of the seventh thoracic vertebra shows the mass infiltrating the spinal canal. Note the compression of the spinal cord (*****) and in the dorsal mediastinum where it completely surrounds the aorta (**O**). Neuroendocrine tumours are rare but the dorsal mediastinum is a common location. They are often extremely invasive.

deformities of the entire skeleton, and pathological fractures. Other osteopenic (Cushing's disease) or osteosclerotic conditions are usually not sufficient to cause clinical signs relating to the thoracic skeleton, although pathological rib fractures are possible.



14.42 Close-up of a DV thoracic radiograph of a 6-year-old Domestic Longhair cat with chronic osteomyelitis of the right tenth rib (arrowhead) as a result of cat bite injuries. There is marked smoothly margined bony proliferation along this rib, consistent with chronic or previous osteomyelitis. Adjacent ribs are also mildly affected.

Hypertrophic osteopathy: In the presence of large chronic masses in the lungs or other thoracic organs, a systemic response can be evoked in the appendicular and, to a lesser extent, in the axial skeleton. It can also be induced by a non-thoracic mass. The distal legs are most commonly affected; the ribs are less commonly affected. Aetiological theories include:

- Circulating toxins from the mass lesion, promoting periosteal response
- Sympathetic stimulation, promoting peripheral vascularization
- Neural reflex originating from the mass, stimulating increased peripheral vascularization of poorly oxygenated blood (shunting through anastomoses in the mass).

Hypertrophic osteopathy is reversible if the original mass is removed.

Radiography: Radiographic findings include:

- Osteomyelitis and abscessation (Figure 14.42):
 - Predominantly, osteoproliferative lesion with irregular periosteal reaction on one or multiple ribs and adjacent soft tissue swelling and/or free gas
 - Local soft tissue opacity with abscess or granuloma formation
 - Pleural effusion or lung changes possible with fistulous tract
 - Hepatozoonosis; signs seen on the proximal long bones in particular.
- Hyperparathyroidism (Figure 14.43):
 - Osteopenic skeleton, spinal curvature deformities and pathological fractures, particularly of the ribs
 - Cushing's disease, osteosclerosis (see Interpretive principles, above).

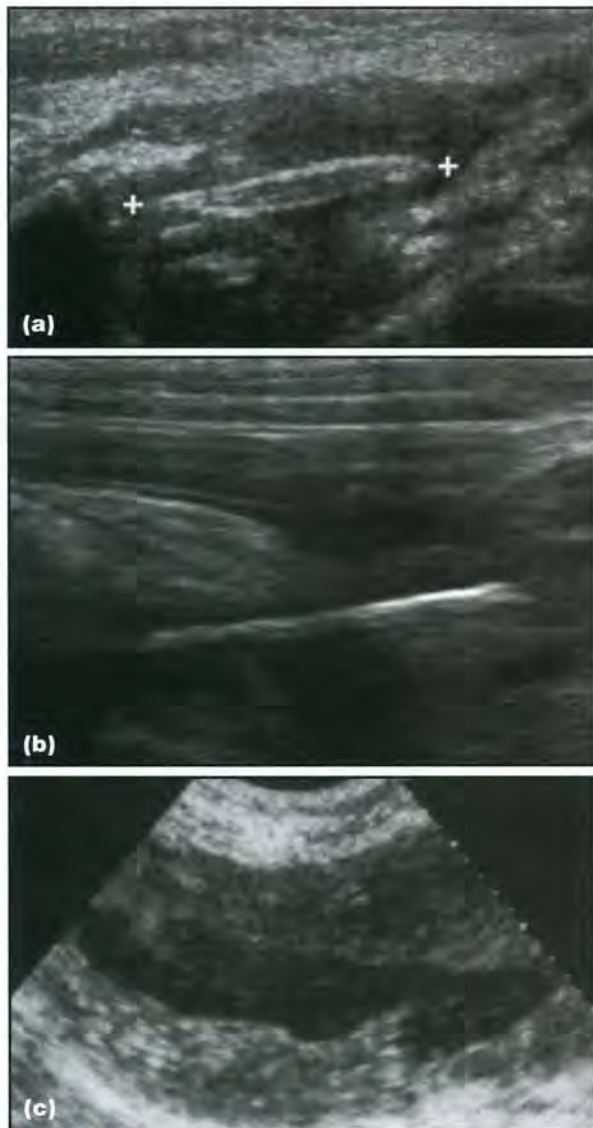


14.43 Lateral thoracic radiograph of a 4-month-old kitten with nutritional hyperparathyroidism. Notice the marked generalized osteopenia, spinal curvature deformity and sternal dislocation.

- Hypertrophic osteopathy:
 - Subtle palisade-like periosteal reaction on multiple ribs
 - More marked changes in the appendicular skeleton.

Contrast studies: Fistulography and sinography may be used to explore the extension of sinuses and connections of fistulous tracts.

Ultrasonography: This is very useful for the identification of foreign material, abscessation and haematomas in the chest wall (Figure 14.44):



14.44 **(a)** Ultrasonographic image of a dog with a migrating grass awn (between white callipers) within the intermuscular layers of the chest wall. Another partially visible grass awn is ventral to it. The spindle-shape appearance is characteristic for this type of plant material. **(b)** Ultrasonographic image of a 2-year-old Dobermann with a wooden skewer foreign body in the pleural cavity. A linear hyperechoic line surrounded by hypoechoic material can be seen. **(c)** Ultrasonographic image of the chest wall of a 5-year-old German Shepherd Dog with a chest wall abscess. There is a hypoechoic area surrounded by a thick hyperechoic capsule, consistent with abscessation.

- Foreign body:
 - Identification of the foreign body (mostly hyperechoic interface): a grass awn is spindle-shaped with two or three echogenic interfaces; a wooden skewer produces a linear hyperechoic interface
 - Surrounding poorly echogenic area represents inflammatory fluid/abscess.
- Abscess:
 - Well defined, hypoechoic or anechoic fluid collection, which may contain varying degrees of echogenic debris
 - Identification of small gas bubbles
 - Hyperechoic surrounding tissue (cellulitis)
 - If chronic, often encapsulated with an irregular internal margin.

An abscess is sometimes indistinguishable from an organized haematoma, necrotic tumour or seroma.

Sternal osteomyelitis

This is uncommon but may be a sequel to trauma (bite, penetrating foreign body) or a complication of midline thoracotomy (sterniotomy). An intermittently discharging sinus may be present.

Radiography: Radiographic findings include:

- Periosteal reaction around the affected sternebra (Figure 14.45)
- Osteolysis or sclerosis
- Soft tissue swelling ventral to sternum; lucent gas tracts may be seen if there is a discharging sinus.
- Pleural thickening and effusion.



14.45 Possible features of sternal osteomyelitis. **(a)** An 8-year-old German Shepherd Dog with an irregular periosteal reaction along several sternebrae, and soft tissue swelling. **(b)** Dog with a smooth periosteal reaction, sternebra fusion and adjacent soft tissue swelling with sinus tract. This is an ongoing chronic infection. (continues)



14.45 (continued) Possible features of sternal osteomyelitis. **(c)** A 3-year-old Weimaraner 5 months after sternotomy, showing predominantly osteolytic changes along several vertebrae, lucencies around the cerclage wires and soft tissue swelling.

Spondylitis and discospondylitis

True vertebral infection is rare. However, discospondylitis is not uncommon in dogs. The thoracic spine is a common location for bacterial discospondylitis; this should be differentiated from intervertebral disc disease. The original nidus of infection is often elsewhere in the body, such as in the prostate.

Radiography: Radiographic findings include:

- Collapsed intervertebral disc space with both endplates irregularly outlined (Figure 14.46)
- Healed discospondylitis shows smooth new bone formation, endplate sclerosis and vertebral fusion
- Can occur at one or multiple sites.

Diseases of the thoracic inlet

For information on diseases of the thoracic inlet, see Chapter 12.

Diseases of the diaphragm

Diaphragmatic rupture

Diaphragmatic ruptures are usually traumatic in origin. They are frequently misnamed as *acquired diaphragmatic hernias*. This is an incorrect term, since the prolapsed organs are not contained within a hernial sac.

The diaphragm normally ruptures at its weakest point, following a sudden increase in intra-abdominal pressure while the glottis is open. The site and size of the rupture are variable. Right-sided tears are reported to be more frequent than left-sided. Tears can extend from one side to the other and be radial or circumferential.

The liver is the most frequently prolapsed organ with right-sided ruptures; the stomach is the most frequently prolapsed organ with left-sided ruptures. Prolapse of the small intestines and omentum can be present with any tear. Less commonly prolapsed organs include the spleen, large intestine, omentum, uterus and kidney.

The most frequent clinical sign is dyspnoea; ranging from mild to severe, depending on the volume of the prolapsed organs and fluid accumulation. Other clinical signs can be present, such as regurgitation or vomiting, and are related to the organ prolapsed in the thoracic cavity. Gastric prolapse is a surgical emergency as sudden strangulation and bloating may quickly become life-threatening.

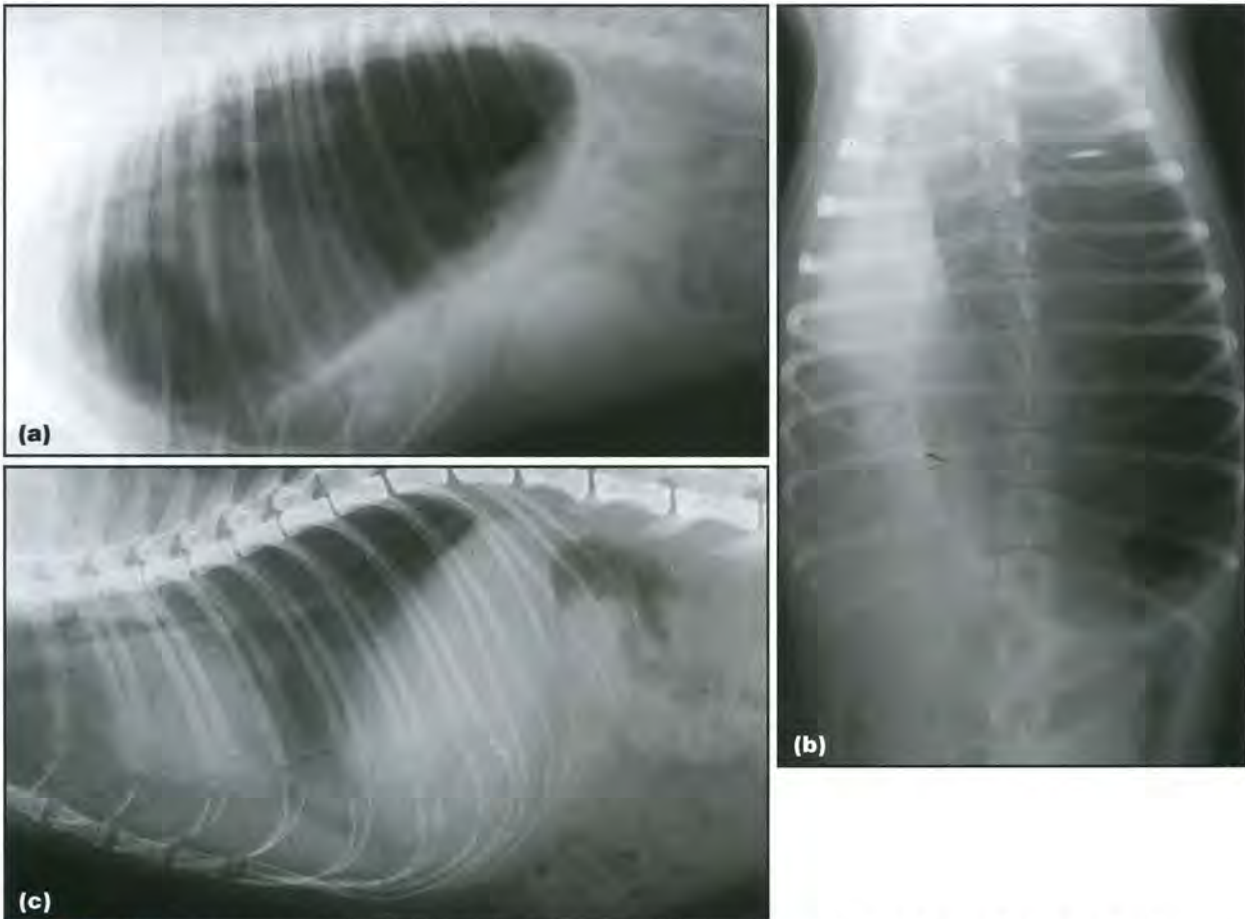
Radiography

A DV view should be taken to avoid further respiratory compromise. Positional radiographs, such as a lateral view using a horizontal beam, should be considered if the respiratory distress worsens in lateral recumbency. It is useful to obtain abdominal radiographs to be able to check for the presence of abdominal organs. One or more of the following radiographic signs can be detected (Figure 14.47):

- Loss or change of contour of the diaphragmatic outline
- Obliteration and/or dorsal displacement of the cardiac shadow
- Increased opacity of the ventral thoracic cavity, with or without elevation of the trachea and/or cardiac silhouette
- Mediastinal shift
- Presence of gas-filled tubular structures and/or speckled mineral opacities, suggestive of the ingesta-filled gastrointestinal tract being located within the thoracic cavity
- Pleural effusion may be present and mask herniated parenchymal organs
- Lung lobe collapse



14.46 Close-up of a lateral thoracic spinal radiograph of a 7-year-old Irish Setter with discospondylitis in the T7–8 intervertebral disc space. The disc space has collapsed and there is an irregular osteolucency in the ventral aspect of the endplates of both adjacent vertebrae (arrowhead). This is a relatively early stage of the disease.



14.47 (a) Lateral and (b) DV thoracic radiographs of an 18-month-old dyspnoeic Jack Russell Terrier that had been involved in a road traffic accident. A large lucent cavitory structure is present in the left hemithorax, consistent with a bloated displaced stomach. Note the absence of a gastric shadow in the cranial abdomen. A distended displaced stomach is a surgical emergency. (c) Lateral thoracic radiograph of a 7-year-old Domestic Shorthair cat. There is loss of the ventral diaphragmatic outline, dorsal displacement of the cardiac silhouette and trachea, increased opacity of the ventral thoracic cavity and cranial displacement of the abdominal organs with loss of visibility of the falciform fat, consistent with a diaphragmatic rupture and abdominal organ prolapse.

- Absence of abdominal organs from the abdominal cavity is often associated with cranioventral displacement of the stomach axis. Some organs may be clearly identified within the thoracic cavity
- In cats, falciform fat may be the only abdominal organ herniated, in which case the fat pad ventral to the liver will appear very small, the liver will be closer to the abdominal wall and the ventral outline of the diaphragm will be lost
- Other radiographic signs of trauma (e.g. rib fractures, lung contusions and appendicular skeleton fractures).

A diaphragmatic tear without organ prolapse cannot be ruled out based on the absence of radiographic signs.

Contrast studies: Contrast studies which may aid diagnosis include:

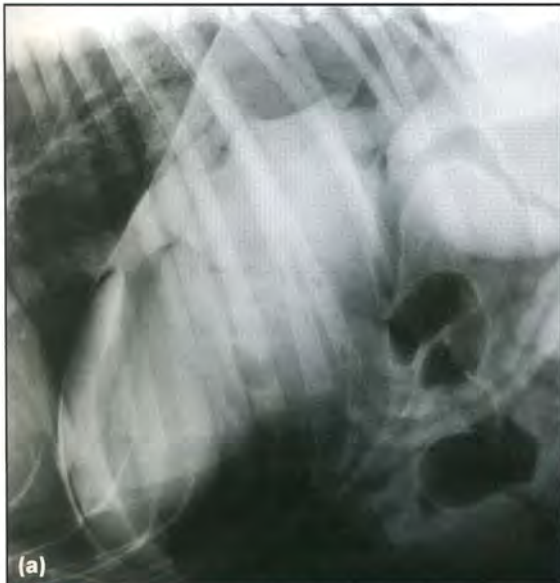
- *Barium transit studies* (Figure 14.48) are useful if survey radiography is equivocal. Radiographs should be repeated over a time period long enough to demonstrate the presence of the

stomach, small and/or large intestines within the thoracic cavity, or cranioventral displacement of the gastric axis if only liver has herniated. Barium studies are contraindicated when perforation of the gastrointestinal tract is suspected in addition to the diaphragmatic rupture. Water-soluble iodinated agents can be used instead

- *Positive-contrast peritoneography.* A positive non-ionic iodine-based contrast medium is injected into, and should remain in, the peritoneal cavity. If positive contrast medium is found in the pleural space, diaphragmatic rupture is confirmed. A negative study does not rule out a diaphragmatic rupture since, in chronic cases, adhesions may obstruct the tear
- *Pneumo- or capnoperitoneography* (Figure 14.49). Positive-contrast studies are preferred and easier to interpret. A small quantity of gas is injected into the peritoneal cavity. If a pneumothorax is then radiographically visible, diaphragmatic rupture is confirmed. Carbon dioxide is preferred due to the reduced risk of vascular air emboli (capnoperitoneography). A negative study does not rule out a diaphragmatic rupture.



14.48 Lateral barium study radiograph of a 9-month-old Domestic Shorthair cat with a diaphragmatic rupture. The barium-filled pyloric antrum and liver are prolapsed into the thorax.



14.49 (a) Lateral and (b) VD radiographs of pneumoperitoneum in a 9-year-old German Shepherd Dog following a laparotomy. The normal diaphragmatic silhouette is outlined by gas on both sides. Pneumo- or capnoperitoneography can be used to outline interruptions in the diaphragmatic silhouette. Spontaneously occurring free peritoneal gas tends to accumulate between the liver and the diaphragm, and should be recognized as abnormal and raise suspicion for an abdominal hollow viscus organ rupture.



Ultrasonography

This is a useful non-invasive method to identify an unclear case of diaphragmatic rupture and organ prolapse. It can be difficult to determine this as the normal diaphragmatic outline is hard to visualize and mirror image artefacts can be confusing. The following should be looked for:

- Visualization of abdominal organs in the pleural cavity. Differentiation between normal

liver and consolidated/collapsed lung may be difficult

- Interruption of the normal echogenic lung–diaphragm interface.

Diaphragmatic hernias

Diaphragmatic hernias are common congenital anomalies in dogs and cats, due to agenesis of a portion of the diaphragm or lack of fusion between the parts of the primitive diaphragm. They include:

- Ventral diaphragmatic hernias
- Hiatal hernias
- Paraoesophageal intramediastinal hernias
- Peritoneopericardial hernias
- Aortic hiatal diaphragmatic hernias.

In contrast to diaphragmatic ruptures, the prolapsed abdominal organs are contained within a peritoneal or pericardial hernial sac, i.e. are *herniated*. Diaphragmatic hernias are usually found in young animals with no history of trauma. They appear in predetermined areas of the diaphragm and may be associated with other congenital defects. No granulation or scar tissue will be found during surgery. Hiatal hernias may be acquired. Hernia of the cranial abdominal wall can lead to a *paracostal hernia*, where the hernial sac is contained between the ribs and soft tissue layers of the thorax.

Paracostal abdominal wall hernia

Herniation of viscera occurs via a body wall defect at the costal arch. Abdominal viscera are contained in the subcutaneous layers of the thoracic wall.

Radiography: There is a soft tissue swelling along the body wall, which may contain gas-filled viscera (Figure 14.50).



14.50 Slightly oblique VD radiograph (lesion-oriented view) of a 3-year-old Siamese cat with a right paracostal body wall hernia. Food and gas-filled loops of intestine can be identified within the hernial sac. Local soft tissue swellings of the chest wall warrant diagnostic imaging procedures.

Ventral diaphragmatic hernia

Ventral (true) diaphragmatic hernias are typically due to a congenital lack of fusion between parts of the primitive diaphragm, which leads to the persistence of an aperture through which abdominal organs herniate into the thoracic cavity. Abdominal organs are contained within a hernial sac, usually the parietal pleura of the diaphragm, which prevents direct communication between the peritoneal and pleural cavities. True ventral diaphragmatic hernias are rare in animals. They are usually small and not associated with clinical signs.

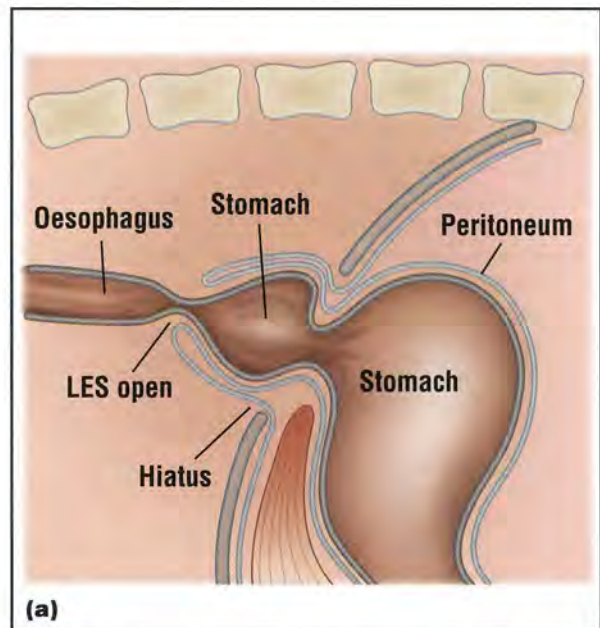
Radiography: There is a cranial bulge in the ventral diaphragmatic silhouette with a possible cardiac shift away from the bulge on a lateral radiograph.

Hiatal hernia

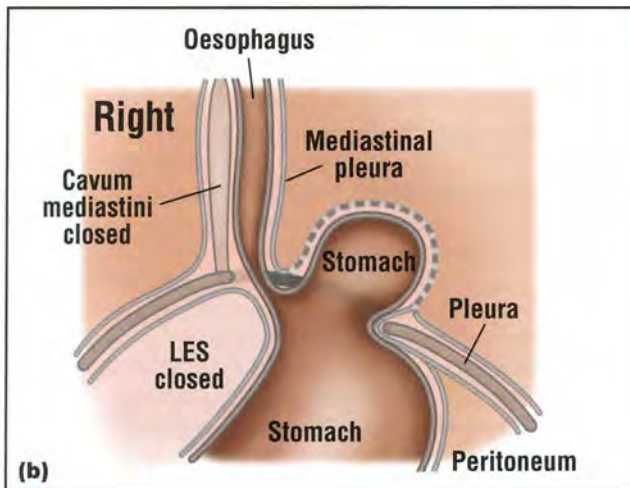
A hiatal hernia corresponds to a herniation of any abdominal organ through the oesophageal hiatus. It is most often congenital in origin but can be acquired, following the repair of a chronic diaphragmatic rupture or secondary to a traumatic event, oesophageal/upper respiratory tract pathologies or neuromuscular disorders. Three main types of hiatal hernia are recognized in animals (Figure 14.51):

- Short oesophagus hiatal hernia
- Sliding hiatal hernia
- Paraoesophageal hiatal hernia.

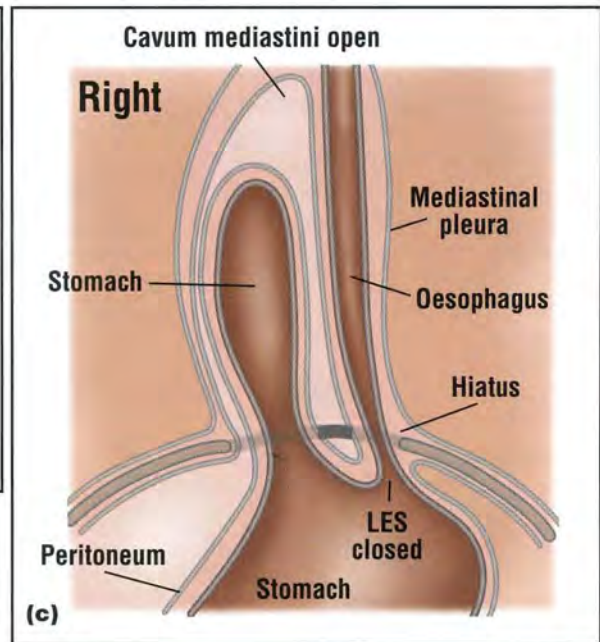
Sliding and paraoesophageal hiatal hernias can coexist. Chinese Shar Pei dogs are predisposed for hiatal hernias.



14.51 Different types of hiatal hernias. **(a)** Sliding hiatal hernia. LES = Lower oesophageal sphincter; ••••• = With or without hernial sac. (Adapted from Suter (1984) with permission) (continues) ▶



14.51 (continued) Different types of hiatal hernias. **(b)** Paraoesophageal hiatal hernia into the pleural space. **(c)** Paraoesophageal hiatal hernia into the Sussdorf's space (*cavum mediastini serosum*). LES = Lower oesophageal sphincter; = With or without hernial sac. (Adapted from Suter (1984) with permission)



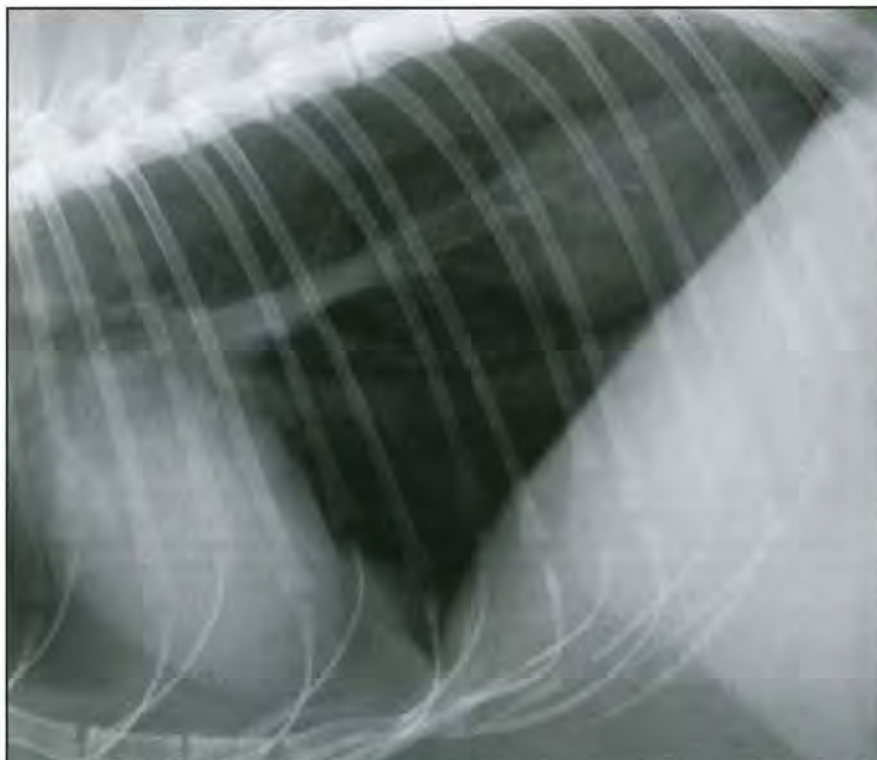
Short oesophagus hiatal hernia: The lower oesophageal sphincter lies in the caudal mediastinum due to a short oesophagus. The cardia is pulled through the oesophageal hiatus. This type of hernia is very rare and has only been described in the dog.

Radiography: Radiographic findings include:

- Ovoid soft tissue opacity in the mid-caudal thorax with a locally obliterated diaphragmatic silhouette on a lateral radiograph.
- Central, slightly left-sided location of opacity on DV/VD views.
- Permanent appearance.

Sliding intramediastinal hiatal hernia: The lower oesophageal sphincter moves freely back and forth into the caudal mediastinum, followed by parts of the stomach, through a loose oesophageal hiatus (see Figure 14.51a). Clinical signs include variable degrees of vomiting or regurgitation, hypersalivation and chronic weight loss. If the stomach is incarcerated, severe respiratory distress can be present. Aspiration pneumonia is frequently associated with this condition.

Radiography: Radiographic findings (Figure 14.52) include:



14.52 Lateral thoracic radiograph of a 4-year-old Domestic Shorthair cat with a sliding intramediastinal hiatal hernia. There is an ovoid soft tissue opacity in the caudodorsal thorax between the aorta and the CdVC, which varied in appearance between different radiographs, consistent with a hiatal hernia. Hiatal hernias may develop secondary to chronic respiratory disease with increased inspiratory effort.

- Semicircular soft tissue mass, merging with the liver shadow localized between the CdVC and the aorta on the lateral view and in the caudal mediastinum on the DV view, superimposed over the hepatic shadow
- Gas present in the herniated stomach may allow recognition of rugal folds. If a large portion of the stomach is herniated and incarcerated, a large hyperlucent cyst-like structure surrounded by a thin soft tissue rim may be seen. In this case, lung collapse and mediastinal shift to the contralateral side is also visible
- Radiographic signs of aspiration pneumonia may be an associated finding.

Radiographic signs might be absent, particularly during expiration, due to the sliding nature of the hernia. Positional radiography is usually unsuccessful in demonstrating a sliding hiatal hernia.

Contrast studies (Figure 14.53) may aid diagnosis:

- A barium oesophagram may confirm suspicion of a sliding hiatal hernia. As the lower oesophageal sphincter moves back and forth, it can be in a normal position at the time of the examination
- Gastric rugae may be visible both in the caudal mediastinum and in the cranial abdomen, separated by a marked narrowing at the level of the oesophageal hiatus
- The lower oesophageal hiatus can be seen cranial to the cardia as a shallow indentation. It also allows assessment of concurrent oesophageal disorders, such as strictures or masses.

Fluoroscopy: This, together with an oesophagram, allows dynamic assessment of the position of the lower oesophageal sphincter and of the stomach. As the lower oesophageal sphincter function is altered due to its abnormal position, gastro-oesophageal reflux of contrast medium may be seen associated with swallowing.

Paraoesophageal hiatal hernia: The lower oesophageal sphincter remains in place and is competent, but part of the stomach surrounded by a peritoneal sac herniates through the oesophageal hiatus parallel to an immobile oesophagus. Two subtypes exist:

- Abdominal organs may herniate to the left of the oesophagus in which case they come to lie in the pleural cavity (see Figure 14.51b)
- Abdominal organs may also slide to the right of the oesophagus and herniate into the potential space between the two mediastinal pleural leaves (Sussdorf's space – *cavum mediastini serosum* or *bursa infracardiaca*) (see Figure 14.51c). This space is normally closed by a thin membrane, which may be congenitally weak or ruptured following trauma. The prolapsed organs, usually part of the stomach, liver or small intestines, can move in and out as the space widens during inspiration and shrinks during expiration.

Clinical signs may range from none to recurrent gastrointestinal signs, including anorexia, retching, vomiting or bloating of the stomach without gastric torsion.

Radiography: Radiographic findings include:

- Left-sided paraoesophageal hernia:
 - Changes in the diaphragmatic contour associated with a mass in the mid-caudal thoracic cavity
 - Extrapleural sign with the base of the mass toward the diaphragm and very sharp margins on the lung side
 - Presence of gas-filled tubular structures in the caudal thoracic cavity
 - Presence of a hyperlucent cyst-like structure surrounded by a thin soft tissue rim filling the left hemithorax, may be seen if the stomach herniates and becomes incarcerated
 - Mediastinal shift to the right and pulmonary atelectasis.



14.53 Lateral barium study of a 4-month-old Cornish Rex cat with a hiatal hernia. The rugal folds are clearly outlined with barium, and the gastric fundus is located in the caudodorsal thorax. Contrast studies can be helpful to confirm the presence of a hiatal hernia.

- Right-sided paraoesophageal hernia:
 - Soft tissue mass in the mid-caudal thorax on the lateral view, caudal to the heart
 - Widening of the caudal mediastinum on the DV view, associated with displacement of the cardiac silhouette to the left. As the pericardium is intact, the cardiac silhouette remains a normal size
 - Gas in the stomach or small intestines may be identified in the caudal mediastinum.

Barium studies can confirm a suspicion of paraoesophageal hiatal hernia by outlining the abnormal position of the stomach or the small intestines in the caudodorsal thorax.

Peritoneopericardial diaphragmatic hernia

Peritoneopericardial diaphragmatic hernia (PPDH) is the most common diaphragmatic hernia in dogs and cats. It is due to an embryological fusion defect in the ventral diaphragm, leading to a communication between the pericardial and the peritoneal cavities. PPDHs are often associated with sternal or cardiac defects. The liver is the most frequently herniated organ, and may be associated with gallbladder, stomach, small intestine or omental herniation.

Clinical signs depend on the organs herniated and the size of the defect, and include respiratory, cardiovascular and gastrointestinal disorders. Auscultation may reveal muffled heart sounds or borborygmy over the cardiac area. Sudden onset of clinical signs may arise secondary to strangulation of a herniated organ. Most frequently no clinical signs are present and a PPDH is found incidentally.

Radiography: Radiographic findings include:

- Moderate to gross enlargement of the cardiac silhouette, merging caudally with the diaphragmatic outline (Figure 14.54) without associated radiographic signs of heart failure
- Dorsal displacement of the trachea
- Dorsal displacement of the CdVC
- Heterogenous opacity of the cardiac shadow due to the presence of falciform or omental fat, and/or gas or mineralized speckled structures contained in the herniated small or large intestines
- Persistence of a dorsal mesothelial remnant between the cardiac silhouette and the diaphragmatic outline, at the level or slightly dorsal to the CdVC, can be seen in cats
- Cranial displacement of the stomach and other abdominal organs
- Sternal abnormalities, including various deformities, reduction in the number of sternebrae and the absence or split of the xiphoid process
- Umbilical hernia or other abdominal wall defects
- Absence of radiographic signs of cardiac failure.

Contrast studies: Barium studies may outline the abnormal position of the stomach or the small intestine in the pericardium if they are herniated (Figure 14.55). Positive- or negative-contrast peritoneography may be useful when barium studies are inconclusive.



14.54 (a) Lateral and (b) VD radiographs of a 16-week-old Persian cat with a PPDH. The cardiac silhouette is grossly enlarged and merges with the diaphragmatic outline ventrally (lateral view) and centrally (VD view). These features distinguish PPDHs from diaphragmatic ruptures.



14.55 Lateral barium study of a 3-year-old Domestic Shorthair cat with a PPDH. The stomach axis is cranioventrally displaced, and the pylorus and proximal duodenum are contained within the pericardial sac.

Fluoroscopy: The normal cardiac and diaphragmatic motion is not visible due to obliteration by herniated soft tissue structures.

Ultrasonography: This is an excellent modality to differentiate between cardiomegaly and a PPDH. An abdominal organ, usually part of the liver, is visible next to the heart, within the pericardial sac (Figure 14.56). Ultrasonography allows evaluation of the herniated organs as well as providing an assessment of cardiac function, if cardiovascular impairment was the reason for investigation.



14.56 Ultrasonographic image of the liver of a 10-year-old British Shorthair cat with an incidental PPDH. The liver (L) lies in direct contact with the left ventricle (LV) without intersecting the diaphragm. Mitral valves are arrowed.

Aortic hilar hernia

The aortic hilus is the only diaphragmatic opening that connects the mediastinum with the retroperitoneal space. Free mediastinal gas can pass through the hilus and enter the retroperitoneal space relatively easily. If defects in this hilus exist, retroperitoneal organs such as the adrenal glands and kidneys can prolapse into the mediastinum. Intramediastinal kidneys are rare in dogs and cats and are usually detected incidentally.

Radiography: Radiographic findings include:

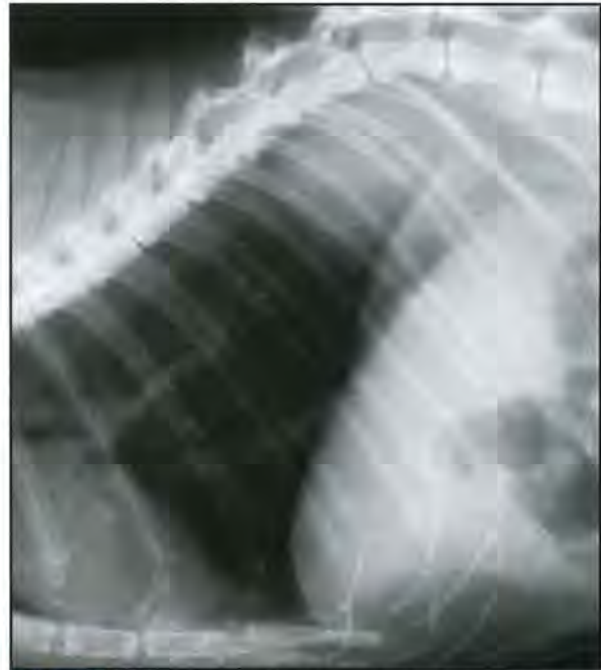
- Caudodorsal mediastinal location of a kidney (Figure 14.57)
- Should be differentiated from a dorsal circumferential diaphragmatic tear and renal prolapse.

Diaphragmatic neoplasia

Diaphragmatic neoplasia is extremely rare in dogs and cats. Neoplasms can be primary or metastatic.

Radiography

An extrapleural soft tissue mass is seen, with the base merging with the diaphragmatic outline and a sharp rounded margin towards the thoracic cavity. If the mass extends strictly towards the abdominal cavity, it will not be radiographically visible on plain radiographs. It can be very difficult to differentiate from other mass lesions or diaphragmatic hernias.



14.57 Lateral thoracic radiograph of a 14-year-old Domestic Shorthair cat with hyperthyroidism. The right kidney is partially herniated into the very dorsocaudal mediastinum and deviates the aorta. This is consistent with an aortic hiatal hernia, which was an incidental finding in this cat.

Diaphragmatic abscess

Diaphragmatic abscesses mainly result from penetrating injuries or migrating foreign bodies penetrating the diaphragm. Less frequently, infection from the abdomen may extend to the peritoneal surface of the diaphragm.

Radiography

An extrapleural soft tissue mass is seen, with the base merging with the diaphragmatic outline and a sharp rounded margin towards the thoracic cavity. If the abscess arises on the peritoneal surface of the diaphragm, it will not be visible on plain radiographs.

Muscular dystrophy

Duchenne muscular dystrophy is a rare inherited disorder in humans, dogs, cats and other animals, leading to a deficiency in the myofibre protein, dystrophin. The deficiency causes excessive intracellular calcium and subsequent myocyte hypertrophy, necrosis and replacement by fibrous tissue. Many skeletal and smooth muscles and the myocardium can be affected, leading to muscular hypertrophy, organomegaly and dystrophic mineralization.

Radiography

Radiographic findings include:

- Convex, scalloped diaphragmatic silhouette (Figure 14.58)
- Abdominal organomegaly
- Cardiomegaly
- Soft tissue mineralization.



14.58 Lateral thoracic radiograph of a Labrador Retriever with muscular dystrophy. Notice the scalloped irregular protrusions of the diaphragm caused by the hypertrophied diaphragmatic musculature. (Courtesy of N. Lester)

Diaphragmatic (phrenic nerve) paralysis

The phrenic nerves arise from the fifth to the seventh cervical nerves, and run through the cranial mediastinum and on each side of the dorsal pericardium. Diaphragmatic paralysis can be uni- or bilateral, temporary or permanent. Diaphragmatic paralysis causes paradoxical diaphragmatic movement; a cranial movement of the affected hemidiaphragm at inspiration and a caudal movement at expiration (Kienbock's phenomenon). Associated inward movement of the abdominal wall at inspiration and outward movement at expiration occurs in bilateral paralysis. Unilateral paralysis of the diaphragm rarely causes any clinical signs, whereas bilateral paralysis often causes moderate to severe signs.

Radiography

Inspiratory and expiratory films should be obtained. Radiographic findings include:

- Increased asymmetry of the diaphragmatic outline on DV/VD views in right hemidiaphragmatic paralysis due to the raised right hemidiaphragm (Figure 14.59)
- Decreased asymmetry of the diaphragmatic outline on DV/VD views in left hemidiaphragmatic paralysis due to the raised left hemidiaphragm
- Right and left costophrenic angles positioned at different levels in the case of unilateral paralysis, with the paralysed side positioned more cranially
- Cranioventral angulation of the ribs on the side of the paralysed hemidiaphragm
- Cranial displacement of the diaphragmatic structures during inspiration and caudal

displacement during expiration in the case of bilateral paralysis, or absence of diaphragmatic displacement at different stages of the respiratory cycle (Figure 14.60)

- Poor pulmonary inflation on the affected side.

Fluoroscopy

This is the imaging modality of choice to observe respiratory excursion of the diaphragm. There is a reduced range of motion of one crus, or paradoxical movement of both crura, during the respiratory cycle.

Diaphragmatic flutter

Flutter of the diaphragm consists of synchronous spastic contractions of one or both hemidiaphragms. It occurs synchronous with the first heart sound. It is thought to be due to a lower threshold of excitability of the phrenic nerves at the level of the pericardium, which allows their stimulation by action currents of the myocardium. It is commonly a self-limiting condition that disappears if the underlying cause is treated, usually an electrolyte imbalance of variable origin. Marked rhythmic movements of the costal arch and the abdominal wall are the only clinical signs of a diaphragmatic flutter. These can last from only a few days to several months.

Fluoroscopy

This allows dynamic visualization of the spastic contractions of one or both hemidiaphragms, synchronous with the heartbeat. This is not detectable radiographically.



14.59 DV thoracic radiograph of a 3-month-old Boxer with right-sided diaphragmatic paralysis. The diaphragm has an increased asymmetry due to the elevated right hemidiaphragm; the right costophrenic angle is positioned more cranially than the left. Note the cranial direction of the ribs of the right thoracic wall.



14.60 (a) Inspiratory lateral thoracic radiographs of a 9-year-old Cocker Spaniel following a pericardectomy and iatrogenic damage to both phrenic nerves. The position of the diaphragm is unchanged between the two stages of the respiratory cycle, but the lungs are more inflated on the inspiratory radiograph. (b) Expiratory lateral thoracic radiographs of a 9-year-old Cocker Spaniel following a pericardectomy and iatrogenic damage to both phrenic nerves. The position of the diaphragm is unchanged between the two stages of the respiratory cycle, but the lungs are more inflated on the inspiratory radiograph.

References and further reading

Baines SJ, Lewis S and White RA (2002) Primary thoracic wall tumours of mesenchymal origin in dogs: a retrospective study of 46 cases. *The Veterinary Record* **150**, 335–339

Berry CR, Gaschen FP and Ackerman N (1992) Radiographic and ultrasonographic features of hypertrophic feline muscular dystrophy in two cats. *Veterinary Radiology and Ultrasound* **33**, 357–364

Berry CR, Koblik PD and Ticer JW (1990) Dorsal peritoneopericardial mesothelial remnant as an aid to the diagnosis of feline congenital diaphragmatic hernia. *Veterinary Radiology* **31**, 239–245

Billier DS, Johnson GC, Birchard SJ and Fingland RB (1987) Aneurysmal bone cyst in a rib of a cat. *Journal of the American Veterinary Medical Association* **190**, 1193–1195

Bright RM, Sackman JE, DeNovo C and Toal C (1990) Hiatal hernia in the dog and cat: a retrospective study of 16 cases. *Journal of Small Animal Practice* **31**, 244–250

Burnie AG, Simpson JW and Corcoran BM (1989) Gastro-oesophageal reflux and hiatus hernia associated with laryngeal paralysis in a dog. *Journal of Small Animal Practice* **30**, 414–416

Caporn TM and Read RR (1996) Osteochondromatosis of the cervical spine causing compressive myelopathy in a dog. *Journal of Small Animal Practice* **37**, 133–137

Dennis R (1993) Radiographic diagnosis of rib lesions in dogs and cats. *Veterinary Annual* **33**, 173–192

Feeney DA, Johnston GR, Grindem CB *et al.* (1982) Malignant neoplasia of canine ribs: clinical, radiographic and pathologic findings. *Journal of the American Veterinary Medical Association* **180**, 927–933

Forrest LJ and Thrall DE (1994) Bone scintigraphy for metastasis detection in canine osteosarcoma. *Veterinary Radiology and Ultrasound* **35**, 124–130

Fossum TW, Boudrieau RJ and Hobson PH (1989) Pectus excavatum in eight dogs and six cats. *Journal of the American Animal Hospital Association* **25**, 595–605

Fowler JD (1998) Thoracic cage defects. In: *BSAVA Manual of Small Animal Cardiorespiratory Medicine and Surgery*, ed. V Luis Fuentes and S Swift, pp. 353–358. BSAVA Publications, Gloucester

Grandage J (1974) The radiology of the dog's diaphragm. *Journal of Small Animal Practice* **15**, 1–17

Hammer AS, Weeren FR, Weisbrode SE and Padgett SL (1995) Prognostic factors in dogs with osteosarcomas of the flat or irregular bones. *Journal of the American Animal Hospital Association* **31**, 321–326

Hardie EM, Clary EM, Kornegay JN *et al.* (1998) Abnormalities of the thoracic bellows: stress fractures of the ribs and hiatal hernia. *Journal of Veterinary Internal Medicine* **12**, 279–287

Heyman SJ, Diefenderfer DL, Goldschmidt MH and Newton CD (1992) Canine axial skeletal osteosarcoma. A retrospective study of 116 cases (1986–1989). *Veterinary Surgery* **21**, 304–310

Hornyak L (1999) Malformation of the processus xiphoideus in two breed cats. *Kleintierpraxis* **44**, 373–378

Jankowski MK, Steyn PF, Lana SE *et al.* (2003) Nuclear scanning with ^{99m}Tc-HDP for the initial evaluation of osseous metastasis in canine osteosarcoma. *Veterinary and Comparative Oncology* **1**, 152–158

Kraje BJ, Kraje AC, Rohrbach BW *et al.* (2000) Intrathoracic and concurrent orthopedic injury associated with traumatic rib fracture in cats: 75 cases (1980–1998). *Journal of the American Veterinary Medical Association* **216**, 51–54

Kramers P, Flückiger MA, Rahn BA and Cordey J (1988) Osteopetrosis in cats. *Journal of Small Animal Practice* **29**, 153–164

Lamb CR (2004) Radiology corner: loss of the diaphragmatic line as a sign of ruptured diaphragm. *Veterinary Radiology and Ultrasound* **45**, 305–306

Langley-Hobbs SJ, Carmichael S, Lamb CR, Bjornson AP and Day MJ (1997) Polyostotic lymphoma in a young dog: a case report and literature review. *Journal of Small Animal Practice* **38**, 412–416

Morgan JP and Stavenborn M (1991) Disseminated idiopathic skeletal hyperostosis (DISH) in a dog. *Veterinary Radiology* **32**, 65–70

Pirkey-Ehrhart N, Withrow SJ, Straw RC *et al.* (1995) Primary rib tumors in 54 dogs. *Journal of the American Animal Hospital Association* **31**, 65–69

Pratschke KM, Hughes JML, Skelly C and Bellenger CR (1998) Hiatal herniation as a complication of chronic diaphragmatic herniation. *Journal of Small Animal Practice* **39**, 33–38

Spattini G, Rossi F, Vignoli M and Lamb CR (2003) Use of ultrasound to diagnose diaphragmatic rupture in dogs and cats. *Veterinary Radiology and Ultrasound* **44**, 226–230

Stickle RL (1984) Positive-contrast cellography (peritoneography) for the diagnosis of diaphragmatic hernia in dogs and cats. *Journal of the American Veterinary Medical Association* **185**, 295–298

Störk CK, Hamaide AJ, Schwedes C *et al.* (2003) Hemiurothorax following diaphragmatic hernia and kidney prolapse in a cat. *Journal of Feline Medicine and Surgery* **5**, 91–96

Sullivan M and Lee R (1989) Radiological features of 80 cases of diaphragmatic rupture. *Journal of Small Animal Practice* **30**, 561–566

Suter PF (1984) Chapter 1 – Normal radiographic anatomy and radiographic examination; Chapter 5 – Lesions of the thoracic wall, extrapleural diseases; Chapter 6 – Abnormalities of the diaphragm. In: *Thoracic Radiography. A Text Atlas of Thoracic Diseases of the Dog and Cat*, ed. PF Suter, pp. 1–45; 161–177; 179–204. Peter F. Suter, Wettswill, Switzerland

The Veterinary Cooperative Oncology Group (1993) Retrospective Study of 26 Primary Tumors of the Osseous Thoracic Wall in Dogs. *Journal of the American Animal Hospital Association* **29**, 68–72

Vignoli M, Toniato M, Rossi F *et al.* (2002) Transient post-traumatic hemidiaphragmatic paralysis in two cats. *Journal of Small Animal Practice* **39**, 312–316

Vincent-Johnson NA (2003) American canine hepatozoonosis. *Veterinary Clinics of North America: Small Animal Practice* **33**, 905–920

Vollmerhaus B, Roos H, Matis U, Veith G and Tassani-Prell M (1999) The specific anatomy and function of the thorax of the domestic cat. *Tierärztliche Praxis K* **27**, 365–370

Appendix 1

M-mode echocardiography reference values for cats

Joanna Dukes-McEwan

Breed	Sedation?	RVd (mm)	IVSd (mm)	IVSs (mm)	LVFWd (mm)	LVFWs (mm)	LVIDd (mm)	LVIDs (mm)	FS (%)	LA (mm)	Ao (mm)	Reference	Comments
Cats	No	0.0–7.0	2.2–4.0	4.7–7.0	2.2–4.0	5.4–8.1	12.0–19.8	5.2–10.8	39.0–61.0	9.3–15.1	7.2–1.19	Jacobs and Knight (1985)	n=30; range given
Cats	No	x	2.8–6.0	x	3.2–5.6	x	11.2–21.8	6.4–16.8	23.0–56.0	4.5–11.2	4.0–11.8	Pipers <i>et al.</i> (1979)	n=25; range given
Cats	No	0.0–8.3	3.0–6.0	4.0–9.0	2.5–6.0	4.3–9.8	10.8–21.4	4.0–11.2	40.0–66.7	7.0–17.0	6.0–12.1	Sisson <i>et al.</i> (1991)	n=79; range given
Cats	No	x	5.0 (0.7)	7.6 (1.2)	4.6 (0.5)	7.8 (1.0)	15.1 (2.1)	6.9 (2.2)	55.0 (10.2)	12.1 (1.8)	9.5 (1.5)	Moise <i>et al.</i> (1986)	n=11; mean (standard deviation) given
Maine Coon	No	x	2.5–5.7	7.2–7.8	2.8–5.9	5.4–10.7	12.1–23.3	5.0–14.5	32.08–69.82	10.3–17.6	8.1–15.7	Drouff <i>et al.</i> (2005)	n=105; range (mean/standard deviation) given
Cats	Anaesthetized, pentobarbital	x	4.0 (0.3)	x	4.0 (4.0)	x	13.0 (1.2)	8.6 (1.6)	34.5 (2.51)	10.0 (0.7)	9 (0.7)	Allen (1982)	n=10; mean (standard deviation) given
Cats	Yes (ketamine)	1.2–7.5	2.2–4.9	x	2.1–4.5	x	10.7–17.3	4.9–11.6	30.0–60.0	7.2–13.3	7.1–11.5	Fox <i>et al.</i> (1985)	n=30; range given
Cats	Yes (xylazine, pentobarbital)	x	x	x	x	x	12.9 (0.9)	8.8 (0.8)	31.1 (4.67)	x	x	Allen and Downey (1983)	n=8; mean (standard deviation) given

A1.1 M-mode echocardiographic reference values for cats. Ao = Aorta; FS = Fractional shortening; LA = Left atrium; LVFWd = Left ventricular free wall in diastole; LVFWs = Left ventricular free wall in systole; LVIDd = Left ventricular internal diameter in diastole; LVIDs = Left ventricular internal diameter in systole; IVSd = Interventricular septum in diastole; IVSs = Interventricular septum in systole; RVd = Right ventricle in diastole; x = No reference value given. (Data from Boon, 1998).

References and further reading

- Allen DG (1982) Echocardiographic study of the anaesthetized cat. *Canadian Journal of Comparative Medicine* **46**, 115–122
- Allen DG and Downey RS (1985) Echocardiographic assessment of cats anaesthetized with xylazine – sodium pentobarbital. *Canadian Journal of Comparative Medicine* **47**, 281–283
- Boon JA (1998) Appendix IV. In: *Manual of Veterinary Echocardiography*, ed. JA Boon, pp. 456–457. Lippincott Williams and Wilkins, Philadelphia
- Drouff L, Lefbom BK, Rosenthal SL and Tyrrell WD (2005) Measurement of M-mode echocardiographic parameters in healthy adult Maine coon cats. *Journal of the American Veterinary Medical Association* **226**, 734–737
- Fox PR, Bond BR and Peterson ME (1985) Echocardiographic reference values in healthy cats sedated with ketamine hydrochloride. *American Journal of Veterinary Research* **46**, 1479–1484
- Jacobs G and Knight DH (1985) M-mode echocardiographic measurements in non-anaesthetised healthy cats: Effects of body weight, heart rate and other variables. *American Journal of Veterinary Research* **46**, 1705–1711
- Moise NS, Dietz AE, Mezza LE *et al.* (1986) Echocardiography, electrocardiography and radiography of cats with dilation cardiomyopathy, hypertrophic cardiomyopathy and hyperthyroidism. *American Journal of Veterinary Research* **47**, 1476–1486
- Pipers FS, Reef V and Hamlin RL (1979) Echocardiography in the domestic cat. *American Journal of Veterinary Research* **40**, 882–886
- Sisson DD, Knight DH, Helinski C *et al.* (1991) Plasma taurine concentrations and M-mode echocardiographic measures in healthy cats and cats with dilated cardiomyopathy. *Journal of Veterinary Internal Medicine* **5**, 232–238

Appendix 2

M-mode echocardiography reference values for dogs

Joanna Duker-McEwan

Breed	RVd (mm)	IVSd (mm)	IVSs (mm)	LVFWd (mm)	LVFWs (mm)	LVIDd (mm)	LVIDs (mm)	FS (%)	EF (%)
Afghan Hound	10.0 *	10.0 *	13.0 *	9.0 *	12.0 *	42.0 *	28.0 *	33.0 *	x
Anatolian Karabash	26–30 kg = 16.0 (1.4); 31–35 kg = 19.8 (2.3); 36–40 kg = 24.7 (3.7); 41–45 kg = 26.7 (2.0); 46–51 kg = 31.2 (0.7)	26–30 kg = 8.5 (0.7); 31–35 kg = 9.8 (0.8); 36–40 kg = 9.9 (0.7); 41–45 kg = 10.8 (1.2); 46–51 kg = 11.7 (0.7)	26–30 kg = 12.5 (0.7); 31–35 kg = 14.5 (0.5); 36–40 kg = 14.8 (1.3); 41–45 kg = 15.5 (0.7); 46–51 kg = 16.5 (0.9)	26–30 kg = 8.5 (0.7); 31–35 kg = 8.6 (0.8); 36–40 kg = 10.0 (0.9); 41–45 kg = 10.6 (0.9); 46–51 kg = 12.2 (1.3)	26–30 kg = 13.5 (0.7); 31–35 kg = 13.6 (0.8); 36–40 kg = 14.8 (1.5); 41–45 kg = 16.3 (0.7); 46–51 kg = 17.0 (0.9)	26–30 kg = 46.0 (1.4); 31–35 kg = 50.5 (1.8); 36–40 kg = 54.1 (1.9); 41–45 kg = 57.3 (1.2); 46–51 kg = 62.1 (2.5)	26–30 kg = 30.0 (0.0); 31–35 kg = 35.0 (1.3); 36–40 kg = 38.1 (1.5); 41–45 kg = 40.8 (1.3); 46–51 kg = 44.6 (1.8)	26–30 kg = 34.5 (2.1); 31–35 kg = 30.3 (2.6); 36–40 kg = 29.6 (1.5); 41–45 kg = 28.7 (1.0); 46–51 kg = 28.1 (1.0)	26–30 kg = 72.0 (2.8); 31–35 kg = 66.8 (3.5); 36–40 kg = 65.1 (2.2); 41–45 kg = 63.8 (1.4); 46–51 kg = 62.8 (2.1)
Beagle	x	6.7 (1.1)	9.6 (1.5)	8.2 (1.9)	11.4 (1.9)	26.3 (3.4)	15.7 (3.4)	40.0 (9.0)	77.0 (10.0)
Boxer	x	9.0 (2.0)	13.0 (2.0)	10.0 (2.0)	15.0 (2.0)	40.0 (5.0)	x	33.0 (8.0)	x
Boxer	x	9.9* (7.1–11.9)	13.1* (10.5–17.1)	9.7* (7.7–12.6)	13.6* (10.3–17.5)	43.1* (36.6–51.8)	29.6* (23.5–36.3)	31* (23–42)	x
Bull Terrier	x	10.0 (2.0)	13.0 (2.0)	10.0 (1.0)	12.0 (1.0)	38.0 (3.0)	LVIDs = body weight (kg) x (14.6 + 0.5)	32.5 (4.5)	x
Cavalier King Charles Spaniel	x	x	x	x	x	28.0 (3.0)	19.3 (2.1)	x	x
Cocker Spaniel	x	0.82 (0.13)	x	0.79 (0.11)	x	3.38 (0.33)	2.22 (0.28)	34.26 (4.54)	x
Corgi (Pembroke)	10.0 *	8.0 *	12.0 *	8.0 *	12.0 *	32.0 *	19.0 *	44.0 *	x
Dobermann	x	10.5 (3.77)	16.5 (1.18)	10.8 (0.987)	16.2 (0.753)	49.7 (5.61)	33.8 (3.601)	31.8 (3.81)	x
Dobermann	x	9.61 (1.19)	14.3 (0.65)	9.59 (0.6)	14.1 (0.84)	46.8 (4.16)	30.8 (3.31)	34.2 (1.81)	x
Dobermann	x	10	16	11	18	39.1	31	20.1	x
Dobermann	x	>7.0	>10.0	>7.0	>10.0	<50.0	x	30.0–36.0	x
Dobermann	x	10.4 (2.0)	14.1 (2.6)	10.0 (2.0)	14.0 (2.8)	41.4 (3.26)	27.3 (3.5)	34.8 (6.3)	x

A2.1 M-mode echocardiographic reference values for dogs. Specific values, where reported, are shown as mean (standard deviation). * = Median value given. Ao = Aorta; EF = Ejection fraction; ET = Ejection time; FS = Fractional shortening; LA = Left atrium; LVFWd = Left ventricular free wall in diastole; LVFWs = Left ventricular free wall in systole; LVIDd = Left ventricular internal diameter in diastole; LVIDs = Left ventricular internal diameter in systole; IVSd = Interventricular septum in diastole; IVSs = Interventricular septum in systole; PEP = Pre-ejection period; RVd = Right ventricle in diastole; √ = Reference value given; x = No reference value given. (continues) ▶

M-mode echocardiography reference values for dogs

Breed	LA (mm)	Ao (mm)	PEP (seconds)	ET (seconds)	PEP:ET ratio	Vcf (circs/s)	Reference	Comments and limitations of study
Afghan Hound	26.0*	26.0 *	x	x	x	x	Morrison <i>et al.</i> (1992)	Regression lines to show influence of body weight. Dogs 2-7 years old
Anatolian Karabash	26-30 kg = 21.5 (0.7); 31-35 kg = 23.5 (1.4); 36-40 kg = 26.0 (1.5); 41-45 kg = 28.0 (0.9); 46-51 kg = 29.0 (1.3)	26-30 kg = 25.5 (0.7); 31-35 kg = 26.5 (0.8); 36-40 kg = 29.0 (1.2); 41-45 kg = 31.5 (1.8); 46-51 kg = 32.2 (1.4)	x	x	x	x	Kayar and Uysal (2004)	n=50 (25 male, 25 female; 2-6 years old; 30-51 kg). Reference values given for weight ranges and body surface area ranges. Mitral M-mode data also given. No follow-up to confirm normality. (Turkish language)
Beagle	x	x	x	x	x	x	Crippa <i>et al.</i> (1992)	EF from cubed formula. Regression line to show influence of body weight
Boxer	23.0 (2.0)	22.0 (2.0)	0.07 (0.01)	0.18 (0.02)	x	x	Herrtage (1994)	Little correlation shown with body weight. Absolute values advocated
Boxer	x (2D reported)	x (2D reported)	x	x	0.4* (0.31-0.5)	1.67* (1.2-2.43)	Schober and Luis Fuentes (2002)	n=66. Healthy Boxers without aortic stenosis. Parameters of diastolic function also provided
Bull Terrier	x (2D reported)	x (2D reported)	x	x	x	x	O'Leary <i>et al.</i> (2003)	n=14 (10 bitches). LVIDs and 2D LA diameter correlated with body weight. Doppler aortic velocity reported as 1.9 (0.2)
Cavalier King Charles Spaniel	x (2D reported)	x (2D reported)	x	x	x	x	Häggström <i>et al.</i> (2000)	Normal animals (n=27) and dogs with class I-IV heart failure reported
Cocker Spaniel	x	x	x	x	x	x	Gooding <i>et al.</i> (1986)	Regression line to show effect of body surface area also. Dogs from a dilated cardiomyopathy kennel - subgroup had low FS%. No repeats
Corgi (Pembroke)	21.0 *	18.0 *	x	x	x	x	Morrison <i>et al.</i> (1992)	Regression lines to show influence of body weight. Dogs 2-7 years old
Dobermann	x	x	x	x	x	x	Calvert <i>et al.</i> (1982)	Minimal data about normal Dobermanns given
Dobermann	26.63 (1.5)	29.9 (2.31)	0.07 (0.01)	0.17 (0.01)	0.44 (0.07)	2.07 (0.16)	Calvert and Brown (1986)	Clinically normal, repeat echocardiography after 1 year
Dobermann	27.0	26.0	x	x	x	x	O'Grady and Horne (1995)	Reference values given
Dobermann	x	x	x	x	x	x	Calvert (1995)	Criteria for normality in this breed
Dobermann	27.3 (4.1)	26.4 (3.8)	x	x	0.38 (0.1)	x	Sottiaux and Amberger (1997)	Normal Dobermanns (n=21). No follow-up scans reported

M-mode echocardiography reference values for dogs

Breed	RVd (mm)	IVSd (mm)	IVSs (mm)	LVFWd (mm)	LVFWs (mm)	LVIDd (mm)	LVIDs (mm)	FS (%)	EF (%)
Dobermann	x	x	x	x	x	<25 kg = <44.6; 25–<30 kg = 44.6–<45.5; 30–<35 kg = 45.5–<46.4; 35–<40kg = 46.4–<47.3; 40–<45kg = 47.3–<48.1; 45–<50 kg = 48.1–<49.0; 50 kg = 49.0–<49.9	<25 kg = <38.8; 25–<30 kg = 38.8–<39.5; 30–<35 kg = 39.5–<40.2; 35–<40 kg = 40.2–<40.9; 40–<45kg = 40.9–<41.6; 45–<50 kg = 41.6–<42.3; 50 kg = 42.3–<43.0 mm	x	x
English Setter	x	8.1 (1.5)	13.2 (1.5)	7.1 (1.7)	11.8 (2.7)	39.7 (6.1)	24.3 (5.7)	39 (10)	x
Estrela Mountain Dog	x	11.0 (1.5)	Male = 15.0 (1.8); Female = 13.6 (2.5)	11.2 (1.6)	14.9 (2.1)	Male = 51.8 (3.9); Female = 48.9 (5.0)	33.0 (4.4)	34.4 (5.7)	x (2D Simpson's calculation reported)
German Shepherd Dog	10.1 (2.6)	9.6 (0.9)	14.0 (0.9)	8.8 (1.1)	13.0 (1.2)	41.7 (5.0)	31.0 (5.1)	28.63 (6.52)	x
German Shepherd Dog	13.5 (0.9)	9.8 (1.4)	14.2 (1.6)	9.5 (1.2)	13.6 (1.1)	49.5 (4.7)	34.3 (3.4)	31.4 (3.4)	x
Golden Retriever	13.0 *	10.0 *	14.0 *	10.0 *	15.0 *	45.0 *	27.0 *	39.0 *	x
Great Dane	x	x	x	x	x	x	x	31.4 (4.0)	57.0 (7.0)
Great Dane	19.0 * (11.0–26.0)	14.5 * (12.0–16.0)	16.5 * (14.0–19.0)	12.5 * (10.0–16.0)	16.0 * (11.0–19.0)	53.0 * (44.0–59.0)	39.5 * (34.0–45.0)	25.0 * (18.0–36.0)	48.0 * (33.0–65.0)
Greyhound	x	13.4 (1.72)	x	11.6 (1.67)	x	46.9 (3.05)	33.3 (2.61)	29.0 (4.2)	x
Greyhound	15.5	11.9	x	12.9	x	42.7	x	24.63	48.93
Irish Wolfhound	17.0 * (10.0–26.0)	12.0 * (9.0–14.5)	15.0 * (11.0–17.0)	10.0 * (9.0–13.0)	14.0 * (11.0–17.0)	50.0 * (46.0–59.0)	36.0 * (33.0–45.0)	28.0 * (20.0–34.0)	54.0 * (38.0–61.0)
Irish Wolfhound	26.7 (5.3)	8.0 (1.9)	13.7 (3.4)	9.5 (2.1)	15.0 (3.3)	53.9 (5.2)	35.2 (4.8)	35.2 (4.9)	x
Irish Wolfhound (males)	x	10.5 (2.23)	12.73 (2.11)	10.19 (1.67)	14.96 (1.91)	51.88 (5.67)	37.81 (4.17)	28.38 (4.71)	x
Irish Wolfhound (females)	x	10.14 (2.2)	12.29 (2.21)	9.75 (1.56)	14.08 (2.03)	49.0 (6.79)	35.75 (5.64)	27.33 (3.78)	x

A2.1 (continued) M-mode echocardiographic reference values for dogs. Specific values, where reported, are shown as mean (standard deviation). * = Median value given. Ao = Aorta; EF = Ejection fraction; ET = Ejection time; FS = Fractional shortening; LA = Left atrium; LVFWd = Left ventricular free wall in diastole; LVFWs = Left ventricular free wall in systole; LVIDd = Left ventricular internal diameter in diastole; LVIDs = Left ventricular internal diameter in systole; IVSd = Interventricular septum in diastole; IVSs = Interventricular septum in systole; PEP = Pre-ejection period; RVd = Right ventricle in diastole; √ = Reference value given; x = No reference value given. (continues) ▶

M-mode echocardiography reference values for dogs

Breed	LA (mm)	Ao (mm)	PEP (seconds)	ET (seconds)	PEP:ET ratio	Vcf (circs/s)	Reference	Comments and limitations of study
Dobermann	x	x	x	x	x	x	O'Grady (2006) (Protect study)	Protect study: screening criteria for Dobermanns of different body weights to identify dogs with dilated cardiomyopathy (Boehringer Ingelheim Vetmedica)
English Setter	27 (3.9)	20.7 (2.4)	x	x	x	x	Pietra <i>et al.</i> (1998)	Apart from LA and Ao, values similar to those predicted from regression lines
Estrela Mountain Dog	x (2D reported)	x (2D reported)	x	x	x	x	Lobo <i>et al.</i> (2007)	n=74 (34 male, 40 female; 18–123 months old; 30–75 kg). 2D and Doppler data also reported. Influence of age, weight and gender reported. No serial data to confirm normality and high prevalence of cardiac disease (26/100 excluded, of which 9/26 had dilated cardiomyopathy and chronic heart failure)
German Shepherd Dog	24.3 (2.1)	25.2 (1.6)	x	x	x	x	Muzzi <i>et al.</i> (2006)	n=60. Significant correlation with body weight (reference values given) and significant difference between sexes. E point to septal separation = 4.9 (1.3 mm). No follow-up to confirm normality
German Shepherd Dog	24.6 (2.3)	27.1 (1.8)	x	x	x	x	Kayar <i>et al.</i> (2006)	n=50 (30 male, 20 female; 1–8 years old; 28–40 kg). Regression equations of influence of body weight. Mitral valve M-mode parameters also reported
Golden Retriever	27.0*	24.0 *	x	x	x	x	Morrison <i>et al.</i> (1992)	Regression lines to show influence of body weight. Dogs 2–7 years old
Great Dane	x	x	x	x	x	x	Borgarelli <i>et al.</i> (1996)	EF from Teicholz formula (see Chapter 2). Published references with regression lines over-estimated left ventricle parameters. FS lower than published values. No follow-up. No figures given
Great Dane	33.0 * (28.0–46.0)	29.5 * (28.0–34.0)	x	0.15 * (0.12–0.18)	x	1.7 * (1.0–2.3)	Koch <i>et al.</i> (1996)	n=15. Results given as median (5–95 percentiles). Dogs re-evaluated for up to 4 years (median age 2.5–3.5 years) (see also Tarducci <i>et al.</i> , 1997)
Greyhound	x	x	0.0685 (0.008)	0.183 (0.016)	0.38 (0.05)	1.6 (0.29)	Snyder <i>et al.</i> (1995)	Regression lines show influence of body weight and body surface area compared with breeds of similar weight (see Morrison <i>et al.</i> , 1992).
Greyhound	24.5	27.1 (systole)	0.07	0.17	0.4	x	Della Torre <i>et al.</i> (2000)	n=20. Standard deviation not given (SEM reported). EF from Teicholz (see Chapter 2) (see also Page <i>et al.</i> 1993)
Irish Wolfhound	31.0 * (22.0–35.0)	30.0 * (29.0–33.0)	x	0.16 * (0.14–0.19)	x	1.7 * (1.0–2.2)	Koch <i>et al.</i> (1996)	n=20. Results given as median (5–95 percentiles). Dogs re-evaluated for up to 4 years (median age 2.5–3.5 years)
Irish Wolfhound	33.7 (5.9)	30.5 (4.0)	x	x	x	x	Vollmar (1996)	E point to septal separation = 7.4 (1.5). No regression analysis
Irish Wolfhound (males)	46.81 (5.66)	33.29 (3.02)	x	x	x	x	Brownlie (unpublished)	LA and Ao from 2D. Personal communication
Irish Wolfhound (females)	44.55 (5.46)	32.66 (2.07)	x	x	x	x	Brownlie (unpublished)	LA and Ao from 2D. Personal communication

M-mode echocardiography reference values for dogs

Breed	RVd (mm)	IVSd (mm)	IVSs (mm)	LVFWd (mm)	LVFWs (mm)	LVIDd (mm)	LVIDs (mm)	FS (%)	EF (%)
Italian Greyhound	7.0	6.4	x	7.1	x	22.2	x	42.72	75.45
Miniature Poodle	4.0 *	5.0 *	8.0 *	5.0 *	8.0 *	20.0 *	10.0 *	47.0 *	x
Newfoundland	x	x	x	x	x	35.0–60.0	22.0–44.0	>25	x
Newfoundland	19.0 * (6.0–28.0)	11.5 * (7.0–15.0)	15.0 * (11.0–20.0)	10.0 * (8.0–13.0)	15.0 * (11.0–16.0)	50.0 * (44.0–60.0)	35.5 * (29.0–44.0)	30.0 * (22.0–37.0)	57.0 * (44.0–66.0)
Newfoundland	8.3 (3.0)	10.66 (1.13)	12.93 (1.38)	10.28 (1.13)	13.69 (1.38)	45.35 (4.03)	34.31 (3.0)	24.47 (3.21)	47.85 (3.45)
Scottish Deerhound	x	10.2	12.4	10.4	13.3	47.9	36.5	27.0	x
Scottish Deerhound	22.6 (5.7)	9.1 (2.8)	14.6 (4.1)	10.0 (1.8)	15.3 (2.2)	51.2 (5.0)	34.0 (5.1)	33.5 (5.8)	54.3 (6.2)
Whippet	11.8	8.6	x	9.0	x	35.9	x	32.17	61.69
Whippet	x	9.4 (1.2)	12.0 (1.5)	8.8 (1.1)	12.4 (1.5)	37.3 (3.8)	26.9 (3.6)	27.7 (5.2)	61.3 (8.1) (Cubed formula)
Mongrels	x	✓	✓	✓	✓	✓	✓	✓	x
Mongrels	x	✓	x	✓	x	✓	✓	x	53.8
Unspecified	x	✓	✓	✓	✓	✓	✓	29.0–45.0	x
Unspecified	✓	✓	✓	✓	✓	✓	✓	39.0 (6.0)	x
Various	x	x	x	x	x	x	x	x	x
Various	x	✓	✓	✓	✓	✓	✓	36.26	x
Various	✓	✓	x	✓	x	✓	✓	30.7 (7.6)	60.8 (7.0)
Various	✓	✓	x	✓	x	✓	✓	39.0 (6.0)	x
Various	x	x	x	x	x	x	x	x	x

A2.1 (continued) M-mode echocardiographic reference values for dogs. Specific values, where reported, are shown as mean (standard deviation). * = Median value given. Ao = Aorta; EF = Ejection fraction; ET = Ejection time; FS = Fractional shortening; LA = Left atrium; LVFWd = Left ventricular free wall in diastole; LVFWs = Left ventricular free wall in systole; LVIDd = Left ventricular internal diameter in diastole; LVIDs = Left ventricular internal diameter in systole; IVSd = Interventricular septum in diastole; IVSs = Interventricular septum in systole; PEP = Pre-ejection period; RVd = Right ventricle in diastole; ✓ = Reference value given; x = No reference value given.

M-mode echocardiography reference values for dogs

Breed	LA (mm)	Ao (mm)	PEP (seconds)	ET (seconds)	PEP:ET ratio	Vcf (cir/s)	Reference	Comments and limitations of study
Italian Greyhound	14.3	14.7 (systole)	0.05	0.15	0.32	x	Della Torre <i>et al.</i> (2000)	n=20. Standard deviation not given (SEM reported). EF from Teicholz
Miniature Poodle	12.0 *	10.0 *	x	x	x	x	Morrison <i>et al.</i> (1992)	Regression lines to show influence of body weight. Dogs 2–7 years old
Newfoundland	x	x	x	x	x	x	Tidholm and Jonsson (1996)	Included dogs 3.5 months old and significant number of animals <2 years old. 10% of normal dogs had FS <22%. Overlap with dilated cardiomyopathy dogs
Newfoundland	30.0 * (24.0–33.0)	29.0 * (26.0–33.0)	x	0.17 * (0.14–0.2)	x	1.7 * (1.1–2.5)	Koch <i>et al.</i> (1996)	n=27. Results given as median (5–95 percentiles). Dogs re-evaluated for up to 4 years (median ages 2.5–3.5 years)
Newfoundland	24.13 (4.06)	29.18 (2.71)	x (Doppler reported)	x (Doppler reported)	x (Doppler reported)	x (Doppler reported)	Dukes-McEwan (1999)	n=86. Parameters influenced by body weight and age (linear regression equations given). Follow-up (1–3 years) confirmed normality. Doppler values also available
Scottish Deerhound	x	x	x	x	x	x	Bodey (1998) (and personal communication)	No standard deviation. No attempts to separate individuals with heart disease. Actual values not given in reference
Scottish Deerhound	28.4 (3.9)	29.6 (3.7)	x	x	x	x	Vollmar (1998)	n=21. EF from Teicholz. No follow-up to confirm normality reported
Whippet	18.8	19.6 (systole)	0.05	0.18	0.3	x	Della Torre <i>et al.</i> (2000)	n=20. Standard deviation not given (SEM reported). EF from Teicholz formula (see Chapter 2)
Whippet	x (2D reported)	x (2D reported)	0.052 (0.01)	0.167 (0.22)	0.31 (0.6)	1.69 (0.39)	Bavegems <i>et al.</i> (2007)	n=105 (51 male, 54 female; 10–169 months old; 9.3–17.2 kg). Racing and show dogs, some trained, some untrained or detoured. Doppler data also reported. Influence of body weight reported
Mongrels	x	x	x	x	x	x	Jacobs and Mahjoub (1988)	Regression line to show influence of body surface area and derivative of heart rate (square root of R–R interval)
Mongrels	x	x	x	x	x	x	Mashiro <i>et al.</i> (1976)	EF from corrected cube method. Correlated stroke volume, etc. with indicator–dilution technique
Unspecified	✓	✓	x	x	x	x	Bonagura <i>et al.</i> (1985)	Regression lines to show influence of body weight. Data repeated by Miller <i>et al.</i> (1989)
Unspecified	✓	✓	x	x	x	x	Lusk and Ettinger (1990)	Data obtained from review of literature
Various	x	x	0.054 (0.007)	0.159(0.015)	0.34(0.05)	2.48(0.5)	Atkins and Snyder (1992)	
Various	✓	✓	x	0.179 (0.018)	x	2.07 (0.37)	Boon <i>et al.</i> (1983)	Regression line to show influence of body surface area. Dogs from 6 months to 6 years old (mean age 16.4 months)
Various	✓	✓	x	x	x	2.0 (0.4)	de Madron (1996)	From review of literature and based on body weight tables derived from regression equations. EF from Teicholz
Various	✓	✓	x	x	x	x	Lombard (1984)	Regression lines to show influence of body weight. Dogs 1–9 years old
Various	x	x	0.069 (0.008)	0.255 (0.01)	0.27 (0.04)	x	Pipers <i>et al.</i> (1978)	Anaesthetized animals. No correction for heart rate

References and further reading

- Atkins CE and Snyder PS (1992) Systolic time intervals and their derivatives for evaluation of cardiac function. *Journal of Veterinary Internal Medicine* **6**, 55–63
- Bavegems V, Duchateau L, Sys SU and De Rick A (2007) Echocardiographic reference values in whippets. *Veterinary Radiology and Ultrasound* **48**, 230–238
- Bodey AR (1998) A study of the relationship between blood pressure and echocardiographic measurements of the left ventricular dimensions in Scottish Deerhounds. *Congress Proceedings of the British Small Animal Association*, p. 248
- Bonagura JD, O'Grady MR and Herring DS (1985) Echocardiography: principles of interpretation. *Veterinary Clinics of North America: Small Animal Practice* **15**, 1177–1194
- Boon J, Wingfield WE and Miller CW (1983) Echocardiographic indices in the normal dog. *Veterinary Radiology* **24**, 214–221
- Borgarelli M, Tarducci A, Bussadori C and Ru G (1996) Echocardiographic and Echo-Doppler parameters in normal Great Danes. *European Society of Veterinary Cardiology Newsletter* **10**, 27–28
- Calvert CA (1995) Diagnosis and management of ventricular tachyarrhythmias in Doberman Pinschers with cardiomyopathy. In: *Kirk's Current Veterinary Therapy, Small Animal Practice XII*, ed. JD Bonagura, pp. 799–806. WB Saunders, Philadelphia
- Calvert CA and Brown J (1986) Use of M-mode echocardiography in the diagnosis of congestive cardiomyopathy in Doberman Pinschers. *Journal of the American Veterinary Medical Association* **189**, 293–297
- Calvert CA, Chapman WL and Toal RL (1982) Congestive cardiomyopathy in Doberman Pinscher dogs. *Journal of the American Veterinary Medical Association* **181**, 598–602
- Calvert CA, Hall G, Jacobs G and Pickus C (1997) Clinical and pathologic findings in Doberman Pinschers with occult cardiomyopathy that died suddenly or developed congestive heart failure: 54 cases (1984–1991). *Journal of the American Veterinary Medical Association* **210**, 505–511
- Crippa L, Ferro E, Melloni E, Brambilla P and Cavalletti E (1992) Echocardiographic parameters and indices in the normal Beagle dog. *Laboratory Animals* **26**, 190–195
- Della Torre PK, Kirby AC, Church DB and Malik R (2000) Echocardiographic measurements in Greyhounds, Whippets and Italian Greyhounds – dogs with similar conformation but different size. *Australian Veterinary Journal* **78**(1), 49–55
- de Madron E (1996) M-mode echocardiographic values in the dog. A review of the recent literature. *European Society of Veterinary Cardiology Newsletter: June 1996* **9**, 10–16
- Dukes-McEwan J (1999) Echocardiographic criteria of normality, the findings in cardiac disease and the genetics of familial dilated cardiomyopathy in Newfoundland dogs. University of Edinburgh, pp. 108–122. PhD thesis
- Gooding JP, Robinson WF and Mews GC (1986) Echocardiographic characterization of a dilatation cardiomyopathy in the English Cocker Spaniel. *American Journal of Veterinary Research* **47**(9), 1978–1983
- Gooding JP, Robinson WF, Wyburn RS and Cullen LK (1982) A cardiomyopathy in the English Cocker Spaniel: a clinico-pathological investigation. *Journal of Small Animal Practice* **23**, 133–149
- Häggström J, Hansson KM, Kvart C, Pedersen HD, Vuolteenaho O and Olsson K (2000) Relationship between different natriuretic peptides and severity of naturally acquired mitral regurgitation in dogs with chronic myxomatous valve disease. *Journal of Veterinary Cardiology* **2**, 7–16
- Herrtage ME (1994) Echocardiographic measurements in the normal Boxer. *Proceedings of the European Society of Veterinary Internal Medicine 4th Annual Congress, Brussels, Belgium* pp. 172–173
- Jacobs G and Mahjoob K (1988) Multiple regression analysis, using body size and cardiac cycle length, in predicting echocardiographic variables in dogs. *American Journal of Veterinary Research* **49**, 1290–1294
- Kayar A, Gonul R, Or ME and Uysal A (2006) M-mode echocardiographic parameters and indices in the normal German Shepherd Dog. *Veterinary Radiology and Ultrasound* **47**, 482–486
- Kayar A and Uysal A (2004) Determination of cardiac reference parameters using M-mode and 2-D echocardiographic techniques in adult Karabash dogs. *Turkish Journal of Veterinary Animal Science* **28**, 39–46
- Koch J, Pedersen HD, Jensen AL and Flagstad A (1996) M-mode echocardiographic diagnosis of dilated cardiomyopathy in giant breed dogs. *Journal of Veterinary Medicine* **43**, 297–304
- Lobo L, Canada N, Bussadori C, Gomes JL and Carvalheira J (2007) Transthoracic echocardiography in Estrela Mountain Dogs: reference values for the breed. *The Veterinary Journal* doi:10.1016/j.tvjl.2007.03.024
- Lombard CW (1984) Normal values of the canine M-mode echocardiogram. *American Journal of Veterinary Research* **45**, 2015–2018
- Lusk RH and Ettinger SJ (1990) Echocardiographic techniques in the dog and cat. *Journal of the American Animal Hospital Association* **26**, 473–488
- Mashiro I, Nelson RR, Cohn JN and Franciosa JA (1976) Ventricular dimensions measured non-invasively by echocardiography in the awake dog. *Journal of Applied Physiology* **41**, 953–959
- Miller et al (1989) – au: please provide full reference
- Morrison SA, Moise NS, Scarlett J, Mohammed H and Yaeger AE (1992) Effect of breed and body weight on echocardiographic values in four breeds of dogs of differing somatotype. *Journal of Veterinary Internal Medicine* **6**, 220–224
- Muzzi RAL, Muzzi LAL, De Araújo RB and Cherem M (2006) Echocardiographic indices in normal German Shepherd Dogs. *Journal of Veterinary Science* **7**(2), 193–198
- O'Grady (2006) ranges for LVIDd and LVIDs in Dobermanns. *Protocol for Investigators on PROTECT study*, p. 22. Boehringer Ingelheim Vetmedica
- O'Grady MR and Horne R (1995) Occult dilated cardiomyopathy in the Doberman Pinscher. *Proceedings of the 13th ACVIM Forum*, pp. 298–299
- O'Leary CA, Mackay BM and Atwell RB (2003) Echocardiographic parameters in 14 healthy English Bull Terriers. *Australian Veterinary Journal* **81**(9), 535–542
- Page A, Edmunds G and Atwell RB (1993) Echocardiographic values in the greyhound. *Australian Veterinary Journal* **70**, 361–364
- Pietra M, Guglielmini C and Cipone M (1998) Normal M-mode and Doppler echocardiographic values in English setter. *European Society of Veterinary Cardiology Newsletter* **16**, 8–14
- Pipers FS, Andryscio RM and Hamlin RL (1978) A totally non-invasive method for obtaining systolic time intervals in the dog. *American Journal of Veterinary Research* **39**, 1822–1826
- Schober KE and Luis Fuentes V (2002) Doppler echocardiographic assessment of left ventricular diastolic function in 74 Boxer dogs with aortic stenosis. *Journal of Veterinary Cardiology* **4**, 7–16
- Snyder PS, Sato T and Atkins CE (1995) A comparison of echocardiographic indices of the non-racing healthy greyhound to reference values from other breeds. *Veterinary Radiology and Ultrasound* **36**, 387–392
- Sottiaux J and Amberger C (1997) Normal echocardiographic values in the Doberman Pinscher (French breeding). *European Society of Veterinary Cardiology Newsletter*, **12**, 8
- Tarducci A, Borgarelli M, Bussadori C, D'Angelo A, Ru G and Dotta U (1997) Valori echocardiografici negli alani normali. *ATTI della società italiana delle scienze veterinarie*. LI, Bologna. **17**(20), 593–594
- Tidholm A and Jönsson L (1996) Dilated cardiomyopathy in the Newfoundland: a study of 37 cases (1983–1994). *Journal of the American Animal Hospital Association* **32**, 465–470
- Vollmar A (1996) Kardiologische Untersuchungen beim Irischen Wolfshund unter besonderer Berücksichtigung des Vorhofflimmerns und der Echokardiographie. *Kleintierpraxis* **41**, 397–408
- Vollmar A (1998) Kardiologische Untersuchungen beim Deerhound, Referenzwerte für die Echodiagnostik. *Kleintierpraxis* **43**, 497–508

Appendix 3

Conversion tables

Weight (kg)	Body surface area (m ²)	Weight (kg)	Body surface area (m ²)
2.0	0.160	27.0	0.909
3.0	0.210	28.0	0.931
4.0	0.255	29.0	0.953
5.0	0.295	30.0	0.975
6.0	0.333	31.0	0.997
7.0	0.370	32.0	1.018
8.0	0.404	33.0	1.029
9.0	0.437	34.0	1.060
10.0	0.469	35.0	1.081
11.0	0.500	36.0	1.101
12.0	0.529	37.0	1.121
13.0	0.553	38.0	1.142
14.0	0.581	39.0	1.162
15.0	0.608	40.0	1.181
16.0	0.641	41.0	1.201
17.0	0.668	42.0	1.220
18.0	0.694	43.0	1.240
19.0	0.719	44.0	1.259
20.0	0.744	45.0	1.278
21.0	0.769	46.0	1.297
22.0	0.785	47.0	1.302
23.0	0.817	48.0	1.334
24.0	0.840	49.0	1.352
25.0	0.864	50.0	1.371
26.0	0.886		

A3.1 Weight (kg) to body surface area (m²) conversion table for dogs. (Reproduced from *BSAVA Manual of Canine and Feline Oncology, 2nd edition*)

Weight (kg)	Body surface area (m ²)	Weight (kg)	Body surface area (m ²)
1.4	0.125	5.8	0.323
1.6	0.137	6.0	0.330
1.8	0.148	6.2	0.337
2.0	0.159	6.4	0.345
2.2	0.169	6.6	0.352
2.4	0.179	6.8	0.360
2.6	0.189	7.0	0.366
2.8	0.199	7.2	0.373
3.0	0.208	7.4	0.380
3.2	0.217	7.6	0.387
3.4	0.226	7.8	0.393
3.6	0.235	8.0	0.400
3.8	0.244	8.2	0.407
4.0	0.252	8.4	0.413
4.2	0.260	8.6	0.420
4.4	0.269	8.8	0.426
4.6	0.277	9.0	0.433
4.8	0.285	9.2	0.439
5.0	0.292	9.4	0.445
5.2	0.300	9.6	0.452
5.4	0.307	9.8	0.458
5.6	0.315	10.0	0.464

A3.2 Weight (kg) to body surface area (m²) conversion table for cats. (Reproduced from *BSAVA Manual of Canine and Feline Oncology, 2nd edition*)

Appendix 4

Differential diagnoses for thoracic mineralization

Tobias Schwarz

Pulmonary and bronchial mineralization (see Chapters 11 and 12)

Generalized, small, well marginated

Possible causes:

- Heterotopic bone
- Granuloma
- Feline bronchiolar microlithiasis (BM)
- Rare forms of metastases (atypical osteosarcoma)

Characteristics:

- Small size, sharply marginated
- Random distribution
- Intrabronchial location in BM
- Very opaque for small size

Local with variable size and margination

Possible causes:

- Primary pulmonary neoplasia
- Abscess
- Old haematoma

Characteristics:

- Neoplasia occurs in older animals and mineralizes more commonly in cats
- Presence of pneumonia supports abscess
- Evidence of trauma supports haematoma
- Rate of progression may differentiate malignant and benign lesions

Diffuse and homogenous

Possible causes:

- Hyperadrenocorticism
- Hyperparathyroidism (primary or secondary)
- Hypercalcaemia of malignancy
- Vitamin D toxicity
- Alveolar microlithiasis (rare)
- Old barium aspiration

Characteristics:

- Lungs may appear normal
- Diffuse interstitial pattern
- Marked diffuse mineralization with alveolar microlithiasis

Bronchial wall mineralization (see Chapter 11)

Possible causes:

- Mild – moderate degree: normal age-related process in dogs
- Moderate – marked: chondrodystrophic dogs
- Chronic bronchitis
- Hyperadrenocorticism

Characteristics:

- Parallel linear orientation in accordance with bronchial anatomy
- Circular end-on bronchial mineralization
- Tapering size towards periphery
- Distal distension in bronchiectasis

Cardiovascular mineralization (see Chapter 7)

Aortic root mineralization

Possible causes:

- Incidental degenerative process in older dogs
- Rottweilers and Irish Setters predisposed

Characteristics:

- Superimposed on the heart at level of fourth rib on lateral radiographs
- Single irregular line of plaques
- Can be circular in aortic valve ring mineralization
- May have money roll appearance
- Can extend to cranial mediastinum into brachiocephalic trunk

Other types of focal cardiovascular mineralization

Possible causes:

- Atherosclerosis (arterial)
- Aberrant spirocercosis (aortic)
- Aortic coarctation (proximal descending aorta)
- Chronic endocarditis (valvular)
- Chronic renal disease (myocardial)
- Old calcified thrombus
- Metaplastic new bone formation

Characteristics:

- Plaque-like, amorphous or ring-shaped

Generalized vascular mineralization

Possible causes:

- Feline chronic renal disease (metastatic)
- Feline systemic hypertension
- Canine severe hypothyroidism (atherosclerosis)
- Chronic hypercalcaemia-inducing diseases

Characteristics:

- Parallel linear mineralization of vascular walls (egg shell-like)
- Sometimes reversible (e.g. post renal transplantation)

Differential diagnoses for thoracic mineralization

Pleural and mediastinal mineralization (see Chapters 11 and 13)

Pleural mineralization

Possible causes:

- Mild: normal age-related process in dogs
- Chronic current or previous pleuritis
- Incidental heterotopic bone (pleural plaque)
- Hernia of mineral-containing organ (kidney, stomach, liver)

Characteristics:

- Very thin but opaque pleural fissure lines
- Small dense nodules in lung periphery (plaques)
- Shape and position consistent with herniated organ

Mediastinal mineralization

Possible causes:

- Chronic marked lymphadenopathy with central necrosis
- Lymph node uptake from old barium aspiration
- Calcified mediastinal nodular fat necrosis in cats
- Mineralized oesophageal foreign body
- Hernia of mineral-containing organ (kidney, stomach, liver)

Characteristics:

- Lesion consistent location
- Egg shell-like mineralization in fat necrosis

Thoracic wall mineralization (see Chapter 14)

Possible causes:

- Soft tissue neoplasia with central necrosis
- Rib neoplasia
- Osteochondromatosis
- Skeletal malformation
- Non- or malunion fracture
- Contaminated haircoat (debris, contrast medium)
- Calcinosis circumscripta (CC)

Characteristics:

- Lesion in a consistent location
- Grape-like in CC
- Streak-like with contaminated haircoat

Acknowledgements

The publication of this Manual could not have been achieved without the cooperation and help of a great number of people. We are extremely grateful and would like to mention some of them here.

We wish to thank the entire editorial team at BSAVA for the patient guidance and encouragement we received throughout the process of editing this book.

We are deeply indebted to all the contributing authors of this Manual. The material these experts provided under stringent deadlines speaks for itself. We are proud to be colleagues of such passionate and professional veterinarians! Many authors went far beyond their Chapter assignments. In particular, Jo Dukes-McEwan was tremendously helpful throughout the entire editing process. Thanks so much Jo for all of your extra time and effort!

We also wish to thank all of the individuals who kindly contributed images for this Manual as stated in the figure legends. We received encouragement for this project from a number of experts in the field who also opened their image archives for us. In particular we would like to thank Drs Peter Suter and James Buchanan for their assistance. The same thanks go to many institutions, such as the Universities of California-Davis, Pennsylvania, Cambridge and the Animal Health Trust to name but a few.

A great number of radiographers and computer experts helped us in obtaining and digitizing radiographs, and in transferring large sets of data between different continents. We are particularly grateful for the help of Amy Lang, Cheryl Baumel, Jo Stacy and Josh Benish. Our anaesthetists provided advice on restraint, sedation and anaesthesia protocols and we would like to especially thank Gabrielle Musk and Anthea Rasis for their time.

Our work colleagues assisted us a great deal whilst working on this Manual by picking up the slack whilst we ran around trying to meet deadlines, by contributing cases and useful information, and by donating their own pets for photographs. We would like to particularly thank Nola Lester, Zoe Lenard, Marie Appleby, Belinda Hopper, Jennifer Richardson, Ruth Dennis, Jennifer Reetz, Jennifer Kinns, Ana Cáceres, Mathieu Spriet, Elizabeth Ballegeer, Daniel Rodriguez and Randi Drees.

We are particularly thankful for the support of our families throughout this project. It has not always been easy on them. We are all happy to return to a normal life!

This book is a tribute to the health of dogs and cats. It was made to help them but it was also created with their help. A final thank you to the pets who patiently sat for photographs and whose thoracic radiographs constitute the core of this Manual.

We wish you pleasant reading.

Tobias Schwarz
Victoria Johnson
January 2008

Index

Numbers in *italic type* indicate figures

Abscess

- chest wall 366
- diaphragmatic 374
- pulmonary 263, 266, 274

Acute respiratory distress syndrome (ARDS) 291–2

Adenocarcinoma

- pulmonary 262
- salivary 67

Age, anatomical variations 15, 62, 247

Air alveolograms 253, 277

Air bronchogram 252

Airway

- computed tomography 67
- obstruction 84–5
- (*see also* Bronchial tree, Lung, Trachea)

Alveolar lung disease 281–3

Alveolar lung pattern 251–3

Alveolar septal metastases 316, 317

Anaesthesia

- for CT 67
- for MRI 72
- for radiography 4

Anatomical variation 14–18

Aneurysmal bone cyst 359

Angiocardiography 12

- aortic coarctation 134
- aortic stenosis 120–1
- atrial septal defect 126
- cor triatum dexter/sinister 133
- first pass radionuclide *see* Scintigraphy
- mitral valve dysplasia 127
- patent ductus arteriosus 112–13, 114
- pulmonic stenosis 117–18
- tetralogy of Fallot 129–30
- tricuspid valve dysplasia 128
- vascular ring anomaly 132
- ventricular septal defect 123–4

Angiography

- coronary artery disease 174, 175
- magnetic resonance 71, 74
- vascular ring anomaly 209

Angiostrongylosis 170–1, 307

Aorta

- echocardiography 31, 33, 35
- radiographic anatomy 96–7

Aortic calcification 106

Aortic coarctation 134

Aortic enlargement 105–7

Aortic hilar hernia 374

Aortic insufficiency 157

Aortic regurgitation 38, 45

Aortic root mineralization 386

Aortic stenosis 45, 120–2

Arrhythmogenic right ventricular cardiomyopathy

- canine 138
- feline 147–8

Arteriosclerosis 175

Aspergillosis 305

Asthma 250, 254, 257, 276, 348

Atelectasis 283–6

Atherosclerosis 175

Atrial septal defect 95–7

Azygos vein, radiographic anatomy 98

Barium contrast media 11

Barium transit studies

- diaphragmatic hernia 373
- diaphragmatic rupture 368, 369

Barrel chest 354

Biopsy

- CT-guided 69, 196
- ultrasound-guided 24

Blastomycosis 304

Body condition 15, 248

Border obliteration sign 18–19

Boxer cardiomyopathy 138

Breeds, anatomical variations 14–15, 247–8

Bronchial calcification 229, 230

Bronchial cartilage dysplasia 240

Bronchial collapse 237

Bronchial dysgenesis 240

Bronchial foreign bodies 237–8

Bronchial lung pattern 253–4

Bronchial microlithiasis 240

Bronchial mineralization 229, 230–4, 386

Bronchial neoplasia 238–9, 330

Bronchial obstruction 231

Index

- Bronchial rupture 239–40
Bronchial tree
 computed tomography 232–3
 radiographic anatomy 228–9
 radiographic interpretive principles 229–33
 ultrasonography 233
Bronchiectasis 229, 230, 232, 235–6
Bronchiolitis obliterans with organizing pneumonia (BOOP) 240
Bronchitis, canine 233
Bronchoalveolar carcinoma 239, 253, 261, 310, 316
Bronchogenic cysts 270
Bronchography 12, 231–2, 265
Broncho-oesophageal fistula 11, 240
Bronchopneumonia 236
Bronchus *see* Bronchial tree
Budd–Chiari-like syndrome 173
Butterfly vertebra 14
- Capnoperitoneography 368
Carcinoma
 bronchoalveolar 239, 253, 261, 310, 316
 pulmonary 260, 262, 266, 310
 tracheal 85
Cardiac cycle 15, 93
Cardiac gating in MRI 73–4
Cardiac neoplasia 164–7
 tracheal deviation 224
Cardiac tamponade 158, 160–1
Cardiomegaly 104
Cardiomyopathy
 canine 135–9
 feline 140–8
 (*see also specific disorders*)
Cardiovascular mineralization 386
Cardiovascular system
 computed tomography 66
 magnetic resonance imaging 71, 73–4
 (*see also Heart and individual vessels*)
Cat muzzle 2
Caudal vena cava
 radiographic anatomy 97–8
 radiographic interpretation 107
Cavitating lung lesions 270–1, 274
Centring 4
Chemodectoma, cardiac 165
Chest wall *see* Thoracic wall
Chondrodysplasias, ribcage 352–3
Chondrosarcoma 362
Chylothorax 332
Coccidioidomycosis 305
Collimation 5
Computed tomography (CT)
 alveolar septal metastases 317
 anaesthetic considerations 67
 -assisted FNA/biopsy 69–70, 196
 bronchial collapse 237
 bronchial foreign bodies 238
 bronchial neoplasia 239
 bronchial rupture 240
 bronchial tree 232–3
 bronchiectasis 236
 bronchiolitis obliterans 240
 Budd–Chiari-like syndrome 173–4
 canine chronic bronchitis 233
 cardiac neoplasia 166
 comparison with MRI 72
 feline chronic lower airway disease 235
 fractures 357, 358
 health and safety 67
 helical 68, 69
 indications 66–7
 interstitial fibrosis 314–15
 interstitial mineralization 318
 lung 68, 69
 lung lobe torsion 279–80
 mediastinal cysts 197
 mediastinal masses 195–6
 mediastinitis 199
 mediastinum 66, 68, 187
 metastatic lung disease 268–70
 multicentric lymphoma 317
 oesophageal neoplasia 206
 patient positioning/restraint 67–8
 pleural effusion 334–5
 pleural space 66, 68
 pneumomediastinum 189
 pneumonia 300
 pneumothorax 339
 primary ciliary dyskinesia 236
 pulmonary masses 266
 pulmonary thromboembolism 172
 spirocercosis 210
 technique 68–9
 thoracic wall 66, 68
 trachea 215–16
 tracheal mass 221
Congestive heart failure 87, 287
Constrictive pericarditis 162
Contrast media 11
Contrast radiography techniques
 angiocardiography 12
 bronchography 11, 231–2
 oesophagography 11–12
Cor pulmonale *see* Pulmonary hypertension
Cor triatum dexter/sinister 132–4
Coronary artery diseases 174–5
Cranial thoracic aperture *see* Thoracic inlet
Cranial vena cava
 radiographic anatomy 98
 syndrome 173–4
Cryptococcosis 305
CT *see* Computed tomography
Cysts
 bone 359
 mediastinal 197
 pericardial 162
 pulmonary 270

- Decubitus view, positioning/technique 8–9
- Degenerative disc disease 351, 352
- Dextrocardia 87
- Diaphragm
 radiographic anatomy 341
 radiographic interpretive principles 345–50
 ultrasonography 23
- Diaphragmatic abscess 374
- Diaphragmatic displacement 346–9
- Diaphragmatic flutter 375
- Diaphragmatic hernias 369–74
- Diaphragmatic neoplasia 374
- Diaphragmatic paralysis 375
- Diaphragmatic rupture 192, 367–9
- Diastole, echocardiography 41, 56–60, 62
- Digital radiography 9–11
- Dilated cardiomyopathy (DCM)
 canine 135–8
 feline 146–7
- Dipyridylum derivate intoxication 316
- Dirofilarium immitis* see Heartworm
- Discospondylitis 367
- Disseminated skeletal hyperostosis (DISH) 351, 352
- Ditzels 269
- Doppler
 lung lobe torsion 279
 (see also Echocardiography)
- Dorsoventral (DV) view
 comparison with VD view 17, 18
 positioning/technique 6–7
- Drowning see Near drowning
- Echocardiography
 angiostrongylosis 171
 aortic coarctation 134
 aortic insufficiency 157
 aortic stenosis 121–2
 atrial septal defect 126
 B-mode (2D) 26
 cardiac function 52–3
 left apical/LPS views 33–6
 RPS/subcostal views 27–32
 cardiac function 41
 diastolic 56–60
 myocardial 56, 61
 systolic 50–5
 cardiac neoplasia 164, 166
 cor triatum dexter/sinister 133–4
 dilated cardiomyopathy
 canine 136–8
 feline 146–7
 Doppler 26, 41, 42–9, 53–8
 pulsed wave tissue 61
 equipment 25
 heartworm 168–40
 hypertrophic cardiomyopathy 140–2, 143–4
 indications 24
 infective endocarditis 156–7
 mitral valve dysplasia 127–8
- M-mode 26
 views 37–40, 50–2
 myocardial infiltrative disease 152
 myxomatous atrioventricular valvular degeneration 154–6
 patent ductus arteriosus 113, 115
 patient restraint/preparation 24–5
 pericardial cysts 162
 pericardial defects 163
 pericardial effusion 160–1
 pericarditis 162
 pulmonary hypertension 150–1
 idiopathic 171
 pulmonic insufficiency 157
 pulmonic stenosis 118–20
 reference values
 canine 378–83
 feline 377
 restrictive cardiomyopathy 145
 systemic hypertension 149
 tetralogy of Fallot 130
 traumatic valvular disease 158
 tricuspid valve dysplasia 128–9
 ventricular septal defect 124
- Echotracheography 215
- Emphysema
 pulmonary 185, 275–6
 subcutaneous 344
- Endocardiosis see Myxomatous atrioventricular valvular degeneration
- Endoscopic ultrasonography (EUS) see Ultrasonography
- Expiration, radiographic features 16
- Exposure 4
- Extrapleural sign 19
- Fat
 intrathoracic 248
 necrosis 193
 pericardial 91–2
 ultrasonography 23, 194
- Feline chronic lower airway disease 234–5
- Film 4
- Fine-needle aspiration
 CT-assisted 69–70
 ultrasound-assisted 23–4, 64
- Flail chest 354
- Flat pup syndrome 354
- Fluid bronchogram 300
- Fluoroscopy
 bronchial collapse 237
 diaphragmatic flutter 375
 diaphragmatic paralysis 375
 equipment 82, 13
 gastro-oesophageal intussusception 211
 hiatal hernia 372
 indications 12
 megaesophagus 203

Index

- oesophageal foreign body 207
- oesophageal stricture 205
- oesophagitis 204
- pulmonary herniation 280, 281
- technique 13
- vascular ring anomaly 208
- Foreign bodies
 - bronchial 237–8
 - oesophageal 188, 207
 - thoracic wall 366
 - tracheal, removal 85
- Fractures
 - ribs 354–6
 - spine 357–8
 - sternum 356–7
- Gastro-oesophageal intussusception 210–11
- Granuloma, pulmonary 263, 264
- Grids 5
- Haemangiosarcoma 362
 - cardiac 159, 164, 165
 - metastatic 268, 316
- Haematomas
 - mediastinal 193, 195
 - pulmonary 263, 265
- Haemothorax 332
- Health and safety
 - in computed tomography 67
 - in fluoroscopy 82
 - in radiography 3
- Heart
 - chambers 88–90
 - enlargement 101–4
 - failure
 - congestive 87
 - left-sided 108–9
 - right-sided 109, 110
 - position 87
 - radiographic anatomy 86–93
 - radiographic interpretive principles 100–5
 - size estimation 93–4
 - (*see also* Cardiac; Echocardiography; and *specific conditions*)
- Heartworm 167–70, 306–7
- Hemivertebrae 351, 352
- Hernias 369–74
- Heterotopic bone 247
- Hiatal hernias 370–3
- Histiocytic sarcoma, pulmonary 261
- Histoplasmosis 256
- Horizontal beam standing view, positioning/technique 9
- Horizontal beam VD/DV views *see* Decubitus view
- Hydrothorax 331–2
- Hyperadrenocorticism 254, 317, 318, 343
- Hypertension
 - pulmonary 149–21
 - idiopathic 171
 - systemic 149
- Hypertrophic cardiomyopathy (HCM)
 - canine 138–9
 - feline 88, 140–4
- Hypertrophic osteodystrophy *see* Metaphyseal osteopathy
- Hypertrophic osteopathy 365–6
- Hypothyroidism 353
- Idiopathic pulmonary fibrosis 314–15
- Infective endocarditis 156–7
- Inspiration, radiographic features 16
- Intensifying screens 4
- Interlobar fissure 324
- Interstitial fibrosis 313–16
- Interstitial lung pattern 255–7
- Interstitial mineralization 317–19
- Interstitial neoplastic infiltrate 316
- Interstitial oedema 312–13
- Interstitial pneumonia 313
- Interventional radiology
 - in airway obstruction 84–5
 - equipment 82–3
 - indications 82
 - in tracheal collapse 83–4
 - for tracheal foreign body removal 85
- Iodinated contrast media 11
- Ischaemic heart disease 175
- Kartagener's syndrome 237
- Kilovoltage (kV) 4
- Kittens, positioning aids 3
- kV 4
- Kyphosis 14
- Lateral views
 - positioning/technique 5–6
 - right/left comparison 16, 17
- Left atrial enlargement 103–4
- Left ventricular enlargement 104
- Levocardia 87
- Lipoma/liposarcoma 361, 362
- Liquidopneumothorax 337, 338
- Lordosis 14
- Lung
 - atelectasis 185
 - computed tomography 67, 68, 69
 - fields 244, 258
 - lobe size 258
 - lobe torsion 276–80
 - magnetic resonance imaging 71, 73
 - opacity 244, 246, 249–50, 258
 - radiographic anatomy 242–8
 - radiographic interpretive principles 248–60
 - scintigraphy 75–6, 78–9
 - ultrasonography 21
 - vascular systems 244–6
 - volume 249–50
 - (*see also* Interstitial, Pulmonary)

- Lungworms 307–8
Luxation, vertebrae 357
Lymph nodes, mediastinal 180–3, 191
Lymphadenopathy 69
Lymphoma 257
 cardiac 166–7
 mediastinal 195, 196
 multicentric 316, 317
Lymphosarcoma, thymic 193
- Magnetic resonance angiography 71, 74
Magnetic resonance imaging
 anaesthetic considerations 72
 angiography 71, 74
 bronchial neoplasia 239
 cardiovascular 66
 cardiac gating 73
 comparison with computed tomography 72
 fat suppression techniques 73
 indications 71
 limitations 72
 lung 71
 mediastinum 71
 patient positioning/restraint 72
 pleural space 71
 pulmonary masses 267
 respiratory gating 73
 technique 72–4
 thoracic wall 71
Main pulmonary artery *see* Pulmonary arteries
Mammary carcinoma 21
mAs 4
Mass
 definition 19
 fine-needle aspiration 24
Mass effect 19
Mediastinal cysts 197
Mediastinal effusion 186–7, 198
Mediastinal masses 71, 185–6, 189–7, 330, 225
Mediastinal mineralization 387
Mediastinal oedema 199
Mediastinal osteosarcoma 6
Mediastinal shift 19, 184–5, 278
Mediastinitis 198–9
Mediastinum
 computed tomography 66, 68, 187
 in juveniles 183
 magnetic resonance imaging 71, 73
 radiographic anatomy 177–84
 radiographic interpretive principles 184–7
 ultrasonography 21–3, 187
Megaesophagus 202–3
Mesothelioma, cardiac 159, 166
Metaphyseal osteopathy 350
Metastatic lung disease 256, 267–70, 316
Microcardia 100–1
Microchips and magnetic resonance imaging 72
Milliampereseconds (mAs) 4
Mineralization, differential diagnosis 386–7
- Mitral regurgitation, echocardiography 40, 43
Mitral stenosis, echocardiography 38
Mitral valve disease
 echocardiography 27
 tracheal deviation 224
Mitral valve dysplasia 97–8
 angiocardiology 97
 echocardiography 43, 97–8
MRA *see* Magnetic resonance angiography
MRI *see* Magnetic resonance imaging
Multiple myeloma 364
Muscular dystrophy 374, 375
Myocardial disease
 canine 135–9
 feline 140–8
 secondary 148–53
 (*see also specific diseases*)
Myocardial performance 91, 92
Myxoma, cardiac 166, 167
Myxomatous atrioventricular valvular degeneration 153–6
- Near drowning 290
Neoplasia *see* Tumours
Nuclear medicine, Nuclear scintigraphy *see* Scintigraphy
Nutritional hyperparathyroidism 365
- Oblique views, positioning/technique 9
Oesophageal diverticulum 205–6
Oesophageal foreign bodies 188, 207
Oesophageal neoplasia 206
Oesophageal perforation 11
Oesophageal stricture 204–5
Oesophagitis 203–4
Oesophagography
 gastro-oesophageal intussusception 211
 megaesophagus 203
 oesophageal diverticulum 206
 oesophageal foreign bodies 207
 oesophageal neoplasia 206
 oesophageal stricture 205
 oesophagitis 204
 pneumonia 301
 pulmonary mass 265
 redundant oesophagus 201
 spirocercosis 210
 technique 11–12
 vascular ring anomaly 132, 208
Oesophagus
 radiographic anatomy 200
 radiographic interpretive principles 200–2
 redundant 201
Oslerus osleri 223
Osteochondroma 358–9
Osteomas 269
Osteomyelitis 364, 365, 366, 367
Osteopenia 343

Index

- Osteopetrosis 343, 344
Osteosarcoma
 mediastinal, CT 66
 rib 343, 344, 360
 scintigraphy 363
- Pacemakers and magnetic resonance imaging 72
Paracostal abdominal wall hernia 370
Paraganglioma 364
Paragonimiasis 274, 307
Paraoesophageal hiatal hernia 372–3
Patent ductus arteriosus (PDA) 36, 81–5
Patient positioning/preparation/restraint
 for radiography
 decubitus view 8
 DV/VD views 6–8
 horizontal beam standing view 9
 lateral views 5–6
 oblique view 9
 for computed tomography 67–8
 for echocardiography 24–5
 for magnetic resonance imaging 72
 for radiography 2–4
 for ultrasonography 20, 63–4
- Pectus carinatum 354
Pectus excavatum 14, 250, 353–4
Peribronchial cuffing 230
Pericardial cysts 162
Pericardial defects 162–3
Pericardial effusion 105, 158–61
Pericardial fat 91–2, 95–6
Pericarditis, constrictive 162
Periosteal reaction 343, 344
Peritoneography 368
Peritoneopericardial diaphragmatic hernia 373–4
Persistent right aortic arch (PRAA) 224–5
Pleural effusion 21, 22, 23, 66, 278, 311, 325–9, 330, 331–5
Pleural line 324
Pleural masses 335
Pleural mineralization 387
Pleural space
 computed tomography 66, 68
 magnetic resonance imaging 71
 radiographic anatomy 321–2
 radiographic interpretive principles 322–31
- Pleural surface, ultrasonography 20
Pleuritis 335
Pneumocystosis 305–6
Pneumomediastinum 187–9
Pneumonia 252, 253
 allergic 308–9
 aspiration/fistulous 300–1
 bacterial, canine 298–300
 feline, non-specific 300
 fungal 264, 267, 303–6
 inhalation 309
 interstitial 313
 leptospiral 302
 lipid/lipoid 309
 mycoplasmal 302
 parasitic 306–8
 viral 302–3
- Pneumo-oesophagram 11, 12, 209
Pneumopericardium 163–4
Pneumoperitoneography 368, 369
Pneumoretroperitoneum 188
Pneumothorax 24, 66, 188, 189, 193, 214, 215, 216–19, 271, 273, 283
Positioning *see* Patient positioning
Positive-contrast peritoneography 368
Primary ciliary dyskinesia 236–7
Protective clothing for fluoroscopy 82
Pseudochylothorax 332
Pseudoeffusion 329
Pseudopneumothorax 330–1
Pulmonary abscesses 263, 266
Pulmonary adenocarcinoma 262
Pulmonary alveolar microlithiasis 297–8
Pulmonary alveolar proteinosis 308–9
Pulmonary arteries/veins
 caudal lobar, radiographic anatomy 99–100
 cranial lobar, radiographic anatomy 98–9
 embolism 293–6
 enlargement 108
 main artery
 radiographic anatomy 98
 radiographic interpretation 107
- Pulmonary bullae/blebs 270, 271, 273, 275
Pulmonary carcinoma 260, 262, 266, 310
Pulmonary collapse 247, 321–4
Pulmonary contusion/laceration 296–7
Pulmonary cysts 270
Pulmonary emphysema 275–6
Pulmonary granulomas 263
Pulmonary haematomas 263
Pulmonary haemorrhage 296, 297
Pulmonary herniation 280–1
Pulmonary hypertension 149
 idiopathic 171
Pulmonary infarction 293
Pulmonary infiltration with eosinophilia (PIE) 263, 264, 308
Pulmonary masses 185, 260–7
Pulmonary mineralization 386
Pulmonary neoplasia 261–3, 265, 310–11
 metastatic 267–70
 (*see also* Pulmonary masses and specific tumours)
- Pulmonary nodules 256, 269, 304
Pulmonary oedema 252, 253, 286–90
Pulmonary thromboembolism 75–6, 79, 171–3, 293–6
Pulmonic insufficiency 157
Pulmonic stenosis 116–20
 ‘hat sign’ 224
Pumice stone lung 297–8
Puppies, positioning aids 3
Pyothorax 332

- QP:QS, scintigraphy 77–8
- Radiation
 lung damage 315
 protection *see* Health and safety
- Radiographic principles
 centring 4
 collimation 5
 exposure 4
 film 4
 grids 5
 health and safety 3
 intensifying screens 4
 patient preparation/positioning 2–4
 views
 decubitus 8–9
 dorsoventral 6–7
 end-expiratory 5
 horizontal beam standing 9
 lateral 5–6
 oblique 9
 terminology 5
 ventrodorsal 7–8
- Radiographic trough
 use in CT 67, 68
 for VD view 8
- Radiography
 contrast 11–12
 (*see also specific techniques*)
 digital 9–11
 indications 1–2
- Radiological principles
 border obliteration (silhouette) sign 18–19
 mass and mass effect 19
 normal anatomical variation 14–18
 Röntgen signs 19
 systematic evaluation 13–14
- Radionuclides 76, 78–9, 80
- Rare earth screens 4
- Respiratory gating in MRI 73
- Respiratory pause imaging (CT) 68, 69
- Restraint *see* Patient restraint
- Restrictive cardiomyopathy (RCM), feline 145
- Ribs/ribcage
 developmental disorders 350, 352–4
 fractures 354–6
 neoplasia 344, 359–61
 osteomyelitis 365
 radiographic anatomy 340
 radiographic interpretive principles 342–4
 ultrasonography 20, 21
- Rickets 350
- Right atrial enlargement 101
- Right ventricular enlargement 101–3
- Röntgen signs 19
- Sandbags 3
- Sarcoma
 chest wall 71
 paraspinal 191
 scapular 66
- Scintigraphy
 atrial septal defect 127
 indications 75
 interstitial mineralization 318
 mediastinal masses 196–7
 mega-oesophagus 203
 metastatic lung disease 270
 patent ductus arteriosus 114, 115
 patient preparation 75–6
 primary ciliary dyskinesia 236–7
 pulmonary thromboembolism 172–3
 techniques
 cranial mediastinal masses 80
 first pass radionuclide angiocardiology 76–8
 mucociliary function 80
 pulmonary scintigraphy 78–80
 tetralogy of Fallot 131
 ventricular septal defect 125
- Sclerosis 343
- Screens 4
- Sedation
 for radiography 3
 for ultrasonography 25
- Sex, anatomical variation 15
- Short oesophagus hiatal hernia 371
- Silhouette sign 18–19
- Sliding intramediastinal hiatal hernia 371–2
- Smoke inhalation 290–1
- Spine (thoracic)
 abnormalities 351–2
 fractures/dislocations 357, 358
 neoplasia 363, 364
 radiographic anatomy 340–1
 radiographic interpretive principles 345
- Spirocercosis 209–10
- Spondylitis/discospondylitis 367
- Spondylosis deformans 351, 352
- Stents, tracheal 82–4, 85
- Sternal abnormalities 350, 351
- Sternal dysraphism 350
- Sternal fractures/dislocations 356, 357
- Sternal neoplasia 362
- Sternal osteomyelitis 366, 367
- Sternum
 radiographic anatomy 340
 radiographic interpretive principles 345
- Sussdorf's space 183, 184
- Systole, echocardiography 41, 50–5
- Tension pneumothorax 337, 338
- Tetralogy of Fallot 129–31
- Thoracic boundaries
 radiographic anatomy 340–2

Index

- radiographic interpretive principles 342–50
(*see also* Diaphragm, Ribs, Spine, Sternum, Thoracic inlet, Thoracic wall)
 - Thoracic duct, radiographic anatomy 68
 - Thoracic inlet, radiographic anatomy 340
 - Thoracic wall
 - computed tomography 66, 68
 - foreign bodies 366
 - magnetic resonance imaging 71, 72, 73
 - mineralization 387
 - neoplasia 73
 - radiographic interpretive principles 344–5
 - Thoracocentesis 333–4
 - Thymoma 190, 195, 196, 225, 352
 - Thymus 183
 - Thyroid masses 226
 - Topography 14
 - Toxoplasmosis 306
 - Trachea
 - and heart size 64–5, 223–4
 - radiographic anatomy 213
 - radiographic interpretive principles 213–16
 - Tracheal carcinoma 85
 - Tracheal collapse 217–20
 - stenting 83–4
 - Tracheal foreign bodies 222
 - removal 85
 - Tracheal haemorrhage 223
 - Tracheal hypoplasia 216–17
 - Tracheal laceration/avulsion 220
 - Tracheal masses 221–2
 - Tracheal obstruction 84–5
 - Tracheal stenosis 217
 - Tracheal stripe sign 200–1, 207
 - Tracheitis 222–3
 - Traumatic valvular disease 158
 - Tricuspid valve
 - dysplasia 128–9
 - echocardiography 46–7
 - Tuberculosis 310
 - Tumours
 - bronchial 238–9
 - cardiac 164–7
 - diaphragmatic 374
 - oesophageal 206
 - pulmonary 69, 73, 261–3, 265, 310–11
 - metastatic 267–70
 - skeletal 344, 359–64
 - thoracic wall 73, 359–62
(*see also specific tumours*)
 - Ultrasonography
 - atelectasis 286
 - and biopsy 24
 - diaphragmatic rupture/hernia 369, 374
 - endoscopic 62–4
 - and fine-needle aspiration 24, 64
 - indications 20
 - lung lobe torsion 278–9
 - mediastinal cysts 197
 - mediastinal effusion 198
 - mediastinal masses 194–5
 - mediastinitis 199
 - mediastinum 187
 - metastatic lung disease 268
 - oesophageal neoplasia 206
 - oesophageal stricture 205
 - patient preparation 20
 - pleural effusion 334
 - pleural masses 336
 - pleuritis 336
 - pneumothorax 339
 - pulmonary masses 265
 - spirocercosis 210
 - technique 20–3
 - thoracic wall 366
(*see also* Echocardiography)
 - Uraemic pneumonitis 292–3
 - Vascular lung pattern 254–5
 - Vascular ring anomaly 101–2, 207–9
 - Ventral diaphragmatic hernia 370
 - Ventricular septal defect 27, 122–5
 - Ventrodorsal (VD) view
 - comparison with DV view 17, 18
 - positioning/technique 6–7
 - Vertebral heart score 94
 - Vertebral neoplasia 363
(*see also* Spine)
 - Views *see* Radiographic principles
 - Wedge vertebra 14
 - X-ray beam, quality/quantity 4
-